

NASA Conference Publication 2457

Sensitivity Analysis in Engineering

*Proceedings of a symposium held at
Langley Research Center
Hampton, Virginia
September 25-26, 1986*

NASA

Sensitivity Analysis in Engineering

Compiled by

Howard M. Adelman
*Langley Research Center
Hampton, Virginia*

Raphael T. Haftka
*Virginia Polytechnic Institute and State University
Blacksburg, Virginia*

Proceedings of a symposium sponsored by
the National Aeronautics and Space
Administration and Virginia Polytechnic
Institute and State University and held at
Langley Research Center
Hampton, Virginia
September 25-26, 1986

NASA
National Aeronautics
and Space Administration
**Scientific and Technical
Information Branch**

PREFACE

This document contains the proceedings of the Symposium on "Sensitivity Analysis in Engineering," held at the NASA Langley Research Center, September 25-26, 1986. The symposium was jointly sponsored by the NASA Langley Research Center and Virginia Polytechnic Institute and State University.

The purpose of the symposium was to disseminate the latest research in the general area of sensitivity analysis, i.e., the systematic calculation of derivatives of the response of a physical model with respect to parameters characterizing the model. A review of recent literature (which the symposium co-chairmen carried out and documented shortly before the symposium) indicated to us that few engineering disciplines are more broadly based across disciplinary lines than is sensitivity analysis. In fact, contributions to research in sensitivity analysis are represented in nearly every major field from chemistry and physics to structural mechanics, aerodynamics, thermodynamics, and behavioral psychology. In recognition of the multidisciplinary nature of sensitivity analysis, the keynote paper was on the subject of sensitivity analysis in chemistry and physics.

The symposium was organized in the following sessions:

- I General and Multidisciplinary Sensitivity
- II Static Structural Sensitivity Analysis and Applications
- III Eigenproblem Sensitivity Methods
- IV Transient Sensitivity Analysis
- V Shape Sensitivity Analysis

Papers in these proceedings are grouped by session and identified in the contents. The order of the papers is the order of presentations at the symposium. The papers contained herein were submitted as camera-ready copy.

The use of trade names or names of manufacturers in this publication does not constitute an official endorsement of such products or manufacturers, either expressed or implied, by the National Aeronautics and Space Administration.

Howard M. Adelman
Raphael T. Haftka
Symposium Co-Chairmen

PRECEDING PAGE BLANK NOT FILMED

CONTENTS

PREFACE	iii
---------------	-----

SESSION I - GENERAL AND MULTIDISCIPLINARY SENSITIVITY

ON DETERMINING IMPORTANT ASPECTS OF MATHEMATICAL MODELS: APPLICATION TO PROBLEMS IN PHYSICS AND CHEMISTRY	1
Herschel Rabitz	
COMPUTABLE OPTIMAL VALUE BOUNDS FOR GENERALIZED CONVEX PROGRAMS	11
Anthony V. Fiacco and Jerzy Kyparisis	
ALTERNATIVE METHODS FOR CALCULATING SENSITIVITY OF OPTIMIZED DESIGNS TO PROBLEM PARAMETERS	19
G. N. Vanderplaats and H. D. Cai	
BEHAVIOR SENSITIVITIES FOR CONTROL AUGMENTED STRUCTURES	33
R. A. Manning, R. V. Lust, and L. A. Schmit	
SENSITIVITY METHOD FOR INTEGRATED STRUCTURE/ACTIVE CONTROL LAW DESIGN	59
Michael G. Gilbert	
THE CASE FOR AERODYNAMIC SENSITIVITY ANALYSIS	77
Jaroslav Sobieszczanski-Sobieski	

SESSION II - STATIC SENSITIVITY ANALYSIS AND APPLICATIONS

SENSITIVITY OF OVERALL VEHICLE STIFFNESS TO LOCAL JOINT STIFFNESS	97
Choon T. Chon	
DESIGN SENSITIVITY ANALYSIS OF NONLINEAR STRUCTURAL RESPONSE	113
J. B. Cardoso and J. S. Arora	
OPTIMAL CONTROL CONCEPTS IN DESIGN SENSITIVITY ANALYSIS	133
Ashok D. Belegundu	
SENSITIVITY AND OPTIMIZATION OF COMPOSITE STRUCTURES USING MSC/NASTRAN	147
Gopal K. Nagendra and Claude Fleury	
OPTIMIZATION OF SHALLOW ARCHES AGAINST INSTABILITY USING SENSITIVITY DERIVATIVES	167
Manohar P. Kamat	

SESSION III - EIGENPROBLEM SENSITIVITY METHODS

SURVEY OF METHODS FOR CALCULATING SENSITIVITY OF GENERAL EIGENPROBLEMS	177
Durbha V. Murthy and Raphael T. Haftka	

MODAL SENSITIVITY FOR STRUCTURAL SYSTEMS WITH REPEATED FREQUENCIES	197
I. U. Ojalvo	
SENSITIVITY DERIVATIVES AND OPTIMIZATION OF NODAL POINT LOCATIONS FOR VIBRATION REDUCTION	215
Jocelyn I. Pritchard, Howard M. Adelman, and Raphael T. Haftka	
ON COMPUTING EIGENSOLUTION SENSITIVITY DATA USING FREE VIBRATION SOLUTIONS	233
B. P. Wang	
APPLICATION OF A SYSTEM MODIFICATION TECHNIQUE TO DYNAMIC TUNING OF A SPINNING ROTOR BLADE	247
C. V. Spain	
SESSION IV - TRANSIENT SENSITIVITY ANALYSIS	
NUMERICAL STUDIES OF THE THERMAL DESIGN SENSITIVITY CALCULATION FOR A REACTION-DIFFUSION SYSTEM WITH DISCONTINUOUS DERIVATIVES	263
Jean W. Hou and Jeen S. Sheen	
APPLICATION OF DESIGN SENSITIVITY ANALYSIS FOR GREATER IMPROVEMENT ON MACHINE STRUCTURAL DYNAMICS	285
Masataka Yoshimura	
DESIGN SENSITIVITY ANALYSIS OF ROTORCRAFT AIRFRAME STRUCTURES FOR VIBRATION REDUCTION	299
T. Sreekanta Murthy	
ON SINGULAR CASES IN THE DESIGN DERIVATIVE OF GREEN'S FUNCTIONAL	319
Robert Reiss	
SESSION V - SHAPE SENSITIVITY ANALYSIS	
3-D MODELING AND AUTOMATIC REGRIDDING IN SHAPE DESIGN SENSITIVITY ANALYSIS	329
Kyung K. Choi and Tse-Min Yao	
ACCURACY OF THE DOMAIN METHOD FOR THE MATERIAL DERIVATIVE APPROACH TO SHAPE DESIGN SENSITIVITIES	347
R. J. Yang and M. E. Botkin	
SENSITIVITY ANALYSIS FOR LARGE-SCALE PROBLEMS	357
Ahmed K. Noor and Sandra L. Whitworth	

ON DETERMINING IMPORTANT ASPECTS OF MATHEMATICAL MODELS:

APPLICATION TO PROBLEMS IN PHYSICS AND CHEMISTRY*

Herschel Rabitz
Princeton University
Department of Chemistry
Princeton, NJ

SUMMARY

Mathematical modelling must always deal with two general problems. First, the form, parameters or distributed functions in a mathematical model are often imprecisely known and their impact on desired objectives or observables is an important issue. Second, even when the components in a model are "known" there always remains the fundamental question concerning the importance and interrelationship between the various components of the system. The use of parametric and functional gradient sensitivity analysis techniques is considered for models described by partial differential equations. By interchanging appropriate dependent and independent variables, questions of inverse sensitivity may be addressed to gain insight into the inversion of observational data for parameter and function identification in mathematical models. It may be argued that the presence of a subset of dominantly strong coupled dependent variables will result in the overall system sensitivity behavior collapsing into a simple set of scaling and self similarity relations amongst elements of the entire matrix of sensitivity coefficients. These general tools are generic in nature, but the present paper will emphasize their application to problems arising in selected areas of physics and chemistry.

INTRODUCTION

Mathematical modelling and analysis has been a traditionally active area in engineering and this is especially true in recent years with the ready availability of high-speed digital computers. Such modelling efforts have many goals, including design, optimization and merely understanding the systems' components. As an adjunct to these efforts, the tools of sensitivity analysis provide a natural means to aid in all of these goals and the development of the subject in engineering has been especially focused on applications to design and optimization. The ultimate driving force behind all these efforts is certainly the practical issues of increased reliability, efficiency, etc.

An interesting contrast with the modelling/sensitivity analysis efforts primarily in engineering occurs upon consideration of analogous problems in the "fundamental" areas of chemistry and physics. The first point of contrast is that issues of design and optimization are frequently not relevant in basic

* The author acknowledges support for this work from the Office of Naval Research.

research studies of chemistry and physics (studies involving problems in applied physics, industrial chemical processes, etc. would be best categorized as engineering). The term "modelling" is also rarely used in the scientific disciplines and the basic thrust is usually for an attainment of system understanding. In particular, control variables frequently found in engineering problems are often absent in the physical and chemical events occurring at atomic and molecular scales. The lack of practical motivation and these inherent differences between engineering and scientific problems has apparently resulted in only a recent realization that the tools of sensitivity analysis have a potentially valuable contribution to make in chemistry and physics.¹⁻⁶

The differences cited above obscure the overall basic similarity between mathematically defined engineering and scientific problems. Their common foundation lies in their basic input-output nature. In addition, the particular mathematical formulations involved can be quite similar even though the physical interpretation is different (e.g., the equations of stationary quantum mechanics are exactly those of classical linear waves). From this general perspective, a common set of tools may be developed within the framework of sensitivity analysis of benefit to all the relevant disciplines making use of mathematical modelling techniques. The present paper will succinctly review current activity with the topics being primarily in the area of chemical physics. Special emphasis will be given viewing problems from a functional perspective rather than treating them as described by a discrete set of input parameters. This approach is essential in many scientific applications and often has a similar broad basis in engineering. Although the particular applications discussed in the paper require more information than provided here for a full appreciation of their significance, they should be viewed in a generic context for analogous applications in other possible areas of interest to the reader. Finally, due to the brief nature of this paper, no attempt will be made to thoroughly review all recent developments in sensitivity analysis as applied to chemical physics problems; a series of recent review articles is available to cover this literature.¹⁻⁶

BASIC CONCEPTS OF FUNCTIONAL SENSITIVITY ANALYSIS

The problems of interest in chemical physics at the atomic scale or macro scale are typically described by differential equations of a boundary value and/or initial value nature. For example, Schrödinger's equation in quantum mechanics has the form

$$\left[\frac{\hbar}{i} \frac{\partial}{\partial t} - \frac{\hbar^2}{2m} \nabla^2 + V(\underline{r}) \right] \psi = 0$$

and the equations of mass conservation in chemical kinetics have the form

$$\frac{\partial}{\partial t} C_i - D_i \nabla^2 C_i - f_i(C) = 0$$

These latter equations follow conventional notation where \hbar is Planck's constant, m is the mass of the particle interacting with potential $V(\underline{r})$ and its wavefunction $\psi(\underline{r}, t)$ is evaluated at point \underline{r} and time t , while C_i is the i -th

chemical species concentration, D_i is the corresponding diffusion coefficient and the reactive flux f_i is generally a nonlinear function of the concentrations. Although Schrödinger's equation is rigorously the only valid approach for treating dynamics at the atomic scale, classical mechanics is a very popular and often quite accurate approach to treating the motion of atoms and molecules. In this case, Hamilton's equations

$$\frac{\partial q_i}{\partial t} = \frac{\partial H}{\partial p_i}, \quad \frac{\partial p_i}{\partial t} = - \frac{\partial H}{\partial q_i}$$

would apply where $H(p,q)$ is the Hamiltonian with i -th coordinate q_i and momentum p_i . Various other dynamical equations also occur in statistical mechanics and in models occurring in all aspects of chemical physics. A general situation commonly arising, included in the equations above, is the appearance of coefficients which are functions of either the system independent or dependent variables. For example, the potential $V(\underline{r})$ plays this role in Schrödinger's equation. These functions may be thought of as input, and two broad categories will arise. First, the form of these functions may be imprecisely known due to a lack of full understanding of the system or simply imprecise measurements defining the structure of the functions. Second, even if the input functions are known precisely, there is typically a very poor understanding of how the form or structure of these functions influences the behavior of the equation solutions or observables. As mentioned in the Introduction, the possibility of varying these functions for the purpose of optimization will not be explicitly considered here since this is not often the case. Therefore, the role of sensitivity analysis in chemistry and physics is largely to provide a means to probe the interrelationship between the input and output functions (i.e., determine the important aspects of the system).

In order to better quantify the above discussion, we may generally write any of the appropriate differential equations in the following form

$$L_i(\underline{r}, t, \underline{\theta}) = 0 \quad (1)$$

where L_i is the i -th differential operator typically being a nonlinear function of the elements of the output solution vector $\underline{\theta}(\underline{r}, t)$. Appropriate initial and/or boundary conditions would be given in order to completely specify the problem. The parametric functional nature of the differential equations is evident through the arguments of L_i in Eq. (1) depending on position \underline{r} and time t . In addition, the boundary conditions may be functions of time and the initial conditions may be functions of position also acting as another class of input functions for consideration. Regardless of the circumstance, we may generally denote the vector of input functions as $\underline{\Omega}(\underline{r}, t)$ and the first variation of Eq. (1) becomes

$$\sum_n \frac{\partial L_i}{\partial \theta_n} \frac{\delta \theta_n(\underline{r}, t)}{\delta \Omega_l(\underline{r}', t')} + \frac{\delta L_i}{\delta \Omega_l} = 0 \quad (2)$$

The first of these terms in Eq. (2) involves the system Jacobian $\partial L_i / \partial \theta_n$, and the second term is the explicit functional derivative of the operator with

respect to the l -th member of the input function set. The solution to this linear differential equation produces the functional derivative matrix $\delta\phi_n(\underline{r},t)/\delta\Omega_l(\underline{r}',t')$ giving the response of the n -th output at position \underline{r} and time t with respect to a disturbance of the l -th input function at a position \underline{r}' and time t' such that

$$\delta\phi_n(\underline{r},t) = \sum_l \int d\underline{r}' dt' \frac{\delta\phi_n(\underline{r},t)}{\delta\Omega_l(\underline{r}',t')} \delta\Omega_l(\underline{r}',t') \quad (3)$$

where $\delta\Omega_l(\underline{r}',t')$ is an arbitrary infinitesimal functional variation. The matrix solution to Eq. (2) constitutes what is sometimes referred to as the forward sensitivity matrix. All of the general applications of sensitivity analysis in chemical physics have focused on an examination of the sensitivity matrix elements and perhaps most importantly their manipulation to address other questions besides mere input-output relations. This point will be emphasized later in this paper.

Since Eq. (2) is linear, it is quite natural to define a Green's function matrix with elements $\delta\phi_n(\underline{r},t)/\delta g_l(\underline{r}',t')$ having the general interpretation of the response of ϕ_n to a disturbance of the flux g_l of the l -th member of the dependent variable set. This matrix satisfies the following equation

$$\sum_n \frac{\partial L_i}{\partial \phi_n} \frac{\delta\phi_n(\underline{r},t)}{\delta g_l(\underline{r}',t')} = \delta_{il} \delta(\underline{r}-\underline{r}') \delta(t-t') \quad (4)$$

The solution to Eq. (2) may be directly expressed in terms of the Green's function solution to Eq. (4). In some cases, this can be a practical numerical procedure but more importantly the elements of the Green's function matrix have direct physical significance and in principle measurements in the laboratory could be performed to determine them. This latter point is especially important since as commented above many basic problems in chemistry and physics do not inherently contain laboratory control functions or variables.

Equation (2) produces the first order functional perturbation coefficients to the nominal solution of Eq. (1) as evidenced by Eq. (3). Due care is needed if the physics corresponds to a degenerative perturbation problem. Standard procedures exist in this case corresponding to the introduction of directional derivatives. A variety of numerical techniques have been developed for solving Eqs. (2) or (4), and detailed information may be found in the literature. In general, it seems most efficient to solve Eq. (2) by maximally taking advantage of its structure in relation to the often employed Newton linearization schemes applied to Eq. (1).

In practice, the coupled differential equations in Eq. (1) are often highly nonlinear and an interesting type of scaling behavior has been found under certain conditions.* This situation has not been explored for the case of functional variations, except for the Green's function, and for that reason we shall consider it here in terms of discrete system parameters denoted by the vector \underline{a} . Supposing that a single dominant dependent variable exists one might expect that a variation in any given system parameter would show up as significant, provided that the dominant variable significantly responded.

*H. Rabitz and M. Smooke, "Scaling Relations and Self Similarity Conditions in Strongly Coupled Dynamical Systems", J. Phys. Chem., in progress.

Without loss of generality, we may take the dominant dependent variable as $\phi_1(t, \underline{\alpha})$ where time t is taken as the only independent "coordinate" for simplicity. Often the identification of this dominant variable seems to be associated with the most strongly coupled nonlinear member entering the differential equations. Under the assumption of strong dominant dependence, we may approximate the remaining dependent variables as

$$\phi_n(t, \underline{\alpha}) \approx \mathcal{F}_n(\phi_1(t, \underline{\alpha})) \quad (5)$$

where \mathcal{F}_n is an appropriate function. The important point is that the parameter dependence of all the remaining dependent variables is approximately driven through that of the dominant dependent variable. This is in keeping with the notion that the dominant variable will pass judgment over any parameter variation regarding its significance to any of the remaining dependent variables. A natural consequence of the approximation in Eq. (5) is the scaling relation

$$\left[\frac{\partial \phi_n}{\partial \alpha_i} \right] \approx \left[\frac{\partial \phi_1}{\partial \alpha_i} \right] \left[\frac{\partial \phi_n}{\partial \phi_1} \right] \left[\frac{\partial \phi_1}{\partial t} \right]^{-1} \quad (6)$$

which expresses all the system sensitivities in terms of those of the dominant dependent variable and simple temporal slope information. The full significance of scaling behavior has not been established although it may have wide applicability in nonlinear systems outside of chemistry and physics.

A MENU OF SENSITIVITY APPLICATIONS IN CHEMICAL PHYSICS

It is beyond the scope and purpose of this paper to present detailed, elaborate physical analyses of particular models or problems. Rather, the examples should be viewed for their generic behavior and as illustrations of the type of sensitivity technology existing in chemical physics (specific citations to the literature can be found in refs. 1-6). The best means to present this information appears to be in the narrative tabular form given below. Finally, many of the examples carried out thus far in chemical physics have considered discrete parameter systems rather than those prescribed from a functional point of view. This approach was taken even though the physical problems were functional in nature. Although these studies were often insightful, a number of cases clearly indicate that the use of a small number of discrete parameters to represent typical continuous input functions can give misleading sensitivity results at times. This comment would most assuredly be applicable to situations outside the realm of chemical physics.

A. Forward Sensitivities

A direct analysis of the gradients introduced in Eq. (2) comprises the forward problem. The name forward results from the fact that the system is being analyzed from the forward direction whereby the response of the output to a disturbance of the input is examined. The magnitude, sign and general

behavior of the sensitivity coefficients as a function of their arguments is of concern. This comment applies to all of the other applications in the following paragraphs. A wealth of information can be gleaned by such an analysis and a number of applications have been carried forth. For example, in the case of molecular collisions, the role of different regions of the potential function upon the collision cross section has been explored. For elastic, inelastic and reactive scattering, a wide variety of problems have been treated in chemical kinetics encompassing temporal, steady-state spatial and unsteady spatial systems.

B. Inverse Sensitivities

The forward sensitivities in paragraph A correspond to the logical definition of the system parameters or input functions as independent variables and the system observables as dependent variables. The original physical problem is, of course, cast in this framework but many laboratory or field measurements are actually done for the purpose of inversion to better quantify a model. In this sense, one may use a "reasonable" zeroth order model and the accompanying forward sensitivities to calculate corresponding inverse sensitivities. These may be denoted as $\partial\Omega_l(\underline{r},t)/\partial\phi_n(\underline{r}',t')$ and it is evident that they give information on the infinitesimal response of the l -th function in the model to a disturbance of the n -th member of the observation set. Knowledge of these gradients can be used as a means to design possible experiments for the ultimate purpose of inversion. In principle, they may also be employed in an iterative inversion process with real data. Thus far, applications in chemical physics have been confined to the former case. Illustrations have been performed for inverse molecular scattering and chemical kinetics mechanism identification. These inverse sensitivities are the first members of what has been referred to as derived sensitivities since they may be derived from the forward set in paragraph A above. The forward and inverse sensitivities are orthogonal complements of each other and more generally they are related through Legendre type transformations familiar in thermodynamics. Exactly the same techniques are employed to generate the specialized sensitivities in paragraph C and D below.

C. Parameter Interrelationships

As implied in paragraph B, one may relax the constraints on the original definition of the system dependent and independent variables or some portion thereof. In this fashion, it is possible to calculate the possible response of one system input function to a disturbance of another corresponding to the gradients $\partial\Omega_l(\underline{r},t)/\partial\Omega_k(\underline{r}',t')$. Nonzero values for these parameter correlation gradients would imply a relationship between the input functions under the particular constraint relaxing the role of the system dependent and independent variables. The behavior of these gradients has implication for the uniqueness of the system model.

D. Observation Interrelationships

A family of gradients exactly analogous to those in paragraph C can be generated to study the relationship between different possible observations or dependent variables in a system. This is a physically meaningful question since all possible observations or system behaviors derive from the same underlying model. The particular gradients in this case have the form $\delta\phi_n(\underline{r},t)/\delta\phi_m(\underline{r}',t')$ where it is understood that an implied exchange of dependent and independent variables has occurred. As with the inverse gradients in paragraph B, these new sensitivities are also of use in the design of laboratory or field measurements. Nonzero values for these gradients imply a relationship between two possible observations and in that case serious consideration should be given to whether it is worthwhile to actually perform both measurements. A hierarchy of observations could be established based on the magnitude of these families of gradients. Little application has thus far been carried out along these lines.

E. Flux Disturbance Sensitivities

The Green's function introduced as the solution to Eq. (4) corresponds to the literal situation of disturbing one of the system dependent variables and monitoring a response in another. Knowledge of such responses provides a detailed map of the interconnectivity produced by the physical model. An interesting point in this regard concerns the fact that the dynamic response of the actual model can be quite distinct from that implied by the kinematic structure of the differential equations. A mapping of the system dependent variable interconnectivity can give valuable insight into which components or portions of a model are of actual significance to the questions or observations of concern. Green's functions are routinely calculated in a variety of applications in chemical physics for these reasons.

F. Objective Function Sensitivity Analysis

As discussed in the Introduction, many problems in chemical physics are not posed with well understood observational objectives before actually investigating the problem. Indeed, the general role of sensitivity analysis in chemical physics is often to simply identify interesting objectives or model components worth further study theoretically and experimentally. This perspective is typically at variance with the situation found in engineering where the problem is often first posed by stating the desired objective. In general, any observable feature or objective of the system may be written as a functional $F[\phi]$ of the system dependent variable vector. Direct functional differentiation of this object will probe the desired quantity of interest in a straightforward fashion. An interesting point occurs when this objective can be identified before actually solving the model. In this circumstance, the well known adjoint sensitivity analysis method may be employed to efficiently calculate the sensitivities of the system objectives. This latter procedure has only been used sparsely in chemical physics thus far for the evident reasons stated above.

G. Model Reduction

A natural objective in all modelling efforts is to reduce the system complexity to a level suitable for the questions or tasks at hand. A procedure such as this is sometimes referred to as lumping, and sensitivity coefficients provide information relevant to this goal. The forward sensitivity coefficients in paragraph A may be examined for this purpose and this is routinely performed. Related more sophisticated manipulation of these forward sensitivities can also be considered but much more work needs to be done in this area to optimally draw on the full variety of sensitivity coefficients. An ever present danger in system reduction is subsequent misuse of the simplified model in situations contrary to the assumptions underlying the lumping procedure; in general, model reduction needs to be performed again for each new objective.

H. Model Expansion

Although model reduction using sensitivity or other techniques represents a well established objective, a much more difficult approach to model improvement entails the expansion of an oversimplified model to a proper level of sophistication. In general, this problem is not well posed, but there is a simple quantitative indicator of model expansion that can be performed using sensitivity analysis. In particular, a common circumstance arises when the actual model calculations are performed on a simplified system drawn from a larger body of facts or information as input. For example in the case of chemical kinetics, often hundreds of possible chemical reactions could be identified as potentially important beforehand while typically only a small subset would actually be included in the first zeroth order model. In essence, one may view the results of such a calculation as involving the full extended model but with the appropriate parameters set to a null value. Although the nominal solution clearly does not contain these parameters, the gradient of the solution may still be nonzero. Therefore, the sensitivity of the additional parameters about their nominal null values can be quite easily calculated if (a) an extended "shopping list" of possible additional system components is available and (b) if the additional components do not introduce further dependent variables. Such a sensitivity to missing model components can be used to que likely new parameters for introduction into the model at their finite realistic values. Limited applications of this type have been carried out in chemical kinetics.

I. Parameter Space Mapping

Both functional and parametric gradient sensitivity analysis techniques are inherently local in nature in that the gradients are evaluated at a nominal point in parameter or input function space. Such an analysis seems often quite adequate to establish which aspects of a model are important. As commented earlier, this latter goal is often the primary motivation for applications in chemistry and physics. On the other hand, in engineering and certain scientific applications optimization is the ultimate objective.

Inherently, an optimization entails a search through parameter space and gradient techniques have an evident limitation. No satisfactory solution is available for circumventing this difficulty, but some interesting new tools involving Lie group techniques seem especially attractive. This approach considers the calculation of a Lie generator (first order differential operator) for prescribing transformations throughout the parameter space. At this stage only preliminary mathematical analysis and elementary applications have been considered.

CONCLUDING COMMENTS

Sensitivity analysis clearly provides a powerful set of systematic tools to analyze models for their physical content and mathematical behavior. Although extensive applications to scientific problems are relatively recent, there is much to be gained by an exchange of techniques and ideas between the engineering and scientific disciplines. Finally, one caveat always worth keeping in mind is that the conclusions of a sensitivity analysis will always be predicated on the significance or validity of the underlying model. However, such caution should never be used as an argument to not perform a sensitivity analysis, since any model calculations without a sensitivity analysis will be far less worthwhile.

REFERENCES

1. H. Rabitz, "Chemical Sensitivity Analysis Theory with Applications to Molecular Dynamics", *Comp. in Chem.*, 5, 167 (1981).
2. J. Tilden, V. Costanza, G. McRae and J. Seinfeld, "Sensitivity Analysis of Chemically Reacting Systems", in Modelling of Chemical Reaction Systems, K. Ebert, P. Deuflhard and W. Jager, Editors, (Springer-Verlag, Berlin, 1981) pg. 69.
3. H. Rabitz, M. Kramer and D. Dacol, "Sensitivity Analysis in Chemical Kinetics", *Ann. Rev. Phys. Chem.*, 34, 419 (1983).
4. H. Rabitz, "Local and Global Parametric Analysis of Reacting Flows", *Physica* 20D, 67 (1986).
5. H. Rabitz, "Sensitivity Analysis of Combustion Systems", in The Mathematics of Combustion, J. Buckmaster, Editor, (SIAM, Philadelphia, 1985).
6. H. Rabitz, "Chemical Dynamics and Kinetics Phenomena as Revealed by Sensitivity Analysis Techniques", *Chem. Rev.*, (1987).

COMPUTABLE OPTIMAL VALUE BOUNDS FOR
GENERALIZED CONVEX PROGRAMS

Anthony V. Fiacco
Department of Operations Research
The George Washington University
Washington, DC

Jerzy Kyparisis
Department of Decision Sciences
Florida International University
Miami, Florida

SUMMARY

It has been shown by Fiacco that convexity or concavity of the optimal value of a parametric nonlinear programming problem can readily be exploited to calculate global parametric upper and lower bounds on the optimal value function. The approach is attractive because it involves manipulation of information normally required to characterize solution optimality. We briefly describe a procedure for calculating and improving the bounds as well as its extensions to generalized convex and concave functions. Several areas of applications are also indicated.

INTRODUCTION

We are concerned here with parametric nonlinear programming problems of the form

$$\min_x f(x,t) \quad \text{s.t.} \quad g(x,t) \geq 0, h(x,t) = 0 \quad P(t)$$

where f is a real valued function, g and h are vector valued functions, and t is a parameter vector. The optimal value function of $P(t)$ is defined by

$$f^*(t) = \min \{ f(x,t) : x \in R(t) \}$$

where $R(t)$ is the feasible set of the problem $P(t)$ given by

$$R(t) = \{ x : g(x,t) \geq 0, h(x,t) = 0 \}$$

In this paper we describe a procedure, originally proposed by Fiacco (refs.1,2), for calculating piecewise-linear continuous global upper and lower parametric bounds on the convex (or concave) optimal value f^* . We also show how these bounds can be improved in a systematic manner until a desired accuracy, as measured by the maximal deviation from the optimal value over the interval of parameter values, is achieved. Extensions of this approach to generalized convex and concave optimal value functions are discussed as well and current experience with applications is described.

COMPUTABLE BOUNDS ON CONVEX OPTIMAL VALUE FUNCTIONS

Consider the parametric problem $P(t)$ and assume that its optimal value function, $f^*(t)$, is convex. This will be the case if $P(t)$ is a jointly convex program, i.e. if f is jointly convex in x and t , the components of g are jointly concave in x and t , and those of h are jointly linear affine in x and t (ref. 3). The assumptions on g and h can actually be generalized by requiring only that the map R is convex (ref. 4).

Suppose now that we have evaluated $f^*(t)$ and its slope at two distinct values t^1 and t^2 of the parameter t , where (for simplicity) t is assumed to be a scalar. Then, global definitional properties of convex functions immediately provide global parametric continuous, piecewise-linear bounds via linear supports and linear interpolation on the graph of f^* over the line segment (t^1, t^2) . This is illustrated in figure 1.

Practical implementation of bounds calculations requires only the information provided by most standard nonlinear programming algorithms. In particular, the solution of the problem $P(t)$ as well as the associated optimal Lagrange multipliers must be determined for two distinct parameter values. The Lagrange multipliers will coincide with derivatives of f^* in case f^* is differentiable and with subgradients of f^* in case when f^* is nondifferentiable and convex. In both cases the multipliers can be used to compute the lower bounds on f^* .

Clearly, if f^* is convex on the convex set $S \subseteq \mathbb{R}^r$, then any supporting hyperplane of the epigraph at any $t \in S$ provides a global lower bound on f^* over S . Both upper and lower bounds calculations obviously apply over any interval (t^1, t^2) in S , provided that f^* is convex over (t^1, t^2) . A standard technique for studying f^* over (t^1, t^2) is to consider $t(a) = at^1 + (1-a)t^2$ and view f^* as a function of the scalar parameter $a \in (0,1)$. This allows for the simultaneous perturbation of all components t_i of t , which are now linear affine functions of the scalar parameter a .

A byproduct of this practical approach is the observation that if the feasible point to set map R is convex then $x(a) = ax^1 + (1-a)x^2 \in R(t(a))$ if $x^1 \in R(t^1)$ and $x^2 \in R(t^2)$. This leads to the simple calculation of a feasible parametric vector $x(a)$ of a problem $P(t(a))$ whenever the condition is met. Hence we also obtain the upper bound $\bar{f}(a) = f(x(a), t(a))$ on $f^*(t(a))$ over (t^1, t^2) . Since the calculation of $x(a)$ does not depend on f , this does not require f to be convex. If f is jointly convex in (x, t) , then f^* is convex and $\bar{f}(a)$ is a convex bound on or above f^* and below the linear upper bound given in figure 1.

The parametric bounds on the optimal value function f^* described above were constrained to one-dimensional perturbations of the parameter vector t . However, it is a simple matter to extend these bounds to multi-dimensional perturbations of t .

Suppose, for example, that f^* is convex on the convex set $S \subseteq \mathbb{R}^r$ and that we are interested in bounds on f^* for t in some polyhedron M contained in S which is determined by its extreme points t^1, t^2, \dots, t^ℓ . To obtain these bounds we need only to determine the values and subgradients of f^* at ℓ points t^1, \dots, t^ℓ . This information will be available if we compute optimal solutions $x^*(t^i)$ and Lagrange multipliers for ℓ nonlinear programs $P(t^i)$, $i=1, \dots, \ell$, similarly to the case of one-dimensional perturbations. If, in addition, R is a convex map, then we can

calculate a feasible parametric vector $x(a)$, for the problem $P(t(a))$ with $t(a) \in M$, as a convex combination of l solutions $x^*(t^i)$, $i=1, \dots, l$ as well as a sharper convex upper bound $\bar{f}(a)$ on f^* .

The described approach for calculating parametric upper and lower bounds on convex f^* can be extended to the case of concave optimal value function f^* . The well known sufficient conditions for concavity of f^* require that f be concave in t for $t \in S$ and the feasible set $R(t) = R_0$ for all $t \in S$ (that is $R(t)$ must be fixed). This result can be generalized to programs with perturbed feasible sets $R(t)$ by assuming that the map R is concave (ref. 4).

If we now assume, similarly to the convex case, that f^* is concave over the interval (t^1, t^2) and the values and slopes of f^* are known at two distinct points t^1 and t^2 , then a linear interpolation on the graph of f^* will provide a lower bound while a piecewise linear upper bound will be determined by the slopes of f^* . Figure 2 illustrates these bounds.

REFINEMENTS OF OPTIMAL VALUE BOUNDS

In the previous section we described a procedure for calculating piecewise-linear optimal value bounds on convex or concave $f^*(t)$ over the interval (t^1, t^2) of parameter values. We also showed that a parametric feasible solution vector $x(a)$, $a \in (0,1)$, is an immediate by-product of this approach. This remarkably regular behavior is exploitable in a number of ways as will be shown next.

Consider a convex $f^*(t(a))$, where $t(a) = at^1 + (1-a)t^2$, and view it as a function of the scalar parameter $a \in (0,1)$ with upper and lower bounds on f^* as depicted in figure 1. Suppose that we solve the program $P(t(a^*))$ at some intermediate value $a^* \in (0,1)$. Then, this additional solution of $P(t(a^*))$ enables us to easily calculate sharper piecewise-linear continuous upper and lower bounds on f^* . These new bounds on f^* along with previous bounds are illustrated in figure 3.

Moreover, we can calculate a more accurate piecewise-linear continuous feasible estimate $x(a)$ of the parametric solution vector, which in this case is the linear interpolation between contiguous optimal solutions of $P(t(a))$ at three values $a=0, a^*, 1$. The feasible solution $x(a)$ allows, in turn, the computation of a sharper piece-convex continuous upper bound on f^* , given by $\bar{f}(a) = f(x(a), t(a))$.

Similar sharper piecewise-linear continuous upper and lower bounds can be computed for a concave optimal value function f^* by solving an additional program $P(t(a^*))$ at some intermediate value $a^* \in (0,1)$. The improved bounds will be analogous to those depicted in figure 3.

It is clear from figure 3 that by repeatedly solving the program $P(t(a))$ at intermediate values of a , the bounds on f^* may be quickly and significantly improved. The value a^* of the parameter at which the problem was solved is the value where the deviation between the current upper bound U and lower bound L , i.e., $U(a) - L(a)$, is the maximum over the considered interval $(0,1)$. This is an appealing choice, although other choices might be dictated by other criteria or user interest; eg. it might be important to know $f^*(a)$ accurately only for certain subintervals or certain choices of a .

EXTENSIONS OF BOUNDS TO GENERALIZED CONVEX OPTIMAL VALUE FUNCTIONS

The approaches for calculating parametric optimal value bounds described earlier can be extended in several ways to include much wider classes of parametric programs. This means that optimal value bounds are much more widely applicable than is apparent from the results of the previous sections.

The first extension is obtained by considering structured classes of generalized convex and concave optimal value functions. Suppose that map R is convex and that f is quasiconvex in (x,t) for $t \in (t^1, t^2)$. Then, f^* is also quasiconvex (ref. 5) and therefore a constant upper bound of f^* , given by $\max \{f^*(t^1), f^*(t^2)\}$, is readily available as well as a sharper quasiconvex upper bound $\bar{f}(a) = f(x(a), t(a))$. Additional classes of convex and nonconvex programs for which parametric upper bounds on f^* can be computed are those where the objective function and, consequently, the optimal value function F^* are strongly convex, strictly quasiconvex and strictly pseudoconvex (ref. 5).

Analogous results can be obtained in the concave case. Assume, for example, that the feasible set R is arbitrary and fixed and that f is quasiconcave in t for $t \in (t^1, t^2)$. Then, quasiconcavity of f^* follows (ref. 5) and $\min \{f^*(t^1), f^*(t^2)\}$ is a constant lower bound on f^* .

The second extension is possible by considering generalized convex programs which are transformable into standard convex programs. Consider program $P(t)$ with a convex feasible map R and an F -convex objective function f . That means that the composed function $f_F(x,t) = F\{f(x,t)\}$ is convex in (x,t) where F is a continuous, one-to-one function (ref. 6). Thus the optimal value function f_F^* of a modified problem $P_F(t)$

$$\min f_F(x,t) \quad \text{s.t.} \quad g(x,t) \geq 0, h(x,t) = 0 \quad P_F(t)$$

is convex and therefore piecewise-linear upper and lower bounds on f_F^* , given by $L(t) \leq f_F^*(t) \leq U(t)$ can be calculated. Then, since $f_F^*(t) = F\{f^*(t)\}$, one immediately obtains the following bounds on $f^*(t)$ (provided that F is nondecreasing): $F^{-1}\{L(t)\} \leq f^*(t) \leq F^{-1}\{U(t)\}$. These bounds are in general nonlinear and nonconvex but, nevertheless, can be calculated without difficulty once the program $P_F(t)$ has been solved.

EXPERIENCE WITH APPLICATIONS

Several preliminary studies have been conducted to investigate some of the more immediate computational and practical implications of the outlined approach for generating global parametric upper and lower optimal value bounds. The procedure for calculating optimal value bounds for both convex and concave optimal value functions was implemented by Fiacco and Ghaemi (ref. 7) as an additional module in the penalty-function based sensitivity-analysis computer program SENSUMT.

Fiacco and Ghaemi (ref. 8) studied a geometric programming model of a stream water pollution abatement system and calculated bounds on the convex optimal value (defined as the annual cost of operation) of an equivalent convex program. The indicated water pollution bounds calculation involved the perturbation of a single right-hand-side parameter, the allowable oxygen deficit level in the final reach of the stream, that proved to be the most influential parameter in the prior sensitivity study.

Subsequently, Fiacco and Kyparisis (refs. 9, 10) utilized SENSUMT to calculate bounds on the optimal value function for the same water pollution abatement model when 30 (not all right-hand-side) most influential constraint parameters were perturbed simultaneously. In this application, the optimal value function was not convex in full neighborhood of the base value of the parameter vector. However, it was possible to show that the restriction of $f^*(t)$ to the subset of parameters involved in the desired perturbation is convex.

In another study involving the convex equivalent of a geometric programming model of a power system energy model, to find the turbine exhaust annulus and condenser system design that minimizes total annual fixed plus operating cost, Fiacco and Ghaemi (ref. 11) used SENSUMT to obtain bounds on the optimal value function for a variety of single objective function and constraint parameter changes. A novelty of this analysis is the exploitation of problem structure to calculate a nonlinear lower bound on the optimal value function. In addition, parametric bounds are computed on the optimal value which is concave for certain perturbations of objective function parameters.

REFERENCES

1. Fiacco, A.V.: Computable Optimal Value Bounds and Solution Vector Estimates for General Parametric NLP Programs. George Washington University (GWU) Technical Paper T-451, 1981.
2. Fiacco, A.V.: Introduction to Sensitivity and Stability Analysis in Nonlinear Programming. Academic Press, New York, 1983.
3. Mangasarian, O.L.; and Rosen, J.B.: Inequalities for Stochastic Nonlinear Programming Problems. Operations Res., vol. 12, no. 1, 1964, pp. 143-154.
4. Fiacco, A.V.; and Kyparisis, J.: Convexity and Concavity Properties of the Optimal Value Function in Parametric Nonlinear Programming. J. Optimiz. Theory Applic., vol. 48, 1986, pp. 95-126.
5. Fiacco, A.V.; and Kyparisis, J.: Generalized Convexity and Concavity Properties of the Optimal Value Function in Parametric Nonlinear Programming. George Washington University (GWU) Technical Paper T-472, 1983.
6. Avriel, M.: Nonlinear Programming: Analysis and Methods. Prentice-Hall, Englewood Cliffs, NJ, 1976.
7. Fiacco, A.V.; and Ghaemi, A.: A User's Manual for SENSUMT: A Penalty Function Computer Program for Solution, Sensitivity Analysis and Optimal Value Bound Calculation in Parametric Nonlinear Programs. GWU Technical Paper T-434, 1980.
8. Fiacco, A.V.; and Ghaemi, A.: Sensitivity Analysis of a Nonlinear Water Pollution Control Model Using an Upper Hudson River Data Base. Operations Res., vol. 30, no. 1, pp. 1-28.
9. Fiacco, A.V.; and Kyparisis, J.: Computable Parametric Bounds for Simultaneous Large Perturbations of Thirty Parameters in a Water Pollution Abatement GP Model, Part I: Optimal Value Bounds. GWU Technical Paper T-453, 1981.

10. Fiacco, A.V.; and Kyparisis, J.: Computable Parametric Bounds for Simultaneous Large Perturbations of Thirty Parameters in a Water Pollution Abatement GP Model, Part II: Refinement of Optimal Value Bounds and Parametric Solution Bounds, GWU Technical Paper T-461, 1981.
11. Fiacco, A.V.; and Ghaemi, A.: Sensitivity and Parametric Bound Analysis of Optimal Steam Turbine Exhaust Annulus and Condenser Sizes. GWU Technical Paper T-437, 1981.

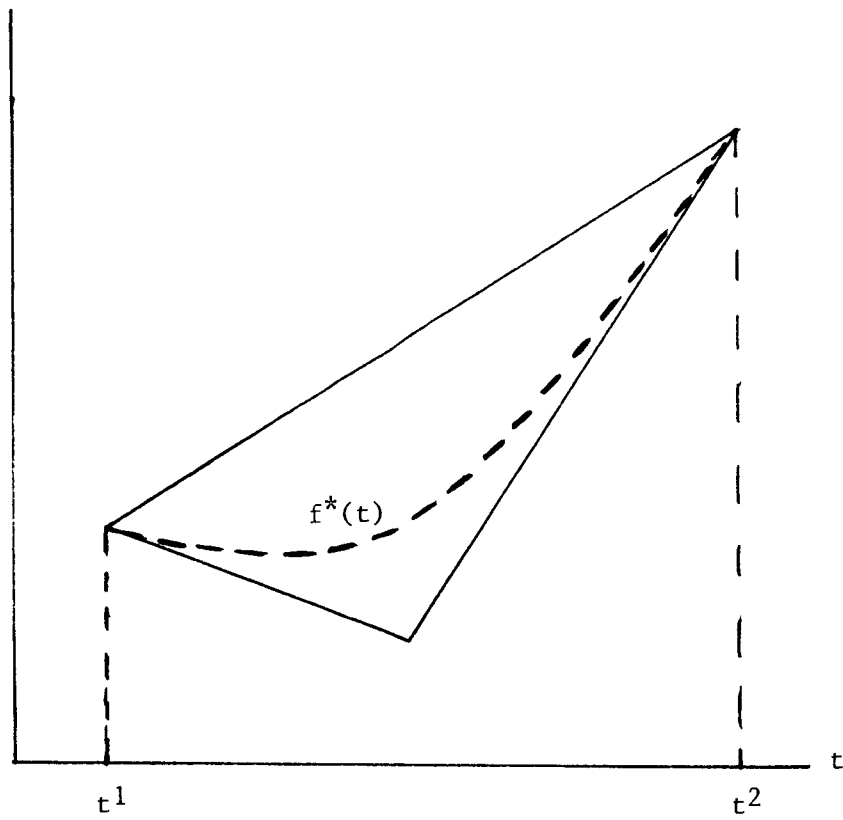


Figure 1. Optimal value bounds on convex f^* .

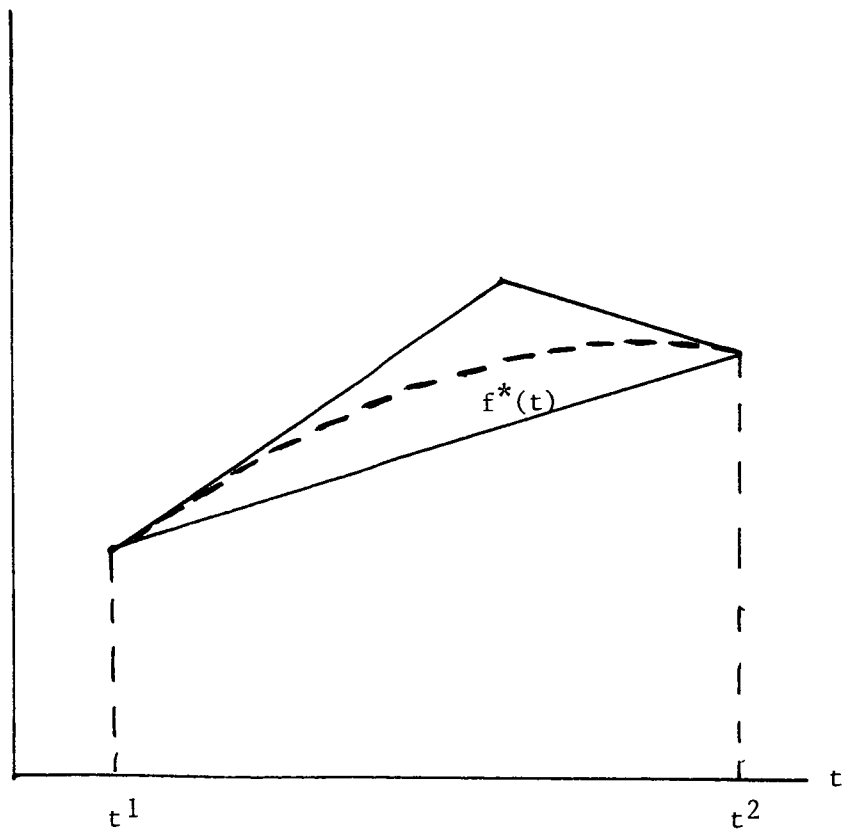


Figure 2. Optimal value bounds on concave f^* .

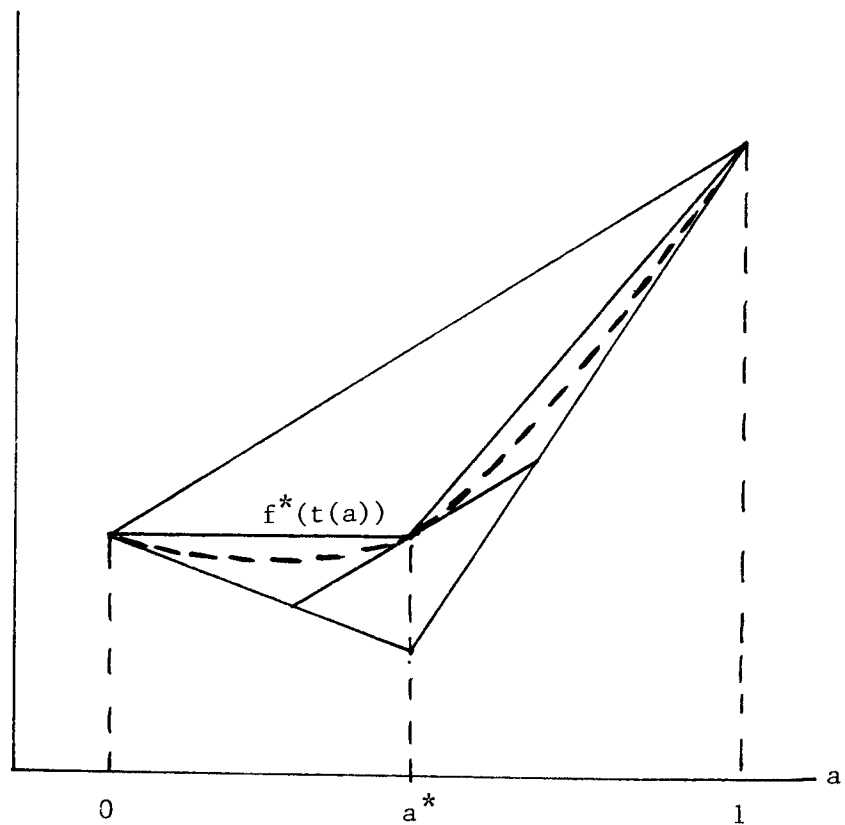


Figure 3. Improved optimal value bounds on convex f^* .

ALTERNATIVE METHODS FOR CALCULATING SENSITIVITY
OF OPTIMIZED DESIGNS TO PROBLEM PARAMETERS

G. N. Vanderplaats
University of California
Santa Barbara, California

H. D. Cai
Engineering Design Optimization, Inc.
Santa Barbara, California

OUTLINE

Optimum sensitivity is defined as the derivative of the optimum design with respect to some problem parameter, P . The problem parameter is usually fixed during optimization, but may be changed later. Thus, we can use optimum sensitivity to estimate the effect of changes in loads, materials or constraint bounds on the design without expensive re-optimization.

Here, we will discuss the general topic of optimum sensitivity, identify available methods, give examples, and identify the difficulties encountered in calculating this information in nonlinear constrained optimization.

1. NEEDS
2. DEFINITIONS
3. AVAILABLE METHODS
4. EXAMPLES
5. CONCLUSIONS

THE NEED FOR OPTIMUM SENSITIVITY

In many situations, we not only want to find the optimum, but we also want to know how sensitive the optimum is relative to a certain parameter (i.e. how stable the optimum is).

When parameter P changes, optimum sensitivity can be used to estimate the changes in the optimum design variables and objective function without expensive re-optimization.

In multi-level optimization, we need the derivative of the lower level optimum with respect to the upper level design variables.

1. FIND THE CHANGE IN THE OPTIMUM DESIGN DUE TO CHANGES IN LOADS, MATERIALS, OR OTHER DESIGN SPECIFICATIONS
2. AVOID RE-OPTIMIZATION
3. PROVIDE NEEDED INFORMATION FOR MULTI-LEVEL OPTIMIZATION

THE DEFINITION OF OPTIMUM SENSITIVITY

The mathematical definition of optimum sensitivity is given here. What makes this unique from what we usually define as sensitivity analysis is that there is an implied inequality constrained sub-problem. Because of this, it is possible that the optimum sensitivity may not be continuous at $P = P^0$.

OPTIMUM SENSITIVITY

$$DF^*/DP = \lim_{\Delta P \rightarrow 0} [F(\underline{X}^* + \underline{\Delta X}^*, P + \Delta P) - F(\underline{X}^*, P)] / \Delta P$$

$$\underline{DX}^*/DP = \lim_{\Delta P \rightarrow 0} [\underline{\Delta X}^* / \Delta P]$$

WHERE $F(\underline{X}^* + \underline{\Delta X}, P + \Delta P)$ IS FOUND FROM;

MINIMIZE $F(\underline{X}, P + \Delta P)$

SUBJECT TO;

$$G_J(\underline{X}, P + \Delta P) \leq 0 \quad J=1, M$$

$$X_I^L \leq X_I \leq X_I^U \quad I=1, N$$

AVAILABLE METHODS

Several methods have been proposed to estimate the optimum sensitivity of a design with respect to parameter P. Each of these methods contains certain assumptions, and these assumptions can be incorrect in some cases. The methods to be discussed here are listed below.

1. BASED ON THE KUHN-TUCKER NECESSARY CONDITIONS FOR AN OPTIMUM
2. BASED ON THE CONCEPT OF A FEASIBLE DIRECTION
3. BASED ON A LINEAR PROGRAMMING METHOD
4. BASED ON A FULL SECOND-ORDER APPROXIMATION

METHOD 1

The assumption contained in this method is that all of the constraints that are critical at the optimum will remain critical when P changes infinitesimally.

Differentiation of the Kuhn-Tucker conditions gives n equations.

The assumption gives another K equation, where K is the number of critical constraints at the optimum.

This method requires second-order information.

Because of the assumption that all critical constraints remain critical, this method does not recognize the discontinuity which may exist in the optimum sensitivity.

This method gives no assurance that the answer obtained is correct.

METHOD 1: BASED ON THE KUHN-TUCKER CONDITIONS

$$\text{AT } \underline{X}^* \quad G_J(\underline{X}^*) = 0 \quad J \in K$$

$$\underline{\nabla} F(\underline{X}^*) + \sum_{J \in K} \lambda_J \underline{\nabla} G_J(\underline{X}^*) = \underline{0}$$

THIS LEADS TO THE SOLUTION OF THE FOLLOWING SET OF EQUATIONS;

$$\begin{bmatrix} A_{N \times N} & B_{N \times K} \\ B_{K \times N}^T & 0_{K \times K} \end{bmatrix} \begin{Bmatrix} S \\ \Delta \lambda \end{Bmatrix} + \begin{Bmatrix} C_{N \times 1} \\ D_{K \times 1} \end{Bmatrix} = \begin{Bmatrix} 0 \\ 0 \end{Bmatrix}$$

WHERE

$$A_{IK} = \frac{\partial^2 F(\underline{X}^*)}{\partial X_I \partial X_K} + \sum_{J \in K} \lambda_J \frac{\partial^2 G_J(\underline{X}^*)}{\partial X_I \partial X_K}$$

WITH SIMILAR EXPRESSIONS FOR B_{IK} , C_I AND D_I

METHOD 2

This method treats the parameter as a new design variable. This enlarges the design space to $n+1$. The assumption contained in this method is that, in the expanded design space, the maximum improvement or minimum degradation in the design is sought.

This method seeks the constrained steepest descent direction in $n+1$ space to give DX^*/DP , and from this DF^*/DP is calculated directly.

This method requires only first-order sensitivity information.

This method accounts for possible discontinuity of the total derivative.

As with the first method, there is no assurance that the result obtained is correct.

LINEAR METHOD BASED ON FEASIBLE DIRECTIONS

LINEAR APPROXIMATION: LET $X_{N+1} = P$

$$\text{MINIMIZE } F(\underline{X}) = F(\underline{X}^*) + \underline{\nabla} F(\underline{X}^*) \cdot \underline{S}$$

SUBJECT TO;

$$G_J(\underline{X}^*) + \underline{\nabla} G_J(\underline{X}^*) \cdot \underline{S} \leq 0 \quad J \in K$$

\underline{S} BOUNDED

WHERE $S_I = X_I - X_I^*$ IS EQUIVALENT TO $S_I = \partial X_I / \partial P$

EQUIVALENT PROBLEM:

$$\text{MINIMIZE } \underline{\nabla} F(\underline{X}^*) \cdot \underline{S}$$

SUBJECT TO;

$$\underline{\nabla} G_J(\underline{X}^*) \cdot \underline{S} \leq 0 \quad J \in K$$

$$\underline{S} \cdot \underline{S} \leq 1$$

METHOD 2B

Two extended forms are available to deal with the possible discontinuity of the optimum sensitivity. This is necessary because the direction in which P is changed will determine the value of the sensitivity. If the value is different, depending on the sign of ΔP , then this indicates that the design will follow one subset of constraints if P is increased but a different set if P is decreased.

This method for dealing with the potential discontinuities of the optimum sensitivity is somewhat dependent on the choice of the parameter C . Numerical difficulties can be encountered in deciding the correct value of C .

DEALING WITH DISCONTINUITY DEPENDENT ON THE SIGN OF P

$$\Delta P \geq 0$$

$$\text{MINIMIZE} \quad \nabla F(\underline{X}^*) \cdot \underline{S} - C \cdot S_{N+1}$$

SUBJECT TO;

$$\nabla G_J(\underline{X}^*) \cdot \underline{S} \leq 0 \quad J \in K$$

$$\underline{S} \cdot \underline{S} \leq 1$$

$$\Delta P \leq 0$$

$$\text{MINIMIZE} \quad \nabla F(\underline{X}^*) \cdot \underline{S} + C \cdot S_{N+1}$$

SUBJECT TO;

$$\nabla G_J(\underline{X}^*) \cdot \underline{S} \leq 0 \quad J \in K$$

$$\underline{S} \cdot \underline{S} \leq 1$$

METHOD 3

Here, we create a Taylor series expansion for the objective function and the critical constraints. Taking the limit as ΔP goes to zero and keeping the lowest order terms only produces the optimum sensitivity according to the original definition. This process requires that we pay close attention to whether ΔP approaches zero from the positive or negative side.

This method requires solving two resultant LP problems.

This method requires first-order sensitivities only.

If the number of the constraints is less than the number of design variables, the LP problems do not have a unique solution.

If a unique solution exists, it is always the correct solution.

LINEAR PROGRAMMING APPROACH

USING THE DEFINITION OF OPTIMUM SENSITIVITY;

$$\text{MINIMIZE } \nabla F(\underline{X}^*) \cdot \underline{\Delta X} + \partial F(\underline{X}^*) / \partial P \cdot \Delta P + O(\underline{\Delta X}, \Delta P)$$

SUBJECT TO;

$$G_J(\underline{X}^*, P) + \nabla G_J(\underline{X}^*) \cdot \underline{\Delta X} + \partial G_J / \partial P \cdot \Delta P + O(\underline{\Delta X}, \Delta P) \leq 0 \quad J=1, M$$

KEEP THE LOWEST ORDER TERMS WHEN $\Delta P \rightarrow 0$. THIS LEADS TO;

IF $\Delta P \rightarrow +0$ ($\Delta P > 0$):

$$\text{MINIMIZE } \nabla F(\underline{X}^*) \cdot \underline{\Delta X} / \Delta P + \partial F(\underline{X}^*) / \partial P$$

SUBJECT TO;

$$\nabla G_J(\underline{X}^*) \cdot \underline{\Delta X} / \Delta P + \partial G_J / \partial P \leq 0 \quad J \in K$$

IF $\Delta P \rightarrow -0$ ($\Delta P < 0$):

$$\text{MINIMIZE } \nabla F(\underline{X}^*) \cdot \underline{\Delta X} / \Delta P - \partial F(\underline{X}^*) / \partial P$$

SUBJECT TO;

$$\nabla G_J(\underline{X}^*) \cdot \underline{\Delta X} / \Delta P - \partial G_J / \partial P \leq 0 \quad J \in K$$

METHOD 4

Just as with method 1, this method requires second derivatives. However, here the second-order information is used directly as an approximate optimization task.

The parameter P may be treated as an independent design variable, or the change in P may be specified.

If a small change in P is specified, the method becomes a finite difference method. When ΔP goes to zero, this method gives the exact answer to a second order approximation.

The set, K , of retained constraints can include all critical and near critical constraints, or even the entire set of constraints. Therefore, as P is changed, a totally new set of constraints can become critical.

Within the limits of numerical precision, this method will always give the correct solution. The disadvantage is that this problem has a quadratic objective and constraints and so must be solved by nonlinear programming. It is, however, quite efficient since it is an explicit problem.

If an attempt is made to simplify this method by linearizing it, the result is the set of two LP problems given in method 3.

FULL SECOND-ORDER APPROXIMATION

SOLVE THE FOLLOWING EXPLICIT APPROXIMATE PROBLEM:

FIND THE CHANGE \underline{S} THAT WILL

$$\text{MINIMIZE } F(\underline{X}^*, P) + \nabla F(\underline{X}^*, P) \cdot \underline{S} + 0.5 \underline{S}^T H_F \underline{S}$$

SUBJECT TO;

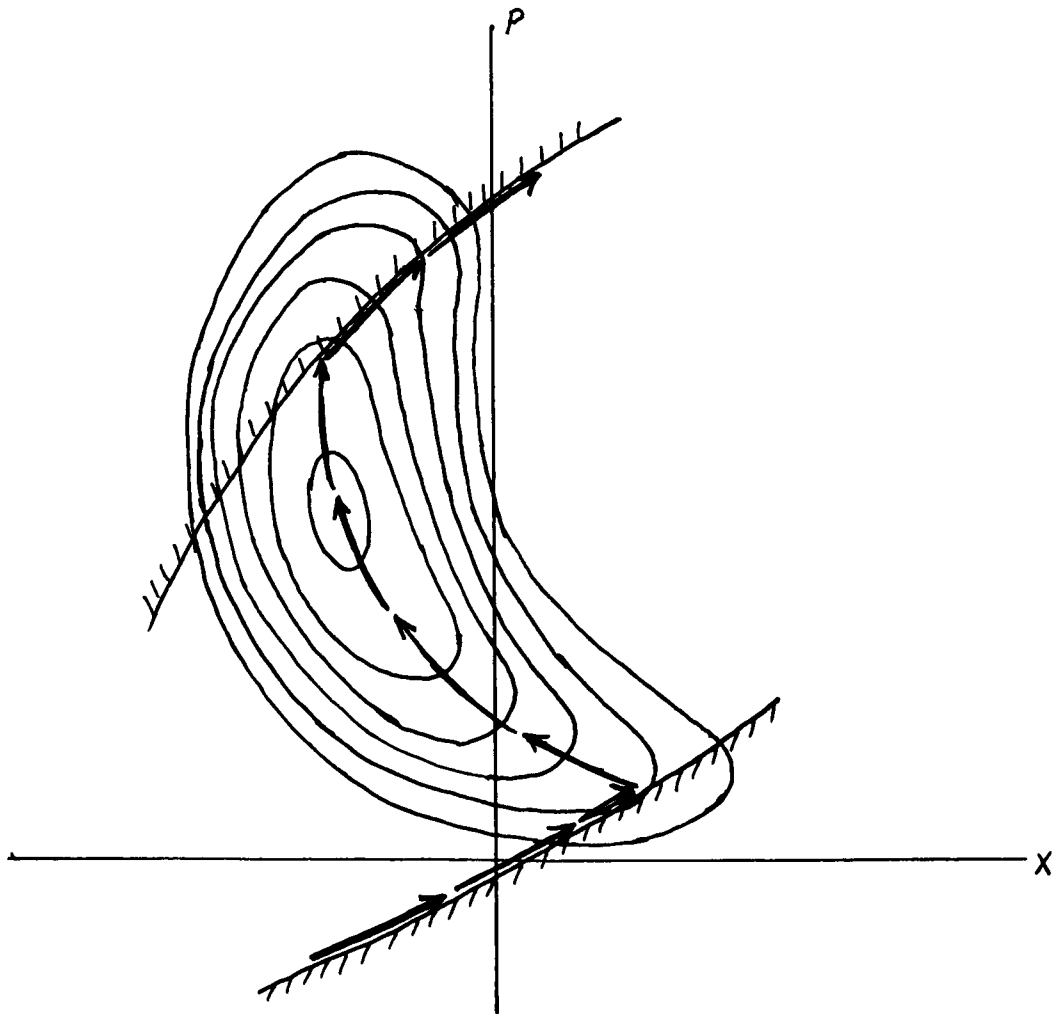
$$G_J(\underline{X}^*, P) + \nabla G_J(\underline{X}^*, P) \cdot \underline{S} + 0.5 \underline{S}^T H_J \underline{S} \leq 0 \quad J \in K$$

\underline{S} BOUNDED

AN OPTIMUM CURVE

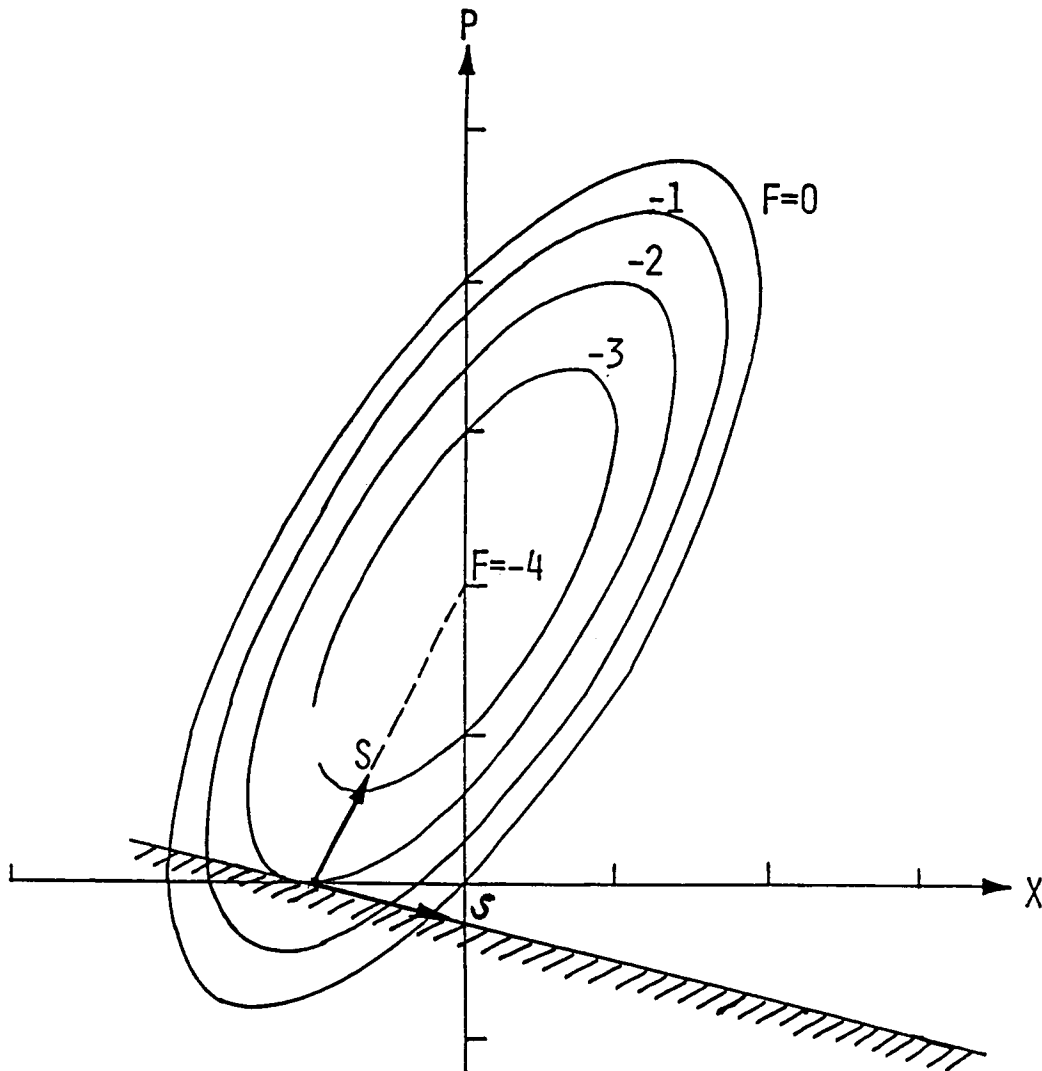
When P changes, the optimum points X^* form a curve in $n+1$ space. The optimum sensitivity DX^*/DP is represented by the tangent of this curve. The curve can be nonsmooth, so DX^*/DP can be discontinuous.

An infinitesimal change in P may cause the curve to leave a currently critical constraint. This demonstrates the potentially discontinuous nature of optimum sensitivity.



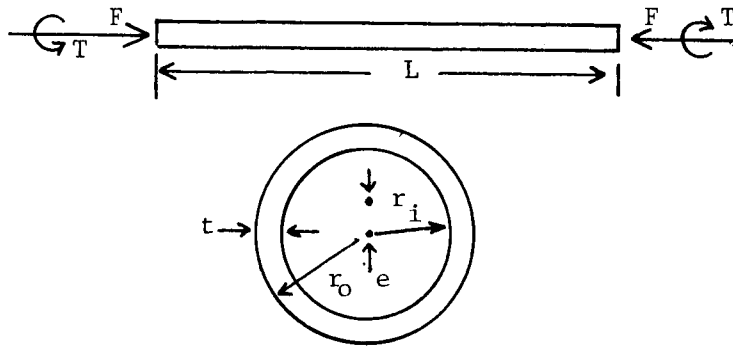
DISCONTINUOUS DERIVATIVES

This is another graphical example of the discontinuous derivative problem. In this case, the constrained optimum is found for $P=0$ to lie on the constraint boundary. Now if P is increased, the optimum sensitivity will point to the unconstrained minimum. On the other hand, if P is decreased, the optimum sensitivity follows the constraint. Since the total derivative is the scalar product of the gradient of the objective function with the vector \underline{S} , it is clear that the optimum sensitivity is not continuous at \underline{X}^* .



ROTATING SHAFT OPTIMIZATION

This example demonstrates the usefulness of optimum sensitivity as an engineering approach to frequency domain avoidance. Assuming it is required that the rotating shaft not vibrate in the domain between 2.8 and 3.5 Hz, the shaft is first optimized with respect to all other constraints. Then the sensitivity with respect to the fundamental frequency is calculated and a new optimum design is projected with a frequency below 2.8 Hz and with a frequency above 3.5 Hz. From this it appears that it is far more economical to drive the frequency up than to drive it down. However, this was not known in advance and so it was not known whether the frequency should be bounded from above or below. Thus, optimum sensitivity provides one means of dealing with a problem in which the design space is disjoint.



OBJECTIVE: MINIMUM WEIGHT. CONSTRAINTS: STRESS, DISPLACEMENT, EULER BUCKLING, SHELL BUCKLING. PARAMETER P: THE FIRST NATURAL FREQUENCY.

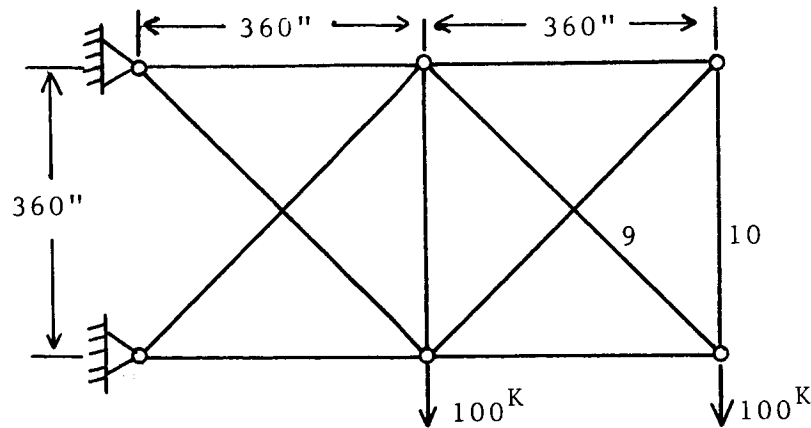
THE OPTIMUM WITHOUT ANY FREQUENCY CONSTRAINTS: $\omega_1 = 3.1$, $W^* = 27,242$

OPTIMUM SENSITIVITY

		METHOD 2	METHOD 3	RE-OPTIMIZE
$\omega_1 \leq 2.8$	W^*	+5,278	+5,278	+6,429
	X_1	-1.65	-1.65	-1.72
	X_2	+0.33	+0.33	+0.44
$\omega_1 \geq 3.5$	W^*	+417	+417	+169
	X_1	+0.17	+0.17	+0.17
	X_2	-0.003	-0.003	-0.011

10-BAR TRUSS

Here the common 10-bar truss was optimized and the sensitivity was calculated with respect to the allowable stress in member 9. It is known that the weight of this structure can be reduced by increasing this allowable stress to a value of 37.5 ksi, but beyond that, no weight reduction is possible. At the initial optimum, member 10 was at its lower bound. Method 1 assumed, incorrectly, that it would stay there, while method 2 recognized that this member dimension should be increased. Using method 3, the allowable stress in member 9 was allowed to change as an independent variable and this method projected that the optimum allowable stress is 38.2 ksi, quite close to the actual value of 37.5 ksi. The case at the bottom of the figure is for optimization at the 37.5 ksi value and shows the discontinuity of the optimum sensitivity.



OBJECTIVE: MINIMUM WEIGHT. CONSTRAINTS: STRESS, MINIMUM GAGE.

PARAMETER P: STRESS LIMIT IN MEMBER 9. INITIAL OPTIMUM $\sigma_9 = 30$ KSI, $W^* = 1545$

SENSITIVITY

CASE 1:	PARAMETER	METHOD 1	METHOD 2	METHOD 3
	$DF^*/D\sigma_9$	-240.5	-238.4	-178.6
	S_{10}	0.00	0.17	0.16
	σ_9	---	---	38.2

CASE 2: $\sigma_9 = 37.5$ KSI, $W^* = 1498$, METHOD 2.

$\Delta\sigma_9 = 0$ $DF^*/D\sigma_9 = 215.7$ $W^*(35) = 1512$ CALCULATED $W^*(35) = 1511$

$\Delta\sigma_9 = 0$ $DF^*/D\sigma_9 = 0.00$

CONCLUSIONS

Optimum sensitivity in linear programming is a common and widely used tool. Research in optimum sensitivity for nonlinear problems has not been this successful and it has been shown here that none of the methods is completely satisfactory. Methods 1-3 often do not provide the correct answer, while method 4 requires second-order information that may be costly to obtain, as well as the nonlinear optimization of the approximating functions.

The reasons for these difficulties are now beginning to be understood. If the optimum design is fully constrained and unique, the optimum sensitivity can be reliably calculated, just as in linear programming. However, if the design is not fully constrained (fewer active constraints than design variables), the optimum sensitivity using first-order information will not be unique and second-order information is essential. Unfortunately, this is the usual case in engineering design. The reason that first-order information is inadequate is that the higher order terms cannot be ignored as ΔP goes to zero in the limit.

The need to calculate the optimum sensitivity is a clear one and often justifies considerable effort. It is this information that is needed to make many fundamental design decisions. Therefore, improved understanding of these concepts is useful in the search to extract the maximum information from the optimization process.

1. IN GENERAL, THERE ARE SITUATIONS WHERE NONE OF THE AVAILABLE METHODS EXCEPT THE FULL SECOND-ORDER APPROXIMATION WILL GIVE THE CORRECT ANSWER
2. ITERATIVE METHODS USING FIRST-AND SECOND-ORDER INFORMATION SHOULD BE INVESTIGATED
3. IF SECOND-ORDER INFORMATION IS AVAILABLE, METHOD 4 WILL PROVIDE USEFUL ENGINEERING WHICH ACCOUNTS FOR NEARBY CONSTRAINTS THAT MAY BECOME CRITICAL WHEN PARAMETER P IS CHANGED
4. FURTHER RESEARCH IS NEEDED; THE USEFULNESS OF OPTIMUM SENSITIVITY HAS BEEN CLEARLY SHOWN IN PAST WORK

Behavior Sensitivities for Control Augmented Structures

R.A. Manning, R.V. Lust, and L.A. Schmit
University of California at Los Angeles
Los Angeles, CA

Introduction

During the past few years it has been recognized that combining passive structural design methods with active control techniques offers the prospect of being able to find substantially improved designs (Refs. 1-3). These developments have stimulated interest in augmenting structural synthesis by adding active control system design variables to those usually considered in structural optimization. An essential step in extending the approximation concepts approach (Refs. 4-6) to control augmented structural synthesis (Ref. 7) is the development of a behavior sensitivity analysis capability for determining rates of change of dynamic response quantities with respect to changes in structural and control system design variables. Behavior sensitivity information is also useful for man-machine interactive design as well as in the context of system identification studies. In this work behavior sensitivity formulations for both steady state and transient response are presented and the quality of the resulting derivative information is evaluated.

Augmented Equations of Motion

Consider a structural/control system that can be modeled as an assemblage of frame, truss and axial actuator elements. When such a system is subjected to harmonic loading conditions the steady state response is of primary interest. It is assumed here that: (1) direct output feedback control is used; (2) actuators and sensors are collocated; and (3) the structure/control system can be represented by a linear model. Let it also be understood that the topology, geometric layout, structural material and actuator positions are preassigned parameters while section properties and gains are selected as design variables.

Dynamic analysis is carried out using the finite element method and Eq. 1 represents the equations of motion including viscous damping $[C]$, structural damping $i\gamma[K]$, harmonic applied loads $\{P(t)\}_k$ and control forces $\{N(t)\}_k$. The control forces $\{N(t)\}_k$ are given by Eq. 2, where $[G_p]_k$ and $[G_v]_k$ denote the system level position and velocity gain matrices for the k^{th} load condition. Substituting Eq. 2 into Eq. 1 gives Eq. 3, the equations of motion for the control augmented system, where $[C_A]_k$ and $[K_A]_k$, respectively (Eqs. 4 and 5) are the augmented damping and the augmented stiffness matrices for the k^{th} load condition. For the case of axial actuators used here the system level position and velocity gain matrices are easily generated following assembly procedures similar to those commonly used in finite element analysis.

$$[M]\{\ddot{X}\}_k + [C]\{\dot{X}\}_k + (1 + i\gamma)[K]\{X\}_k = \{N(t)\}_k + \{P(t)\}_k \quad (1)$$

$$k = 1, 2, \dots, K_d$$

$$\{N(t)\}_k = -[G_v]_k\{\dot{X}\}_k - [G_p]_k\{X\}_k \quad (2)$$

$$[M]\{\ddot{X}\}_k + [C_A]_k\{\dot{X}\}_k + [K_A]_k\{X\}_k + i\gamma[K]\{X\}_k = \{P(t)\}_k \quad (3)$$

$$[C_A]_k = [C] + [G_v]_k \quad (4)$$

$$[K_A]_k = [K] + [G_p]_k \quad (5)$$

Dynamic Response Solution

The steady state dynamic response for harmonically loaded (see Eq. 6) damped structures augmented by a linear direct output feedback control system can be obtained via a frequency response analysis as follows. Substituting Eq. 6 into the control augmented equations of motion (Eq. 3) leads to Eq. 7, where the complex displacements $\{\bar{X}\}_k$ are represented by Eq. 8. It is well known that the steady state solution of Eqs. 7 has the form shown in Eq. 9. Substituting Eq. 9 into Eq. 7, eliminating $e^{i\Omega_k t}$ from both sides, and equating the real and imaginary parts leads to a partitioned matrix equation (Eq. 10). For the general case, Eq. 10 represents a $2n \times 2n$ set of indefinite, non-symmetric linear simultaneous algebraic equations in the unknowns $\{C_R\}_k$ and $\{C_I\}_k$, where n equals the number of degrees of freedom in the system model. For the special case treated here (i.e. collocated axial actuators and sensors) the efficiency of the solution process can be improved because $[K_A]_k$ and $[C_A]_k$ are symmetric and Eq. 10 can be rewritten in the symmetric form shown in Eq. 11.

$$\{P(t)\}_k = \{P\}_k e^{i\Omega_k t} \quad (6)$$

$$[M]\{\ddot{\bar{X}}\}_k + [C_A]_k\{\dot{\bar{X}}\}_k + [K_A]_k\{\bar{X}\}_k + i\gamma[K]\{\bar{X}\}_k = \{P\}_k e^{i\Omega_k t} \quad (7)$$

$$\{\bar{X}\}_k = \{X_R\}_k + i \{X_I\}_k \quad (8)$$

$$\{\bar{X}\}_k = \{\bar{C}\}_k e^{i\Omega_k t} = (\{C_R\}_k + i\{C_I\}_k) e^{i\Omega_k t} \quad (9)$$

$$\left[\begin{array}{c|c} \frac{[K_A]_k - \Omega_k^2[M]}{\Omega_k[C_A]_k + \gamma[K]} & \frac{-\Omega_k[C_A]_k - \gamma[K]}{[K_A]_k - \Omega_k^2[M]} \end{array} \right] \left\{ \begin{array}{c} \{C_R\}_k \\ \{C_I\}_k \end{array} \right\} = \left\{ \begin{array}{c} \{P\}_k \\ \{0\} \end{array} \right\} \quad (10)$$

$$k = 1, 2, \dots, K_d.$$

Dynamic Response Solution (cont.)

The amplitude of the steady state dynamic displacements can be obtained as follows. Solve Eq. 11 for the primary unknowns $\{C_R\}_k$ and $\{C_I\}_k$. Note that $e^{i\Omega_k t}$ can be expressed in the alternate form given by Eq. 12. Then it follows from Eqs. 8 and 9 that the steady state dynamic response is given by Eq. 13 where $\{X_R\}_k$ and $\{X_I\}_k$ solve Eq. 1 when the loading function has the form of a cosine or a sine respectively. When the loading function is sinusoidal the amplitude of the dynamic displacement for the j^{th} degree of freedom is given by Eq. 14. It is worth noting that Eq. 14 is a relatively simple explicit nonlinear expression for the amplitude of the steady state dynamic response in terms of the primary unknowns of the analysis, namely $\{C_R\}_k$ and $\{C_I\}_k$.

$$\left[\begin{array}{c|c} \Omega_k[C_A]_k + \gamma[M] & [K_A]_k - \Omega_k^2[M] \\ \hline [K_A]_k - \Omega_k^2[M] & -\Omega_k[C_A]_k - \gamma[M] \end{array} \right] \left\{ \begin{array}{c} \{C_R\}_k \\ \{C_I\}_k \end{array} \right\} = \left\{ \begin{array}{c} \{0\} \\ \{P\}_k \end{array} \right\} \quad (11)$$

$$e^{i\Omega_k t} = \cos\Omega_k t + i \sin \Omega_k t \quad (12)$$

$$\begin{aligned} \{\bar{X}\}_k &= \{X_R\}_k + i\{X_I\}_k = (\{C_R\}_k \cos\Omega_k t - \{C_I\}_k \sin\Omega_k t) \\ &\quad + i(\{C_R\}_k \sin\Omega_k t + \{C_I\}_k \cos\Omega_k t) \end{aligned} \quad (13)$$

$$\left| X_{Ijk} \right| = \left(C_{Rjk}^2 + C_{Ijk}^2 \right)^{1/2} \quad (14)$$

Behavior Sensitivity Analysis

Approximate values of the amplitude for the j^{th} degree of freedom under the k^{th} load condition ($|\tilde{X}_{jk}|$) will be obtained by constructing first order Taylor series approximations for the primary unknowns of the steady state response, namely \tilde{C}_{Rjk} and \tilde{C}_{Ijk} . Equations (15a) and (15b) show the first order Taylor series approximations for the primary unknowns of the steady state response analysis and they are linear in the design variables (i.e. element properties). Note that the subscript 0 refers to the base design for which an analysis is available. Substituting Eqs. (15 a,b) into Eq. (14') gives the desired explicit approximation for the amplitude of the j^{th} degree of freedom under the k^{th} load condition. It is apparent that the first partial derivatives of the primary unknowns evaluated at the base design must be known in order to evaluate approximate values of the amplitude. These behavior sensitivity derivatives are readily found by implicit differentiation of Eq. 11' (i.e. Eq. 11 written in compact notation where $[A]_k = \Omega_k[C_A]_k + \gamma[M]$ and $[B]_k = [K_A]_k - \Omega_k^2[M]$) with respect to the design variables d_r , which leads to Eq. 16.

$$|\tilde{X}_{jk}| = (\tilde{C}_{Rjk}^2 + \tilde{C}_{Ijk}^2)^{1/2} \quad (14')$$

$$\tilde{C}_{Rjk} = (C_{Rjk})_o + \sum_r \left[\frac{\partial C_{Rjk}}{\partial d_r} \right]_o (d_r - d_{ro}) \quad (15a)$$

$$\tilde{C}_{Ijk} = (C_{Ijk})_o + \sum_r \left[\frac{\partial C_{Ijk}}{\partial d_r} \right]_o (d_r - d_{ro}) \quad (15b)$$

$$\begin{bmatrix} [A] & [B] \\ [B] & -[A] \end{bmatrix}_k \begin{Bmatrix} \{C_R\}_k \\ \{C_I\}_k \end{Bmatrix} = \begin{Bmatrix} \{0\} \\ \{P\}_k \end{Bmatrix} \quad (11')$$

$$\begin{bmatrix} \frac{\partial [A]}{\partial d_r} & \frac{\partial [B]}{\partial d_r} \\ \frac{\partial [B]}{\partial d_r} & -\frac{\partial [A]}{\partial d_r} \end{bmatrix}_k \begin{Bmatrix} \{C_R\}_k \\ \{C_I\}_k \end{Bmatrix} + \begin{bmatrix} [A] & [B] \\ [B] & -[A] \end{bmatrix}_k \begin{Bmatrix} \frac{\partial \{C_R\}_k}{\partial d_r} \\ \frac{\partial \{C_I\}_k}{\partial d_r} \end{Bmatrix} = \begin{Bmatrix} \{0\} \\ \{0\} \end{Bmatrix} \quad (16)$$

Behavior Sensitivity Analysis (cont.)

Equation 16 is written in a more compact notation in Eq. 17 and it becomes apparent on examining Eq. 17 that the form of this sensitivity analysis is very similar to that which arises for the case of linear static analysis (i.e. $K \frac{\partial \{X\}_k}{\partial d_r} = \{V\}_{rk} = - \left[\frac{\partial K}{\partial d_r} \right] \{X\}_k$). The terms on the right hand side of Eq. 17 play the role of pseudo-load vectors that are easily evaluated once the primary unknowns of the analysis have been determined for a base design by solving Eq. 11. The solution of Eq. 17 for the desired first derivatives $\left[\frac{\partial \{C_R\}_k}{\partial d_r} \text{ and } \frac{\partial \{C_I\}_k}{\partial d_r} \right]$ require relatively little effort because the $2n \times 2n$ matrix in Eq. 17 was previously decomposed into LDL^T form when the primary analysis was executed by solving Eq. 11. Furthermore, the computational efficiency of the primary sensitivity analysis (solving Eq. 17) can be enhanced by employing the well known partial inverse method to obtain only the desired partial derivatives. (Ref. 5).

$$\left[\begin{array}{c|c} [A] & [B] \\ [B] & -[A] \end{array} \right]_k \left\{ \begin{array}{c} \frac{\partial \{C_R\}_k}{\partial d_r} \\ \frac{\partial \{C_I\}_k}{\partial d_r} \end{array} \right\} = \left\{ \begin{array}{c} \{V_I\}_{rk} \\ \{V_R\}_{rk} \end{array} \right\} \quad (17)$$

$$\{V_I\}_{rk} = - \frac{\partial [A]_k}{\partial d_r} \{C_R\}_k - \frac{\partial [B]_k}{\partial d_r} \{C_I\}_k \quad (18)$$

$$\{V_R\}_{rk} = - \frac{\partial [B]_k}{\partial d_r} \{C_R\}_k + \frac{\partial [A]_k}{\partial d_r} \{C_I\}_k \quad (19)$$

$$\frac{\partial}{\partial d_r} [A]_k = \frac{\partial}{\partial d_r} \left[\Omega_k [C_A]_k + \gamma [K] \right] = \Omega_k \frac{\partial [C_A]_k}{\partial d_r} + \gamma \frac{\partial [K]}{\partial d_r} \quad (20)$$

$$\frac{\partial}{\partial d_r} [B]_k = \frac{\partial}{\partial d_r} \left[[K_A]_k - \Omega_k^2 M \right] = \frac{\partial [K_A]_k}{\partial d_r} - \Omega_k^2 \frac{\partial [M]}{\partial d_r} \quad (21)$$

Numerical Example - Steady-State Response

The quality of the steady state dynamic response behavior sensitivities is evaluated for the planar grillage shown in Figure 1. The grillage consists of nine aluminum box beams and is cantilevered at node 1. A dynamic load $P(t) = 100.0 \text{ N} \sin(5.0 \text{ Hz})t$ is applied slightly off the centerline of the grillage at node 8 so that both symmetric and anti-symmetric modes participate in the response. Three active control elements placed at nodes 5, 6, and 7 act in the vertical direction. Two percent structural damping is assumed.

Taylor series approximations based on direct and reciprocal element properties are compared with the exact results for the maximum steady state vertical displacements at node 7 for various design variables (See Figures 2 through 6). One can see that the difference between the approximations and the exact displacements is relatively small even when considering 30 to 40% changes in the primary load-carrying member (i.e., 30 to 40% changes in the bending inertia for element 1).

In order to study the behavior of the approximations in a near-resonance condition, a harmonic loading of frequency 20 Hz is applied at node 8. This loading will excite the flapping - type 5th mode ($f_5 = 19.63 \text{ Hz}$) of the grillage.

Figures 7 and 8 bring out two major difficulties associated with resonance or near-resonance situations: (1) the high nonlinearity of the exact response curve; and (2) the non-convexity of the design space. Nonlinearity of the response curve results in the Taylor series approximations being of acceptable quality in only a limited interval near the base point (i.e. $\pm 10\%$). Nonconvexity of the design space could lead to local minima in an optimization context. These difficulties lead one to use frequency constraints to avoid the near-resonance conditions in optimum design problems.

Transient Response Equations of Motion

In applications where the external loading is either not harmonic or cannot be conservatively replaced with an equivalent harmonic loading, peak transient response is a primary concern. Furthermore, nonlinear on/off controls are well suited to controlling transient response and they are practical for space-based structures.

The dynamic equations of motion for a finite element representation of a linear structure augmented by a discrete actuator control system are given in equation 22 where $\{P(t)\}$ is the nodal load time history, $\{u\}$ is a vector of actuator output forces, and $[B]$ is a matrix of zeroes and ones locating the discrete actuators at nodal degrees of freedom. Vectors of observed displacements and velocities, $\{Y\}$ and $\{\dot{Y}\}$, respectively, are available from the control system sensors and are given in equation 23 where $[C]$ is a matrix of zeroes and ones locating the discrete sensors at nodal degrees of freedom. The actuator output forces, $\{u\}$, are chosen in a manner which reduces the system response based on the sensor measurements. In particular, the output force for the n th actuator is given in equation 24 where \bar{u}_n is the output magnitude for the control system and ϵ_n is the velocity threshold.

Transformation of equation 22 from physical space to modal space yields equation 25b where modal damping has been introduced into the system through the ζ parameter. The uncoupled modal equations in 25b are easily solved for the modal coordinates using the Wilson- θ time-stepping scheme and physical displacements are recovered using the modal transformation in 25a.

The k th modal second order equation of motion can be written in the equivalent first order form given by equation 26 where $n_1 = q$ and $n_2 = \dot{q}$.

$$[M]\{\ddot{X}\} + [K]\{X\} = \{P(t)\} + [B]\{u\} \quad (22)$$

$$\{Y\} = [C]\{X\} \quad \{\dot{Y}\} = [C]\{\dot{X}\} \quad (23)$$

$$u_n = \begin{cases} 0 & \text{if } |\dot{Y}_n| \leq \epsilon_n \\ -\bar{u}_n & \text{if } |\dot{Y}_n| \geq \epsilon_n \text{ and } \dot{Y}_n > 0 \\ \bar{u}_n & \text{if } |\dot{Y}_n| \geq \epsilon_n \text{ and } \dot{Y}_n < 0 \end{cases} \quad (24)$$

$$\{X\} = [\Phi]\{q\} \quad (25a) \quad \ddot{q}_k + 2\zeta_k\omega_k\dot{q}_k + \omega_k^2 q_k = Q_k + Z_k \quad (25b)$$

$$\begin{Bmatrix} \dot{n}_1 \\ \dot{n}_2 \end{Bmatrix}_k = \begin{Bmatrix} 0 & 1 \\ -\omega_k^2 & -2\zeta_k\omega_k \end{Bmatrix} \begin{Bmatrix} n_1 \\ n_2 \end{Bmatrix}_k + \begin{Bmatrix} 0 \\ 1 \end{Bmatrix} Q_k + \begin{Bmatrix} 0 \\ 1 \end{Bmatrix} Z_k \quad (26)$$

Calculation of Behavior Sensitivities

Time dependent transient response sensitivities can be obtained by differentiating the modal transformation given in equation 25a with respect to each design variable (beam element section properties and actuator output force levels) to yield equation 27. The first term in equation 27 is known from the system response solution and the eigenvector sensitivities. The $\{\frac{\partial q}{\partial d_r}\}$ quantity in the second term is the last desired quantity.

The direct way of obtaining these partial derivatives is to differentiate equation 26 (or equation 25b) with respect to each design variable to obtain equation 28 and time step on these equations. The computational effort needed to obtain $\{\frac{\partial q}{\partial d_r}\}$ would be KR time stepping solutions where K is the number of retained modes and R is the number of independent design variables.

A more efficient way to obtain this last desired quantity is to exploit the special form of equation 26 by applying the Wilkie-Perkins essential parameter method (Ref. 8). Writing equation 26 in compact notation yields equation 29a where the [A] matrix in equation 29b is in Frobenius canonical form with $\alpha_1 = \omega^2$ and $\alpha_2 = 2\zeta\omega$ being referred to as essential parameters. A sensitivity matrix $[\xi]$ can be defined as in equation 30. As a consequence of the [A] matrix being in canonical form, two beneficial properties of the sensitivity matrix are: (1) the sensitivity matrix has a total symmetry property resulting in all terms on a single anti-diagonal being equal; and (2) the sensitivity matrix has a complete simultaneity property resulting in all sensitivity functions for the canonical system being linear combinations of the modal response, n_1 and n_2 , and $\frac{\partial n_1}{\partial \alpha_1}$ and $\frac{\partial n_1}{\partial \alpha_2}$. The equations shown in 31a and 31b result from these two properties.

$$\left\{ \frac{\partial X}{\partial d_r} \right\} = \left[\frac{\partial \phi}{\partial d_r} \right] \left\{ q \right\} + \left[\phi \right] \left\{ \frac{\partial q}{\partial d_r} \right\} \quad (27)$$

$$\left\{ \frac{\partial \dot{n}_i}{\partial d_r} \right\}_k = \begin{bmatrix} 0 & 0 \\ -\frac{\partial \omega_k^2}{\partial d_r} & -\frac{\partial (2\zeta_k \omega_k)}{\partial d_r} \end{bmatrix} \left\{ \begin{matrix} n_1 \\ n_2 \end{matrix} \right\}_k + \begin{bmatrix} 0 & 1 \\ -\omega_k^2 & -2\zeta_k \omega_k \end{bmatrix} \left\{ \frac{\partial n_i}{\partial d_r} \right\}_k + \left\{ \begin{matrix} 0 \\ 1 \end{matrix} \right\} \frac{\partial Q_k}{\partial d_r} + \left\{ \begin{matrix} 0 \\ 1 \end{matrix} \right\} \frac{\partial Z_k}{\partial d_r} \quad (28)$$

$$\{\dot{n}\} = [A]\{n\} + \{b\} Q + \{b\} Z \quad (29a)$$

$$A = \begin{bmatrix} 0 & 1 \\ -\alpha_1 & -\alpha_2 \end{bmatrix} \quad (29b)$$

$$\left[\xi \right] = \begin{bmatrix} \frac{\partial n_1}{\partial \alpha_1} & \frac{\partial n_1}{\partial \alpha_2} \\ \frac{\partial n_2}{\partial \alpha_1} & \frac{\partial n_2}{\partial \alpha_2} \end{bmatrix} \quad (30)$$

$$\frac{\partial n_1}{\partial \alpha_2} = \frac{\partial n_2}{\partial \alpha_1} \quad (31a)$$

$$\frac{\partial n_2}{\partial \alpha_2} = -n_1 - \alpha_1 \frac{\partial n_1}{\partial \alpha_1} - \alpha_2 \frac{\partial n_2}{\partial \alpha_1} - \alpha_2 \frac{\partial n_1}{\partial \alpha_2} \quad (31b)$$

Calculation of Behavior Sensitivities (cont.)

Evaluation of the $\left\{ \frac{\partial q}{\partial d_r} \right\}$ term utilizing the Wilkie-Perkins essential parameter method is done by: (1) differentiating equation 29a with respect to α_1 to yield equation 32; (2) time stepping on equation 32; (3) chain ruling from essential parameter space to design variable space via equation 33. Thus the computational effort needed to obtain $\left\{ \frac{\partial q}{\partial d_r} \right\}$ has been reduced from KR time stepping solutions to K.

It should be noted that this method of obtaining behavior sensitivities can only be used for the passive structural design variables since the essential parameters are independent of the active control design variables. Sensitivities of the transient dynamic response with respect to the active control design variables can be obtained by differentiating equation 26 with respect to the active control design variables to yield 34. Equation 34 is time-stepped for the desired terms.

$$\begin{Bmatrix} \frac{\partial \dot{n}_1}{\partial \alpha_1} \\ \frac{\partial \dot{n}_2}{\partial \alpha_1} \end{Bmatrix} = \begin{bmatrix} 0 & 0 \\ -1 & 0 \end{bmatrix} \begin{Bmatrix} n_1 \\ n_2 \end{Bmatrix} + \begin{bmatrix} 0 & 1 \\ -\alpha_1 & -\alpha_2 \end{bmatrix} \begin{Bmatrix} \frac{\partial n_1}{\partial \alpha_1} \\ \frac{\partial n_2}{\partial \alpha_1} \end{Bmatrix} \quad (32)$$

$$\left\{ \frac{\partial q}{\partial d_r} \right\} = \frac{\partial q}{\partial \alpha_1} \frac{\partial \alpha_1}{\partial d_r} + \frac{\partial q}{\partial \alpha_2} \frac{\partial \alpha_2}{\partial d_r} \quad (33)$$

$$\begin{Bmatrix} \frac{\partial \dot{n}_1}{\partial d_r} \\ \frac{\partial \dot{n}_2}{\partial d_r} \end{Bmatrix}_k = \begin{bmatrix} 0 & 1 \\ -\omega_k^2 & -2\zeta_k \omega_k \end{bmatrix} \begin{Bmatrix} \frac{\partial n_1}{\partial d_r} \\ \frac{\partial n_2}{\partial d_r} \end{Bmatrix}_k + \begin{Bmatrix} b \end{Bmatrix} \frac{\partial Z_k}{\partial d_r} \quad (34)$$

Numerical Example - Transient Response

The same aluminum planar grillage (see Fig. 1) used for the steady state response sensitivities is used to examine the quality of the peak transient response sensitivities. The loading consists of the force time history shown in Figure 9 applied at node 8. A single collocated sensor/actuator pair is located at node 6 and acts in the vertical direction. Peak transient response and peak transient response sensitivities were calculated by time-stepping through 1 second in 0.0005 second increments using ten retained modes (frequency content up to 100 Hz) and 2% modal damping.

Exact results for the peak positive and negative displacements at nodes 5 and 7 are compared with both direct and reciprocal element property Taylor series approximations in Figures 10 through 22 for a number of different design variables. For design variable changes up to $\pm 20\%$ the approximations are seen to be of acceptable accuracy. Furthermore, the direct approximations for peak displacements as functions of the actuator force level agree extremely well with the exact response curve (see Figures 19 through 22).

It should be noted that the degree of conservatism present in either the direct or the reciprocal section property approximations is not necessarily correlated with its accuracy. For instance, in Figure 15, the reciprocal approximation is more conservative than the direct approximation, but is far less accurate for design variable changes greater than 20%.

Conclusions

In this work behavior sensitivity formulations for both steady state and transient response were developed and the quality of the resulting derivative information was assessed.

Derivatives of the steady state response with respect to both structural and control design variables for harmonically loaded structures augmented by a linear direct output feedback control system were presented. The base design dynamic response was calculated using a frequency response method which reduced the solution of the complex dynamical equations of motion to the solution of a $2n \times 2n$ set of linear algebraic equations. The response quantity sensitivities were obtained directly using the psuedo-load method in its partial inverse form. Taylor series approximations in both direct and reciprocal element properties were constructed using this sensitivity information and shown to yield high quality approximations for 30 to 40% design variable changes provided near-resonance conditions are not encountered. When resonance or near-resonance conditions are present, the approximations for the response quantities are of acceptable quality for a relatively restricted interval around the base design.

Using a normal mode method of analysis, peak transient response and peak transient response sensitivities were calculated for arbitrarily loaded structures augmented by nonlinear on/off control actuators. The special form of the modal equations of motion was exploited to reduce the computational effort needed to obtain transient response sensitivities. These sensitivities were used to construct Taylor series approximations in both direct and reciprocal element properties for peak transient response. The approximations are of acceptable quality for structural design variable changes of up to 20%. The direct approximations in terms of the controller variables compare very well with the exact response for up to 50% changes in the design variables.

The results of this paper show that for control augmented structural systems, high quality approximations for both steady state dynamic response and peak transient response can be constructed. Therefore, the approximation concepts approach for structural synthesis can be extended to include both steady state dynamic response (Ref. 7) and peak transient response.

References

1. Venkayya, V.B. and Tischler, V.A., "Frequency Control and the Effect on Dynamic Response of Flexible Structures," *Proceedings of the 25th AIAA/ASME/ASCE/AHS Structures, Structural Dynamics and Materials Conference*, Palm Springs, California, May 14-16, 1984, pp. 431-441.
2. Haftka, R.T., Martinovic, Z.N. and Hallauer, W.L., "Enhanced Vibration Controllability by Minor Structural Modifications," *AIAA Journal*, Vol. 23, No. 8, August, 1985, pp. 1260-1266.
3. Haftka, R.T., Martinovic, Z.N., Hallauer, W.L. and Schamel, G., "Sensitivity of Optimized Control Systems to Minor Structural Modification," *Proceedings of the 26th AIAA/ASME/ASCE/AHS Structures, Structural Dynamics and Materials Conference*, Orlando, Florida, April 15-17, 1985, pp. 642-650.
4. Schmit, L.A. and Farshi, B., "Some Approximation Concepts for Efficient Structural Synthesis," *AIAA Journal*, Vol. 12, No. 5, 1974, pp. 692-699.
5. Schmit, L.A. and Miura, H., "Approximation Concepts for Efficient Structural Synthesis," NASA CR 2552, March, 1976.
6. Lust, R.V. and Schmit, L.A., "Alternative Approximation Concepts for Space Frame Synthesis," *Proceedings of the 26th AIAA/ASME/ASCE/AHS Structures, Structural Dynamics and Materials Conference*, Orlando, Florida, April 15-17, 1985, pp. 333-348.
7. Lust, R.V. and Schmit, L.A., "Control Augmented Structural Synthesis", AIAA Paper No. 86-1014-CP, presented at the 27th AIAA/ASME/ASCE/AHS Structures, Structural Dynamics, and Materials Conference, San Antonio, Texas, May 19-21, 1986.
8. Wilkie, D.F. and Perkins, W.R., "Essential Parameters in Sensitivity Analysis", *Automatica*, Vol. 5, 1969, pp. 191-197.

PLANAR GRILLAGE STRUCTURE

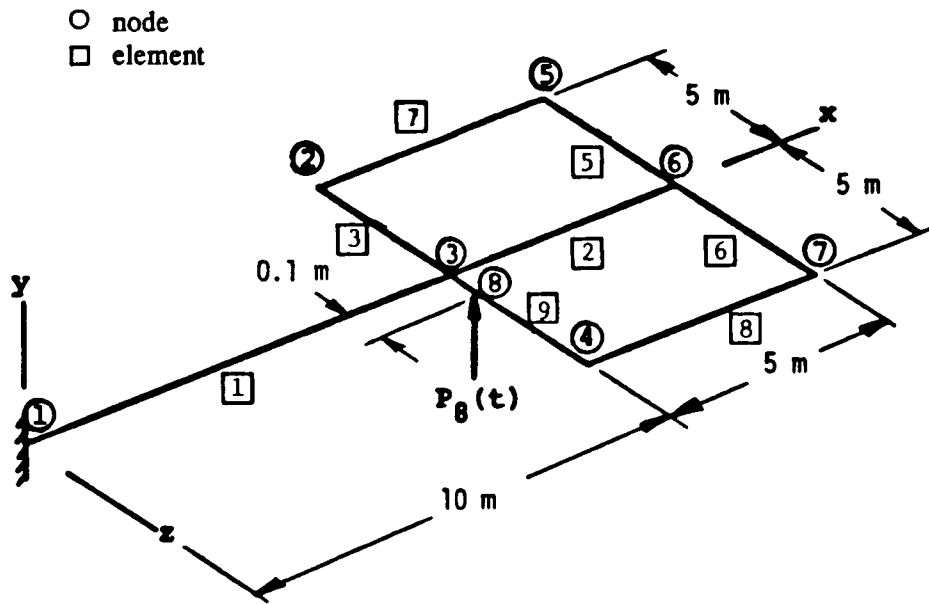


Fig. 1

MAXIMUM VERTICAL DISPLACEMENT AT NODE 7

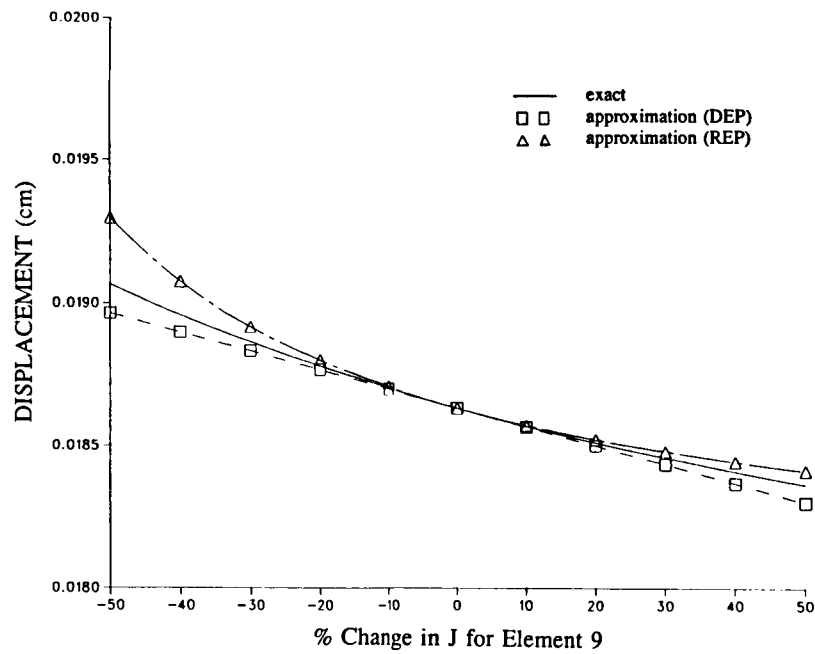


Fig. 2

MAXIMUM VERTICAL DISPLACEMENT AT NODE 7

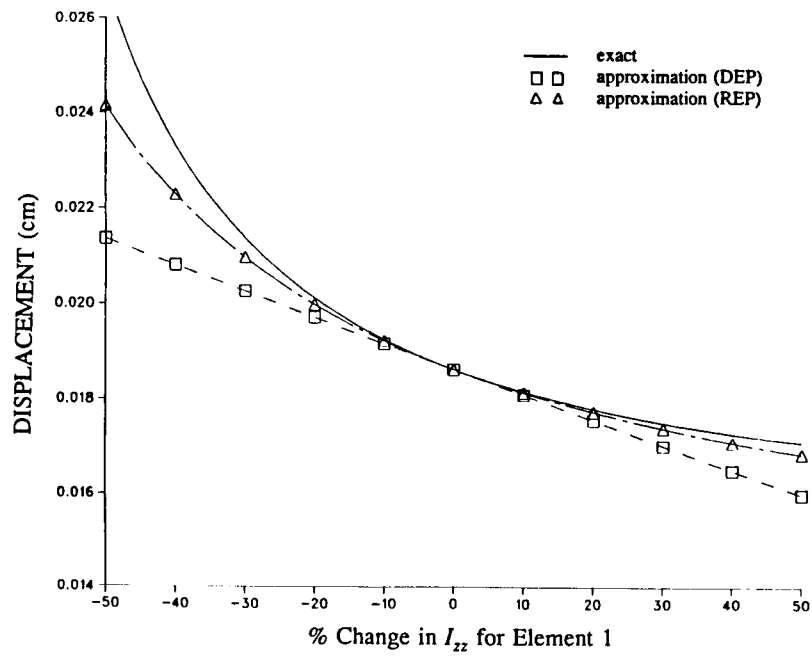


Fig. 3

MAXIMUM VERTICAL DISPLACEMENT AT NODE 7

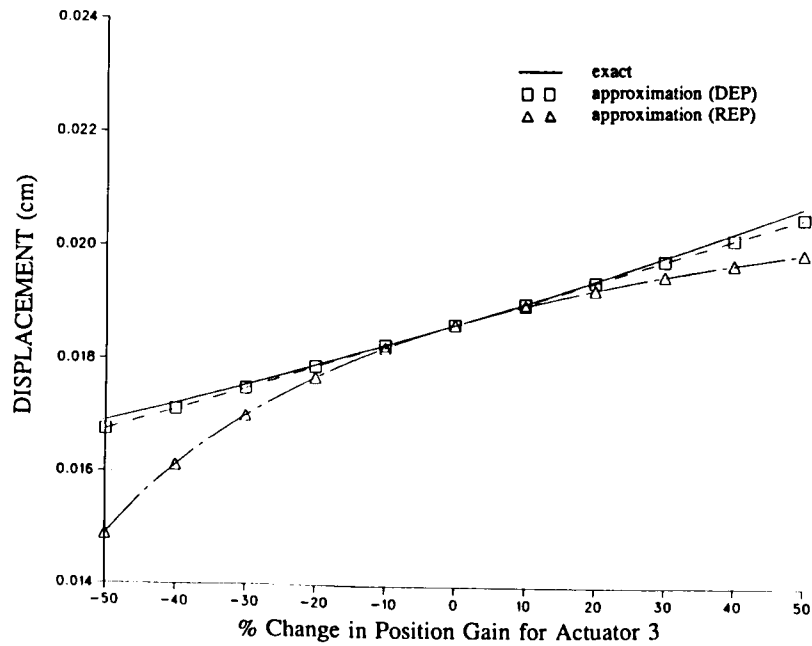


Fig. 4

MAXIMUM VERTICAL DISPLACEMENT AT NODE 7

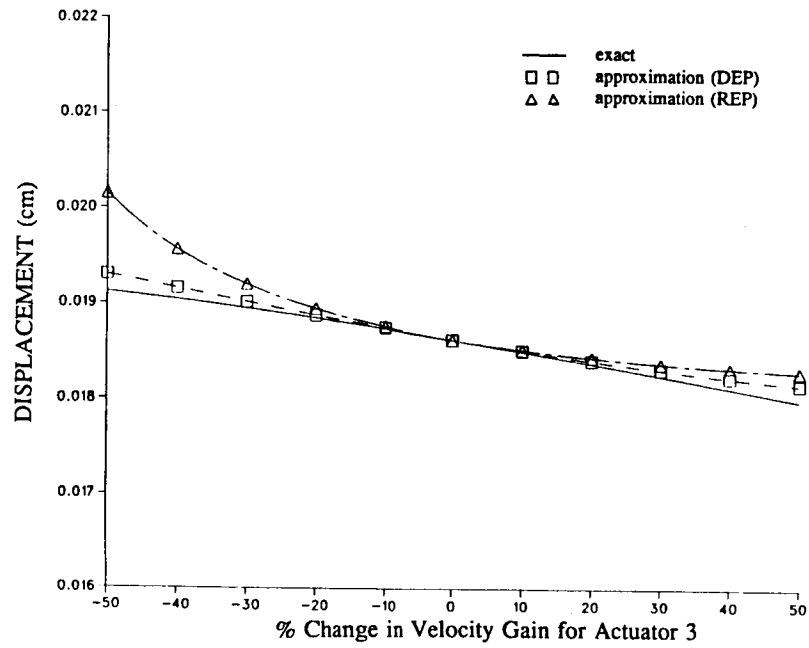


Fig. 5

MAXIMUM VERTICAL DISPLACEMENT AT NODE 7

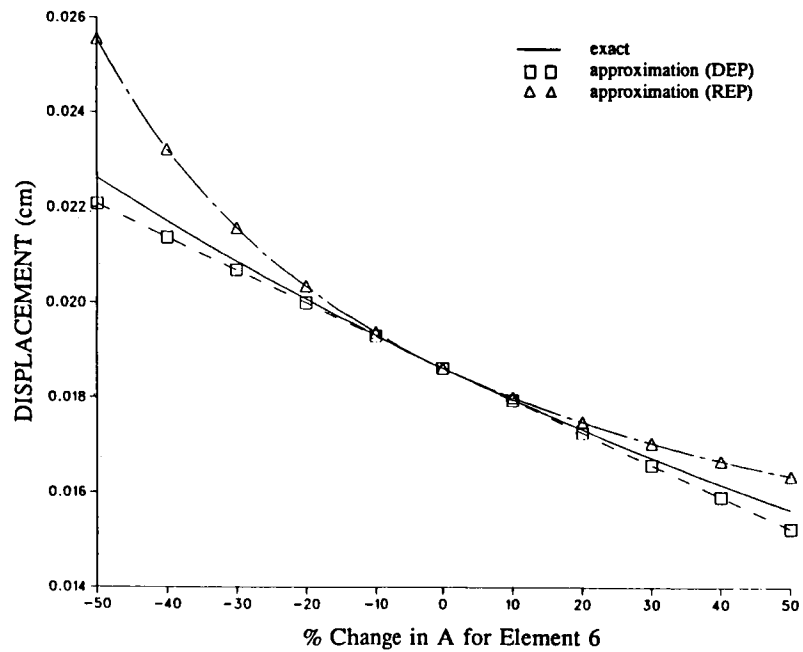


Fig. 6

MAXIMUM VERTICAL DISPLACEMENT AT NODE 5

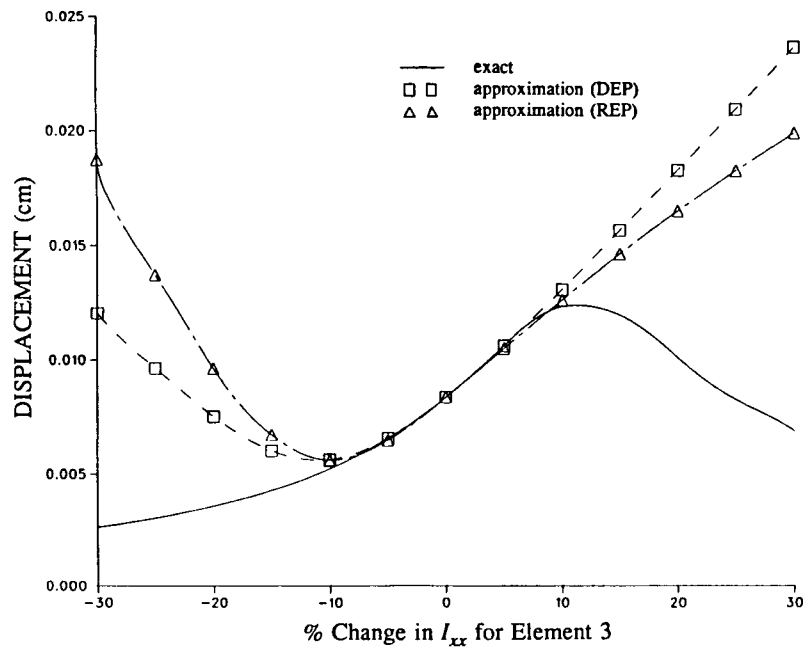


Fig. 7

MAXIMUM VERTICAL DISPLACEMENT AT NODE 5

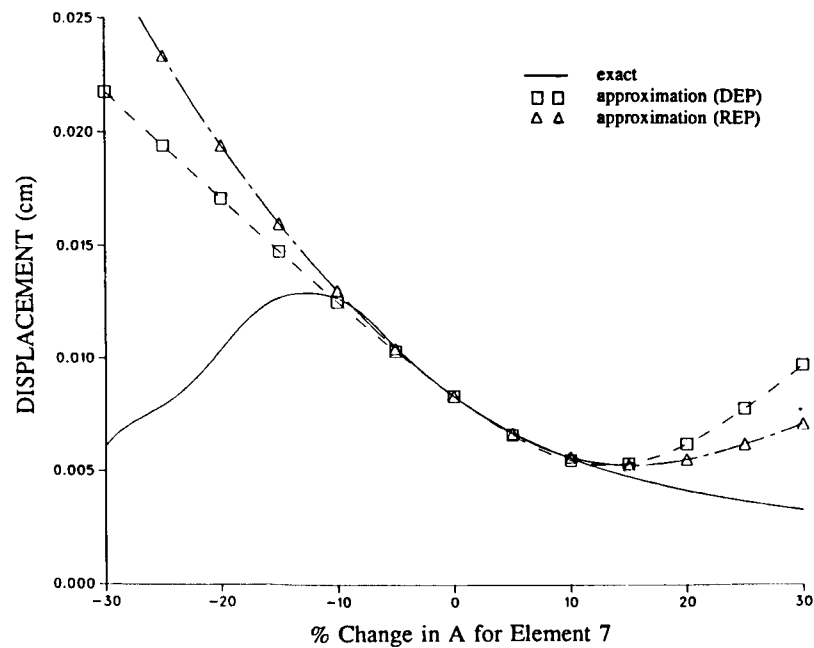


Fig. 8

APPLIED LOAD TIME HISTORY

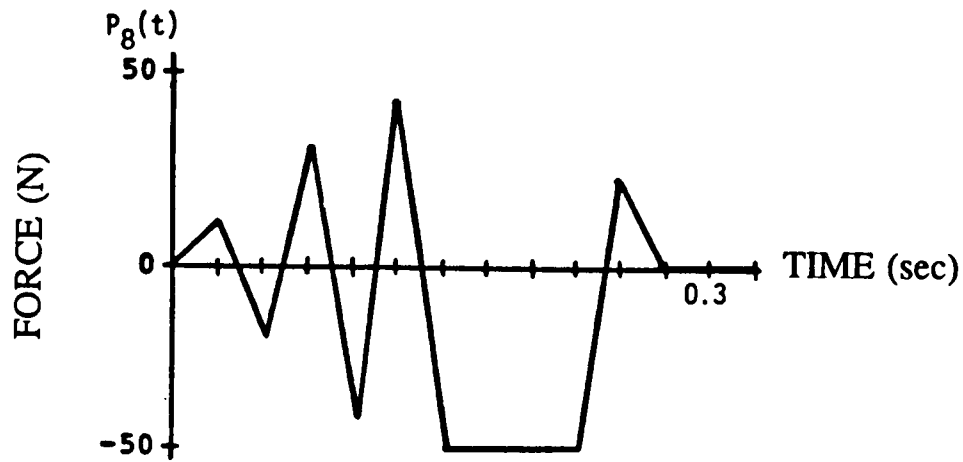


Fig. 9

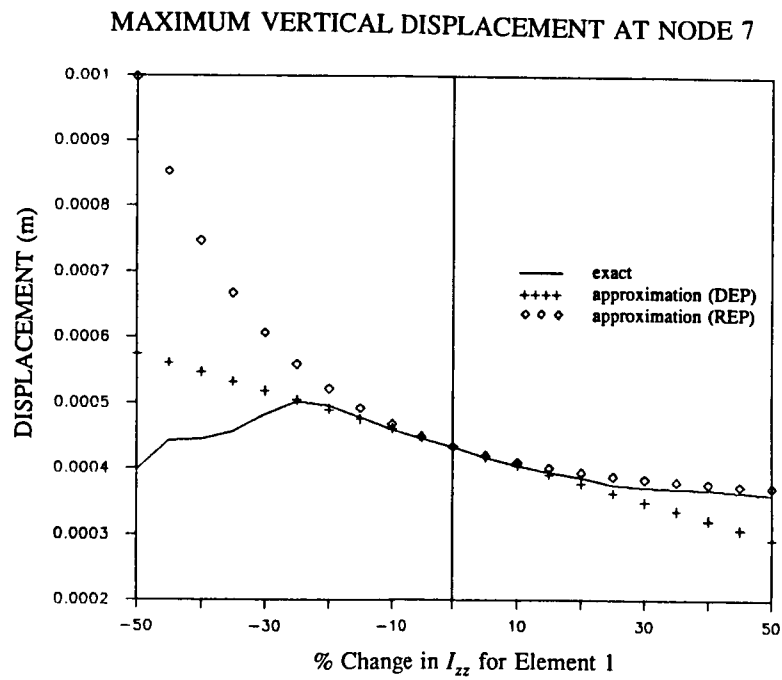


Fig. 10

MAXIMUM VERTICAL DISPLACEMENT AT NODE 7

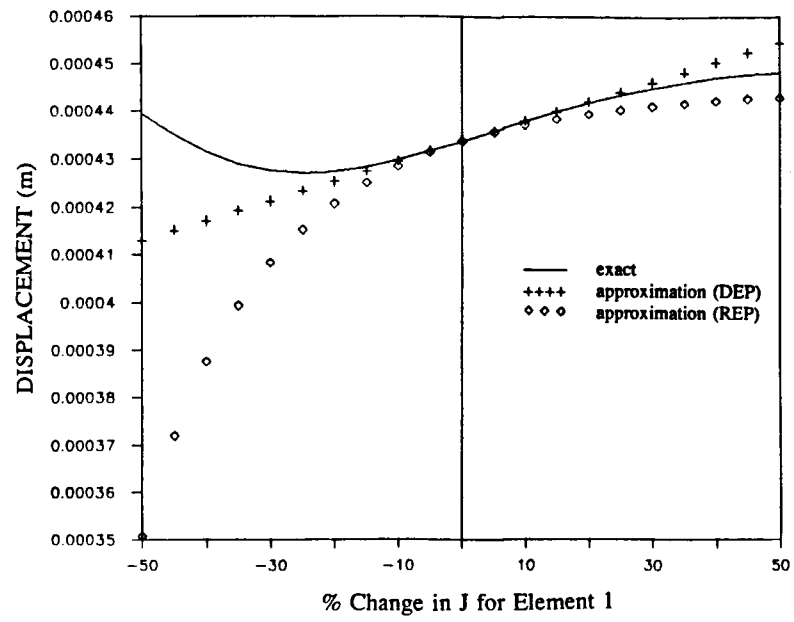


Fig. 11

MAXIMUM VERTICAL DISPLACEMENT AT NODE 7

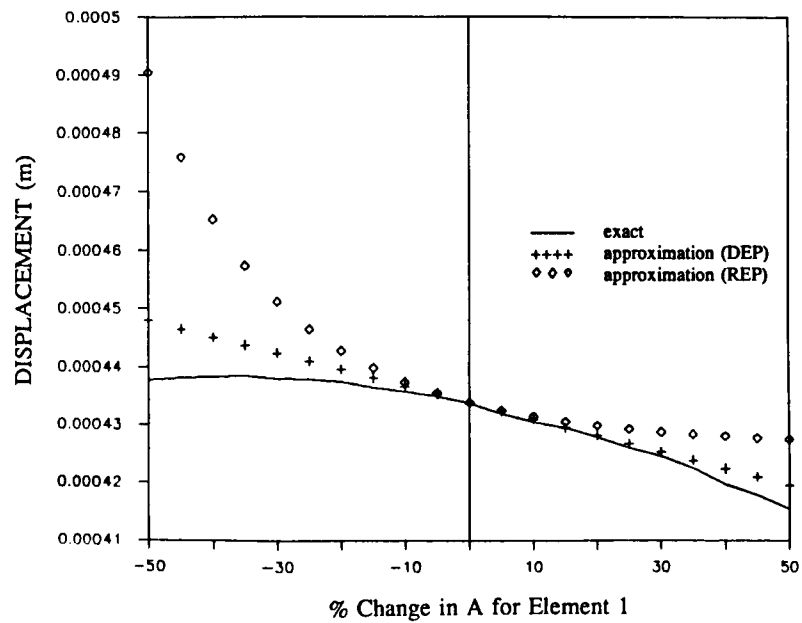


Fig. 12

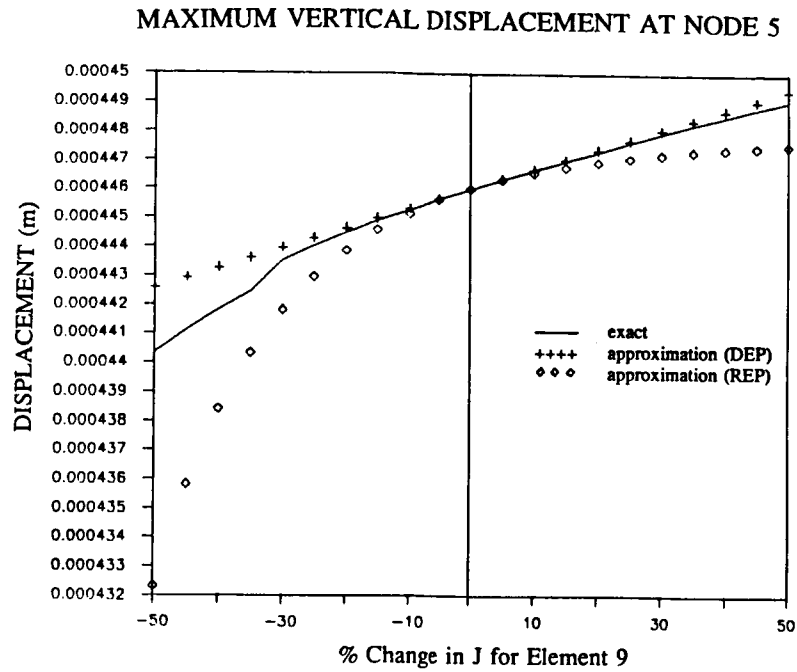


Fig. 13

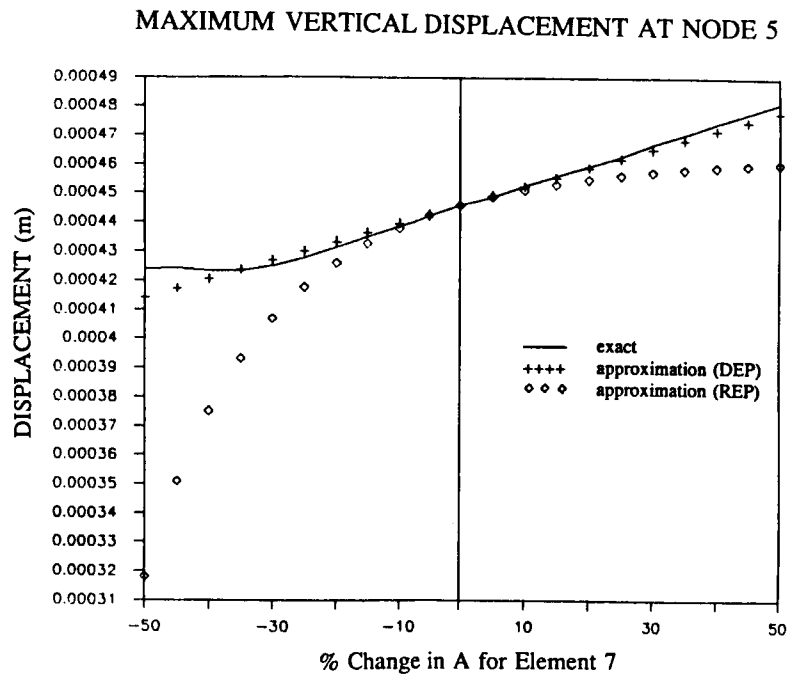


Fig. 14

MAXIMUM VERTICAL DISPLACEMENT AT NODE 5

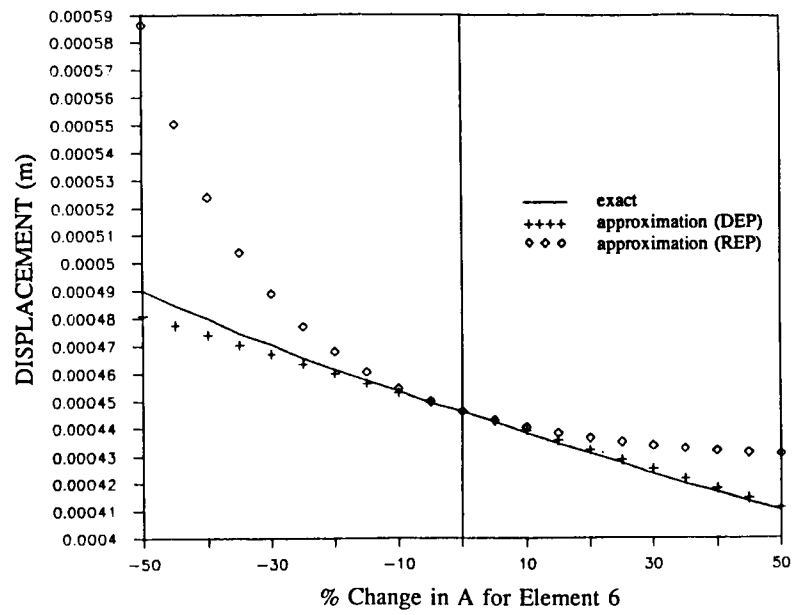


Fig. 15

MINIMUM VERTICAL DISPLACEMENT AT NODE 7

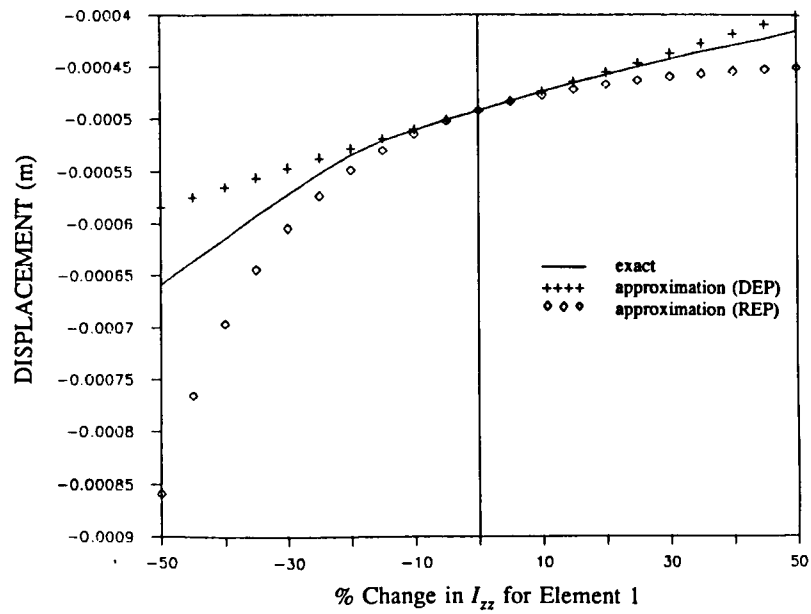


Fig. 16

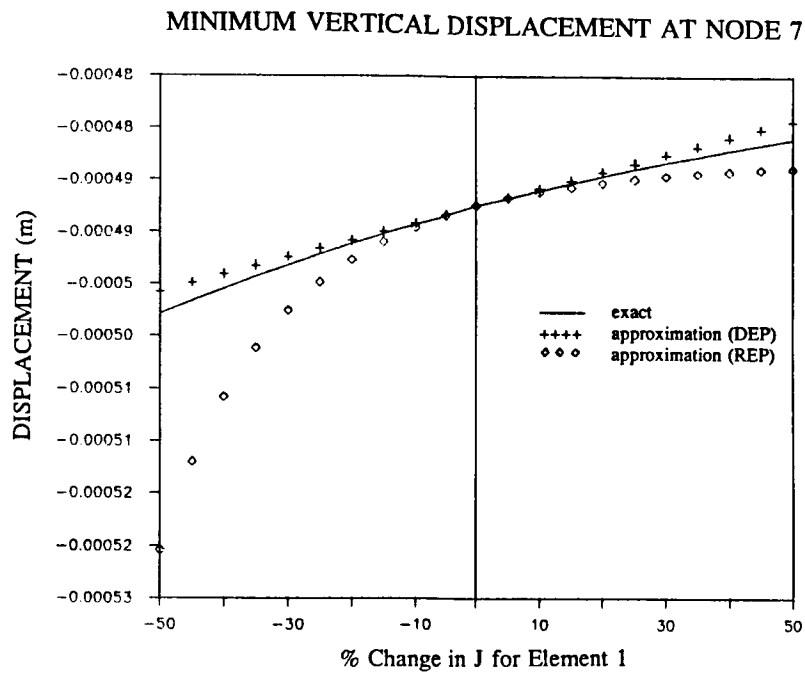


Fig. 17

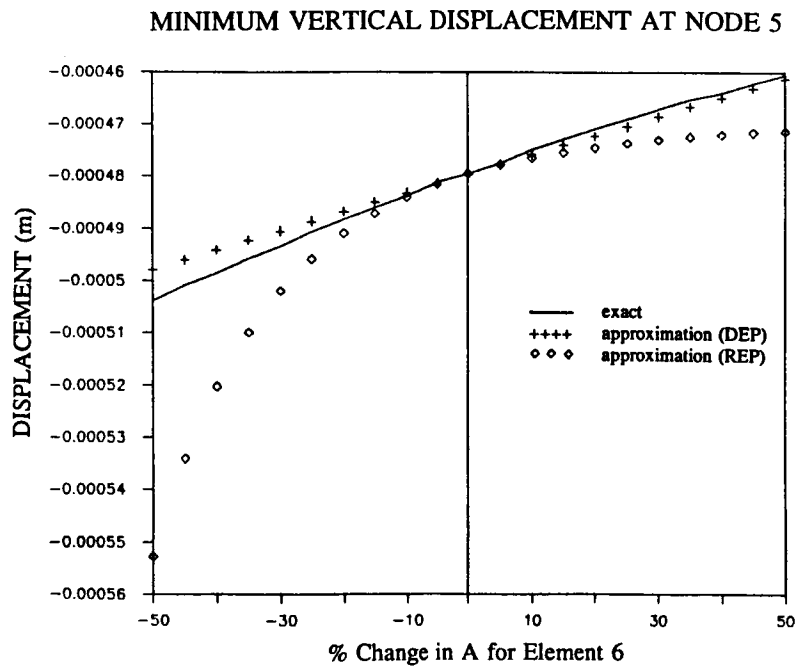


Fig. 18

MAXIMUM VERTICAL DISPLACEMENT AT NODE 5

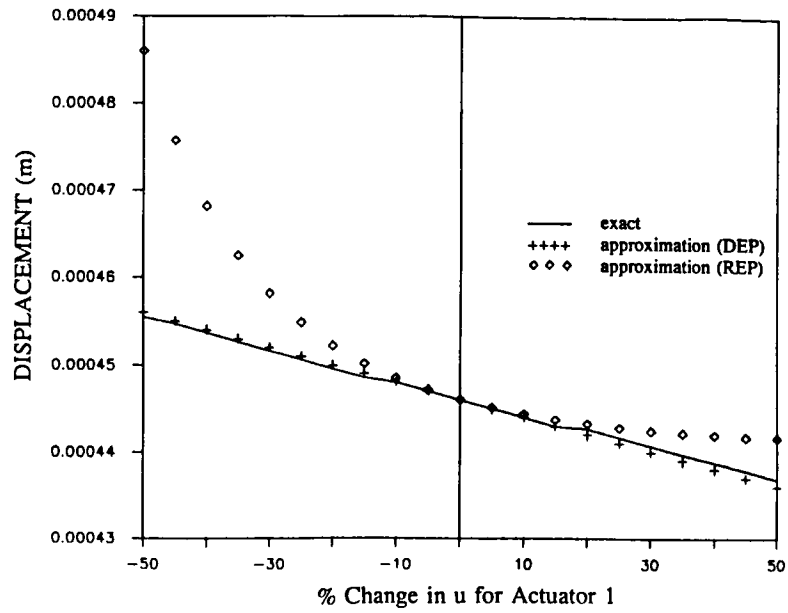


Fig. 19

MINIMUM VERTICAL DISPLACEMENT AT NODE 5

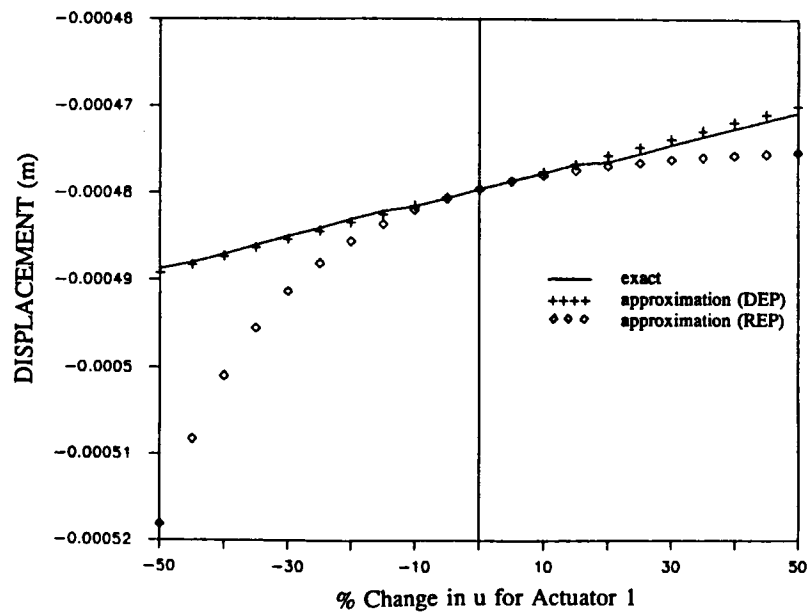


Fig. 20

MAXIMUM VERTICAL DISPLACEMENT AT NODE 7

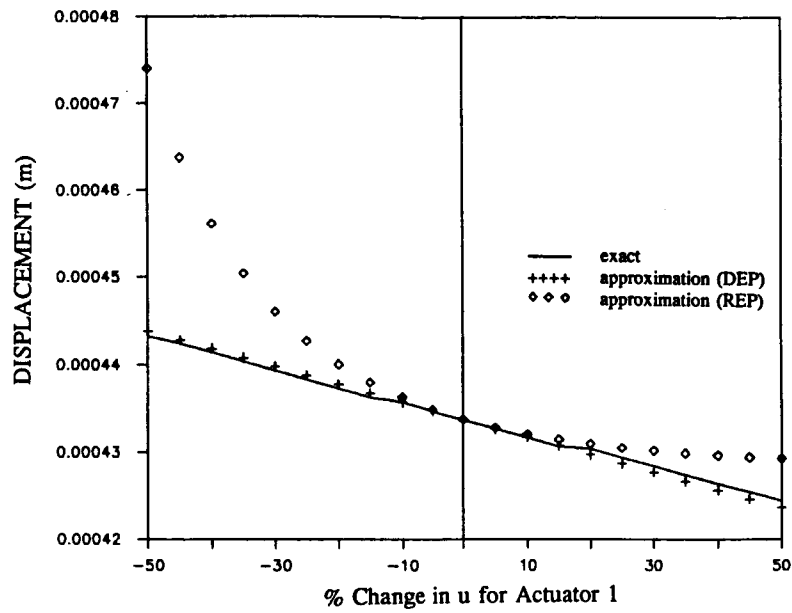


Fig. 21

MINIMUM VERTICAL DISPLACEMENT AT NODE 7

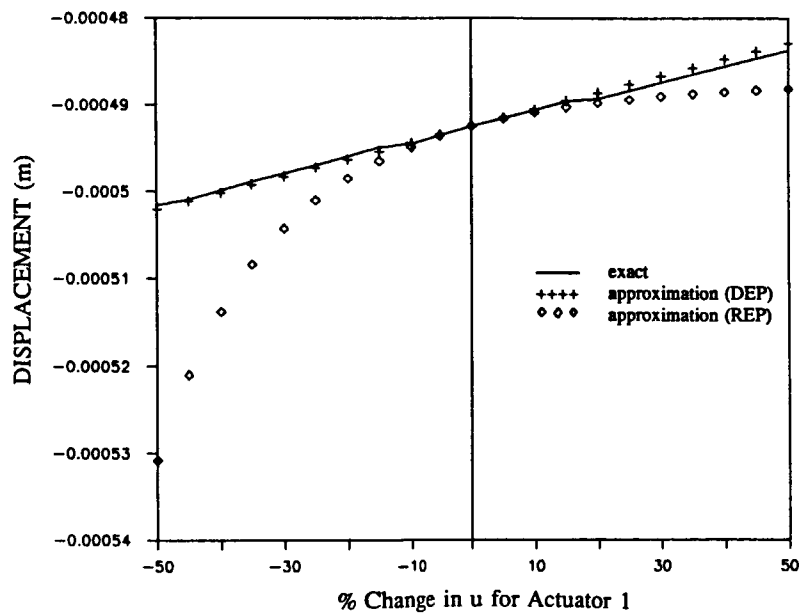


Fig. 22

SENSITIVITY METHOD FOR INTEGRATED
STRUCTURE/ACTIVE CONTROL LAW DESIGN

Michael G. Gilbert
NASA Langley Research Center
Hampton, VA

OUTLINE

This paper describes the development of an integrated structure/active control law design methodology for aeroelastic aircraft applications. The paper gives a short motivating introduction to aeroservoelasticity and the need for integrated structures/controls design algorithms. Three alternative approaches to development of an integrated design method are briefly discussed with regards to complexity, coordination and tradeoff strategies, and the nature of the resulting solutions. This leads to the formulation of the proposed approach which is based on the concepts of sensitivity of optimum solutions and multi-level decompositions. The concept of sensitivity of optimum is explained in more detail and compared with traditional sensitivity concepts of classical control theory. The analytical sensitivity expressions for the solution of the linear, quadratic cost, Gaussian (LQG) control problem are summarized in terms of the linear regulator solution and the Kalman Filter solution. Numerical results for a state-space aeroelastic model of the DAST ARW-II vehicle are given, showing the changes in aircraft responses to variations of a structural parameter, in this case first wing bending natural frequency.

- Introduction
- Design Approach
- Sensitivity of Optimum
- Sensitivity of LQG Solution
- Integrated Design Results
- Concluding Remarks

INTRODUCTION

Aeroservoelasticity is defined as the interaction of unsteady aerodynamics, elastic structure, and automatic control systems of an aircraft. This interaction can be either favorable and unfavorable, that is it can be the source of dynamic responses of the aircraft which force the redesign of the structure or flight control system, or it can actually improve the performance of the aircraft. Examples of aircraft which exhibited aeroservoelastic problems include the F-16, F-18, and the X-29, all of which required flight control system changes before flight. The Lockheed L1011-500 on the other hand employs an active load alleviation system to reduce wing loads and improve range.

The state of the art in aeroservoelastic analysis is now to the point where it is possible in many cases to predict aeroservoelastic interactions before flight test of the vehicle. With this capability in hand, the next logical step is to develop design methodologies which use aeroservoelastic interactions to improve aircraft performance. This paper describes the initial development of one approach to this interdisciplinary design problem, concentrating on integrated design of aircraft structures and control laws.

- Aeroservolasticity Is The Interaction
Of Aerodynamics, Structures, And Controls
- Favorable And Unfavorable Interactions
- Analysis Methods Maturing
- Integrated Design Methods In Infancy

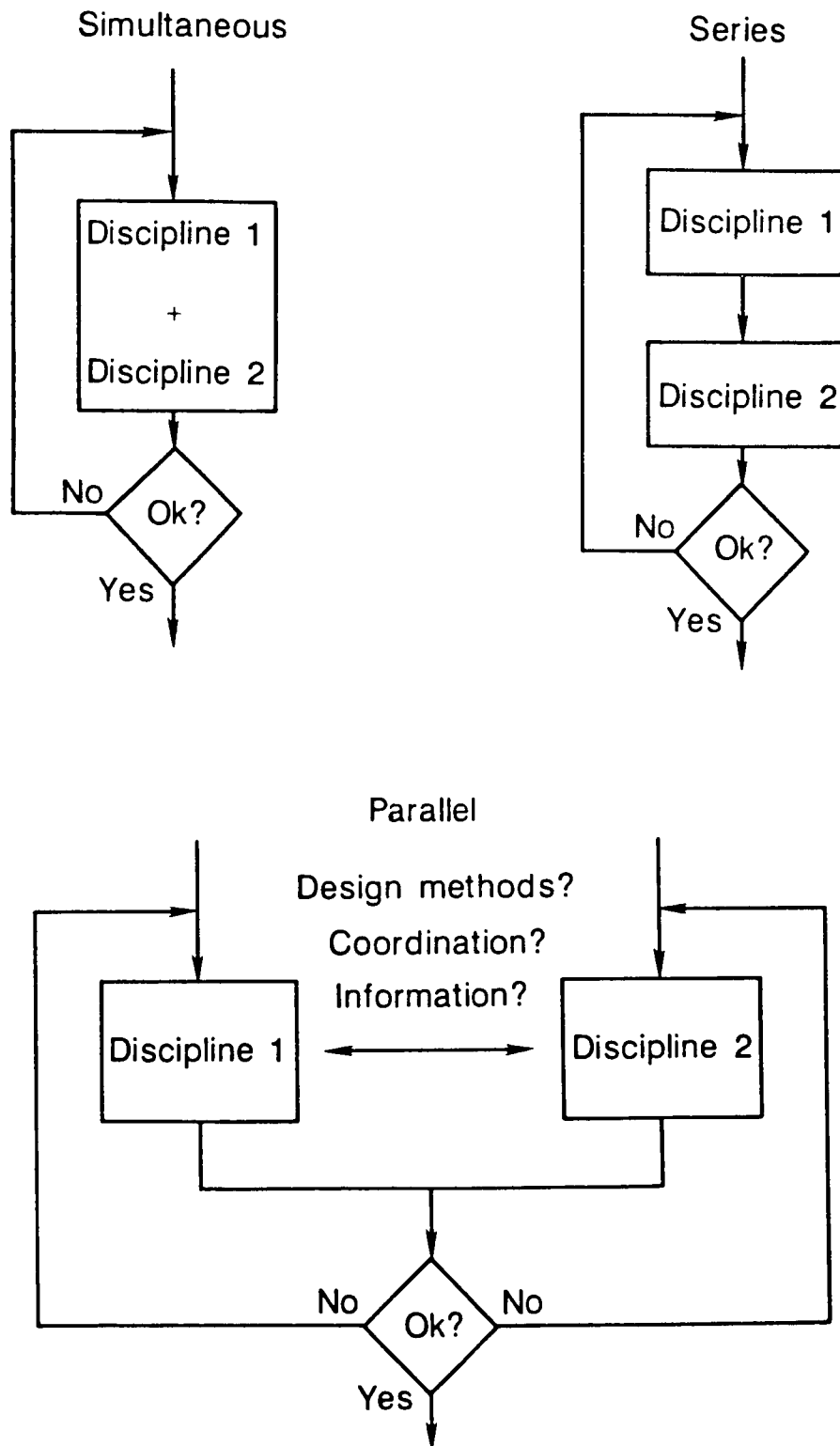
DESIGN APPROACHES

There are three possible approaches to integrated structure/control law design, or for that matter, any integrated design. These are the simultaneous or combined approach, the series or sequential approach, and the parallel approach. In the simultaneous approach, the design problem is formulated as a single problem by combining the objectives, requirements, and design variables of the various disciplines into a single set. The design variables are then selected simultaneously to satisfy the design requirements and objectives. The drawbacks to this approach are the resulting size of the design problem and the difficulty of making reasonable tradeoffs when all the design criteria are not satisfied.

In the series approach, the individual disciplinary designs are performed in a logical sequence or series, with each discipline selecting its own design variables to satisfy its own design requirements. System performance is assessed at the end of the sequence, and the process is repeated if necessary in an iterative manner. Again, one of the drawbacks with this approach is difficulty in making tradeoffs between disciplines, although a more serious drawback is that the overall system design is dominated by the discipline which is first in the sequence. For example, if an aircraft structural design is completed first, followed by the flight control design, and unfavorable dynamic interactions occur, most often the flight control system design is changed extensively to improve the overall dynamics while the structural design is held fixed, even though moderate structural changes may be more effective.

A parallel approach to integrated design has the individual disciplines performing their designs simultaneously but independently. At the completion of the design iteration, the overall system performance is checked and the individual designs undergo iterations. Of course, some form of coordination must occur during the iteration process or no improvement in the system design will be possible. The coordination activity requires that information about the individual designs and the relationships of those designs to the other disciplines must be available. This information is dependent on the actual design methods that are used as well as the type and form of the design requirements, objectives, and design variables. The kinds of information, coordination, and design methods necessary for the successful development of a parallel integrated design methodology are still open research questions.

DESIGN APPROACHES



PARALLEL DESIGN

The successful development of a parallel integrated interdisciplinary design methodology requires a coordination strategy, the determination of disciplinary design information requirements, and the selection of design tools for each discipline which are compatible with the coordination strategy and information requirements. Based on research conducted at NASA - Langley Research Center and elsewhere, a multi-level problem decomposition approach [1,2] is used to define a coordination strategy for the integrated structures/control law design method proposed here. This approach breaks the integrated design problem down into a hierarchical structure that naturally reflects the individual disciplinary design requirements as well as the integrated system design requirements and objectives. Selecting optimization techniques for the individual disciplinary design methods allows the use of the concept of the sensitivity of an optimum solution to fixed parameters [3] to define the information requirements of the hierarchical decomposition. That is, for the case of integrated structure/control law design, the sensitivity of the optimum structural design to control law design variables is passed to the coordination level, as is the sensitivity of the optimum control law design to structural design variables. This information is used at the system design level to make design tradeoffs between the disciplines in the interest of improving the system design.

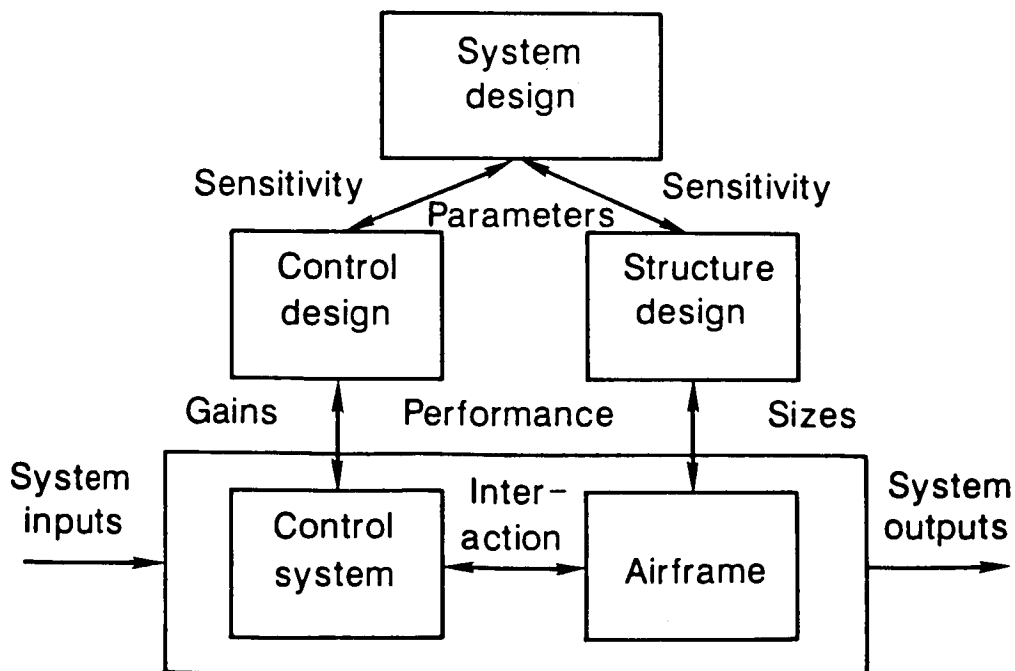
Design Methods: Optimization Techniques

Information: Sensitivity Of Optimum Designs^[3]

Coordination: Multilevel Problem Decompositions^[1,2]

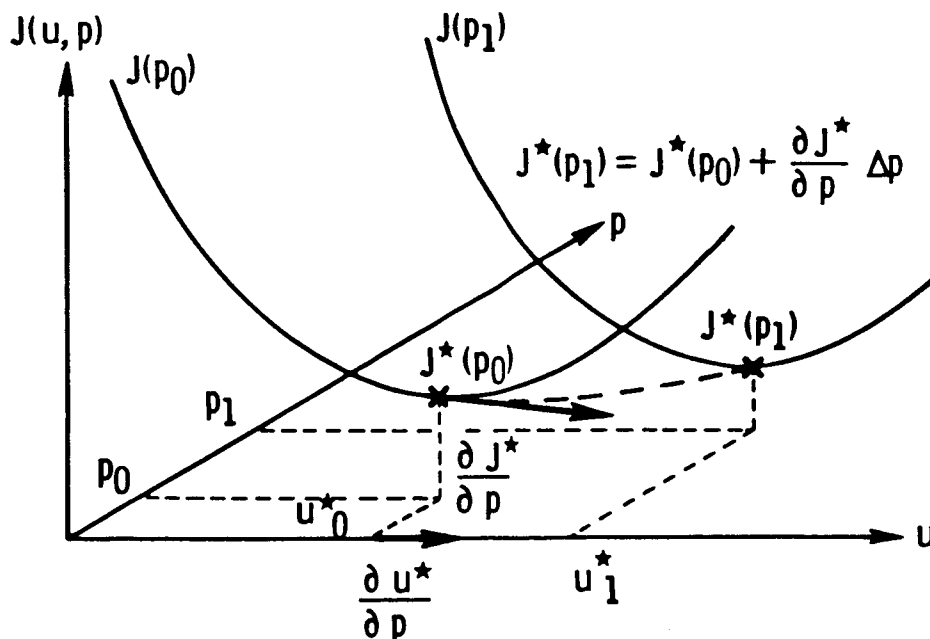
INTEGRATED STRUCTURE/CONTROL DESIGN

The selection of multi-level hierarchal problem decompositions, optimization techniques, and the sensitivities of optimum solutions leads to the integrated structure/control law design methodology shown below. The control law and structure designs occur simultaneously and in parallel, with the recognition that the two disciplines interact in the actual aircraft. These designs proceed on the basis of the individual discipline design objectives and variables. For example, the structural design might determine structural element sizing to minimize weight while maintaining stress levels, while the control design picks control gains to minimize control energy and maintain adequate stability margins. The sensitivity of the optimum control design to the structural element sizes, and the sensitivity of the optimum structural design to the control law gains are then computed, either by finite differencing of neighboring designs, or by analytical sensitivity of optimum derivative expressions, and passed on to the system level. This sensitivity data are then used as gradient information at the higher level to determine the most effective tradeoffs to achieve desired system performance. A key aspect of the research reported here is the development of analytical sensitivity expressions for the LQG optimal control law problem, eliminating the need for finite difference derivative calculations.



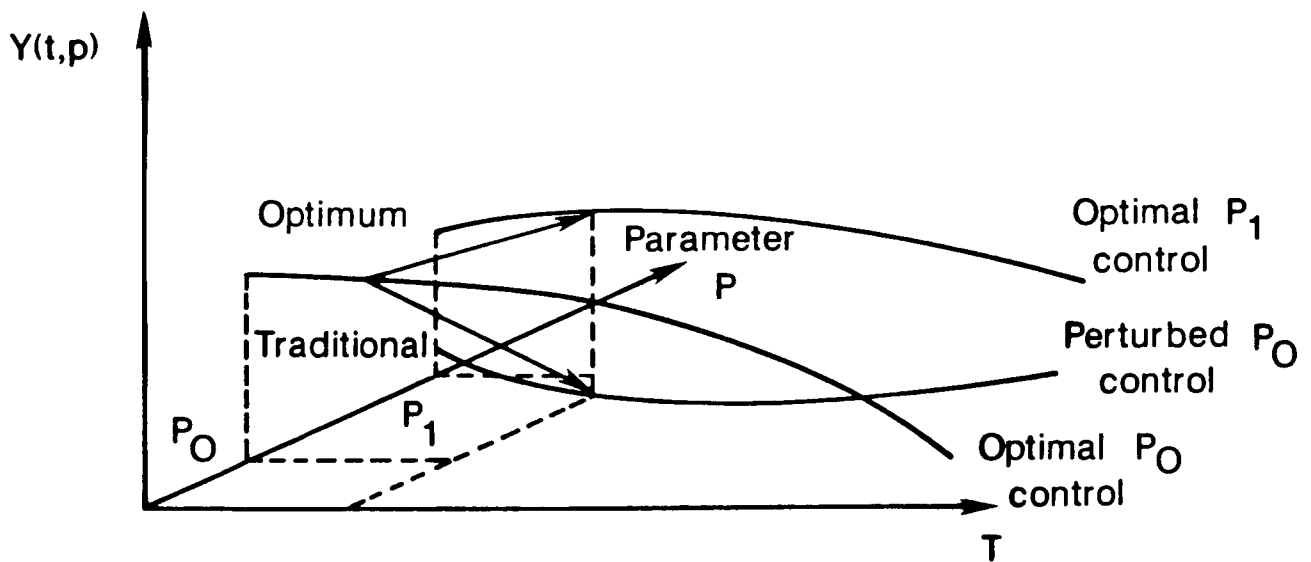
GEOMETRICAL INTERPRETATION OF OPTIMUM SENSITIVITY

The concept of the sensitivity of an optimum solution of an optimization problem to problem parameters which were held fixed during the optimization is illustrated below. Consider a conceptual optimization problem where an objective function $J(u, p)$ is to be minimized by choice of a design variable u , with some design parameter p held fixed at some nominal value p_0 . For a different nominal value of the design parameter, say p_1 , the optimum solution of the problem will be different, as shown. The sensitivity of the optimum solution with respect to the design parameter p is then the change of the optimum value of the objective function and the change of the design variable at optimum due to changes in the parameter. One approach to calculating these sensitivities is to finite difference solutions of the problem due to perturbations in the parameter. Another approach is to obtain analytical sensitivity expressions by differentiation of the necessary conditions of optimality with respect to the design parameter, and evaluating those expressions at the optimum solution, as advocated in [3]. This approach eliminates the need for numerous perturbed solutions of the problem and the inaccuracies of numerical approximations of the sensitivities.



COMPARISON OF SENSITIVITY TYPES

The difference between the sensitivity of optimum analysis and a traditional sensitivity analysis in controls applications can be highlighted as follows. Consider the time response of some output $Y(t,p)$ of an optimally controlled dynamic system due to a specified input. For the nominal value of the design parameter p_0 , the optimal control law is computed and the time response is calculated. If the value of the design parameter was to change to p_1 , but the control law was to remain the same (that is the control law that is optimal for p_0), then the time response to the same input would change, and a traditional sensitivity analysis could be used to predict that change. On the other hand, if a new control law which is optimal for p_1 is used, the time response would again be different from the original, and from the perturbed control law time response as well. The sensitivity of optimum analysis results can be used to predict this new optimally controlled system time response analytically.



LQG PROBLEM FORMULATION

The optimal control law formulation to be used in the integrated structure/control law design algorithm is the standard linear time invariant system, quadratic cost, Gaussian distributed noise (LQG) optimal control problem. For the purposes of this integrated design methodology, the formulation consists of state space equations of motion, where A is the system state matrix, B is the control input matrix, C is the controlled output matrix, D is disturbance input matrix, and M is the measurement matrix defining the signals to be used for feedback. The vector x is the system state vector, u is the control input, r is a vector of external commands, and w_D , w_U , and v are Gaussian distributed white noise vectors with noise intensity matrices W_D , W_U , and V respectively. The objective function J to be minimized is the expected value of a quadratic function of the controlled outputs y and the control inputs u , where the weighting matrices Q and R are positive semi-definite and positive definite, respectively. It is assumed that the matrices A , B , C , M , Q , R , and W_U are functions of the fixed design parameters p , for which the functional dependence and the derivatives of the matrix elements with respect to the parameters are known. The solution to this optimal control problem is known to be the interconnection of the optimal linear regulator with the optimal Kalman Filter state estimator [4, pg. 390].

$$\dot{x} = A(\bar{p})x + B(\bar{p})(u + r) + Dw_D + B(\bar{p})w_U$$

$$y = C(\bar{p})x$$

$$z = M(\bar{p})x + v$$

$$J = \lim_{T \rightarrow \infty} \epsilon \left\{ \frac{1}{2T} \int_0^T (y^T Q(\bar{p})y + u^T R(\bar{p})u) dt \right\}$$

$$\bar{p} = \{ . \quad . \quad . \quad . \quad p \quad . \quad . \quad . \}^T = \text{vector of fixed parameters}$$

LQ REGULATOR SOLUTION AND OPTIMUM SENSITIVITY

The solution of the LQG optimal control problem is the interconnection of the optimal linear regulator and the optimal Kalman Filter state estimator. The solution of the optimal regulator problem is an optimal feedback gain matrix G determined by the solution for S of a nonlinear matrix Riccati equation, where both equations come directly from the necessary conditions of optimality [5, pg. 148]. The interconnection with the Kalman Filter is defined by feeding back estimates of the system states rather than the actual (unmeasurable) system states. Differentiating the LQG solution equations with respect to the parameter p gives an expression for the sensitivity of the optimal gain matrix G which is in terms of the sensitivity of the Riccati equation solution matrix S . The Riccati sensitivity is obtained from the solution of the linear Lyapunov equation that results from differentiation of the matrix Riccati equation with respect to p . (Note that all the other derivative matrices in the two equations are assumed to be known as part of the problem formulation.) A property of the regulator solution is that the matrix $(A-BG)$ is asymptotically stable, guaranteeing that a unique solution to the Lyapunov equation exists [4, pg. 103].

Necessary conditions

$$u = -R^{-1} B^T S \hat{x} = -G \hat{x}$$

$$0 = A^T S + SA - SBR^{-1} B^T S + C^T Q C$$

Differentiate necessary conditions with respect to p

$$\frac{\partial G}{\partial p} = -R^{-1} \frac{\partial R}{\partial p} R^{-1} B^T S + R^{-1} \frac{\partial B^T}{\partial p} S + R^{-1} B^T \frac{\partial S}{\partial p}$$

$$\begin{aligned} 0 = & (A-BG)^T \frac{\partial S}{\partial p} + \frac{\partial S}{\partial p} (A-BG) + \left\{ \frac{\partial A^T}{\partial p} S + S \frac{\partial A}{\partial p} + \frac{\partial C^T}{\partial p} Q C + C^T \frac{\partial Q}{\partial p} C \right. \\ & \left. + C^T Q \frac{\partial C}{\partial p} - S \left(\frac{\partial B}{\partial p} R^{-1} B^T - B R^{-1} \frac{\partial R}{\partial p} R^{-1} B^T + B R^{-1} \frac{\partial B^T}{\partial p} \right) S \right\} \end{aligned}$$

KALMAN FILTER AND OPTIMUM SENSITIVITY

The optimal Kalman Filter solution is similar to the optimal regulator solution in that the optimal filter gain matrix K is given in terms of the solution T to the filter nonlinear matrix Riccati equation. Differentiation of these two equations with respect to the parameter p gives the filter gain matrix K sensitivity in terms of the sensitivity of the matrix Riccati equation solution T . This sensitivity is calculated from a linear Lyapunov equation obtained by differentiation of the Riccati equation, which again is known to have a unique solution because of the asymptotic stability properties of the coefficient matrix $(A-KM)$.

Necessary conditions :

$$K = TM^T V^{-1}$$

$$0 = AT + TA^T + DW_D D^T + BW_U B^T - TM^T V^{-1} MT$$

Differentiate necessary conditions with respect to p :

$$\frac{\partial K}{\partial p} = \frac{\partial T}{\partial p} M^T V^{-1} + T \frac{\partial M^T}{\partial p} V^{-1}$$

$$\begin{aligned} 0 = & (A-KM) \frac{\partial T}{\partial p} + \frac{\partial T}{\partial p} (A-KM)^T + \left\{ \frac{\partial A}{\partial p} T + T \frac{\partial A^T}{\partial p} + \frac{\partial B}{\partial p} W_U B^T \right. \\ & \left. + B \frac{\partial W_U}{\partial p} B^T + BW_U \frac{\partial B^T}{\partial p} - T \left(\frac{\partial M^T}{\partial p} V^{-1} M + M^T V^{-1} \frac{\partial M}{\partial p} \right) T \right\} \end{aligned}$$

OPTIMALLY CONTROLLED SYSTEM EQUATIONS

The state-space equations of the optimally controlled system can be written in terms of the optimal gain matrices G and K by defining a state estimation error vector e which in turn is used to define a new augmented system state vector. The closed-loop system equations are then as shown, with the new system state matrix shown in partitioned form as a function of K and G . The sensitivity of the new system state matrix with respect to p is calculated in terms of known sensitivity derivative matrices and the optimal gain sensitivities which have already been calculated. These results are used with analytical performance sensitivity expressions, such as for eigenvalues and time responses, to find the changes in optimally controlled system performance due to changes in system design parameters p .

Define: $e \triangleq x - \hat{x}$, $\bar{x}^T = \{x^T \mid e^T\}$, $\bar{w}^T = \{w^T \mid v^T\}$

Closed Loop

$$\dot{\bar{x}} = \bar{A}\bar{x} + \bar{D}\bar{w}$$

$$y = \bar{C}\bar{x}$$

$$u = \bar{G}\bar{x}$$

$$\bar{A} = \left[\begin{array}{c|c} A - BG & BG \\ \hline 0 & A - KM \end{array} \right] \quad \frac{\partial \bar{A}}{\partial p} = \left[\begin{array}{c|c} \frac{\partial A}{\partial p} - \frac{\partial B}{\partial p} G - B \frac{\partial G}{\partial p} & \frac{\partial B}{\partial p} G + B \frac{\partial G}{\partial p} \\ \hline 0 & \frac{\partial A}{\partial p} - \frac{\partial K}{\partial p} M - K \frac{\partial M}{\partial p} \end{array} \right]$$

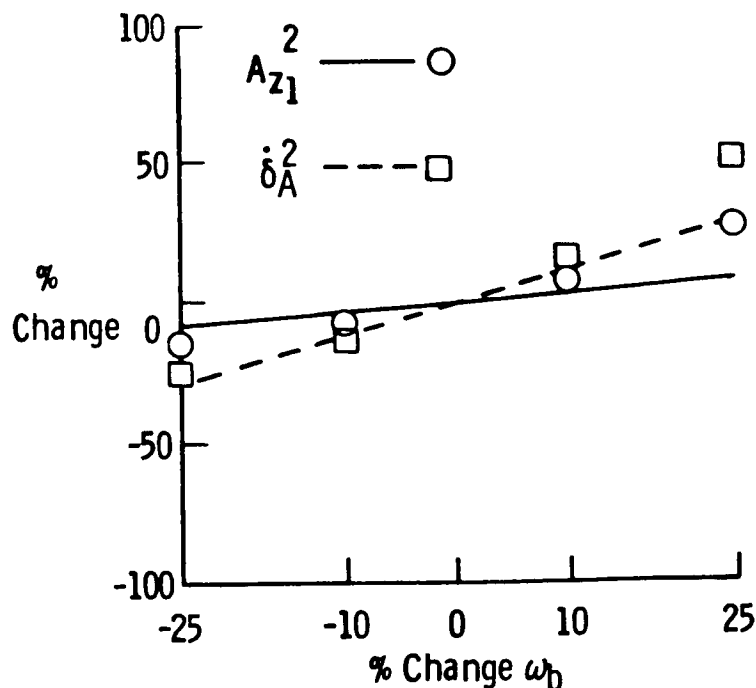
ANALYTICAL PERFORMANCE SENSITIVITIES

Analytical performance sensitivity expressions exist for numerous dynamic system performance measures in terms of the sensitivity matrices of state-space systems. These include eigenvalue and eigenvector sensitivities [6], trajectory (time) and frequency response sensitivities [7], sensitivity of covariance responses due to random system inputs and disturbances [8], and singular value sensitivities [9]. These results are used in the integrated structure/control algorithm at the upper level as gradient information to predict performance changes due to changes in the structural design parameters.

- Eigenvalues/Eigenvectors
- Trajectory Responses
- Covariance Responses
- Frequency Responses
- Singular Value Decompositions

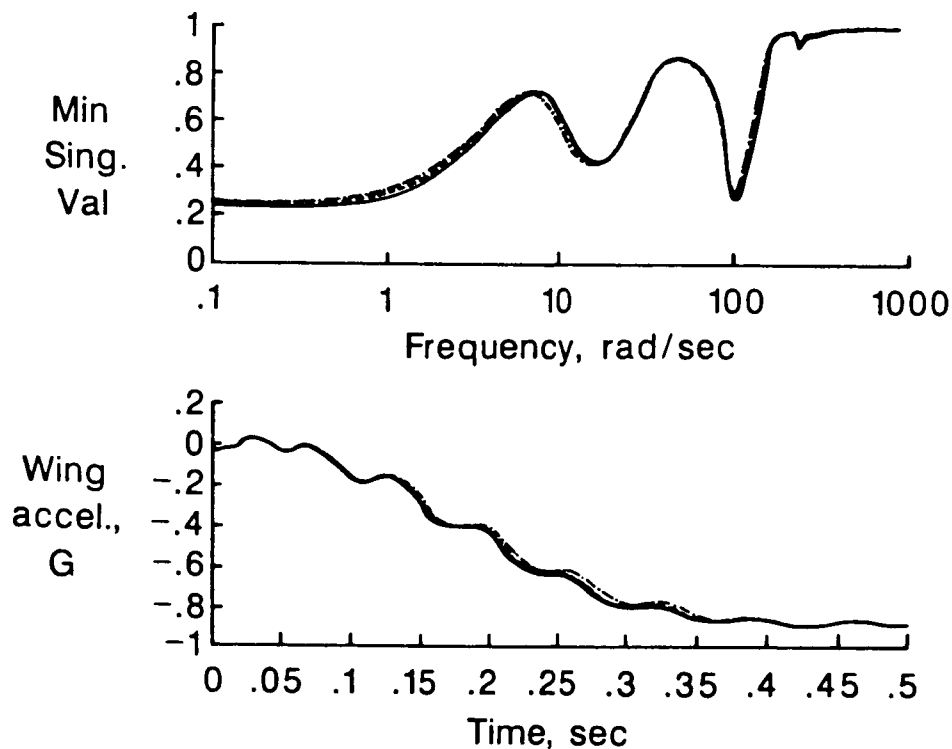
COMPARISON OF PREDICTED AND ACTUAL CHANGES

Numerical results have been calculated for an integrated design study of the DAST ARW-II flight test vehicle. This application involved the design of an optimal LQG control law and the prediction of changes in the optimally controlled response of the vehicle due to changes in a structural design parameter, in this case first wing bending natural frequency. For example, changes in mean square wing tip acceleration and mean square aileron deflection rate due to changes in wing first bending frequency for a 12 ft/sec RMS random wind gust environment are shown below. The sensitivities of the mean square responses to the structural parameter are the slopes of the solid and dashed lines, with the lines themselves showing the predicted change in performance if a new optimal control law was implemented for various changes in the parameter. The symbols show the actual change in performance which occurred when the parameter was varied and the resulting new optimal control law was computed and implemented. For $\pm 10\%$ variations in the wing first bending frequency the sensitivity based predictions were reasonably accurate. For larger variations, the predictions were not as accurate, although the trends were correct. Note that for reductions in wing first bending frequency, both the acceleration and the control surface deflection rate were reduced, whereas if changes were made only in the control law, the acceleration could only be reduced at the expense of increased aileron deflection rate. This indicates the potential benefit of an integrated structure/control law design approach to improved system performance.



WING BENDING FREQUENCY VARIATIONS

Shown are two controlled system performance measure changes due to changes in wing first bending frequency. The top plot is of changes in the minimum singular value of the loop return difference matrix with the control loops broken at the input to the system. This measure is an indication of the stability robustness of the system with respect to gain and phase variations and unmodelled higher order dynamics, with larger values over the frequency range implying greater robustness. For reductions of 10% and 25% in the wing first bending natural frequency, there is a slight rise in the minimum singular value at the critical low regions between .1 and 1 rad/sec and again near 100 rad/sec. The lower plot shows wing tip acceleration in g's due to a commanded pitch over of the vehicle. For 10% and 25% reductions of nominal wing bending frequency there is a small reduction in transient wing tip acceleration response to the same maneuver, although the steady-state acceleration is the same. These results again indicate the possibility for improvements in overall system performance due to integrated structure/control law design, although other structural parameters may provide more significant changes in performance and thus be more useful from a design standpoint.



CONCLUSIONS AND FUTURE RESEARCH

An approach to parallel integrated interdisciplinary design using hierarchical decompositions and sensitivity of optimum solution concepts is under development at NASA-Langley Research Center. An implementation of this approach for integrated structure/control law design problems of aeroservoelastic aircraft is currently under way, and numerical results for an example problem indicate that an integrated design could lead to better overall system performance. The development and implementation of the methodology have also shown that sensitivity of optimum solutions to problem parameters is required for accurate gradient information at the top (system) level when the parallel disciplinary design approaches are optimization based, and that accurate predictions of performance changes due to reasonable (+ or - 10%) variations in parameters are obtained from the optimum sensitivity results. The continuing research program is working toward the inclusion of more formal structural optimization techniques, and to the development of sensitivity expressions for other, more realistic, optimal control law problem formulations.

- Sensitivity of Optimum Analysis Required When Design Iterations Use Optimization
- Performance Changes Accurately Predicted For Reasonable Parameter Variations
- Overall System Performance Can Be Improved By Parallel Intergrated Design
- Need To Develop Analytical Sensitivity Expressions For More Optimal Control Problems
- Need To Exercise Parallel Design Methodology Fully

REFERENCES

- [1] Sobieszczanski-Sobieski, J., "A Linear Decomposition Method for Large Optimization Problems - A Blueprint for Development", NASA TM-83248, Feb. 1982.
- [2] Mesarovic, M. D., Macko, D., and Takahara, Y., "Theory of Hierarchical, Multilevel, Systems", Academic Press, 1970.
- [3] Sobieszczanski-Sobieski, J., Barthelemy, J. F., and Riley, K. M., "Sensitivity of Optimum Solutions of Problem Parameters", AIAA Journal, Vol. 20, No. 9, pg. 1291-1299.
- [4] Kwakernaak, H., and Sivan, R., "Linear Optimal Control Systems", Wiley-Interscience, 1972.
- [5] Bryson, A. E., and Ho, Y. C., "Applied Optimal Control", Halstead Press, 1975.
- [6] Nelson, R. B., "Simplified Calculations of Eigenvector Derivatives", AIAA Journal, Vol. 14, No. 9, pg. 1201-1205
- [7] Frank, P. M., "Introduction to System Sensitivity Theory", Academic Press, 1978.
- [8] Schaecter, D. B., "Closed-Loop Control Performance Sensitivity to Parameter Variations", Journal of Guidance, Control, and Dynamics, Vol. 6, No. 5, pg. 399-402.
- [9] Newsom, J. R., and Mukhopadhyay, V., "The Use of Singular Value Gradients and Optimization Techniques to Design Robust Controllers for Multiloop Systems", AIAA 83-2121, AIAA Guidance and Control Conference, August 1983.

THE CASE FOR AERODYNAMIC SENSITIVITY ANALYSIS

Jaroslav Sobieszczanski-Sobieski
NASA Langley Research Center
Hampton, Va

This paper is somewhat unusual since it does not offer any specific solutions, verified by applications, for its subject problem which is sensitivity analysis in Computational Fluid Dynamics (CFD). Instead, the paper makes a plea to the CFD community for extending their present capability to include sensitivity analysis. The plea is made from the viewpoint of an aeronautical engineer, not an expert in CFD methods, who needs the sensitivity information when working at the junction of aerodynamics, structures, active controls, and other disciplines whose inputs need to be integrated in aircraft design. The principal message of the paper is displayed on figure 1.

THE MESSAGE

- Computational fluid mechanics is advancing rapidly its capability to calculate aerodynamic forces on wing-body-nacelle-empennage configurations
- Next logical step: capability to compute sensitivity of these forces to configuration geometry, i.e., sensitivity derivatives
- Example: $\partial(\text{lift})/\partial(\text{wing sweep angle})$
- Urgent need:
 - Intradisciplinary: aerodynamic shape optimization
 - Interdisciplinary: integrating aerodynamics with other disciplines

Fig. 1

PRECEDING PAGE BLANK NOT FILMED

The intradisciplinary applications of the postulated sensitivity analysis are obvious enough. It has now become quite common to optimize aerodynamic shapes (illustrated at the bottom of figure 2 by the inset showing an airfoil and an aircraft planform) by formal algorithms that iteratively change geometrical variables shown in the inset. Figure 2 depicts one such procedure composed of an OPTIMIZER which determines the increment of each geometrical variable (design variable, x), TERMINATOR containing a logic for stopping the iteration, and ANALYZER (a CFD program) whose task is to calculate the aerodynamic objective function (F) and constraints (g) for the geometry modified by the optimizer. Since most of the OPTIMIZER algorithms commonly in use require derivatives of F and g with respect to the design variables (x), it would be advantageous for the efficiency and accuracy of the aerodynamic optimization, if these derivatives were available in the ANALYZER's output. Thus, the need for a finite difference approximation to the derivatives, and the associated, costly, repetitive analysis would be eliminated.

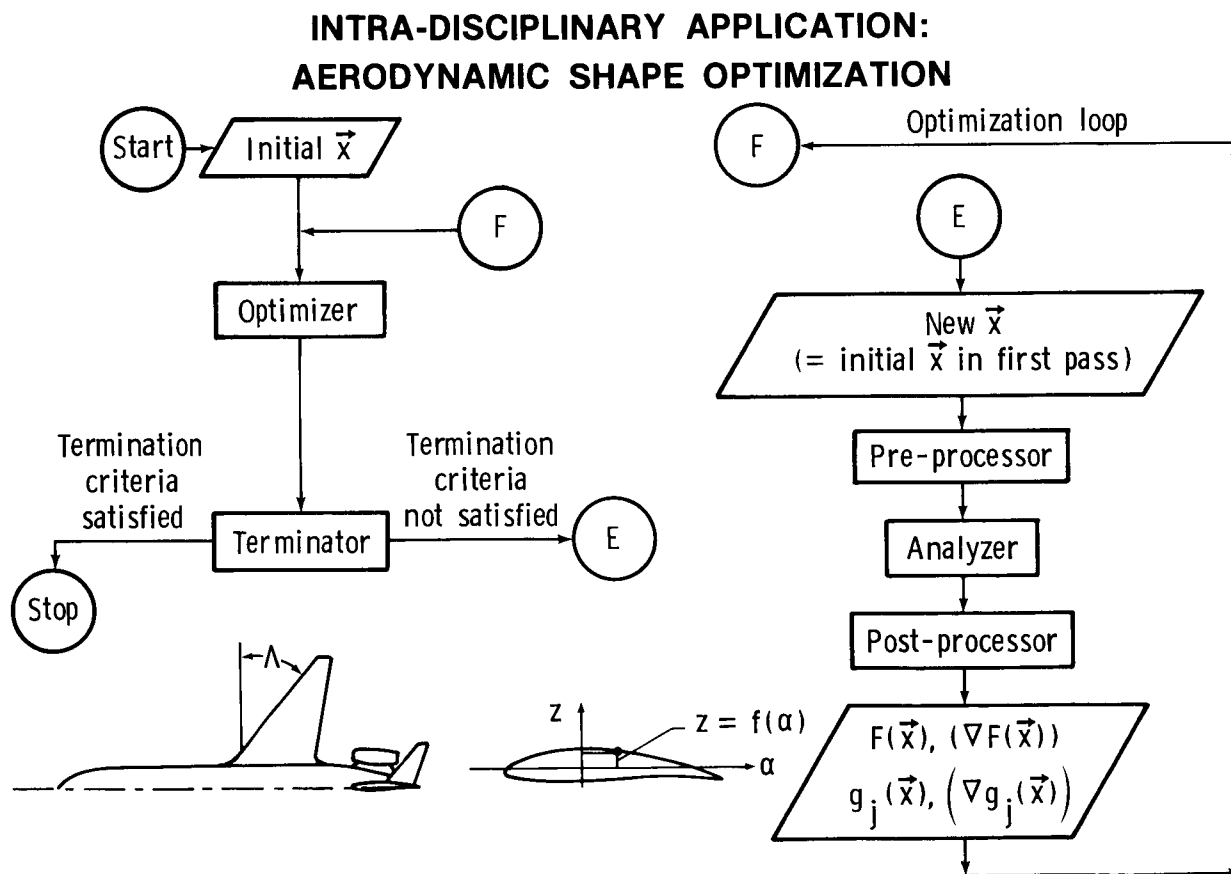


Fig. 2

Going beyond the confines of the discipline of aerodynamics, the aerodynamic sensitivity information is needed to quantify the effect of the changes in aerodynamic shape on other disciplines coupled to aerodynamics in the design process. Figure 3 shows aerodynamics at a central position in the process, its interactions with other disciplines depicted by two-headed arrows. The meaning of the arrows may be illustrated by an example of a coupling between the aerodynamics and structures. A change of the aerodynamic shape causes a change in the structural response, directly through the geometry and, indirectly, through the aerodynamic loads. In the opposite direction, the change in structural response will, of course, influence the aerodynamic loads through the change of deformation pattern.

To stay within a limited scope, the remainder of this discussion will concentrate on the interaction among only three disciplines: aircraft performance, aerodynamics, and structures, to show how the sensitivity information, including the aerodynamic sensitivity, could be used toward improving aircraft performance.

AERODYNAMICS INTERACTION WITH OTHER DISCIPLINES IN AIRCRAFT DESIGN

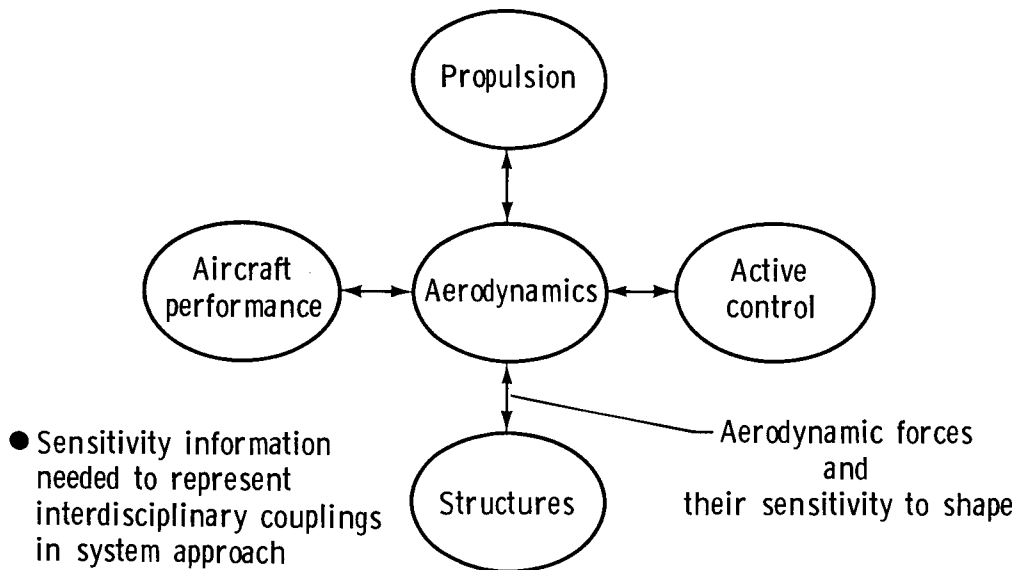


Fig. 3

To demonstrate that, figure 4 and the next two figures show what may happen when a problem encountered in one subsystem, or engineering discipline, is fixed by the means local to that subsystem or discipline. An example of a particular stage in the process of aircraft design will illustrate the point. Suppose that at that stage, the configuration designers had already set the value of the aspect ratio (AR), a typical configuration design variable, so as to maximize the aircraft range (R) under the constraint on the take-off gross weight (TOGW or T). In that decision, they accounted for the influence of the aerodynamic drag, represented by c_D , fuel weight W_f , and structural weight, W_s on R and TOGW. Of course, many more variables are involved in the real problem, but simplification of the example will help to make the point.

In the above set of quantities, c_D and W_f came from the analysis and experimentation carried out by the group of engineers working with the configuration and performance aerodynamics. In contrast, the value of structural weight was available to that group only as a rough estimate. Now, suppose that the process moves on into the phase of more detailed structural analysis and design.

A CONVENTIONAL APPROACH: LOCAL PROBLEM — LOCAL FIX

$$\text{Aircraft: Range } R = f_1(W_s, c_D, \dots) \quad (1)$$

R is objective function, $R \rightarrow R_{\max}$

W_s — structural weight

Constraint:

$$\text{TOGW: } T = f_2(W_s, W_f, \dots) \leq T_0 \quad (2)$$

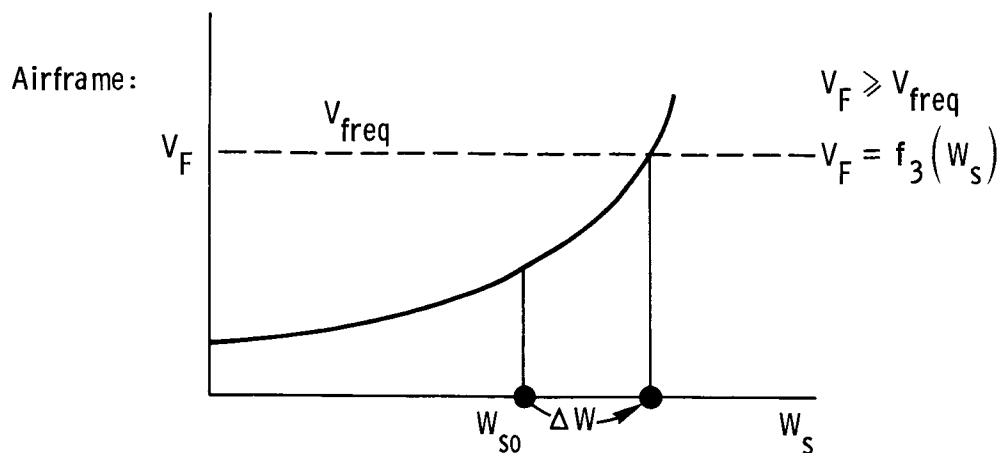
W_f — fuel weight

f_1, f_2 — computable functions, may be analytical expressions or computer programs

Fig. 4

At that stage, illustrated by figure 5 below, structural design has advanced to the point where a flutter analysis was carried out. Let us assume that it showed the flutter speed V_F falling short of the required value V_{freq} . With the wing geometry (AR) having been already set and frozen, the structural group fixed the flutter problem by stiffening the wing at the weight penalty made as small as possible, ΔW_{min} .

LOCAL PROBLEM, FLUTTER, FIXED BY A LOCAL MEANS A STRUCTURAL STIFFENING



Aeroelastic optimization: $\Delta W \rightarrow \Delta W_{min}$

ΔW — weight penalty

Fig. 5

The flutter weight penalty was sent back to the aircraft performance group who added it to the initial estimate of W_s and had to compensate for it by reducing the fuel weight W_f to keep TOGW within constraint (assuming constant payload). The result is a change in performance (R) estimated by eqs. 1 and 2 in figure 6.

GLOBAL (SYSTEM) CONSEQUENCES OF LOCAL FIX

Aircraft: $W_s \rightarrow W_s + \Delta W_{\min}$ requires reduced

fuel $W_f \rightarrow W_f - \Delta W_f$ because of

constrained TOGW,

$$T = f_2(W_s, W_f, \dots) = T_0, \text{ hence}$$

$$\text{Range reduction: } R = R_0 + \frac{\partial R}{\partial W_f} \cdot \Delta W_f \quad \text{to the first order approximation} \quad (1)$$

$$\text{Since } \Delta W_f = -\Delta W_{\min}$$

$$R = R_0 + \frac{\partial R}{\partial W_s} \cdot \Delta W_{\min} \quad (2)$$

Fig. 6

Examination of the example unfolded thus far leads to the two observations, shown in figure 7, that summarize what may happen when a local problem is fixed by local means, but has an impact on the system performance.

TWO OBSERVATIONS

1. $\partial R / \partial W_s < 0$ (of course), hence $R \rightarrow R - \Delta R$. $(-\Delta R)$ is the system performance penalty for a subsystem modification.
2. The system configuration was not touched. The constraint (flutter) was satisfied by purely local, subsystem, means. Since $\Delta W = \Delta W_{\min}$, the system performance penalty is the smallest achievable by the local means. To reduce it further, one needs modification at system level.

Fig. 7

This, and the next three figures, will show the potential for improving the system performance by correcting the subsystem problem by design modifications at both the local and system levels - a system approach. In our example, that means unfreezing the configuration geometry (AR) and using it together with added structural material ΔW_{\min} to meet the flutter constraint, while reducing the penalty in the system performance (R) subjected to the constraint on TOGW.

The upper box in figure 8 symbolizes the performance and configuration aerodynamics group who sends the data on geometry (AR) and on the aerodynamic loads magnitude and distribution $c_p(\alpha, \beta)$ to the structures group depicted by the lower box. The former group's objective is to maximize R under the constraint on TOGW by means of changing the configuration geometry AR. The latter group manipulates the structural cross-section dimensions to meet the flutter constraint at the minimum weight penalty. That penalty is a computable function of the geometry, (AR), and aerodynamic loads, c_p (the next to the last line on the figure). To the structures group these quantities are constants, but the configuration group can control them by means of AR, thus influencing the ΔW_{\min} . That influence can be quantified by the chain differentiation shown on the bottom line on the figure.

In that line, the derivatives of f_4 are derivatives of the optimum design with respect to the constant parameters of the optimization - a type of constrained derivative. Algorithms exist (refs. 1 and 2) for computing such derivatives quasi-analytically, without engaging in repeated optimization of perturbed geometry. The derivative of c_p is a CFD sensitivity derivative postulated in this presentation.

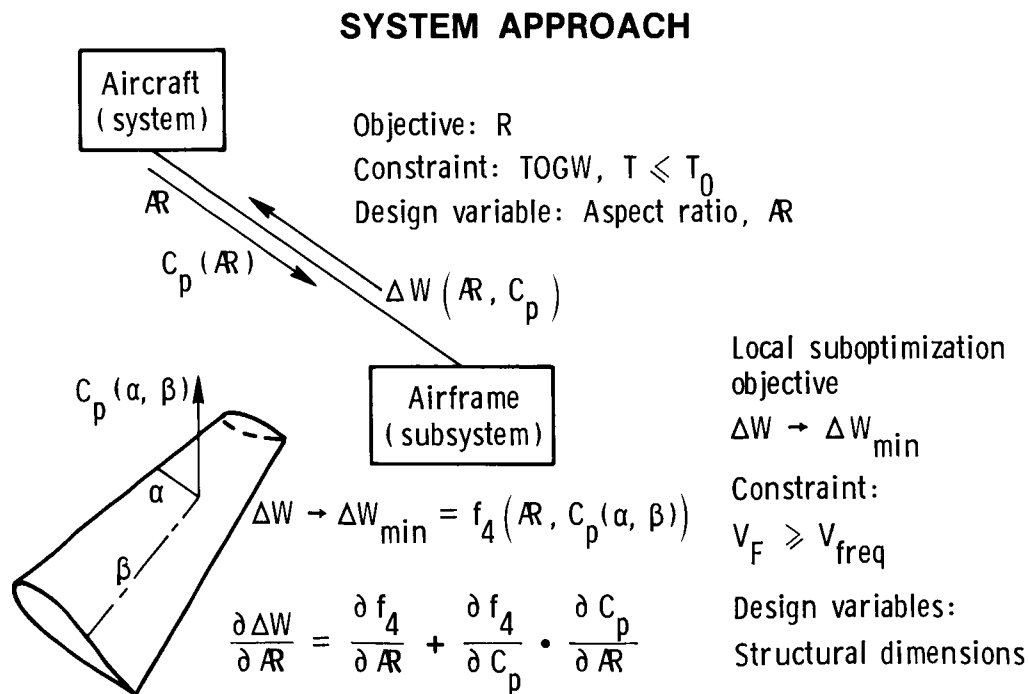


Fig. 8

Here, we return to the system level with the information generated in the discipline of structures. Under the system approach, the information has been enhanced by the sensitivity of the flutter weight penalty to geometry, quantified by the derivative of ΔW_{\min} with respect to AR. The information now available to the performance and configuration group, and originating in that group's own work, is shown on line 1, figure 9 (subscript/superscript "0" refers to the design that has been accomplished and is now to be modified). The first two derivatives are computable from the performance analysis, and the third one was discussed at the end of the preceding figure. The chain differentiation relates the range to geometry.

The extrapolation in eq. 2 using the optimum sensitivity derivative for ΔW_{\min} with respect to AR establishes an approximation to the flutter weight penalty as a function of geometry. Substitutions shown by arrows into the linear extrapolation for R in eq. 3 lead to the approximation of R as a function of geometry in eq. 4. The first two terms represent the result obtained previously under the rule of frozen AR. The square parentheses term reflects the cumulative, first order effect of geometry on performance, exerted through a multitude of interdisciplinary effects, each quantified by a particular term in the parentheses.

SYSTEM SENSITIVITY AND OPTIMIZATION: OBJECTIVE

$$R_0, \frac{\partial R}{\partial \Delta W}, \frac{\partial R}{\partial C_D}, \frac{\partial C_D}{\partial AR}; \frac{\partial R}{\partial AR} = \frac{\partial R}{\partial C_D} \cdot \frac{\partial C_D}{\partial AR} \quad (1)$$

Approximate:

$$\Delta W_{\min} = \Delta W_{\min}^0 + \frac{\partial \Delta W_{\min}}{\partial AR} \cdot \Delta AR \quad (2)$$

$$R = R_0 + \frac{\partial R}{\partial (\Delta W)} \cdot \Delta W_{\min} + \frac{\partial R}{\partial AR} \Delta AR \quad (3)$$

$$R = R_0 + \frac{\partial R}{\partial (\Delta W)} \Delta W_{\min}^0 + \left[\frac{\partial R}{\partial (\Delta W)} \cdot \frac{\partial (\Delta W_{\min})}{\partial AR} + \frac{\partial R}{\partial (\Delta W_{\min})} \frac{\partial (\Delta W_{\min})}{\partial C_p} \cdot \frac{\partial C_p}{\partial AR} + \frac{\partial R}{\partial C_D} \cdot \frac{\partial C_D}{\partial AR} \right] \cdot \Delta AR \quad (4)$$

Fig. 9

A similar development is shown in figure 10 for the system level constraint on TOGW leading to a linear approximation in of the constraint as a function of geometry in eq. 4. Again, the terms in eq.4 quantify the several, interdisciplinary influences involved.

$$\text{TOGW, } T \leq T_0; \frac{\partial T}{\partial (\Delta W)}, \frac{\partial T}{\partial (W_f)}, \frac{\partial W_f}{\partial C_D}, \frac{\partial C_D}{\partial R}; \quad (1)$$

Approximate:

$$T = T_0 + \frac{\partial T}{\partial (\Delta W)} \cdot \Delta W_{\min} + \frac{\partial T}{\partial W_f} \cdot \frac{\partial W_f}{\partial C_D} \cdot \frac{\partial C_D}{\partial R} \cdot \Delta R \quad (2)$$

$$\Delta W_{\min} = \Delta W_{\min}^0 + \frac{\partial \Delta W_{\min}}{\partial R} \cdot \Delta R \quad (3)$$

↑ From optimum sensitivity analysis

$$T = T_0 + \frac{\partial T \cdot \Delta W_{\min}^0}{\partial (\Delta W_{\min})} + \left[\frac{\partial T}{\partial (\Delta W_{\min})} \cdot \left(\frac{\partial (\Delta W_{\min})}{\partial R} + \frac{\partial (\Delta W_{\min})}{\partial C_p} \cdot \frac{\partial C_p}{\partial R} \right) + \frac{\partial T}{\partial W_f} \cdot \frac{\partial W_f}{\partial C_D} \cdot \frac{\partial C_D}{\partial R} \right] \cdot \Delta R \leq T_0 \quad (4)$$

Fig. 10

Derivation of R and T as approximate functions of geometry (bottom line equations in fig. 9 and 10) enables the configuration group to modify the geometry (AR) toward better performance (R). When modifying AR, the group is assured that the flutter constraint will be kept satisfied to the first order of accuracy, because the flutter weight penalty will follow the change of AR in a way prescribed by eq. 2, figure 9. The change of AR may be obtained formally by solving an optimization problem defined by eqs. 1 and 2, figure 11. The resulting performance improvement over the previous case of the frozen AR is shown by the last term in eq. 4. The improvement comes about because we traded structural weight and aerodynamic drag for each other while modifying the geometry (a typical design trade-off), and we did it in a measured way on the basis of the sensitivity derivatives.

SYSTEM SENSITIVITY AND OPTIMIZATION

Conclusion

Find ΔR , such that

$$R = R_0 + \frac{\partial R}{\partial (\Delta W)} \cdot \Delta W_{\min}^0 + \frac{\partial R}{\partial AR} \cdot \Delta AR \rightarrow \max \quad (1)$$

Subject to

$$T = T_0 + \frac{\partial T}{\partial (\Delta W_{\min})} \cdot \Delta W_{\min}^0 + \frac{\partial T}{\partial AR} \cdot \Delta AR \leq T_0 \quad (2)$$

Obtain $(\Delta AR)_{\text{opt}}$ from 1 and 2, to get R_{\max} :

$$R_{\max} = R_0 + \frac{\partial R}{\partial (\Delta W)} \cdot \Delta W_{\min}^0 + \frac{\partial R}{\partial AR} \cdot \Delta AR \quad (3)$$

$$R_{\max} = \underbrace{R_0 - \Delta R}_{\text{Obtained previously}} + \underbrace{\frac{\partial R}{\partial AR} \cdot \Delta AR}_{\text{Additional term}} \quad (4)$$

Fig. 11

The sensitivity of R to geometry represented by the derivative in the last term on the preceding figure is the key piece of information necessary to reduce the system performance penalty paid for the fix of the subsystem problem (flutter). The expression for the derivative is reproduced in figure 12 (see eq. 4, figure 9), with the source of each partial identified by a letter code inscribed beneath.

DISCUSSION OF THE OPTIMAL SOLUTION

Total chain-derivative expression for $\partial R / \partial \mathcal{R}$ is:

$$\frac{\partial R}{\partial \mathcal{R}} = \underbrace{\frac{\partial R}{\partial (\Delta W)}}_P \cdot \underbrace{\frac{\partial (\Delta W_{\min})}{\partial \mathcal{R}}}_S + \underbrace{\frac{\partial R}{\partial (\Delta W_{\min})}}_P \cdot \underbrace{\frac{\partial (\Delta W_{\min})}{\partial C_p}}_{ASF} \cdot \underbrace{\frac{\partial C_p}{\partial \mathcal{R}}}_A + \underbrace{\frac{\partial R}{\partial C_D}}_P \cdot \underbrace{\frac{\partial C_D}{\partial \mathcal{R}}}_A$$

U
ST

- Existence of the additional term in equation for R_{\max} allows to recover a part of the performance penalty —
- Sources of derivatives: P - performance, S - structures, ASF - aeroelasticity and flutter, A - aerodynamics, ST - steady, U - unsteady

Fig. 12

Before we take a closer look at availability of the derivatives at the appropriate sources, let us devote one figure (fig. 13) to address the obvious question that arises at this point: "Why not to get whatever derivatives are needed by a straightforward finite difference technique ?". To supplement the figure, let us assure the reader that we do not dogmatically favor the quasi-analytical way over the finite difference way of computing the derivatives. If someone overcomes the computational cost impediment in a finite difference technique built on top of a CFD analysis - the resulting tool will certainly be eagerly accepted. However, the point is that a quasi-analytical alternative to finite difference techniques exists, and due to experience garnered in other disciplines it deserves a serious consideration. We will come back to this point again, soon after we examine, briefly, the derivative availability under the state of the art.

SENSITIVITY DERIVATIVES BY FINITE DIFFERENCE?

- For N variables, the simplest finite difference technique requires, at least, $N + 1$ repetitions of analysis
- In real world of engineering design, that erects a time n and cost barrier
- Experience from other engineering disciplines suggests an alternative: quasi-analytical algorithms
- Only one paper in this symposium program refers to aerodynamic sensitivity analysis — that fact is symptomatic for the state of the art in CFD

Fig. 13

Although it is quite clear where each derivative should originate, the availability is distributed very unevenly, as shown in figure 14. Most of the pertinent capability exists in structures for derivatives with respect to cross-sectional dimensions and overall shape (see survey in ref. 3). Some of that capability became available in production level codes. In aeroelasticity, algorithms exist for computation of the flutter velocity derivatives with respect to the cross-sectional dimensions (ref. 4), but not with respect to the overall shape variables. Unfortunately, to the best of available information, sensitivity analysis in CFD is currently limited to the capability described in ref. 5 that applies only to linear subsonic aerodynamics.

AVAILABILITY OF DERIVATIVES

- Performance: Finite difference is inexpensive
- Structures: Analytical derivatives available in production codes
(e. g., NASTRAN)
- Aeroelasticity
and flutter: Analytical derivatives of V_F available
- Aerodynamics: A beginning made in steady, subsonic, NASA CR 3713,
1983 (Bristow, MCDAC)
 - Nothing in transonic
 - Nothing in supersonic
 } Steady
 - Nothing in unsteady
 - Nothing in production level codes

Fig. 14

Let us contrast, in figure 15, the finite difference technique with a quasi-analytical manner of computing the derivatives. Both techniques apply to a set of equations that, in general, govern a physical problem (this is a generic discussion, not limited to aerodynamics). The set of equations appears as the topmost equation on the figure, with y denoting the vector of solution variables (behavior variables), and x standing for a vector of design variables that are constant in the process of solving the equations F , but may vary in the associated design (optimization) problem.

The computational cost of the finite difference approach (line 1) was noted before. That cost may be avoided by means of a quasi-analytical approach described by line 2. It begins with setting to zero the first variation of F with respect to perturbation of an element of the vector x , and leads to a universal sensitivity equation (eq. 2). That equation can be directly solved to obtain the vector of derivatives which, in effect, relate change of the output (y) of the solution of the governing equations ($F(y,x) = 0$) to the input (x). Three comments on the nature of the sensitivity equation (eq.2) are noted at the bottom of the figure. Appendix A provides a self-contained elaboration on the generic quasi-analytical approach, and Appendix B illustrates that approach in linear static structural analysis.

ANALYTICAL DERIVATIVES VERSUS FINITE DIFFERENCES

$F(y,x) = 0, \rightarrow y; y = y(x)$ implicitly

e.g., $y = C_p$ (location), $x = AR$, $F(\)$ — an algorithm

$$1. \text{ Finite difference: } x \rightarrow x + \Delta x \rightarrow F(y,x) \rightarrow y + \Delta y; \quad \frac{\partial y}{\partial x} \cong \frac{\Delta y}{\Delta x} \quad (1)$$

$N + 1$ times for N x 's

$$2. \text{ Analytical: } \frac{\partial}{\partial x} (F(y,x)) = 0 \rightarrow \frac{\partial F}{\partial y} \cdot \frac{\partial y}{\partial x} = - \frac{\partial F}{\partial x} \quad (2)$$

- Eq. 2 is linear with respect to $\partial y / \partial x$, even though $F(y,x)$ may be nonlinear
- Eq. 2 is noniterative, even if $F(y,x) = 0$ is iterative
- In eq. 2, $\partial F / \partial y$ and $\partial F / \partial x$ obtainable either analytically or by finite difference, then $F(y,x)$ is evaluated, rather than solved $F(y,x) = 0$

Fig. 15

The conclusion we are now arriving at is that demonstratable improvements in aircraft performance are achievable by including interdisciplinary interactions in the configuration shaping decisions. Much of the potential for these improvements remains either unused, or its exploitation is being achieved at an excessive computational cost because of the lack of sensitivity analysis capability in CFD. The postulated remedy is development of a capability for computation of derivatives with respect to shape as a routinely available option in the CFD codes. Hence, the challenge to the CFD community posed in figure 16 closes this paper.

A CHALLENGE FOR COMPUTATIONAL AERODYNAMICS COMMUNITY

- Derivatives of: $C_p(x,y)$, C_D , C_L , C_M
- With respect to: Configuration variables,
e. g. , Aspect ratio
Sweep angle
Taper
Airfoil shape
Camber . . .
Twist, etc. . . .
- For sub-, tran-, supersonic, steady, unsteady wing + full configuration
- Basic formulation + production codes

Fig. 16

REFERENCES

1. Sobieszczanski-Sobieski, J.; Barthelemy, J.-F. M.; and Riley, M. F.: Sensitivity of Optimum Solutions to Problem Parameters. AIAA Paper No. 81-0548R. AIAA Journal, Vol. 20, No. 9, September 1982, pp. 1291-1299.
2. Barthelemy, J.-F. M.; and Sobieszczanski-Sobieski, J.: Optimum Sensitivity Derivatives of Objective Functions in Nonlinear Programming. AIAA Journal, Vol. 21, No. 6, June 1983, pp. 913-915.
3. Adelman, Howard M.; and Haftka, Raphael T.: Sensitivity Analysis and Discrete Structural Systems. AIAA Journal, Vol. 24, No. 5, May 1986, pp. 823-832.
4. Rudisill, C. S.; and Bhatia, K. G.: Second Derivatives of the Flutter Velocity and the Optimization of Aircraft Structures. AIAA Journal, Vol. 10, 1972, pp. 1569-1572.
5. Bristow, D. R.; and Hawk, J. D.: Subsonic Panel Method for Designing Wing Surfaces from Pressure Distributions. NASA CR-3713, 1983.

APPENDIX A

GENERAL EQUATION FOR SENSITIVITY

This Appendix is a self-contained tutorial on sensitivity analysis arising in a generic problem whose governing equations are given. Let

$$F(y,x) = 0 \quad (1)$$

represent governing equations of a problem in which y is a vector of unknowns to be obtained by solving eq. 1, and x is a vector of given constants. The quantities y and x may be vectors, and F may be a vector of functions. If y is a vector, eq. 1 implies a set of equations whose number is equal to the length of vector y ; however, the x vector may be shorter than y . Existence of the solution of eq. 1 makes, implicitly, $y = f(x)$. The functions F may be anything computable: linear algebraical equations, PD equations, integral equations, or integral-differential equations, transcendental functions, etc. It may be nonlinear, and may require an iterative method for solution of eq. 1.

If eq. 1 governs a physical system being designed, then the designer wants to know not only the y for a given x , but also the sensitivity of y to those x -quantities that he controls as design variables. For instance, $F(y,x)$ might be the Euler equations from which to compute y - the pressure distribution on a body in airflow, and x might be the body geometry variables. The designer of the body shape needs to know $\partial y/\partial x$.

One way to obtain $\partial y/\partial x$ is by finite differences. This requires solving eq. 1 for given x to obtain y . Then assume, for one element of x , a perturbation $x + \Delta x$, and repeat solution of eq. 1 to get $y + \Delta y$. Approximation to $\partial y/\partial x$ is

$$\partial y/\partial x = \Delta y/\Delta x; \quad (2)$$

This operation must be repeated for all x -quantities of interest and may be prohibitively computer-intensive, if eq. 1 is expensive to solve. In addition, the accuracy of $\partial y/\partial x$ will depend on the proper choice of Δx .

An alternative is a quasi-analytical approach. It is called "quasi-" because the $y(x)$ is known only numerically. However, we know that for Δx , we must have

$$F(y+\Delta y, x+\Delta x) = 0; \quad (3)$$

in other words, increase of x must be compensated for by change in y to preserve the zero value of F . Hence, recognizing that the total derivative (TD) of F with respect to x is according to the textbook rules of differentiation for implicit functions

$$dF/dx = \partial F/\partial x + \partial F/\partial y \partial y/\partial x; \quad (4)$$

eq. 3 will be satisfied if

$$dF/dx \Delta x = 0 \quad (5)$$

Substituting eq. 4 into 5, and rearranging, yield

$$\partial F / \partial y \partial y / \partial x = - \partial F / \partial x \quad (6)$$

Eq. 6 is a general sensitivity equation in which the desired sensitivity appears directly as the unknown $\partial y / \partial x$. For vector y of length n , the term $\partial F / \partial y$ is a matrix $n * n$ whose each column is a vector of gradients with respect to y (a Jacobian matrix), the term $\partial y / \partial x$ is a vector of unknown derivatives of y with respect to one particular x variable, and the term $\partial F / \partial x$ is a vector of derivatives with respect to the same particular variable x . Computation of the derivatives of y with respect to several variables x requires solutions of eq. 6 with many right hand sides - one per each variable x . Since the Jacobian matrix remains the same for all variables x , a solution algorithm arranged so as to factor the matrix only once will be preferred for computational economy.

It is important that eq. 6 is simply a set of linear, algebraical equations even though eq.1 may be far more complicated than that. The terms $\partial F / \partial y$ and $\partial F / \partial x$ may still not be obtainable analytically. If so, they can be computed by finite difference, i.e., assuming perturbation $x = x + \Delta x$ and $y = y + \Delta y$ for each element of x and each element of y separately, and substituting into eq. 1, one obtains the respective ΔF values (upon substitution of $x + \Delta x$, or $y + \Delta y$, F in eq. 1 is no longer equal zero, it becomes ΔF) from which the terms $\partial F / \partial y$ and $\partial F / \partial x$ can be computed as in eq. 2.

Computation of the terms $\partial F / \partial y$ and $\partial F / \partial x$ by finite difference is accomplished by repetitive evaluations of $F(y, x)$ for known y and x , as opposed to repetitive solutions of $F(y, x) = 0$ (eq.1) for unknown y required by eq.2. Hence, the quasi-analytical approach is inherently less computer intensive than the finite difference procedure based on eq. 2.

APPENDIX B

Application of the generic, quasi-analytical algorithm for sensitivity derivatives is illustrated with one example from linear, static, structural analysis. The governing equations - the counterpart of $F(y,x) = 0$ - are the load-deflection equations involving a stiffness matrix K , unknown displacements y , and the cross-sectional dimensions x as design variables. The structural sensitivity equation recursively connects to the load-deflection equations through the solution vector y . Since the matrix K has to be factored (decomposed) in the process of solving for y , significant computational economy may be realized by saving the factored matrix and reusing it in the solution of the sensitivity equation.

ANALYTICAL DERIVATIVES IN LINEAR STATIC STRUCTURAL ANALYSIS

Generic	Structural
$F(y,x) = 0; y = y(x)$ $\frac{\partial f}{\partial y} \cdot \frac{\partial y}{\partial x} = -\frac{\partial f}{\partial x}$	$K(x) \cdot y = P(x); y = y(x)$ $K \cdot \frac{\partial y}{\partial x} = -\frac{\partial K}{\partial x} \cdot y + \frac{\partial P}{\partial x}$ <p>y — displacement</p> <p>x — cross-section dimension</p> <p>$\frac{\partial K}{\partial x}, \frac{\partial P}{\partial x}$ Analytically or by finite differences</p>

SENSITIVITY OF OVERALL VEHICLE STIFFNESS
TO LOCAL JOINT STIFFNESS

Choon T. Chon
Vehicle Methods and Components Department
Engineering and Manufacturing Staff
Ford Motor Company
Dearborn, Michigan

SUMMARY

The present paper discusses how overall vehicle stiffness is affected by local joint stiffness. By using the principle of virtual work and the minimum strain energy theorem, a closed form expression for the sensitivity coefficient has been derived. The insensitivity of the vehicle stiffness to a particular joint, when its stiffness exceeds a certain value (or threshold value), has been proved mathematically. In order to investigate the sensitivity of the structure to the joint stiffness, a so-called "stick" model has been created, and the modeling technique is briefly described. Some data on joint stiffness of tested vehicles are also presented.

INTRODUCTION

Over the years, the study of the joint behavior of vehicle structures has been identified as one of the most important subjects in the automotive industry. It is widely known that the flexibility of structural joints can affect not only the NVH (Noise, Vibration and Harshness) characteristics of the vehicle, but also other vital structural performance characteristics under various loading conditions (e.g. crash loads, road loads, jacking load, towing load, etc.).

The first study which accounted for the effect of flexible joints on automotive structural responses was by Chang [1] who used a two-dimensional frame model for a static analysis. He found that the structural response is far more sensitive to reducing joint stiffnesses (relative to the baseline values) than to increasing them. Recently a similar phenomenon was reported by Du and Chon [2], and it was claimed that there might exist a threshold stiffness value in a given joint of a vehicle structure. In other words, if a joint stiffness exceeds the threshold value, then the overall stiffness of the structure becomes insensitive to the particular joint.

The objective of the present paper is to demonstrate this phenomenon theoretically by showing that the derivative of the total strain energy with respect to a particular joint stiffness decreases and becomes zero as the joint stiffness approaches infinity. It should be noted that under the same loading and boundary conditions, the structure which contains higher strain energy is less stiff than the structure with lower strain energy. In this paper, a closed form expression for the sensitivity coefficient has been derived, using the principle of minimum strain energy and the principle of virtual work. In order to investigate the sensitivity of the structure to joint stiffness, a so-called "stick" model has been created, and the modeling technique is described. The last section discusses joint behavior, in general, by comparing the analytical results with test data. Discussion of other component behavior is also given based on the sensitivity coefficients derived in the paper.

SYMBOLS

P_i	generalized force vector
Q_j	generalized stress vector
u_i	generalized displacement vector
q_j	generalized strain vector
S	surface of the structure
S_p	surface where the force vector, p_i , is prescribed
S_u	surface where the displacement vector, u_i , is prescribed
D_{jk}	compliance matrix
U	total strain energy
Q_j^w	free component of Q_j
Q^r	reactant component of Q_j
N_r	total number of redundancies
b_m	m -th parameter
N_b	total number of parameters
n_l	vector normal to the boundary surface S as shown in Fig. 1
V_m	volume in which D_{jk} depends on b_m .

U_m	strain energy stored in the volume V_m due to the external loads p_i
J_m	m-th joint stiffness
U_s	total strain energy stored in a "stick" model under prescribed loading conditions
U_{sm}	strain energy stored in the m-th joint under given external loads
N	number of joints
α_p	joint stiffness multiplication factor

BASIC CONCEPTS

This section summarizes the basic concepts of the general sensitivity study reported in Refs. [3.5]. They will then be applied to joint behavior in the later section.

(i) THEORETICAL BACKGROUND - Linearity of the equilibrium and strain-displacement relations will permit the principle of virtual work to be written as:

$$\int_V Q_j q_j^* dV = \int_S p_i u_i^* dS \quad (1)$$

where p_i and Q_j are any statically admissible fields, and u_i^* and q_j^* are any kinematically admissible fields. In the current paper, the body forces are assumed to be negligible. Note that $S = S_p + S_u$ (Fig. 1).

Let the solution of a structural problem for an elastic material be given by u_i , Q_j , and q_j . These quantities constitute, by definition, both a statically admissible field and a kinematically admissible field. In addition, q_j and Q_k satisfy Hooke's law:

$$q_j = D_{jk} Q_k \quad (2)$$

Note that if the deformations are small, the total strain energy stored in the loaded system will be equal to the work done by the applied forces. Thus the

total strain energy U may be expressed in terms of generalized stresses as:

$$U = 1/2 \int_V D_{jk} Q_j Q_k dV \quad (3)$$

Since a structure is, in general, statically indeterminate, one may divide the generalized stress $Q_j(x_l)$ at any point x_l into two parts:

$$Q_j(x_l) = Q_j^w(x_l) + \sum_{r=1}^{N_r} \lambda_j^r(x_l) Q^r \quad (4)$$

where $\lambda_j^r(x_l)$ ($r = 1, \dots, N_r$) are linear functions of x_l . Then substituting Eq. (2) into Eq. (1) and using the principle of virtual work (Eqs. (1) and (4)), one can prove that

$$\frac{\partial U}{\partial Q^r} = \int_V D_{jk} \lambda_j^r Q_k dV = 0 \quad (5)$$

Eq. (5) implies that the quantity U is minimized with respect to the values of each of the redundancies; Eq. (5) thus yields exactly N_r equations from which the values of the redundancies may be found.

(ii) SENSITIVITY ANALYSIS - The objective, then, is to derive a closed form expression for the sensitivity coefficient $\partial U / \partial b_m$. Differentiating the total strain energy, U , which is defined in Eq. (3), with respect to the m -th variable b_m , leads to the following expression:

$$\begin{aligned} \frac{\partial U}{\partial b_m} = & 1/2 \int_S D_{jk} Q_j Q_k \frac{\partial x_l}{\partial b_m} n_l dS + 1/2 \int_V \frac{\partial D_{jk}}{\partial b_m} Q_j Q_k dV \\ & + \int_V D_{jk} \frac{\partial Q_j}{\partial b_m} Q_k dV \end{aligned} \quad (6)$$

Here Eq. (6) may be considered as material derivative of volume integral [6].

Eq. (6) can be greatly simplified, if one chooses certain types of parameters. For example, an appropriate choice of cross-sectional properties (e.g., material property, area, moment of inertia, etc.) of either beam or

plate/shell structures, makes the first term of Eq. (6) identical to zero. And since the free components Q_j^w in Eq. (4) are the solutions of the statically determinate structures, they are independent of cross-sectional properties, which results in:

$$\frac{\partial Q_j}{\partial b_m} = \sum_{r=1}^{N_r} \lambda_j^r \frac{\partial Q^r}{\partial b_m} \quad (7)$$

Then using the minimum strain energy principle (Eq. (5)) and Eq. (7), it can be shown that the last term of Eq. (6) also vanishes. Finally one can rewrite Eq. (6) as:

$$\frac{\partial U}{\partial b_m} = 1/2 \int_{V_m} \frac{\partial D_{jk}}{\partial b_m} Q_j Q_k dV \quad (8)$$

It should be noted that the integration in Eq. (8) need only be performed over the region V_m in which D_{jk} depends on b_m .

In addition, if one can express the compliance tensor D_{jk} as inversely proportional to b_m (i.e., $D_{jk} \propto 1/b_m$) in the region V_m , then Eq. (8) can be further simplified:

$$\frac{\partial U}{\partial b_m} = - \frac{1}{b_m} \left(1/2 \int_{V_m} D_{jk} Q_j Q_k dV \right) = - \frac{U_m}{b_m} \quad (9)$$

VEHICLE STRUCTURAL MODEL

Before proceeding further, it is necessary to describe a vehicle structural model for the purpose of studying the sensitivity of local joint stiffness to the overall structural stiffness.

"STICK" MODEL - A "stick" model has been created according to the concept described in [2] (Fig. 2). This modeling concept is based on the assumption that beams/frames are the primary load carrying members in a structure.

The model consists of 188 grid points and 259 beam elements. Beams are modeled with proper offset vectors, which are often very useful when modeling beams containing eccentricity [7]. Even though there are no shell elements, per

se, several equivalent beam elements are introduced to simulate the sheet metal structures (e.g., floor panel, dashboard, wheel housing, rear quarter panel, etc.). By equivalent beam elements we mean that sectional properties are computed as if panels were beams. The Ford Computer Graphics System is used to create the model. The software for the Ford Graphics System is called PDGS (Product Design Graphics System) which is a general purpose three-dimensional design and drafting system. FAST (Finite element Analysis SysTem), which is embedded in PDGS, can be accessed from the main menu of the PDGS and allows the user to build and modify a finite element model.

TESTS - Bending and torsional tests were performed on the body structure in accordance with the Company Test Procedure. The structure was supported at the center of front and rear wheels. In order to apply the bending load across each seat position (so-called H-point), a heavy beam was laid on three points (on both left and right rocker panels and the middle tunnel) with spacers underneath so that the beam can be levelled with respect to the ground. The beam weighs 4,448.2 N (1,000 lb.). For the torsional test, the applied torque was 3.39×10^6 N-mm (2,500 ft-lb.) at both centers of the front wheels, while the rear wheel axle was supported.

ANALYSES - Elastic analyses under bending and torsional loads were performed using the "stick" model described above with the following boundary conditions and material properties.

Loading (L.C.) and Boundary (B.C.) Conditions :

(a) Static Bending Analysis

L.C. : Unit downward (-z direction) displacements are prescribed at both the right and left rocker panels, and the middle tunnel. This simulates the dead weight applied in the test setup and these points coincide with the H-point of the "stick" model. Since displacements are prescribed instead of forces as the loading condition, reaction forces at the loading points are computed, and the deflections are proportionally adjusted so that the sum of the reaction forces equals 4448.2 N (1000 lbs.).

B.C. : Simply supported at both the front and rear wheel centerlines with one end allowed to move freely in the x-direction.

(b) Static Torsional Analysis

L.C. : Two vertical loads, 4945.0 N (1111.7 lbs.) each, in opposite directions, which are equivalent to 3.39×10^6 N-mm (2500 ft-lb torque) were applied at the centerline of the front wheel axle.

B.C. : Simply supported at the centerline of the rear wheel axle.

Material and Cross-Sectional Properties:

Young's modulus (E) and Poisson's ratio (ν) used in the model are:

$$E = 2.07 \times 10^5 \text{ N/mm}^2 \quad (30.0 \times 10^6 \text{ psi})$$

$$\nu = 0.3$$

ACCURACY OF THE MODEL - In this subsection, the analytical results were compared to the test data to investigate the accuracy of the model.

The overall deformed shapes obtained from the analyses and the tests for both bending and torsion are compared in Figs. 3a and 3b. The dotted and solid lines represent the test data and the analysis results, respectively. The abscissa denotes the x-coordinate of the body structure from the front to the rear wheel axles and thus represents the length of the wheel base. The ordinates denote normalized deflections for the bending analysis and twist angles for the torsional analysis. Note that these values were measured along the bottom rails of the structure in the actual test.

Even though the overall deformed shape from the analysis is in good agreement with that of the test, the analytical and test curves show a slight discrepancy in the rear of the vehicle. This may have resulted from the slight difference in the boundary conditions between the analysis and the test setup. The torsional curve from the analysis gives a good agreement with the test data. It should be noted that the curve obtained from the test data has more local fluctuation in magnitude. Studying the reasons of it is beyond the scope of this report.

A rationale which justifies the concept of a "stick" model approximation for predicting the overall stiffness of a vehicle structure is established in a separate paper*. In this paper, it is shown that the upper bounds as well as the lower bounds of total strain energy are the same for both the vehicle structure and the corresponding "stick" model.

SENSITIVITY STUDY OF JOINTS

Thus far, the basic concept of derivation of the sensitivity coefficients and the concept of the "stick" model approximation have been presented. This section

*Chon, C. T.: "Rationalization of "Stick" Model Approximation," work in progress.

describes the application of the above results to the sensitivity study of joints which affects the overall vehicle stiffness. As mentioned above, it has been analytically and experimentally demonstrated in [1 & 2] that the joint behavior is one of the most important factors for the overall stiffness of the body structure. For the sake of clarity, this section is divided into two subsections: the cases of a single joint and multiple joints.

A SINGLE JOINT - In the model analyzed, the joint which connects the rocker panel and the bottom of the B-pillar (see Fig. 4) was identified as the joint to which the total strain energy was most sensitive. This was done by comparing the amount of strain energy stored in the joints. After introducing a joint magnification factor which was used in [2] (see Fig. 4 for the joint locations), a parametric study of the joint behavior was performed. Fig. 5 shows how the total strain energy of the structure is affected by the joint stiffness of the B-pillar and the rocker panels. Note that the total strain energy becomes insensitive as the joint stiffness becomes large. This phenomenon can be explained using the sensitivity coefficient derived in the previous section (see Eq. (9)) as follows:

Let $b_m = J_m$ and let U_s be the total strain energy stored in the model under the prescribed loading conditions (either bending or torsion). Then Eq. (8) can be rewritten as:

$$\frac{\partial U_s}{\partial J_m} = \frac{1}{2} \int_{V_m} \frac{\partial D_{jk}}{\partial J_m} Q_j Q_k dV \quad (10)$$

Note that integration in Eq. (10) needs only be performed over the volume in which the m-th joint is contained. Moreover, since the compliance tensor D_{jk} is inversely proportional to the m-th joint stiffness, J_m , the final form of Eq. (10) is:

$$\frac{\partial U_s}{\partial J_m} = - \frac{U_{sm}}{J_m} \quad (11)$$

It is very important to note from Eq. (11) that the sensitivity coefficient $\partial U_s / \partial J_m$ goes to zero as the m-th joint stiffness, J_m , approaches infinity. Mathematically one can write this as:

$$\lim_{J_m \rightarrow \infty} \frac{\partial U_s}{\partial J_m} = \lim_{J_m \rightarrow \infty} \left(- \frac{U_{sm}}{J_m} \right) = 0 \quad (12)$$

Eq. (12) proves the phenomenon shown in Fig. 5 for a large value of J_m (see region "C"). In addition, it should be noted that the total strain energy also becomes insensitive to J_m as the magnification factor approaches to zero (see region "A" in Fig. 5). This will be discussed in the next section.

MULTIPLE JOINTS - Eq. (12) can be generalized to compute a derivative of the strain energy with respect to more than one joint stiffness. Given a group of joints which are of interest, the associated joint stiffness multiplier, α_p , is defined as:

$$(J_p, \dots, J_{p+N}) = \alpha_p (J_p, \dots, J_{p+N}) \quad (13)$$

The number of joints, N , in one group can be completely arbitrary. Then Eq. (10) can be modified as:

$$\frac{\partial U_s}{\partial \alpha_p} = \sum_{l=p}^N \left(1/2 \int_{V_l} \frac{\partial D_{jk}}{\partial \alpha_p} Q_j Q_k dV \right) \quad (14)$$

Again since $D_{jk} \propto 1/\alpha_p$, Eq. (14) becomes

$$\frac{\partial U_s}{\partial \alpha_p} = - \frac{1}{\alpha_p} \sum_{l=p}^N \left(1/2 \int_{V_l} D_{jk} Q_j Q_k dV \right) = - \frac{1}{\alpha_p} \sum_{l=p}^N U_l \quad (15)$$

Note that the individual strain energy has to be summed in this case. Therefore one can conclude that the following expression is also true:

$$\lim_{\alpha_p \rightarrow \infty} \frac{\partial U_s}{\partial \alpha_p} = 0 \quad (16)$$

Eq. (15) implies that the strain energy U_s is a hyperbolic function of the multiplication factor of the joint stiffnesses. Fig. 6 shows the total strain energy variation as functions of the multiplication factor, α_p . Again, the total strain energy becomes far less sensitive if α_p exceeds a certain value. This is the proof of the findings reported in Refs. [1] and [2].

DISCUSSION AND CONCLUSIONS

EFFECTS OF A SINGLE JOINT - When a single joint is varied, the overall vehicle stiffness becomes sensitive to the local joint stiffness only within a certain stiffness range (region "B", Fig. 5). In other words, the structure loses sensitivity not only when the magnification factor is small (region "A"), but also when the magnification factor is large (region "C"). The latter case has been proven in the previous section. For an explanation of the former case, one may consider the concept of a "failure mechanism" which has been used extensively in the literature on Limit Analysis [8]. Since the structure can sustain the given load with one or more "yield hinges", as long as the structure does not form a "mechanism", the structure can be said to have a finite stiffness, which is shown in the region "A" of Fig. 5. This means that, even if one removes the particular joint, the structure will still sustain a load within given limits.

EFFECTS OF MULTIPLE JOINTS - In the case of multiple joints, flexible joints have been introduced by adding 24 rotational spring elements at 12 structural joints in the model. The joints added in this fashion are shown in Fig. 4. A joint stiffness magnification factor (see α_p in Eq. (13)) was introduced and a parametric study of the joint behavior was performed. Fig. 6 shows a diagram of the total strain energy of the "stick" model versus the joint stiffness magnification factor for both bending and torsional loading cases. Published values for the joint stiffness obtained from three vehicle tests [9] (see Table 1) were used in the analyses. Table 2 as well as Fig. 6 compares the strain energy of the "stick" model (which has rigid joints) with strain energy computed using those three sets of joint stiffness. It is interesting to note that the strain energy values using the three sets of joint stiffness are all within a range of 3% and that those values, compared with the values of the "stick" model which has rigid joints, differ by a maximum of 11%. This means that the actual values of joint stiffness may be equal to or slightly smaller than the corresponding threshold values. Unlike in the case of a single joint, the total strain energy becomes infinitely large as the multiplication factor approaches to zero; this indicates that the joints shown in Fig. 4 may form a "failure mechanism".

"STICK" MODEL - These findings of the joints support the following hypothesis: A structure consisting of thin panels surrounded by frames, as is typical of automotive structures, may not be stiffened substantially by the panels under usual loading conditions, for the panels will buckle or deform like thin membranes, offering no support at the interior points. Even under these conditions, however, the part of the panel near the edge remains relatively undeformed, and acts as a gusset which stiffens the joint. This, then, implies the following modeling technique for the "stick" model of a vehicle structure: (i) The joints can be treated as rigid in the model, reflecting the fact that the panels act as gussets; this allows the joint stiffness to exceed the threshold value, and (ii) Since the panels contribute negligibly to the stiffness of the structure away from the joints, they do not have to be explicitly included in the model.

EFFECTS OF OTHER COMPONENTS - This idea, which has been applied to the joints, can be extended to other components. Similar phenomena can be seen by varying stiffness values of other components instead of varying those of just the joints. Figs. 7a and 7b show how the overall bending stiffness (solid lines) and torsional stiffness (dotted lines) change with the stiffness of the rocker panels or the tunnel. Figs. 7a and 7b were generated by varying the stiffness (abscissa) of the rocker panels and the tunnel, respectively. The ordinates represent the maximum deflections for bending and the twist angles for torsion, respectively. It is obvious from both Figs. 7a & 7b that the overall vehicle stiffness is much more sensitive to the rocker panel than to the tunnel under bending as well as torsional loadings. One can, however, see that the curves of both figures become flat as the stiffness of these two components increases. This phenomenon can also be shown using the equations derived in the previous section by replacing the variable b_m with the stiffness of either the rocker panels or the tunnel.

REFERENCES

1. Chang, D. C.: "Effects of Flexible Connections on Body Structural Response", SAE Transactions, Vol. 83, Paper No. 740071, pp 233-244, 1974.
2. Du, H. A. and Chon, C. T.: "Modeling of a Large-Scale Vehicle Structure", Proc. of the 8th Conf. on Electronic Computation, University of Houston, Houston, TX. ed. by J. K. Nelson Jr., ASCE, pp 326-335, 1983.
3. Chon, C. T.: "Design Sensitivity Analysis via Strain Energy Distribution", AIAA J. Vol. 22, No. 4, pp 559, 1984.
4. Chon, C. T. and Du, H. A.: "An Alternative Approach to Design Sensitivity Analysis for Large Scale Structures", Computers in Engineering, Vol. 3, ed. by D. E. Dietrich, pp 233, 1983.
5. DeVries, R. I. and Chon, C. T.: "Structural Design Sensitivity Analysis via Strain Energy Variations", 5th Int. Conf. on Vehicle Structural Mechanics, Detroit, MI. April 2-4, 1984, pp 135-141, 1984.
6. Malvern, L. E.: "Introduction to the Mechanics of a Continuous Medium", Prentice-Hall, Inc., Englewood Cliffs, N. J., 1969.
7. "MSC/NASTRAN - User's Manual", Version 62, ed. by C. W. McCormick, The MacNeal-Schwendler Corporation, April, 1982.
8. Hodge, P. G., Jr.: "Plastic Analysis of Structures", McGraw-Hill Book Co., N. Y., pp 20, 1959.
9. Crabb, H. C. et al.: "Structural Joint Performance", Advanced Structural & Safety Technology, Vehicle Development Technology, September 16, 1980.

TABLE 1.- MEASURED JOINT STIFFNESS VALUES.*

JOINTS	STIFFNESS ($\times 10^7$ N-mm/rad)		
	Vehicle A	Vehicle B	Vehicle C
1	2.12/1.61	3.96/3.48	5.12/3.38
2	3.55/2.46	2.45/3.69	3.48/2.84
3	14.4/3.92	28.7/15.6	18.0/5.14
4	20.1/3.26	39.3/4.51	27.4/4.12
5	2.35/0.18	2.75/0.12	7.41/0.20
6	10.1/0.54	22.6/1.25	16.9/1.29

(Fore-Aft/In-Outboard)

*(See Fig. 4 for corresponding joint numbers.)

TABLE 2.- COMPARISON OF STRAIN ENERGIES OF "STICK" MODEL AND STRAIN ENERGY COMPUTED USING JOINT STIFFNESS LISTED IN TABLE 1.

STRAIN ENERGY	BENDING	TORSION
U ("STICK" MODEL)	7.04×10^3 (1.00)	2.88×10^4 (1.00)
U (Vehicle A)	7.79×10^3 (1.11)	3.17×10^4 (1.10)
U (Vehicle B)	7.69×10^3 (1.09)	3.07×10^4 (1.07)
U (Vehicle C)	7.57×10^3 (1.08)	3.11×10^4 (1.08)

N-mm

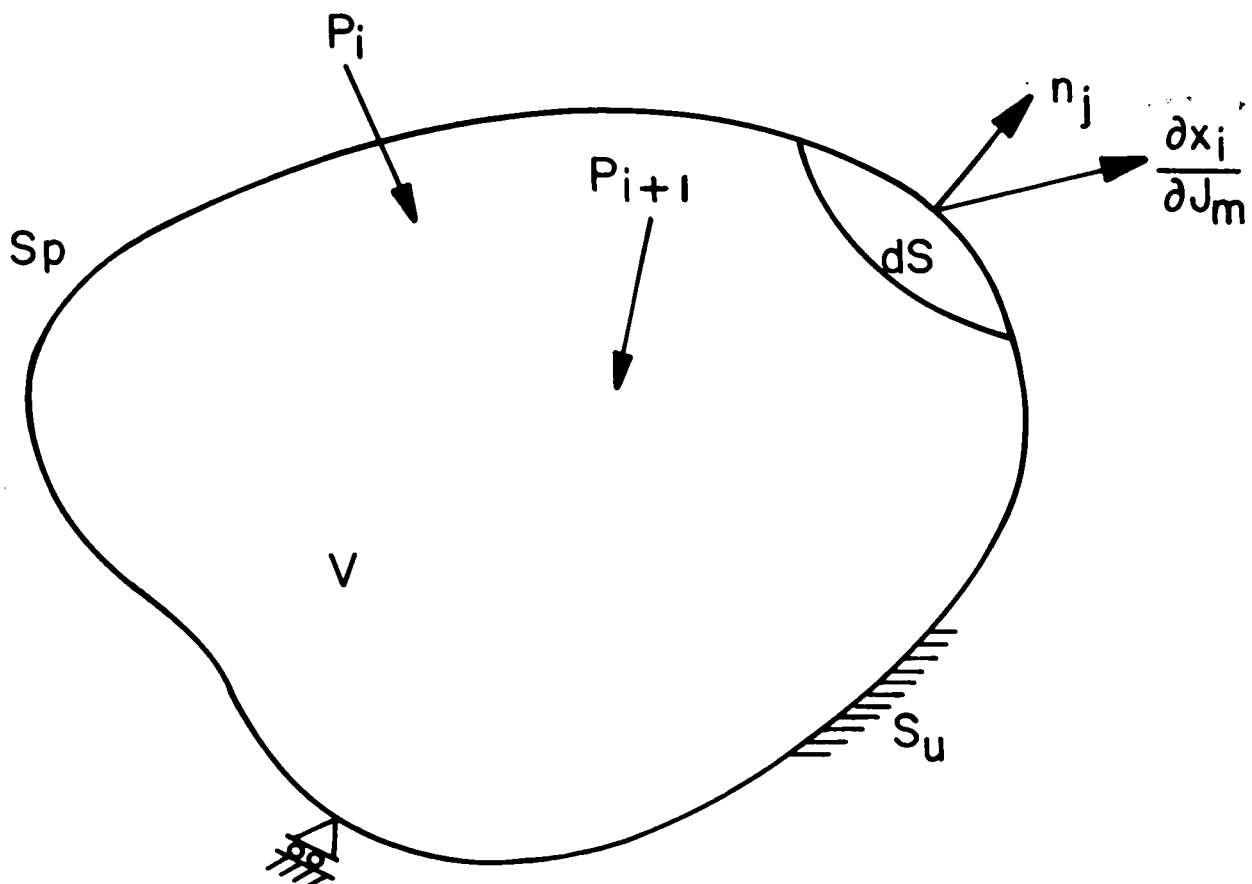


Figure 1 - A general body surface S consists of two parts, S_p and S_u . Over S_p , forces are prescribed and over S_u , displacements are prescribed. The term n is the unit vector normal to the surface.

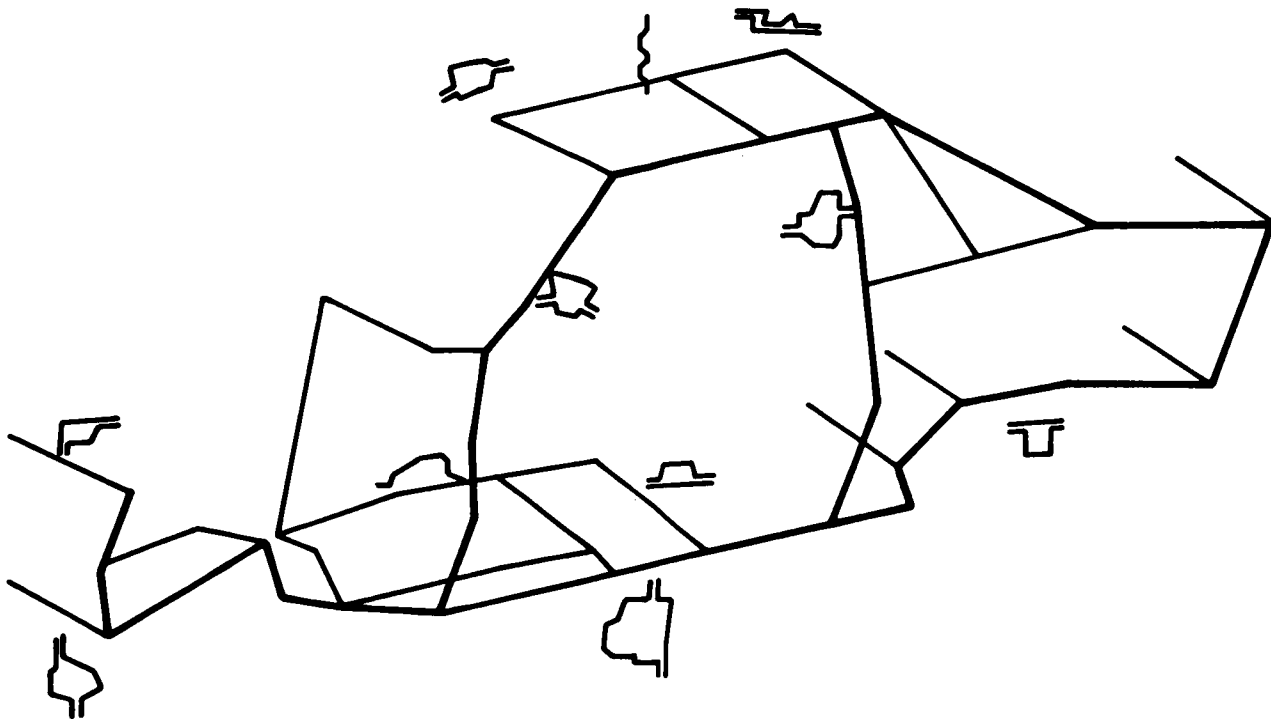


Figure 2 - A typical "STICK" model with cross-sectional shapes of beam elements.

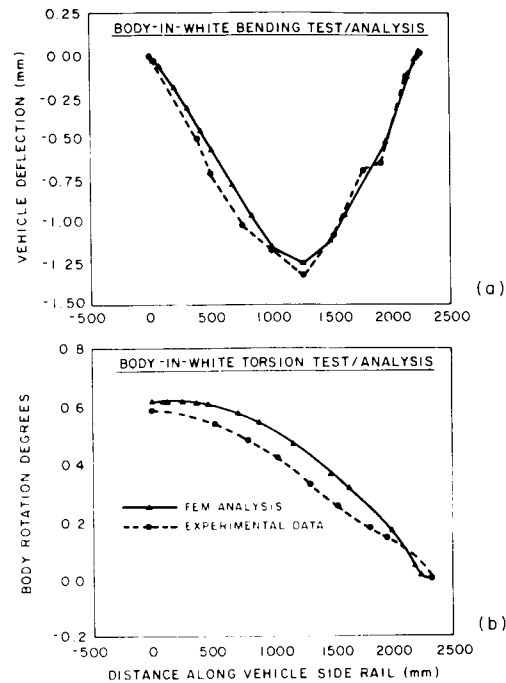
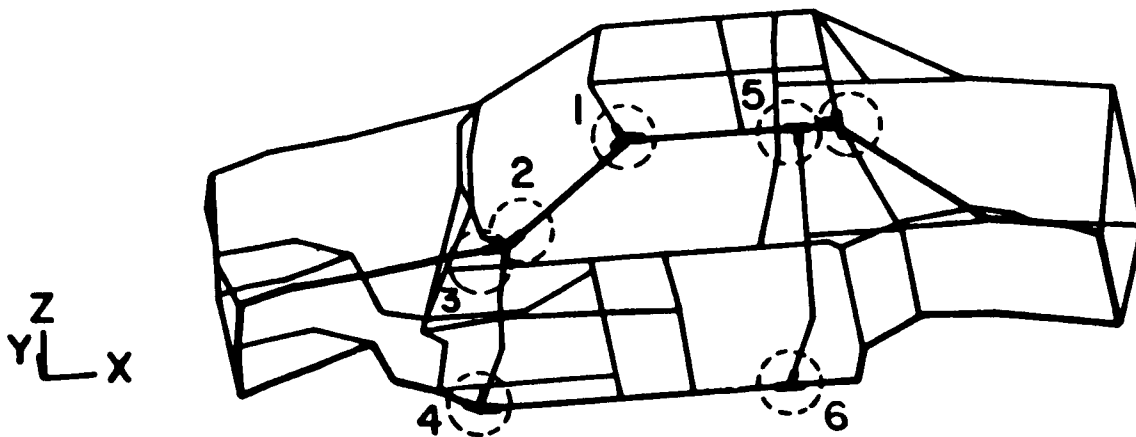


Figure 3 - Deflection versus wheel base length a "STICK" model for bending and torsion. Solid and dotted lines represent analytical results and test data, respectively.



- | | |
|---------------------------------|--------------------------|
| 1) A-PILLAR TO ROOF RAIL | 5) B-PILLAR TO ROOF RAIL |
| 2) A-PILLAR TO FRT HINGE PILLAR | 6) B-PILLAR TO ROCKER |
| 3) SHOTGUN TO FRT HINGE PILLAR | |
| 4) FRT HINGE PILLAR TO ROCKER | |

Figure 4 - Joint locations.

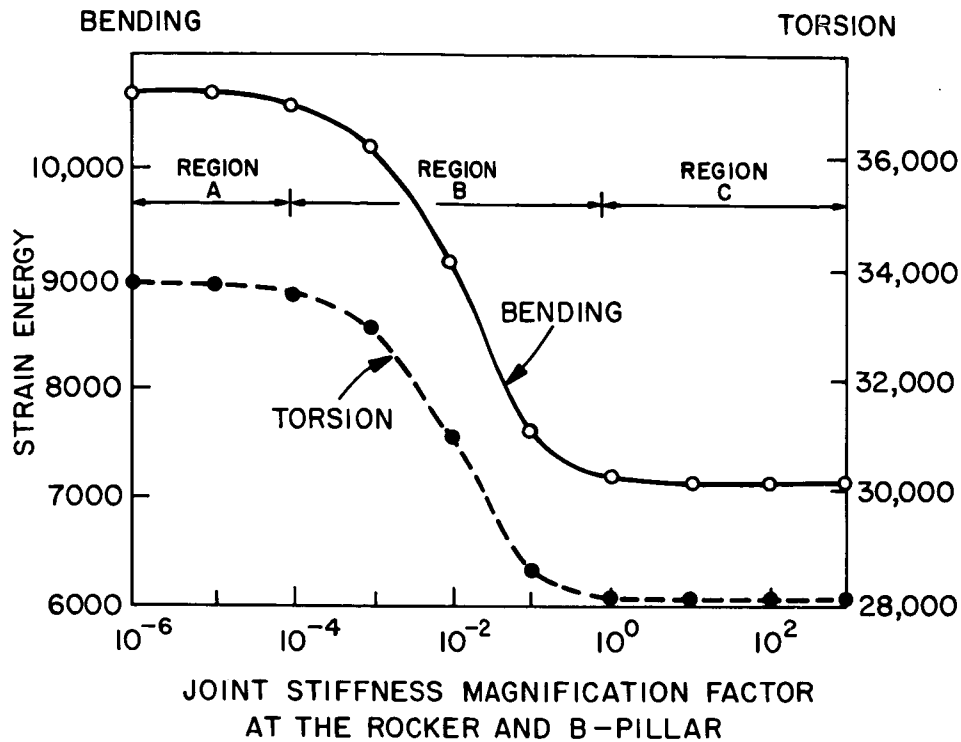


Figure 5 - Strain energy versus stiffness of the joint between the rocker panels and the B-pillar.

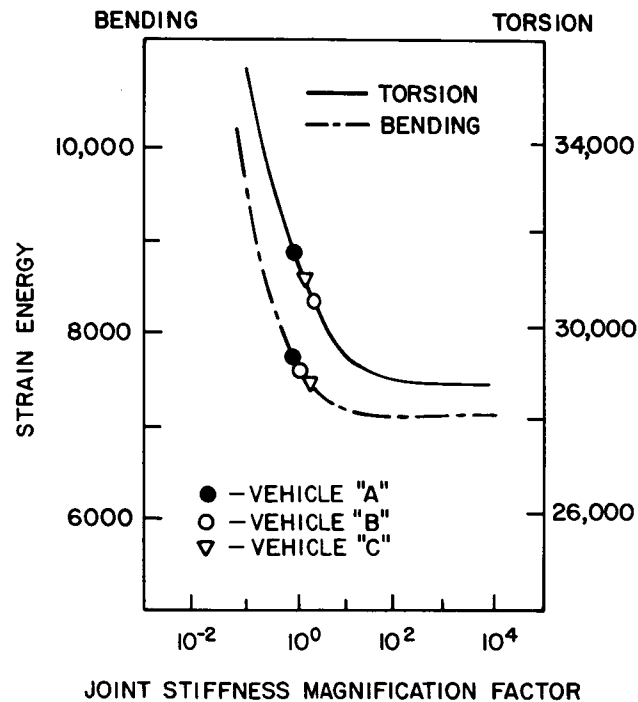
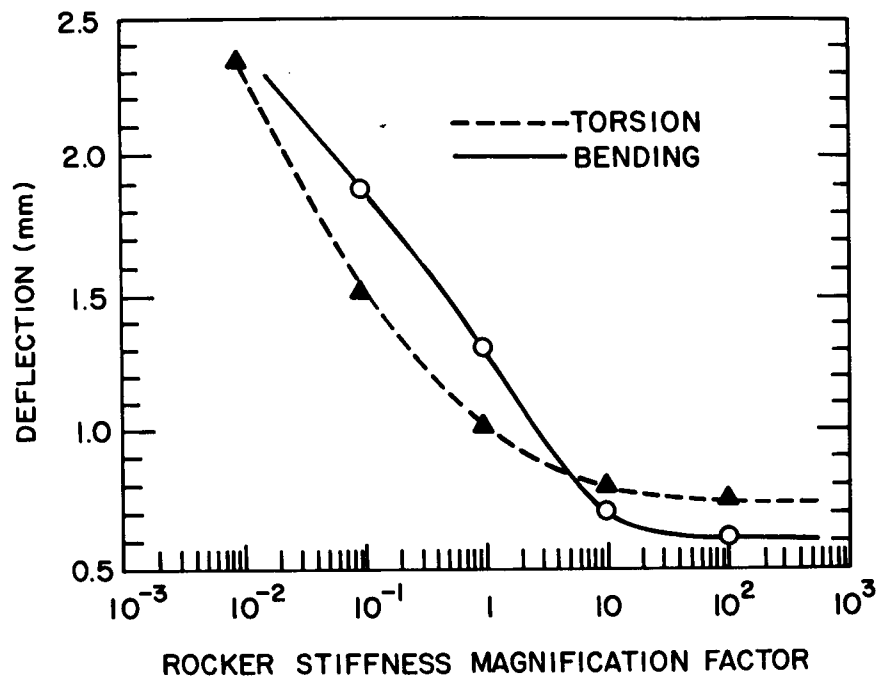
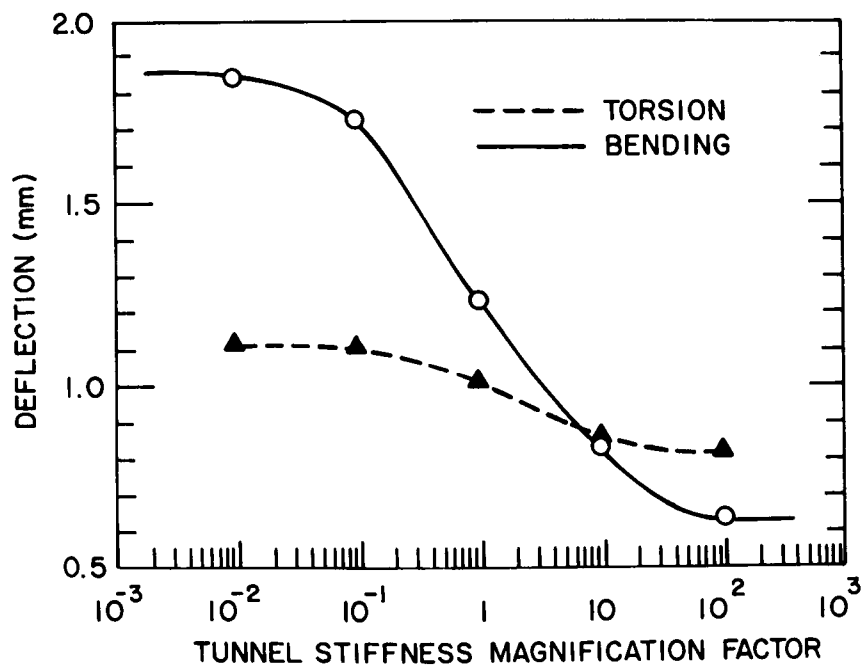


Figure 6 - Strain energy versus joint stiffness magnification factor. Strain energy obtained using measured joint stiffnesses from three vehicle structures is also shown.



a - Maximum deflection versus rocker stiffness magnification factor.



b - Maximum deflection versus tunnel stiffness magnification factor.

Figure 7 - Maximum deflections versus rocker stiffness and tunnel stiffness magnification factor.

DESIGN SENSITIVITY ANALYSIS OF NONLINEAR

STRUCTURAL RESPONSE

J.B. Cardoso and J.S. Arora
Optimal Design Laboratory
College of Engineering
The University of Iowa
Iowa City, IA

ABSTRACT

This paper describes a unified theory of design sensitivity analysis of linear and nonlinear structures for shape, nonshape and material selection problems. The concepts of reference volume and adjoint structure are used to develop the unified viewpoint. A general formula for design sensitivity analysis is derived. Simple analytical linear and nonlinear examples are used to interpret various terms of the formula and demonstrate its use.

1. INTRODUCTION

Design sensitivity analysis gives trend information that can be used in the conventional or optimal design process. The subject, therefore, has received considerable attention in recent years. For a thorough review of the subject Refs. 1 and 2 should be consulted.

The present paper describes a unified variational theory of design sensitivity analysis of linear and nonlinear structures (geometric as well as physical nonlinearities) including shape, nonshape and material selection problems. The adjoint variable approach is utilized although the direct differentiation method can be also easily developed. In Section 2, equations of continuum mechanics for nonlinear analysis are summarized. They are needed in design sensitivity analysis. A unified viewpoint for shape and nonshape design sensitivity analysis is described in Section 3. The concept of a reference volume is explained in Section 4. The variational theory of design sensitivity analysis using adjoint variable approach is developed in Section 5. The theory is used to solve several simple analytical problems in Section 6. Finally concluding remarks are given in Section 7.

2. NONLINEAR ANALYSIS

Nonlinearities in structural systems can be due to large displacements, large strains, material behavior and boundary conditions. Consistent theories to treat these nonlinearities have been developed^{3,4}. We will use the developments and notations of Ref. 4, and follow the Total Lagrangian (or Lagrangian) formulation, although updated Lagrangian formulation can also be used. One of the major difficulties in describing nonlinear analysis is the complexity of notation. We will mostly use standard symbols from the literature for various quantities. Matrix and

tensor notations will be used. One major departure from linear analysis is that quantities must be measured in a deformed configuration. Also, a reference configuration for the quantities must be defined. We will use a left superscript to indicate the configuration in which the quantity occurs and a left subscript to indicate the reference configuration.

A starting point for theory of nonlinear analysis is the principle of virtual work for the body in the deformed configuration at time t (load level t):

$$\int_{0V} {}^t_0 \mathbf{S} \cdot \delta {}^t_0 \boldsymbol{\epsilon} {}^0 dV - \int_{0V} {}^t_0 \mathbf{f} \cdot \delta {}^t_0 \mathbf{u} {}^0 dV - \int_{0\Gamma_T} {}^t_0 \mathbf{T} \cdot \delta {}^t_0 \mathbf{u} {}^0 d\Gamma_T = 0 \quad (1)$$

where left subscript 0 refers to the undeformed configuration, a '.' refers to the standard tensor product and

0V = undeformed volume of the body

${}^t_0 \mathbf{S}$ = Second Piola-Kirchhoff stress tensor

${}^t_0 \boldsymbol{\epsilon}$ = Green-Lagrange strain tensor

${}^t_0 \mathbf{f}$ = body force per unit volume

${}^t_0 \mathbf{u}$ = displacement field

${}^t_0 \mathbf{T}$ = surface traction specified on part of the surface Γ_T

${}^0\Gamma$ = surface of the body

δ = variation in the state fields

Let \mathbf{u}^0 be the specified displacement on the part Γ_u of the surface. The variations of the state fields in Eq. (1) are arbitrary but kinematically admissible. They can be replaced by any kinematically admissible fields. In particular they will be replaced by adjoint structure state fields in later derivations. The virtual work equation can also be written using Cauchy stress tensor and other quantities referred to the deformed configuration. Transformation can be used to recover Cauchy stresses from second Piola-Kirchhoff stresses and vice versa. However, in all the derivations given in this paper we will use the undeformed configuration as the reference configuration.

The Green-Lagrange strain tensor is given as

$${}^t_0 \boldsymbol{\epsilon} = \frac{1}{2} [{}^t_0 \nabla \mathbf{u}^T + ({}^t_0 \nabla \mathbf{u}^T)^T + ({}^t_0 \nabla \mathbf{u}^T) ({}^t_0 \nabla \mathbf{u}^T)^T] \quad (2)$$

The nonlinear stress strain law, in general, can be written as

$${}^t_0 \mathbf{S} = \boldsymbol{\phi}({}^t_0 \boldsymbol{\epsilon}, b) \quad (3)$$

where b is a design variable. Note that for many applications, functional form for $\boldsymbol{\phi}$ is not known. In numerical implementations, the explicit form is not needed. Only an incremental stress-strain relation is required.

Equations (1) to (3) are nonlinear in the displacement field ${}^t\mathbf{u}$. There are several methods for solving such system of equations.⁵ The incremental/iterative procedure based on Newton methods is the most commonly used and effective procedure. This will be summarized here. In the derivation of the procedure, it is assumed that equilibrium is known at t and it is desired at $t+\Delta t$. The state fields are decomposed as⁴

$$\begin{aligned} {}^{t+\Delta t}\mathbf{u} &= {}^t\mathbf{u} + \mathbf{u}; \quad {}^{t+\Delta t}{}_0\mathbf{S} = {}^t{}_0\mathbf{S} + {}_0\mathbf{S}; \quad {}_0\mathbf{S} = \boldsymbol{\phi}_{,\epsilon} {}_0\boldsymbol{\epsilon} \\ {}^{t+\Delta t}{}_0\boldsymbol{\epsilon} &= {}^t{}_0\boldsymbol{\epsilon} + {}_0\boldsymbol{\epsilon}, \quad {}^{t+\Delta t}{}_0\mathbf{f} = {}^t{}_0\mathbf{f} + {}_0\mathbf{f}; \quad {}^{t+\Delta t}{}_0\mathbf{T} = {}^t{}_0\mathbf{T} + {}_0\mathbf{T} \end{aligned} \quad (4)$$

where \mathbf{u} = increment in the displacement field
 ${}_0\mathbf{S}$ = increment in the Second Piola-Kirchhoff stress
 ${}_0\boldsymbol{\epsilon}$ = increment in the Green-Lagrange strain
 ${}_0\mathbf{f}$ = increment in the body force
 ${}_0\mathbf{T}$ = increment in the surface traction

Variation of the strain field is given as

$$\delta {}^{t+\Delta t}{}_0\boldsymbol{\epsilon} = \delta {}_0\boldsymbol{\epsilon} \quad (5)$$

The incremental strain field from Eq. (2) is given as

$${}_0\boldsymbol{\epsilon} = {}_0\mathbf{e} + {}_0\boldsymbol{\eta} \quad (6)$$

$${}_0\mathbf{e} = \frac{1}{2} [({}_0\mathbf{v}\mathbf{u}^T + ({}_0\mathbf{v}\mathbf{u}^T)^T + ({}_0\mathbf{v}\mathbf{u}^T) ({}_0\mathbf{v}^t\mathbf{u}^T)^T + ({}_0\mathbf{v}^t\mathbf{u}^T) ({}_0\mathbf{v}\mathbf{u}^T)^T)] \quad (7)$$

$${}_0\boldsymbol{\eta} = \frac{1}{2} [({}_0\mathbf{v}\mathbf{u}^T) ({}_0\mathbf{v}\mathbf{u}^T)^T] \quad (8)$$

Substituting Eqs. (4) - (6) in the virtual work principle, Eq. (1), written at $t+\Delta t$ and using the fact that state at t is in equilibrium, we obtain the following incremental virtual work principle:

$$\int ({}_0\mathbf{S} + {}_0\mathbf{S}) \cdot \delta {}_0\boldsymbol{\epsilon} {}^0dV - \int {}_0\mathbf{f} \cdot \delta \mathbf{u} {}^0dV - \int {}_0\mathbf{T} \cdot \delta \mathbf{u} {}^0d\Gamma_T = 0 \quad (9)$$

Equation (9) is still a nonlinear in incremental displacement field \mathbf{u} . It is linearized by assuming

$$\delta {}_0\boldsymbol{\epsilon} = \delta {}_0\mathbf{e}; \quad {}_0\mathbf{S} = \boldsymbol{\phi}_{,\epsilon} \cdot {}_0\mathbf{e} \quad (10)$$

and iteration is used within the load increment to satisfy the equilibrium exactly at $t+\Delta t$. The finite element procedure has been used to implement the preceding equations into a computer program ADINA.⁶

3. UNIFICATION OF DIMENSIONAL AND SHAPE DESIGN SENSITIVITY ANALYSIS

In the literature, shape and dimension design sensitivity analysis problems have been treated independently. In the shape problem, domain of the problem is allowed to vary whereas in the dimensional problem domain is fixed but cross-sectional dimensions are allowed to vary. It will be seen here that when variational formulation is used and volume integrals are used, there is no distinction between the two problems.

Consider the general functional requiring design sensitivity analysis:

$$\psi = \int_0^{V(b)} \bar{G}({}_0^t \mathbf{S}, {}_0^t \boldsymbol{\epsilon}, {}_0^t \mathbf{u}, b) {}^0 dV + \int_0^{r_u(b)} \bar{g}({}_0^t \mathbf{T}, b) {}^0 dr_u + \int_0^{r_T(b)} \bar{h}({}_0^t \mathbf{u}, b) {}^0 dr_T \quad (11)$$

It can be seen that when design b is changed, the volume of the body as well as its surface change. As examples, consider optimal design of two simple bodies shown in Fig. 1. Are these shape or dimensional optimization problems? Our contention is that although length of the members is not treated as a design variable in these problems, volume of the body changes whenever any of the indicated design variables is changed. We must account for variations of the domain of the body while writing variations of the functional ψ in Eq. (11). Thus the variational concept for design sensitivity analysis is slightly different from the corresponding concept used in purely analysis problems where domain of the body remains fixed (at least in linear problems). This distinction is important in maintaining generality of the variational design sensitivity analysis theory where variation of the domain should be always considered.

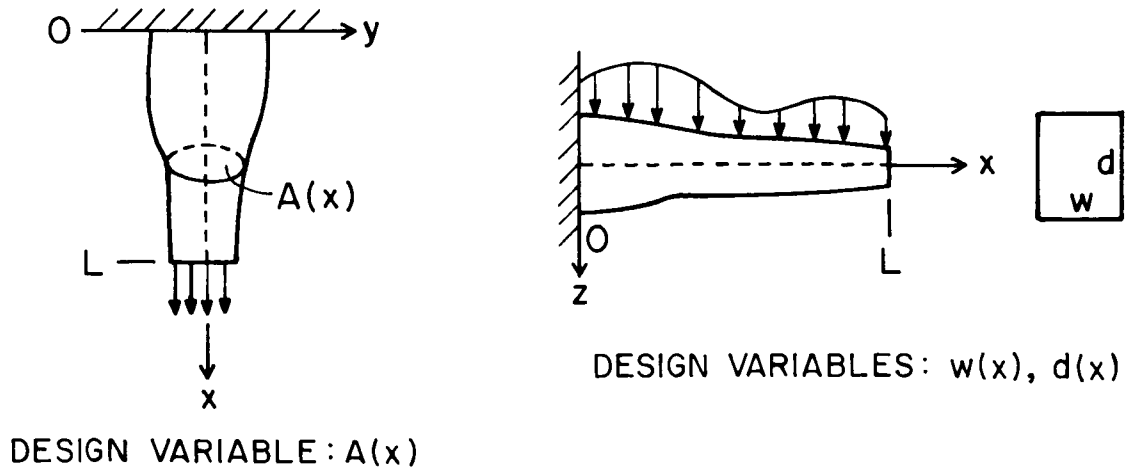


Figure 1. Examples of Optimal Design

4. CONCEPT OF REFERENCE VOLUME

The concept of a reference volume is extremely useful in problems where the volume of the body is changing. The idea, introduced recently in Ref. 7, is to map volume of the body in various configurations to a reference volume \bar{V} . This is shown in Fig. 2. The original volume of the body ${}^0V(b^0)$ moves to a volume ${}^tV(b^0)$ under a nonlinear motion. However, both the volumes can be mapped to the fixed reference volume \bar{V} under the mappings $F_1(b^0)$ and $F_2(b^0)$ respectively. The design process changes shape of the body so that its volume becomes ${}^0V(b^1)$ at the new design b^1 . This volume moves to ${}^tV(b^1)$ under the nonlinear motion. Both these volumes can also be mapped to the fixed reference volume \bar{V} .

The concept of reference volume is also quite useful in design sensitivity analysis. All the integrals of the problem are transformed to the reference volume using the proper transformation of the independent variables. The mapping to the fixed volume keeps changing under state or design variations. However, the reference volume never changes. Thus, when variations of various integrals are taken, the variations of the reference volume need not be considered. In numerical implementations, this concept is also very useful. It allows us to discretize the design problem into design elements that keep the same shape even when the real shape for

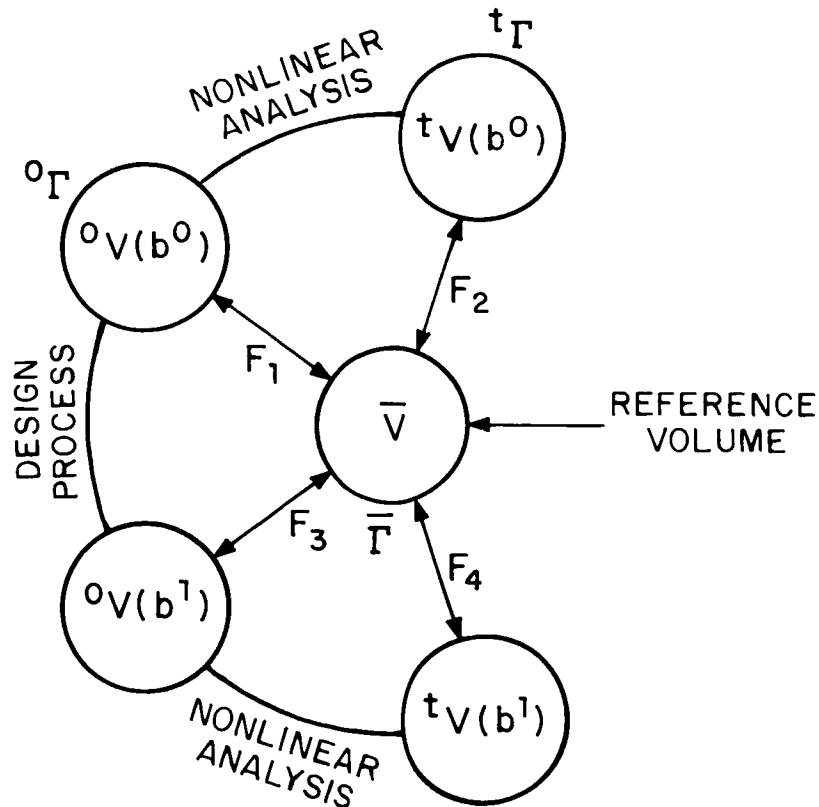


Figure 2. Concept of Reference Volume

the structure changes during the optimization process. Using the transformation of independent variables, various expressions are given as

Virtual Work Equation at Load Level t :

$$\int_0^t \mathbf{S}_0 \cdot \delta_0 \boldsymbol{\epsilon} J d\bar{V} - \int_0^t \mathbf{f}_0 \cdot \delta \mathbf{u} J d\bar{V} - \int_0^t \mathbf{T}_0 \cdot \delta \mathbf{u} \bar{J} d\bar{\Gamma}_T = 0 \quad (12)$$

Incremental Virtual Work Equation at Load Level $t+\Delta t$:

$$\int_0^t (\mathbf{S}_0 + \mathbf{S}) \cdot \delta_0 \boldsymbol{\epsilon} J d\bar{V} - \int_0^t \mathbf{f}_0 \cdot \delta \mathbf{u} J d\bar{V} - \int_0^t \mathbf{T}_0 \cdot \delta \mathbf{u} \bar{J} d\bar{\Gamma}_T = 0 \quad (13)$$

Green-Lagrange Strain Tensor:

$$\mathbf{e}_0^t = \frac{1}{2} [\bar{\mathbf{X}}^T (\mathbf{r} \nabla \mathbf{u}^T) + (\mathbf{r} \nabla \mathbf{u}^T)^T \bar{\mathbf{X}} + \bar{\mathbf{X}}^T (\mathbf{r} \nabla \mathbf{u}^T) (\mathbf{r} \nabla \mathbf{u}^T)^T \bar{\mathbf{X}}] \quad (14)$$

Incremental Strains:

$$\begin{aligned} \mathbf{e}_0 = \frac{1}{2} [\bar{\mathbf{X}}^T (\mathbf{r} \nabla \mathbf{u}^T) + (\mathbf{r} \nabla \mathbf{u}^T)^T \bar{\mathbf{X}} + \bar{\mathbf{X}}^T (\mathbf{r} \nabla \mathbf{u}^T) (\mathbf{r} \nabla \mathbf{u}^T)^T \bar{\mathbf{X}} \\ + \bar{\mathbf{X}}^T (\mathbf{r} \nabla \mathbf{u}^T) (\mathbf{r} \nabla \mathbf{u}^T)^T \bar{\mathbf{X}}] \end{aligned} \quad (15)$$

$$\mathbf{n}_0 = \frac{1}{2} [\bar{\mathbf{X}}^T (\mathbf{r} \nabla \mathbf{u}^T) (\mathbf{r} \nabla \mathbf{u}^T)^T \bar{\mathbf{X}}] \quad (16)$$

Functional for Sensitivity Analysis:

$$\psi = \int G(\mathbf{S}_0, \mathbf{e}_0, \mathbf{u}, b) J d\bar{V} + \int g(\mathbf{T}_0, b) \bar{J} d\bar{\Gamma}_u + \int h(\mathbf{u}, b) \bar{J} d\bar{\Gamma}_T \quad (17)$$

Jacobian of Transformation:

$$\mathbf{X} = \frac{\partial (\mathbf{x}_0, \mathbf{y}_0, \mathbf{z}_0)}{\partial (\mathbf{r}_x, \mathbf{r}_y, \mathbf{r}_z)} ; \quad J = |\mathbf{X}| ; \quad \bar{\mathbf{X}} = \mathbf{X}^{-1} ; \quad \bar{J} = J |\bar{\mathbf{X}}^T \mathbf{n}| \quad (18)$$

In the above equations superscript or subscript r refers to the reference coordinates, \bar{J} is the area metric, and \mathbf{n} is the unit surface normal. Note that all quantities in the above integrals are functions of the reference coordinates. Also for oriented bodies such as bars and beams, J and $|\mathbf{X}|$ may be different from each other if we use volume integrals throughout the sensitivity analysis. This can be observed in the examples discussed later in the paper.

5. ADJOINT STRUCTURE APPROACH FOR GENERAL DESIGN SENSITIVITY ANALYSIS

Discrete form of the adjoint variable method has been discussed by several researchers.^{1,8-13} Variational form of the approach based on material derivative

concept is described in Ref. 13 where sensitivity with respect to shape variations is also considered. Adjoint structure approach is described in Refs. 14-17. The approach has been applied to some nonlinear and shape variation problems in Refs. 18-20. Recently, Belegundu²¹ has traced roots of the adjoint variable method to methods of sensitivity analysis in optimal control literature. In addition, he has shown that sensitivity analysis methods for static, dynamic, shape and distributed parameter problems can be viewed as the general Lagrange multiplier method. This shows that the adjoint variable is also a Lagrange multiplier for the state equations which gives a sensitivity interpretation for it.²² This interpretation is extremely useful and leads to some insights into the adjoint variable method. It also has implications in practical applications and numerical implementations of the method.

In the following derivation we combine the adjoint structure approach with the fixed reference volume concept to develop a general theory of design sensitivity analysis of linear or nonlinear structures. To avoid confusion, we use δ and $\bar{\delta}$ to indicate arbitrary variations of the state fields and variations with respect to design variable, respectively. Also, the notation $G_{,S}$ will be used to indicate partial derivative of G with respect to \mathbf{S}_0^t . Note that design sensitivity analysis is performed at the final state of the system denoted by left superscript t on various variables. Thus the virtual work equation (12) holds for the deformed configuration.

Now taking variation of the functional ψ in Eq. (17) with respect to design, we obtain

$$\begin{aligned} \bar{\delta}\psi = & \int \bar{\delta}G J d\bar{V} + \int G \bar{\delta}J d\bar{V} + \int \bar{\delta}g \bar{J} d\bar{\Gamma}_u \\ & + \int g \bar{\delta}\bar{J} d\bar{\Gamma}_u + \int h \bar{\delta}\bar{J} d\bar{\Gamma}_T + \int \bar{\delta}h \bar{J} d\bar{\Gamma}_T + \bar{\delta}\psi_I \end{aligned} \quad (19)$$

where $\bar{\delta}\psi_I$ represents implicit design variation of ψ given as

$$\begin{aligned} \bar{\delta}\psi_I = & \int (G_{,S} \cdot \bar{\delta}_0^t \mathbf{S} + G_{,\epsilon} \cdot \bar{\delta}_0^t \boldsymbol{\epsilon} + G_{,\mathbf{u}} \cdot \bar{\delta}_0^t \mathbf{u}) J d\bar{V} \\ & + \int g_{,T} \cdot \bar{\delta}_0^t \mathbf{T} \bar{J} d\bar{\Gamma}_u + \int h_{,\mathbf{u}} \cdot \bar{\delta}_0^t \mathbf{u} \bar{J} d\bar{\Gamma}_T \end{aligned} \quad (20)$$

The basic idea of the adjoint structure approach is to replace the implicit design variations of the state fields in Eq. (20) by explicit design variations and the adjoint state fields. To accomplish this we write design variations of various equations as follows:

Design Variations of the Constitutive Law (Eq. 3):

$$\bar{\delta}_0^t \mathbf{S} = \boldsymbol{\phi}_{,\epsilon} \cdot \bar{\delta}_0^t \boldsymbol{\epsilon} + \bar{\delta}\boldsymbol{\phi} \quad (21)$$

Design Variations of Strains:

$$\bar{\delta}_0^t \epsilon = \bar{\delta}_0^t \epsilon + \bar{\bar{\delta}}_0^t \epsilon \quad (22)$$

where

$$\begin{aligned} \bar{\delta}_0^t \epsilon = & \frac{1}{2} [\bar{\bar{X}}^T ({}_r \nabla \bar{\delta}^t \mathbf{u}^T) + ({}_r \nabla \bar{\delta}^t \mathbf{u}^T)^T \bar{\bar{X}} \\ & + \bar{\bar{X}}^T ({}_r \nabla \bar{\delta}^t \mathbf{u}^T) ({}_r \nabla \bar{\delta}^t \mathbf{u}^T)^T \bar{\bar{X}} + \bar{\bar{X}}^T ({}_r \nabla \bar{\delta}^t \mathbf{u}^T) ({}_r \nabla \bar{\delta}^t \mathbf{u}^T)^T \bar{\bar{X}}] \end{aligned} \quad (23)$$

$$\begin{aligned} \bar{\bar{\delta}}_0^t \epsilon = & \frac{1}{2} [\bar{\delta} \bar{\bar{X}}^T ({}_r \nabla \bar{\delta}^t \mathbf{u}^T) + ({}_r \nabla \bar{\delta}^t \mathbf{u}^T)^T \bar{\delta} \bar{\bar{X}} \\ & + \bar{\delta} \bar{\bar{X}}^T ({}_r \nabla \bar{\delta}^t \mathbf{u}^T) ({}_r \nabla \bar{\delta}^t \mathbf{u}^T)^T \bar{\bar{X}} + \bar{\delta} \bar{\bar{X}}^T ({}_r \nabla \bar{\delta}^t \mathbf{u}^T) ({}_r \nabla \bar{\delta}^t \mathbf{u}^T)^T \bar{\bar{X}}] \end{aligned} \quad (24)$$

Here $\bar{\delta}$ represents implicit design variations of the displacements and $\bar{\bar{\delta}}$ the explicit design variations of the strain fields.

Design Variations of Equilibrium Equation (12):

$$\begin{aligned} & \int \bar{\delta}_0^t \mathbf{S} \cdot \epsilon^a J d\bar{V} + \int {}_0^t \mathbf{S} \cdot \bar{\bar{\delta}} \epsilon^a J d\bar{V} + \int {}_0^t \mathbf{S} \cdot \epsilon^a \bar{\delta} J d\bar{V} - \int \bar{\delta}_0^t \mathbf{f} \cdot \mathbf{u}^a J d\bar{V} \\ & - \int {}_0^t \mathbf{f} \cdot \mathbf{u}^a \bar{\delta} J d\bar{V} - \int \bar{\delta}_0^t \mathbf{T} \cdot \mathbf{u}^a \bar{J} d\bar{\Gamma}_T - \int {}_0^t \mathbf{T} \cdot \mathbf{u}^a \bar{\delta} \bar{J} d\bar{\Gamma}_T = 0 \end{aligned} \quad (25)$$

where arbitrary variations of the primary state fields in Eq. (12) have been replaced by the corresponding fields for the adjoint structure denoted by the superscript 'a'. The adjoint structure and the corresponding state fields are defined later. Substitute for $\bar{\delta}_0^t \mathbf{S}$ from Eq. (21) into Eq. (25), use Eq. (22) and collect terms:

$$\begin{aligned} & \int [\epsilon^a \cdot \phi_{,\epsilon} (\bar{\delta}_0^t \epsilon + \bar{\bar{\delta}}_0^t \epsilon) + {}_0^t \mathbf{S} \cdot \bar{\bar{\delta}} \epsilon^a - \bar{\delta}_0^t \mathbf{f} \cdot \mathbf{u}^a + \epsilon^a \cdot \bar{\delta} \phi] J d\bar{V} \\ & - \int ({}_0^t \mathbf{f} \cdot \mathbf{u}^a - {}_0^t \mathbf{S} \cdot \epsilon^a) \bar{\delta} J d\bar{V} - \int (\bar{\delta}_0^t \mathbf{T} \cdot \mathbf{u}^a \bar{J} + {}_0^t \mathbf{T} \cdot \mathbf{u}^a \bar{\delta} \bar{J}) d\bar{\Gamma}_T = 0 \end{aligned} \quad (26)$$

Now, let us define the adjoint structure as follows:

Loads and Boundary Conditions:

$$\begin{aligned} \text{Initial strain field} & : \epsilon^{ai} = G_{,S} \\ \text{Initial stress field} & : \mathbf{S}^{ai} = G_{,\epsilon} \\ \text{Body force} & : \mathbf{f}^a = G_{,u} \\ \text{Specified Traction} & : \mathbf{T}^{a0} = h_{,u} \text{ on } \Gamma_T \\ \text{Specified Displacements} & : \mathbf{u}^{a0} = -g_{,T} \text{ on } \Gamma_u \end{aligned} \quad (27)$$

Constitutive Law (Linear):

$$\mathbf{S}^a = \boldsymbol{\phi}_{,\epsilon}^T \cdot (\boldsymbol{\epsilon}^a - \boldsymbol{\epsilon}^{ai}) - \mathbf{S}^{ai}; \quad \mathbf{S}^a = \text{the adjoint stress field.} \quad (28)$$

Virtual Work Equation:

$$\int \mathbf{S}^a \cdot \delta_0^t \boldsymbol{\epsilon} J \, d\bar{V} - \int \mathbf{f}^a \cdot \delta^t \mathbf{u} J \, d\bar{V} - \int \mathbf{T}^a \cdot \delta^t \mathbf{u} \bar{J} \, d\bar{\Gamma}_T = 0 \quad (29)$$

Substitute Eq. (28) into Eq. (29):

$$\begin{aligned} \int (\boldsymbol{\epsilon}^a \cdot \boldsymbol{\phi}_{,\epsilon} \cdot \delta_0^t \boldsymbol{\epsilon} - \boldsymbol{\epsilon}^{ai} \cdot \boldsymbol{\phi}_{,\epsilon} \cdot \delta_0^t \boldsymbol{\epsilon} - \mathbf{S}^{ai} \cdot \delta_0^t \boldsymbol{\epsilon} - \mathbf{f}^a \cdot \delta^t \mathbf{u}) J \, d\bar{V} \\ - \int \mathbf{T}^a \cdot \delta^t \mathbf{u} \bar{J} \, d\bar{\Gamma}_T = 0 \end{aligned} \quad (30)$$

Strain Field (Linear in \mathbf{u}^a):

$$\begin{aligned} \boldsymbol{\epsilon}^a = \frac{1}{2} [\bar{\mathbf{X}}^T (\mathbf{r} \mathbf{v} \mathbf{u}^a)^T + (\mathbf{r} \mathbf{v} \mathbf{u}^a)^T \bar{\mathbf{X}} + \bar{\mathbf{X}}^T (\mathbf{r} \mathbf{v} \mathbf{u}^a)^T (\mathbf{r} \mathbf{v}^t \mathbf{u}^T)^T \bar{\mathbf{X}} \\ + \bar{\mathbf{X}}^T (\mathbf{r} \mathbf{v}^t \mathbf{u}^T) (\mathbf{r} \mathbf{v} \mathbf{u}^a)^T \bar{\mathbf{X}}] \end{aligned} \quad (31)$$

Substitute the adjoint equilibrium equation (30) into Eq. (26):

$$\begin{aligned} \int [\boldsymbol{\epsilon}^a \cdot \boldsymbol{\phi}_{,\epsilon} \cdot \bar{\delta}_0^t \boldsymbol{\epsilon} + {}_0^t \mathbf{S} \cdot \bar{\delta} \boldsymbol{\epsilon}^a - \bar{\delta}_0^t \mathbf{f} \cdot \mathbf{u}^a + \boldsymbol{\epsilon}^{ai} \cdot \boldsymbol{\phi}_{,\epsilon} \cdot \bar{\delta}_0^t \boldsymbol{\epsilon} + \boldsymbol{\epsilon}^a \cdot \bar{\delta} \boldsymbol{\phi} \\ + \mathbf{S}^{ai} \cdot \bar{\delta}_0^t \boldsymbol{\epsilon} + \mathbf{f}^a \cdot \bar{\delta}^t \mathbf{u}] J \, d\bar{V} - \int ({}_0^t \mathbf{f} \cdot \mathbf{u}^a - {}_0^t \mathbf{S} \cdot \boldsymbol{\epsilon}^a) \bar{\delta} J \, d\bar{V} \\ + \int (\mathbf{T}^a \cdot \bar{\delta}^t \mathbf{u} - \bar{\delta}_0^t \mathbf{T} \cdot \mathbf{u}^a) \bar{J} \, d\bar{\Gamma}_T - \int {}_0^t \mathbf{T} \cdot \mathbf{u}^a \bar{\delta} \bar{J} \, d\bar{\Gamma}_T = 0 \end{aligned} \quad (32)$$

Note that the variations of the state fields in Eq. (30) are arbitrary. So, they have been replaced as $\delta_0^t \boldsymbol{\epsilon} = \bar{\delta}_0^t \boldsymbol{\epsilon}$ and $\delta^t \mathbf{u} = \bar{\delta}^t \mathbf{u}$.

Substitute the adjoint loads from Eq. (27) into Eq. (20):

$$\begin{aligned} \bar{\delta} \psi_I = \int (\boldsymbol{\epsilon}^{ai} \cdot \bar{\delta}_0^t \mathbf{S} + \mathbf{S}^{ai} \cdot \bar{\delta}_0^t \boldsymbol{\epsilon} + \mathbf{f}^a \cdot \bar{\delta}^t \mathbf{u}) J \, d\bar{V} \\ + \int - \mathbf{u}^{a0} \cdot \bar{\delta}_0^t \mathbf{T} \bar{J} \, d\bar{\Gamma}_u + \int \mathbf{T}^{a0} \cdot \bar{\delta}^t \mathbf{u} \bar{J} \, d\bar{\Gamma}_T \end{aligned} \quad (33)$$

Substitute for $\bar{\delta}_0^t \mathbf{S}$ from Eq. (21) into Eq. (33):

$$\begin{aligned}\bar{\delta}\psi_I = & \int (\epsilon^{ai} \cdot \phi_{,\epsilon} \cdot \bar{\delta}_0^t \epsilon + \epsilon^{ai} \cdot \bar{\delta}\phi + S^{ai} \cdot \bar{\delta}_0^t \epsilon + f^a \cdot \bar{\delta}^t \mathbf{u}) J \, d\bar{V} \\ & + \int -u^{a0} \cdot \bar{\delta}_0^t T \bar{J} \, d\bar{\Gamma}_u + \int T^{a0} \cdot \bar{\delta}^t \mathbf{u} \bar{J} \, d\bar{\Gamma}_T\end{aligned}\quad (34)$$

Substitute for $\bar{\delta}_0^t \epsilon$ from Eq. (22) into Eq. (34):

$$\begin{aligned}\bar{\delta}\psi_I = & \int [(\epsilon^{ai} \cdot \phi_{,\epsilon} + S^{ai}) \cdot \bar{\delta}_0^t \epsilon + (\epsilon^{ai} \cdot \phi_{,\epsilon} + S^{ai}) \cdot \bar{\delta}_0^t \epsilon + \epsilon^{ai} \cdot \bar{\delta}\phi \\ & + f^a \cdot \bar{\delta}^t \mathbf{u}] J \, d\bar{V} + \int -u^{a0} \cdot \bar{\delta}_0^t T \bar{J} \, d\bar{\Gamma}_u + \int T^{a0} \cdot \bar{\delta}^t \mathbf{u} \bar{J} \, d\bar{\Gamma}_T\end{aligned}\quad (35)$$

Substitute Eq. (32) into Eq. (35) and use Eq. (28) to obtain

$$\begin{aligned}\bar{\delta}\psi_I = & \int [\bar{\delta}_0^t \mathbf{f} \cdot \mathbf{u}^a - (\epsilon^a - \epsilon^{ai}) \cdot \bar{\delta}\phi - S^a \cdot \bar{\delta}_0^t \epsilon - {}_0^t \mathbf{S} \cdot \bar{\delta} \epsilon^a] J \, d\bar{V} \\ & + \int ({}_0^t \mathbf{f} \cdot \mathbf{u}^a - {}_0^t \mathbf{S} \cdot \epsilon^a) \bar{\delta} J \, d\bar{V} + \int ({}_0^t \mathbf{T} \cdot \mathbf{u}^a \bar{\delta} \bar{J} + \bar{\delta}_0^t \mathbf{T} \cdot \mathbf{u}^a \bar{J}) d\bar{\Gamma}_T \\ & - \int \bar{\delta}_0^t \mathbf{T} \cdot \mathbf{u}^{a0} \bar{J} \, d\bar{\Gamma}_u\end{aligned}\quad (36)$$

Substitute Eq. (36) into Eq. (19):

$$\begin{aligned}\bar{\delta}\psi = & \int [\bar{\delta}_0^t \mathbf{f} \cdot \mathbf{u}^a - (\epsilon^a - \epsilon^{ai}) \cdot \bar{\delta}\phi - \mathbf{S}^a \cdot \bar{\delta}_0^t \epsilon - {}_0^t \mathbf{S} \cdot \bar{\delta} \epsilon^a + \bar{\delta} G] J \, d\bar{V} \\ & + \int ({}_0^t \mathbf{f} \cdot \mathbf{u}^a - {}_0^t \mathbf{S} \cdot \epsilon^a + G) \bar{\delta} J \, d\bar{V} + \int (\bar{\delta} g \bar{J} + g \bar{\delta} \bar{J} - \bar{\delta}_0^t \mathbf{T} \cdot \mathbf{u}^{a0} \bar{J}) d\bar{\Gamma}_u \\ & + \int [(h + {}_0^t \mathbf{T} \cdot \mathbf{u}^a) \bar{\delta} \bar{J} + (\bar{\delta} h + \bar{\delta}_0^t \mathbf{T} \cdot \mathbf{u}^a) \bar{J}] d\bar{\Gamma}_T\end{aligned}\quad (37)$$

Equation (37) is a general design sensitivity formula for linear and nonlinear structures (geometric and material nonlinearities), and shape, non-shape and material selection problems. Formula also gives sensitivity interpretations of the adjoint state fields. For example, it shows that the adjoint displacement field is sensitivity of functional ψ with respect to variations of the body force and surface tractions. This interpretation has been also derived in Refs. 21 and 22 for linear systems using the Lagrangian approach. Formula (37) also shows that the adjoint strain field gives variations of the functional ψ with respect to the constitutive law, the adjoint stress field is related to variations of ψ with respect to explicit design variations of the strain field, and variations of ψ with respect to variations of J can be recovered using adjoint and primary fields. These sensitivity interpretations will be observed in the example problems solved in the next section. These interpretations can be invaluable in practical applications and numerical implementations.

6. EXAMPLE PROBLEMS

Several analytical linear and nonlinear examples are solved to show use of Eq. (37) and interpretation of various terms. Although these examples are simple, they can be valuable in gaining insights into numerical implementation for larger complex problems. Also in using Eq. (37), we will use standard symbols σ for stress and ϵ for strain.

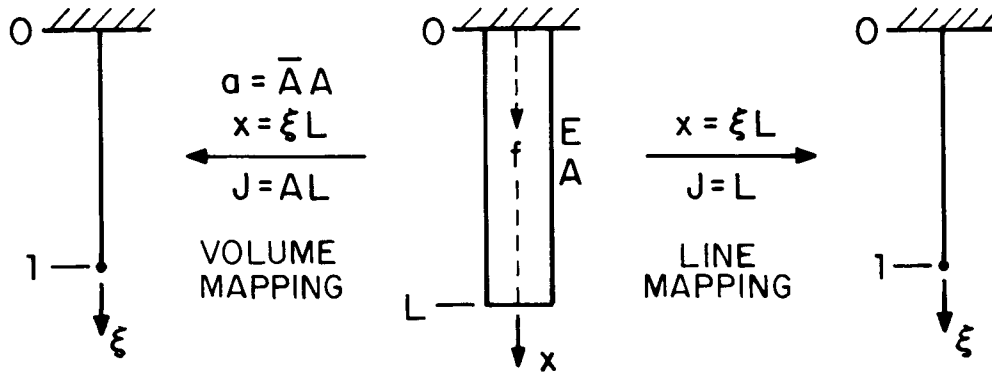
Example 1. Bar Under Self Weight

This example is taken from Ref. 7 where sensitivity of tip displacement with respect to length L is calculated. We will calculate sensitivities with respect to all parameters of the problem to demonstrate use of formula (37) for material, cross-sectional and length variations. The problem definition and various transformations are shown in Fig. 3. Small displacements and linear stress-strain law are assumed. The displacement field for the bar is given as $u(x) = fx(2L-x)/2E$ where f is the body force per unit volume. Thus

$$\begin{aligned} u(L) &= fL^2/E; \quad \bar{\delta}u(L) = (L^2/2E)\bar{\delta}f + (fL/E)\bar{\delta}L \\ &\quad + (0)\bar{\delta}A - (fL^2/2E^2)\bar{\delta}E \end{aligned} \quad (38)$$

There are at least two interpretations of this problem and both can be treated using Eq. (37).

First Interpretation. In this case, Eq. (37) can be interpreted as a line integral with x as the only independent variable. The stress-strain law of Eq. (3) must be interpreted as force-strain law, as the structure is only a line element. Note that this must be done with the formulas given in Refs. 14, 16, 18 and 20 when



DESIGN VARIABLES: f, E, A, L

Figure 3. Bar Under Self Weight

variations with respect to the cross-sectional area are needed. While using Eq. (37), the tip displacement can be treated as a boundary term or the interior term. We will use the latter approach. The functional for sensitivity analysis is given as

$$\psi = \int_0^1 u(\xi) J^{-1} \hat{\delta}(\xi-1) J d\xi; \quad G = u(\xi) J^{-1} \hat{\delta}(\xi-1); \quad G_{,u} = J^{-1} \hat{\delta}(\xi-1) \quad (39)$$

where $\hat{\delta}(\xi-1)$ is the Dirac delta function. The primary and adjoint fields can be obtained as

$$\begin{aligned} u(\xi) &= fL^2 \xi(2-\xi)/2E; & u^a(\xi) &= L\xi/EA \\ \epsilon(\xi) &= fL^2(1-\xi)/E; & \epsilon^a(\xi) &= L/EA \\ \epsilon &= \epsilon(\xi) J^{-1} = fL(1-\xi)/E; & \epsilon^a &= \epsilon^a(\xi) J^{-1} = 1/EA \\ N &= EA\epsilon = fAL(1-\xi); & N^a &= EA\epsilon^a = 1 \end{aligned} \quad (40)$$

where N is the axial force and $\phi = EA\epsilon$. Equation (37) reduces to

$$\begin{aligned} \bar{\delta}\psi &= \int_0^1 (\bar{\delta}\tilde{f}u^a - \epsilon^a \bar{\delta}\phi - N^a \bar{\delta}\epsilon - N\bar{\delta}\epsilon^a + \bar{\delta}G) J d\xi \\ &+ \int_0^1 (\tilde{f}u^a - N\epsilon^a + G) \bar{\delta}J d\xi \end{aligned} \quad (41)$$

Note that since we are using line integrals, the body force $\tilde{f} = fA$ must be used. Various quantities for use in Eq. (41) are

$$\begin{aligned} \bar{\delta}\phi &= (A\delta E + E\delta A) J^{-1} fL^2(1-\xi)/E; & \bar{\delta}\tilde{f} &= A\delta f + f\delta A \\ \bar{\delta}G &= -u(\xi) J^{-2} \hat{\delta}(\xi-1) \delta L; & \bar{\delta}\epsilon &= \epsilon(\xi) \bar{\delta}J^{-1} = -f(1-\xi) \delta L/E \\ \bar{\delta}\epsilon^a &= \epsilon^a(\xi) \bar{\delta}J^{-1} = -\delta L/EAL \end{aligned} \quad (42)$$

Substituting all the quantities in Eq. (41) and carrying out the integrations, we obtain the required sensitivity equation which is the same as Eq. (38). The sensitivity interpretations of the adjoint fields can be directly observed.

Second Interpretation. In this case, Eq. (3) will be treated as a volume integral. The functional for sensitivity analysis is given as

$$\psi = \int_0^1 \int_{\bar{A}} (AL)^{-1} u(\xi) \hat{\delta}(\xi-1) J d\bar{A} d\xi; \quad G = (AL)^{-1} u(\xi) \hat{\delta}(\xi-1) \quad (43)$$

The displacement and strain fields are the same as given in Eq. (40). However, the stress-strain law is the usual Hooke's Law:

$$\sigma = E\epsilon = fL(1-\xi); \quad \sigma^a = 1/A \quad (44)$$

Equation (37) reduces to

$$\begin{aligned} \bar{\delta}\psi = & \int_0^1 \int_{\bar{A}} (\bar{\delta}fu^a - \epsilon^a \bar{\delta}\phi - \sigma^a \bar{\delta}\epsilon - \sigma \bar{\delta}\epsilon^a + \bar{\delta}G) J d\bar{A} d\xi \\ & + \int_0^1 \int_{\bar{A}} (fu^a - \sigma \epsilon^a + G) \bar{\delta}J d\bar{A} d\xi \end{aligned} \quad (45)$$

Various quantities for use in Eq. (45) are

$$\bar{\delta}\phi = fL\delta E(1-\xi)/E; \quad \bar{\delta}J = L\delta A + A\delta L; \quad \bar{\delta}G = -(A^{-1} + L^{-1})G \quad (46)$$

Substituting various quantities from Eqs. (40), (42) and (46) into Eq. (45), we again obtain the sensitivity expression given in Eq. (38). The sensitivity interpretation of the adjoint fields can be easily observed.

Example 2. Cantilever Beam

This example is also discussed in Ref. 7 where sensitivity of tip deflection with respect to the length is given. Figure 4 defines the problem and the transformations to the reference volume. The design variables are chosen as $b = (E, s, h, L)$.

The tip deflection using small displacements beam theory is given as $w(L) = PL^3/3EI$ and its variation with respect to the design variables is given as

$$\bar{\delta}w(L) = -\frac{PL^3}{3E^2I} \bar{\delta}E - \frac{PL^3h^3}{36EI^2} \bar{\delta}s - \frac{PL^3sh^2}{12EI^2} \bar{\delta}h + \frac{PL^2}{EI} \bar{\delta}L \quad (47)$$

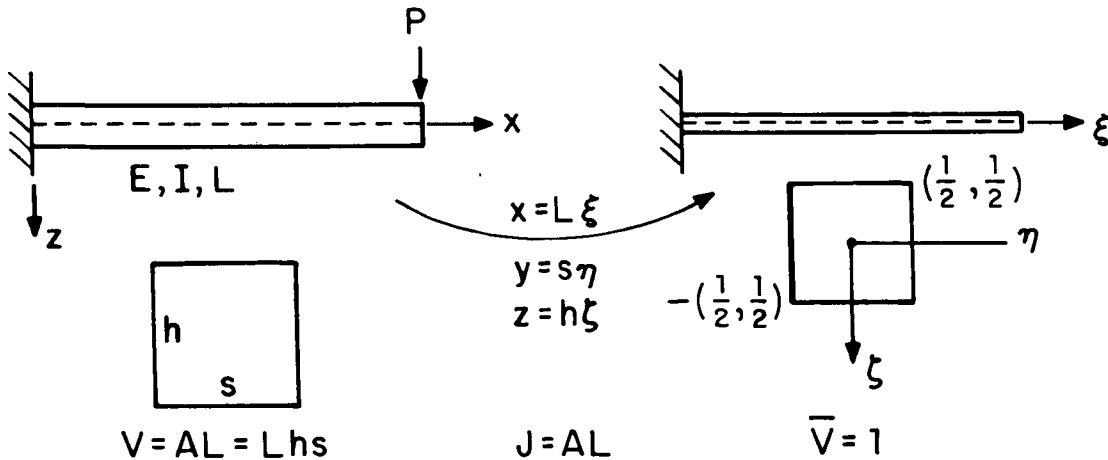


Figure 4. Cantilever Beam

The functional for the tip deflection and the function G are given as

$$\psi = \int_0^1 \int_{\bar{A}} (AL)^{-1} w(\xi) \hat{\delta}(\xi-1) AL d\bar{A} d\xi \quad (48)$$

$$G = (AL)^{-1} w(\xi) \hat{\delta}(\xi-1); \quad G_{,w} = (AL)^{-1} \hat{\delta}(\xi-1) \quad (49)$$

The primary and adjoint structure solutions are given

$$w_{,\xi\xi} = \frac{PL^3}{EI} (1-\xi); \quad w(\xi) = \frac{PL^3 \xi^2}{6EI} (3-\xi) \quad (50)$$

$$w^a_{,\xi\xi} = \frac{L^3}{EI} (1-\xi); \quad w^a(\xi) = \frac{L^3 \xi^2}{6EI} (3-\xi) \quad (51)$$

The sensitivity formula of Eq. (37) is reduced to

$$\begin{aligned} \bar{\delta}\psi = & \int_0^1 \int_{\bar{A}} (-\epsilon^a \bar{\delta}\phi - \sigma \bar{\delta}\epsilon^a - \sigma^a \bar{\delta}\epsilon + \bar{\delta}G) AL d\bar{A} d\xi \\ & + \int_0^1 \int_{\bar{A}} (-\sigma \epsilon^a + G) \bar{\delta}(AL) d\bar{A} d\xi \end{aligned} \quad (52)$$

The following quantities are needed to complete integrations in Eq. (52):

$$\epsilon = \zeta w_{,\xi\xi} hL^{-2}; \quad \epsilon^a = \zeta w^a_{,\xi\xi} hL^{-2}; \quad \bar{\delta}G = \hat{w} \hat{\delta}(\xi-1) \bar{\delta}(AL)^{-1}$$

$$\sigma = E\epsilon; \quad \bar{\delta}\phi = \epsilon \delta E; \quad \sigma^a = E \epsilon^a$$

$$\bar{\delta}\epsilon = \zeta w_{,\xi\xi} \bar{\delta}(hL^{-2}); \quad \bar{\delta}\epsilon^a = \zeta w^a_{,\xi\xi} \bar{\delta}(hL^{-2})$$

Substituting these quantities in Eq. (52) and carrying out the integrations we get the sensitivity expression given in Eq. (47). It is interesting to again note that the adjoint displacement field given in Eq. (51) represents the sensitivity of the primary displacement field (Eq. 52) with respect to the load parameters P; i.e. $u^a(\xi) = d\psi/dP$.

Example 3. Materially Nonlinear Problem

Consider the bar of Fig. 3 subjected to a load P in the x direction at the free end. The material for the bar obeys a nonlinear stress-strain law $\sigma = E\epsilon^{1/2} (\epsilon > 0)$; so $\phi = E\epsilon^{1/2}$. We will consider E, A and L as design variables and determine sensitivity of the tip deflection. Transformation to the reference volume gives $x = L\xi$, $a = AA$, $J = AL$, $V = AL$, and $\bar{V} = 1$. Nonlinear analysis of the primary structure yields:

$$u(\xi) = \frac{P^2 L \xi}{A^2 E^2}; \quad \bar{u}(L) = -\frac{2P^2 L}{A^2 E^3} \bar{\delta} E - \frac{2P^2 L}{A^3 E^2} \bar{\delta} A + \frac{P^2}{A^2 E^2} \bar{\delta} L \quad (53)$$

The functional for sensitivity analysis is given as

$$\psi = \int_0^1 \int_{\bar{A}} \bar{A}^{-1} L^{-1} u(\xi) \hat{\delta}(\xi-1) (AL) d\bar{A} d\xi \quad (54)$$

$$G = A^{-1} L^{-1} u(\xi) \hat{\delta}(\xi-1); \quad G_{,u} = A^{-1} L^{-1} \hat{\delta}(\xi-1) \quad (55)$$

The adjoint structure is linear with the stress-strain law as

$$\sigma^a = \phi_{,\epsilon} \epsilon^a = \frac{1}{2} E \epsilon^{1/2} \epsilon^a = \frac{AE^2}{2P} \epsilon^a \quad (56)$$

The equilibrium equation for the adjoint structure gives

$$u^a(\xi) = \frac{2PL\xi}{A^2 E^2}, \quad u_{,\xi}^a = \frac{2PL}{A^2 E^2} \quad (57)$$

The sensitivity formula of Eq. (37) reduces to

$$\begin{aligned} \bar{\delta}\psi = & \int_0^1 \int_{\bar{A}} (-\epsilon^a \bar{\delta}\phi - \sigma^a \bar{\delta}\epsilon - \sigma \bar{\delta}\epsilon^a + \bar{\delta}G) J d\bar{A} d\xi \\ & + \int_0^1 \int_{\bar{A}} (-\sigma \epsilon^a + G) \bar{\delta} J d\bar{A} d\xi \end{aligned} \quad (58)$$

Various quantities for Eq. (58) are

$$\epsilon = u_{,\xi} L^{-1} = \frac{P^2 L}{A^2 E^2}; \quad \epsilon^a = u_{,\xi}^a L^{-1} = \frac{2PL}{A^2 E^2}; \quad \bar{\delta}G = u \hat{\delta}(\xi-1) \bar{\delta}(AL)^{-1}$$

$$\sigma = E \epsilon^{1/2}; \quad \phi_{,\epsilon} = (1/2) E \epsilon^{-1/2}, \quad \bar{\delta}\phi = \epsilon^{1/2} \bar{\delta}E; \quad \sigma^a = \phi_{,\epsilon} \epsilon^a$$

$$\bar{\delta}\epsilon = u_{,\xi} \bar{\delta}L^{-1} = -L^{-2} u_{,\xi} \delta L; \quad \bar{\delta}\epsilon^a = -L^{-2} u_{,\xi}^a \delta L$$

Substituting these quantities into Eq. (58), we obtain the sensitivity formula of Eq. (53). It is interesting to observe sensitivity meaning of the adjoint displacement field in Eq. (57); i.e. $u^a(\xi) = d\psi/dP$.

Example 4. Geometrically Nonlinear Problem

Consider the two bar structure shown in Fig. 5. The material for the structure is linear, so $\sigma = E\epsilon$. Transformation to the reference volume is shown in the

figure. The design variables for the problem are $\mathbf{b} = (E, A, L)$. The strain for the problem is given as

$$t_o \epsilon = (t_L - o_L)/o_L = \frac{1}{2} w^2 L^{-2} \equiv \epsilon \quad (59)$$

The deflection at the center and member strains are calculated as

$$w = \frac{P^{1/3} L}{(EA)^{1/3}}; \quad \bar{\epsilon} = \epsilon L^2 = \frac{1}{2} w^2 = \frac{P^{2/3} L^2}{(EA)^{2/3}} \quad (60)$$

The incremental equilibrium equation in terms of displacement at the center is $3EA w^2 L^{-3} \delta w = \delta P$. The functional for sensitivity analysis is given as

$$\psi = \int_0^1 \int_{\bar{A}} (AL)^{-1} w(\xi) \hat{\delta}(\xi-1) AL d\bar{A} d\xi \quad (61)$$

$$G = (AL)^{-1} w(\xi) \hat{\delta}(\xi-1); \quad G_{,w} = (AL)^{-1} \hat{\delta}(\xi-1) \quad (62)$$

The equilibrium equation for the adjoint structure (using the incremental equilibrium equation of the primary structure) is given as

$$3EA L^{-3} w^2 w^a = \int_0^1 \int_{\bar{A}} (AL)^{-1} \hat{\delta}(\xi-1) AL d\bar{A} d\xi = 1$$

$$w^a = \frac{L^3}{3EA w^2} = \frac{L}{3E^{1/3} A^{1/3} P^{2/3}} \quad (63)$$

Total axial displacement and displacement at any point are given as

$$u^a(L) = w^a \sin \theta = w^a w L^{-1}; \quad u^a(\xi) = w^a w L^{-1} \xi \quad (64)$$

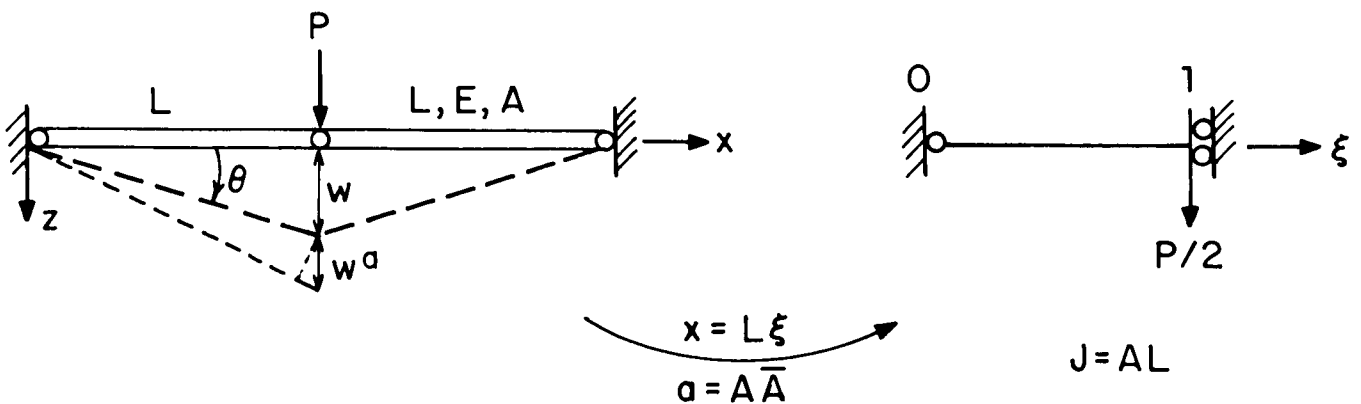


Figure 5. Two Member Structure

The adjoint strains are given as

$$\epsilon^a = w^a w_L^{-2} = \bar{\epsilon}^a L^{-2}, \quad \bar{\epsilon}^a = w^a w \quad (65)$$

The sensitivity formula of Eq. (37) reduces to

$$\begin{aligned} \bar{\delta}\psi = & 2 \int_0^1 \int_{\bar{A}} (-\epsilon^a \bar{\delta}\phi - \sigma^a \bar{\delta}\epsilon - \sigma \bar{\delta}\epsilon^a + \bar{\delta}G) J d\bar{A} d\xi \\ & + 2 \int_0^1 \int_{\bar{A}} (-\sigma \epsilon^a + G) \bar{\delta}J d\bar{A} d\xi \end{aligned} \quad (66)$$

Note that factor of 2 is used because volume integrals in Eq. (37) are for the entire structure. Various quantities for Eq. (66) are

$$\begin{aligned} \bar{\delta}\phi &= \epsilon \delta E; \quad \bar{\delta}\epsilon = \bar{\epsilon} \delta L^{-2} = -w^2 L^{-3} \delta L; \quad \bar{\delta}\epsilon^a = \bar{\epsilon}^a \delta L^{-2} = -2w w^a L^{-3} \delta L \\ \sigma &= E\epsilon = \frac{1}{2} E w^2 L^{-2}; \quad \sigma^a = E\epsilon^a = E w w^a L^{-2}; \quad \bar{\delta}J = L\delta A + A\delta L \end{aligned} \quad (67)$$

Substituting these quantities into Eq. (66), we get

$$\bar{\delta}\psi = - \frac{P^{1/3} L}{3E^{4/3} A^{1/3}} \bar{\delta}E - \frac{P^{1/3} L}{3E^{1/3} A^{4/3}} \bar{\delta}A + (P/EA)^{1/3} \bar{\delta}L \quad (68)$$

which can also be obtained directly from Eq. (60). Comparing w and w^a in Eqs. (60) and (63), we again observe the sensitivity interpretation of the adjoint displacement field.

Next, consider the member stress given in Eq. (67) as $\sigma = (P^{2/3} E^{1/3}) / (2A^{2/3})$. Its design sensitivity is given as

$$\bar{\delta}\sigma = \frac{P^{2/3}}{6E^{2/3} A^{2/3}} \bar{\delta}E - \frac{P^{2/3} E^{1/3}}{3A^{5/3}} \bar{\delta}A + (0) \bar{\delta}L \quad (69)$$

The functional for design sensitivity analysis is given as

$$\psi = \int_0^1 \int_{\bar{A}} (AL)^{-1} \sigma AL d\bar{A} d\xi = \int_0^1 \int_{\bar{A}} G(\sigma) AL d\bar{A} d\xi \quad (70)$$

The adjoint load G, \mathbf{u} in this case is zero but initial strain in the adjoint structure and stress strain law are given as $\epsilon^{ai} = G, \sigma = (AL)^{-1}$, $\sigma^a = E(\epsilon^a - \epsilon^{ai})$. The adjoint equilibrium equation in terms of central displacement gives $w^a = (wA)^{-1} L/3$ and $\epsilon^a = w w^a L^{-2} = (AL)^{-1}/3$. Substituting appropriate quantities in Eq. (37), it can be verified that Eq. (69) is obtained. It can be also directly verified that $w^a = d\psi/dP \equiv d\sigma/dP$.

7. CONCLUDING REMARKS

A general formula for design sensitivity analysis of linear and nonlinear structures using variational approach has been developed. Equations of continuum mechanics are used and the concepts of reference volume and adjoint structure are exploited. Use of the formula is demonstrated on a few simple analytical problems. The theory can be easily adapted for finite element modelling of structures. The finite element models for the primary and adjoint structures can be independent of each other. For modelling of design optimization problems, the concept of a reference volume is translated to the concept of a design element that is invariant with respect to design changes. These observations can have considerable implications in numerical implementations for design sensitivity analysis and optimization of complex structures.

Considerable numerical work has been done for design sensitivity analysis and optimization of linear structures.¹ Material derivative approach has been exploited for shape optimization. In this regard recent work of Choi and Co-workers,²³ Yang and Co-workers²⁴ and Hou and Co-workers²⁵ is significant. Yang and Co-workers²⁴ have shown equivalence of variational and finite element formulations of design sensitivity analysis of shape problems for linear structures. This equivalence can also be shown for nonlinear problems. Hou and Co-workers²⁵ have discussed some difficulties with the material derivative approach of design sensitivity analysis of linear shape problems. They have suggested numerical procedures to improve accuracy of the approach.

Design sensitivity analysis and optimization with nonlinear response is just beginning to be studied. Finite element approach for nonlinear stresses, strains, displacements and the buckling load has been recently studied.²⁶⁻³² More research needs to be done to fully develop this area.

REFERENCES

¹Adelman, H.M. and Haftka, R.T., "Sensitivity Analysis of Discrete Structural Systems," AIAA Journal, Vol. 24, No. 5, May 1986, pp. 823-832.

²Adelman, H.M. and Haftka, R.T. (Eds.), "Sensitivity Analysis in Engineering," Proceedings of the NASA Symposium, NASA Langley Research Center, Hampton, VA, NASA CP 2457, 1987.

³Gadala, M.S., Dokainish, M.A., and Oravas, A.E.G., "Formulation Methods of Geometric and Material Nonlinear Problems," International Journal for Numerical Methods in Engineering, Vol. 20, 1984, pp. 887-914.

⁴Bathe, K.J., Finite Element Procedures in Engineering Analysis, Prentice-Hall, Englewood Cliffs, N.J., 1982.

⁵Ryu, Y.S. and Arora, J.S., "Review of Nonlinear FE Methods with Substructures," Journal of Engineering Mechanics Division, ASCE, Vol. 111, No. 11, November 1985, pp. 1361-1379.

⁶Bathe, K.J. (Ed.), "Proceedings of the 5th ADINA Conference," Computers and Structures, Vol. 21, Nos. 1/2, 1985.

⁷Haber, R.B., "Application of The Eulerian Lagrangian Kinematic Description to Structural Shape Optimization," Proceedings of NATO Advanced Study Institute on Computer-Aided Optimal Design, C.A. Mota Soares (Ed.), Troia, Portugal, June 29 - July 11, 1986, pp. 297-307.

⁸Arora, J.S. and Govil, A.K., "Design Sensitivity Analysis with Substructuring," Journal of Engineering Mechanics Division, ASCE, Vol. 103, No. EM4, 1977, pp. 537-548.

⁹Arora, J.S. and Haug, E.J., "Methods of Design Sensitivity Analysis in Structural Optimization," AIAA Journal, Vol. 17, Sept. 1979, pp. 970-974.

¹⁰Haug, E.J. and Arora, J.S., "Design Sensitivity Analysis of Elastic Mechanical Systems," Computer Methods in Applied Mechanics and Engineering, Vol. 15, 1978, pp. 35-62.

¹¹Haug, E.J. and Arora, J.S., Applied Optimal Design, Wiley-Interscience, John Wiley and Sons, New York, N.Y. 1979.

¹²Hsieh, C.C. and Arora, J.S., "Structural Design Sensitivity Analysis with General Boundary Conditions: Static Problem," International Journal for Numerical Methods in Engineering, Vol. 20, 1984, pp. 1661-1670.

¹³Haug, E.J., Choi, K.K., and Komkov, V., Design Sensitivity Analysis of Structural Systems, Academic Press, Orlando, FL, 1986.

¹⁴Dems, K. and Mroz, Z., "Variational Approach by Means of Adjoint Systems to Structural Optimization and Sensitivity Analysis - I. Variation of Material Parameters Within Fixed Domain," International Journal of Solids and Structures, Vol. 19, No. 8, 1983, pp. 677-692.

¹⁵Dems, K. and Mroz, Z., "Variational Approach by Means of Adjoint Systems to Structural Optimization and Sensitivity Analysis - II: Structure Shape Variation," International Journal of Solids and Structures, Vol. 6, 1984, pp. 527-552.

¹⁶Dems, K. and Mroz, Z., "Variational Approach to First- and Second-Order Sensitivity Analysis of Elastic Structures," International Journal for Numerical Methods in Engineering, Vol. 21, 1985, pp. 637-661.

¹⁷Dems, K., "Sensitivity Analysis in Thermoelasticity," Proceedings of NATO Advanced Study Institute on Computer-Aided Optimal Design, C.A. Mota Soares (Ed.), Troia, Portugal, June 29 - July 11, 1986, pp. 287-297.

¹⁸Haftka, R.T. and Mroz, Z., "First and Second Order Sensitivity Analysis of Linear and Nonlinear Structures," AIAA Journal, Vol. 24, No. 7, July 1986, pp. 1187-1192.

¹⁹Mroz, Z., Kamat, M.P., and Plant, R.H., "Sensitivity Analysis and Optimal Design of Nonlinear Beams and Plates," Journal of Structural Mechanics, Vol. 13, Nos. 3/4, 1985, pp. 245-266.

²⁰Mroz, Z., "Sensitivity Analysis and Optimal Design with Account for Varying Shape and Support Conditions," Proceedings of NATO Advanced Study Institute on Computer-Aided Optimal Design, C.A. Mota Soares (Ed.), Troia, Portugal, June 29 - July 11, 1986, pp. 109-144.

²¹Belegundu, A.D., "Lagrangian Approach to Design Sensitivity Analysis," Journal of Engineering Mechanics Division, ASCE, Vol. 111, No. 5, May 1985, pp. 680-695.

²²Belegundu, A.D. and Arora, J.S., "A Sensitivity Interpretation of Adjoint Variables in Optimal Design," Computer Methods in Applied Mechanics and Engineering, Vol. 48, 1985, pp. 81-89.

²³Choi, K.K., "Shape Design Sensitivity Analysis and Optimal Design of Structural Systems," Proceedings of NATO Advanced Study Institute on Computer-Aided Optimal Design, C.A. Mota Soares (Ed.), Troia, Portugal, June 29 - July 11, 1986, pp. 54-108.

²⁴Yang, R.J. and Botkin, M.E., "Comparison between the Variational and Implicit Differentiation Approaches to Shape Design Sensitivities," AIAA Journal, Vol. 24, No. 6, June 1986, pp. 1027-1032.

²⁵Hou, J.W., Chen, J.L., and Sheen, J.S., "Computational Method for Optimization of Structural Shapes," AIAA Journal, Vol. 24, No. 6, June 1986, pp. 1005-1012.

²⁶Ryu, Y.S., Haririan, M., Wu, C.C., and Arora, J.S., "Methods of Design Sensitivity Analysis for Nonlinear Response," Computers and Structures, Vol. 21, No. 1/2, 1985, pp. 245-255.

²⁷Haririan, M. and Arora, J.S., "Use of ADINA for Design Optimization of Nonlinear Structures," Computers and Structures, 1987.

²⁸Wu, C.C. and Arora, J.S., "Simultaneous Analysis and Design Optimization of Nonlinear Response," Engineering with Computers, 1987.

²⁹Wu, C.C. and Arora, J.S., "Design Sensitivity Analysis of Nonlinear Response Using Incremental Procedure," AIAA Journal, 1987.

³⁰Wu, C.C. and Arora, J.S., "Design Sensitivity Analysis of Nonlinear Buckling Load," Computational Mechanics, 1987.

³¹Arora, J. and Wu, C.C., "Design Sensitivity Analysis of Nonlinear Structures," Proceedings of NATO Advanced Study Institute on Computer-Aided Optimal Design, C.A. Mota Soares (Ed.), Troia, Portugal, June 29 - July 11, 1986, pp. 228-246.

³²Kamat, M.P., "Optimization of Shallow Arches Against Instability Using Sensitivity Derivatives," Proceedings of the NASA Symposium on Sensitivity Analysis in Engineering, H.M. Adelman and R.T. Haftka (Eds.), Langley Research Center, Hampton, VA, NASA CP 2457, 1987.

OPTIMAL CONTROL CONCEPTS IN DESIGN SENSITIVITY ANALYSIS

Ashok D. Belegundu
Mechanical Engineering Department
The Pennsylvania State University
University Park, PA

ABSTRACT

In this paper, a close link is established between open loop optimal control theory and optimal design by noting certain similarities in the gradient calculations. The resulting benefits include a unified approach, together with physical insights in design sensitivity analysis, and an efficient approach for simultaneous optimal control and design. Both matrix displacement and matrix force methods are considered, and results are presented for dynamic systems, structures, and elasticity problems.

1. INTRODUCTION

Considerable interest is being shown in recent years on control of flexible systems such as robots and space structures. In control theory and optimal control in particular, the geometry (dimensions and shape) is given, and the task is to develop a control law so as to ensure proper operation of the system in an uncertain environment. In design, and optimal design in particular, the task is to determine the geometry. Evidently, at least in the preliminary design stages, there is interaction between optimal control and optimal design. There is a need for better understanding of this interaction. In this paper, a close link is established between these two disciplines. Specifically, the similarity of the sensitivity calculations and adjoint equations is examined. Practical benefits and new possibilities are discussed. Dynamic systems, structures, and continuum elasticity models are considered. Both displacement and matrix force methods of structural analysis are treated.

2. THE LAGRANGE MULTIPLIER RULE FOR CALCULATING SENSITIVITY COEFFICIENTS

The Lagrange multiplier rule is a well-known method for obtaining optimality conditions in the presence of constraints. The rule, however, serves equally well in obtaining expressions for sensitivity coefficients (or derivatives) of implicit functions, as shown below.

Consider the scalar valued function $f = f(x, b)$, where x is an $(n \times 1)$ vector of 'state' variables and b is a $(k \times 1)$ vector of design variables. The function f is implicit in that for every vector b , x satisfies the state

equation

$$\underline{g}(\underline{x}, \underline{b}) = \underline{0} \quad (1)$$

where \underline{g} is $(n \times 1)$ vector function. It is desired to obtain the sensitivity vector df/db . In design of structural and mechanical systems, f often represents the stress or displacement of a point and Eq. (1) is the equation of equilibrium. To illustrate the Lagrange multiplier rule for calculating df/db , we first form the scalar valued function H as

$$H = f + \underline{\lambda}^T \underline{g} \quad (2)$$

where $\underline{\lambda}$ is an $(n \times 1)$ vector of Lagrange multipliers or 'adjoint' variables. Noting that f , \underline{g} and H are functions of \underline{x} and \underline{b} , we have, upon differentiating H with respect to \underline{b} ,

$$dH/db = \partial H/\partial b + \partial H/\partial \underline{x} \quad d\underline{x}/db \quad (3)$$

The idea behind the Lagrange multiplier rule is to require that $\underline{\lambda}$ satisfy the equations

$$\partial H/\partial \underline{x} = \underline{0} \quad (4)$$

Assuming that $\partial \underline{g}/\partial \underline{x}$ is a nonsingular matrix -- which is necessary for \underline{x} to be a unique solution to Eq. (1) -- and using Eq. (4), we can obtain $\underline{\lambda}$ from the following 'adjoint equations':

$$[\partial \underline{g}/\partial \underline{x}]^T \underline{\lambda} = - \partial f/\partial \underline{x}^T \quad (5)$$

Equation (3) now provides the result

$$df/db = \partial H/\partial b \quad (6)$$

or,

$$df/db = \partial f/\partial b + \underline{\lambda}^T \partial \underline{g}/\partial b. \quad (7)$$

In Eq. (7), the term $\underline{g}^T \partial \underline{\lambda}/\partial b$ does not appear because of Eq. (1).

The fact that the Lagrange multiplier rule offers a unified approach to design sensitivity analysis has been discussed in Ref. 1. Further, the adjoint method of design sensitivity analysis given in Ref. 2 results in the exact same equations as obtained using the Lagrange multiplier rule. In this paper, the use of this rule to obtain expressions for sensitivity coefficients helps to establish a close link between optimal design and optimal control, as discussed in the next section.

3. OPTIMAL CONTROL AND OPTIMAL DESIGN

Optimal Control

To present the basic concepts, consider a dynamic system described by the following nonlinear differential equations

$$\dot{\underline{x}} = \underline{q}(\underline{x}(t), \underline{u}(t), t); \underline{x}(t_0) \text{ given, } t_0 \leq t \leq t_f \quad (8)$$

where the 'state' $\underline{x}(t)$, an $(n \times 1)$ vector function, is determined by the 'control' $\underline{u}(t)$, a $(k \times 1)$ vector function. Consider a performance index given by the scalar functional

$$F = \int_{t_0}^{t_f} f(\underline{x}(t), \underline{u}(t), t) dt \quad (9)$$

The optimal control problem is to find $\underline{u}(t)$ that minimizes (or maximizes) F [3]. The Lagrange multiplier rule as discussed in the previous section, is used to do this. Adjoin the system in Eq. (8) to F with multiplier functions (or adjoint variables) $\underline{\lambda}(t)$:

$$\bar{F} = \int_{t_0}^{t_f} [f + \underline{\lambda}^T (\underline{q} - \dot{\underline{x}})] dt \quad (10)$$

If we define the scalar function H , the Hamiltonian, as

$$H = f + \underline{\lambda}^T \underline{q} \quad (11)$$

and integrate the last term on the right side of Eq. (10) by parts, we obtain

$$\begin{aligned} \bar{F} = & - \underline{\lambda}^T(t_f) \underline{x}(t_f) + \underline{\lambda}^T(t_0) \underline{x}(t_0) \\ & + \int_{t_0}^{t_f} [H + \dot{\underline{\lambda}}^T \underline{x}] dt \end{aligned} \quad (12)$$

Now, consider the variation in F due to variation in the control vector $\underline{u}(t)$ for fixed times t_0 and t_f and fixed initial conditions,

$$\begin{aligned} \delta \bar{F} = & - \underline{\lambda}^T \delta \underline{x} \Big|_{t=t_f} + \underline{\lambda}^T \delta \underline{x} \Big|_{t=t_0} + \int_{t_0}^{t_f} (\partial H / \partial \underline{x} + \dot{\underline{\lambda}}^T) \delta \underline{x} dt \\ & + \int_{t_0}^{t_f} \frac{\partial H}{\partial \underline{u}} \delta \underline{u} dt \end{aligned} \quad (13)$$

Since it is tedious to determine the variations $\delta \underline{x}(t)$ produced by a given $\delta \underline{u}(t)$, we choose the multiplier functions $\underline{\lambda}(t)$ to satisfy

$$\dot{\underline{\lambda}}^T = - \frac{\partial H}{\partial \underline{x}} = - \frac{\partial f}{\partial \underline{x}} - \underline{\lambda}^T \frac{\partial g}{\partial \underline{x}} \quad (14)$$

with boundary conditions

$$\underline{\lambda}^T(t_f) = \underline{0} \quad (15)$$

In view of the adjoint equations in (14) and (15), Eq. (13) yields

$$\delta F = \int_{t_0}^{t_f} \frac{\partial H}{\partial \underline{u}} \delta \underline{u} dt \quad (16)$$

The functions $\partial H / \partial \underline{u}$ can be interpreted as impulse response functions since each component of $\partial H / \partial \underline{u}$ represents the variation in F due to a unit impulse in the corresponding component of \underline{u} at time t [3]. Furthermore, $\partial H / \partial \underline{u}$ can be interpreted as the function-space gradient of F with respect to \underline{u} . This last interpretation is useful when using gradient methods to extremize F . For example, choosing $\underline{u}(t) = -\alpha \partial H / \partial \underline{u}$ corresponds to a steepest descent step to minimize F .

Finally, it should be noted that setting $\partial H / \partial \underline{u} = 0$ yields the optimality conditions. In the special case when F is quadratic in \underline{x} and \underline{u} and Eqs. (8) are linear, the optimality conditions together with the state equations (8) and adjoint equations (14) and (15) can be solved in closed form, leading to the Ricatti equations, which are very attractive in closed loop control since the feedback law is independent of the state vector \underline{x} and can be computed 'off-line'.

Optimal Design

In optimal design of mechanical systems, it is required to obtain the sensitivity vector dF/db where F is a cost or constraint functional of the form

$$F = \int_{t_0}^{t_f} f(\underline{x}(t), \underline{b}, t) dt \quad (17)$$

with \underline{b} a $(k \times 1)$ vector of design variables. For example, F represents a time-averaged performance measure of a vehicle traversing a rough terrain. Most gradient-based nonlinear programming codes require input of the vector

dF/db . In Eq. (17), for a given \underline{b} , \underline{x} should satisfy the equations of motion given by

$$\dot{\underline{x}} = \underline{q}(\underline{x}(t), \underline{b}, t); \underline{x}(t_0) \text{ given}, t_0 \leq t \leq t_f \quad (18)$$

As before, the use of the Lagrange multiplier rule requires the function

$$\bar{F} = \int_{t_0}^{t_f} [f + \underline{\lambda}^T (\underline{q} - \dot{\underline{x}})] dt \quad (19)$$

Integrating the last term on the right side of Eq. (19) by parts yields

$$\begin{aligned} \bar{F} = & - \underline{\lambda}^T(t_f) \underline{x}(t_f) + \underline{\lambda}^T(t_0) \underline{x}(t_0) \\ & + \int_{t_0}^{t_f} [H + \dot{\underline{\lambda}}^T \underline{x}] dt \end{aligned} \quad (20)$$

where H is defined in Eq. (11). Now, consider the variation in F due to variations (or differentials) in \underline{b} for fixed times t_0 and t_f , and fixed initial conditions:

$$\begin{aligned} \delta \bar{F} = & - \underline{\lambda}^T \delta \underline{x} \Big|_{t_f} + \underline{\lambda}^T \delta \underline{x} \Big|_{t_0} + \int_{t_0}^{t_f} (\partial H / \partial \underline{x} + \dot{\underline{\lambda}}^T) \delta \underline{x} dt \\ & + \int_{t_0}^{t_f} \partial H / \partial \underline{b} \delta \underline{b} dt \end{aligned} \quad (21)$$

If we choose $\lambda(t)$ to satisfy the same adjoint equations as in the optimal control problem in (14) and (15), we obtain

$$\delta F = \int_{t_0}^{t_f} \partial H / \partial \underline{b} \delta \underline{b} dt \quad (22)$$

Since \underline{b} is not a function of time, Eq. (22) yields the sensitivity coefficient vector

$$dF/db = \int_{t_0}^{t_f} \partial H / \partial b \, dt \quad (23)$$

Expressions as in Eq. (23) can then be fed into nonlinear programming codes to obtain improved design vectors \underline{b} . The main emphasis here, however, is to show that the calculation of design sensitivity vectors is simply a special case of open loop optimal control. That is, treating the control variables $u(t)$ as design variables enables us to obtain expressions for the sensitivity vectors.

The following advantages result from this observation:

- (1) A general approach to design sensitivity analysis is established.
- (2) Physical significance of the adjoint variables is established. In particular, in the above discussion, the functions $\partial H / \partial u$ are interpreted to be influence functions. The importance of such a physical interpretation in structural design is discussed subsequently.
- (3) The fact that the adjoint equations are the same in the optimal control and optimal design problems motivates an efficient gradient approach for simultaneous handling of control variables and design parameters. That is, functionals of the form

$$F = \int_{t_0}^{t_f} f(x(t), u(t), b, t) \, dt \quad (24)$$

where both control variables $u(t)$ and design parameters b have to be optimally chosen, can be treated efficiently. Such problems may arise, for example, when designing both a control law as well as determining the dimensions and shape for a robot or for a flexible space structure.

4. STRUCTURES

Matrix Displacement Method

The general results discussed in the preceding section lead to special insights when applied to structural systems. Consider a scalar function

$$f \equiv f(\underline{x}, \underline{b}) \quad (25)$$

where f typically represents the stress or displacement at some point in the structure, \underline{b} is a $(k \times 1)$ vector of design variables, and \underline{x} is the nodal

displacement vector. If a finite element model of the structure exists, then the (nx1) vector \underline{x} is obtained from the matrix displacement (finite element) equations

$$\underline{K}(\underline{b})\underline{x} = \underline{P}(\underline{b}) \quad (26)$$

where \underline{K} is an (nxn) structural stiffness matrix and \underline{P} is a vector of applied nodal loads.

The importance of applying optimal control concepts to structural systems described by (25) and (26) will now be shown. The sensitivity vector df/db will be obtained by using the Lagrange multiplier rule. Define the function H as

$$H = f + \underline{\lambda}^T (\underline{P} - \underline{K} \underline{x}) \quad (27)$$

where $\underline{\lambda}$ is the (nx1) adjoint vector. The variation of H due to a variation in \underline{b} is given by

$$\delta H = \partial H / \partial \underline{b} \delta \underline{b} + \partial H / \partial \underline{x} \delta \underline{x} \quad (28)$$

Choosing $\underline{\lambda}$ to satisfy

$$\partial H / \partial \underline{x} = 0 \quad (29)$$

which can also be written as $\underline{K} \underline{\lambda} = \partial f / \partial \underline{x}^T$, we have from Eq. (28),

$$\delta f = \partial H / \partial \underline{b} \delta \underline{b} \quad (30)$$

which yields

$$df / d\underline{b} = \partial H / \partial \underline{b} \quad (31)$$

Now, in the foregoing analysis, let us consider the variation in H due to a variation in \underline{P} . That is, we consider variations in the 'control' vector \underline{P} instead of the design vector \underline{b} . We have

$$\delta H = \partial H / \partial \underline{P} \delta \underline{P} + \partial H / \partial \underline{x} \delta \underline{x} \quad (32)$$

Choosing $\underline{\lambda}$ to satisfy the adjoint equation in (29), and noting that f and \underline{K} do not depend explicitly on \underline{P} for linear structures, we get

$$\delta f = \underline{\lambda}^T \delta \underline{P} \quad (33)$$

or,

$$\underline{\lambda}^T = df / d\underline{P} \quad (34)$$

Since the adjoint equations in (29) are the same regardless of whether the fundamental variation is in \underline{b} or \underline{P} , Eq. (34) shows that the adjoint vector

λ used in structural design sensitivity analysis represents the sensitivity of the function f to variations in the applied loads P . Further, if f is linear in P , then λ_i = value of f due to $P_i = 1$. In civil engineering, λ is the influence coefficient vector associated with the function f , as discussed in Ref. 4. Further, since Eqs. (29) can be written as

$$\underline{K} \underline{\lambda} = \partial f / \partial \underline{x}^T \quad (35)$$

we can think of λ as a displacement vector associated with the load vector $\partial f / \partial \underline{x}$. This motivates the use of element shape functions to obtain expressions for λ within the elements from knowing the nodal values. Thus, we can write

$$\lambda(\xi) = \sum_i \lambda_i N_i(\xi) \quad (36)$$

where λ_i are the nodal values obtained by solving Eq. (35) and N_i are the familiar shape functions used in finite element analysis.

The beam in Fig. 1(a) is solved to illustrate this. A finite element model of the beam is shown in Fig. 1(b). The function f is taken to be the moment at support b . The adjoint vector λ , representing the values of f due to unit loads along each degree of freedom, is obtained by solving Eq. (35). Equation (36) is used to obtain expressions for λ along the beam, which is used to draw the influence line as shown in Fig. 1(c). The results are in agreement with those in Ref. 5, and show that the adjoint method is a new and powerful approach for determining influence lines.

Some other interesting aspects relating to Eqs. (34) and (35) may now be noted. If we let f be the strain energy function U given by

$$U = \frac{1}{2} \underline{x}^T \underline{K} \underline{x} \quad (37)$$

then Eq. (35) yields $\underline{K} \underline{\lambda} = \underline{K} \underline{x}$, from which $\underline{\lambda} = \underline{x}$. Equation (34) then yields

$$\underline{x}^T = dU/d\underline{P} \quad (38)$$

which is a discrete version of Castigliano's theorem for linear structures.

Also, letting $f = \frac{1}{2} \underline{x}^T \underline{K} \underline{x} - \underline{x}^T \underline{F}$ = potential energy, results in $\underline{\lambda} = \underline{0}$ and $d\pi/d\underline{P} = 0$, which is a statement of the minimum potential energy theorem.

Matrix Force Method

The systematic use of the Lagrange multiplier rule or adjoint method for design sensitivity analysis and physical significance of adjoint variables, which was discussed in the context of displacement finite element analysis, will now be extended to structures analyzed by the the matrix force method.

For indeterminate structures, the equilibrium equations in the matrix force method take the form [6]

$$n_F \underline{F} + n_X \underline{X} = \underline{P} \quad (39)$$

where \underline{X} is a vector of 'redundant' or independent forces (and reactions), \underline{F} is a vector of dependent forces, and \underline{P} is the vector of externally applied forces. The redundants \underline{X} are obtained from compatibility conditions of the form

$$\underline{X} = C(\underline{b}) \underline{P} + \underline{d}(\underline{b}) \quad (40)$$

Consider now a function $f(\underline{b}, \underline{F}, \underline{X})$. Note that matrices C and d also depend on the design vector \underline{b} . Form the function H as

$$\begin{aligned} H = f(\underline{b}, \underline{F}, \underline{X}) &+ \underline{\lambda}^T (\underline{P} - n_F \underline{F} - n_X \underline{X}) \\ &+ \underline{\mu}^T (\underline{X} - C \underline{P} - \underline{d}) \end{aligned} \quad (41)$$

Consider the variation in H due to a variation in \underline{b} :

$$\begin{aligned} \delta H = \partial f / \partial \underline{b} \delta \underline{b} &+ (\partial f / \partial \underline{F} - \underline{\lambda}^T n_F) \delta \underline{F} \\ &+ (\partial f / \partial \underline{X} - \underline{\lambda}^T n_X + \underline{\mu}^T) \delta \underline{X} - \underline{\mu}^T (\delta C \cdot \underline{P} + \delta \underline{d}) \end{aligned} \quad (42)$$

Choosing $\underline{\lambda}$ to satisfy

$$n_F^T \underline{\lambda} = \partial f / \partial \underline{F}^T \quad (43)$$

and letting

$$\underline{\mu}^T = \underline{\lambda}^T n_X - \partial f / \partial \underline{X} \quad (44)$$

we have

$$\delta f = \partial f / \partial \underline{b} \delta \underline{b} - \underline{\mu}^T (\delta C \cdot \underline{P} + \delta \underline{d}) \quad (45)$$

from which the sensitivity vector is obtained as

$$df/d\underline{b} = \partial f / \partial \underline{b} - \underline{\mu}^T \partial / \partial \underline{b} (C \underline{P} + \underline{d}) \quad (46)$$

The physical significance of the adjoint variables $\underline{\lambda}$ and $\underline{\mu}$ is obtained in the usual manner by considering the variation of H in Eq. (41), due to a variation $\delta \underline{P}$ is \underline{P} . Upon defining $\underline{\lambda}$ as in Eq. (43) and $\underline{\mu}$ as in Eq. (44), we get

$$\delta f = (\underline{\lambda}^T - \underline{\mu}^T C) \delta \underline{P} \quad (47)$$

Thus, $(\underline{\lambda} - C^T \underline{\mu})$ is now the influence coefficient vector.

For statically determinate structures, the terms n_X , $\underline{\lambda}$ and $\underline{\mu}$ vanish, and Eq. (47) becomes

$$\delta f = \underline{\lambda}^T \delta \underline{P} \quad (48)$$

which is analogous to Eq. (33) that was obtained in the displacement method of analysis. In this case, λ_i = value of f due to $P_i = 1$, provided f is linear and homogeneous in \underline{P} .

5. ELASTICITY

This section will focus on elasticity problems. Consider a functional

$$F = \int_{\Omega} f(\sigma_{ij}) d\Omega \quad (49)$$

where σ_{ij} is the stress tensor, Ω is the domain of the elastic body, and the equilibrium equations in variational form are

$$\int_{\Omega} \sigma_{ij}(u) \epsilon_{ij}(\phi) d\Omega = \int_{\Gamma} \phi_i T_i d\Gamma + \int_{\Omega} \phi_i B_i d\Omega \quad (50)$$

Equation (50) is satisfied for every displacement field ϕ satisfying $\phi_i = 0$ on Γ_1 , u is the actual displacement field due to traction forces T_i and body forces B_i , and kinematic boundary conditions $u = 0$ is imposed on a portion Γ_1 of the total boundary. Equation (50) is simply the principle of virtual work, with $\epsilon_{ij}(\phi)$ being the virtual strain due to a kinematically admissible virtual displacement ϕ . As before, form the functional H as

$$H = \int_{\Omega} [f(\sigma_{ij}) - \sigma_{ij}(u) \epsilon_{ij}(\lambda)] d\Omega + \int_{\Gamma} \lambda_i T_i d\Gamma + \int_{\Omega} \lambda_i B_i d\Omega \quad (51)$$

where λ satisfies $\lambda = 0$ on Γ_1 . Consider a variation δT_i in T_i , and δB_i in B_i , and let $\sigma_{ij}(v)$ and $\epsilon_{ij}(v)$ be the corresponding variations in stress and strain, respectively. The variation in H is given by

$$\begin{aligned} \delta H = & \int_{\Omega} [\partial f / \partial \sigma_{ij} \sigma_{ij}(v) - \sigma_{ij}(v) \epsilon_{ij}(\lambda)] d\Omega \\ & + \int_{\Gamma} \lambda_i \delta T_i d\Gamma + \int_{\Omega} \lambda_i \delta B_i d\Omega \end{aligned} \quad (52)$$

Equation (52) holds true for all kinematically admissible λ , and consequently holds true for a λ determined from the following adjoint equations:

$$\int_{\Omega} \sigma_{ij}(\lambda) \epsilon_{ij}(\Psi) d\Omega = \int_{\Omega} \partial f / \partial \sigma_{ij} \sigma_{ij}(\Psi) d\Omega \quad (53)$$

which is satisfied for all Ψ , $\Psi = 0$ on Γ_1 . Since

$$\int_{\Omega} \sigma_{ij}(\lambda) \epsilon_{ij}(\Psi) d\Omega = \int_{\Omega} \sigma_{ij}(\Psi) \epsilon_{ij}(\lambda) d\Omega$$

putting $\Psi = v$ in Eq. (53), Eq. (52) yields

$$\delta F = \int_{\Gamma} \lambda_i \delta T_i + \int_{\Omega} \lambda_i \delta B_i d\Omega \quad (54)$$

Equation (54) is essentially a variational principle. If we let the functional F be the complementary strain energy density, that is, we let

$$F = \int_{\Omega} \left[\int_0^{\sigma_{ij}} \epsilon_{ij} d\sigma_{ij} \right] d\Omega \quad (55)$$

then Eq. (54) yields (upon using Leibnitz's rule)

$$\int_{\Omega} \epsilon_{ij} \delta \sigma_{ij} d\Omega = \int_{\Gamma} \lambda_i \delta T_i d\Gamma + \int_{\Omega} \lambda_i \delta B_i d\Omega \quad (56)$$

which is the principle of complementary virtual work [7]. Finally, sensitivity expressions can be readily obtained if variation of H due to design variations is considered as done in previous sections. This approach holds true for a changing domain, as in shape optimal design [1]. From Eq. (54), we can see that λ_i at a point represents the value of F due to a unit load at that point. This fact can be written in terms of Green's function as

$$\lambda_i = \int_{\Omega} f(\sigma_{ij}(G_i)) d\Omega \quad (57)$$

where the Green's function G is the displacement field due to a unit load.

6. FUTURE WORK

In both optimal control and optimal design, it is shown that the Hamiltonian function and the Lagrange multiplier rule play a similar role. Optimal control theory helps to obtain a unified framework for design sensitivity analysis and physical understanding of adjoint variables. Some areas which may merit future investigation are noted below.

1. This work motivates an efficient gradient approach for optimal design of systems with control in mind. That is, both control variables and geometric design parameters can be considered simultaneously in the preliminary design stages.
2. In structures, the adjoint method provides a powerful method for constructing influence lines in the framework of finite element analysis. Also, the equation $\lambda^T = df/d\bar{p}$ can be used to design structures which are insensitive to loads P_i by minimizing λ_i^2 , or can be used to optimally locate the loads for maximum utilization of the structure, by maximizing $\lambda^T \bar{p}$ subject to suitable constraints.
3. The stability analysis of the adjoint equations that has been carried out extensively in optimal control theory may turn out to be of importance to the design engineer.

7. REFERENCES

1. A. D. Belegundu, "Lagrangian Approach to Design Sensitivity Analysis", ASCE J. of Engr. Mech., Vol. 111, No. 5, May 1985, pp. 680-695.
2. E. J. Haug and J. S. Arora, Applied Optimal Design, Wiley, 1979.
3. A. E. Bryson, Jr. and Y. C. Ho, Applied Optimal Control, Hemisphere Publ. Corp., 1975.
4. A. D. Belegundu, "Interpreting Adjoint Equations in Structural Optimization", ASCE J. of Str. Engr., Vol. 112, No. 8, Aug. 1986, pp. 1971-1976.
5. C. H. Norris and J. B. Wilbur, Elementary Structural Analysis, McGraw-Hill, 1960.
6. J. S. Przemieniecki, Theory of Matrix Structural Analysis, McGraw-Hill, 1968.
7. C. L. Dym and I. H. Shames, Solid Mechanics: A Variational Approach, McGraw-Hill, 1973.

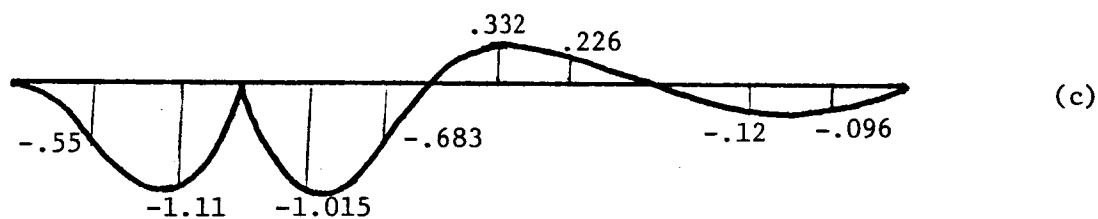
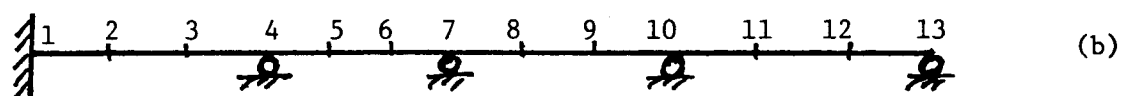
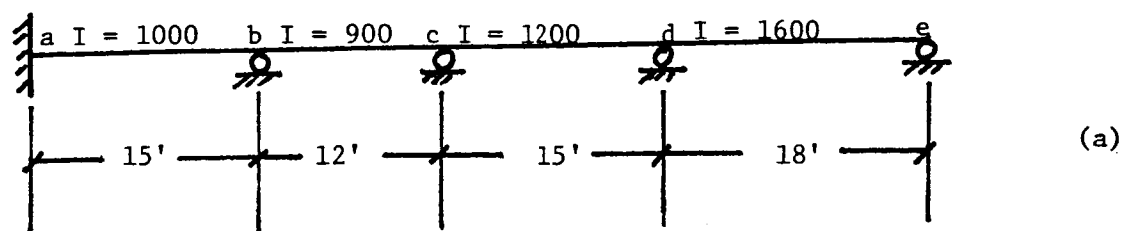


Figure 1. (a) Beam Problem,
 (b) Finite Element Model of Beam,
 (c) Influence Line for Moment at Support b of Beam

SENSITIVITY AND OPTIMIZATION OF COMPOSITE STRUCTURES USING MSC/NASTRAN

Gopal K. Nagendra* and Claude Fleury**

* The MacNeal-Schwendler Corporation, Los Angeles, CA

**UCLA
Los Angeles, CAABSTRACT

Design sensitivity analysis for composites will soon be available in MSC/NASTRAN. The design variables for composites can be lamina thicknesses, orientation angles, material properties or a combination of all three. With the increasing use of composites in aerospace and automotive industries, this general capability can be used in its own right for carrying out sensitivity analysis of complicated real-life structures.

As part of a research effort, the sensitivity analysis has been coupled with a general-purpose optimizer. This preliminary version of the optimizer is capable of dealing with minimum weight structural design with a rather general design variable linking capability at the element level or system level. Only sizing type of design variables (i.e., lamina thicknesses) can be handled by the optimizer.

Test cases have been run and validated by comparison with independent finite element packages. The linking of design sensitivity capability for composites in MSC/NASTRAN with an optimizer would give designers a powerful automated tool to carry out practical optimization design of real-life complicated composite structures.

PRECEDING PAGE BLANK NOT FILMED

INTRODUCTION

The purpose of this paper is to present the considerations and the resultant approach used to implement design sensitivity capability for composites into MSC/NASTRAN. MSC/NASTRAN is a large-scale, general-purpose computer program which solves a wide variety of engineering problems by the finite-element method. In addition, as part of a research effort, MSC/NASTRAN has been coupled with a general-purpose optimizer CONLIN to optimize composite structures with sizing type variables.

The following sections will cover:

- The analysis of laminated composites in MSC/NASTRAN
- Theory for design sensitivity analysis for composites
- The program architecture and considerations that go into implementing such a capability into a large-scale general-purpose computer program
- Basic optimization concepts and a brief description of the optimizer CONLIN used for this study
- Numerical studies to validate the results

THE ANALYSIS OF LAMINATED COMPOSITE MATERIALS IN MSC/NASTRAN

Laminated composites may be conceptually viewed as a "stack" of laminae with different orientations of the principal material directions in the individual lamina. An exploded view of three cross-ply laminated plates is illustrated in Figure 1. The n -laminae ($n = 2,3,4$) of each of the three configurations are normal to the z -axis of the indicated coordinate system and the 1- and 2-axes appended to the individual lamina denote principal material axis directions. The directions of the principal material axes of each lamina alternate as implied by the use of the word "cross-ply" to describe the configuration. The xy -plane of the coordinate axes is defined in the geometric middle plane of the laminae.

An entire "stack" of laminae may be modeled with a single plate or shell element because the material properties of the "stack" are completely reflected in the matrices of elastic moduli for the element. These matrices are automatically calculated in MSC/NASTRAN from user-supplied definitions of the thickness, the material properties, and the relative orientation of these properties for the individual lamina. Once these matrices of elastic moduli are calculated, the analysis proceeds in a standard manner. This capability for the automatic representation of laminated composites is available in linear static analysis, real and complex eigenvalue analysis, buckling analysis, geometric nonlinear analysis, and a dynamic analysis [1].

In the analysis of isotropic materials, strength is independent of the orientation of the body under load and one may compare the largest computed principal stress with an allowable stress to establish the integrity of the structure. Laminated composites, on the other hand, are orthotropic materials and may exhibit unequal properties in tension and compression. Thus, the strengths of these orthotropic laminae are a function of body orientation relative to the imposed stresses.

As the evaluation of the matrices of material moduli for laminated composites provides sufficient information to determine the actual stress field sustained by the material, the determination of structural integrity will depend on the definition of an allowable stress field. The basic ingredient of this definition is the establishment of a set of allowable stresses or strengths in the principal material directions.

X_t = Allowable tensile stress in the principal x(or 1)-direction of the material

X_c = Allowable compressive stress in the principal x(or 1)-direction of the material

Y_t = Allowable tensile stress in the principal y(or 2)-direction of the material

Y_c = Allowable compressive stress in the principal y(or 2)-direction of the material

S = Allowable shear stress in the principal material system

Failure index of an element is a measure designed to test whether the state of stress in the worst-stressed lamina is within or outside the lamina's failure envelope.

In addition, the interlaminar shear stress will be checked against the allowable bonding stress (S_b) specified by the user.

The failure index for the laminate is the larger of the two values so obtained. Three failure criteria are available in MSC/NASTRAN. They are Hill, Hoffman and Tsai-wu. In this paper Hill's failure criterion will be used, i.e.,

$$\frac{\sigma_1^2}{X^2} + \frac{\sigma_2^2}{Y^2} - \frac{\sigma_1 \sigma_2}{X^2} + \frac{\sigma_{12}^2}{S^2} = 1$$

$X = X_t$ if σ_1 is tensile
 $= X_c$ if σ_1 is compressive

$Y = Y_t$ if σ_2 is tensile
 $= Y_c$ if σ_2 is compressive

For the product term, $X = X_t$ if σ_1 and σ_2 are of the same sign; $X = X_c$

otherwise. Basically the equation represents a failure envelope in the stress space (figure 2).

If the state of stress in the orthotropic lamina ($\sigma_1, \sigma_2, \sigma_{12}$) is such that the stress point is within or on the envelope, the lamina is said to be "safe"; if the point is outside, the lamina is said to have "failed".

DESIGN SENSITIVITY CAPABILITY FOR COMPOSITES IN MSC/NASTRAN

Design sensitivity analysis for composites will soon be available in MSC/NASTRAN. The design variable for composites can be lamina thicknesses, orientation angles, material properties, or a combination of all three. With the increasing use of composites in aerospace and automotive industries, this general capability can be used in its own right for carrying out sensitivity analysis of complicated real-life structures.

Design sensitivity analysis estimates the effects of interrelated design variables such as element properties and materials on the structural response quantities, such as displacement, stress, natural frequency, buckling loads, and for composites lamina stresses and failure indices. Design sensitivity coefficients are defined as the gradients of the design constraints with respect to the design variables at the current design point. The method chosen for incorporation into MSC/NASTRAN is called the Pseudo load technique, based on a first variation (finite-difference scheme) of the systems equilibrium equations with respect to the design variables.

Let $\psi_i(b_j, u_g)$ be a set of design constraints which are functions of b_j design variables and displacements u_g . The design constraints are expressed as

$$\psi_i(b_j, u_g) < 0$$

The first variation in ψ_i is given as

$$\delta\psi_i = \left[\frac{\partial\psi_i}{\partial b_j} \right]_{ixj} \{ \delta b_j \}_{jx1} + \left[\frac{\partial\psi_i}{\partial u_g} \right]_{ixn} \{ \delta u_g \}_{nx1} \quad \begin{matrix} \text{u-fixed} & & \text{b-fixed} \end{matrix}$$

consider u_g as a function of b_j , then

$$\{ \delta u_g \}_{nxj} = \left[\frac{\partial u_g}{\partial b_j} \right]_{nxj} \{ \delta b_j \}_{jx1}$$

Thus

$$\{\delta\psi_i\} = \left(\left[\frac{\partial\psi_i}{\partial b_j} \right] + \left[\frac{\partial\psi_i}{\partial u_g} \right] \left[\frac{\partial u_g}{\partial b_j} \right] \right) \{\delta b_j\}$$

or

$$\frac{\delta\psi_i}{\delta b_j} = \frac{\Delta\psi_i}{\Delta b_j} = \left[\frac{\partial\psi_i}{\partial b_j} \right] + \left[\frac{\partial\psi_i}{\partial u_g} \right] \left[\frac{\partial u_g}{\partial b_j} \right]$$

The matrix $\frac{\partial u_g}{\partial b_j}$ can be evaluated by taking the first variation of the systems equilibrium equation

$$[K_g]\{u_g\} = \{P_g\}$$

or

$$[K_g]\{\Delta u_g\} + [\Delta k_g]\{u_g\} = \{\Delta P_g\}$$

or

$$\{\Delta u_g\} = [K_g]^{-1} (\{\Delta P_g\} - [\Delta k_g]\{u_g\})$$

or

$$[\Delta u_g] = [K_g]^{-1} (\{\Delta P_g(\Delta b_1)\}, \{\Delta P_g(\Delta b_2)\}, \dots, \{\Delta P_g(\Delta b_j)\}) \\ - [K_g]^{-1} ([\Delta k_g(\Delta b_1)]\{u_g\}, [\Delta k_g(\Delta b_2)]\{u_g\}, \dots, [\Delta k_g(\Delta b_j)]\{u_g\})$$

The elements of $\left[\frac{\partial\psi_i}{\partial u_g} \right]$ matrix for an element constraint, such as stress, force, or a failure index, can be expressed by the relationship

$$\{\psi_i\} = [S]_e \{u_g\}$$

or

$$\left[\frac{\partial\psi_i}{\partial u_g} \right] = [S]_{ig}$$

The design sensitivity coefficient matrices may thus be expressed as

$$\begin{aligned} [\Lambda_{ij}] = & \left(\left\{ \frac{\Delta \psi_i}{\Delta b_1} \right\}, \left\{ \frac{\Delta \psi_i}{\Delta b_2} \right\}, \dots, \left\{ \frac{\Delta \psi_i}{\Delta b_j} \right\} \right) |_{u_{\text{fixed}}} \\ & + [S_{ig}] \left(\left\{ \frac{\Delta U_{g1}}{\Delta b_1} \right\}, \left\{ \frac{\Delta U_{g2}}{\Delta b_2} \right\}, \dots, \left\{ \frac{\Delta U_{gj}}{\Delta b_j} \right\} \right) |_{b_{\text{fixed}}} \end{aligned}$$

From this equation it is easy to see that the number of additional case control records (additional loading cases) required for design sensitivity analysis is equal to the number of design variables for each subcase (Pseudo-Load Technique).

A typical term of the coefficient matrix may thus be written as

$$\Lambda_{ij} = \left(\frac{S_{uB}^{B+\Delta B}}{\Delta B} - \frac{S_{uB}^B}{\Delta B} \right) + \left(\frac{S_{uB}^B + \Delta B}{\Delta B} - \frac{S_{uB}^B}{\Delta B} \right)$$

where B represents the base line or original state and B + ΔB represents the perturbed state. The first expression in parentheses on the right-hand side is thus the change in response quantity due to a change in design variable for the original solution vector. The second term represents the change in response quantity due to a change in displacement for the unperturbed design variable. For displacement constraints, the first term in parentheses on the right-hand side is identically zero.

The design constraints for composites can be lamina stresses or failure indices, displacements, frequency, buckling loads, or forces. The design variables can be lamina thicknesses, orientation angles or material properties.

PROGRAM ARCHITECTURE

In order to understand the reasons behind how a development is introduced into a large finite-element program, a knowledge of the program architecture and technical purpose is necessary. A brief description of MSC/NASTRAN is presented as background.

The cornerstone of MSC/NASTRAN's architecture is its Executive System, whose essential functions are to establish and control and sequence of calculations, to allocate files, and to maintain a restart capability. Engineering calculations are performed by approximately 200 functional modules which communicate only with the Executive System and not with each other. Flexibility is maintained by a macro-instruction language called DMAP, which

is under user control, but which also serves to establish preformatted calculation sequences for the major types of analysis, including linear analysis, buckling, vibration mode analysis, and design sensitivity.

The calculation of finite element data is concentrated exclusively in a few modules. The element matrices for stiffness, structural damping, and differential stiffness for elements of the structural model are generated in the Element Matrix Generator (EMG) module. These element matrices are subsequently assembled to form the elastic stiffness matrix, the structural damping matrix, the mass matrix, or the differential stiffness matrix.

The element contribution to the load vector is generated in the SSG1 module and the element stress and force are generated in the SDR2 module. In all these modules, the finite element descriptions are defined in the Element Summary Table, the EST table. The EST table contains the element connection, material property and sectional property information.

Taking advantage of the table-driven concept used by the element modules, much of the element dependent development could be avoided in implementing design sensitivity if a procedure could be developed which would involve only building EST tables that would cause existing modules to form the necessary element data.

How a given capability is introduced into a commercial general-purpose finite-element program is as important an issue to the user as its theoretical sophistication. If the user views a capability as hard to use, as having an insufficient capacity to solve his problem, or taking an inordinate time to comprehend its output, the product is of little practical use. In addition, the program developer, while heeding the user's needs, has to keep sight of the program as a whole when adding new capabilities. This involves interfacing well with existing capabilities, maintaining program reliability and generality, and producing software that makes effective use of computer resources.

The user interface is a major consideration in the design of a new capability. The following issues were considered in DSA:

1. DSA input should be straightforward, but allow flexibility to model complex structural design concepts
2. DSA output should be concise and easily understood
3. Avoid arbitrary program limits which restrict the allowable element types, constraint quantities, and problem size
4. Provide an interface for external optimization postprocessors

A brief discussion of the processes involved in a typical DSA STATIC analysis in MSC/NASTRAN will help bring into perspective the work involved in the various parts of the DSA solution.

DSA in a STATICS analysis is based on solving for $\{\Delta u_g\}$ in the first-order variation of the nodal equilibrium equation:

$$[K_{gg}^0]\{\Delta u_g\} = \{\Delta P_g\} - [\Delta K_{gg}]\{u_g^0\}$$

The DSA problem in the paper is considered to be the additional task required after the solution of primary analysis. By restarting from the primary STATIC analysis, the solution of the DSA system equation only involves the calculation of the right-hand side and the backward pass operation in the solution of Δu .

The work involved in solving the system equations (backward pass operation) is a function of the product of the number of design variables and loading conditions. The following DSA tasks are required in addition to solving the system equations:

1. DSA Data Organization
2. DSA Data Assembly
3. DSA Data Recovery

These tasks are functions of the triple product of the number of design variables, design constraints and loading conditions. For large DSA problems, the data organization, assembly and recovery tasks are the dominant users of computer resources.

Another major consideration was to support all structural finite-element types in MSC/NASTRAN. Since a large number of the elements developed are semiempirical, the determination of consistent element derivative formulations cannot be practically accomplished. Therefore, a method was developed to calculate element derivatives by a differencing scheme about the current design point. This method involved the calculation of the element matrix at the design point plus or minus the user-specified design variable increment. These element data are differenced with the data at the design point to determine the corresponding element derivatives. For example, the following shows the change in element stiffness due to a change in the design variable.

$$[\Delta K_{gg}] = [K_{gg} + \Delta B] - [K_{gg}^0]$$

Another benefit of differencing about the design point is that it avoids most potential numerical problems. This is because the evaluation of the perturbed element data is computed near a design point which has already been determined to be numerically acceptable in the primary analysis.

To get an idea of the magnitude of the task involved, about 15 existing subroutines comprising approximately 6000 lines of Fortran had to be modified, in addition to coding approximately 10 new subroutines comprising 1000 lines of Fortran. There are approximately 15 tables created for data organization and manipulation.

An initial analysis is carried out to identify critical constraints and a data base created. In the succeeding run, information about constraints, design variables, and maximum and minimum side constraints is supplied. A special DMAP package was created which exploits the data base technology.

The user can control the number of iterations performed. He can restart from the previous step. This is especially convenient, as he can scan the output and intervene manually to either add or delete constraints or modify design variables. Table 1 gives a schematic diagram of the program flow.

OPTIMIZATION CONCEPTS AND CONVEX LINEARIZATION

In order to validate the new design sensitivity capability for composite structures, it was decided to introduce a numerical optimization module in a special version of MSC/NASTRAN. It has then become possible to solve some well-documented structural optimization problems, and to compare the results with those produced by other finite-element systems having similar sensitivity and optimization capabilities. In our opinion this pilot implementation represents the most complete and reliable way of verifying that the sensitivity analysis results are correct and accurate enough for a meaningful exploitation. It should however be mentioned that only sizing types of design variables (i.e., lamina thicknesses) are permitted in our optimization module. This is because no proper formulation is currently available to deal with optimization problems involving other types of design variables (e.g., orientation angles and material properties).

Structural optimization methods using finite-element models have now reached a high level of reliability and efficiency. These methods can currently address practical problems involving various types of design variables (e.g., component transverse sizes, shape variables) and design constraints (e.g., geometry requirements, maximum allowable stresses, bounds on deflections, or frequencies). In addition the types of finite-element models tractable by these methods have recently been largely extended so that virtually all finite-element models that can be analyzed can now be addressed by optimization techniques (e.g., bar, beam, membrane, plate, and shell).

A numerical optimization problem is characterized by a given objective function $f(x)$, which is to be minimized by determining the magnitudes of design variables x , such that certain constraints on the x_i 's are achieved. This leads to a mathematical programming problem of the "primal" form:

$$\begin{array}{ll} \text{minimize} & f(x) \\ \text{such that} & h_j(x) > 0 \quad j=1,2,\dots,m \\ & x_i^- > x_i > x_i^+ \quad i=1,2,\dots,n \end{array}$$

where m is the number of behavior constraints and n , the number of design variables.

Such a problem can be solved iteratively by using numerical optimization techniques. Each iteration begins with a complete analysis of the system behavior in order to evaluate the objective function and constraint values along with their sensitivities to changes in the design variables (i.e., first derivatives). A design iteration is concluded by employing the results of these behavioral and sensitivity analyses in a primal minimization algorithm which searches the n -dimensional design space for a new primal point that decreases $f(x)$ while remaining feasible (i.e., satisfying the constraints $h_j(x)$). Many such iterations are usually required before achieving the optimum design. Until recently, because of the high-computation cost of each iteration (full FEM analysis), structural optimization techniques based on primal algorithms have been only conceivable on power mainframe computers.

An alternative to this primal formulation is the so-called "dual" approach [2], in which the constrained primal minimization problem is replaced by maximizing a quasi-unconstrained dual function depending only on the Lagrangian multipliers associated with the behavior constraints. These multipliers are the dual variables subject to simple non-negativity constraints. The efficiency of this dual formulation is due to the fact that maximization is performed in the dual space whose dimensionality is relatively low and depends on the active constraint at each design iteration. The dual approach is especially powerful when used in conjunction with approximation concepts [3]. In particular, the convex linearization scheme (CONLIN) [4], recently introduced to solve general structural optimization problems, exhibits very good performance, even when dealing with the inherently difficult problems involving changes in geometry.

In CONLIN each function defining the optimum design problem is linearized with respect to appropriate intermediate variables (called "mixed" variables) yielding a convex, separable problem approximation. The initial problem is therefore transformed into a sequence of explicit subproblems having a simple algebraic structure. The convex linearization scheme exhibits remarkable properties that makes it attractive to replace the original primal subproblem by its dual [2]. CONLIN can be viewed as a generalization of well-established approaches to pure sizing structural optimization problems, namely "approximation concepts" and "optimality criteria" techniques [5], and as such it is capable of addressing a broader class of problems with considerable facility of use.

Because of its many attractive features the CONLIN algorithm has been selected to implement optimization capabilities in our pilot program. At each successive iteration point, the CONLIN method only requires evaluation of the objective and constraint functions and their first derivatives with respect to the design variables. This information is provided by the FEM analysis and sensitivity analysis results. The CONLIN optimizer will then select by itself an appropriate approximation scheme on the basis of the sign of the derivatives. CONLIN benefits from many interesting features.

- The CONLIN approach is very general, requiring only values and derivatives of the functions describing the optimization problem to be solved; it permits therefore straight interfacing to the FEM software;

- Because it is based on conservative approximation concepts, CONLIN does not demand a high level of accuracy for the sensitivity analysis results, which can therefore be obtained by finite differencing;
- CONLIN usually generates a nearly optimal design with less than 10 FEM analyses;
- CONLIN has an inherent tendency to produce a sequence of steadily improving feasible designs;
- The CONLIN method is simple enough to lead to a relatively small computer code, and well organized to avoid high core requirements.

These features have considerably facilitated the implementation of reliable and efficient optimization capabilities in our special version of MSC/NASTRAN.

NUMERICAL EXAMPLES

Two example problems were chosen to validate the capability and to highlight some of the salient features.

EXAMPLE 1 RECTANGULAR PLATE WITH A CIRCULAR HOLE.

A rectangular plate with a circular hole is subjected to a specified displacement along the x-direction. The quarter model of the plate is shown in Figure 3. The plate is modelled using QUADRILATERAL elements. Each element consists of 4 laminae stacked at 0° , 45° , 90° and -45° , respectively. The region near the hole is divided into 13 regions. The 0° lamina for each of the 13 regions is treated as a single design variable. The laminae at 45° and -45° are linked and are treated as a single design variable for each of the 13 regions. Similarly the 90° lamina is treated as single design variable for each of the 13 regions. Thus there are a total of 39 design variables for this problem. The model consists of 288 QUADRILATERAL elements and 317 grids.

The design constraints are the failure indices using the Hill criterion selected for different lamina in specified elements. The model was optimized for these selected constraints. The results are shown in Table 2. The results were examined after iteration 5 to examine if the failure index exceeded 1 for any of the elements which were not specified as constraints originally. The violated elements were input as constraints and the optimization loop started from this point onward. The algorithm converged in 9 loops. As can be seen, the user can intervene at specific points in the algorithm and monitor the progress. This capability is particularly important and convenient for realistic design of structures.

EXAMPLE 2

The second demonstration problem is a delta wing structure with graphite/epoxy skins and titanium webs subjected to pressure loading and temperature loading. The wing is shown in Figure 4. The problem has been previously studied for frequency constraint in Reference 3. The structure is symmetric

with respect to its middle surface which corresponds to the x-y plane in Figure 4. The skins are assumed to be made up of 0° , $\pm 45^\circ$ and 90° high strength graphite/epoxy laminates. It is understood that orientation angles are given with respect to the x reference co-ordinate in Figure 4, that is, material oriented at 0° has fibers running spanwise while material at 90° has fibers running chordwise. The skins are represented by QUADRILATERAL and TRIANGULAR membrane elements and the webs are represented by shear panels. According to the linking scheme depicted in Figure 5, it can be seen that the total number of independent design variables is equal to 60 made up as follows: 16 for 0° material, 16 for $\pm 45^\circ$ material, 16 for 90° material and 12 for the web material. The model contains 56 QUADRILATERAL elements, 12 TRIANGULAR elements and 142 shear panels. The total number of nodes is 132.

The design constraint was the maximum deflection at the tip of the wing equal to 10.0 in. The results are shown in Figure 6 for the objective function and the tip deflection for the number of iterations.

After the Delta-wing was optimized for tip deflection of 10.00 in., parametric studies were carried out to study the effect of ΔB on the response quantity. The fundamental frequency was chosen as the constraint and ply-angle chosen as the design variable. All the 0° laminae in the wing were linked together, as were the $45^\circ/-45^\circ$ and 90° laminae. The value of ΔB was varied from 10.0 to 10^{-7} and the results are shown in Table 3. As can be seen from Table 3, the sensitivity coefficients gradually converge till ΔB equal to 10^{-5} and then begin to diverge. Thus for ΔB less than 10^{-5} , round off errors become significant enough to degrade the solution. The robustness of the finite difference approach is, however, evident since even for ΔB as large as 0.1, the % error is only of the order of magnitude of 1%.

It was also decided to investigate the effect of linked design variables on fundamental frequency as a constraint. The results are shown in Table 4, where ply-thicknesses, orientation angles and Young's modulus along the principal direction were chosen as the design variables. The sensitivity analysis, by itself has little value unless used in an optimization context.

Table 5 gives the CPU times on the VAX-11/780 machine for the two example problems. As can be seen, the optimizer itself takes very little time. Since normally, 5 to 10 iterations are required for optimization, sensitivity analysis and the reanalysis after updating the design variables constitute the expensive portions of the design process. Efforts to enhance efficiency for sensitivity and reanalysis would go a long way toward making the design of realistic structures a viable proposition.

CONCLUSIONS

The design sensitivity capability for composites to be available in the next release of MSC/NASTRAN was designed for generality, whereby the design variables can be laminae thicknesses, orientation angles, material properties or a combination of all three. It is envisaged that this capability would constitute a powerful first step toward optimizing composite structures.

Furthermore as part of a research effort MSC/NASTRAN was linked to a general-purpose optimizer CONLIN for fully automated structural design synthesis. It has been demonstrated that the coupling of a large-scale finite element package like MSC/NASTRAN with a powerful optimizer will give designers a powerful tool to carry out practical optimization of real-life complicated structures. It should however be mentioned that only sizing type of design variables (i.e. lamina thicknesses) are permitted in our optimization module. This is because no proper formulation is currently available to deal with optimization problems involving other types of design variables (e.g., orientation angles and material properties).

A unique feature of the coupling is the capability for the user to intervene at any stage of the redesign process and to modify design constraints or design variables and to carry on from the previous stage. Man-machine interaction is an essential ingredient for realistic optimization of structural problems.

REFERENCES:

- [1] G. K. Nagendra, "The Analysis of Laminated Composite Materials in MSC/NASTRAN", Chapter 6 of Computer-Aided Engineering of Composite Materials and Structures (J. Backlund), Elsevier, 1987.
- [2] C. Fleury, "Structural Weight Optimization by Dual Methods of Convex Programming", International Journal for Numerical Methods in Engineering, Vol. 14, 1979, pp. 1761-1783.
- [3] C. Fleury and L. A. Schmit, "Dual Methods and Approximation Concepts in Structural Synthesis", NASA Contractor Report, NASA-CR-3226, 1980, 196 pages.
- [4] C. Fleury and V. Braibant, "Structural Optimization - A New Dual Method Using Mixed Variables", Int. J. Num. Meth. Eng., Vol. 23, No: 3 1986, pp. 409-428.
- [5] C. Fleury, "Reconciliation of Mathematical Programming and Optimality Criteria Approaches to Structural Optimization", Chapter 10 of Foundations of Structural Optimization: a Unified Approach (A. J. Morris, ed.), John Wiley and Sons, 1982, pp. 363-404.

TABLE 1. FLOW CHART FOR OPTIMIZATION PROCEDURE

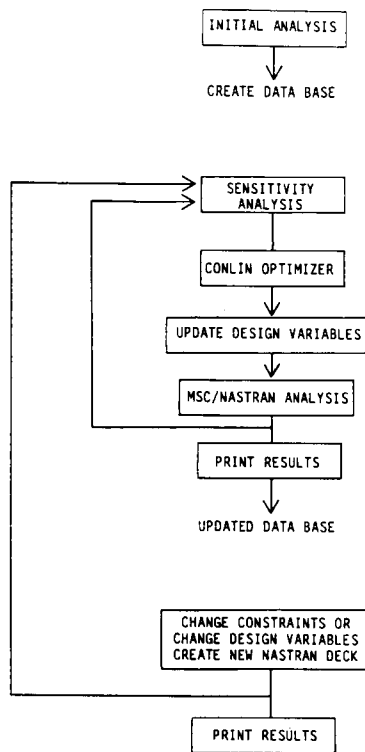


TABLE 2. RESULTS OF OPTIMIZATION

ANALYSIS NUMBER	WEIGHT	σ_1 1(00)	σ_2 1(45)	σ_3 2(00)	σ_4 (2-45)	σ_5 3(00)
1	.3575	1.1632	1.1421	-	-	-
2	.3562	.9446	.9076	-	-	-
3	.3545	.9886	.9238	-	-	-
4	.3541	.9948	.9160	-	-	-
5	.3540	.9982	.9164	-	-	-
6*	.3539	.9990	.9983	1.0999	1.1053	1.1634
7	.3554	.9388	.9469	.9799	.9921	.9871
8	.3552	.9552	.9651	.9855	.9994	.9805
9	.3552	.9585	.9690	.9854	.9999	.9769
10	.3552	.9594	.9700	.9853	1.0000	.9757

*User Intervention

TABLE 3. VARIATION OF SENSITIVITY COEFFICIENTS WITH RESPECT TO ΔB

ΔB	Λ
10.0	-.072539
1.0	-.082207
.1	-.082766
.01	-.082803
.001	-.082819
.0001	-.082836
.00001	-.082940
.000001	-.079559*
.0000001	-.098504

*Degrades

TABLE 4. SENSITIVITY COEFFICIENTS FOR FUNDAMENTAL FREQUENCY

DESIGN VARIABLE	SENSITIVITY COEFFICIENTS	
Ply-Thickness	0°	0.38200
	45°/-45°	-0.89380
	90°	-0.01774
Ply-Angles	0°	-0.08280
	45°/-45°	-0.10490
	90°	-0.00633
Material Properties	0°	1.48870
	45°/-45°	0.22640
	90°	0.00444

TABLE 5. ESTIMATE OF CPU TIME ON VAX 11-780

	Example 1	Example 2
	Rectangle with Cutout	Delta Wing
	650 DOF	400 DOF
	39 Design Variables	60 Design Variables
Initial Analysis	430 Secs.	300 Secs.
{ Sensitivity Analysis	257 Secs. (39 Constraints)	180 Secs. (6 Constraints)
	190 Secs. (10 Constraints)	
Optimization	3 Secs.	3 Secs.
Analysis	135 Secs.	115 Secs.
Per Iteration	395 Secs. (39 Constraints) 330 Secs. (10 Constraints)	300 Secs. (6 Constraints)

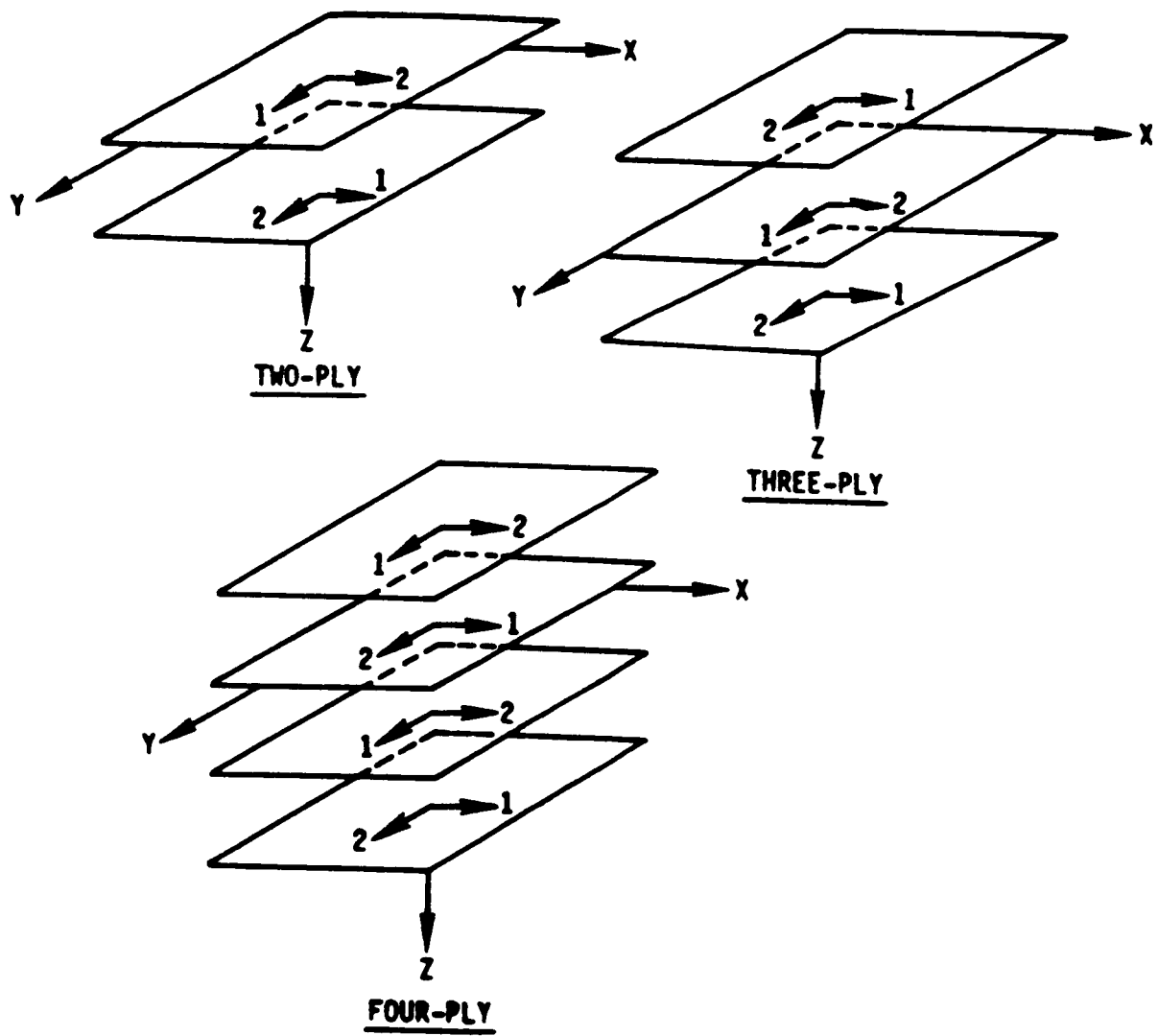


Figure 1. Exploded view of three cross-ply laminated plane structures.

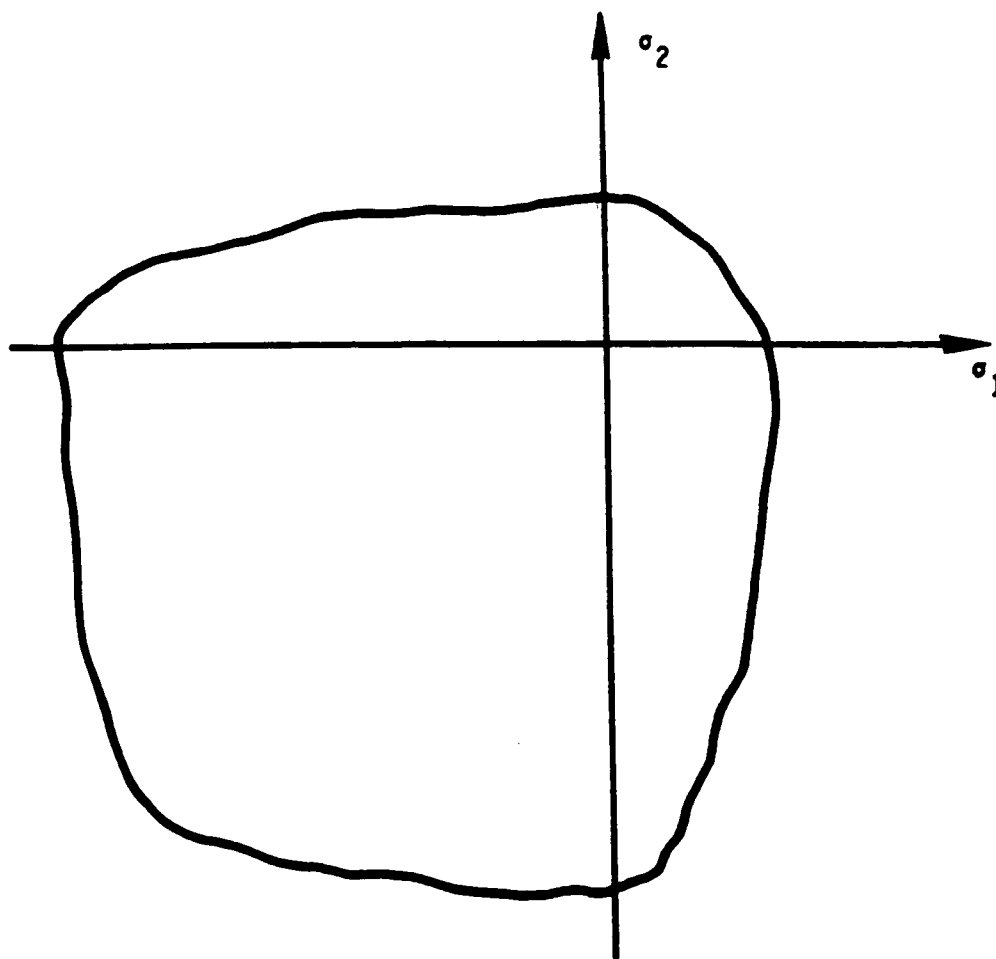


Figure 2. Typical failure envelope for a material such as concrete.

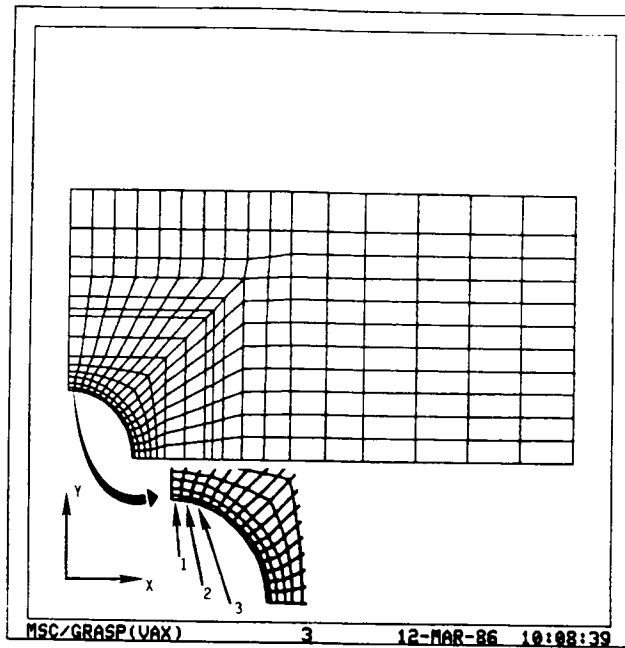


Figure 3. Finite-element model of one-quarter plate.

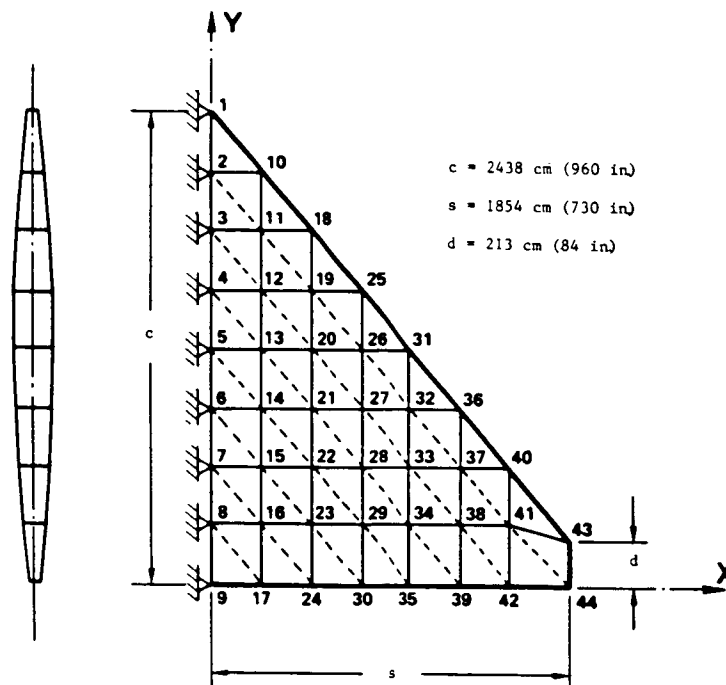


Figure 4. Delta wing analysis model (problem 2).

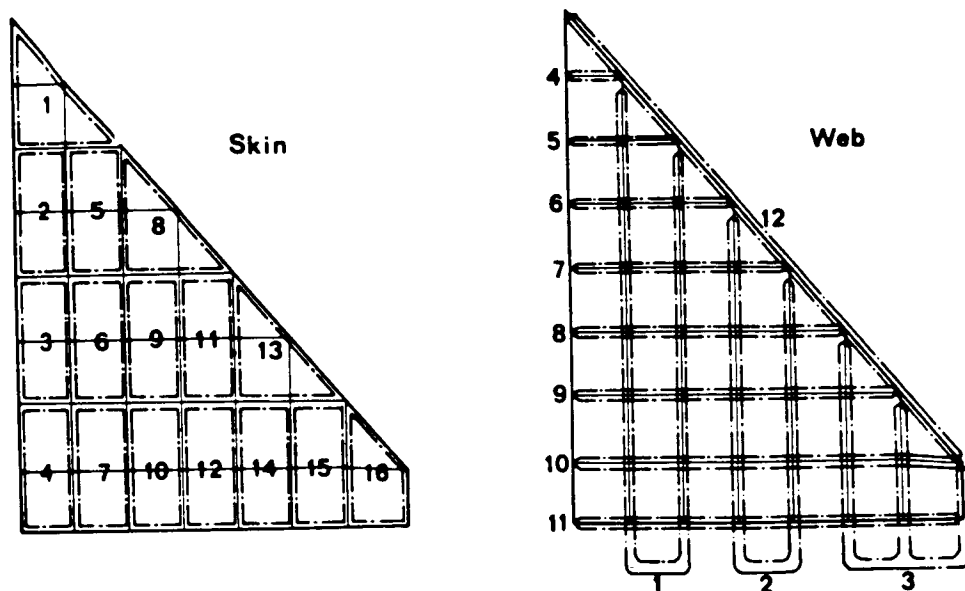


Figure 5. Delta wing design model (problem 2).

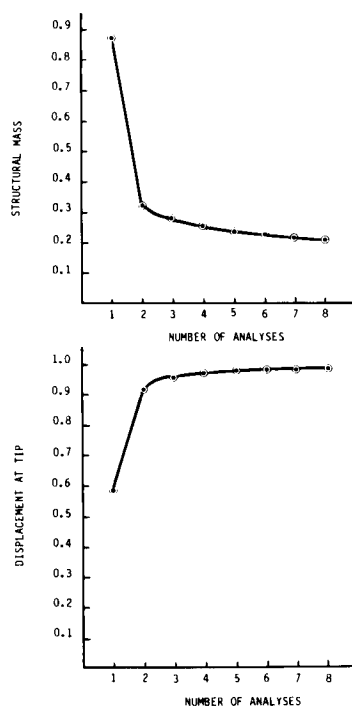


Figure 6. Convergence of delta wing design.

OPTIMIZATION OF SHALLOW ARCHES
AGAINST INSTABILITY USING SENSITIVITY DERIVATIVES⁺

Manohar P. Kamat
Georgia Institute of Technology
Atlanta, GA

SUMMARY

In this paper the author discusses the problem of optimization of shallow frame structures which involve a coupling of axial and bending responses. A shallow arch of a given shape and of given weight is optimized such that its limit point load is maximized. The cross-sectional area, $A(x)$ and the moment of inertia, $I(x)$ of the arch obey the relationship $I(x) = \rho [A(x)]^n$, $n = 1, 2, 3$ and ρ is a specified constant. Analysis of the arch for its limit point calculation involves a geometric nonlinear analysis which is performed using a corotational formulation.

The optimization is carried out using a second-order projected Lagrangian algorithm and the sensitivity derivatives of the critical load parameter with respect to the areas of the finite elements of the arch are calculated using implicit differentiation. Results are presented for an arch of a specified rise to span ratio under two different loadings and the limitations of the approach for the intermediate rise arches are addressed.

INTRODUCTION

With the advent of highly flexible large space structures the nonlinearity of response of such structures plays a dominant role in the control of such structures. Naturally, optimization of structures in nonlinear response is gaining prominence. This paper addresses the issue of optimizing shallow frame structures in nonlinear response involving a coupling of axial and bending actions. The objective is to optimize a shallow arch of a given shape and given weight such that its limit point load is maximized. Besides having to perform a nonlinear analysis in calculating the limit point load an issue of even greater concern is that of calculating the sensitivity derivatives of the critical load parameter with respect to the design variables, namely the cross-sectional areas of the elements of the discretized model of the arch. Two approaches are available for the calculation of sensitivity derivatives: the direct and the adjoint approach [1]. In general, the adjoint approach is preferred for problems involving nonlinear response [2] - [4]. The popularity of the adjoint approach stems from the fact that the differential equations governing the adjoint variable are linear even though the corresponding equilibrium equations in terms of the true displacement variables are nonlinear. But to date the author is unaware of the use of the adjoint approach for problems involving limit point instability. The present work outlines a direct approach

⁺ This work was supported by the National Science Foundation under Grant No. ECE-8596016.

similar to that used by the author and his co-worker in the case of shallow space trusses [5]. In this approach the sensitivity derivatives of the critical load parameter are obtained through an implicit differentiation of the nonlinear equilibrium equations as explained below. The present discussion is restricted to finite-element models of shallow arches whose cross sections obey the relationship

$$I(x) = \rho [A(x)]^n, \quad n = 1, 2, 3, \quad \rho = \text{specified constant} \quad (1)$$

SENSITIVITY DERIVATIVES OF THE CRITICAL LOAD PARAMETER

Consider a shallow arch under a given distribution of loading. Assume that λ_{cr} is the smallest value of the parameter by which the given distribution of loading must be scaled in order to produce instability of the arch. The parameter λ is then defined by the solution of the following system of equations of a finite-element model of the arch.

$$\frac{\partial \pi}{\partial q_j} = 0 \quad (2)$$

$$\left| \frac{\partial^2 \pi}{\partial q_i \partial q_j} \right| = 0 \quad (3)$$

where π denotes the total potential energy of the model undergoing finite displacements and q_j , $j = 1, 2 \dots N$ denote the generalized nodal displacements of the model. The load parameter λ occurs implicitly in Eqs. (2) and (3). Assume that A_k for $k = 1, 2 \dots m$ are the m design variables, which for the arch are the cross-sectional areas of the finite elements. To obtain $\frac{\partial \lambda}{\partial A_k}$ we proceed as follows:

Rewrite Eqs. (2) and (3) as

$$f_l(q_j(A_k), \lambda(A_k), A_k) = 0 \quad (4)$$

$$g(q_j(A_k), \lambda(A_k), A_k) = 0 \quad (5)$$

$$j, l = 1, 2 \dots N$$

$$k = 1, 2 \dots m$$

An implicit differentiation of Eqs. (4) and (5) with respect to A_k leads to

$$\begin{bmatrix} \frac{\partial f_1}{\partial q_1} & \frac{\partial f_1}{\partial q_2} & \dots & \frac{\partial f_1}{\partial q_N} & \frac{\partial f_1}{\partial \lambda} \\ \frac{\partial f_2}{\partial q_1} & \frac{\partial f_2}{\partial q_2} & \dots & \frac{\partial f_2}{\partial q_N} & \frac{\partial f_2}{\partial \lambda} \\ \vdots & \vdots & & \vdots & \vdots \\ \frac{\partial f_N}{\partial q_1} & \frac{\partial f_N}{\partial q_2} & \dots & \frac{\partial f_N}{\partial q_N} & \frac{\partial f_N}{\partial \lambda} \\ \frac{\partial g}{\partial q_1} & \frac{\partial g}{\partial q_2} & \dots & \frac{\partial g}{\partial q_N} & \frac{\partial g}{\partial \lambda} \end{bmatrix} \begin{pmatrix} \frac{\partial q_1}{\partial A_k} \\ \frac{\partial q_2}{\partial A_k} \\ \vdots \\ \frac{\partial q_N}{\partial A_k} \\ \frac{\partial \lambda}{\partial A_k} \end{pmatrix} = \begin{pmatrix} -\frac{\partial f_1}{\partial A_k} \\ -\frac{\partial f_2}{\partial A_k} \\ \vdots \\ -\frac{\partial f_N}{\partial A_k} \\ -\frac{\partial g}{\partial A_k} \end{pmatrix} \quad (6)$$

for every $k = 1, 2 \dots m$. These equations may be written symbolically as

$$\begin{bmatrix} \underline{H} & \underline{F} \\ \underline{G} & 0 \end{bmatrix} \begin{pmatrix} \frac{\partial \underline{q}}{\partial A_k} \\ \frac{\partial \lambda}{\partial A_k} \end{pmatrix} = \begin{pmatrix} -\frac{\partial \underline{f}}{\partial A_k} \\ -\frac{\partial g}{\partial A_k} \end{pmatrix} \quad (7)$$

where \underline{H} is the Hessian matrix of the potential energy of the finite-element model of the arch, \underline{F} is the given vector of nodal forces, and \underline{G} is the row matrix of derivatives of the determinant g of the Hessian matrix with respect to nodal displacements. Equations (7) assume that $\frac{\partial g}{\partial \lambda}$ is equal to zero since for constant directional loading parameter λ does not occur explicitly in the stability criterion. The elements of \underline{G} can be evaluated by using the formula

$$\frac{\partial g}{\partial q_j} = \text{trace} \left\{ (\text{adj } (\underline{H})) \left[\frac{\partial \underline{H}}{\partial q_j} \right] \right\} \quad (8)$$

where $\left[\frac{\partial \underline{H}}{\partial q_j} \right]$ is the matrix obtained by differentiating each element of the determinant of \underline{H} with respect to a typical component q_j . With this, the sensitivity derivative $\frac{\partial \lambda}{\partial A_k}$ can be calculated by the solution of Eqs. (7) at a given (\underline{q}, λ) .

Incidentally, Eqs. (7) apply everywhere along the loading path including the limit point. It is only at a bifurcation point that the determinant of \underline{H} is not differentiable. For very shallow arches instability typically occurs through snap-through and hence Eqs. (7) clearly apply.

SPECIALIZATION TO A FRAME ELEMENT MODEL OF THE ARCH

We illustrate the derivation of the sensitivity derivatives for a finite element model with 3-D frame elements. For its kinematic description the frame element uses the co-rotational formulation as outlined in great detail in reference [6]. According to this formulation, which permits large rigid body motion of the element, the total motion is decomposed into a rigid body component and a strain-producing component. For an element p-q of length L, the displacements of the end q relative to the end p in the body fixed axes can be shown to be

$$\begin{Bmatrix} \delta_u \\ \delta_v \\ \delta_w \end{Bmatrix} = [T]_p \begin{Bmatrix} x_q - x_p \\ y_q - y_p \\ z_q - z_p \end{Bmatrix} - \begin{Bmatrix} L \\ 0 \\ 0 \end{Bmatrix} + [T]_p \begin{Bmatrix} U_q - U_p \\ V_q - V_p \\ W_q - W_p \end{Bmatrix} \quad (9)$$

$U_i, V_i,$ and W_i ($i = p$ or q) denote the global displacements of the nodes and matrix $[T]_p$ is [6].

$$[T]_p = [T_1(\phi_x, \phi_y, \phi_z)][T_1(\theta_{xp}, \theta_{yp}, \theta_{zp})] \quad (10)$$

with

$$[T_1(\alpha_x, \alpha_y, \alpha_z)] = \begin{bmatrix} c_y c_z & c_y s_z & -s_y \\ -c_x s_z + s_x s_y c_z & c_x c_z + s_x s_y s_z & s_x c_y \\ s_x s_z + c_x s_y c_z & -s_x c_z + c_x s_y s_z & c_x c_y \end{bmatrix} \quad (11)$$

$c_i = \cos \alpha_i$, $s_i = \sin \alpha_i$ for $i = x, y$ and z . Angles ϕ_x, ϕ_y and ϕ_z are the initial orientation angles of the frame element and the angles θ_{xp}, θ_{yp} and θ_{zp} are the rigid-body rotations of the end p. In deriving Eqs. (10) Euler angle transformation is implied with the order of the rotations being α_z, α_y and α_x .

Similarly, with the restriction of small relative rotation within the element, the rotations ψ_x, ψ_y and ψ_z of the end q relative to the end p are

$$\begin{Bmatrix} \psi_x \\ \psi_y \\ \psi_z \end{Bmatrix} = [T]_p \begin{Bmatrix} \theta_{xq} - \theta_{xp} \\ \theta_{yq} - \theta_{yp} \\ \theta_{zq} - \theta_{zp} \end{Bmatrix} \quad (12)$$

Assuming the relative axial and transverse displacements to be linear and cubic, respectively, the strain energy of the (p-q)th or the e-th element, $e = 1, 2, \dots, m$ can be shown to be [6].

$$U_e = U_{(p-q)} = \frac{E}{2L_e} \left\{ A_e (\delta_u)^2 + \frac{12}{L_e^2} \rho_z A_e^n [(\delta_v)^2 + \frac{L_e^2}{3} \psi_z^2 - L_e (\delta_v)(\psi_z)] \right. \\ \left. + \frac{12}{L_e^2} \rho_y A_e^n [(\delta_w)^2 + \frac{L_e^2}{3} \psi_y^2 + L_e (\delta_w)(\psi_y)] \right\} \quad (13)$$

Hence

$$\pi = \sum_{e=1}^m U_e - \underline{F}^T \underline{q} \quad (14)$$

where $\underline{q}^T = (U_p, V_p, W_p, \theta_{xp}, \theta_{yp}, \theta_{zp}, U_q, V_q, W_q, \theta_{xq}, \theta_{yq}, \theta_{zq})$. All the expressions for the evaluation of matrices in Eqs. (7) are now available and, in principle, can be evaluated even though the algebra may be rather tedious. The above expressions, especially the $[T]_p$ matrix, can be simplified using the assumption of small rigid body motions within a load step.

Indeed, Updated Lagrangian formulation for the kinematic description may have simplified matters quite a bit especially if the expressions are linearized within a load step but the above expressions using the co-rotational formulation permit truly large displacements and with an highly efficient algorithm for the solution of nonlinear equations like for instance the BFGS algorithm [7], it can permit relatively large load steps resulting in a fewer number of load steps to attain a given load level.

CONSTRAINED OPTIMIZATION

The optimization problem consists of maximizing the critical value of the load parameter λ subject to the constraint on total volume of the structure and side constraints on member sizes. Although it is perfectly permissible to pose the problem as

$$\min (f(\underline{A}) = -\lambda) \quad (15)$$

Subject to

$$\frac{\partial \pi}{\partial q_j} = 0 \quad (16)$$

$$\left| \frac{\partial^2 \pi}{\partial q_i \partial q_j} \right| = 0 \quad (17)$$

$$\sum_{i=1}^m A_i L_i - V_0 = 0 \quad (18)$$

$$A_i - A_{\min} \geq 0 \quad (19)$$

experience suggests the following well-posed problem

$$\min (-\lambda_{cr}) \quad (20)$$

subject to

$$\sum_{i=1}^m A_i L_i - V_0 = 0 \quad (21)$$

$$A_i - A_{\min} \geq 0 \quad (22)$$

where λ_{cr} is located by incrementing the load parameter and locating its level at which the determinant of the Hessian vanishes. This can be done by monitoring either the determinant or the inertia of the eigenvalues of the Hessian matrix H . Once an interval is located where the critical point is supposed to lie its exact location is determined by a root-finding technique. With Eqs. (15)-(19) there is no guarantee that the lowest value of λ that satisfies Eqs. (17) will always be found.

The problem as posed by Eqs. (20)-(22) is solved by using Powell's variable metric algorithm for constrained optimization (VMCON) [8]. The required gradient of the Lagrangian function corresponding to Eqs. (20)-(22) involves the gradient of the load parameter which is calculated using the expressions derived in the previous section.

DISCUSSION OF RESULTS AND CONCLUSIONS

The first step was to validate the accuracy of the sensitivity derivatives. This validation was performed by comparing the analytically calculated derivatives using the expressions (6)-(8) with those calculated using central differences. Since no previous studies exist that address the problem being discussed herein, it was essential to generate a basis for comparison. Such a basis was provided by designs that corresponded to maximum potential energy of the nonlinear deformations. Even though previous studies on shallow trusses [5] have confirmed the non-optimality of such designs they are relatively easy to generate and provide a basis for comparison with truly optimum designs.

It can be easily verified that designs which correspond to maximum potential energy satisfy the condition

$$S_e = \frac{(U_e^s + n U_e^b)}{V_e} = C = \text{constant}; \quad e = 1, 2, \dots, m \quad (23)$$

where U_e^s , U_e^b and V_e are the strain energy due to stretching, the strain energy due to bending, and the volume of the eth element, respectively.

Relations (23) can be easily met by a recurrence procedure that evolves design for the $(r+1)$ st iteration from that of the r th iteration according to

$$A_e^{r+1} = \alpha A_e^r \left(\frac{S_e}{S_{avg}} \right)^p \quad (24)$$

where

$$S_{avg} = \left(\sum_{e=1}^m U_e^s + n U_e^b \right) / V_0 \quad (25)$$

α is a constant such that

$$\sum_{e=1}^m A_e^{r+1} L_e = V_0$$

and p is a suitable exponent usually chosen to be equal to $1/2$. Several designs for a concentrated load at the crown and a uniformly distributed vertical loading were generated for $n = 1, 2, 3$ using the mathematical programming procedure, VMCON and the recurrence relations (23)-(24). Table 1 provides a comparison of these designs. Differences between the two designs are indeed drastic especially for $n = 3$. A curious phenomenon was observed during the recurrence procedure namely, that several non-converged intermediate designs had higher critical (limit) loads than the final fully covered designs with a uniform specific energy density distribution. This is to be expected since the fully converged designs are non-optimal. Table 2 provides the material distributions in terms of the non-dimensional areas of the five frame elements used to model half the arch.

An attempt to optimize a five element arch model with $y(x) = 5 \sin \frac{\pi x}{100}$ failed for $n = 2, 3$ because no limit point load could be determined. This is not surprising since for very low rise to span ratios the arch is likely to behave more like a flexible nonlinear beam with no susceptibility to snap-through. Likewise for arches with high rise to span ratios instability occurs by bifurcation at load levels far below their limit points and hence the problem belongs to the class of linear eigenvalue problems. For arches with intermediate rise to span ratios the type of instability can change from the initial limit point to a bifurcation type at convergence. In fact the two points may coincide during optimization at which point the critical load parameter is no longer differentiable with respect to the design variables. Recourse must be then made to techniques of nondifferentiable optimization [8].

REFERENCES

1. Haftka, R. T. and Kamat, M. P., Elements of Structural Optimization, Martinus Nijhoff Publishers, 1984.
2. Mroz, Z., Kamat, M. P., and Plaut, R. H., "Sensitivity Analysis and Optimal Design of Nonlinear Beams and Plates", Journal of Structural Mechanics, Vol. 13, No. 3, 1985, pp. 245-266.
3. Mroz, Z. "Sensitivity Analysis and Optimal Design with Account for Varying Shape and Support Conditions", Computer Aided Optimal Design, NATO Advanced Study Institute, Portugal, 1986, Vol. 2, pp. 109-144.
4. Arora, J. S. and Wu, C. C., "Design Sensitivity Analysis of Nonlinear Structures, Computer Aided Optimal Design, NATO Advanced Study Institute, Portugal, 1986, Vol. 2, pp. 228-246.
5. Kamat, M. P. and Ruangsilasingha, P., "Optimization of Space Trusses Against Instability Using Design Sensitivity Derivatives", Engineering Optimization Vol. 8, 1985, pp. 177-188.
6. Kamat, M. P., "Nonlinear Transient Analysis by Energy Minimization,- Theoretical Basis for the ACTION Computer Code, NASA-CR-3287, July 1980.
7. Avriel, M., "Nonlinear Programming", Prentice Hall, Englewoods Cliff, N. J. 1979.
8. Wardi, Y. Y., and Polak, E., "A Nondifferentiable Optimization Algorithm for Structural Problems with Eigenvalue Inequality Constraints", Journal of Structural Mechanics, Vol. 11, No. 4, 1984, pp. 561-577.

Table 1. Comparison of Designs for Different Loadings on an Arch

$$y(x) = a \sin \frac{\pi x}{L}; \quad a = 10, \quad L = 100$$

Type of Design	$(\lambda_{cr})_{OPT} / (\lambda_{cr})_{unif.}$					
	Concentrated Load at the Crown			Uniformly Distributed Vertical Loading		
	n = 1	n = 2	n = 3	n = 1	n = 2	n = 3
VMCON with Sensitivity Derivatives	1.033	1.305	2.15	1.0013	1.207	1.932
Max. Potential Energy with Recurrence Procedure	1.047	1.064	1.092	1.005	1.024	1.048

Table 2. Material Distributions for the Optimal Arch Designs of Table 1 Using VMCON

Type of Loading	n	$(A_e)_{OPT} / (A_e)_{unif.}$				
		e = 1	e = 2	e = 3	e = 4	e = 5
Concentrated Load at the Crown	1	0.8774	0.8662	0.8839	1.0452	1.340
	2	0.7036	0.8370	0.9963	1.1577	1.3153
	3	0.5780	0.8860	1.0700	1.1953	1.2907
Uniformly Distributed Vertical Loading	1	0.9471	1.0240	1.0455	1.0080	0.9760
	2	0.7662	0.9526	1.0663	1.1080	1.1168
	3	0.6122	0.9285	1.0927	1.1738	1.2095

Survey of Methods for Calculating Sensitivity of General Eigenproblems

Durbha V. Murthy and Raphael T. Haftka
Department of Aerospace and Ocean Engineering
Virginia Polytechnic Institute and State University
Blacksburg, VA

SUMMARY

A survey of methods for sensitivity analysis of the algebraic eigenvalue problem for non-Hermitian matrices is presented. In addition, a modification of one method based on a better normalizing condition is proposed. Methods are classified as Direct or Adjoint and are evaluated for efficiency. Operation counts are presented in terms of matrix size, number of design variables and number of eigenvalues and eigenvectors of interest. The effect of the sparsity of the matrix and its derivatives is also considered, and typical solution times are given. General guidelines are established for the selection of the most efficient method.

Introduction

The behavior of many physical systems is completely determined by the eigenvalues of the system. Variations in parameters lead to changes in these eigenvalues and hence in response characteristics. Thus derivatives of eigenvalues and eigenvectors are of immense interest in several fields of physical sciences and engineering.

The derivatives (or synonymously, sensitivities) are of interest for a variety of uses. Design optimization is intimately connected with sensitivity analysis and the cost of calculating derivatives is the dominant contributor to the total cost in many optimization procedures. Most optimization algorithms require many analyses of the system and derivatives can be effectively used to approximate the eigenvalues and eigenvectors of a modified system and thus reduce the cost of reanalysis, especially in large systems. In addition, derivatives are very useful in design trend studies and for gaining understanding of and insight into the behavior of physical systems.

PRECEDING PAGE BLANK NOT FILMED

Finally, derivatives of eigenvalues are valuable in calculating the statistics of eigenvalue locations in probabilistic analyses.

The application of derivatives is not restricted to design-oriented activities. Sensitivity analysis is also playing an increasing role in determining the analytical model itself. In the areas of system identification and analytical model improvement using test results, sensitivity analysis is of growing importance. Much recent work in these fields is directly dependent on the calculation of eigensystem derivatives.

It has been found in certain cases that second order derivatives are effective in improving accuracy of approximations[1-7] and efficiency of design[3,8,9]. Eigenvalues are usually non-linear functions of design parameters and a second order approximation offers a much wider range of applicability compared to the first order approximation. Intermediate variables which may improve the quality of first order approximations are not generally available for eigenvalue approximations. Also, some optimization algorithms require second order derivatives, and first order derivatives of optimal solutions require second order derivatives of constraints[7]. The use of second derivatives can also greatly reduce the number of reanalyses required for the convergence of an optimization procedure[8,10]. Further, in certain optimization algorithms, second order approximations for eigenvalue constraints can drastically relax the move limits, thus achieving a nearly optimum trajectory, and can virtually eliminate the need for trial and error adjustment of move limits, thus improving the performance of the optimizer[10]. Looking at another aspect, in problems where instabilities are to be avoided, a first order calculation may completely fail to detect instabilities[2]. References [11,12] also offer examples of the usefulness of second order derivatives.

The problem of calculating the derivatives of symmetric and Hermitian eigenproblems is relatively simple and solution procedures are well-established, e.g.[13-17]. However, many physical problems give rise to non-self-adjoint formulations and thus lead to general matrices. An important example is aeroelastic stability which requires the solution of eigenproblems with complex, general and fully populated matrices. General systems are also obtained in damped structural systems and in network analysis and control system design where the eigenvalues are usually called poles. This study presents a comparative analysis of the various methods available for calculating the derivatives of the general eigenproblem and propose some modifications to existing techniques. A considerable amount of literature is available on the subject and a comparative analysis of the various methods will be of value for selecting the most efficient technique for a particular application. The purpose of this paper is to summarize the more efficient techniques proposed so far and to establish guidelines for the selection of the appropriate method for a given problem. Only the essentials of these methods are presented with details referred to the original references. Attention is restricted to the general eigenproblem and techniques that are useful only for the self-adjoint problem are not considered. The present discussion is limited to the case of distinct eigenvalues.

Problem Definition

The matrix eigenproblem is defined as follows:

$$\mathbf{A}\mathbf{u}^{(k)} = \lambda^{(k)}\mathbf{u}^{(k)} \quad (1)$$

and the corresponding adjoint problem is

$$\mathbf{v}^{(k)T}\mathbf{A} = \lambda^{(k)}\mathbf{v}^{(k)T} \quad (2)$$

where \mathbf{A} is a general complex matrix of order n and $\lambda^{(k)}$, $\mathbf{u}^{(k)}$ and $\mathbf{v}^{(k)}$ are the k -th eigenvalue and right and left eigenvectors respectively. The superscript T denotes the transpose. All eigenvalues are assumed to be distinct.

The matrix \mathbf{A} and hence, $\lambda^{(k)}$, $\mathbf{u}^{(k)}$ and $\mathbf{v}^{(k)}$ are functions of design parameter vector \mathbf{p} with individual parameters denoted by Greek subscripts, e.g. p_α . Derivatives with respect to p_α are denoted by the subscript, α e.g., $\frac{\partial \mathbf{A}}{\partial p_\alpha} = \mathbf{A}_{,\alpha}$. All the design variables are assumed to be real.

The well-known biorthogonality property of the eigenvectors is given by

$$\mathbf{v}^{(i)T}\mathbf{u}^{(j)} = 0 \text{ iff } i \neq j \quad (3)$$

Note that, the left hand side of eq. (3) is not an inner product as usually understood, since $\mathbf{v}^{(i)}$ and/or $\mathbf{u}^{(j)}$ may be complex vectors. The left eigenvectors of \mathbf{A} are the right eigenvectors of \mathbf{A}^T and vice versa.

Normalization of Eigenvectors

The eigenvectors $\mathbf{u}^{(k)}$ and $\mathbf{v}^{(k)}$ are not completely defined by eqs. (1) and (2). A normalization condition has to be imposed to obtain unique eigenvectors. For brevity, let us consider only the normalization of the right eigenvector. A normalizing condition frequently imposed in the self-adjoint case is the following:

$$\mathbf{u}^{(k)T}\mathbf{u}^{(k)} = 1 \quad (4)$$

However, it is not always possible to use eq. (4) for non-self-adjoint problems as $\mathbf{u}^{(k)T}\mathbf{u}^{(k)}$ can equal zero or a very small number causing numerical difficulties. This is true even if the matrix \mathbf{A} is real. Unfortunately, considerable confusion exists in the literature regarding this point and several authors arbitrarily adopted eq.(4) as a normalizing condition for non-self-adjoint problems, e.g.[8,9,11,18-21]. In this respect, the formulations of these references are not rigorous for general matrices.

One possible way to avoid the above difficulty is to replace eq.(4) by

$$\mathbf{u}^{(k)*}\mathbf{u}^{(k)} = 1 \quad (5)$$

where superscript $*$ denotes a conjugate-transpose. Eq. (5) is not prone to the difficulties of eq. (4) because $\mathbf{u}^{(k)*}\mathbf{u}^{(k)}$ is always guaranteed to be non-zero. But, eq.(5) is not a complete normalizing condition as it does not render the eigenvector unique.

If \mathbf{u} satisfies eq.(5), then $\mathbf{w} = \mathbf{u}e^{ic}$, where $i = \sqrt{-1}$ and c is an arbitrary real number, also satisfies eq.(5).

Another normalization condition, inspired by the biorthogonality property of the left and right eigenvectors, is

$$\mathbf{v}^{(k)T} \mathbf{u}^{(k)} = 1 \quad (6)$$

Eq.(6) also does not render the eigenvectors unique. It must be emphasized that if the eigenvector is not unique, neither is its derivative.

The normalization condition

$$u_m^{(k)} = 1 \quad (7)$$

is very attractive because it renders the eigenvectors unique and at the same time, the index m can be chosen easily to avoid ill-conditioning. Apparently, only Nelson[22] used this normalizing condition in obtaining the derivatives of eigenvectors. The index, m , may be chosen such that

$$|u_m^{(k)}| = \max_i |u_i^{(k)}| \quad (8)$$

Another choice for m , used by Nelson[22], is

$$|u_m^{(k)}| |v_m^{(k)}| = \max_i |u_i^{(k)}| |v_i^{(k)}| \quad (9)$$

The nature of uncertainty of the derivative of the eigenvector is of some interest. Without a normalizing condition, an eigenvector is uncertain to the extent of a non-zero constant multiplier. The derivative of an eigenvector is uncertain to the extent of an additive multiple of that eigenvector. To show this, let $\mathbf{u}^{(k)}$ be an eigenvector so that $\mathbf{w}^{(k)} = c\mathbf{u}^{(k)}$ is also an eigenvector. Then, if p_α is a design parameter,

$$\frac{\partial \mathbf{w}^{(k)}}{\partial p_\alpha} = \frac{\partial (c\mathbf{u}^{(k)})}{\partial p_\alpha} = c \frac{\partial \mathbf{u}^{(k)}}{\partial p_\alpha} + d\mathbf{u}^{(k)} \quad (10)$$

where $d = (\partial c / \partial p_\alpha)$ is arbitrary. In practice, the constant d depends on the way the eigenvectors $\mathbf{u}^{(k)}$ and $\mathbf{w}^{(k)}$ are normalized.

Methods of Calculation

The various methods of calculating the derivatives of eigenvalues and eigenvectors can be divided into three categories:

1. *Adjoint Methods*, which use both the right and the left eigenvectors.
2. *Direct Methods*, which use only the right eigenvectors.
3. *Iterative Methods*, which use an iterative algorithm that converges to the required derivatives.

Adjoint Methods

The first expressions for the derivatives of eigenvalues of a general matrix seem to have been derived by Lancaster[23]. Considering only a single parameter, Lancaster obtained the following expressions for the first and second derivatives of an eigenvalue:

$$\lambda_{,\alpha}^{(k)} = \frac{\mathbf{v}^{(k)T} \mathbf{A}_{,\alpha} \mathbf{u}^{(k)}}{\mathbf{v}^{(k)T} \mathbf{u}^{(k)}} \quad (11)$$

$$\lambda_{,\alpha\alpha}^{(k)} = \frac{\mathbf{v}^{(k)T} \mathbf{A}_{,\alpha\alpha} \mathbf{u}^{(k)}}{\mathbf{v}^{(k)T} \mathbf{u}^{(k)}} + 2 \sum_{\substack{j=1 \\ j \neq k}}^n \left[\frac{(\mathbf{v}^{(k)T} \mathbf{A}_{,\alpha} \mathbf{u}^{(j)}) (\mathbf{v}^{(j)T} \mathbf{A}_{,\alpha} \mathbf{u}^{(k)})}{(\lambda^{(k)} - \lambda^{(j)}) (\mathbf{v}^{(k)T} \mathbf{u}^{(k)}) (\mathbf{v}^{(j)T} \mathbf{u}^{(j)})} \right] \quad (12)$$

An expression corresponding to eq. (11) for a generalized quadratic eigenvalue problem was obtained by Pedersen and Seyranian[24].

Morgan[25] obtained an expression for the derivative of an eigenvalue without requiring the eigenvectors explicitly. His expression is equivalent to

$$\lambda_{,\alpha}^{(k)} = \frac{\text{trace of } \{ [\text{adj}(\mathbf{A} - \lambda^{(k)} \mathbf{I})] \mathbf{A}_{,\alpha} \}}{\text{trace of } \text{adj}(\mathbf{A} - \lambda^{(k)} \mathbf{I})} \quad (13)$$

The corresponding expression for derivatives with respect to matrix elements was derived by Nicholson[26].

It can however be shown that[27]

$$\text{adj}(\mathbf{A} - \lambda^{(k)} \mathbf{I}) = t_k \mathbf{u}^{(k)} \mathbf{v}^{(k)T} \quad (14)$$

where t_k is a constant and that[28]

$$\begin{aligned} \text{trace of } \{ [\text{adj}(\mathbf{A} - \lambda^{(k)} \mathbf{I})] \mathbf{A}_{,\alpha} \} &= t_k \mathbf{v}^{(k)T} \mathbf{A}_{,\alpha} \mathbf{u}^{(k)} \\ \text{trace of } \text{adj}(\mathbf{A} - \lambda^{(k)} \mathbf{I}) &= t_k \mathbf{v}^{(k)T} \mathbf{u}^{(k)} \end{aligned} \quad (15)$$

Thus, in the computation of $\text{adj}[\mathbf{A} - \lambda^{(k)} \mathbf{I}]$, both right and left eigenvectors are implicitly computed, in view of eq. (14). Eqs. (15) also show that Morgan's eq. (13) is equivalent to Lancaster's eq. (11). Woodcock[29] also obtained formulas involving the adjoint matrix for the first and second derivatives of eigenvalues. An operation count shows that calculation of the adjoint matrix is several times more expensive than the explicit calculation of right and left eigenvectors so that Lancaster's formula is preferable to formulas requiring the adjoint matrix. This conclusion is also supported by sample computations[30]. In addition, although eq. (13) was used satisfactorily for small problems[31,32], numerical difficulties were reported for reasonably large problems[33]. Woodcock's formula for the second derivative of the eigenvalue requires a partial derivative of the adjoint matrix and this is so complicated that Woodcock himself recommends the finite difference method. Formulas due to Morgan and Woodcock are not therefore considered in the following.

To obtain the second derivatives of eigenvalues, the first derivatives of left and right eigenvectors are calculated either implicitly[9,11,23] or explicitly[1,8,12,34,35]. Since the eigenvalues are assumed to be distinct, the first derivatives of eigenvectors can be expressed as

$$\mathbf{u}_{,\alpha}^{(k)} = \sum_{j=1}^n c_{kja} \mathbf{u}^{(j)} \quad \text{and} \quad \mathbf{v}_{,\alpha}^{(k)} = \sum_{j=1}^n d_{kja} \mathbf{v}^{(j)} \quad (16)$$

Rogers[36] obtained the coefficients c_{kja} and d_{kja} as

$$c_{kja} = \frac{\mathbf{v}^{(j)T} \mathbf{A}_{,\alpha} \mathbf{u}^{(k)}}{(\lambda^{(k)} - \lambda^{(j)}) \mathbf{v}^{(j)T} \mathbf{u}^{(j)}} \quad k \neq j \quad (17)$$

$$d_{kja} = \frac{\mathbf{v}^{(k)T} \mathbf{A}_{,\alpha} \mathbf{u}^{(j)}}{(\lambda^{(k)} - \lambda^{(j)}) \mathbf{v}^{(j)T} \mathbf{u}^{(j)}} \quad k \neq j \quad (18)$$

It can be observed that

$$d_{kja} = -c_{jka} \frac{\mathbf{v}^{(k)T} \mathbf{u}^{(k)}}{\mathbf{v}^{(j)T} \mathbf{u}^{(j)}} \quad (19)$$

Reddy[37] derived an equivalent expression for the response derivative by casting the derivative as the solution of a forced response problem for the same system.

Note that, in view of eq. (10), the coefficients c_{kka} and d_{kka} in eq. (16) are arbitrary and depend on the normalization of the eigenvectors. For example, if eq. (7) is used to normalize the right eigenvectors, then

$$c_{kka} = - \sum_{\substack{j=1 \\ j \neq k}}^n c_{kja} u_m^{(j)} \quad (20)$$

and if eq. (6) is used to normalized the left eigenvectors, then

$$d_{kka} = -c_{kka} \quad (21)$$

It has been proposed[38,39] that the eigenvector derivative be approximated by using less than the full set of eigenvectors in the expansion of eq. (16) so that the evaluation of eigenvector derivative by Adjoint Method could become cheaper. This variant of Adjoint Method has received mixed reports in the literature[22,38]. The quality of such an approximation is difficult to assess beforehand and the selection of eigenvectors to be retained in the expansion is problem dependent. It has not been considered in this work because a meaningful comparison with other methods cannot easily be made. However, this consideration should not be ignored while implementing the sensitivity calculations for particular problems.

The expressions for the second derivatives of eigenvalues were obtained by Plaut and Huseyin[35]. For the sake of simplicity in expressions, let us assume, without loss of generality, that the left eigenvectors are normalized as in eq. (6).

Plaut and Huseyin[35] obtained the second derivatives of eigenvalues with respect to uncorrelated parameters p_α and p_β as

$$\lambda_{,\alpha\beta}^{(k)} = \mathbf{v}^{(k)T} \mathbf{A}_{,\alpha\beta} \mathbf{u}^{(k)} + \mathbf{v}^{(k)T} \mathbf{A}_{,\alpha} \mathbf{u}_{,\beta}^{(k)} + \mathbf{v}_{,\beta}^{(k)T} \mathbf{A}_{,\alpha} \mathbf{u}^{(k)} \quad (22)$$

which can be equivalently written, without involving the derivative of the left eigenvector, as

$$\lambda_{,\alpha\beta}^{(k)} = \mathbf{v}^{(k)T} \mathbf{A}_{,\alpha\beta} \mathbf{u}^{(k)} + \mathbf{v}^{(k)T} (\mathbf{A}_{,\alpha} - \lambda_{,\alpha} \mathbf{I}) \mathbf{u}_{,\beta}^{(k)} + \mathbf{v}^{(k)T} (\mathbf{A}_{,\beta} - \lambda_{,\beta} \mathbf{I}) \mathbf{u}_{,\alpha}^{(k)} \quad (23)$$

For a diagonal second derivative, eq.(22) is simplified to

$$\lambda_{,\alpha\alpha}^{(k)} = \mathbf{v}^{(k)T} \mathbf{A}_{,\alpha\alpha} \mathbf{u}^{(k)} + 2\mathbf{v}^{(k)T} \mathbf{A}_{,\alpha} \mathbf{u}_{,\alpha}^{(k)} \quad (24)$$

Eq. (22) can be rewritten using eqs. (17) and (18) as

$$\lambda_{,\alpha\beta}^{(k)} = \mathbf{v}^{(k)T} \mathbf{A}_{,\alpha\beta} \mathbf{u}^{(k)} + \sum_{\substack{j=1 \\ j \neq k}}^n (\lambda^{(k)} - \lambda^{(j)}) (c_{kj\alpha} d_{kj\beta} + c_{kj\beta} d_{kj\alpha}) \quad (25)$$

Crossley and Porter[1,40] derived similar expressions for derivatives with respect to the elements of the matrix. Expressions for N -th order diagonal derivatives were derived by Elrazaz and Sinha[5].

In calculating the derivatives using eqs. (11), (16)-(25),

- the first derivative of an eigenvalue requires the corresponding right and left eigenvectors.
- the first derivative of an eigenvector requires *all* the left and right eigenvectors.
- the second derivative of an eigenvalue requires the corresponding right and left eigenvectors and their first derivatives.

Direct Methods

The second category comprises methods that evaluate the derivatives using only the right eigenproblem. Direct Methods typically involve either the evaluation of the characteristic polynomial or the solution of a system of linear simultaneous equations without requiring all the left and right eigenvectors. Methods requiring the evaluation of the characteristic polynomial and the derivative of the determinant[33,41] are $O(n^5)$ processes while other methods considered here are at most $O(n^3)$ processes. In addition, the determination of the characteristic polynomial is, in general, an unsatisfactory process with respect to numerical stability, even when all the eigenvalues are well-conditioned[42]. While numerically stable algorithms have been proposed for evaluation of the characteristic polynomial[43], the computational expense still seems to be formidable. Hence, we do not consider these methods. Methods requiring the solution of a system of equations have the particularly attractive feature that the coefficient matrix needs to be factored only once for each eigenvalue regardless of the number of parameters and the order of the derivatives

required. Thus, they are very useful in applications where higher order derivatives are required.

The earliest method in this class is due to Garg[18] who obtained the first derivatives of the eigenvalue and the eigenvector by solving two systems of $(n + 1)$ equations each in the real domain, without requiring any left eigenvectors. However, his formulation involves several matrix multiplications. Rudisill[19] proposed a scheme in which only the corresponding left and right eigenvectors are required to calculate the first derivative of the eigenvalue and the eigenvector. This was refined by Rudisill and Chu[20] to avoid calculating the left eigenvectors altogether. Solution of a system of only $(n + 1)$ equations is required (though in the complex domain) to obtain the first derivatives of eigenvalue as well as eigenvector. Extension to higher order derivatives is straightforward. Cardani and Mantegazza[21] proposed solution methods of the same formulation for sparse matrices and extended it to the quadratic eigenproblem.

One weakness that is common to all the above formulations that do not require left eigenvectors[18-21] is that they rely on the normalization condition given by eq. (4), which is unreliable for general eigenproblems as discussed earlier.

Nelson[22] circumvented this difficulty by using the normalizing conditions

$$\mathbf{v}^{(k)T} \mathbf{u}^{(k)} = 1 \quad \text{and} \quad u_m^{(k)} = 1$$

However, the formulation of Rudisill and Chu is superior to Nelson's formulation in that it does not require any left eigenvectors.

In this paper, we propose a variation of the Rudisill and Chu formulation which does not rely on the questionable normalizing condition of eq. (4) and at the same time requires no left eigenvectors.

Differentiating eq. (1), we get

$$\mathbf{A}_{\alpha} \mathbf{u}^{(k)} + \mathbf{A}_{,\alpha} \mathbf{u}^{(k)} = \lambda^{(k)} \mathbf{u}_{,\alpha}^{(k)} + \lambda_{,\alpha}^{(k)} \mathbf{u}^{(k)} \quad (26)$$

which can be rewritten in partitioned matrix form as

$$[\mathbf{A} - \lambda^{(k)} \mathbf{I} \mid -\mathbf{u}^{(k)}] \left\{ \frac{\mathbf{u}_{,\alpha}^{(k)}}{\lambda_{,\alpha}^{(k)}} \right\} = -\mathbf{A}_{,\alpha} \mathbf{u}^{(k)} \quad (27)$$

Now, we impose the normalizing condition of eq. (7). Differentiation of eq. (7) yields,

$$u_{m,\alpha}^{(k)} = 0 \quad (28)$$

Because of eq. (28), the m -th column of the coefficient matrix in eq. (27) can be deleted. Eq. (28) also reduces the number of unknowns by one so that eq. (27) is now a system of n equations in n unknowns. Eq. (27) is rewritten as

$$\mathbf{B} \mathbf{y}_1 = \mathbf{r} \quad (29)$$

where

$$\begin{aligned} \mathbf{B} &= [\mathbf{A} - \lambda^{(k)} \mathbf{I} \mid -\mathbf{u}^{(k)}]_{m\text{-th column deleted}} \\ \mathbf{y}_1 &= \left\{ \begin{array}{c} \mathbf{u}_{,\alpha}^{(k)} \\ -\lambda_{,\alpha}^{(k)} \end{array} \right\} \text{ with } m\text{-th element deleted} \\ \mathbf{r} &= -\mathbf{A}_{,\alpha} \mathbf{u}^{(k)} \end{aligned} \quad (30)$$

To get second derivatives, differentiate (27) with respect to p_β and get,

$$\begin{aligned} (\mathbf{A} - \lambda^{(k)} \mathbf{I}) \mathbf{u}_{,\alpha\beta}^{(k)} - \mathbf{u}^{(k)} \lambda_{,\alpha\beta}^{(k)} &= -\mathbf{A}_{,\alpha\beta} \mathbf{u}^{(k)} - (\mathbf{A}_{,\alpha} - \lambda_{,\alpha}^{(k)} \mathbf{I}) \mathbf{u}_{,\beta}^{(k)} \\ &\quad - (\mathbf{A}_{,\beta} - \lambda_{,\beta}^{(k)} \mathbf{I}) \mathbf{u}_{,\alpha}^{(k)} \end{aligned} \quad (31)$$

or, in partitioned matrix form,

$$\begin{aligned} [\mathbf{A} - \lambda^{(k)} \mathbf{I} \mid -\mathbf{u}^{(k)}] \left\{ \begin{array}{c} \mathbf{u}_{,\alpha\beta}^{(k)} \\ -\lambda_{,\alpha\beta}^{(k)} \end{array} \right\} &= -\mathbf{A}_{,\alpha\beta} \mathbf{u}^{(k)} - (\mathbf{A}_{,\alpha} - \lambda_{,\alpha}^{(k)} \mathbf{I}) \mathbf{u}_{,\beta}^{(k)} \\ &\quad - (\mathbf{A}_{,\beta} - \lambda_{,\beta}^{(k)} \mathbf{I}) \mathbf{u}_{,\alpha}^{(k)} \end{aligned} \quad (32)$$

Following the same reasoning as before, eq. (32) is written as

$$\mathbf{B} \mathbf{y}_2 = \mathbf{s} \quad (33)$$

where

$$\begin{aligned} \mathbf{y}_2 &= \left\{ \begin{array}{c} \mathbf{u}_{,\alpha\beta}^{(k)} \\ -\lambda_{,\alpha\beta}^{(k)} \end{array} \right\} \text{ with } m\text{-th element deleted} \\ \mathbf{s} &= -\mathbf{A}_{,\alpha\beta} \mathbf{u}^{(k)} - (\mathbf{A}_{,\alpha} - \lambda_{,\alpha}^{(k)} \mathbf{I}) \mathbf{u}_{,\beta}^{(k)} - (\mathbf{A}_{,\beta} - \lambda_{,\beta}^{(k)} \mathbf{I}) \mathbf{u}_{,\alpha}^{(k)} \end{aligned} \quad (34)$$

Note that, if $\lambda^{(k)}$ is a simple eigenvalue of \mathbf{A} and if $u_m^{(k)} \neq 0$, then the matrix \mathbf{A} is of rank $(n - 1)$ and the m -th column that is deleted is linearly dependent on the other columns. Hence the matrix \mathbf{B} is non-singular. The matrix \mathbf{B} will also be well-conditioned if $u_m^{(k)}$ is the largest component in the eigenvector $\mathbf{u}^{(k)}$ and the matrix \mathbf{A} is itself not ill-conditioned. The vectors \mathbf{y}_1 and \mathbf{y}_2 can be obtained by standard solution methods. If the matrix \mathbf{A} is banded or if the derivatives of both right and left eigenvectors are required, it may be more efficient to use a partitioning scheme as described in the appendix.

In summary, we note that, in calculating derivatives by Direct Method,

- left eigenvectors are not used.
- a complete solution of the eigenvalue problem is not required, if the derivatives of only a few of the eigenvalues and eigenvectors are sought. This is in contrast to the Adjoint Method which requires all the left and right eigenvectors to calculate the first derivative of any eigenvector.

- calculation of any derivative requires the solution of a system of linear equations.
- only one matrix factorization needs to be performed for all orders of derivatives of an eigenvalue and its corresponding right and left eigenvectors.

Iterative Methods

Andrew[44] proposed an iterative algorithm to calculate the first derivatives of eigenvalues and eigenvectors. This algorithm is a refined and generalized version of the iterative scheme developed by Rudisill and Chu[20]. Except for the dominant eigenvalue, the convergence of this algorithm seems to be very much dependent on the choice of the initial values for the derivatives. To be efficient for non-Hermitian matrices, this iterative method requires a complex eigenvalue shifting strategy which is not easy to implement. Hence this method is not considered.

Relative Computational Cost

In this section, we compare the efficiency of calculating the derivatives of eigensystems as a function of the size of the matrix n , number of design parameters m and number of eigenvalues of interest l .

To start with, let us consider the operation counts (flops) for the Adjoint Methods given by eqs. (11),(16)-(25) and the Direct Methods given by eqs.(29)-(34). They are summarized in Table 1. It should be noted that the operation counts represent an estimate of the actual number of operations performed by a solution routine and include only the most significant terms. The actual number of operations will vary slightly depending on programming details. The effect of the sparsity of the matrix derivative $A_{,\alpha}$ is modeled by the parameter κ , defined such that the the number of operations in evaluating the product $A_{,\alpha}u$ is equal to κn^2 (that is, $\kappa = 1$ corresponds to a full $A_{,\alpha}$).

The eigenvalues are calculated using the EISPACK subroutine package [45] by first reducing the matrix to upper Hessenberg form using unitary similarity transformations and then applying the QR algorithm. The number of operations and CPU time for calculating the eigenvalues are not counted in the following results as they are not relevant in comparing the methods to calculate the derivatives.

The right eigenvectors are calculated by inverse iteration on the same upper Hessenberg matrix used for calculating the eigenvalues and back transformation using standard subroutines in the package EISPACK. The corresponding operation count is given in Table 1. For the calculation of left eigenvectors, it is important to note that there is no need to repeat the process with the transposed matrix. The left eigenvectors are obtained cheaply using forward substitution in place of backward substitution in the inverse iteration process. There is also no need to repeat the matrix factorization. A subroutine was written to calculate the right and left eigenvectors in this manner and the corresponding operation count is given in Table 1.

Table 1 gives the operation count of evaluating the individual steps. To obtain the number of operations involved in evaluating the derivatives, we must add the operation counts for all the steps required in the calculations. These counts are given in the following discussion.

CPU Time Statistics

In the following tables, computational cost for the calculation of the first and second derivatives of eigensystems are compared for matrices of order 20, 40 and 60. The CPU time statistics are obtained on the IBM 3084 computer using the VS-FORTRAN compiler with no compiler optimization. The ratio of operation count(OC) and CPU time for various operations is about 10^5 operations per CPU second with a variability of 27 percent.

The matrices are generated for the dynamic stability analysis of a compressor stage rotor with mistuned blades. The geometric and structural parameters of the rotor and formulation and method of analysis are the same as those of NASA Test Rotor 12 described in reference[46] except that the number of blades and the torsional frequencies are varied. The torsional frequency values are selected randomly from a population of mean 1.0 and standard deviation 0.01. The standard deviations of the actual samples are slightly different.

Calculation of First Derivatives of Eigenvalues Only

Operation Count	
Adjoint Method	$O(\frac{7}{2}n^2 + \kappa mn^2)$
Direct Method	$O[\frac{n^3}{3} + (\kappa + 1)mn^2]$

It is clear from the operation count that the Adjoint Method, which is an $O(n^2)$ process, is superior to Direct Method, an $O(n^3)$ process, for large n . The number of design variables and the number of eigenvalues of interest have no bearing on this conclusion. As the order of the matrix increases, the Direct Method becomes more expensive. For example, for 5 design variables and 10 eigenvalues of interest, the CPU time for the Direct Method is 2.3 times more expensive than for the Adjoint Method for $n = 20$, and for $n=60$, the ratio is 3.0.

Calculation of First Derivatives of Eigenvalues and Eigenvectors

Operation Count	
Adjoint Method	$\frac{7}{2}n^3 + lmn^2(\kappa + 2)$
Direct Method	$\frac{ln^3}{3} + lmn^2(\kappa + 1)$

When the derivatives of both eigenvalues and right eigenvectors are required, the choice of method is dependent on the values of l and m . When very few eigenvalues are of interest, the Direct Method is cheaper. When many eigenvalues are of interest, the Direct Method is more expensive than the Adjoint Method. However, this effect of the number of eigenvalues of interest is less significant when the number of design variables is large. As the number of design variables increases, the Direct Method becomes more competitive, even when all eigenvalues are of interest. For a 60 x 60 full ($\kappa = 1$) matrix, this is illustrated in Figure 1.

The operation count shows that the computation by Adjoint Method of eigenvector derivative, which is necessary for the second derivative of eigenvalue, is an $O(n^3)$ process and is more expensive than the computation of the eigenvector itself which is an $O(n^2)$ process using the procedure described above. This fact is significant as some authors have stated the opposite[2,3].

Calculation of First and Second Derivatives of Eigenvalues only

Operation Count

Adjoint Method	$\frac{7}{2}n^3 + (\kappa + 1)mn^3 + l \binom{m}{2} n^2\kappa$
Direct Method	$l\frac{n^3}{3} + l \binom{m}{2} n^2(3\kappa + 1)$
Direct-Adjoint Method	$l\frac{n^3}{3} + l \binom{m}{2} n^2\kappa + lmn^2(2\kappa + 1)$

The Direct-Adjoint Method denotes the calculation of the eigenvector derivatives by the Direct Method and the eigenvalue derivatives by the Adjoint Method. The third term in the operation count for the Direct-Adjoint Method is significant only when m is small. From the operation count, it is seen that the Direct-Adjoint Method is always cheaper than the Direct Method. Hence, the choice is between the Adjoint Method and the Direct-Adjoint Method. Here, considerations similar to those of the last section hold and the choice of method depends on the values of l and m . When few eigenvalues are of interest, the Direct-Adjoint Method is cheaper. When many eigenvalues are of interest, the Adjoint Method is superior. But this advantage of Adjoint Method diminishes as the number of design variables increases. This is again illustrated for a 60 x 60 full matrix ($\kappa = 1$) in Figure 2.

Concluding Remarks

The normalization of the eigenvector needs to be properly related to its derivative. In practice, this means that the derivative of the eigenvector is to be normalized before it is used, to conform to the normalization of the eigenvector itself. When the eigenvector is not normalized in a unique manner, its derivative cannot be evaluated. Fixing one of the components of the eigenvector is the best normalizing condition for computation of the derivative. The methods found in the literature are extended to apply to eigenvectors normalized in this manner.

Various methods for calculation of derivatives of eigenvalues and eigenvectors are surveyed and classified as Direct or Adjoint. Adjoint Methods use both the left and the right eigenvectors whereas the Direct Methods use only the right eigenvectors. Their relative efficiency is evaluated as a function of matrix size, number of eigenvalues of interest and the number of design parameters. General recommendations are made for the cases when (a) eigenvalue first derivatives are required, (b) eigenvalue and eigenvector first derivatives are required, and (c) eigenvalue second derivatives are required.

When only eigenvalue first derivatives are required, the calculation of left eigenvectors is worth the expense as the Adjoint Method is shown to be superior to the Direct Method. When first derivatives of eigenvectors are also required, the decision is dependent on the problem size, the number of design variables and the number of eigenvalues of interest. When the first and second derivatives of eigenvalues are required, similar considerations hold. It is also shown that once the first derivatives of eigenvectors are calculated, the second derivatives of eigenvalues are calculated more efficiently by the Adjoint Method than by the Direct Method.

Acknowledgment

This work was sponsored by NASA grants NAG-3-347 and NAG-1-224.

Appendix

Modification of Direct Method for Banded Matrices

Equations (29) and (33) can be written as

$$(\mathbf{A} - \lambda^{(k)} \mathbf{I})_{m\text{-th column deleted}} \mathbf{u}_{,\alpha}^{(k)} - \lambda_{,\alpha} \mathbf{u} = \mathbf{r} \quad (\text{A1})$$

Let $\mathbf{u}^{(k)}$ be normalized so that $u_m^{(k)} = 1$

Eq. (A1) is a system of n equations. Writing the m -th equation separately, we have, if the superscript (k) is omitted for notational convenience,

$$\mathbf{C} \mathbf{x}_{,\alpha} - \lambda_{,\alpha} \mathbf{x} = \mathbf{t} \quad (\text{A2})$$

and

$$\mathbf{a}_m^T \mathbf{x}_{,\alpha} - \lambda_{,\alpha} = r_m \quad (\text{A3})$$

where

$$\mathbf{C} = (\mathbf{A} - \lambda \mathbf{I})_{m\text{-th row and column deleted}}$$

$$\mathbf{x}_{,\alpha} = \mathbf{u}_{,\alpha} \text{ } m\text{-th row deleted}$$

$$\mathbf{x} = \mathbf{u}_{m\text{-th row deleted}}$$

$$\mathbf{t} = \mathbf{r}_{m\text{-th row deleted}}$$

$$\mathbf{a}_m^T = m\text{-th row of } \mathbf{A} \text{ with the } m\text{-th column deleted}$$

From (A3),

$$\lambda_{,\alpha} = \mathbf{a}_m^T \mathbf{x}_{,\alpha} - r_m \quad (\text{A4})$$

From (A2),

$$\mathbf{x}_{,\alpha} = \mathbf{C}^{-1}(\lambda_{,\alpha}\mathbf{x} + \mathbf{t}) \quad (\text{A5})$$

Eliminating $\mathbf{x}_{,\alpha}$, we have

$$\lambda_{,\alpha} = \frac{\mathbf{t}^T \mathbf{b}_m - r_m}{1 - \mathbf{x}^T \mathbf{b}_m} \quad (\text{A6})$$

where

$$\mathbf{b}_m = [\mathbf{C}^T]^{-1} \mathbf{a}_m$$

Proceeding in a similar manner for the left eigenvector,

$$\mathbf{y}_{,\alpha} = [\mathbf{C}^T]^{-1}(\lambda_{,\alpha}\mathbf{y} + \mathbf{t}_l) \quad (\text{A7})$$

where

$$\mathbf{y}_{,\alpha} = \mathbf{v}_{,\alpha} \text{ } m\text{-th row deleted}$$

$$\mathbf{y} = \mathbf{v} \text{ } m\text{-th row deleted}$$

$$\mathbf{t}_l = (\mathbf{r}_l) \text{ } m\text{-th row deleted}$$

\mathbf{r}_l being the appropriate right hand side.

Thus the following procedure can be used to obtain the derivatives $\lambda_{,\alpha}$ and $\mathbf{u}_{,\alpha}$.

1. Form a LU decomposition of the matrix \mathbf{C} .
2. Solve $\mathbf{b}_m = [\mathbf{C}^T]^{-1} \mathbf{a}_m$ by forward substitution.
3. Calculate $\lambda_{,\alpha}$ from (A6).
4. Calculate $\mathbf{x}_{,\alpha}$ from (A5) by backward substitution.
5. Expand $\mathbf{x}_{,\alpha}$ to $\mathbf{u}_{,\alpha}$ setting $\mathbf{u}_{m,\alpha} = 0$.

If the derivatives $\mathbf{v}_{,\alpha}$ of the left eigenvectors are also required, only three further steps are needed.

6. Calculate $\mathbf{y}_{,\alpha}$ from (A7) by forward substitution.
7. Expand $\mathbf{y}_{,\alpha}$ to $\mathbf{v}_{,\alpha}$ setting $\mathbf{v}_{m,\alpha} = 0$.
8. Normalize $\mathbf{v}_{,\alpha}$ appropriately depending on the normalization of \mathbf{v} . For example, to obtain the derivative of the left eigenvector that satisfies the normalization condition of eq. (6), subtract $(\mathbf{v}^T \mathbf{u}_{,\alpha} + \mathbf{v}_{,\alpha}^T \mathbf{u}) \mathbf{v}$.

The matrix \mathbf{C} needs to be factored only once. Also, the matrix \mathbf{C} retains the bandedness characteristics of the original matrix \mathbf{A} . Furthermore, higher derivatives can be obtained by merely substituting an appropriate right hand side vector, \mathbf{r} . However, higher order derivatives can suffer in accuracy because of accumulated round-off error.

The conditioning of matrix \mathbf{C} needs some comment. Note that \mathbf{C} is obtained from the singular matrix $(\mathbf{A} - \lambda^{(k)}\mathbf{I})$ by deleting both the row and column corresponding to index m . Hence, for matrix \mathbf{C} to be non-singular, one must make sure that the m -th row is linearly dependent on the other rows as well as that the m -th column is linearly dependent on the other columns. In other words, \mathbf{C} is non-singular iff $u_m^{(k)} \neq 0$ and $v_m^{(k)} \neq 0$. If $v_m^{(k)}$ is very small compared to the largest element in $\mathbf{v}^{(k)}$, steps 2 and 4 in the above procedure will give inaccurate results even if $u_m^{(k)}$ is the largest element in $\mathbf{u}^{(k)}$. In general, it is not possible to make a good choice for m without the knowledge of the left eigenvector. Since the calculation of left eigenvector by forward substitution is cheap, it is suggested that the left eigenvector be calculated and the index m be chosen as in eq.(9). This is the same criterion used by Nelson[22] and will assure as well-conditioned a matrix \mathbf{C} as possible.

References

1. Crossley, T.R. and Porter, B., "High-order Eigenproblem Sensitivity Methods: Theory and Applications to the Design of Linear Dynamical Systems", Intl. J. of Control, Vol.10, No. 3, 1969, pp.315-329.
2. Zein El-Din, H.M., Alden, R.T.H. and Chakravarti, P.C., "Second Order Eigenvalue Sensitivities Applied to Multivariable Control Systems", Proc. of the IEEE, Vol. 65, Feb. 1977, pp.277-278.
3. Zein El-Din, H.M. and Alden, R.T.H., "Second Order Eigenvalue Sensitivities Applied to Power System Dynamics", IEEE Trans. on Power Apparatus and Systems, Vol. PAS-96, No. 6, Nov./Dec. 1977, pp.1928-1936.
4. Flax, A.H., "Comment on 'Estimation of Fundamental Frequencies of Beams and Plates with Varying Thickness'", AIAA Journal, Vol. 16, Sept.1978, pp.1022-1024.
5. Elrazaz, Z. and Sinha, N.K., "Dynamic Stability Analysis of Power Systems for Large Parameter Variations", IEEE PES Summer Meeting, Vancouver, Canada, July 15-20, 1979.
6. Elrazaz, Z. and Sinha, N.K., "Dynamic Stability Evaluation for Multimachine System: An Efficient Eigenvalue Approach", IEE Proceedings-D, Vol. 128, No. 6, Nov. 1981, pp.268-274.
7. Haftka, R.T. and Kamat, M.P., "Elements of Structural Optimization", Martinus Nijhoff Publishers, 1985.
8. Rudisill, C.S. and Bhatia, K.G., "Second Derivatives of the Flutter Velocity and the Optimization of Aircraft Structures", AIAA Journal, Vol.10, No.12, Dec.1972, pp.1569-1572.
9. Bhatia, K.G., "An Automated Method for Determining the Flutter Velocity and the Matched Point", J. Aircraft, Vol.11, No.1, Jan.1974, pp.21-27.
10. Miura, H. and Schmit, L.A., "Second Order Approximation of Natural Frequency Constraints in Structural Synthesis", Intl. Journal for Numerical Methods in Engineering, Vol. 13, 1978, pp.337-351.
11. Rudisill, C.S. and Cooper, J.L., "An Automated Procedure for Determining the Flutter Velocity", J. Aircraft, Vol.10, No.7, Jul.1973, pp.442-444.
12. Junkins, J.L., Bodden, D.S. and Kamat, M.P., "An Eigenvalue Optimization Approach for Feedback Control of Flexible Structures", Proc. of SECTAM XII, May 10-11, 1984, Vol. II, pp.303-308.

13. Jacobi, C.G.J., "Über ein leichtes Verfahren die in der Theorie der Saecular stoerungen vorkommenden Gleichungen numerisch aufzuloesen", Zeitschrift fur Reine unde Angewandte Mathematik, Vol.30, 1846, pp.51-95.
14. Wittrick, W.H., "Rates of Change of Eigenvalues with Reference to Buckling and Vibration Problems", J. Royal Aeronautical Society, Vol.66, 1962, pp.590-591.
15. Fox, R.L. and Kapoor, M.P., "Rates of Change of Eigenvalues and Eigenvectors", AIAA Journal, Vol.6, No.12, 1968, pp.2426-2429.
16. Zarghamee, M.S., "Minimum Weight Design with Stability Constraint", J. of the Struct.Divn./ASCE, Vol.96, ST8, 1970, pp.1697-1710.
17. Fox, R.L., "Optimization Methods for Engineering Design", Addison-Wesley Pub. Co. Inc., 1971.
18. Garg, S., "Derivatives of Eigensolutions for a General Matrix", AIAA Journal, Vol.11, No.8, Aug.1973, pp.1191-1194.
19. Rudisill, C.S., "Derivatives of Eigenvalues and Eigenvectors for a General Matrix", AIAA Journal, Vol.12, No.5, May 1974, pp.721-722.
20. Rudisill, C.S. and Chu, Y., "Numerical Methods for Evaluating the Derivatives of Eigenvalues and Eigenvectors", AIAA Journal, Vol.13, No.6, Jun.1975, pp.834-837.
21. Cardani, C. and Mantegazza, P., "Calculation of Eigenvalue and Eigenvector Derivatives for Algebraic Flutter and Divergence Problems", AIAA Journal, Vol.17, No.4, Apr.1979, pp.408-412.
22. Nelson, R.B., "Simplified Calculation of Eigenvector Derivatives", AIAA Journal, Vol. 14, No. 9, Sept.1976, pp.1201-1205.
23. Lancaster, P., "On Eigenvalues of Matrices Dependent on a Parameter", Numerische Mathematik, Vol. 6, No. 5, 1964, pp.377-387.
24. Pedersen, P. and Seyranian, A.P., "Sensitivity Analysis for Problems of Dynamic Stability", International Journal of Solids and Structures, Vol. 19, No.4, 1983, pp.315-335.
25. Morgan, B.S., "Computational Procedure for Sensitivity of an Eigenvalue", Electronics Letters, Vol. 2, 1966, pp.197-198.
26. Nicholson, H., "Eigenvalue and State-Transition Sensitivity of Linear Systems", Proc. of IEE, London, Vol. 114, 1967, pp.1991-1995.
27. Frazer, R.A., Duncan, W.J. and Collar, A.R., "Elementary Matrices", Cambridge University Press, London.
28. Reddy, D.C., "Evaluation of the Sensitivity Coefficient of an Eigenvalue", IEEE Trans. on Automatic Control, AC-12, Dec.1967, p.792.
29. Woodcock, D.L., "The Rates of Change of Eigenvalues of a Lambda Matrix and their Use in Flutter Investigations", Journal of the Royal Aeronautical Society, Vol. 70, Feb. 1966, pp.364-365.
30. Vetter, W.J., "Reply to R. G. Rains' Comments on 'An Extension to Gradient Matrices'", IEEE Trans. on Systems, Man and Cybernetics, Vol. SMC-2, No. 2, 1972, p.285.
31. Nagraj, V.T., "Changes in the Vibration Characteristics Due to Changes in the Structure", J. Spacecraft, Vol. 7, No. 12, Dec. 1970, pp.1499-1501.
32. Paraskevopoulos, P.N., Christodoulou, M.A. and Tsakiris, M.A., "Eigenvalue Eigenvector Sensitivity Analysis of Linear Time-Invariant Singular Systems", IEEE Trans. on Automatic Control, AC-29, No. 4, Apr.1984, pp.344-346.
33. Nail, J.B., Mitchell, J.R. and McDaniel Jr., W.L., "Determination of Pole Sensitivities by Danilevskii's Method", AIAA Journal, Vol. 15, No. 10, Oct.1977, pp.1525-1527.

34. Taylor, D.L. and Kane, T.R., "Multiparameter Quadratic Eigenproblems", J. of Applied Mechanics/ASME, Vol.42, Jun.1975, pp.478-483.
35. Plaut, R.H. and Huseyin, K., "Derivatives of Eigenvalues and Eigenvectors in Non-self-adjoint Systems", AIAA Journal, Vol. 11, No. 2, Feb.1973, pp.250-251.
36. Rogers, L.C., "Derivatives of Eigenvalues and Eigenvectors", , AIAA Journal, Vol.8, No. 5, May 1970, pp.943-944.
37. Reddy, D.C., "Eigenfunctions and the Solution of Sensitivity Equations", Electronics Letters, Vol. 4, 1968, pp.262-263.
38. Hasselman, T.K. and Hart, G.C., "Modal Analysis of Random Structural Systems", Journal of the Engineering Mechanics Division/Proc. of the ASCE, Vol. 98, No. EM3, June 1972, pp.561-579.
39. Adelman, H.M. and Haftka, R.T., "Sensitivity Analysis for Discrete Structural Systems-A Survey", NASA TM-86333, Dec. 1984.
40. Crossley, T.R. and Porter, B., "Eigenvalue and Eigenvector Sensitivities in Linear Systems Theory", Intl. J. of Control, Vol.10, No.2, 1969, pp.163-170.
41. Mitchell, J.R., Nail, J.B. and McDaniel, Jr.,W.L., "Computation of Cofactors of [sI-A] with Applications", IEEE Trans. on Automatic Control, AC-24, No. 4, Aug.1979,pp.637-638.
42. Wilkinson, J.H., "The Algebraic Eigenvalue Problem", Clarendon Press, Oxford, 1965.
43. Werner, W., "A Generalized Companion Matrix of a Polynomial and Some Applications", Linear Algebra and Its Applications, Vol. 55, 1983, pp.19-36.
44. Andrew, A.L., "Convergence of an Iterative Method for Derivatives of Eigensystems", J. of Comput. Physics, Vol.26, 1978, pp.107-112.
45. Smith, B.T., Boyle, J. M., Garbow, B.S., Ikebe, Y. and Kleme, V.C., "Matrix Eigensystem Routines - EISPACK Guide", Lecture Notes in Computer Science, Vol. 6, Springer-Verlag, Heidelberg, 1974, pp. 95-97.
46. Kaza, K.R.V. and Kielb, R.E., "Flutter and Response of a Mistuned Cascade in Incompressible Flow", AIAA Journal, Vol. 20, No. 8, Aug. 1982, pp.1120-1127.

Table 1. Operation Counts

Eigenvectors	
Operation	Operation Count
Evaluation of right eigenvectors	$l(2n^2)$
Evaluation of left eigenvectors	$l(\frac{3}{2}n^2)$
Adjoint Methods	
Operation	Operation Count
Evaluation of eq. (11)	$lmn^2\kappa$
Evaluation of eqs. (16),(17),(18)	$lmn^2(\kappa + 2)$
Evaluation of eq. (25)	$l \binom{m}{2} n^2\kappa$
Direct Methods	
Operation	Operation Count
LU decomposition of matrix B	$l(n^3/3)$
Formulation and solution of eq.(29)	$lmn^2(\kappa + 1)$
Formulation and solution of eq.(33)	$l \binom{m}{2} n^2(3\kappa + 1)$

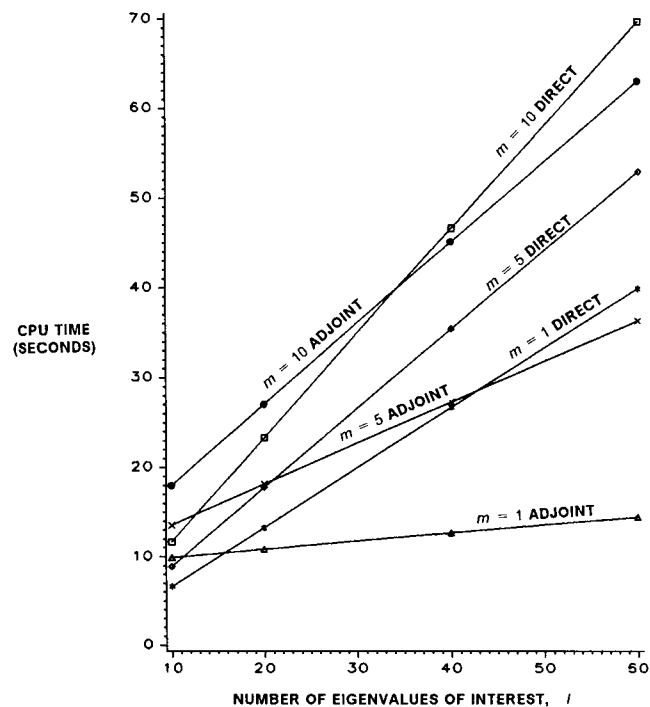


Figure 1. CPU Times for calculation of first derivatives of eigenvalues and eigenvectors for a 60×60 matrix

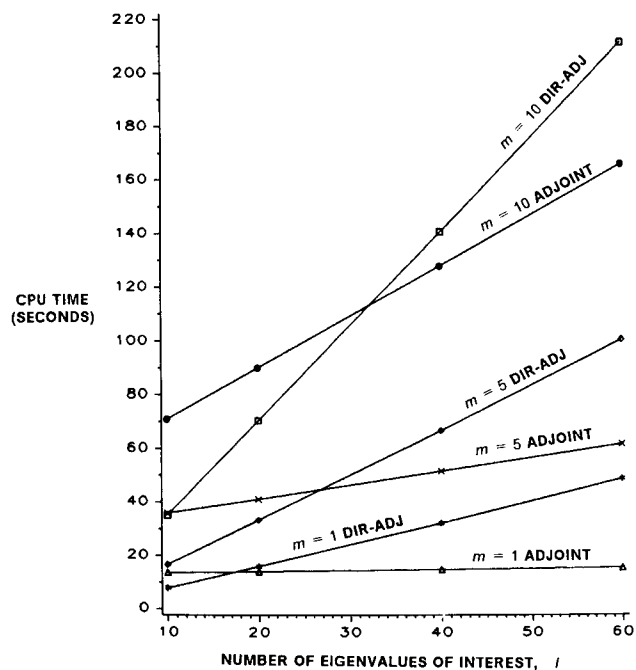


Figure 2. CPU Times for calculation of second derivatives of eigenvalues for a 60×60 matrix

MODAL SENSITIVITY FOR
STRUCTURAL SYSTEMS WITH REPEATED FREQUENCIES

I. U. Ojalvo
University of Bridgeport
Bridgeport, Conn.

ABSTRACT

Repeated or closely packed modal frequencies are common physical occurrences for vibrating structures which are complex or possess multi-planes of symmetry. The computation of the sensitivity to structural modifications for these frequencies and mode shapes is made difficult by the fact that the mode shapes are not unique, since any linear combination of eigenvectors corresponding to a repeated eigenvalue is also an eigenvector.

This paper extends the work of Chen and Pan [1], who used modal expansion techniques for accommodating the sensitivity analysis of structures with repeated eigenvalues. Starting with a discussion of the physical significance of sensitivity analysis for repeated frequency modes, the paper presents a derivation of the governing equations for the derivatives of a repeated eigenvalue. This is followed with a small example to illustrate the results. An efficient computation procedure, based upon an expansion of Nelson's ideas [2] for large banded systems, is then proposed for systems with repeated or closely spaced eigenvalues.

IMPORTANCE OF THE PROBLEM

The importance of obtaining gradients for eigenvalue problems stems from the fact that gradients, or derivatives with respect to system parameters, represent solution sensitivities. A knowledge of these sensitivities permits efficient design modifications, yields insight into the reasons for discrepancies between structural analyses and dynamic tests, and suggests model changes to improve correlations.

KNOWLEDGE OF GRADIENTS:

YIELDS INSIGHT RE. PARAMETER SENSITIVITIES

PERMITS EFFICIENT DESIGN MODIFICATIONS

UNDERSTAND TEST/ANALYSIS DISCREPANCIES

SUGGESTS MODEL CHANGES TO IMPROVE CORRELATION

WHEN DO REPEATED FREQUENCIES OCCUR?

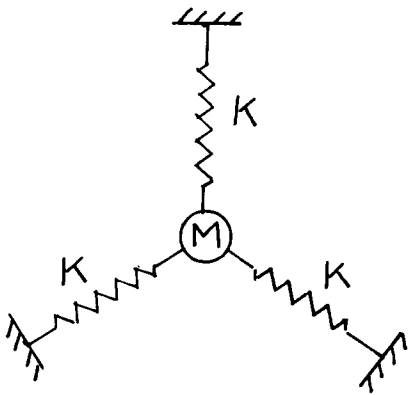
While a procedure for obtaining gradients efficiently was presented a decade ago by Nelson [2], the problems associated with repeated roots have not been adequately addressed.

The problem of repeated frequencies, or identical frequencies with different mode shapes, occurs in many physical situations. The most common circumstances under which multiple eigenvalues occur in engineering are cases where system symmetry exists, such as structures with two or more planes of reflective or cyclic symmetry (see Figure 1) or axis symmetry (see Figure 2).

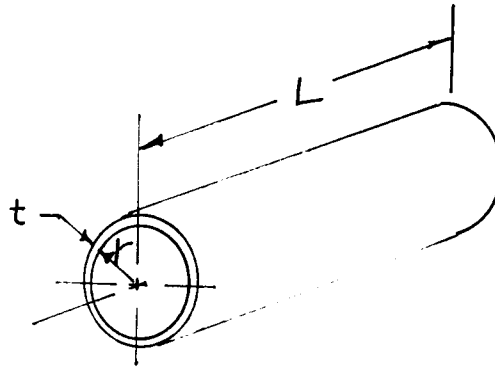
It is also possible for repeated or closely spaced eigenvalues to occur when physical symmetry is not present, such as with classical wing flutter when the first bending and twisting frequencies coalesce.

COINCIDENTAL PARAMETERS (E.G. WING TWIST/BENDING FLUTTER)

SYMMETRY: REFLECTIVE, CYCLIC, AXISYMMETRY



SYMMETRICALLY SUPPORTED MASS



RIGHT CIRCULAR CYLINDRICAL SHELL

TECHNICAL BACKGROUND

Assume $[A]$ and $[B]$ are symmetric $n \times n$ matrices and λ_i is a repeated eigenvalue with $m+1$ distinct orthogonal eigenvectors. Then $\{z_i\}$ is also an eigenvector corresponding to λ_i where

$$\{z_i\} = \sum_{j=0}^m \alpha_{i+j} \{x_{i+j}\} = [X] \{\alpha\}$$

and

$$[X] \equiv \begin{bmatrix} | & | & & | \\ x_i & x_{i+1} & \dots & x_{i+m} \\ | & | & & | \end{bmatrix}$$

SYMMETRIC EIGENVALUE PROBLEM

$$([A] - \lambda_i [B]) \{x_i\} = \{0\}$$

ORTHONORMALIZATION

$$\{x_i\}^T [B] \{x_j\} = \delta_{ij}$$

MULTIPLE EIGENVALUE

λ_i REPEATS $m + 1$ TIMES

CORRESPONDING EIGENVECTORS

$$\{x_i\}, \{x_{i+1}\}, \dots, \{x_{i+m}\}$$

NONUNIQUENESS OF EIGENVECTORS

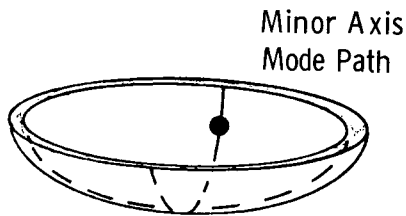
$$\{z_i\} = \sum_{j=0}^m \alpha_{i+j} \{x_{i+j}\} = [X] \{\alpha\}$$

$$[X] \equiv \begin{bmatrix} | & | & \dots & | \\ x_i & x_{i+1} & \dots & x_{i+m} \\ | & | & \dots & | \end{bmatrix}$$

FRICTIONLESS PARTICLE IN A SHALLOW ELLIPTIC DISH PHYSICAL INTERPRETATION

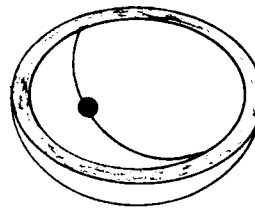
A simple physical interpretation of repeated eigenvalues was presented by Crandall [3] in which he considered a shallow elliptical bowl in which a frictionless mass particle is allowed to slide in the bottom of the bowl (left figure). The eigenvalue problem for this system consists in determining the paths and frequencies of back-and-forth motion in which each motion is repeated on the same path. The natural mode solution is obviously along the major and minor axes of the ellipse.

Next imagine that the elliptical bowl is gradually transformed into a spherical bowl (right figure). The eigenvalues will approach one another and any straight path, through the bottom of the bowl, is equally a natural mode. Thus, when $m+1$ eigenvalues coalesce, there is an infinity of mode shapes composed of a linear combination of the $m+1$ dependent, but somewhat arbitrary, basis modes.



Elliptic Dish - Unique Modes

Any Diametral Path Is A
Natural Mode



Spherical Dish - Nonunique Modes

Natural Frequencies Coalesce As Dish Becomes Spherical

Distinct Mode Shapes Vanish As Ellipticity Disappears

Crandall (ref. 3)

MODAL GRADIENT EQUATIONS PRESENT AN ENIGMA

The modal sensitivity equations for a small change in a typical parameter, R , upon which certain matrix elements of $[A]$ and $[B]$ depend, are well known and summarized below. The problems are that they cannot be easily interpreted for the repeated eigenvalue problem since $\{x_i\}$ is not unique, and matrix $([A] - \lambda_i [B])$ is not of order $n-1$ but lower (i.e., $n-(m+1)$) depending on the multiplicity, m , of eigenvalue λ_i .

$$(\quad)' = \frac{\partial(\quad)}{\partial R}$$

$$\lambda_i' = \{x_i\}^T ([A]' - \lambda_i [B]') \{x_i\}$$

$$([A] - \lambda_i [B]) \{x_i'\} = \{F_i\}$$

$$\{x_i\}^T [B] \{x_i'\} = b$$

$$\{F_i\} = - ([A] - \lambda_i [B])' \{x_i\}$$

$$b = -\frac{1}{2} \{x_i\}^T [B]' \{x_i\}$$

INTERPRETATION PROBLEMS

There are ambiguities associated with the gradient equations since $\{x_i\}$ is not unique and λ_i depends upon which $\{x_i\}$ is chosen. In addition, the rank of $([A] - \lambda_i [B])$ is not $n-1$, but lower. Therefore, inclusion of the derivative of the normalization condition alone is not sufficient to uniquely determine $\{x_i\}$.

WHICH $\{x_i\}$ SHOULD BE USED? Is $\{x_i\}$ DIFFERENTIABLE IN R?

USE OF DIFFERENT $\{x_i\}$ WILL YIELD DIFFERENT RESULTS.

RANK OF $([A] - \lambda_i [B])$ IS TOO LOW TO UNIQUELY DETERMINE $\{x_i'\}$.

WHICH ADDITIONAL EQUATIONS SHOULD BE USED?

REPEATED FREQUENCY SENSITIVITY EQUATION

To determine how the eigenvectors are perturbed by the infinitesimal change in R, we postulate an arbitrary vector $\{Z_i\}$ which is linearly composed of all the $\{x_j\}$ ($j = i, i+1, \dots, i+m$) and premultiply the eigenvector gradient equations by the transpose of all the eigenvectors corresponding to λ_i .

This yields an auxiliary matrix eigenvalue equation in λ'_i , which is of order $m+1$, the solution of which defines the specific eigenvectors, through the eigenvectors $\{\alpha(i)\}$, affected by the change in parameter R.

$$\text{LET } \{Z_i\} = \sum_{j=0}^M \alpha_{i+j} \{x_{i+j}\} = [X] \{\alpha\}$$

$$([A] - \lambda_i [B]) \{Z'_i\} = \{F_i\} = - ([A] - \lambda'_i [B])' \{Z_i\}$$

$$[X]^T ([A] - \lambda_i [B]) = [0]$$

$$[X]^T \{F_i(Z)\} = \{0\} \Leftrightarrow [D] \{\alpha\} = \lambda'_i \{\alpha\}$$

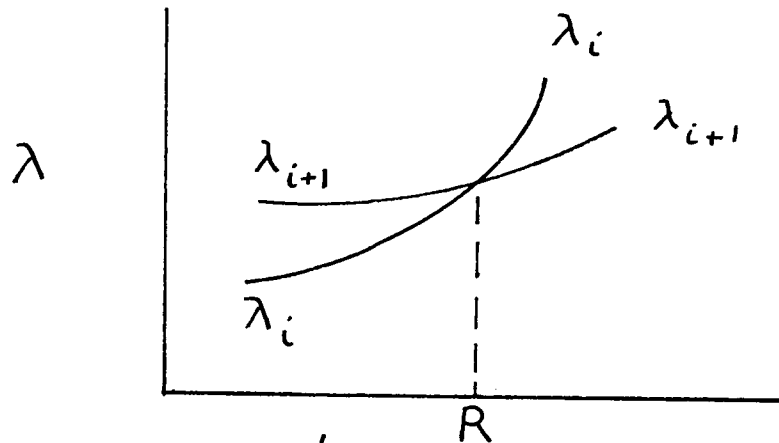
$$[D] \equiv [X]^T ([A]' - \lambda'_i [B]') [X]$$

(M+1) x (M+1)

PHYSICAL INTERPRETATION

Solution of the $(m+1)$ eigenvalues and eigenvectors of the $[D]$ matrix will yield the $m+1$ gradients of λ_i as well as the eigenvectors $\{Z_i\}$ to which they correspond. The figure below displays how the eigenvalues coalesce for a particular value of the parameter R and also shows how they correspond to different gradients. In general, there will be as many derivatives as there are curves intersecting at a particular parameter value R .

$$\begin{matrix} m + 1 \\ \text{SOLUTIONS} \end{matrix} \quad [D] \{ \alpha \} = \lambda'_i \{ \alpha \}$$



NOTE: THERE ARE TWO λ'_i WHERE λ_i COALESCES WITH λ_{i+1}

DETERMINATION OF λ'_i AND CORRESPONDING $\{ \alpha \}$

UNIQUELY DETERMINES MODE FOR GRADIENT SOUGHT

PROPOSED SOLUTION PROCEDURE: OVERVIEW

The solution procedure proposed is an extended version of Nelson's method for non-repeated roots. The method maintains the original matrix bandwidth while eliminating $m+1$ equation redundancies in the original eigenvalue system.

The equations to be eliminated are determined by examining each eigenvector which corresponds to the eigenvalue whose gradients are desired, and establishing which elements are the maximum for each vector. These then correspond to which $m+1$ rows of $([A] - \lambda_i [B])$ should be considered as redundant. If the maximum elements of any two eigenvectors correspond to the same row, then it is necessary to go to the next smaller element until a set of $m+1$ equations for removal is obtained.

Rather than eliminate these rows and upset the system bandedness, we propose to extend Nelson's ideas by zeroing out the corresponding element of $\{F_j\}$ and then solve for $\{V_j\}$.

BASED UPON MAXIMUM ELEMENTS OF $\{Z_i\}, \{Z_{i+1}\}, \dots, \{Z_{i+m}\}$

ZERO-OUT $m+1$ ROWS AND COLUMNS OF $([A] - \lambda_i [B])$

ZERO-OUT $m+1$ ELEMENTS FROM $\{F_j\}$, $j = i, i+1, \dots, i+m$

SOLVE: $(\overline{[A] - \lambda_i [B]}) \{V_j\} = \{\bar{F}_j\}$

NOTE: $(\overline{[A] - \lambda_i [B]})$ HAS SAME BANDWIDTH AS $([A] - \lambda_i [B])$

SOLUTION PROCEDURE: AUGMENTATION OF EQUATION

The process described on the previous page yields a solution vector $\{V_j\}$ with $m+1$ zeroes. To this we append the $m+1$ eigenvectors $\{Z_\ell\}$ with appropriate constants $C_{j\ell}$. This combination is then substituted into the derivatives of the $m+1$ orthonormalization equations and the (m) additional optional equations to uniquely determine the $m+1$ constants $C_{j\ell}$.

INTRODUCE $m+1$ ADDITIONAL EQUATIONS:

$$(\{Z_j\}^T [B] \{Z_i\} - \delta_{ij})' = 0$$

$$i, j = i, i+1, i+2, \dots, i+m$$

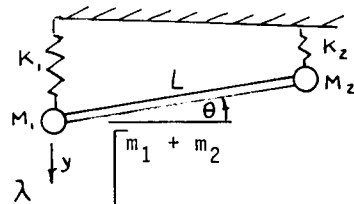
$$\text{LET } \{Z_j'\} = \{V_j\} + \sum_{\ell=i}^{i+m} C_{j\ell} \{Z_\ell\}$$

$$\text{AND } \{Z_j\}^T [B] \{Z_k'\} = \{Z_k\}^T [B] \{Z_j'\} \quad k \neq j \text{ (OPTIONAL)}$$

$$\text{THEN } C_{kj} = -\frac{1}{2} \{Z_k\}^T [B] \{Z_j\} - \{Z_j\}^T [B] \{V_k\}$$

SIMPLE EXAMPLE: BASIC DESCRIPTION

As a very simple application of this procedure consider a weightless straight bar of length L with end masses supported by linear springs. As the spring stiffnesses and masses approach one another, so do the two system frequencies. Thus, depending upon the method by which the normal modes are obtained, the mode shapes may vary. For the mode shapes presented below, either both masses vibrate simultaneously up and down together $\{x_1\}$, or in opposition, $\{x_2\}$.

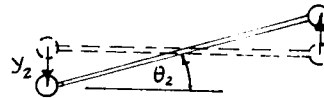
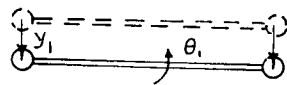
$$\begin{bmatrix} k_1 + k_2 & -k_2 \\ -k_2 & k_2 \end{bmatrix} \begin{Bmatrix} y \\ \theta L \end{Bmatrix} = \lambda \begin{bmatrix} m_1 + m_2 & -m_2 \\ -m_2 & m_2 \end{bmatrix} \begin{Bmatrix} y \\ \theta L \end{Bmatrix}$$


For $k_1 = k_2 \equiv k$, $m_1 = m_2 \equiv m$

$$\lambda_1 = \lambda_2 = \frac{k}{m}$$

$$\{x_1\} = \begin{Bmatrix} y_1 \\ L\theta_1 \end{Bmatrix} = \frac{1}{\sqrt{2m}} \begin{Bmatrix} 1 \\ 0 \end{Bmatrix}$$

$$\{x_2\} = \begin{Bmatrix} y_2 \\ L\theta_2 \end{Bmatrix} = \frac{1}{\sqrt{2m}} \begin{Bmatrix} 1 \\ 2 \end{Bmatrix}$$



SIMPLE EXAMPLE: NORMAL MODES

If we follow the procedure outlined earlier, and compute the system frequency gradients with respect to changes in m_2 , we obtain normal modes $\{Z_1\}$ and $\{Z_2\}$. These modes are associated with motions for which only m_1 moves, and motions for which only m_2 moves.

$$(\quad)' = \frac{\partial(\quad)}{\partial m_2}, \quad [D]\{\alpha\} = \lambda'\{\alpha\}$$

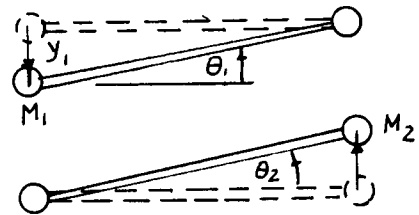
$$-\frac{k}{2M^2} \begin{bmatrix} 1 & -1 \\ -1 & 1 \end{bmatrix} \begin{Bmatrix} \alpha_1 \\ \alpha_2 \end{Bmatrix} = \lambda' \begin{Bmatrix} \alpha_1 \\ \alpha_2 \end{Bmatrix}$$

$$\lambda' = 0 \quad \text{AND} \quad -\frac{k}{M^2} = \frac{\partial(\frac{k}{M})}{\partial M}$$

$$\{\alpha^{(1)}\} = \frac{1}{\sqrt{2}} \begin{Bmatrix} 1 \\ 1 \end{Bmatrix}, \quad \{\alpha^{(2)}\} = \frac{1}{\sqrt{2}} \begin{Bmatrix} -1 \\ 1 \end{Bmatrix}$$

$$\{Z_1\} = \alpha_1^{(1)} \{X_1\} + \alpha_2^{(1)} \{X_2\} = \frac{1}{\sqrt{M}} \begin{Bmatrix} 1 \\ 1 \end{Bmatrix}$$

$$\{Z_2\} = \alpha_1^{(2)} \{X_1\} + \alpha_2^{(2)} \{X_2\} = \frac{1}{\sqrt{M}} \begin{Bmatrix} 0 \\ 1 \end{Bmatrix}$$



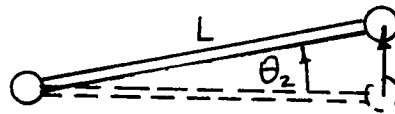
SIMPLE EXAMPLE: EIGENVECTOR GRADIENTS

Following the computation procedure outlined earlier, the eigenvector gradients, $\{Z'_1\}$ and $\{Z'_2\}$, for changes in m_2 are the null vector and the value of $\partial \{Z_2\} / \partial m_2$ shown below.

$$\{Z'_1\} = C_{11}\{Z_1\} + C_{12}\{Z_2\} = \begin{Bmatrix} 0 \\ 0 \end{Bmatrix}, \text{ I.E. } \{Z_1\} \text{ NOT AFFECTED BY } m_2 \text{ CHANGE}$$

$$\{Z'_2\} = C_{21}\{Z_1\} + C_{22}\{Z_2\} = \begin{Bmatrix} 0 \\ -\frac{1}{2m^{3/2}} \end{Bmatrix}$$

$$\text{I.E. } \{Z_2\} = \frac{1}{\sqrt{m}} \begin{Bmatrix} 0 \\ 1 \end{Bmatrix}$$

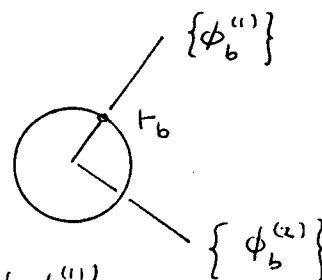
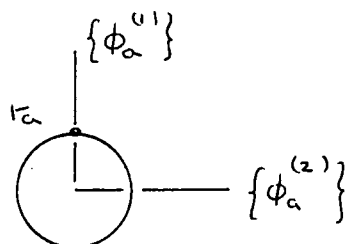


$$\frac{\partial \{Z_2\}}{\partial m_2} = \begin{Bmatrix} 0 \\ -\frac{1}{2} m^{-3/2} \end{Bmatrix}$$

USE CAUTION WHEN WORKING WITH THE TOTAL DIFFERENTIAL

$$d\{\phi_a^{(1)}\} = \frac{\partial \{\phi_a^{(1)}\}}{\partial r_a} dr_a$$

$$d\{\phi_b^{(1)}\} = \frac{\partial \{\phi_b^{(1)}\}}{\partial r_b} dr_b$$



$$d\{\phi^{(1)}\} \neq \frac{\partial \{\phi_a^{(1)}\}}{\partial r_a} dr_a + \frac{\partial \{\phi_b^{(1)}\}}{\partial r_b} dr_b$$

THE TOTAL DIFFERENTIAL MAY NOT EXIST EVEN THOUGH THE PARTIAL DERIVATIVES DO.

CONCLUSIONS

The coordinate system and mode shapes initially selected for this example gave little physical insight regarding how the initial system would decompose due to a change in m_2 . Yet, this example yields a simple demonstration of the insight to be gained by following the proposed procedure. Thus, it is seen that the proposed mathematical procedure automatically yields $m+1$ distinct gradients for repeated frequencies and $m+1$ distinct modes, without requiring user dependence.

The computational efficiencies suggested by Nelson³ have been expanded. These include: maintaining system bandwidth and consideration of only the $m+1$ repeated root frequencies.

EIGENVALUE GRADIENTS FOR REPEATED FREQUENCIES

GENERALLY YIELD MULTIPLE DISTINCT VALUES

EFFICIENT COMPUTATION OF EIGENVECTOR GRADIENTS

FOR REPEATED FREQUENCIES IS POSSIBLE

I.E. BANDWIDTH MAY BE MAINTAINED

MODAL EXPANSION IS NOT NECESSARY

BUT, MUST INTRODUCE MODAL ORTHOGONALITY CONDITIONS IN
ADDITION TO NORMALIZATION CONDITION

EXERCISE CAUTION WHEN USING A TOTAL DIFFERENTIAL WHICH IS A COMBINATION OF
PARTIAL DERIVATIVES FOR REPEATED FREQUENCIES.

REFERENCES

1. Chen, S.H. and Pan, H.H., "Design Sensitivity Analysis of Vibration Modes by Finite Element Perturbation", 4th International Modal Analysis Conference (IMAC), Los Angeles, CA, February 1986, pp 38-43.
2. Nelson, R.B., "Simplified Calculation of Eigenvector Derivatives", AIAA J., Vol. 14, September 1976, pp 1201-1205.
3. Crandall, S. H., "Engineering Analysis", McGraw-Hill, New York, 1956.

SENSITIVITY DERIVATIVES AND OPTIMIZATION OF
NODAL POINT LOCATIONS FOR VIBRATION REDUCTION

Jocelyn I. Pritchard and Howard M. Adelman
NASA Langley Research Center
Hampton, Virginia

Raphael T. Haftka
Virginia Polytechnic Institute and
State University
Blacksburg, Virginia

ABSTRACT

A method is developed for sensitivity analysis and optimization of nodal point locations in connection with vibration reduction. A straightforward derivation of the expression for the derivative of nodal locations is given, and the role of the derivative in assessing design trends is demonstrated. An optimization process is developed which uses added lumped masses on the structure as design variables to move the node to a preselected location; for example, where low response amplitude is required or to a point which makes the mode shape nearly orthogonal to the force distribution, thereby minimizing the generalized force. The optimization formulation leads to values for added masses that adjust a nodal location while minimizing the total amount of added mass required to do so. As an example, the node of the second mode of a cantilever box beam is relocated to coincide with the centroid of a prescribed force distribution, thereby reducing the generalized force substantially without adding excessive mass. A comparison with an optimization formulation that directly minimizes the generalized force indicates that nodal placement gives essentially a minimum generalized force when the node is appropriately placed.

RECORDING PAGE BLANK NOT FILMED

INTRODUCTION

The current trend in engineering design of aircraft and spacecraft is to incorporate in an integrated manner various design requirements and to do so at an early stage in the design process (refs. 1, 2). Incorporation of vibration design requirements is one example of this. Work in this area is ongoing in the Interdisciplinary Research Office at the Langley Research Center, particularly for vibration reduction in rotorcraft.

In helicopter rotor blade and fuselage design, stringent requirements on ride comfort, stability, fatigue life of structural components, and stable locations for electronic equipment and weapons lead to design constraints on vibration levels (refs. 3-5). Some of the methods previously used to control structural vibration in rotor blades include pendulum absorbers (ref. 6), active isolation devices (ref. 7), additional damping (refs. 5, 8), vibration absorbers which create "anti-resonances" (refs. 9, 10), and tuning masses to place frequencies away from driving frequencies (refs. 5, 11-14). Efforts to incorporate the above concepts for vibration reduction in systematic optimization techniques are described in references 10, 15-19. References 20, 21 contain surveys of applications of optimization methods for vibration control of helicopters.

The objectives of this paper are to develop and demonstrate the concept of nodal point placement and develop a mathematical optimization procedure based on this concept to reduce vibration. An important ingredient in the optimization procedure is the derivative of the nodal point location with respect to a design variable. This derivative quantifies the sensitivity of a nodal location to a change in a design variable. The sensitivity derivative of the nodal location is derived in this paper. The equation involves the derivative of the vibration mode with respect to the design variable and the slope of the mode shape at the nodal point and is easily implemented in a vibration analysis program using available or easily computed quantities. Analytical results are presented for the sensitivity derivatives for a beam model of a rotor blade and compared with finite differences for an independent check. The sensitivity derivatives have been employed in an optimization procedure for placing a node at a specified location by varying the sizes of lumped masses while minimizing the sum of these masses. Optimization results are shown for placement of a node at a prescribed location on the beam model.

Recently, the concept of "modal shaping" has been proposed as a method to reduce structural vibration, especially in helicopters (refs. 3, 4). In this method, vibration modes of rotor blades are altered through structural modification to make them nearly orthogonal to the air load distribution - thus reducing the generalized (modal) force. This paper deals with the concept of nodal point placement which is related to modal shaping and consists of modifying the mass distribution of a structure to place the node of a mode at a desirable location. Typical candidates for nodal point placement are locations where low response amplitude is required such as pilot or passenger seats, locations of sensitive electronic equipment, weapon platforms, or engine mounts. Nodal point placement also has the potential for reducing overall response by placing a node at a strategic location of a force distribution to reduce the generalized force.

MOTIVATION FOR DERIVATIVES OF NODAL POINT LOCATIONS

A method has been developed for calculating the sensitivity derivatives of node locations (points of zero displacement on a mode shape). These derivatives are used in optimization procedures to place nodes for the purpose of reducing vibrations. There are two general cases of nodal placement (figure 1). The first case places a node at a point where low response is desirable such as the pilot or passenger seat, the location of sensitive electronics, or weapon platforms, for example. The second case places the node at a point to minimize the generalized force. By placing the node at certain locations, the major components of the force vector are cancelled out and, therefore, the generalized force is reduced. Two possible candidates for placement of the node in this case are the point of maximum force or the centroid of the force. An example of the latter will be shown. The derivatives of nodal locations, besides being used in optimization procedures to place nodes, provide valuable information about the effect of a design change in moving the location of the node.

● Application of nodal placement

Points desirable for low response

- Pilot or passenger seat
- Location of sensitive electronics
- Weapon platform

Minimize generalized force, $\Phi^T F$

● Design application

Tells which design variables are most effective in
changing nodal location

Figure 1

DERIVATIVES OF NODAL POINT LOCATIONS

The derivation of the analytical expression used to calculate the derivatives of node point locations is developed for an arbitrary design variable, v . The modal deflection normal to the length of a one-dimensional structure is denoted $u(x, v)$ and represented by the solid line in the sketch of figure 2. The deflection, u and the nodal point location denoted by $x_n(v)$ are both functions of a design variable. When the design variable is perturbed, the deflection shape changes to the shape shown by the dashed line. The derivative of the nodal location is obtained by expanding the perturbed mode in a Taylor series about the nominal nodal point. Neglecting the higher order terms,

$$u(x_n + dx_n, v + dv) = u(x_n, v) + \left. \frac{\partial u}{\partial x} \right|_{x_n, v} dx_n + \left. \frac{\partial u}{\partial v} \right|_{x_n, v} dv \quad (1)$$

The term on the left side of the equation and the first term on the right are deflections at the nodal points of the perturbed and nominal mode shapes, respectively, which are zero. Since x_n is a function of v , it

follows that $dx_n = \frac{dx_n}{dv} dv$. Therefore, from (1)

$$\left. \frac{\partial u}{\partial x} \right|_{x_n, v} dx_n + \left. \frac{\partial u}{\partial v} \right|_{x_n, v} dv = \left(\left. \frac{\partial u}{\partial x} \right|_{x_n, v} \frac{dx_n}{dv} + \left. \frac{\partial u}{\partial v} \right|_{x_n, v} \right) dv = 0 \quad (2)$$

Noting that dv is arbitrary and solving for dx_n/dv leads to the formula for

the nodal point derivative

$$\frac{dx_n}{dv} = - \left[\frac{\partial u / \partial v}{\partial u / \partial x} \right]_{x_n, v} \quad (3)$$

The two ingredients in the formula are $\partial u / \partial v$, the derivative of the mode shape at the nodal point and $\partial u / \partial x$, the slope of the mode shape at the nodal point. The value of $\partial u / \partial x$ is obtained from the nominal mode shape; and the value of $\partial u / \partial v$ is obtained by Nelson's method (ref. 22) which will be described in the next figure.

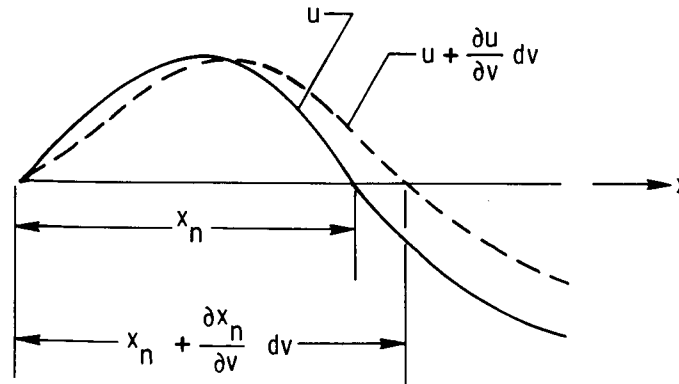


Figure 2

DERIVATIVES OF EIGENVECTORS - NELSON'S METHOD *

A free-vibration problem with no damping is governed by equation (4) of figure 3 where K is the stiffness matrix, M is the mass matrix, ϕ is the eigenvector, and λ is the eigenvalue (square of the circular frequency). The eigenvector is normalized such that the generalized mass is unity (eq. (5)). By taking the derivative of equation (4) with respect to a design variable v , equation (6) is obtained. Because this equation is singular, a direct solution for $\frac{\partial \phi}{\partial v}$ is not possible. However, the general solution to equation (6) is expressible in the form of equation (7) as the sum of a complementary solution, ϕ and a particular solution, Q . The particular solution is found by setting one component of the eigenvector derivative equal to zero and deleting the corresponding row and column from equation (6) and solving for the remaining components. The constant C is found by taking the derivative of the normalization condition in equation (5) and substituting equation (7) into the resulting expression.

$$\bullet \{K - \lambda M\} \phi = 0 \quad (4)$$

$$\bullet \phi^T M \phi = 1 \quad (5)$$

• Take derivative of Eq. (4)

$$\{K - \lambda M\} \frac{\partial \phi}{\partial v} = \frac{\partial \lambda}{\partial v} M \phi - \frac{\partial K}{\partial v} \phi + \lambda \frac{\partial M}{\partial v} \phi \quad (6)$$

$$\bullet \text{Solution: } \frac{\partial \phi}{\partial v} = Q + C \phi \quad (7)$$

• C is determined from derivative of Eq. (5)

$$2 \phi^T M \frac{\partial \phi}{\partial v} = - \phi^T \frac{\partial M}{\partial v} \phi$$

$$\bullet C = - \phi^T M Q - \frac{1}{2} \phi^T \frac{\partial M}{\partial v} \phi$$

*Ref. 22

Figure 3

DERIVATIVES OF NODAL LOCATIONS FOR SPINNING STRUCTURES

For calculating derivatives of nodal locations of spinning structures such as rotor blades, a modification of the previous development is necessary. The basic expression for the nodal point derivative is unaffected (see eq. (3)), and Nelson's method is still used to calculate the eigenvector derivative. However, the details of Nelson's method when applied to a spinning structure are different because the eigenvalue problem has additional stiffness terms (refs. 23, 24). As shown in figure 4, the new terms are K_C , the centrifugal stiffness matrix and K_D , the differential stiffness matrix. K_C contains products of masses m and angular velocity Ω . K_D contains stresses associated with the extension of the spinning structure. (Details may be found in refs. 23 and 24.) Presently, the derivative of the stiffness matrix is calculated by finite differences, but methods for calculating this derivative analytically are being investigated.

● Stiffness matrix for spinning structures

$$K = K_E + K_C + K_D$$

- K_E = elastic stiffness matrix
- K_C = centrifugal stiffness matrix = (m, Ω)
- K_D = differential stiffness matrix = $K_D(\sigma)$

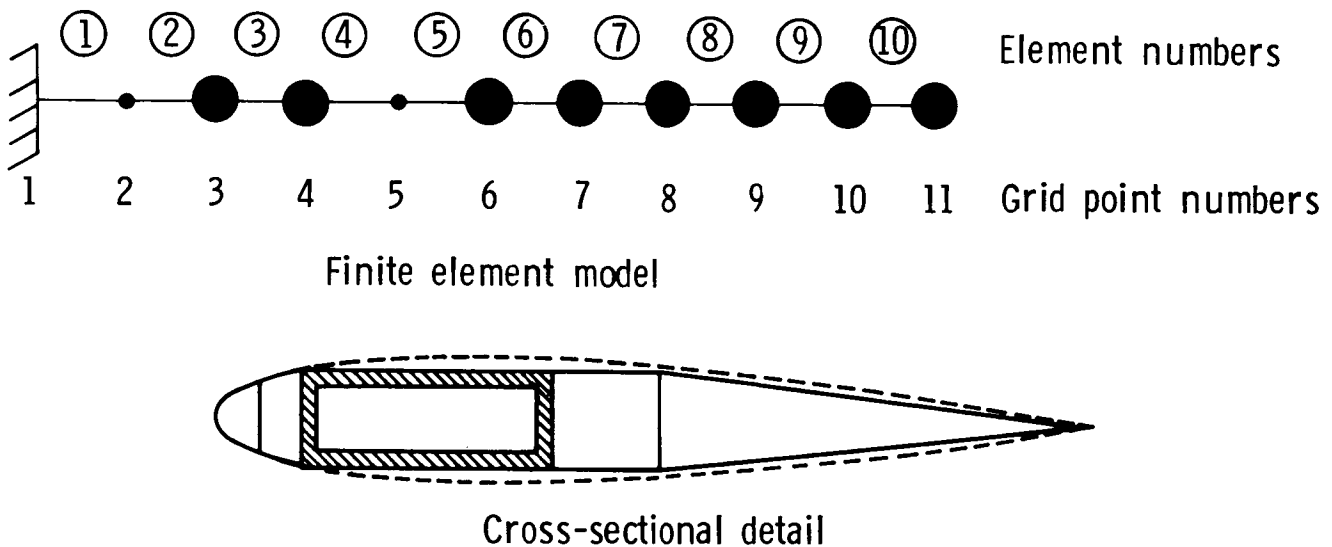
● Compute $\partial(K_E + K_C + K_D)/\partial v$ by finite differences

● Plans are to develop derivative of $K_E + K_C + K_D$ analytically

Figure 4

SENSITIVITY DERIVATIVE TEST PROBLEM

The example problem used to test the sensitivity analysis is a cantilever beam representation of a rotor blade developed in reference 25 and shown in figure 5. The beam is 193 inches long and is modeled by ten finite elements of equal length. The model contains both structural mass and lumped (non-structural) masses. The beam has a box cross section as shown in the figure. Additional details of the model are given in reference 26. There are eight lumped masses at various locations along the length of the beam and the values of the masses are the design variables. The derivatives of the nodal location with respect to these lumped masses are computed for the second mode. The second mode is chosen because it is a prime contributor to the vibrations transmitted from the rotor to the fuselage (ref. 3).



- Compute derivatives of node location for second mode
- Design variables - masses at grid points

Figure 5

RESULTS OF SENSITIVITY ANALYSIS

Derivatives of the nodal point location with respect to the lumped masses for the second mode were calculated using equation (3). The sensitivity analysis included the model with spin ($\Omega=425$ rpm), as well as without ($\Omega=0$). For an independent check on the implementation of equation (3), the derivatives were also calculated by forward finite differences with a step size of .1 percent. The sensitivity results are shown in figure 6. The two methods generally agreed within one percent. Examination of the table shows both positive and negative values of the derivatives. A positive value indicates that an increase in the mass moves the nodal point to the right of the nominal location and a negative value indicates that an increase in mass moves the node to the left. The derivatives show, for example, that changes in the masses at grid points 10 and 11 are the most effective ways (per unit mass) to move the node. The derivatives for the spinning model follow the same basic trends as the non-spinning model even though the derivatives are somewhat different.

dx_n/dv (inch/lbm)				
Mass no.	$\Omega = 0$		$\Omega = 425$ rpm	
	Analytical	Finite difference	Analytical	Finite difference
3	-0.028	-0.028	-.050	-.050
4	-0.088	-0.088	-.129	-.129
6	-0.231	-0.230	-.261	-.261
7	-0.236	-0.236	-.221	-.221
8	-0.166	-0.165	-.096	-.096
9	-0.004	-0.004	.062	.062
10	0.309	0.309	.280	.280
11	0.828	0.826	.778	.777

Figure 6

OPTIMIZATION TO PLACE NODES

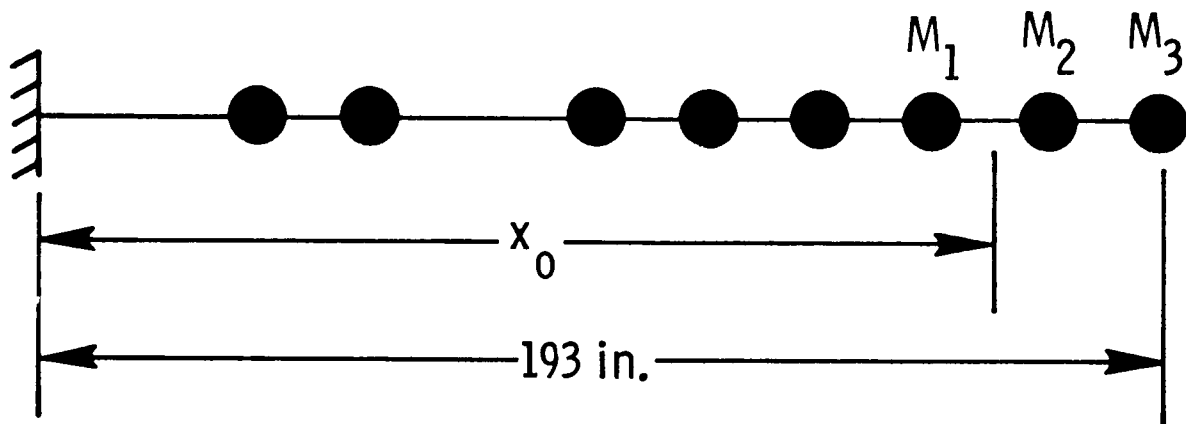
The optimization problem is to place the node at a desired location by varying the magnitudes of lumped masses while minimizing the total lumped mass. CONMIN, a general-purpose optimization program (ref. 27), is utilized. The formulation of the problem consists of defining an objective function (the quantity to be minimized); the constraints (limitations on the behavior of the model); and the design variables (the parameters of the model to be changed in order to find the optimum design). The optimizer requires derivatives of both the objective function and the constraints. The formulation for this problem, summarized in figure 7, is as follows: The objective function, f , is the sum of the lumped masses. The constraint, g , which must be negative or zero for an acceptable design, expresses the requirement that the nodal point x_n be placed within a distance δ from a desired location x_0 . The design variables consist of the sizes of the lumped masses. Constraints on the largest and smallest acceptable values of the design variables are optional. These values are arbitrarily set in this case. The derivatives of the objective function with respect to the design variables are all equal to 1.0 and the derivatives of the constraints are equal to positive or negative values of the nodal point sensitivity derivatives calculated from equation (3).

- Problem: Place node x_n within δ of x_0 by varying masses M_i
- Objective function, $f = \sum_{i=1} M_i$
- Constraint, $g = |x_n - x_0| - \delta \leq 0$
- Design variables, $v_i = M_i$
- Use CONMIN
- Derivatives of objective function: $\partial f / \partial v_i = 1.0$
- Derivatives of constraints: $\partial g / \partial v_i = \pm \partial x_n / \partial v_i$

Figure 7

OPTIMIZATION TEST PROBLEM

The model used in the optimization procedure is shown in figure 8 and is the same beam structure of figure 5. The node for the second mode is to be placed within $\delta = 1.0$ inch of $x_0 = 164$ inches. The location x_0 is chosen because it is the centroid of a representative air load distribution given in reference 3 for a rotor blade. In reference 26, it is shown that the centroid of a load distribution is a desirable location for the node. The design variables are the masses at joints 9, 10, and 11 having initial values of 5.21 lbm, 6.55 lbm, and 6.60 lbm, as given in reference 25 - a total of 18.36 pounds. The initial location of the node is 154.7 inches. The upper and lower bounds on the design variables are 50.0 and 0.5 lbm, respectively.



- Desired node location : $x_0 = 164.0$ in.
- Allowable distance: $\delta = 1.0$ in.
- Design variables: M_1 M_2 M_3
- Upper bounds on design variables: 50 lb
- Lower bounds on design variables: 0.5 lb

Figure 8

CONVERGENCE OF OPTIMIZATION PROCEDURE FOR NODAL LOCATION

Initially, the constraint is not satisfied since the node is nine inches from the desired location (instead of one inch). The optimization history is shown in figure 9. The optimizer initially adds mass to bring the nodal point to within one inch of the desired location. After ten cycles, the constraint is satisfied, but the mass is increased to about 36 lbm. For the remainder of the cycles, the optimizer concentrates on minimizing the total mass by shifting mass among the three locations, finally reaching the optimum design with a mass of 24.45 lbm.

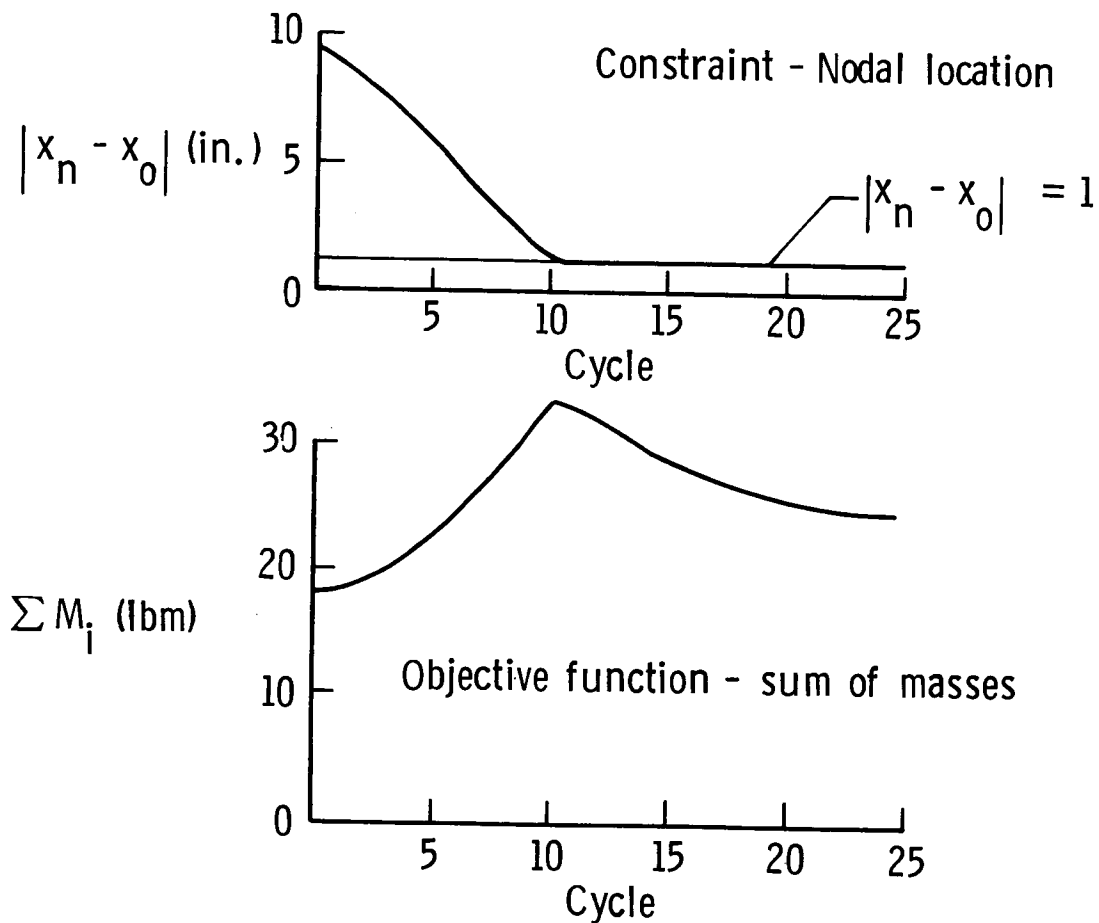


Figure 9

INITIAL AND FINAL DESIGN FOR NODAL POINT OPTIMIZATION

The optimization procedure converged to the final design shown in figure 10 in which the masses are 0.5 lbm, 3.70 lbm, and 20.25 lbm, for a total of 24.45 lbm, and the nodal point is located at 163 inches. Basically, mass was shifted from the two inboard locations to the tip where mass is most effective in moving the nodal point. For example, the mass at grid point 9 is reduced from 5.21 lbs to 0.5 lbs; while the tip mass is increased from 6.6 lbs to 20.25 lbs. Excessive addition of mass is avoided (only 6 additional pounds were needed) because of the effectiveness of relocating mass to the tip.

$$x_0 = 164.0 \text{ in.} \quad \delta = 1.0 \text{ in.}$$

	Initial	Final
M_1 (lbm)	5.21	0.50
M_2 (lbm)	6.55	3.70
M_3 (lbm)	6.60	20.25
M_{TOT} (lbm)	18.36	24.45
Nodal location x_n (in.)	154.7	163.0

Figure 10

GENERALIZED FORCE STUDY

One of the potential applications of nodal point placement is the reduction of overall vibration response by generalized force minimization. A study is performed in which the generalized force for the second mode is calculated using the force distribution F , shown in figure 11. This generalized force is $\phi_2^T F$ where ϕ_2 is the mode shape from the final design based on the nodal point placement optimization. The force distribution in figure 11 is taken from reference 3 as representative of the air loading on a rotor blade and is adjusted so that the centroid is near the location of the nodal point; i.e., (164 ± 1) inches. Locating the node at the centroid results in a low value for the generalized force (ref. 26). To assess how well nodal placement reduces generalized force, the generalized force from node placement optimization is compared with the value obtained when the generalized force is directly minimized (ref. 26).

Centroid of distribution at $x/L = .85$ (164 inches)

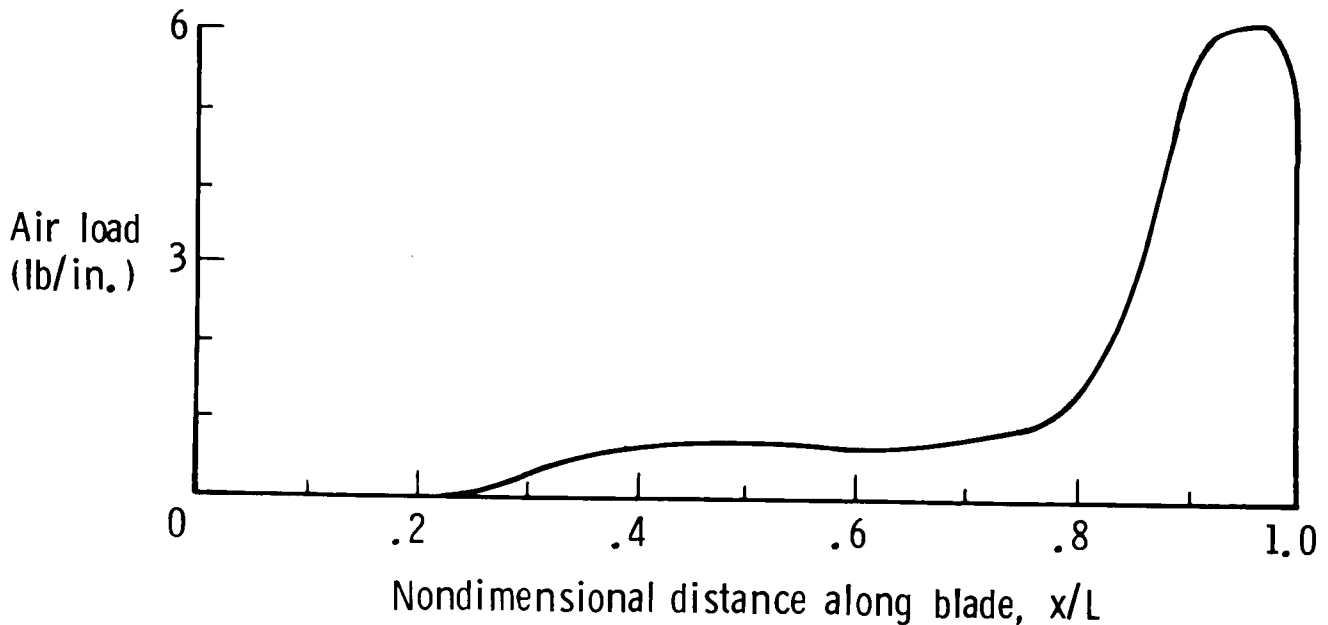


Figure 11

DESIGN CHARACTERISTICS FROM NODAL POINT OPTIMIZATION

Figure 12 contains design variables, total mass, generalized force, and nodal point locations for three designs: the initial design, the final design from nodal placement, and the final design from the direct minimization of the generalized force (ref. 26). The nodal placement procedure is very effective in minimizing the generalized force - giving 10.8 lbf, compared to 10.0 lbf from the direct method when both were started at a design with a generalized force of 20.8 lbf. The direct minimization procedure, while not dealing directly with the nodal location, nevertheless places the node essentially at the same point as the nodal placement design: 163.8 inches versus 163.0 inches.

	Initial	Nodal placement	Direct minimization
Generalized force (lbf)	20.8	10.8	10.0
Nodal location x_n (inch)	154.70	163.0	163.8
M_1 (lbm)	5.21	0.50	0.50
M_2 (lbm)	6.55	3.70	1.75
M_3 (lbm)	6.60	20.25	22.20
M_{TOT} (lbm)	18.36	24.45	24.45

Figure 12

CONCLUDING REMARKS

This paper has described sensitivity analysis and optimization methods for adjusting mode shape nodal point locations with application to vibration reduction. The paper begins with a derivation of an expression for the derivative of the nodal location with respect to a design variable. Sensitivity analyses were performed on a demonstration problem which consisted of a box beam model of a helicopter rotor blade. In these analyses, the derivatives of the nodal location for the second mode with respect to the magnitudes of lumped masses on the beam were calculated. It was shown that these derivatives gave useful information about the effect of the masses on the nodal location and indicated which masses were most effective in moving the nodal point. Next, the paper described an optimization procedure to place a node at a prescribed location by adjusting the magnitudes of lumped masses while minimizing the sum of these masses. A general-purpose optimization program was used and the nodal point derivatives were a key ingredient in the procedure. This optimization procedure was demonstrated in an example where the nodal point for the second mode of a cantilever beam model of a rotor blade was placed at a location close to the centroid of a force distribution. The procedure was successful in moving the node to the desired location requiring only six additional pounds of lumped mass on a 193-inch beam that weighed 117 pounds.

Finally, to demonstrate the potential for nodal placement to reduce vibration, the generalized force for the second mode was calculated and compared to the minimum generalized force obtained by a separate optimization procedure. It was found that the nodal placement procedure gave a generalized force which was very close to the minimum. The results in this paper suggest that adjusting the mode shapes of structures by relocating nodal points has potential for reducing both overall and local response levels in vibrating structures.

REFERENCES

1. Sobieszczanski-Sobieski, J.: Structural Optimization: Challenges and Opportunities. Paper presented at International Conference on Modern Vehicle Design Analysis, London, England, June 1983.
2. Sobieszczanski-Sobieski, J.; James B. B.; and Riley, M. F.: Structural Optimization by Generalized, Multilevel Optimization. AIAA Paper No. 85-0697-CP.
3. Taylor, R. B.: Helicopter Vibration Reduction by Rotor Blade Modal Shaping. Presented at the 38th Annual Forum of the American Helicopter Society, Anaheim, CA, May 1982.
4. Taylor, R. B.: Helicopter Rotor Blade Design for Minimum Vibration. NASA CR-3825, 1984.
5. Blackwell, R. H.: Blade Design for Reduced Helicopter Vibration. Journal of the American Helicopter Society, Vol. 28, No. 3, July 1983.
6. Hamouda, M. H.; and Pierce, G. A.: Helicopter Vibration Suppression Using Simple Pendulum Absorbers on the Rotor Blade. Presented at the American Helicopter Society Northeast Region National Specialists' Meeting on Helicopter Vibration, Hartford, CT, November 1981.
7. Reichert, G.: Helicopter Vibration Control - A Survey. Vertica, Vol. 5, 1981, pp. 1-20.
8. Rogers, L.: Damping as a Design Parameter. Mechanical Engineering, Vol. 108, No. 1, January 1986.
9. Wang, B. P.; Kitis, L.; Pilkey, W. D.; and Palazzolo, A.: Synthesis of Dynamic Vibration Absorbers. Journal of Vibration, Acoustics, Stress, and Reliability in Design, Vol. 107, April 1985, pp. 161-166.
10. Kitis, L.; Pilkey, W. D.; and Wang, B. P.: Optimal Frequency Response Shaping by Appendant Structures. Journal of Sound and Vibration, Vol. 95, No. 2, 1984, pp. 161-175.
11. Davis, M. W.: Optimization of Helicopter Rotor Blade Design for Minimum Vibration. NASA CP-2327, Part 2, September 1984, pp. 609-625.
12. McCarty, J. L.; and Brooks, G. W.: A Dynamic Model Study of the Effect of Added Weights and Other Structural Variations on the Blade Bending Strains of an Experimental Two-Blade Jet-Driven Helicopter in Hovering and Forward Flight. NACA TN--3367, May 1955.
13. Hirsh, H.; Hutton, R. E.; and Rasamoff, A.: Effect of Spanwise and Chordwise Mass Distribution on Rotor Blade Cyclic Stresses. Journal of the American Helicopter Society, Vol. 1, No. 2, April 1965, pp. 37-45.

14. Peers, D. A.; Rossow, M. P.; Korn, A.; and Ko, T.: Design of Helicopter Rotor Blades for Optimum Dynamic Characteristics. Comp. and Maths. with Appls., Vol. 12A, No. 1, 1986, pp. 85-109.
15. Friedmann, P. P.: Application of Modern Structural Optimization to Vibration Reduction in Rotorcraft. NASA CP-2327, Part 2, 1984, pp. 553-566.
16. Bennett, R. L.: Application of Optimization Methods to Rotor Design Problems. Vertica, Vol. 7, Part 3, 1983, pp. 201-208.
17. Friedmann, P. P.; and Shanthakumaran, P.: Aeroelastic Tailoring of Rotor Blades for Vibration Reduction in Forward Flight. Presented at 24th Structures, Structural Dynamics and Materials Conference, Lake Tahoe, NV, May 2-4, 1983.
18. Friedmann, P. P.; and Shanthakumaran, P.: Optimum Design of Rotor Blades for Vibration Reduction in Forward Flight. Journal of the American Helicopter Society, October 1984.
19. Sutton, L. R.; and Bennett, R. L.: Aeroelastic/Aerodynamic Optimization of High-Speed Helicopter/Compound Rotor. NASA CP-2327, Part 2, September 1984, pp. 643-662.
20. Miura, H.: Applications of Numerical Optimization Methods to Helicopter Design Problems: A Survey. NASA TM-86010, October 1984.
21. Friedmann, P.: Application of Modern Structural Optimization to Vibration Reduction in Rotorcraft. Vertica, Vol. 9, No. 4, 1985, pp. 363-376.
22. Nelson, R. B.: Simplified Calculation of Eigenvector Derivatives. AIAA Journal, Vol. 14, No. 9, September 1976, pp. 1201-1205.
23. Laurenson, R. M.: Modal Analysis of Rotating Flexible Structures. AIAA Journal, Vol. 14, No. 10, October 1976, pp. 1444-1450.
24. Patel, J. S.; and Seltzer, S. M.: NASTRAN: User's Experiences. NASA TMX-2378, September 1971.
25. Peters, D. A.; Ko, T.; Korn, A.; and Rossow, M. P.: Design of Helicopter Rotor Blades for Desired Placement of Natural Frequencies. Presented at 39th Annual Forum of the American Helicopter Society, May 1983.
26. Pritchard, J. I.; Adelman, H. M.; and Haftka, R. T.: Sensitivity Analysis and Optimization of Nodal Point Placement for Vibration Reduction. NASA TM-87763, 1986.
27. Vanderplaats, G. N.: CONMIN - A FORTRAN Program for Constrained Function Minimization - User's Manual. NASA TMX-62282, 1973.

ON COMPUTING EIGENSOLUTION SENSITIVITY DATA USING FREE

VIBRATION SOLUTIONS

B. P. Wang

Department of Mechanical Engineering
The University of Texas at Arlington
Arlington, Texas

SUMMARY

A simplified method of computing eigensolution sensitivity derivatives in structural dynamics is developed in this paper. It is shown that if the elements of stiffness and mass matrices associated with a design variable are homogeneous functions of that design variable, then eigenvalue derivatives can be computed from element strain and kinetic energies. Furthermore, if cross-mode energies are known, eigensolution derivatives of modified systems can be computed approximately using assume mode reanalysis formulation. A ten bar truss example is used to illustrate the present formulations.

INTRODUCTION

The usefulness of eigensolution sensitivity derivatives in structural dynamics research is well known. The sensitivity data can be used for approximate reanalysis, analytical model improvement, assessment of design trend as well as structural optimization with eigenvalue constraints. When applied to larger discrete structural models, these applications typically require long and expensive computer runs and usually the predominate contributor to the computing time was the calculation of derivatives. Thus efficient eigensolution sensitivity analysis procedures would be very useful in structural dynamic research. It is the purpose of this paper to develop, under certain conditions, efficient eigensolution analysis procedures using free vibration data.

The equations for computing derivatives of eigenvalues and eigenvectors for free vibration of undamped structures were known for a long time. Only recently have these methods been implemented in some general-purpose finite-element programs. In this paper, a simple method is developed which can be used to compute the eigenvalue derivatives for a large class of problems by exploiting the similarity between the equations for eigenvalue derivatives and element strain and kinetic energies. Furthermore, if the cross-mode element energy data are available, the approximate eigenvector derivatives can also be computed using a truncated modal expansion expression. The approximate second derivatives of eigenvalues can then be computed. Additionally, with the cross-mode strain energy data, the eigenvalue derivatives of a modified structure can be computed using assumed mode reanalysis formulation. Numerical examples will be presented to illustrate the various formulations.

EIGENSOLUTION SENSITIVITY IN STRUCTURAL DYNAMICS

The general problem is to compute the rate of change (or derivatives) of eigenvalues and eigenvectors with respect to design variables for the following generalized eigenvalue problem in structural dynamics.

$$K \phi = \lambda M \phi \quad (1)$$

Much research has addressed this problem in the past two decades. A comprehensive survey of literature can be found in a recent paper by Adelman and Haftka [1]. The equations for first order eigenvalue and eigenvector derivatives as well as second order eigenvalue derivatives are summarized below:

Eigenvalue Derivative:

$$\frac{\partial \lambda_\ell}{\partial x_r} = \phi_\ell^T \frac{\partial K}{\partial x_r} \phi_\ell - \lambda_\ell \phi_\ell^T \frac{\partial M}{\partial x_r} \phi_\ell \quad (2)$$

Eigenvector Derivative:

$$\frac{\partial \phi_\ell}{\partial x_r} = \sum_{j=1}^n A_{\ell ij} \phi_j \quad (3)$$

where for $\ell \neq j$

$$A_{\ell rj} = \phi_j^T \frac{\partial Z_\ell}{\partial x_r} \phi_\ell / (\lambda_\ell - \lambda_j) \quad (4)$$

$$Z_\ell = K - \lambda_\ell M \quad (5)$$

$$\text{and} \quad A_{\ell r\ell} = -\frac{1}{2} \phi_\ell^T \frac{\partial M}{\partial x_r} \phi_\ell \quad (6)$$

Second Derivative of Eigenvalues:

$$\frac{\partial^2 \lambda_\ell}{\partial x_r \partial x_s} = Y_\ell + \phi_\ell^T \left(\frac{\partial Z_\ell}{\partial x_r} \frac{\partial \phi_\ell}{\partial x_s} + \frac{\partial Z_\ell}{\partial x_s} \frac{\partial \phi_\ell}{\partial x_r} \right) \quad (7)$$

where

$$Y_\ell = \phi_\ell^T \left(\frac{\partial^2 K}{\partial x_r \partial x_s} - \lambda_\ell \frac{\partial^2 M}{\partial x_r \partial x_s} - \frac{\partial \lambda_\ell}{\partial x_s} \frac{\partial M}{\partial x_r} - \frac{\partial \lambda_\ell}{\partial x_r} \frac{\partial M}{\partial x_s} \right) \phi_\ell \quad (8)$$

Note that in the above equations, the mode shapes are normalized to unit generalized mass, i.e.

$$\phi_\ell^T M \phi_\ell = 1.0$$

For the eigenvector derivatives, if less than full modes are used, Eq. (2) is an approximate expression. These will lead to approximate second order derivatives of eigenvalues.

The above equations have been developed in the literature for some time. For example, Equations (2) and (3) can be found in Fox and Kapoor [2] and Eq. (7) was reported by Miura and Schmit [3]. It should be noted in passing that there are some recently developed algebraic methods [4-5] which can be used to compute eigenvector derivatives without using modal expansions.

The difficulty of applying the aforementioned equations appears to be the calculation of derivatives of stiffness and mass matrices with respect to design variables. In the next section it will be shown that under certain assumptions, we can circumvent the calculation of $\partial K/\partial x_i$ and $\partial M/\partial x_i$ in implementing these above equations.

SIMPLIFYING ASSUMPTIONS

In general, the system stiffness and mass matrices in Eq. (1) can be written as

$$K = K_c + \sum_{i=1}^{ND} K_i \quad (9)$$

$$M = M_c + \sum_{i=1}^{ND} M_i \quad (10)$$

where

K_c = contribution to stiffness matrix due to structural elements that are to remain constant during the design process.

M_c = contribution to mass matrix due to the masses of the unchanged elements as well as nonstructural masses.

K_i, M_i = contributions to stiffness and mass matrices respectively due to elements controlled by design variable x_i .

To develop simplified efficient methods for eigensolution sensitivity analysis, the elements of the matrices K_i and M_i are assumed to be homogeneous functions of design variables. That is the matrices K_i and M_i have the form

$$K_i = (x_i)^{\beta_i} K_i^* \quad (11)$$

$$M_i = (x_i)^{\gamma_i} M_i^* \quad (12)$$

where K_i^* and M_i^* are constant matrices. Furthermore, define non-dimensional design parameters

$$\alpha_i = \left(\frac{x_i}{x_{i0}}\right)^{\beta_i} \quad (13)$$

$$\bar{\alpha}_i = \left(\frac{x_i}{x_{i0}}\right)^{\gamma_i} \quad (14)$$

Then

$$K_i = (x_i)^{\beta_i} K_i^* = \left(\frac{x_i}{x_{i0}}\right)^{\beta_i} (x_{i0})^{\beta_i} K_i^*$$

or

$$K_i = \alpha_i K_{i0} \quad (15)$$

Similarly,

$$M_i = \bar{\alpha}_i M_{i0} \quad (16)$$

where K_{i0} and M_{i0} are stiffness and mass matrices due to design variable x_i at its nominal value x_{i0} .

Based on the above assumptions, the derivatives of stiffness and mass matrices with respect to design variables can be computed readily:

$$\frac{\partial K}{\partial x_i} = \frac{\partial K_i}{\partial x_i} = \frac{\partial \alpha_i}{\partial x_i} K_{i0}$$

or

$$\frac{\partial K_i}{\partial x_i} = \frac{\beta_i}{x_i} K_{i0} \quad (17)$$

Similarly, we can derive

$$\frac{\partial M}{\partial x_i} = \frac{\gamma_i}{x_i} M_{i0} \quad (18)$$

It should be noted that at the nominal design, $\alpha_i = \bar{\alpha}_i = 1$. With these simplifications, the eigenvalue derivatives can be computed readily.

RATE OF CHANGE OF EIGENVALUES

Using (17) and (18) with $\alpha = \bar{\alpha}_i = 1$, the eigenvalue derivative, eq. (2) becomes

$$\frac{\partial \lambda_\ell}{\partial x_r} = \frac{\beta_r}{x_r} \phi_\ell^T K_{r0} \phi_\ell - \frac{\gamma_r}{x_r} \lambda_\ell \phi_\ell^T M_{r0} \phi_\ell \quad (19)$$

Define

$$V_{\ell r \ell} = \frac{1}{2} \phi_{\ell}^T K_{r0} \phi_{\ell} \quad (20)$$

$$T_{\ell r \ell} = \frac{1}{2} \lambda_{\ell} \phi_{\ell}^T M_{r0} \phi_{\ell} \quad (21)$$

Then Eq. (19) can be written as

$$\frac{\partial \lambda_{\ell}}{\partial x_r} = 2 \left(\frac{\beta_r}{x_r} V_{\ell r \ell} - \frac{\gamma_r}{x_r} T_{\ell r \ell} \right) \quad (22)$$

Note that from Eqs. (20) and (21), $V_{\ell r \ell}$ and $T_{\ell r \ell}$ can be interpreted as the strain and kinetic energy respectively of elements associated with design variable x_r .

Thus, given β_r and γ_r , the rate of change of eigenvalues can be computed from the energies associated with this design variable. Since most general-purpose finite-element codes provide element strain energy as an output option, one way to implement (22) is to calculate $V_{\ell r \ell}$ and $T_{\ell r \ell}$ by summing strain energy and kinetic energy for all elements controlled by design variable x_r .

In the above formulation, we have made use of the form of the stiffness and mass matrices, Eqs. (11), (12). Not all structural elements can fit into these models but some important cases do. Some of these are tabulated in Table 1.

Using Eqs. (15) to (18), it is possible to derive explicit equations for eigenvector derivatives as well as second-order derivatives of eigenvalues in terms of energies associated with various design variables. These are quite tedious and have not been accomplished so far. In the following, we will discuss the special case of $\beta_i = \gamma_i$.

EIGENSOLUTION SENSITIVITIES FOR THE CASE $\beta_i = \gamma_i$

For this special case, we can use chain rules to rewrite sensitivity derivatives as:

$$\frac{\partial \lambda_{\ell}}{\partial x_r} = \frac{\partial \lambda_{\ell}}{\partial \alpha_r} \frac{\partial \alpha_r}{\partial x_r} \quad (23)$$

$$\frac{\partial \phi_{\ell}}{\partial x_r} = \frac{\partial \phi_{\ell}}{\partial \alpha_r} \frac{\partial \alpha_r}{\partial x_r} \quad (24)$$

$$\frac{\partial^2 \lambda_{\ell}}{\partial x_r \partial x_s} = \frac{\partial^2 \lambda_{\ell}}{\partial \alpha_r \partial \alpha_s} \frac{\partial \alpha_r}{\partial x_r} \frac{\partial \alpha_s}{\partial x_s} \quad (25)$$

Thus, it remains to find $\partial \lambda_{\ell} / \partial \alpha_r$, $\partial \phi_{\ell} / \partial \alpha_r$ and $\partial^2 \lambda_{\ell} / \partial \alpha_r \partial \alpha_s$. Note that

$$\frac{\partial K_r}{\partial \alpha_r} = K_{r0} \quad (26)$$

$$\frac{\partial M_r}{\partial \alpha_r} = M_{r0} \quad (27)$$

Using Eqs. (26), (27) and replacing all x_r, x_s in Eqs. (2) to (8) by α_r and α_s , and making use of the orthogonality properties of normal modes

$$\phi_\ell^T M \phi_j = 0 \quad \text{if } \ell \neq j$$

as well as the linearity assumptions (Eqs. (15) and (16)), we can derive, after considerable algebraic manipulation, the following results:

$$\frac{\partial \lambda_\ell}{\partial \alpha_r} = c_{\ell r \ell} \quad (28)$$

$$\frac{\partial \phi_\ell}{\partial \alpha_r} = \sum_{j=1}^n \bar{c}_{\ell r j} \phi_j \quad (29)$$

$$\frac{\partial^2 \lambda_\ell}{\partial \alpha_r \partial \alpha_s} = 2 \left[\left(\frac{\partial \lambda_\ell}{\partial \alpha_s} c_{\ell r \ell} + \frac{\partial \lambda_\ell}{\partial \alpha_r} c_{\ell s \ell} \right) + \sum_{\substack{j=1 \\ j \neq \ell}}^n \bar{c}_{\ell r j} c_{\ell s j} \right] \quad (30)$$

where

$$c_{\ell r j} = 2(V_{\ell r j} - T_{\ell r j}) \quad (31)$$

$$V_{\ell r j} = \frac{1}{2} \phi_\ell^T K_{ro} \phi_j \quad (32)$$

$$T_{\ell r j} = \frac{1}{2} \lambda_\ell \phi_\ell^T M_{ro} \phi_j \quad (33)$$

$$\bar{c}_{\ell r j} = \frac{c_{\ell r j}}{\lambda_\ell - \lambda_j} \quad \ell \neq j \quad (34)$$

$$\bar{c}_{\ell r \ell} = - \frac{T_{\ell r \ell}}{\lambda_\ell} \quad (35)$$

It should be noted that $V_{\ell r j}$ can be considered as the "cross mode" strain energy, since it is the work done by the elastic force in j th mode (i.e. $K_r \phi_j$) moving through displacement in the ℓ th mode. Similarly, $T_{\ell r j}$ can be considered as the "cross mode" kinetic energy. Thus, eigensolution sensitivity derivatives can be computed readily when these energy terms become available.

SENSITIVITY DERIVATIVES FOR MODIFIED SYSTEMS

In iterative analysis, we frequently require the eigensolution derivatives of a system different from the nominal design. In these situations, assumed mode reanalysis [6-7] appears to be very efficient. Let ΔK and ΔM denote the change to stiffness and mass matrices, respectively. Then, in term of α_i , we have

$$\Delta K = \sum_{i=1}^{ND} (\alpha_i - 1) K_{i0} \quad (36)$$

and

$$\Delta M = \sum_{i=1}^{ND} (\alpha_i - 1) M_{i0} \quad (37)$$

Following the development in Ref. 7, the eigensolution of the modified system can be computed approximately by solving the following reduced eigenvalue problem

$$\bar{K} q = \lambda \bar{M} q \quad (38)$$

where

$$\begin{aligned} \bar{K} &= \Phi^T (K + \Delta K) \Phi \\ &= [\lambda_0] + \sum (\alpha_i - 1) \tilde{K}_i \end{aligned} \quad (39)$$

$$\bar{M} = [I] + \sum (\alpha_i - 1) \tilde{M}_i \quad (40)$$

where Φ is the truncated modal matrix of the original system, and

$$\tilde{K}_i = \Phi^T K_{i0} \Phi \quad (41)$$

$$\tilde{M}_i = \Phi^T M_{i0} \Phi \quad (42)$$

Once (37) is solved, the eigenvectors of the modified system ψ_i , in terms of physical coordinates, can be completed from

$$\psi_i = \Phi q_i \quad (43)$$

For modified systems, the eigenvalue derivatives, Eqs. (28) and (30) are still applicable except $V_{\ell r j}$ and $T_{\ell r j}$ are now defined by

$$V_{\ell r j} = \frac{1}{2} q_{\ell}^T \tilde{K}_r q_{\ell} \quad (44)$$

$$T_{\ell r j} = \frac{1}{2} \lambda_{\ell} q_{\ell}^T \tilde{M}_r q_{\ell} \quad (45)$$

and the eigenvector derivatives can be computed from

$$\frac{\partial \psi_{\ell}}{\partial \alpha_r} = \Phi \frac{\partial q_{\ell}}{\partial \alpha_r} \quad (46)$$

where

$$\frac{\partial q_\ell}{\partial \alpha_r} = \sum_{j=1}^n \bar{c}_{\ell r j} q_j \quad (47)$$

$\bar{c}_{\ell r j}$ is as defined by (34) or (35) with $v_{\ell r j}$, $T_{\ell r j}$ defined by (44) and (45).

DISCUSSION

In Eq. (7), the second-order derivatives of eigenvalues are shown to be dependent on eigenvector derivatives. In the present formulation, we can compute $\partial^2 \lambda_\ell / \partial \alpha_r \partial \alpha_s$ Using Eq. (34) without the need to compute eigenvector derivatives explicitly. Once the derivatives with respect to α 's are known, chain rules can be used to compute the derivatives with respect to design variables x 's (Eqs. (23) to (25)).

NUMERICAL EXAMPLE

The assumed mode reanalysis sensitivity derivative formulation has been implemented in a program which post-processes MSC/NASTRAN generated data. The first-order sensitivity data have been applied to improve analytical model using measured modal data [8] as well as synthesis of structures with multiple frequency constraints [9]. Recently the second order derivatives of eigenvalues (Eq. (30)) has also been implemented.

A ten-bar cantilever truss structure, Fig. 1, is used to test the program. The ten members are grouped into 4 design variables as indicated in Figure 1. Starting with a uniform structure with cross sectional area 10 in^2 for all design variables, the optimal design program described in Ref. 7 is used to mode the first two natural frequencies from 13.3 and 37.8 Hz to 16 and 39.3 Hz, respectively. This is accomplished by a sequential linear programming formulation [7,9]. At each intermediate design, the eigenvalue derivatives are computed using reanalysis formulations. Table 2 defines the design history. Specifically, the designs at iteration No. A-0 and B-0 are analyzed exactly using MSC/NASTRAN. Three iterations are shown after each exact analysis. The eigensolution at designs A-1 to A-3 and B-1 to B-3 are computed using assumed mode reanalysis formulations. Four modes are used in each case. The first two natural frequencies are tabulated in Table 3. Also shown in Table 3 are the corresponding exact frequencies. From Table 3, it can be seen that the accuracy in frequency of assumed mode reanalysis formulation is very good. Tables 4 to 7 summarize $\partial \lambda_1 / \partial x_1$, $\partial \lambda_1 / \partial x_2$, $\partial \lambda_2 / \partial x_1$ and $\partial \lambda_2 / \partial x_2$, respectively. The results of these tables indicate that the sensitivity derivatives of modified system can be predicted quite accurately using the assumed-mode reanalysis formulation.

CONCLUDING REMARKS

General procedures for computing eigensolution sensitivity derivatives for a class of problems have been proposed in this paper. Detailed formulations have been carried out for a special case. It is shown that the eigenvalue derivative with a design variable can be computed from strain energy and kinetic energy for that design variable. Furthermore, when the cross mode energy terms are available, assumed mode method can be used for eigensolution as well as associated sensitivity reanalysis. This efficient formulation has proved to be very effective in synthesis of structures with multiple frequency constraints [7,9]. Additionally, the present approach can be implemented in a post-processor of any finite-element programs without the need to modify the source code.

Since the current formulation provides an efficient approach for computing second-order eigenvalue derivatives, it would appear that a second-order method for structural optimization with frequency constraints could be implemented efficiently. Finally, in view of the success of the formulation for the special case of $\beta_i = \gamma_i$, further development for the general case of $\beta_i \neq \gamma_i$ seems to be warranted.

SYMBOLS

K	= system stiffness matrix
M	= system mass matrix
ϕ_l	= eigenvector of the l th mode
λ_l	= eigenvalue of the l th mode
Φ	= modal matrix of original system
$V_{l r j}$	= cross-mode strain energy
$T_{l r j}$	= cross-mode kinetic energy
x_r	= r th design variable
ΔK	= modification in stiffness matrix
ΔM	= modification in mass matrix
ψ_l	= eigenvector of the l th mode of the modified systems
N	= number of dof of the system
n	= number of modes computed, $n < N$
ND	= number of design variables

REFERENCES

1. Adelman, H. M. and Haftka, R. T., "Sensitivity Analysis of Discrete Structural Systems," AIAA Journal, Vol. 24, No. 5, May 1986, pp. 823-832.
2. Fox, R. L. and Kapoor, M. P., "Rates of Change of Eigenvalues and Eigenvectors," AIAA Journal, Vol. 6, No. 12, December 1968, pp. 2425-2429.
3. Miura, H. and Schmit, L. A., "Second Order Approximation of Natural Frequency Constraints in Structural Synthesis," International Journal for Numerical Methods in Engineering, Vol. 13, 1978, pp. 337-351.
4. Nelson, R. B., "Simplified Calculation of Eigenvector Derivatives," AIAA Journal, Vol. 14, No. 9, September 1976, pp. 1201-1205.
5. Chen, S. Y. and Wei, F. S., "Systematic Approach for Eigensensitivity Analysis," Proceedings of AIAA/ASME/ASCE/AHS 26th Structures, Structural Dynamics and Materials Conference, Part 2, Orlando, Florida, April 15-17, 1985, pp. 178-183.
6. Wang, B. P., Pilkey, W. D. and Palazzolo, A. B., "Reanalysis, Modal Synthesis and Dynamic Design," Chapter 8 of State-of-the-Art Survey on Finite Element Technology, Edited by A. K. Noor and W. D. Pilkey, The American Society of Mechanical Engineers, 1983, pp. 225-295.
7. Wang, B. P., "Structural Dynamic Optimization Using Reanalysis Techniques," ASME AMD-vol. 76, Reanalysis of Structural Dynamic Models (B. P. Wang, ed.), 1986, pp. 1-19.
8. Wang, B. P., "Synthesis of Structures with Multiple Frequency Constraints," AIAA Paper No. 0951-CP, Proceedings of AIAA/ASME/ASCE/AHS 27th Structures, Structural Dynamics and Materials Conferences, Vol. 1, pp. 394-397.
9. Wang, B. P., Chen, T. Y. and Chu, F. H., "Model Refinement Using Test Data," Proceedings of 4th International Modal Analysis Conferences, Los Angeles, CA 1986 Vol. II, pp. 1052-1057.

TABLE I. - STIFFNESS AND MASS EXPONENTS FOR SEVERAL COMMON STRUCTURAL ELEMENTS

Element	Design variable	β	γ
Truss	Cross	1	1
Membrane	Thickness	1	1
Plate bending	Thickness	3	1
Beam bending	Cross-sectional area*	2	1
Beam bending	Section area moment of inertia*	1	0.5

*Circular cross section

TABLE II. - DESIGN HISTORY OF TEN BAR TRUSS

Iteration No.	x_1	2	x_3	x_4
A-0	10.0	10.0	10.0	10.0
A-1	12.76	8.88	5.0	5.0
A-2	10.39	8.15	5.0	5.0
A-3	10.44	8.29	5.0	5.0
B-0	10.44	8.29	5.0	5.0
B-1	7.92	7.80	3.44	3.44
B-2	7.47	7.18	2.90	2.90
B-3	7.19	7.0	2.68	2.68

TABLE III. - COMPARISONS OF NATURAL FREQUENCIES

Case No.	f_1 (Hz)		Error (%)	f_2 (Hz)		Error (%)
	Approximate	Exact		Approximate	Exact	
A-1	16.88	16.60	1.71	40.16	39.03	2.88
A-2	15.96	15.78	1.14	39.85	38.99	2.19
A-3	15.99	15.82	1.10	40.00	39.11	1.27
B-1	15.90	15.89	0.11	40.23	39.87	0.88
B-2	15.99	15.98	0.03	39.98	39.44	1.37
B-3	15.99	15.99	0.00	40.00	39.33	1.71

TABLE IV. - COMPARISON OF $\partial\lambda_1/\partial x_1$

Case No.	$\partial\lambda/\mu x$	$\partial\lambda/\mu x$	Error (%)
	Eq. (28)	Exact	
A-1	418.9	454.0	7.7
A-2	494.2	509.2	2.9
A-3	495.8	505.9	1.9
B-1	557.2	578.3	3.7
B-2	607.3	609.2	0.3
B-3	635.8	620.0	2.6

TABLE V. - COMPARISON OF $\partial\lambda_1/\partial x_2$

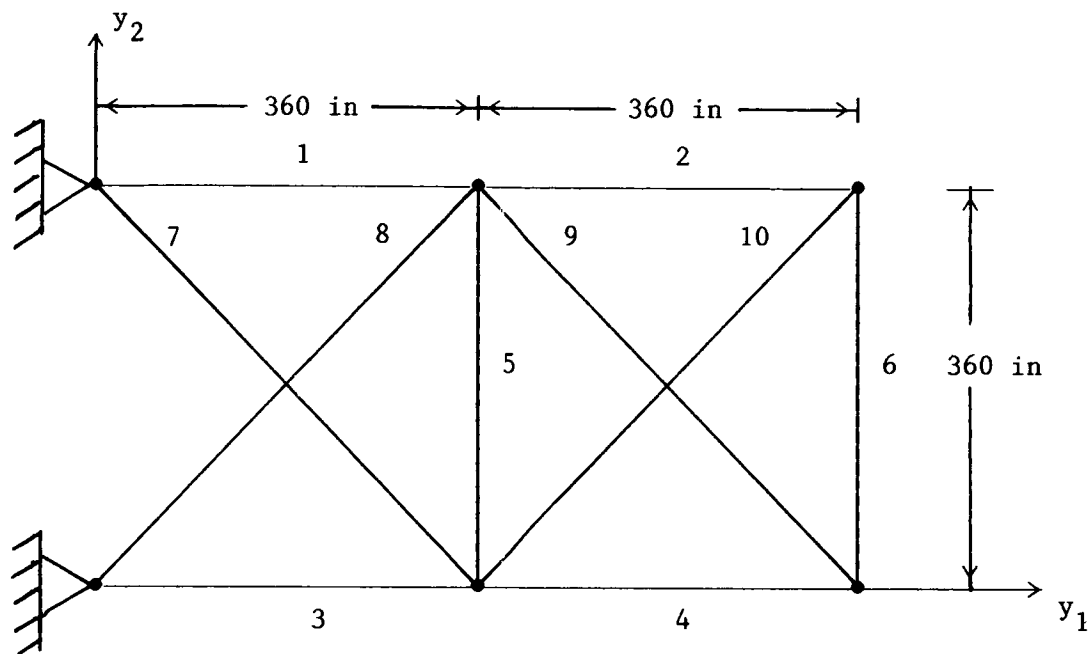
Case No.	$\partial\lambda/\partial x$	$\partial\lambda/\partial x$	Error (%)
	Eq. (28)	Exact	
A-1	216.7	294.6	26.5
A-2	208.8	269.9	22.5
A-3	202.3	262.7	23.5
B-1	203.8	205.2	0.7
B-2	203.8	222.9	8.6
B-3	196.0	221.0	11.3

TABLE VI. - COMPARISON OF $\partial\lambda_2/\partial x_1$

Case No.	$\partial\lambda/\mu x$	$\partial\lambda/\mu x$	Error (%)
	Eq. (28)	Exact	
A-1	-812.2	-786.9	3.2
A-2	-747.4	-793.9	5.8
A-3	-764.7	-805.2	9.0
B-1	-1232.3	-1247.8	1.2
B-2	-1387.7	-1320.2	5.1
B-3	-1482.4	-1435.7	3.2

TABLE VII. - COMPARISON OF $\partial\lambda_2/\partial x_2$

Case No.	$\partial\lambda/\partial x$	$\partial\lambda/\partial x$	Error (%)
	Eq. (28)	Exact	
A-1	3337.9	3652.3	31.35
A-2	3678.3	2917.2	26.1
A-3	3647.5	2876.9	26.8
B-1	3523.5	2928.3	20.3
B-2	3874.9	3038.0	27.5
B-3	4025.3	3043.1	32.3



Modulus of elasticity = 10^4 ksi

Material density = 0.1 lbm/in^3

Design variable $x_1 = 1, 2, 3, 4$
 $x_2 = 5, 6$
 $x_3 = \text{member } 7, 8, 9, 10$

Figure 1. Ten Member Cantilever Truss

APPLICATION OF A SYSTEM MODIFICATION TECHNIQUE TO
DYNAMIC TUNING OF A SPINNING ROTOR BLADE

C. V. Spain
PRC Kentron, Inc.
Aerospace Technologies Division
Hampton, Virginia

INTRODUCTION

An important consideration in the development of modern helicopters is the vibratory response of the main rotor blade. One way to minimize vibration levels is to ensure that natural frequencies of the spinning main rotor blade are well removed from integer multiples of the rotor speed. This report demonstrates a technique for dynamically tuning a finite-element model of a rotor blade to accomplish that end.

Rotor blades are an ideal subject for this type of analysis because a good structural representation can be achieved with a single string of beam elements and relatively few degrees of freedom. This means that the numerous system stiffness and mass matrices required can be formed with relatively low central processor time. The technique is valid, however, for larger and more complex models.

Because the tuning process involves the independent redistribution of mass and stiffness, it is especially applicable to composite blade designs in which mass and stiffness can be controlled independently by fiber orientation and the use of nonstructural mass.

In the following sections, a brief overview is given of the general purpose finite element system known as Engineering Analysis Language (EAL, ref. 1) which was used in this work. A description of the EAL System Modification (SM) processor is then given along with an explanation of special algorithms developed to be used in conjunction with SM. Finally, this technique is demonstrated by dynamically tuning a model of an advanced composite rotor blade.

This work was accomplished in support of the Interdisciplinary Research Office of NASA Langley Research Center and the objectives were threefold. The first was to establish a technique for tuning the natural frequencies of a spinning rotor blade. The second was to demonstrate the usefulness of the EAL SM processor and to be able to perform sensitivity and modification operations without dependence on additional software. The final objective was to provide guidelines on advanced use of the SM processor, i.e., use beyond the scope of currently available documentation.

ENGINEERING ANALYSIS LANGUAGE (EAL)

EAL is a general purpose finite element system produced by Engineering Information Systems, Inc. It evolved from an earlier finite element program known

as SPAR (ref. 2). In its present form, EAL consists of an Executive Control System (ECS) in which the user can execute work flow logic, looping, branching and data storage; and processors (similar to subroutines) which actually perform structural and utility computations. Data input or computations result in data sets which are stored in binary data bases or libraries which can be saved and referred to indefinitely. The user communicates with and uses these features with input known as runstreams.

Reference 1 is the current EAL reference manual, however, the older SPAR reference manual (ref. 2) must be used for the SM processor. EAL version 209 was used in this work.

EAL SYSTEM MODIFICATION (SM) FOR FREQUENCY MODIFICATION

The approach in modifying frequencies is to first specify a set of target (required) eigenvalues corresponding to natural frequencies of the original model. Parameters to be changed must be identified along with limits on acceptable changes. Sensitivities of the eigenvalues to parameter changes must then be calculated. To determine the actual structural changes, the statistical method described in reference 3 is used.

SM operates in 4 phases as described below. The notation used here is generally consistent with the SM description contained in reference 2.

Phase 1: The differences (ΔX) between the eigenvalue targets (X_T) and current eigenvalues (X) are calculated. That is:

$$\Delta X = X_T - X \quad (1)$$

Phase 2: The purpose of phase 2 is to approximate the sensitivities of eigenvalues ($\text{radians}^2/\text{sec}^2$) to specified changes in structural parameters which affect stiffness and/or mass. These specified changes are known as unit parameters. System stiffness change (ΔK) and mass change (ΔM) matrices are formed for each unit parameter.

Because the original model eigenvalue solution is based on equation 2 below, where λ_i is the i th eigenvalue and M , K and Y_i are the system mass, system stiffness and the i th mode shape, respectively, then the modified system can be described by equation 3.

$$\lambda_i M Y_i - K Y_i = 0 \quad (2)$$

$$(\lambda_i + \Delta \lambda_i)(M + \Delta M) - (K + \Delta K)(Y_i + \Delta Y_i) = 0 \quad (3)$$

With some simplifying assumptions (i.e. changes in mode shapes and products of the changes (Δ 's) are very small), a reasonable approximation of eigenvalue sensitivity is expressed by equation (4).

$$\Delta \lambda_i = Y_i^T \Delta K Y_i - \lambda_i Y_i^T \Delta M Y_i \quad (4)$$

The ΔK , ΔM and $\Delta \lambda_i$ are therefore the results of phase 2 which is computationally the most costly phase because the system mass and stiffness matrices must be formed for each unit parameter. Computations in the other 3 phases are trivial in terms of central processor time.

Equation 4 is valid only for a nonspinning structure and must be augmented for a spinning structure as described later.

Phase 3: The actual structural changes needed to realize the targeted eigenvalues are estimated based on equation (5) below which is an adaptation of the work presented in reference 3.

$$\{\Delta P\} = [S_{rr}] [NT]^T \left\{ [NT] [S_{rr}] [NT]^T + [S_{ee}] \right\}^{-1} [N] \{\Delta x\} \quad (5)$$

where:

ΔP is a set of multipliers which reflects the total estimated structural modifications needed in terms of corresponding unit parameters.

S_{rr} is the covariance or weighting matrix. The diagonal terms, each corresponding to the unit parameters in sequence, allow for the relative weighting of those parameters. In this application, values are set at unity and reset in later iterations if the parameter change limits are being exceeded.

N is a matrix containing reciprocals of the current eigenvalues ($1/\lambda_i$).

T is the sensitivity matrix consisting of ($\Delta\lambda_i$'s) with the rows corresponding to the number of targets and the columns to the number of unit parameters.

S_{ee} is the target tolerance matrix associated with acceptable variances of the resulting eigenvalues from the targets.

ΔX is as described in equation (1).

The purpose of using this method is to achieve the targeted eigenvalues with minimum change to the structure. S_{rr} can be used to influence how much a particular unit parameter is changed. For example, a unit parameter which can be changed with small penalty or is not likely to exceed the prescribed change limits may be assigned an S_{rr} value of 1.0, whereas, a unit parameter which should be changed as little as possible may be assigned a value of 0.1. S_{ee} values normally range from 0.0 (when a more exact attainment of the targeted eigenvalue is being sought) to 0.1 (when only an approximate result is needed). As described in reference 4, S_{ee} values of 0.001 when most S_{rr} values are 1.0 normally provide satisfactory results.

Phase 4: Each term of the ΔP matrix is compared to the parameter change limits data set (described below). If any of the limits are exceeded, a ΔPX matrix is formed where the smaller terms (from ΔP or limits) are used. ΔPX (ΔP if no limits were exceeded) is then used to actually change the structural parameter data sets of the finite-element model.

To test the results after the completion of phase 4, new mass and stiffness matrices must be formed, and the original process of computing mode shapes and frequencies is repeated. Normally, two or three iterations are sufficient to achieve the desired results if reasonable targets, unit parameters and change limits were selected. A complete iteration is the execution of phases 1-4 and testing of the results by calculating frequencies of the modified structure.

Prior to executing SM, EAL data sets must be established defining the targets, parameters, change limits, weighting and target tolerances. The EAL data set names for these inputs are given below followed by brief descriptions.

TVAL - Target (desired) eigenvalues ($\text{radian}^2/\text{sec}^2$) preceded by mode sequence numbers.

PARA - Each PARA data set is a group of changes (incremental element parameter or rigid mass) expressed as a fraction of the existing value. Each data set is then considered a unit parameter in SM computations.

SEE - Target tolerance matrix (S_{ee}).

SRR - Covariance or weighting matrix (S_{rr}).

DPLI - Parameter change limits (minimums and maximums) expressed as multiples (+ or -) of unit parameters defined in the PARA data sets.

AUGMENTATION TO THE SM PROCESSOR

In this application, it was necessary to develop three algorithms to augment the SM processor. These were implemented in the EAL Arithmetic Utility System (AUS) processor. The first was to add the centrifugal stiffening effect of the mass change (ΔM) matrices to the sensitivity matrix. The second was to revise the weighting matrix (S_{rr}) when the original values resulted in too many values of the change limits data set (DPLI) being violated by the ΔP matrix, thus causing structural changes which were inadequate in achieving targeted results. The third was to update the change limits after a complete iteration so that in the next iteration, the change limits data set (DPLI), which is based on a fraction of the current structural data set values, expresses the same engineering limits in terms of mass or stiffness originally intended.

To correct the sensitivity matrix, an additional system stiffness matrix must be formed for each nonzero ΔM matrix formed in phase 2. This matrix $[\Delta KC]$ reflects the centrifugal effect of the spinning ΔM and is formed using the AUS SPIN command to calculate a centrifugal force matrix and the elastic and centripetal contributions to stiffness. The Static Solution (SSOL) processor is used to calculate deflections due to the centrifugal force. The resulting stresses are embedded in the element state data sets by the GSF processor. Geometric stiffness changes are then calculated using the KG processor. The elastic, centripetal and geometric stiffness contributions are then summed to form $[\Delta KC]$ which is used to finalize the sensitivities as follows:

$$\Delta \lambda_{i\text{TOTAL}} = \lambda_i + Y_i [\Delta KC] Y_i^T \quad (6)$$

where λ_i is given by equation 4.

The weighting matrix (S_{rr}) is revised when limits (DPLI) are violated by (ΔP). This is accomplished simply by multiplying each term of the (S_{rr}) matrix by the ratios of corresponding terms of the ΔPX and ΔP matrices. That is,

$$\begin{bmatrix} S_{rr} \end{bmatrix}_{NEW} = \begin{bmatrix} S_{rr} \end{bmatrix}_{OLD} \begin{bmatrix} \frac{\delta PX_1}{\bar{\delta P}_1} & & \\ & \frac{\delta PX_2}{\bar{\delta P}_2} & \\ & & \ddots \end{bmatrix} \quad (7)$$

which has the effect of reducing those S_{rr} terms corresponding to unit parameters which are tending to be changed beyond their allowable limits in phase 3. This process is repeated until the resulting ΔPX matrix resulting from phase 4 does not, in the judgement of the user, differ too greatly from the ΔP matrix. If this cannot be achieved, the targets may be unachievable based on the selected parameters and change limits.

The updating of the change limits (DPLI) for the subsequent iteration is achieved by the following process which updates each term of the DPLI matrix to retain the original engineering value.

$$[\Delta PLI]_{NEW} = \begin{bmatrix} \frac{L_{1OLD} - \Delta PX_1}{1 + f_1 \Delta PX_1} & \frac{L_{2OLD} - \Delta PX_2}{1 + f_2 \Delta PX_2} & \dots \\ \frac{U_{1OLD} - \Delta PX_1}{1 + f_1 \Delta PX_1} & \dots & \dots \end{bmatrix} \quad (8)$$

(Etc for each parameter)

where:

ΔPLI_{NEW} = New parameter change limits data set.

L_{1OLD}, L_{2OLD} = Old lower limits for parameters 1 and 2.

U_{1OLD} = Old upper limit for parameter 1.

$\Delta PX_1, \Delta PX_2$ = The final changes for parameters 1 and 2 produced in SM phases 3 and 4.

f_1, f_2 = The fraction used in defining a unit change for parameters 1 and 2 in the PARA data sets. For this process to work, the fraction must be uniform within a given PARA data set.

DEMONSTRATION

The finite element model (see figure 1) used in this report is based on a preliminary design of an advanced composite main rotor blade developed by Mark W. Nixon of the U.S. Army Aerostructures Research Group at Langley Research Center. Table I gives the mass and stiffness properties of the baseline model which resulted from a composite analysis program also developed by Mr. Nixon. Table II provides the constraints or parameter changes which cannot be exceeded during the tuning

process. These constraints are based on the designer's estimate of what changes can be reasonably made without sacrificing the structural integrity or performance of the rotor blade.

Additional constraints on the problem were that bending stiffness, if modified, must be changed uniformly over large segments of the blade. The minimum allowable mass moment of inertia about the hub was 19000 lb-in-sec² for autorotation capability.

The objective of the tuning process was to minimize resonances caused when flexible mode frequencies were too close to integer multiples of the rotor speed up to eight per revolution (8P). The main rotor speed was 263 RPM (4.3833 HZ) and a criterion of at least .2P separation was used. Table III lists the unacceptable frequency ranges along with the natural frequencies of the original model and those of the modified model following the first and second tuning iterations.

The overall process which was conducted interactively is depicted in figure 2. Figure 3 contains the actual EAL runstreams used in the process. The runstreams in combination with this paper and the references should provide adequate guidelines for a new SM user.

Modes 1 and 2 are the flatwise and edgewise rigid body modes, and due to the physics of a spinning rotor blade, cannot be significantly altered. Modes 3 through 7 were therefore targeted for modification. Due to blade twist, modes 3, 5, 6 and 7 are combined flatwise/edgewise bending modes whereas mode 4 is predominantly torsion. It appeared reasonable to drive all of the bending mode frequencies to approximately .25P below the nearest P multiple while allowing the torsion mode to remain close to its original frequency. A study of the sensitivities indicated that to drive frequencies in opposite directions would have required unacceptably large changes in certain parameters. The selected target frequencies are listed in Tables III and IV. Table IV also lists all of the SM inputs.

Results of two complete iterations are summarized in Table III and figure 4. Figure 4 shows the ratio of calculated to target frequencies plotted against the iteration number ("0" iteration being the original model). A ratio of 1.0 would indicate complete convergence with the target value. The first iteration did not move all of the frequencies to acceptable ranges (Table III) but did move all of them towards the targets as shown in figure 4. The second iteration produced frequencies out of the unacceptable ranges and very close to the targeted frequencies. The total weight of the blade increased from 250.54 lb to 265.30 lb and the mass moment of inertia about the hub increased from 19007.1 to 19780.7 lb-in-sec². Table V summarizes the final structural properties of the modified rotor blade model.

CONCLUDING REMARKS

A sensitivity technique useful in minimizing vibrations associated with helicopter rotor blades has been demonstrated. This and similar techniques can be

effective in achieving desired performance with minimum change to the basic structure. This is especially true for spinning structures because centrifugal stiffening complicates the intuitive process of changing mass and stiffness to tune natural frequencies.

An advantage of the process described in this report is that the modification capability is built into the structural analysis program. This eliminates the need for data transfer and development or use of external software.

The EAL System Modification processor has applications beyond that for which it was originally produced and documented, as demonstrated here for a spinning structure. As long as the equations for calculating appropriate sensitivities are known, structural modification can be computed to achieve any targeted response such as mode shapes, static deflections, stress and bending moments and loads due to dynamic loads.

REFERENCES

1. Whetstone, W. D.: EISI-EAL Engineering Analysis Language Reference Manual. Engineering Information Systems, Inc., San Jose, CA, July, 1983.
2. Whetstone, W. D.: EISI/SPAR Reference Manual, Volume 1 Program Execution. Engineering Information Systems, Inc., Saratoga, CA, January, 1979.
3. Collins, Jon D.; Hart, Gary C.; Hassleman, T. K.; and Kennedy, Bruce: Statistical Identification of Structures. AIAA Journal, Vol. 12, No. 2, Feb. 1974, pp. 185-190.
4. Robinson, James C.: Application of a Systematic Finite-Element Model Modification Technique to Dynamic Analysis of Structures, AIAA Paper No. 82-0730. Presented at 23rd AIAA/ASME/ASCE/AHS SDM Conference, May 10-12, 1982, New Orleans, LA.

TABLE I. - MODEL PROPERTIES

Joint No.	Joint Location (z,in)	Lumped Mass (lb)	Lumped inertia about z-axis (lb-in-sec ²)
1	0	0	.2415
2	16.1	0	.2700
3	18.0	0	.0585
4	20.0	0	.1230
5	26.2	0	.1860
6	32.4	0	.1860
7	38.6	0	.1905
8	45.1	0.32	.1551
9	51.5	0.645	.1161
10	58.0	0.645	.1161
11	64.4	1.93	.3474
12	96.6	3.22	.5796
13	128.8	3.22	.5796
14	161.0	3.22	.5796
15	193.2	2.415	.4347
16	209.3	1.61	.2898
17	225.4	1.61	.2898
18	241.5	1.61	.31395
19	257.6	1.61	.36225
20	273.7	1.61	.3864
21	289.8	1.125	.2700
22	296.2	0.645	.1548
23	302.7	0.645	.1548
24	309.1	0.32	.2068
25	315.6	0.35	.2580
26	322.0	0.35	.1280

Beam Section	Joints Spanned	Edgewise Stiffness EI_{11}^* (LBF-in ²)	Flatwise Stiffness EI_{22}^* (LBF-in ²)	Twist Angle LE Down (DEGR)	Distributed Weight (Lbs/in)	Cross Sectional Area In ²	Torsional Stiffness GJ (LBF-in ²)
1	1 - 2	900.0	900.0	26.0	2.29	44.44	100.00
2	2 - 3	.0001	.0001	25.34	2.29	44.44	87.50
3	3 - 4	.0001	.0001	25.26	2.29	44.44	87.50
4	4 - 5	580.0	360.0	25.17	2.20	44.44	75.50
5	5 - 6	580.0	360.0	24.92	2.20	44.44	75.50
6	6 - 7	580.0	360.0	24.66	2.20	44.44	75.50
7	7 - 8	580.0	298.0	24.41	2.60	44.44	60.00
8	8 - 9	1260.0	25.89	24.14	0.35	78.84	17.125
9	9 - 10	1260.0	25.89	23.87	0.35	78.84	17.125
10	10 - 11	1260.0	25.89	23.60	0.35	78.84	17.125
11	11 - 12	1260.0	25.89	23.34	0.35	78.84	17.125
12	12 - 13	1260.0	25.89	22.01	0.35	78.84	17.125
13	13 - 14	1260.0	25.89	20.68	0.35	78.84	17.125
14	14 - 15	1260.0	25.89	19.35	0.35	78.84	17.125
15	15 - 16	1260.0	25.89	18.02	0.35	78.84	17.125
16	16 - 17	1260.0	25.89	17.34	0.35	78.84	17.125
17	17 - 18	1260.0	25.89	16.69	0.35	78.84	17.125
18	18 - 19	1260.0	25.89	16.03	0.35	78.84	17.125
19	19 - 20	1260.0	25.89	15.67	0.35	78.84	17.125
20	20 - 21	1260.0	25.89	14.70	0.35	78.84	17.125
21	21 - 22	1260.0	25.89	14.03	0.35	78.84	17.125
22	22 - 23	1260.0	25.89	13.77	0.35	78.84	17.125
23	23 - 24	1260.0	25.89	13.51	0.35	78.84	17.125
24	24 - 25	580.0	24.0	13.23	0.90	44.44	60.00
25	25 - 26	580.0	24.0	12.77	3.3706	44.44	60.00

Total mass moment of inertia about x axis (hub): 19007.1 lb in sec². Total weight: 250.54 lb.

* Stiffness paramaters are with respect to a local reference frame which is rotated the amount of the twist angle from the global frame shown on figure 1.

TABLE II. - CHANGE LIMITS ORIGINAL PAGE IS
OF POOR QUALITY

Joint No.	Lumped Mass %	Edgewise		
		Section No.	Stiffness %	Flatwise Stiffness
1	0	1	0	0
2	0	2	0	0
3	0	3	0	0
4	0	4	0	0
5	0	5	0	0
6	0	6	0	0
7	0	7	0	0
8	0	8	+20	+10
9	-50 +100	9	+20	+10
10	-50 +100	10	+20	+10
11	-50 +100	11	+20	+10
12	-50 +100	12	+20	+10
13	-50 +100	13	+20	+10
14	-50 +100	14	+20	+10
15	-50 +100	15	+20	+10
16	-50 +100	16	+20	+10
17	-50 +100	17	+20	+10
18	-50 +100	18	+20	+10
19	-50 +100	19	+20	+10
20	-50 +100	20	+20	+10
21	-50 +100	21	+20	+10
22	-50 +100	22	+20	+10
23	-50 +100	23	+20	+10
24	-50 +100	24	0	0
25	+100	25	0	0
26	+100			

Minimum Allowable Mass Moment of Inertia About X Axis: 19000 lb in sec²

* Items in brackets must be changed uniformly as a group.

TABLE III. - MODEL NATURAL FREQUENCIES
COMPARED TO UNACCEPTABLE RANGES

MULTIPLE, M	UNACCEPTABLE RANGES, HZ (MP±.2P)
1	3.507 - 5.260
2	7.890 - 9.643
3	12.273 - 14.027
4	16.657 - 18.410
5	21.040 - 22.793
6	25.423 - 27.177
7	29.807 - 31.560
8	34.190 - 35.943

WHERE P=263rpm OR 4.3833HZ

FREQUENCIES

MODE	TARGET	ORIGINAL	ITER 1	ITER 2
3	12.054	12.488*	12.067	12.030
4	16.0896	16.090	16.010	15.988
5	20.8208	22.460*	21.062*	20.928
6	23.0125	25.056	23.158	22.949
7	33.9708	36.368	34.326*	34.114

*IN UNACCEPTABLE RANGE

TABLE IV. - SYSTEM MODIFICATION INPUT DATA

SEQUENCE NO.	TARGET FREQUENCIES (TVAL SM) ¹		TARGET TOLERANCES (SEE SM)		
	MODE NO.	EIGENVALUE	TARGET NO.	MODE NO.	TOLERANCE
1	3	5736.3299 (12.05 HZ)	1	3	.001
2	4	10219.9920 (16.09 HZ)	2	4	.1 ⁴
3	5	17114.1744 (20.82 HZ)	3	5	.001
4	6	20906.7892 (23.01 HZ)	4	6	.001
5	7	45558.7855 (33.97 HZ)	5	7	.001

UNIT PARAMETERS (PARA SM n)					INITIAL COVARIANCE ⁵ AND CHANGE LIMITS (SRR SM AND DPLI SM)		
n	DATA TYPE	LINE ² NO.	FRACTION	COLUMN ³ NO.	UNIT PARAMETER NO.	COVARIANCE	LIMITS ⁶
1	RIGID MASS	25	.1	1 TO 3	1	1	-10,+10
2	RIGID MASS	26	.1	1 TO 3	2-15	1	-5,+10
3	RIGID MASS	9	.1	1 TO 3	16	1	-2,+2
4	RIGID MASS	10	.1	1 TO 3	17	1	-1,+1
5	RIGID MASS	11	.1	1 TO 3	18	1	-1,+1
6	RIGID MASS	12	.1	1 TO 3			
7	RIGID MASS	13	.1	1 TO 3			
8	RIGID MASS	14	.1	1 TO 3			
9	RIGID MASS	15	.1	1 TO 3			
10	RIGID MASS	16	.1	1 TO 3			
11	RIGID MASS	17	.1	1 TO 3			
12	RIGID MASS	18	.1	1 TO 3			
13	RIGID MASS	19	.1	1 TO 3			
14	RIGID MASS	20	.1	1 TO 3			
15	RIGID MASS	21	.1	1 TO 3			
16	RIGID MASS	22	.1	1 TO 3			
17	RIGID MASS	23	.1	1 TO 3			
18	RIGID MASS	24	.1	1 TO 3			
19	EDGEWISE STIFFNESS (EI ₁₁)	8 TO 23	.1	4			
20	FLATWISE STIFFNESS (EI ₂₂)	16 TO 23	.1	6			
21	FLATWISE STIFFNESS (EI ₂₂)	8 TO 15	.1	6			

NOTES: These data correspond to the input in the EAL runstream in figure 3b.

- Names in parentheses are EAL data set names.
- Line number of structural data set corresponds to joint for rigid masses and beam segment number for stiffnesses.
- The unit parameter is a set of numbers computed from multiplying the fraction times the structural values in the indicated lines and columns.
- A tolerance value of 0.1 rather than 0.001 indicates that it is less critical for the final frequency to be very close to the target value.
- These values were modified in the iteration process.
- Limits of -5 to plus 10 means that the structural parameter cannot be reduced by more than 5 x (FRACTION) x (EXISTING VALUE) nor increased more than 10 x (FRACTION) x (EXISTING VALUE).

TABLE V. - FINAL MODIFIED STRUCTURAL PROPERTIES

JOINT NO.	LUMPED MASS (lb)	BEAM SECTION	EDGEWISE STIFFNESS EI ₁₁ (LBF in ²)	FLATWISE STIFFNESS EI ₂₂ (LBF in ²)
9	1.284	8	1046.96	23.311
10	1.284	9	1046.96	23.311
11	3.785	10	1046.96	23.311
12	6.440	11	1046.96	23.311
13	6.286	12	1046.96	23.311
14	6.401	13	1046.96	23.311
15	1.883	14	1046.96	23.311
16	1.025	15	1046.96	23.32
17	1.881	16	1046.96	23.32
18	3.190	17	1046.96	23.32
19	3.220	18	1046.96	23.32
20	3.201	19	1046.96	23.32
21	0.5713	20	1046.96	23.32
21	0.3225	21	1046.96	23.32
23	0.3225	22	1046.96	23.32
24	0.1815	23	1046.96	23.32
25	0.1275			
26	0.1275			

TOTAL MASS MOMENT OF INERTIA ABOUT X AXIS (HUB): 19780 lb-in sec².

TOTAL WEIGHT: 265.30 lb

NOTE: All other properties unchanged from Table I.

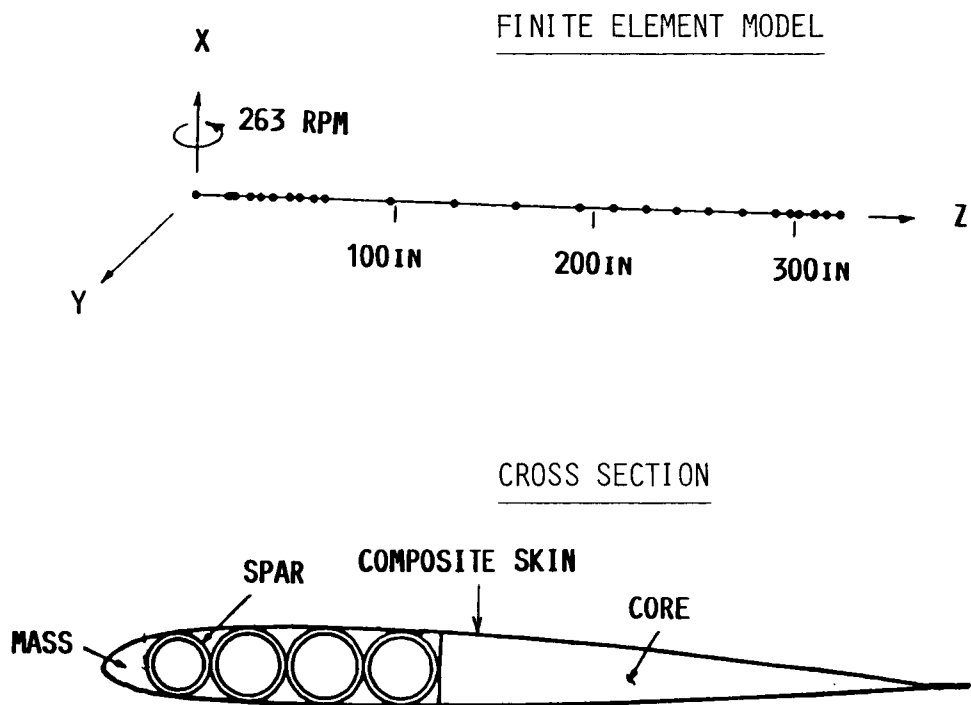


Figure 1.- Rotor blade model.

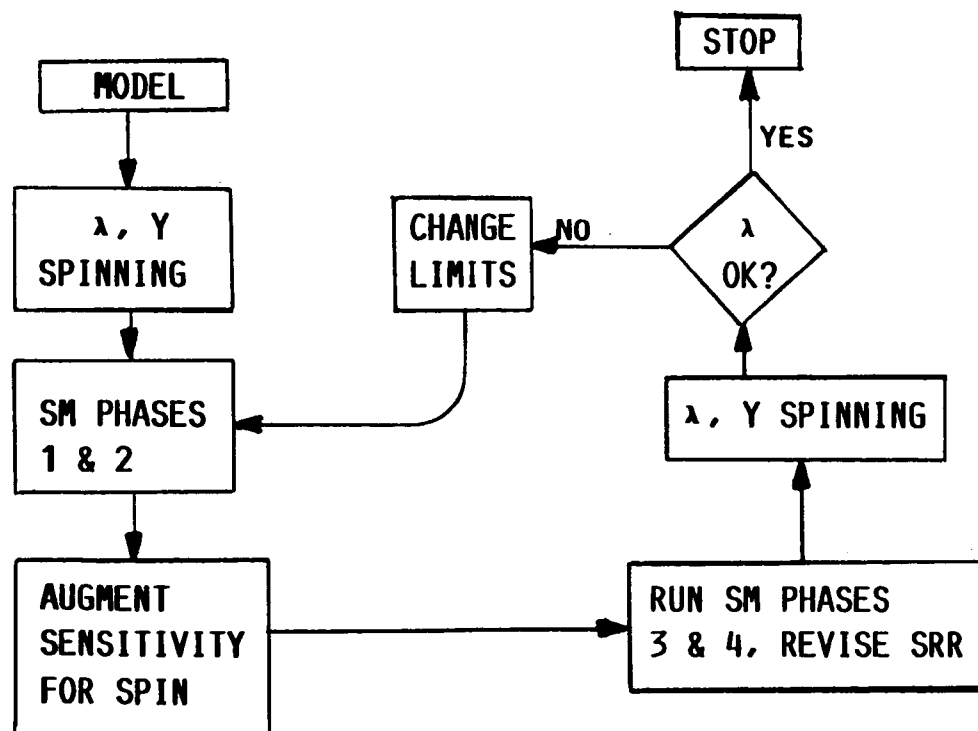


Figure 2.- Procedure for tuning frequencies of a spinning structure.

```

XXQT TAB
START 26
JLOC
1 0. 0. 00.
2 0. 0. 16.1
3 0. 0. 18.0
4 0. 0. 20.0
5 0. 0. 25.20
6 0. 0. 32.40
7 0. 0. 38.60
8 0. 0. 45.10
9 0. 0. 51.50
10 0. 0. 58.00
11 0. 0. 64.40
12 0. 0. 96.60
13 0. 0. 128.80
14 0. 0. 161.00
15 0. 0. 193.20
16 0. 0. 209.30
17 0. 0. 225.40
18 0. 0. 241.50
19 0. 0. 257.60
20 0. 0. 273.70
21 0. 0. 289.80
22 0. 0. 296.20
23 0. 0. 302.70
24 0. 0. 309.10
25 0. 0. 315.60
26 0. 0. 322.00
CON-1
ZERO 1 2 3 4 5 6:1
MATC
1 1.+6 .25 0. 80-.4+6
BA
$GIUM I1 A1 I2 A2 A F
GIUM 1 900.0 0. 900.0 0. 44.44 100.00
GIUM 2 .0001 0. .0001 0. 44.44 87.500
GIUM 3 .0001 0. .0001 0. 44.44 87.500
GIUM 4 580.0 0. 360.0 0. 44.44 75.000
GIUM 5 580.0 0. 360.0 0. 44.44 75.000
GIUM 6 580.0 0. 360.0 0. 44.44 75.000
GIUM 7 580.0 0. 298.0 0. 44.44 60.000
GIUM 8 1260. 0. 25.89 0. 78.84 17.125
GIUM 9 1260. 0. 25.89 0. 78.84 17.125
GIUM 10 1260. 0. 25.89 0. 78.84 17.125
GIUM 11 1260. 0. 25.89 0. 78.84 17.125
GIUM 12 1260. 0. 25.89 0. 78.84 17.125
GIUM 13 1260. 0. 25.89 0. 78.84 17.125
GIUM 14 1260. 0. 25.89 0. 78.84 17.125
GIUM 15 1260. 0. 25.89 0. 78.84 17.125
GIUM 16 1260. 0. 25.89 0. 78.84 17.125
GIUM 17 1260. 0. 25.89 0. 78.84 17.125
GIUM 18 1260. 0. 25.89 0. 78.84 17.125
GIUM 19 1260. 0. 25.89 0. 78.84 17.125
GIUM 20 1260. 0. 25.89 0. 78.84 17.125
GIUM 21 1260. 0. 25.89 0. 78.84 17.125
GIUM 22 1260. 0. 25.89 0. 78.84 17.125

```

```

7 2.60
8 0.35
9 0.35
10 0.35
11 0.35
12 0.35
13 0.35
14 0.35
15 0.35
16 0.35
17 0.35
18 0.35
19 0.35
20 0.35
21 0.35
22 0.35
23 0.35
24 0.90
25 3.3706
XXQT ELD
E21
GROUP 1' ROTOR BLADE
NSECT=1:NMAT=1:NMNU=1
INC NSECT=1
INC NMNU=1
INC NREF=1
1 2 1 25
XXQT E
RESET G=386.
XXQT AUS
TABL(NI=6 NJ=26):ING
I=6: J= 1: .241500E+00
I=6: J= 2: .270000E+00
I=6: J= 3: .585000E-01
I=6: J= 4: .123000E+00
I=6: J= 5: .186000E+00
I=6: J= 6: .186000E+00
I=6: J= 7: .190500E+00
I=6: J= 8: .155100E+00
I=6: J= 9: .116100E+00
I=6: J= 10: .116100E+00
I=6: J= 11: .347400E+00
I=6: J= 12: .579600E+00
I=6: J= 13: .579600E+00
I=6: J= 14: .579600E+00
I=6: J= 15: .434700E+00
I=6: J= 16: .289800E+00
I=6: J= 17: .289800E+00
I=6: J= 18: .313950E+00
I=6: J= 19: .362250E+00
I=6: J= 20: .386400E+00
I=6: J= 21: .270000E+00
I=6: J= 22: .154800E+00
I=6: J= 23: .154800E+00
I=6: J= 24: .206800E+00
I=6: J= 25: .258000E+00
I=6: J= 26: .128000E+00

```

```

GIUM 23 1260. 0. 25.89 0. 78.84 17.125
GIUM 24 580.0 0. 24.00 0. 44.44 60.000
GIUM 25 580.0 0. 24.00 0. 44.44 60.000
NREF
1 1 1 -1 .89879
2 1 1 -1 .90378
3 1 1 -1 .90438
4 1 1 -1 .90505
5 1 1 -1 .90690
6 1 1 -1 .90880
7 1 1 -1 .91061
8 1 1 -1 .91255
9 1 1 -1 .91447
10 1 1 -1 .91636
11 1 1 -1 .91817
12 1 1 -1 .92712
13 1 1 -1 .93557
14 1 1 -1 .94351
15 1 1 -1 .95095
16 1 1 -1 .95455
17 1 1 -1 .95787
18 1 1 -1 .96112
19 1 1 -1 .96281
20 1 1 -1 .96727
21 1 1 -1 .97017
22 1 1 -1 .97126
23 1 1 -1 .97234
24 1 1 -1 .97346
25 1 1 -1 .97527
RMAS5
CM .00259067 .00259067
8 0.32
9 0.645
10 0.645
11 1.93
12 3.22
13 3.22
14 3.22
15 2.415
16 1.61
17 1.61
18 1.61
19 1.61
20 1.61
21 1.125
22 0.645
23 0.645
24 0.32
25 .35
26 .35
NSUB NON STRUCT WT DISTR
1 2.29
2 2.29
3 2.29
4 2.20
5 2.20
6 2.20
DEM2=SUM(DEM IN6)
M+RM = SUM(RMAS DEM2 )
XXQT DCU
DISA 1 EQNF
XXQT EKS
XXQT TAN
XXQT K
SPDP=2
XXQT AUS
SPIN: M+RM K 27.5413 0.0 0. 0. 0. 0. 8 27.5413 RAD/SEC
XXQT RSI
RESET K-KSPN
XXQT SSOL
RESET K-KSPN
XXQT GSF
RESET EMBED=1
XXQT KG
SPDP=2
XXQT AUS
KECG=SUM(KSPN KG)
XXQT RSI
RESET K-KECG
XXQT EIG
RESET INIT=11 NREQ=7 M=M+RM K=KECG OUTL=1
XXQT AUS
RIG=RIGID(1)
MR=PROD(M+RM RIG)
GM=XTYD(RIG MR)
GMUT=UNION(386. GM)
XXQT DCU
PRINT 1 GM
PRINT 1 GMUT
XXQT EXIT

```

ORIGINAL PAGE IS
OF POOR QUALITY

Figure 3a.- EAL runstream for calculation of natural frequencies of the spinning structure.

ORIGINAL PAGE IS OF POOR QUALITY

```

XXQT AUS
TABL(NI=2 NJ=5):TVAL SM
J=113. 5736.3299 $12.054 MZ
J=214. 10219.9920 $ 16.0896
J=315. 17114.1744 $ 20.8208
J=416. 20906.7892 $ 23.0125
J=517. 45558.7855 $ 33.97082
TABL(NI=5 NJ=2):PARA SM 11J=1118. 25. .1 1. 3.
J=2118. 26. .1 1. 3.
TABL(NI=5 NJ=2):PARA SM 21J=1118. 09. .1 1. 3.
J=2118. 10. .1 1. 3.
TABL(NI=5 NJ=1):PARA SM 31J=1118. 11. .1 1. 3.
TABL(NI=5 NJ=1):PARA SM 41J=1118. 12. .1 1. 3.
TABL(NI=5 NJ=1):PARA SM 51J=1118. 13. .1 1. 3.
TABL(NI=5 NJ=1):PARA SM 61J=1118. 14. .1 1. 3.
TABL(NI=5 NJ=1):PARA SM 71J=1118. 15. .1 1. 3.
TABL(NI=5 NJ=1):PARA SM 81J=1118. 16. .1 1. 3.
TABL(NI=5 NJ=1):PARA SM 091J=1118. 17. .1 1. 3.
TABL(NI=5 NJ=1):PARA SM 101J=1118. 18. .1 1. 3.
TABL(NI=5 NJ=1):PARA SM 111J=1118. 19. .1 1. 3.
TABL(NI=5 NJ=1):PARA SM 121J=1118. 20. .1 1. 3.
TABL(NI=5 NJ=1):PARA SM 131J=1118. 21. .1 1. 3.
TABL(NI=5 NJ=2):PARA SM 141J=1118. 22. .1 1. 3.
J=2118. 23. .1 1. 3.
TABL(NI=5 NJ=1):PARA SM 151J=1118. 24. .1 1. 3.
TABL(NI=5 NJ=16):PARA SM 161J=1 16
9. 8. .1 4. 4.
9. 9. .1 4. 4.
9. 10. .1 4. 4.
9. 11. .1 4. 4.
9. 12. .1 4. 4.
9. 13. .1 4. 4.
9. 14. .1 4. 4.
9. 15. .1 4. 4.
9. 16. .1 4. 4.
9. 17. .1 4. 4.
9. 18. .1 4. 4.
9. 19. .1 4. 4.
9. 20. .1 4. 4.
9. 21. .1 4. 4.
9. 22. .1 4. 4.
9. 23. .1 4. 4.
TABL(NI=5 NJ=8):PARA SM 171J=1 8
9. 16. .1 6. 6.
9. 17. .1 6. 6.
9. 18. .1 6. 6.
9. 19. .1 6. 6.
9. 20. .1 6. 6.
9. 21. .1 6. 6.
9. 22. .1 6. 6.
9. 23. .1 6. 6.
TABL(NI=5 NJ=8):PARA SM 181J=1 8
9. 8. .1 6. 6.
9. 9. .1 6. 6.
9. 10. .1 6. 6.
9. 11. .1 6. 6.
9. 12. .1 6. 6.

```

```

9. 13. .1 6. 6.
9. 14. .1 6. 6.
9. 15. .1 6. 6.
TABL(NI=1 NJ=5):SEE SM1J=1 5:0.001 .1 .001 .001 .001
TABL(NI=1 NJ=18):SRR SM1J=1 18:1.
TABL(NI=2 NJ=18):DPL1 SM1J=11-10. 10.
J=2 151-5.0 10.
J=161-2. 2.
J=171-1. 1.
J=181-1. 1.

```

XXQT EXIT

Figure 3b.- EAL runstream for input to the SM processor.

```

XXQT SM $DEVELOP DM FOR EACH PARAM
RESET NPARA=18 G=386. OUTL=1 NUUX=2
OPER 1 1 0 0
XXQT RSI
RESET K=K$LAST KECC
XXQT AUS$ DEVEL INERTIAL STIFFNESS FOR PARAM 1
DEFINE DMT=DM SM 1 1:DMA=UNION(DMT)
SPIN:DMA K 27.5413 0. 0. 0. 0. 0.
XXQT SSOL
RESET K=K$SPN
XXQT GSF
RESET EMBED=1
XXQT KG
XXQT DCU
CHAN 1 KG SPAR 36 0 DK1 SPAR 36 1
XXQT AUS$ DEVEL INERTIAL STIFFNESS FOR PARAM 2
DEFINE DMT=DM SM 2 1:DMA=UNION(DMT)
SPIN:DMA K 27.5413 0. 0. 0. 0. 0.
XXQT SSOL
RESET K=K$SPN
XXQT GSF
RESET EMBED=1
XXQT KG
XXQT DCU
CHAN 1 KG SPAR 36 0 DK2 SPAR 36 2
XXQT AUS$ DEVEL INERTIAL STIFFNESS FOR PARAM 3
DEFINE DMT=DM SM 3 1:DMA=UNION(DMT)
SPIN:DMA K 27.5413 0. 0. 0. 0. 0.
XXQT SSOL
RESET K=K$SPN
XXQT GSF
RESET EMBED=1
XXQT KG
XXQT DCU
CHAN 1 KG SPAR 36 0 DK3 SPAR 36 3
XXQT AUS$ DEVEL INERTIAL STIFFNESS FOR PARAM 4
DEFINE DMT=DM SM 4 1:DMA=UNION(DMT)
SPIN:DMA K 27.5413 0. 0. 0. 0. 0.
XXQT SSOL
RESET K=K$SPN
XXQT GSF
RESET EMBED=1
XXQT KG
XXQT DCU
CHAN 1 KG SPAR 36 0 DK4 SPAR 36 4
XXQT AUS$ DEVEL INERTIAL STIFFNESS FOR PARAM 5
DEFINE DMT=DM SM 5 1:DMA=UNION(DMT)
SPIN:DMA K 27.5413 0. 0. 0. 0. 0.
XXQT SSOL
RESET K=K$SPN
XXQT GSF
RESET EMBED=1
XXQT KG
XXQT DCU
CHAN 1 KG SPAR 36 0 DK5 SPAR 36 5
XXQT AUS$ DEVEL INERTIAL STIFFNESS FOR PARAM 6
DEFINE DMT=DM SM 6 1:DMA=UNION(DMT)

```

```

SPIN:DMA K 27.5413 0. 0. 0. 0. 0.
XXQT SSOL
RESET K=K$SPN
XXQT GSF
RESET EMBED=1
XXQT KG
XXQT DCU
CHAN 1 KG SPAR 36 0 DK6 SPAR 36 6
XXQT AUS$ DEVEL INERTIAL STIFFNESS FOR PARAM 7
DEFINE DMT=DM SM 7 1:DMA=UNION(DMT)
SPIN:DMA K 27.5413 0. 0. 0. 0. 0.
XXQT SSOL
RESET K=K$SPN
XXQT GSF
RESET EMBED=1
XXQT KG
XXQT DCU
CHAN 1 KG SPAR 36 0 DK7 SPAR 36 7
XXQT AUS$ DEVEL INERTIAL STIFFNESS FOR PARAM 8
DEFINE DMT=DM SM 8 1:DMA=UNION(DMT)
SPIN:DMA K 27.5413 0. 0. 0. 0. 0.
XXQT SSOL
RESET K=K$SPN
XXQT GSF
RESET EMBED=1
XXQT KG
XXQT DCU
CHAN 1 KG SPAR 36 0 DK8 SPAR 36 8
XXQT AUS$ DEVEL INERTIAL STIFFNESS FOR PARAM 9
DEFINE DMT=DM SM 9 1:DMA=UNION(DMT)
SPIN:DMA K 27.5413 0. 0. 0. 0. 0.
XXQT SSOL
RESET K=K$SPN
XXQT GSF
RESET EMBED=1
XXQT KG
XXQT DCU
CHAN 1 KG SPAR 36 0 DK9 SPAR 36 9
XXQT AUS$ DEVEL INERTIAL STIFFNESS FOR PARAM 10
DEFINE DMT=DM SM 10 1:DMA=UNION(DMT)
SPIN:DMA K 27.5413 0. 0. 0. 0. 0.
XXQT SSOL
RESET K=K$SPN
XXQT GSF
RESET EMBED=1
XXQT KG
XXQT DCU
CHAN 1 KG SPAR 36 0 DK10 SPAR 36 10
XXQT AUS$ DEVEL INERTIAL STIFFNESS FOR PARAM 11
DEFINE DMT=DM SM 11 1:DMA=UNION(DMT)
SPIN:DMA K 27.5413 0. 0. 0. 0. 0.
XXQT SSOL
RESET K=K$SPN
XXQT GSF
RESET EMBED=1
XXQT KG
XXQT DCU
CHAN 1 KG SPAR 36 0 DK11 SPAR 36 11

```

Figure 3c.- EAL runstream for developing the sensitivity matrix.

```

$XQT AUS$ DEVEL INERTIAL STIFFNESS FOR PARAM 12
DEFINE DMT=DM SM 12 1:DMA=UNION(DMT)
SPIN:DMA K 27.5413 0. 0. 0. 0.
$XQT SSOL
RESET K-KSPN
$XQT GSF
RESET EMBED=1
$XQT KG
$XQT DCU
CHAN 1 KG SPAR 36 0 DK12 SPAR 36 12
$XQT AUS$ DEVEL INERTIAL STIFFNESS FOR PARAM 13
DEFINE DMT=DM SM 13 1:DMA=UNION(DMT)
SPIN:DMA K 27.5413 0. 0. 0. 0.
$XQT SSOL
RESET K-KSPN
$XQT GSF
RESET EMBED=1
$XQT KG
$XQT DCU
CHAN 1 KG SPAR 36 0 DK13 SPAR 36 13
$XQT AUS$ DEVEL INERTIAL STIFFNESS FOR PARAM 14
DEFINE DMT=DM SM 14 1:DMA=UNION(DMT)
SPIN:DMA K 27.5413 0. 0. 0. 0.
$XQT SSOL
RESET K-KSPN
$XQT GSF
RESET EMBED=1
$XQT KG
$XQT DCU
CHAN 1 KG SPAR 36 0 DK14 SPAR 36 14
$XQT AUS$ DEVEL INERTIAL STIFFNESS FOR PARAM 15
DEFINE DMT=DM SM 15 1:DMA=UNION(DMT)
SPIN:DMA K 27.5413 0. 0. 0. 0.
$XQT SSOL
RESET K-KSPN
$XQT GSF
RESET EMBED=1
$XQT KG
$XQT DCU
CHAN 1 KG SPAR 36 0 DK15 SPAR 36 15
$XQT AUS$ DEVEL INERTIAL STIFFNESS FOR PARAM 16
$DEFINE DMT=DM SM 16 1:DMA=UNION(DMT)
$SPIN:DMA K 27.5413 0. 0. 0. 0.
$XQT SSOL
$RESET K-KSPN
$XQT GSF
$RESET EMBED=1
$XQT KG
$XQT DCU
$CHAN 1 KG SPAR 36 0 DK16 SPAR 36 16
$XQT AUS$ DEVEL INERTIAL STIFFNESS FOR PARAM 17
$DEFINE DMT=DM SM 17 1:DMA=UNION(DMT)
$SPIN:DMA K 27.5413 0. 0. 0. 0.
$XQT SSOL
$RESET K-KSPN
$XQT GSF
$RESET EMBED=1

$XQT KG
$XQT DCU
$CHAN 1 KG SPAR 36 0 DK17 SPAR 36 17
$XQT AUS
DEFI UMS=UIBR MODE 1 1 3 7
VK1=PROD(DK1 UMS)
VK2=PROD(DK2 UMS)
VK3=PROD(DK3 UMS)
VK4=PROD(DK4 UMS)
VK5=PROD(DK5 UMS)
VK6=PROD(DK6 UMS)
VK7=PROD(DK7 UMS)
VK8=PROD(DK8 UMS)
VK9=PROD(DK9 UMS)
VK10=PROD(DK10 UMS)
VK11=PROD(DK11 UMS)
VK12=PROD(DK12 UMS)
VK13=PROD(DK13 UMS)
VK14=PROD(DK14 UMS)
VK15=PROD(DK15 UMS)
$VK16=PROD(DK16 UMS)
$VK17=PROD(DK17 UMS)
SE01=XTVD(UMS VK1 )
SE02=XTVD(UMS VK2 )
SE03=XTVD(UMS VK3 )
SE04=XTVD(UMS VK4 )
SE05=XTVD(UMS VK5 )
SE06=XTVD(UMS VK6 )
SE07=XTVD(UMS VK7 )
SE08=XTVD(UMS VK8 )
SE09=XTVD(UMS VK9 )
SE10=XTVD(UMS VK10)
SE11=XTVD(UMS VK11)
SE12=XTVD(UMS VK12)
SE13=XTVD(UMS VK13)
SE14=XTVD(UMS VK14)
SE15=XTVD(UMS VK15)
$SE16=XTVD(UMS VK16)
$SE17=XTVD(UMS VK17)
TABL(NI=5 NJ=1):SE16
TABL(NI=5 NJ=1):SE17
TABL(NI=5 NJ=1):SE18
SEMK=UNION(SE01 SE02 SE03 SE04 SE05 SE06 SE07)
SE08 SE09 SE10 SE11 SE12 SE13)
SE14 SE15 SE16 SE17 SE18)
SENB=SUM(SEMK SENB)
$XQT DCU
CHAN 1 SENB AUS 1 1 SENS MATR 0 1
$XQT AUS
DEFI BA9=BA BTAB 2 9:BA9=UNION(BA9)
DEFI RM18=RMAS BTAB 2 18:R18=UNION(RM18)
$XQT SM
RESET OUTL=2 NUUX=2 NUDP=2 NPARA=18 G=386.
OPER 0 0 1 1
$XQT AUS
BA BTAB 2 9=UNION(BA9)
RMAS BTAB 2 18=UNION(R18)
$XQT DCU
PRINT 1 SRR
PRINT 2 DP SM
PRINT 2 DPX
$XQT EXIT

```

Figure 3c.- EAL runstream for developing the sensitivy matrix (concluded).

```

$XQT AUS
DEFI DPA=2 DP SM 1 1
DEFI DPXA=2 DPX REV 1 1
RA=RECIP(DPA)
RAX=PROD(RA DPXA)
RAXT=RTRAN(RAX)
RAX2=PROD(SRR RAXT)
SRR SM 1 1=UNION(RAX2)
DEFI BA9=BA BTAB 2 9:BA9=UNION(BA9)
DEFI RM18=RMAS BTAB 2 18:R18=UNION(RM18)
$XQT SM
RESET OUTL=2 NUUX=2 NUDP=2 NPARA=18 G=386.
OPER 0 0 1 1
$XQT AUS
BA BTAB 2 9=UNION(BA9)
RMAS BTAB 2 18=UNION(R18)
$XQT DCU
PRINT 1 SRR
PRINT 2 DP SM
PRINT 2 DPX
$XQT EXIT

```

ORIGINAL PAGE IS
OF POOR QUALITY

Figure 3d.- EAL runstream for revision of the covariance (weighting) matrix.

```

$XQT SM
RESET OUTL=2 NUUX=2 NUDP=2 NPARA=18 G=386.
OPER 0 0 0 1
$XQT AUS
TABL(NI=1 NJ=18):SRR SM:J=1 18:1.
DEFI DPSM 2 DPM REV
DPST=TRAN(DPSM)
TABL(NI=2 NJ=18):DPCH
TRAN(SOUR=DPST ILIM=1 JLIM=18 DSKIP=1 SBASE=0 DBASE=0)
TRAN(SOUR=DPST ILIM=1 JLIM=18 DSKIP=1 SBASE=0 DBASE=1)
DEFI DPO=DPLI
DPNE=SUM(DPO -1. DPCH)
DPFR=SUM(SRR -1. DPSM)
DPRE=RECIP(DPFR)
TABL(NI=2 NJ=18):RADP
TRAN(SOUR=DPRE ILIM=1 JLIM=18 DSKIP=1 SBASE=0 DBASE=0)
TRAN(SOUR=DPRE ILIM=1 JLIM=18 DSKIP=1 SBASE=0 DBASE=1)
DPN2=PROD(RADP DPNE)
DPLI SM=UNION(DPN2)
$XQT E
RESET G=386.
$XQT EKS
$XQT K
$XQT AUS
MNEU=SUM(DEM2 RMAS)
MDIF=SUM(MNEU -1. M+RM)
M+RM=SUM(DEM2 RMAS)
SPIN:M+RM K 27.5413 0. 0. 0. 0.
$XQT RSI
RESET K-KSPM
$XQT SSOL
RESET K-KSPM
$XQT GSF
RESET EMBED=1
$XQT KG
$XQT AUS
KECG=SUM(KSPM KG)
$XQT RSI
RESET K-KECG
$XQT EIG
RESET INLIB=1 M=M+RM K=KECG
$XQT AUS
RIG=RIGID(1)
MR=PROD(M+RM RIG)
GM=XTYD(RIG MR)
GMUT=UNION(386. GM)
RMUT=UNION(386. RMAS)
$XQT DCU
PRINT 1 GM
PRINT 1 GMUT
PRINT 1 RMUT
PRINT 1 BA BTAB 2 9
PRINT 2 SENS:PRINT 2 DP
$XQT EXIT

```

Figure 3e.- EAL runstream for calculation of frequencies of the modified structure and recomputation of the change limits for the next iteration.

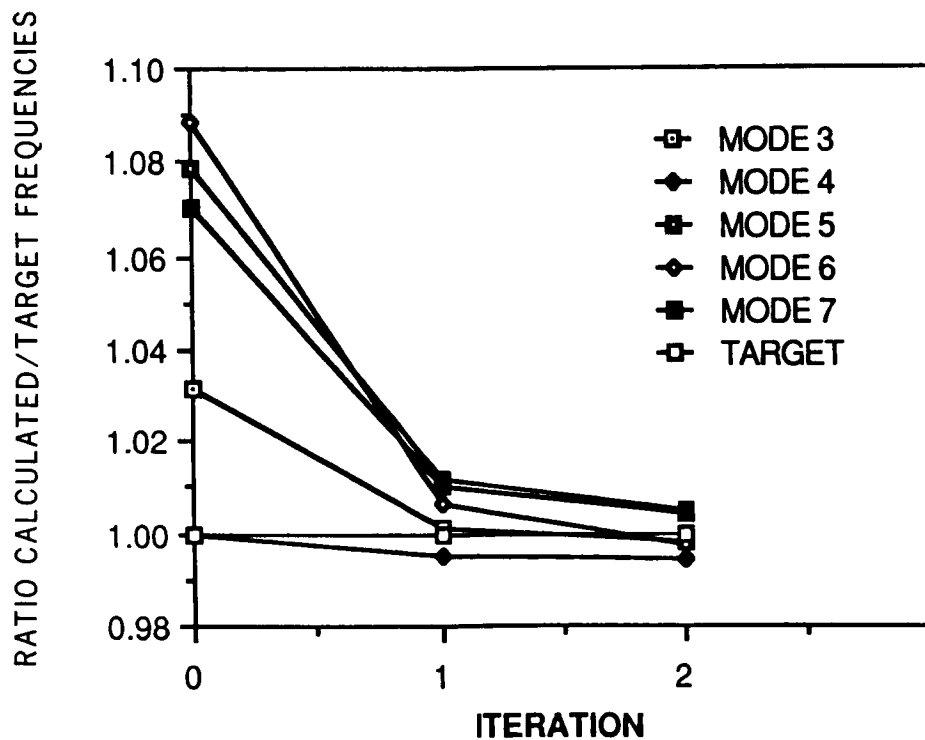


Figure 4.- Results of modification.

NUMERICAL STUDIES OF THE THERMAL DESIGN SENSITIVITY
CALCULATION FOR A REACTION-DIFFUSION SYSTEM WITH
DISCONTINUOUS DERIVATIVES*

Jean W. Hou and Jeen S. Sheen
Department of Mechanical Engineering and Mechanics
Old Dominion University
Norfolk, VA

SUMMARY

The aim of this study is to find a reliable numerical algorithm to calculate thermal design sensitivities of a transient problem with discontinuous derivatives. The thermal system of interest is a transient heat conduction problem related to the curing process of a composite laminate. A logical function which can smoothly approximate the discontinuity is introduced to modify the system equation. Two commonly used methods, the adjoint variable method and the direct differentiation method, are then applied to find the design derivatives of the modified system. The comparisons of numerical results obtained by these two methods demonstrate that the direct differentiation method is a better choice to be used in calculating thermal design sensitivity.

I. INTRODUCTION

High-performance polymeric composites have been used widely in the aerospace and automobile industries. Such materials are commonly composed of long or chopped fibers embedded in the thermosetting resin matrix. Changes in physical and chemical properties of such composite materials during the curing process are rather complex. Thus, it is not a trivial task to properly design a cure cycle (temperature and pressure profiles) for a curing process. The material should be cured uniformly and completely with the lowest void content; the temperature inside the laminate must not exceed some maximum value; and the curing process should be completed within the shortest amount of time. In the past, most cure cycle designs for newly developed composite systems are based upon the technique of trial and error. Several simulation models [1-3] have been developed recently for curing various epoxy matrix composites. This development represents a significant advancement in computerizing the cure cycle design. An attempt [4] has been made recently to incorporate thermal optimal design techniques with such analysis capabilities to systematically establish the "best" curing process. The research progress regarding the computational aspects of the thermal design sensitivity analysis is reported in this paper.

*The research reported here is sponsored by NASA Langley Research Center under NASA Grant NAG-1-561.

The derivative of the thermal response with respect to the design variable is usually called the thermal design derivative or sensitivity. The information of the design derivative is not only very useful for the trade-off design, but it is also required for an iterative design optimization. The calculation of design derivatives in thermal problems has attracted research interests in such areas as design of space structures subject to temperature constraints [5], and chemical process control [6,7]. The thermal system studied in this paper can be stated as a heat conduction problem coupled with chemical-kinetic reaction during the cure process, while the temperature of cure cycle is considered as a design variable.

II. MATHEMATICAL FORMULATION OF CURING PROCESS

During the curing process, the temperature distribution $T(x,t)$ and the degree of cure $\alpha(x,t)$ of the resin inside the composite depend on the rate at which heat is transmitted from the environment into the material. The heat conduction model for a piled composite with its thickness $2h$ during the curing process can be found as

$$\rho c \frac{\partial T}{\partial t} = k \frac{\partial^2 T}{\partial x^2} + \rho H_R \dot{\alpha} \quad (1)$$

with the boundary conditions,

$$\frac{\partial T(0,t)}{\partial x} = 0 \quad 0 \leq t \leq T \quad (2)$$

$$T(h,t) = T_c(t), \quad 0 \leq t \leq T$$

and the initial condition

$$T(x,0) = T_0(x), \quad 0 \leq x \leq h, \quad (3)$$

where ρ is the mass density, c is the coefficient of heat capacity, k is the heat conduction coefficient, and H_R is the total or ultimate heat of reaction during the curing process. The last term in equation (1), $\rho H_R \dot{\alpha}$, denotes the rate of heat generated by chemical reaction which can be expressed by cure kinetics.

Two models of cure kinetics are investigated here. One is the chemical-kinetic reaction of Hercules 3501 during press processing [1]. The chemical-kinetic reaction can be determined in terms of the degree of cure, α , which is given experimentally from reference [2] as

$$\dot{\alpha} = \begin{cases} f_1(\alpha, T, t) = (K_1 + K_2 \alpha) (1 - \alpha) (B - \alpha), & 0 \leq \alpha \leq 0.3 \\ f_2(\alpha, T, t) = K_3 (1 - \alpha), & 0.3 < \alpha \end{cases} \quad (4)$$

with the initial condition $\alpha(x,0) = 0$ and the following definitions:

$$K_1 = \Delta A_1 \cdot \text{Exp}(-\Delta E_1/RT)$$

$$K_2 = \Delta A_2 \cdot \text{Exp}(-\Delta E_2/RT)$$

$$K_3 = \Delta A_3 \cdot \text{Exp}(-\Delta E_3/RT)$$

where $\Delta A_1, \Delta A_2, \Delta A_3, \Delta E_1, \Delta E_2, \Delta E_3$, R and B are material constants, and T is K° temperature. Note that the rate of cure presents discontinuity at $\alpha=0.3$.

The second example is taken from the results of compression molding of a polyester [3]. The degree of cure of resin in terms of temperature is given as

$$\dot{\alpha} = (K_1 + K_2 \alpha^m) (1-\alpha)^n \quad (5)$$

where m and n are constants, and K_1 and K_2 are exponential functions of temperature.

Note that in equation (2), the temperature $T_c(t)$ on the surface of the piled pre-pregs is called the cure temperature. The cure temperature can be controlled by the processor and is considered as a design variable. Moreover, the performance index of interest is the temperature uniformity ψ which may be defined as the least square of the deviation between the pointwise temperature and the averaged temperature as

$$\psi = \int_0^T \left\{ \int_0^h T^2 dx - \left(\int_0^h T dx \right)^2 / h \right\} dt \quad (6)$$

Some observations of interest are mentioned here:

1. The state equations of the cure process are coupled with two state variables, the temperature distribution $T(x,t)$ and the degree of cure $\alpha(x,t)$.
2. The nonhomogenous boundary value, $T_c(t)$, is the design variable.
3. The rate of cure, $\dot{\alpha}$ in equation (4), exhibits discontinuity, as does the last term $\rho H_R \dot{\alpha}$ in the equation of heat conduction.

The heat conduction problem stated in equations (1) to (3) can be simplified to an equation of $\bar{T}(x,t)$,

$$\rho c \frac{\partial \bar{T}}{\partial t} = k \frac{\partial^2 \bar{T}}{\partial x^2} - \rho c \dot{T}_c + \rho H_R \dot{\alpha} (\bar{T} + T_c) \quad (7)$$

with the homogeneous boundary conditions,

$$\frac{\partial \bar{T}(0,t)}{\partial x} = 0, \quad 0 \leq t \leq T \quad (8)$$

$$\bar{T}(h,t) = 0, \quad 0 \leq t \leq T$$

and the initial condition,

$$\bar{T}(x,0) = T_0(x) - T_c(0), \quad 0 \leq x \leq h, \quad (9)$$

by introducing the following replacement of the temperature $T(x,t)$:

$$T(x, t) = \bar{T}(x, t) + T_c(t) \quad (10)$$

It is noted that the initial temperature $T_0(x)$ of the composite laminate is identical with the initial cure temperature for most applications. Therefore, equation (7) might have not only homogeneous boundary conditions but also a homogeneous initial condition. Moreover, the design variable $T_c(t)$ now appears on the right side of equation (7). In other words, the design variable is now involved in terms of heat generation, instead of being a boundary condition. It is also noted that the replacement of $T(x, t)$ doesn't change the structure of the performance index ϕ , i.e.,

$$\phi = \int_0^T \left\{ \int_0^h \bar{T}^2 dx - \left(\int_0^h \bar{T} dx \right)^2 / h \right\} dt \quad (11)$$

In general, the cure temperatures recommended by resin manufacturers consist of linear segments. As an example, the cure temperature recommended for the Hercules 3501-6 resin is shown in Fig. 1. Consequently, the right side of heat conduction equation (7) has discontinuous terms of $\rho c \dot{T}_c$ as well as $\rho H_R \dot{\alpha}$. The term $\rho H_R \dot{\alpha}$ shows discontinuities in both x and t dimensions. The term $\rho c \dot{T}_c$, on the other hand, is discontinuous along the t dimension only. Such discontinuities pose numerical difficulties for calculating the design derivatives, especially, when the time or the place at which these discontinuities occur is subjected to change due to the perturbation of the design variable. It is easy to see that the term $\rho H_R \dot{\alpha}$ is of this nature. Note that the discontinuity of α is determined by a state variable-dependent jump condition at $\alpha(x, t) = 0.3$. Thus, the discontinuity of the term $\rho H_R \dot{\alpha}$ will take place at the new critical time \tilde{t} and the new position \tilde{x} so that $\tilde{\alpha}(\tilde{x}, \tilde{t}) = 0.3$ for a perturbed state variable $\tilde{\alpha}$. Also the discontinuous point of the term $\rho c \dot{T}_c$ can be shifted, if the time interval of the junction point of constant and variable temperatures of the cure temperature profile, such as T_1 in Fig. 1, is considered as a design variable.

III. LOGICAL FUNCTION MODELLING

Quite a few engineering examples whose state variables show discontinuities in derivatives can be found in the multi-state control problems [8], and the mechanical systems with intermittent motion [9, 10]. However, the derivative discontinuities of those examples are associated with time dimension only.

The intermittent motion is characterized by the occurrence of nearly discontinuous force and velocity caused by impulsive force, impact, mass capture, and mass release. The optimal design problems of mechanisms with intermittent motion have been discussed by Huang, Huag and Andrews [9]. Their method is based on the identification of critical times at which discontinuities in forces or velocities occur [8]. The overall time interval of analysis can be divided into a number of subintervals based on those critical times. The jump conditions of state variables are then employed in an adjoint variable approach to determine the discontinuities of adjoint variables. The adjoint variables are then used for the calculation of design sensitivity coefficients. In employing this approach, an a priori knowledge of the critical times is required. The determination of the critical times of jump conditions, however, may lead to a rather complex logic for

digital computer programming. In order to avoid these complexities, Ehle and Huag [10] introduced a "logical function" to smoothly approximate discontinuities, and then calculated the design derivatives by the standard adjoint variable technique. An example in their work shows that the proper selection of the sizes of the time step and the transient zone used for discontinuity approximation is crucial to the accuracy of design sensitivity calculation. However, making such a selection is difficult. Nevertheless, the logical function approach is used in this study. The reason is that $\dot{\alpha}$ is a function of time as well as spatial position. As a result, keeping track of the $\dot{\alpha}$ discontinuity at every spatial position is a very difficult task for numerical analysis.

As mentioned earlier, logical functions can be used to represent a sequence of logical events. A logical function $L(z, \epsilon)$ is a continuous function which smoothly approximates a Heaviside step function $H(z)$ within a given region $0 < z < \epsilon$ for a small number ϵ . The symmetrical step function $H(z)$ is defined as:

$$H(z) = \begin{cases} 0, & z < 0 \\ \frac{1}{2}, & z = 0 \\ 1, & z > 0. \end{cases}$$

The logical function employed here is given in reference [10] as:

$$L(z, \epsilon) = \frac{1}{2} \frac{|z|^{2n+1} + z^{2n+1}}{|z|^{2n+1} + \frac{1}{2} [|z-\epsilon|^{2n+1} - (z-\epsilon)^{2n+1}]}$$

where n is an integer selected in order to ensure the continuity of the derivative up to order d , i.e., $2n+1 > d$. The n is taken as 1 in this study. The approximation of the logical function is shown in Fig. 2. Note that the values of a logical function $L(z, \epsilon)$ are 0, 1/2 and 1 for $z=0$, $\epsilon/2$ and ϵ , respectively, and the transition width ϵ defines the region of approximation. The value of the logical function is exactly identical with the Heaviside step function outside the approximation region.

In using the logical function method, one is free to choose a wide variety of arguments that determine the transition point for a logical function. As an example, the transition condition $\alpha=0.3$ for the degree of cure can be used to define a logical function $L(\alpha-0.3, \epsilon)$ such that $L(\alpha-0.3, \epsilon) = 1$ when $\alpha > 0.3 + \epsilon$, and $L(\alpha-0.3, \epsilon) = 0$ when $\alpha < 0.3$. Based on this definition, the logical function can be used to compress the equation of cure kinetics into a compact form:

$$\dot{\alpha} = f_1 \cdot [1 - L(\alpha-0.3, \epsilon)] + f_2 \cdot L(\alpha-0.3, \epsilon) \quad (12)$$

Note that the above single equation of cure kinetics is the same as the original equation over the entire time interval of analysis outside the transition period. Furthermore, since the logical function is a smooth function of α , there is no discontinuity in the $\dot{\alpha}$ of the preceding equation. Thus, the analysis of the design sensitivity can be simplified to a great extent, because there is no need to monitor the perturbation of $\dot{\alpha}$ discontinuity. Note that the value of $\alpha(x, t)$ in equation (12) can be calculated by the linear combination of shape functions and nodal values obtained by the finite element analysis. Similarly, the discontinuity in \dot{T}_c can be smoothed out in the same manner. Again, using the cure temperature profile

indicated in figure 1 as an example, the first discontinuity at $t=T_1$ can be expressed as

$$\dot{T}_c = a[1 - L(t - T_1, \epsilon)] \quad (13)$$

It is then easy to consider the junction point T_1 as a design variable based upon the above equation.

Finally, the heat conduction equation stated in equation (7) can be expressed as

$$\begin{aligned} \rho c \frac{\partial \bar{T}}{\partial t} &= k \frac{\partial^2 \bar{T}}{\partial x^2} + g(\bar{T}, \alpha, T_1) \\ &= k \frac{\partial^2 \bar{T}}{\partial x^2} - \rho c a \cdot [1 - L(t - T_1, \epsilon)] \\ &\quad + \rho H_R f_1 \cdot [1 - L(\alpha - 0.3, \epsilon)] + \rho H_R f_2 \cdot L(\alpha - 0.3, \epsilon) \end{aligned} \quad (14)$$

for the cure cycle given in figure 1. Similarly, the equation of the degree of cure given in equation (12) can be rewritten here,

$$\begin{aligned} \dot{\alpha} &= f(\bar{T}, \alpha, T_1) \\ &= f_1 \cdot [1 - L(\alpha - 0.3, \epsilon)] + f_2 \cdot L(\alpha - 0.3, \epsilon) \end{aligned} \quad (15)$$

The finite element discretization is then introduced to convert the above initial-boundary value equations into a set of first order differential equations:

$$[C] \{\dot{\bar{T}}\} + [K] \{\bar{T}\} = \{F(\{\bar{T}\}, \{\alpha\})\} \quad (16)$$

and

$$[N] \{\dot{\alpha}\} = \{G(\{\bar{T}\}, \{\alpha\})\} \quad (17)$$

Quadratic and linear polynomials are used to interpolate the states of temperature distribution and degree of cure, respectively. Note that the right side vectors of the above two matrix equations are different. This is because the trial functions for equations (14) and (15) are different.

The finite-element discretization can also be used to simplify the expression for the performance index of concern into a single integral:

$$\psi = \int_0^T (\{\bar{T}\}^T [C] \{\bar{T}\} - \{\bar{T}\}^T \{P\} \{P\}^T \{\bar{T}\} / h) dt \quad (18)$$

where the $[C]$ is same as the one defined in equation (16), and the components of the vector $\{P\}$ are obtained by integrating the quadratic shape functions of temperature.

This set of equations (16) and (17) is then solved simultaneously by a numerical integration code called DE [11]. The DE program is one of predictor-

corrector integration algorithms using the Adams family of formulas. The truncation error is controlled by varying the step size and the order of the method. The DE program has the capability to handle moderately stiff equations which often occur in the problems of chemical kinetics. To preserve the accuracy of analysis, the temperature distribution and the degree of cure are subjected to the same numerical error tolerance during the numerical integration.

IV. DESIGN SENSITIVITY ANALYSIS

In general, there are four ways to calculate the thermal design derivatives, i.e., the finite-difference method, Green's function approach, the direct differentiation method and the adjoint variable technique. The last two are often mentioned in the literature [12-15]. Both methods lead to a set of linear equations that have a structure similar to the original system.

The computational efforts regarding the direct differentiation method and the adjoint variable method depend mainly on the numbers of constraints and design variables of concern. The direct differentiation method requires the solution of a differential equation for each design variable; while the adjoint variable method requires the solution of an adjoint equation for each constraint. Consequently, the direct differentiation method is more efficient in calculating the design derivatives than the adjoint variable method when the number of design variables is less than the number of constraints, or vice versa.

It is known that the direct differentiation method provides equations of design derivatives which can be integrated forward, instead of backward to solve the adjoint variables. The equations of design derivatives can, therefore, be solved simultaneously with the original system of equations and are subjected to the same numerical error tolerance. Furthermore, the approach of direct differentiation provides, without extra efforts, the time histories of design derivatives of functionals and state variables. This information can be used by a designer to reconstruct the design space. One may check this information to see whether a design variable of concern contributes to the perturbation of the performance index consistently over a long or short period of time. As an example, the time histories of design derivatives of various pollutants' concentrations with respect to emission and meteorological parameters are studied and used in reference [16] to improve the mathematical model of air quality. In this study, the direct differentiation method and the adjoint variable technique, in conjunction with the logical function method, is used for the calculation of thermal design sensitivities.

The calculation of design derivatives using the direct differentiation method is straightforward. For example, let T_1 in Fig. 1 be the design variable. The direct differentiation of equations (14) and (15) yields

$$\rho c \frac{\partial \bar{T}'}{\partial t} = k \frac{\partial^2 \bar{T}'}{\partial x^2} - \rho c a L'(t-T_1, \epsilon) \\ + \rho H_R \left(\frac{\partial f_1}{\partial \alpha} \alpha' + \frac{\partial f_1}{\partial \bar{T}} T' \right) \cdot [1 - L(\alpha - 0.3, \epsilon)]$$

$$+ \rho H_R \left(\frac{\partial f_2}{\partial \alpha} \alpha' + \frac{\partial f_2}{\partial \bar{T}} \bar{T}' \right) L(\alpha - 0.3, \epsilon) + \rho H_R \frac{dL}{d\alpha} \alpha' \cdot (f_2 - f_1) \quad (19)$$

and

$$\begin{aligned} \dot{\alpha}' &= \left(\frac{\partial f_1}{\partial \alpha} \alpha' + \frac{\partial f_1}{\partial \bar{T}} \bar{T}' \right) \cdot [1 - L(\alpha - 0.3, \epsilon)] \\ &+ \left(\frac{\partial f_2}{\partial \alpha} \alpha' + \frac{\partial f_2}{\partial \bar{T}} \bar{T}' \right) \cdot L(\alpha - 0.3, \epsilon) \\ &+ \frac{dL}{d\alpha} \alpha' (f_2 - f_1) \end{aligned} \quad (20)$$

where the prime indicates the design derivative with respect to T_1 . The derivative of the logical function $dL/d\alpha$ is an approximation of a delta function which can be derived from the definition of the logical function L . From equations (8-9) and the initial condition of $\alpha(x, 0) = 0$, the boundary and initial conditions for design derivatives, \bar{T}' and α' , can be derived as

$$\frac{\partial \bar{T}'(0, t)}{\partial x} = 0, \quad 0 \leq t \leq T \quad (21)$$

$$\bar{T}'(h, t) = 0, \quad 0 \leq t \leq T$$

and

$$\bar{T}'(x, 0) = -T_c'(0), \quad 0 \leq x \leq h \quad (22)$$

$$\alpha'(x, 0) = 0, \quad 0 \leq x \leq h$$

where $T_c'(0)$ is usually zero unless the initial control temperature $T_c'(0)$ is considered as a design variable. With these boundary and initial conditions, the last two coupled linear equations can be solved numerically for the design derivatives \bar{T}' and α' .

Based on the same finite element discretization as used in solving the original system, equations (19) and (20) can be converted into a set of linear ordinary differential equations:

$$[C] \{\dot{\bar{T}}'\} + [K] \{\bar{T}'\} = \{H(\{\bar{T}\}, \{\alpha\}, \{\bar{T}'\}, \{\alpha'\})\} \quad (23)$$

and

$$[N] \{\dot{\alpha}'\} = \{Q(\{\bar{T}\}, \{\alpha\}, \{\bar{T}'\}, \{\alpha'\})\} \quad (24)$$

Note that the coefficient matrices of equations (23) and (24) are similar to those of equations (16) and (17). However, $\{\bar{T}\}$ and $\{\alpha\}$ appear in equations (23) and

(24). Thus, the numerical integration of equations (16) - (17) and (23) - (24) can be performed simultaneously so as to maintain equal accuracy between state variables ($\{\bar{T}\}$, $\{\alpha\}$) and design derivatives ($\{\bar{T}'\}$, $\{\alpha'\}$). The DE program, mentioned previously, is employed as an integrator to obtain the numerical results of design derivatives.

The values of the design derivative of temperature $\{\bar{T}'\}$ can then be directly substituted into the following equation to calculate the thermal design derivative of the performance index:

$$\psi' = 2 \int_0^T \{\bar{T}\}^T [C] \{\bar{T}'\} - \{\bar{T}\}^T \{P\} \{P\}^T \{\bar{T}'\} / h \, dt \quad (25)$$

The above equation is derived from equation (18) by using the direct differentiation method.

Regarding the computational efficiency of the direct differentiation method, it is worthwhile mentioning two notes here:

1. Because the coefficient matrices of $\{\dot{\bar{T}}'\}$ and $\{\dot{\alpha}'\}$ are identical to those of $\{\dot{\bar{T}}\}$ and $\{\dot{\alpha}\}$, the triangular factorizations of matrices $[C]$ and $[M]$ need to be done once only. The calculation of $\{\dot{\bar{T}}\}$ and $\{\dot{\alpha}\}$ can be carried out by back substitution for each of design variables.
2. Compared to the original system equations, the right side of equations for computing $\{\bar{T}'\}$ and $\{\alpha'\}$, such as equations (23) and (24), may have different frequency contents. Thus, to maintain the same numerical accuracy, a smaller time step Δt may be required for the DE program to solve the pairs $(\{\bar{T}\}, \{\alpha\})$ and $(\{\bar{T}'\}, \{\alpha'\})$ simultaneously.

A major step in the adjoint variable method is deriving the adjoint equations to solve the design derivatives of equations (18) in terms of state and adjoint variables. In order to do so, one may extend the performance index ψ of equation (11) as, using T_1 as a design variable,

$$\begin{aligned} \psi &= \int_0^T \int_0^h \left\{ \left[\bar{T} - \int_0^h \frac{\bar{T}}{h} dx \right] \bar{T} \right\} dx \, dt \\ &= \int_0^T \int_0^h \left\{ \bar{T} - \int_0^h \frac{\bar{T}}{h} dx \right\} \bar{T} \, dx \, dt \\ &+ \int_0^T \int_0^h \left\{ \lambda \left[\rho c \frac{\partial \bar{T}}{\partial t} - k \frac{\partial^2 \bar{T}}{\partial x^2} - g(\bar{T}, \sigma, T_1) \right] + \right. \\ &\quad \left. s \left[\frac{\partial \alpha}{\partial t} - f(\bar{T}, \alpha, T_1) \right] \right\} dx \, dt \end{aligned}$$

where $\alpha(x,t)$ and $s(x,t)$ are two arbitrary functions. Note that the last integral is zero because of state equations (14-15). Taking the design derivative of the above equation with respect to T_1 and integrating by parts, it follows that

$$\begin{aligned}
 \psi' = & \int_0^T \int_0^h \left(-\lambda \frac{\partial g}{\partial T_1} - s \frac{\partial f}{\partial T_1} \right) dx dt \\
 & + \int_0^T \int_0^h \left[-\rho c \frac{\partial \lambda}{\partial t} - k \frac{\partial^2 \lambda}{\partial x^2} - \lambda \frac{\partial g}{\partial \bar{T}} - s \frac{\partial f}{\partial \bar{T}} + 2 \left(\bar{T} - \int_0^h \frac{\bar{T}}{h} dx \right) \right] \bar{T}' dx dt \\
 & + \int_0^T \int_0^h \left\{ \left[-\frac{\partial s}{\partial t} - s \frac{\partial f}{\partial \alpha} - \lambda \frac{\partial g}{\partial \alpha} \right] \alpha' \right\} dx dt \\
 & + \int_0^T \left(-k\lambda \frac{\partial \bar{T}'}{\partial x} + k \frac{\partial \lambda}{\partial x} \bar{T}' \right) \Big|_0^h dt \\
 & + \int_0^h \left(\rho c \lambda \bar{T}' + s \alpha' \right) \Big|_0^T dx
 \end{aligned} \tag{25}$$

Note that the only two unknowns in the above equation are the design derivatives \bar{T}' and α' . One may now specify the variables λ and s in such a way that all terms associated with \bar{T}' and α' are dropped. This can be accomplished by introducing the following adjoint equations for λ and s :

$$0 = \rho c \frac{\partial \lambda}{\partial t} + k \frac{\partial^2 \lambda}{\partial x^2} + \lambda \frac{\partial g}{\partial \bar{T}} + s \frac{\partial f}{\partial \bar{T}} - 2 \left(\bar{T} - \int_0^h \frac{\bar{T}}{h} dx \right) \tag{26}$$

and,

$$0 = \frac{\partial s}{\partial t} + \lambda \frac{\partial g}{\partial \alpha} + s \frac{\partial f}{\partial \alpha} \tag{27}$$

with the terminal conditions,

$$\lambda(x, T) = 0, \quad 0 \leq x \leq h, \tag{28}$$

$$s(x, T) = 0 \quad 0 \leq x \leq h, \tag{29}$$

and the boundary conditions,

$$\frac{\partial \lambda}{\partial x}(0, t) = 0 \quad 0 \leq t \leq T, \tag{30}$$

$$\lambda(h, t) = 0, \quad 0 \leq t \leq T, \tag{31}$$

Then, the combination of equations (25 - 31) provides a simple formula for the design derivative of the functional,

$$\begin{aligned} \psi' = & \int_0^T \int_0^h \left(-\lambda \frac{\partial g}{\partial T_1} - s \frac{\partial f}{\partial T_1} \right) dx dt \\ & + \int_0^h \rho c \lambda(x,0) T_c'(0) dx \end{aligned} \quad (32)$$

Equation (32) shows that the design derivative of ψ , namely, ψ' , is a functional of the state variables α and \bar{T} , and the adjoint variables λ and s . Since the adjoint variables of equations (26 - 27) form an "adjoint" diffusion-reaction system similar to the original one, the same numerical scheme used to solve the state variables α and \bar{T} can be extended here to compute the adjoint variables s and λ . For instance, using the shape functions of α and \bar{T} in equations (16 - 17) to interpolate the adjoint variables λ and s obtains the following matrix equations for nodal values of λ and s ,

$$[C] \{\dot{\lambda}\} = [K] \{\lambda\} + \{R(\{\bar{T}\}, \{\alpha\}, \{\lambda\}, \{s\})\} \quad (33)$$

$$[N] \{\dot{s}\} = \{S(\{\bar{T}\}, \{\alpha\}, \{\lambda\}, \{s\})\} \quad (34)$$

with the proper boundary and terminal conditions.

In general, the adjoint equations cannot be solved simultaneously with the original system equations. Because of the terminal conditions, the adjoint equations can be solved by either the backward integration along the real-time t -axis directly or the forward integration along the artificial time t^* -axis by changing the independent variable t to t^* as $t^* = T - t$. However, both approaches require the solutions of the original system equations prior to solving the adjoint equations.

In the derivation of design derivatives, it has been assumed that $T(x,b,t)$ and $\alpha(x,b,t)$ have enough regularity in the time-spatial domain and in the design space.

V. NUMERICAL EXAMPLES AND RESULTS

Four examples are presented in this section to discuss the numerical accuracy of the logical function approximation and the methods for calculating the thermal design derivatives. The accuracy of the thermal design sensitivity analysis is checked, based on the fundamental definition of design derivatives which states that they can be approximated by the finite difference. In other words, it is mathematically true for a small perturbation of design variable ΔT_c so that:

$$\psi' \equiv \frac{d\psi}{dT_c} \approx \frac{\Delta\psi}{\Delta T_c}$$

The perturbation of the design variable ΔT_c is defined as the difference between a perturbed design T_c^* and the nominal design T_c , i.e.,

$$\Delta T_c = T_c^* - T_c$$

As a result of the above definitions, it follows that

$$\begin{aligned}\Delta\psi &\equiv \psi(T_c^*) - \psi(T_c) \\ &\approx \psi' \cdot \Delta T_c\end{aligned}\quad (35)$$

The above equation provides a simple means to check the accuracy of the design sensitivity analysis.

The first example presented here deals with the curing process of compression molding (equation (1) and (5)) in which the cure temperature of the process is assumed to be a constant temperature. The nominal cure temperature is taken as 423°K, and there is no discontinuity involved. According to the approximation defined in equation (35), the results shown in figure 3 demonstrate the validity of the direct differentiation method for the thermal design sensitivity analysis.

The second example, on the other hand, refers to the curing process of press processing (equation (1) and (4)) in which a jump condition appears in the derivative of the degree of cure. The profile of the cure temperature is assumed to be $T_c(t) = b_0 + b_1 t$ where the initial temperature b_0 and heating rate b_1 are considered as design variables. The nominal values of b_0 and b_1 are taken as 290°K and 1.7°K/sec. The changes of the performance index with respect to the values of b_0 and b_1 are calculated by using the direct differentiation method as

$$\Delta\psi = -0.3158 \cdot \Delta b_0$$

$$\Delta\psi = 2.6336 \cdot \Delta b_1$$

However, using the adjoint variable technique obtains

$$\Delta\psi = -0.0367 \cdot \Delta b_0$$

$$\Delta\psi = 8.099 \cdot \Delta b_1$$

The results indicated in Tables 1 and 2 show that the direct differentiation method, in conjunction with the logical function approximation, performs very well even for a thermal problem with discontinuous derivatives. It is also shown in Table 2 that the relation between the performance index and the heating rate b_1 is highly nonlinear. In this example, the transient width ϵ of equation (15) is defined as 10^{-4} second which is the smallest time step size allowed in the DE program.

Next, the thermal design derivative of the compression molding is studied, with the cure temperature being given in figure 4. The value of T_1 , where the rate of the cure temperature changes, is considered as a design variable. In this study, the nominal value and the perturbation of T_1 are taken as 40 seconds and 1 second, respectively. The discontinuity of \dot{T}_c at T_1 can be smoothed by equation (13). The upper curve shown in figure 5 is obtained by using the direct differentiation method based on equation (13). On the other hand, the lower curve displayed in figure 5 is obtained by using the following expression for the design derivative of \dot{T}_c :

$$\frac{dT_c}{dT_1} = \begin{cases} 0, & t < T_1 \\ a, & t > T_1 \end{cases}$$

The design derivative of \dot{T}_c at the junction point, T_1 , is a delta function which is not included in the above equation. The results in figure 5 clearly show that the design derivative of the jump condition should be considered in the sensitivity calculation.

It is easy to obtain the time histories of design derivatives of state variables using the direct differentiation approach. Using this information, the processor can investigate whether a design variable of concern contributes to the change of system performance consistently over a long or short period of time so as to reconstruct the design space. For example, figures 6 and 7 show that the change of the design variable T_1 has a significant effect on the temperature and the degree of cure on the surface of the pre-pregs when the time is 42 seconds.

The distribution of thermal design derivatives α' and T' along the thickness of the pre-pregs is shown in figures 8 and 9 for different instants of time. It is of great interest to see that the most significant changes of T and α due to the change of the junction point T_1 happen around 80 seconds and at 2.5 mm from the surface of pre-pregs.

In this example, the various values of transient width, regioned from 10^{-2} second to 10^{-4} second are chosen to be used in the logical function approximation. The sensitivity results obtained accordingly are essentially the same. This indicates that the value of the transition width in the range of study has no significant effect on the accuracy of the sensitivity analysis. The transition width ϵ is taken as 10^{-3} second in the results reported in figures 6 to 9.

Finally, the cure temperature of the press process studied herein is again the same as the one shown in figure 1. With 100 minutes as the nominal value, T_1 is considered as a design variable. Thus, both equations (12) and (13) should be used to approximate the jumps in $\dot{\alpha}$ and \dot{T}_c smoothly for the thermal problem of the press process. The results of sensitivities calculated by the direct differentiation method are in good agreement with the actual changes calculated by the finite difference method as shown in figure 10. The transition regions used in this example are 10^{-4} second and 10^{-2} second for equations (12) and (13), respectively.

VI. CONCLUSIONS

It is quite common to have empirical formulations appear in the state equations modelling the composite curing process. These empirical formulations may introduce discontinuous state derivatives into the state equations. A simple method which uses the logical function approximation is introduced in this paper to perform the thermal design sensitivity analysis for such state equations.

Based on the numerical study, it is obvious that the direct differentiation method provides more accurate results than the adjoint variable method does. The direct differentiation method also yields the time histories of the design derivatives. In addition, the information of design derivatives of the pointwise

constraints can be obtained by using the direct differentiation method without extra cost. It is thus concluded that for the transient problem in this study, the direct differentiation method is superior to the adjoint variable technique in terms of accuracy and physical interpretation of results.

REFERENCES

1. Loos, A. C., and Springer, G. S., "Curing of Epoxy Matrix Composites," J. of Composite Materials, Vol. 17, pp. 135-169, 1983.
2. Lee, W. I., Loos, A. C., and Springer, G. S., "Heat of Reaction, Degree of Cure, and Viscosity of Hercules 3501-6," J. of Composite Materials, Vol. 16, pp. 510, 1982.
3. Barone, M. E., and Caulk, D. A., "The Effect of Deformation and Thermoset Cure on Heat Conduction in a Chopped-Fiber Reinforced Polyester During Compression Molding," Int. J. Heat Mass Transfer, Vol. 22, pp. 1021-1032, 1979.
4. Hou, J. W., "Optimal Cure Cycle Design for Autoclave Processing of Thick Composite Laminates: A Feasibility Study," Progress Report, ODU Research Foundation, November 1985.
5. Haftka, R. T., "Techniques for Thermal Sensitivity Analysis," Int. J. Num. Meth. Engng., Vol. 17, pp. 71-80, 1981.
6. Biegler, L. T., "Solution of Dynamics Optimization Problems by Successive Quadratic Programming and Orthogonal Allocation," Report No. DRC-06-45-83, Design Research Center, Carnegie-Mellon University, Pittsburgh, PA, 1983.
7. Irwin, C. L., and Komkov, V., "Sensitivity Analysis and Model Optimization for Reaction-Diffusion Systems," Journal of Optimization Theory and Applications, Vol. 44, No. 4, pp. 569-584, 1984.
8. Bryson, A. E., and Ho, Y. C., Applied Optimal Control, Ginn and Co., MA, 1969.
9. Huang, R. C., Haug, E. J. and Andrews, J. G., "Sensitivity Analysis and Optimal Design of a Mechanical System with Intermittent Motion," ASME J. Mech. Design, Vol. 100, No. 3, pp. 492-499, 1978.
10. Ehle, P. E. and Haug, E. J., "A Logical Function Method for Dynamic and Design Sensitivity Analysis of Mechanical System with Intermittent Motion," ASME J. Mech. Design, Vol. 104, No. 1, pp. 90-100, 1982.
11. Shampine, L. F., and Gordon, M. K., Computer Solution of Ordinary Differential Equations: The Initial Value Problem, W. H. Freeman and Co., San Francisco, CA., 1975.
12. Adelman, H. M., Haftka, R. T., Camarda, C. J., and Walsh, J. L., "Structural Sensitivity Analysis: Methods, Applications and Needs," NASA TM-85827, June 1984.

13. Hsieh, C. C., and Arora, J. S., "Design Sensitivity Analysis and Optimization of Dynamic Response," *Computer Methods in Applied Mechanics and Engineering*, No. 2, Vol. 43, pp. 195-219, 1984.
14. Haug, E. J., Mani, N. K., and Krishnaswami, P., "Design Sensitivity Analysis and Optimization of Dynamically Driven Systems," Computer-Aided Analysis and Optimization of Mechanical System Dynamics, (ed. E. J. Haug) Springer-Verlag, 1984.
15. Krishnaswami, P., Wahage, R. A., and Haug, E. J., "Design Sensitivity Analysis of Constrained Dynamic Systems of Direct Differentiation," Technical Report No. 83-5, Center for Computer-Aided Design, The University of Iowa, Iowa City, 1983.
16. Tilden, J. W., and Seinfeld, J. H., "Sensitivity Analysis of a Mathematical Model for Photochemical Air Pollution," *Atmospheric Environment*, Vol. 16, No. 6, pp. 1357-1364, 1982.

**TABLE 1 DESIGN SENSITIVITY RESULTS FOR DESIGN
VARIABLE b_o IN EXAMPLE 1**

b_o	ψ	$\Delta\psi$	$\psi^1 \cdot \Delta b_o$ (Direct Diff)	(Adjoint)
290.0	26.217	--	--	--
289.9	26.248	0.0315	0.0316	0.0037
289.8	26.280	0.0628	0.0632	0.0073
289.7	26.311	0.0940	0.0948	0.0110
289.5	26.313	0.1559	0.1579	0.0183
289	26.525	0.3077	0.3157	0.0367

**TABLE 2 DESIGN SENSITIVITY RESULTS FOR DESIGN
VARIABLE b_1 IN EXAMPLE 1**

b_1	ψ	$\Delta\psi$	$\psi^1 \cdot \Delta b_1$ (Direct Diff.)	(Adjoint)
1.700	26.217	--	--	--
1.702	26.222	0.00497	0.00527	0.01620
1.706	26.230	0.01312	0.01580	0.04859
1.708	26.233	0.01633	0.02107	0.06479
1.710	26.236	0.01898	0.02637	0.08099
1.730	26.234	0.01713	0.07901	0.24297
1.750	26.189	-0.02805	0.13168	0.4050
1.800	26.962	-0.25457	0.26336	0.8099

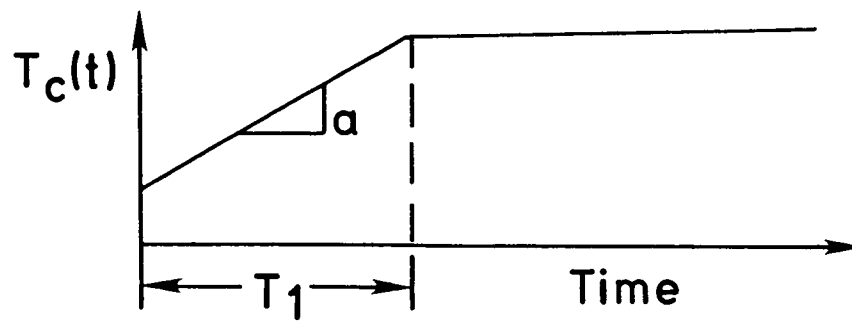


Figure 1. A typical cure temperature.

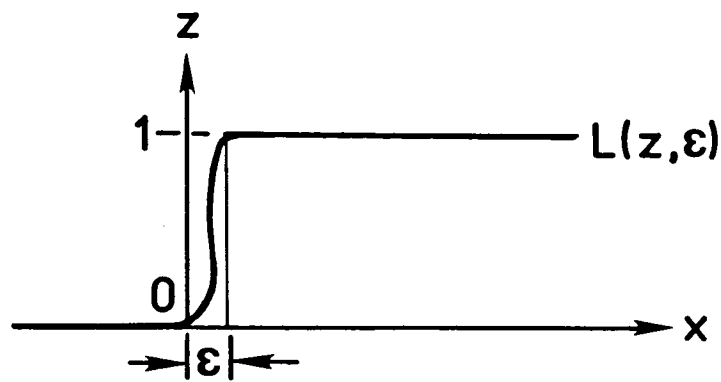


Figure 2. The approximation of logical function.

C-4

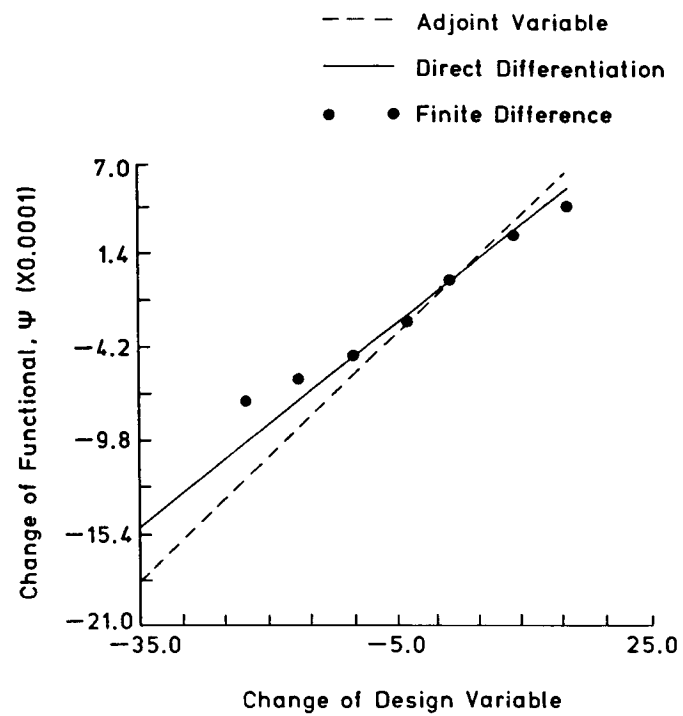


Figure 3. Thermal design derivatives for compression molding with respect to the mold temperature.

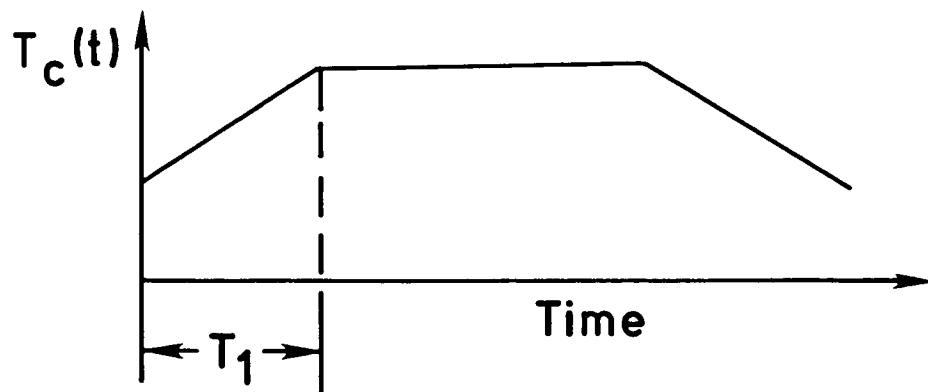


Figure 4. The cure temperature for compression molding.

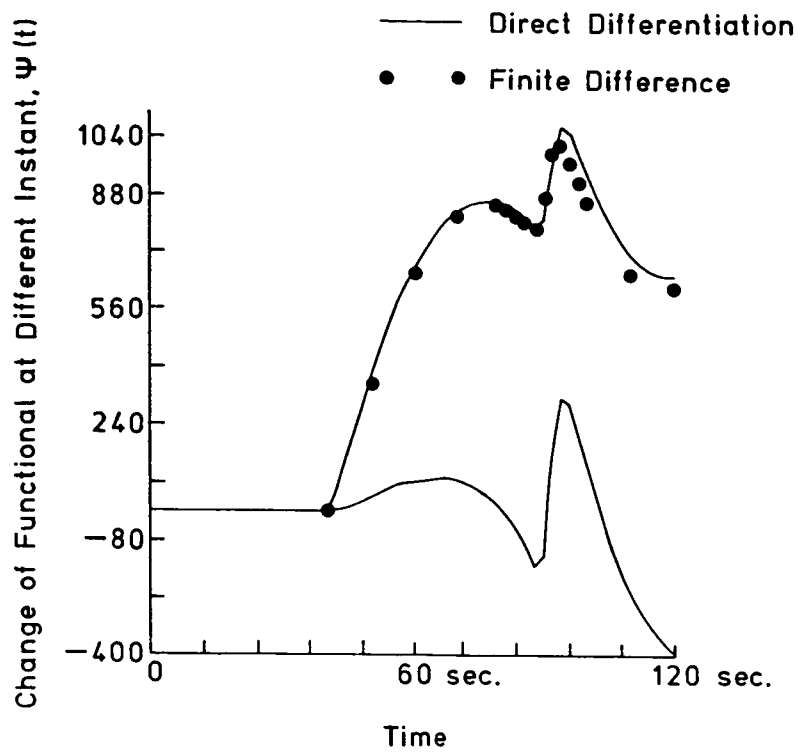


Figure 5. Thermal design derivatives for compressive molding with a jump in \dot{T}_c .

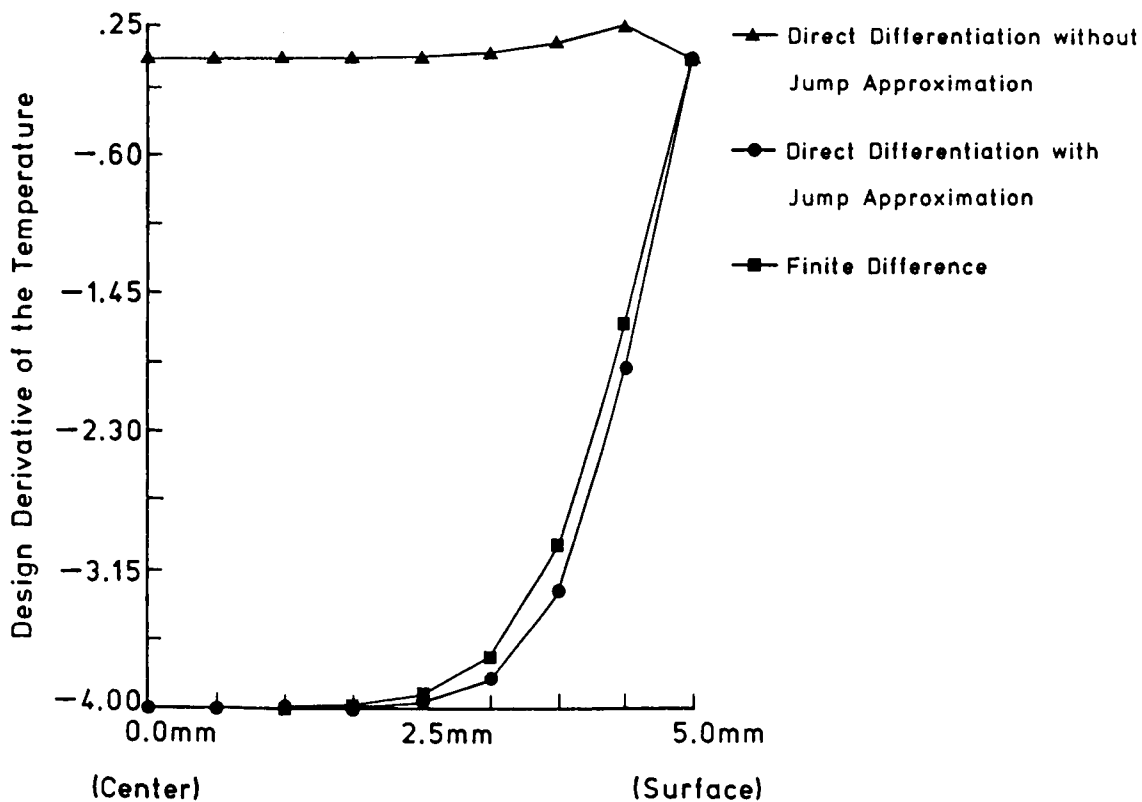


Figure 6. Design derivatives of temperature at time equal to 42 sec.

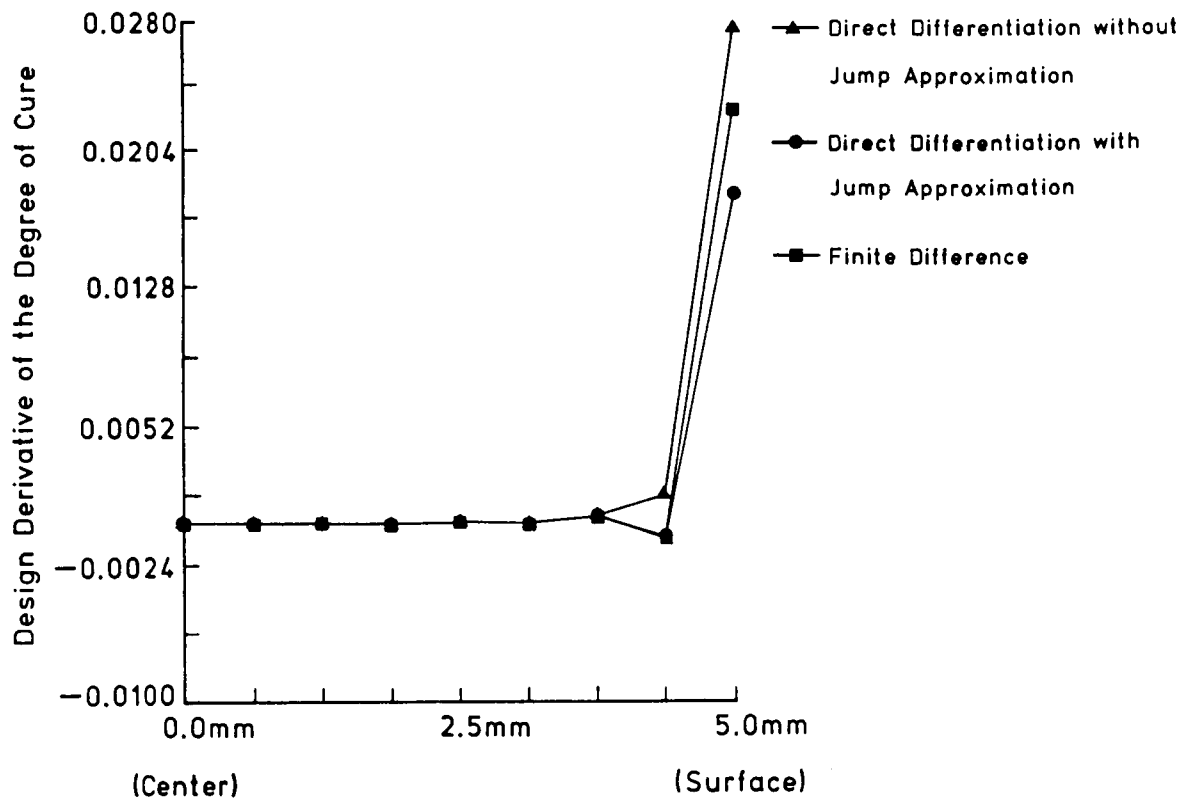


Figure 7. Design derivative of degree of cure at time equal to 42 sec.

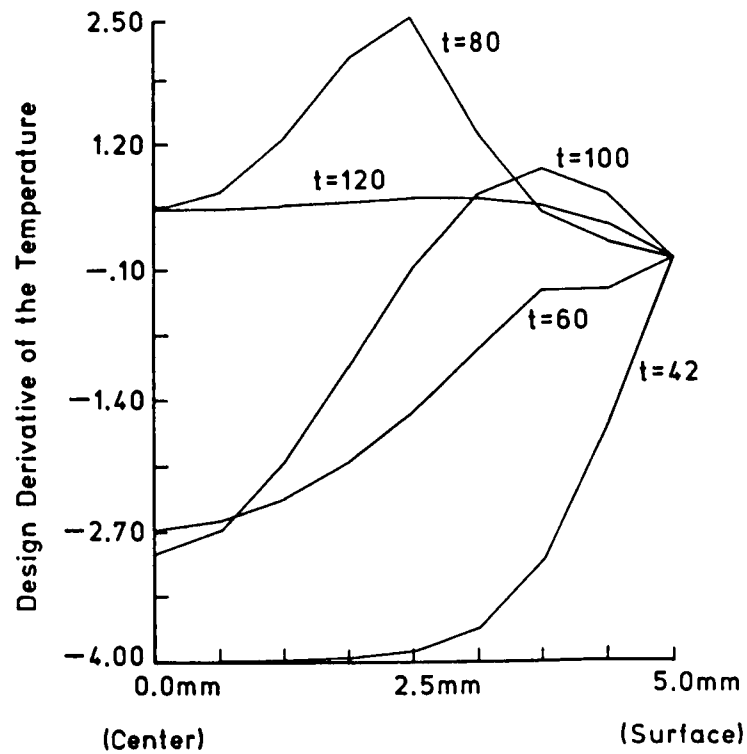


Figure 8. Distribution of T' at different time instants.

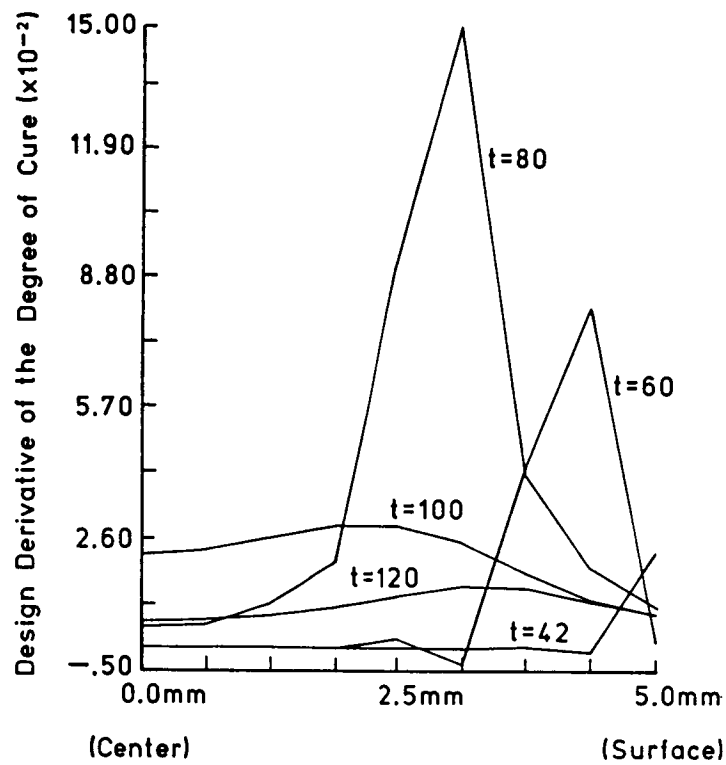


Figure 9. Distribution of α' at different time instants.

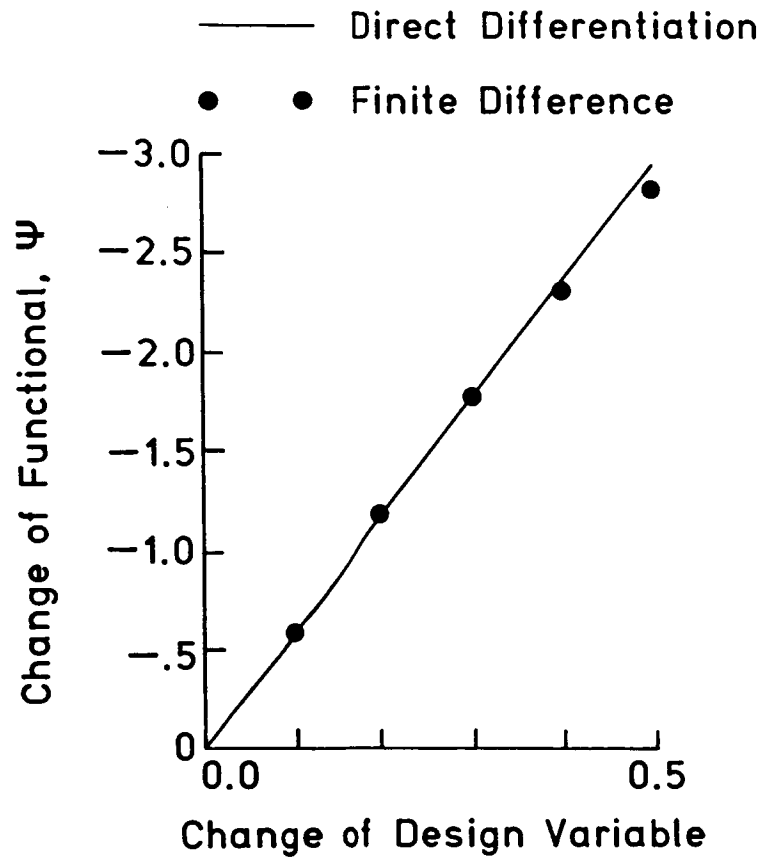


Figure 10. Thermal design derivatives for press molding with a jump in T_c .

APPLICATION OF DESIGN SENSITIVITY ANALYSIS FOR GREATER IMPROVEMENT ON MACHINE STRUCTURAL DYNAMICS

Masataka YOSHIMURA
Department of Precision Engineering
School of Mechanical Engineering
Kyoto University
Kyoto, JAPAN

SUMMARY

This paper presents methodologies for greatly improving machine structural dynamics by using design sensitivity analyses and evaluative parameters. First, design sensitivity coefficients and evaluative parameters of structural dynamics are described. Next, the relations between the design sensitivity coefficients and the evaluative parameters are clarified. Then, design improvement procedures of structural dynamics are proposed for the following three cases: (1) addition of elastic structural members, (2) addition of mass elements, and (3) substantial changes of joint design variables. Cases (1) and (2) correspond to the changes of the initial framework or configuration, and (3) corresponds to the alteration of poor initial design variables. Finally, numerical examples are given for demonstrating the availability of the methods proposed in this paper.

1. INTRODUCTION

In usual design optimization of machine structures, a framework pattern for the complete structure is definite and initial design variables which are usually tentatively given are modified so that the objective function is improved. In such design optimization, design sensitivity coefficients of evaluative parameters can be used for finding the most preferable design change directions. However, improvement of the product performance or characteristics, which is attained under the condition of a constant framework and using poor initial design variables, often is not satisfactory. Furthermore, machine structural dynamics depend on characteristics at many natural modes, and on damping characteristics which are yet unclear. Hence, the relationships between the machine structural dynamics and design variables are very complicated. Application of design sensitivity analyses to optimization of structural dynamics is not simple.

This paper proposes design decision making methods of structural dynamics which intend to greatly increase product performance of machine structures. First, evaluative parameters of structural dynamics are listed, and design sensitivity coefficients of the parameters are derived. Next, the relations between the design sensitivity coefficients and the parameters of displacement, internal vibratory force, and energy distributions are analyzed. Based on the analyses, priorities among the evaluative parameters are clarified. Then, using the design sensitivity analyses and the relations between parameters, design improvement procedures of structural dynamics are constructed for each of the three cases: (1) addition of elastic structural members, (2) addition of mass elements, and (3) substantial changes of joint design variables. Addition of elastic structural members and mass elements on the original design is utilized for decreasing the static compliance and for balancing the frequency response over the frequency range, respectively. Substantial changes of joint design variables are made for balancing the frequency response and for increasing damping ratios. Finally, the effectiveness of the procedures is demonstrated by applying them to a structural model.

2. EVALUATIVE PARAMETERS FOR STRUCTURAL DYNAMICS AND INFORMATION FOR DESIGN CHANGES

A machine structure has point E where vibrational (excitational) force or static force generates, and point G where vibrational or static displacement produced by that force causes reduction of the machine performance. The transfer function of a vibrational system defining the relation between the input force at point E and the displacement output at point G is expressed as the "frequency response".

Fig. 1 shows an example of the receptance frequency response $R(=D/F)$ which is obtained from the displacement D at point G caused by the harmonic force F at point E.

According to the requirements for the product performance, the following changes of the characteristics are required:

- (1) decrease the static compliance f_s ,
- (2) increase/decrease a natural frequency ω_n ,
- (3) increase the damping ratio ζ_n at a natural mode,
- (4) decrease the receptance value R_n at a natural mode.

In the case of machine tools, the maximum receptance value $R_{n-\max}$ at the cutting point is evaluated for increasing the stability against regenerative chatter (refs. 1 and 2), and natural frequencies are evaluated for diminishing the forced vibrational troubles. Even in other machines' cases concerned with transient dynamic response, some treatment among (1) through (4) can be applied. Hence, the "frequency response" is the most fundamental characteristic of structural dynamics.

In the following nomenclature, "direct" means that the point and direction of the exciting (or static) force are the same as the pick-up point and direction of displacement, while "cross" means that those points and directions are not the same.

2.1 Evaluative Parameters of Frequency Response

The equation of motion in a linear vibrational system having multiple-degrees of freedom is expressed by the following equation:

$$[M]\{\ddot{X}\} + [C]\{\dot{X}\} + i[H]\{X\} + [K]\{X\} = \{F\} \quad (1)$$

where $[M]$, $[K]$, $[C]$, and $[H]$ are the mass, stiffness, viscous damping, and hysteretic damping matrices, respectively; where $\{X\}$ and $\{F\}$ are the column vectors representing the displacements and the forces; and where i designates the imaginary unit.

The angular natural frequency at an arbitrary n th natural mode is denoted as ω_n . For easy expansion of equations, a displacement eigenvector $\{X_n\}$ at each of the natural modes is normalized as follows:

$$\{X_n\}^T [M] \{X_n\} = 1 \quad (\text{then, } \{X_n\}^T [K] \{X_n\} = \omega_n^2)$$

The equation showing the relation between $\{X\}$ and $\{F\}$ at a given angular frequency ω is expressed using receptance matrix $[R(\omega)]$ as follows:

$$\{X\} = [R(\omega)] \{F\} \quad (2)$$

The receptance matrix under the assumption of the proportional damping vibrational system is obtained using the orthogonality relations of displacement eigenvectors:

$$[R(\omega)] = \sum_{m=1}^{\infty} \left[\frac{[f_m]}{1 - \left(\frac{\omega}{\omega_m}\right)^2 + 2i \frac{\omega}{\omega_m} \zeta_m} \right] \quad (3)$$

where $[f_m]$, ω_m , and ζ_m are respectively the modal flexibility matrix, angular natural frequency, and damping ratio at the m th natural mode. The modal flexibility matrix (ref. 3) is obtained using the displacement eigenvector $\{X_m\}$ and stiffness matrix $[K]$ as follows:

$$[f_m] = \frac{\{X_m\} \{X_m\}^T}{\{X_m\}^T [K] \{X_m\}} \quad (4)$$

Damping ratio ζ_m at the m th natural mode is obtained for a viscous damping vibrational system as follows:

$$\zeta_m = \frac{\omega_m \{X_m\}^T [C] \{X_m\}}{2 \{X_m\}^T [K] \{X_m\}} \quad (5)$$

When no other natural frequencies having large modal flexibility exist near the n th natural frequency, the receptance value at the n th angular natural frequency, ω_n , is approximated from equation (3) using the following equation:

$$[R(\omega_n)] \doteq -\frac{i[f_n]}{2\zeta_n} + \sum_{\substack{m=1 \\ m \neq n}}^{\infty} \left[\frac{[f_m]}{1 - (\frac{\omega_n}{\omega_m})^2} \right] \quad (6)$$

Since $[R(0)]$ is equivalent to static compliance $[f_s]$ by substituting zero for ω in eq. (3), the following relation is established between the modal flexibility matrix, $[f_m]$, and the static compliance matrix, $[f_s]$.

$$[f_s] = \sum_{m=1}^{\infty} [f_m] \quad (7)$$

By selecting diagonal elements at the j -row and j -column of matrices $[f_s]$ and $[f_m]$ in eq. (7), the following relation is obtained (ref. 3).

$$f_{s(j,j)} = \sum_{m=1}^{\infty} f_{m(j,j)} \quad (8)$$

Since the values of $f_{m(j,j)}$ are always positive, the relation in eq. (8) means that the summation of $f_{m(j,j)}$ at all natural modes is equal to the value of static compliance $f_{s(j,j)}$.

2.2 Design Sensitivity Coefficients of Evaluative Parameters (ref. 3)

The design variables are denoted by a vector $\mathbf{b} = \{b_1, b_2, \dots, b_N\}^T$, where N is the number of design variables. Design sensitivity coefficients, $\partial\omega_n/\partial\mathbf{b}$, and $\partial\{X_n\}/\partial\mathbf{b}$ of an angular natural frequency, ω_n , and a displacement eigenvector, $\{X_n\}$, with respect to a design variable vector, \mathbf{b} , are obtained by applying the orthogonality relations of displacement eigenvectors to the eigenvalue equation of motion partially differentiated with respect to \mathbf{b} , as follows:

$$\frac{\partial\omega_n}{\partial\mathbf{b}} = \frac{1}{2\omega_n} \frac{\partial\omega_n^2}{\partial\mathbf{b}} = \frac{1}{2\omega_n} \{X_n\}^T \left[\frac{\partial[K]}{\partial\mathbf{b}} - \omega_n^2 \frac{\partial[M]}{\partial\mathbf{b}} \right] \{X_n\} \quad (9)$$

$$\frac{\partial\{X_n\}}{\partial\mathbf{b}} = -\frac{1}{2} \{X_n\}^T \frac{\partial[M]}{\partial\mathbf{b}} \{X_n\} \{X_n\} + \sum_{\substack{m=1 \\ m \neq n}}^{\infty} \left\{ \frac{\{X_m\}^T \left[\frac{\partial[K]}{\partial\mathbf{b}} - \omega_n^2 \frac{\partial[M]}{\partial\mathbf{b}} \right] \{X_n\} \{X_m\}}{\omega_n^2 - \omega_m^2} \right\} \quad (10)$$

Using equations (9) and (10), design sensitivity coefficients of modal flexibilities are derived from eq. (4):

$$\begin{aligned} \frac{\partial[f_n]}{\partial\mathbf{b}} = & -\frac{1}{\omega_n^4} \{X_n\} \{X_n\}^T \{X_n\}^T \frac{\partial[K]}{\partial\mathbf{b}} \{X_n\} \\ & + \frac{1}{\omega_n^2} \sum_{\substack{m=1 \\ m \neq n}}^{\infty} \left[\frac{\{X_m\}^T \left[\frac{\partial[K]}{\partial\mathbf{b}} - \omega_n^2 \frac{\partial[M]}{\partial\mathbf{b}} \right] \{X_n\} [\{X_m\} \{X_n\}^T + \{X_n\} \{X_m\}^T]}{\omega_n^2 - \omega_m^2} \right] \end{aligned} \quad (11)$$

Similarly, design sensitivity coefficients of damping ratios ζ_n for a viscous damping vibrational system are derived from eq. (5) as follows:

$$\frac{\partial\zeta_n}{\partial\mathbf{b}} = \frac{1}{\{X_n\}^T [K] \{X_n\}} \left\{ \frac{1}{4\omega_n} \frac{\partial\omega_n^2}{\partial\mathbf{b}} \{X_n\}^T [C] \{X_n\} \right.$$

$$\begin{aligned}
& + \omega_n \frac{\partial \{X_n\}^T}{\partial b} [C] \{X_n\} + \frac{1}{2} \omega_n \{X_n\}^T \frac{\partial [C]}{\partial b} \{X_n\} \\
& - 2\zeta_n \frac{\partial \{X_n\}^T}{\partial b} [K] \{X_n\} - \zeta_n \{X_n\}^T \frac{\partial [K]}{\partial b} \{X_n\} \Big\} \quad (12)
\end{aligned}$$

Design sensitivity coefficients with respect to fundamental structural elements of spring elements, concentrated mass elements, and damping elements are obtained from eqs. (11) and (12).

(i) Spring element

Spring stiffness k of a spring element at point J (for example, a joint) in the machine structural model is considered as a design variable. The design sensitivity coefficient of the direct modal flexibility $f_{n(C, C)}$ at the n th natural mode at point C is:

$$\frac{\partial f_{n(C, C)}}{\partial k} = -f_{n(C, J)}^2 + 2 \sum_{\substack{m=1 \\ m \neq n}}^{\infty} \left(\frac{f_{m(C, J)} \cdot f_{n(C, J)}}{\frac{\omega_n^2}{\omega_m^2} - 1} \right) \quad (13)$$

where $f_{n(C, J)}$ and $f_{m(C, J)}$ are the cross modal flexibilities at the n th and the m th natural modes, respectively. The design sensitivity coefficient of the damping ratio at the n th natural mode is:

$$\frac{\partial \zeta_n}{\partial k} = -\frac{\zeta_n}{2} f_{n(J, J)} \quad (14)$$

where $f_{n(J, J)}$ is the direct modal flexibility at point J.

(ii) Concentrated mass element

The mass, M_I , of a concentrated mass element at point I in a machine structural model is considered as a design variable. The design sensitivity coefficient of the direct modal flexibility $f_{n(C, C)}$ at point C is:

$$\frac{\partial f_{n(C, C)}}{\partial M_I} = 2\omega_n^2 f_{n(C, I)} \sum_{\substack{m=1 \\ m \neq n}}^{\infty} \left(\frac{f_{m(C, I)}}{1 - \frac{\omega_n^2}{\omega_m^2}} \right) \quad (15)$$

(iii) Damping element

In a viscous damping vibrational system, the design sensitivity coefficient of the damping ratio with respect to viscous damping coefficient c of a damping element at point J is:

$$\frac{\partial \zeta_n}{\partial c} = \frac{\omega_n}{2} f_{n(J, J)} \quad (16)$$

2.3 Information of Energy Distributions

2.3.1 Relationships between changes of natural frequencies and energy distribution rates (ref. 4)

It is assumed that the stiffness matrices at subsystems s and r of the machine structure are $[K_s]$ and $[K_r]$, the mass matrices at subsystems s and r are $[M_s]$ and $[M_r]$, and the displacement eigenvectors corresponding to subsystems s and r are $\{X_n\}_s$ and $\{X_n\}_r$. Now, the values of the stiffness matrix $[K_s]$ at subsystem s increase (or decrease) α times to become $[K'_s]$, and the values of the mass matrix $[M_r]$ at subsystem r increase (or decrease) β times to become $[M'_r]$ as shown in eqs. (17) and (18):

$$[K'_s] = [K_s] + \alpha[K_s] \quad (17)$$

$$[M_r'] = [M_r] + \beta[M_r] \quad (18)$$

α and β being small values. The variable component $d\omega_n^2$ of the square of an angular natural frequency ω_n is obtained as follows:

$$d\omega_n^2 = \frac{\alpha \{X_n\}_s^T [K_s] \{X_n\}_s - \beta \omega_n^2 \{X_n\}_r^T [M_r] \{X_n\}_r}{\{X_n\}^T [M] \{X_n\}} \quad (19)$$

The following equation is obtained multiplying both sides of eq. (19) by $1/\omega_n^2$:

$$\frac{d\omega_n^2}{\omega_n^2} = \frac{\alpha \{X_n\}_s^T [K_s] \{X_n\}_s - \beta \omega_n^2 \{X_n\}_r^T [M_r] \{X_n\}_r}{\omega_n^2 \{X_n\}^T [M] \{X_n\}} \quad (20)$$

In eq. (20), $\{X_n\}_s^T [K_s] \{X_n\}_s$ and $\omega_n^2 \{X_n\}_r^T [M_r] \{X_n\}_r$ are respectively twice the potential energy (strain energy) at subsystem s and the kinetic energy at subsystem r in the initial structural design. Hence, those have positive values. $\omega_n^2 \{X_n\}^T [M] \{X_n\}$ is twice the maximum kinetic energy in the complete structure which also has a positive value.

The following rule is established from eq. (20): when the design change is conducted so that the rigidity is increased (that is, α has a positive value) / decreased (that is, α has a negative value) at the member or the element which has the larger potential energy distribution, or the mass is decreased (that is, β has a negative value) / increased (that is, β has a positive value) at the member or the element which has the larger kinetic energy distribution, the natural frequency increases / decreases more effectively.

2.3.2 Relationships between design sensitivity coefficients and energy distribution rates

The maximum potential energies stored in the whole machine structure and in the spring element with spring stiffness k at point J at the n th natural mode are denoted as V_{Tn} and V_{Jn} , respectively. The design sensitivity coefficients of the natural frequency ω_n and the damping ratio ζ_n at the natural mode with respect to spring stiffness k have the relation with the potential energy distribution rate, V_{Jn}/V_{Tn} , as shown in the following equations.

$$\frac{\partial \omega_n^2}{\partial k} = \frac{\omega_n^2}{k} \left(\frac{V_{Jn}}{V_{Tn}} \right) \quad (21)$$

$$\frac{\partial \zeta_n}{\partial k} = - \frac{\zeta_n}{2k} \left(\frac{V_{Jn}}{V_{Tn}} \right) \quad (22)$$

A similar relation for the modal flexibility at point C is derived when the modal flexibility at a natural mode is far greater than that at any other natural mode (ref. 3):

$$\frac{\partial f_{n(C,C)}}{\partial k} \cong - \frac{f_{n(C,C)}}{k} \left(\frac{V_{Jn}}{V_{Tn}} \right) \quad (23)$$

In this case, the modal flexibility at the natural mode can be decreased by increasing the spring stiffness of the spring element having the high potential energy distribution.

2.4 Information of Static Displacement and Internal Vibratory Force

(i) Static displacement

It is assumed that a machine structural model is installed in a hypothetical system T which is filled with a substance having a sufficiently small rigidity, as shown in Fig. 2. Now, two points, P_1 and P_2 , are chosen on the machine structural model, and between the two points a thin circular tube (or a thin square bar) is conceived. Then, it can be considered that a circular tube (or a square bar) member exists between points P_1 and P_2 .

When the evaluative parameter is the direct static compliance $f_{s(C,C)}$ at point C , the design sensitivity coefficient

of $f_s(C, C)$ with respect to the spring stiffness k_P in the axial direction of the member between points P_1 and P_2 is obtained as follows:

$$\frac{\partial f_s(C, C)}{\partial k_P} = - \left(\frac{X_C \cdot (X_{P_1} - X_{P_2})}{2V_s} \right)^2 = - f_s^2(C, P) \quad (24)$$

where X_C is the relative displacement between points A and B caused by the static force at point C, X_{P_1} and X_{P_2} are the displacements at points P_1 and P_2 in the axial direction of the member between points P_1 and P_2 , and V_s is the total strain energy of the structural model at the displacement state; $f_s(C, P)$ is the cross static compliance between points C and P. As understood from eq. (24), the design sensitivity of the direct static compliance $f_s(C, C)$ with respect to a hypothetical spring between two points having the largest relative displacement is greatest. Hence, the displacement distribution on the machine structural model can be used as the information for adding an elastic member when the static compliance is required to be decreased.

(ii) Internal vibratory force

When the internal vibratory force at a structural member or a joint is small, it can be understood that the member or the joint has a small effect on the vibrational characteristics. If the force is negligibly small, removal of the member or the joint may have negligible influence on the dynamic characteristics.

On the other hand, when the internal vibratory force F_J is great at a joint, the following two cases exist:

- (1) the potential energy distribution rate at the joint is great,
- (2) the potential energy distribution rate at the joint is small.

In case (1), the joint has a great effect on the vibrational characteristics, and even small changes of the joint design variables bring about a great change of the characteristics. In case (2), such small changes of the joint design variables cause little change of the vibrational characteristics. Great changes of the joint design variables are necessary for a great change of the characteristics.

The relation on the frequency domain between the excitational input force F_E and the internal vibratory force F_J at a joint similar to the relation between the excitational input force and the displacement shown in eq. (3), is obtained as follows:

$$\frac{F_J}{F_E}(\omega) = \sum_{m=1}^{\infty} \frac{h_{EJm}}{1 - \left(\frac{\omega}{\omega_m} \right)^2 + 2i \frac{\omega}{\omega_m} \zeta_m} \quad (25)$$

where h_{EJm} is the modal internal force coefficient at the m th natural mode. The value of h_{EJm} is subject to very little change due to variations in damping. Hence, values of h_{EJm} can be used for relatively evaluating magnitudes of internal vibratory forces.

Spring stiffness k_J of a spring element at a joint of a machine structural model generally has the relation with the angular natural frequency ω_n at the n th natural mode and the modal internal force coefficient h_{EJn} of the spring element as shown in Fig. 3. Case (1) corresponds to the design at (hypothetical) point Q within the region S, while case (2) corresponds to the design at (hypothetical) point H within the region T.

It can be understood from Fig. 3 that a joint spring element having a great internal vibratory force but a small potential energy distribution rate has a great latent effect on the vibrational characteristics, although the value of the design sensitivity coefficient at that design point is small.

2.5 Considerations on the Evaluative Parameters and Information for Design Improvement

The following concluding remarks are obtained for the evaluative parameters:

- (1) As can be understood from eq. (8), the static compliance f_s has a direct influence on the modal flexibility values at natural modes.
- (2) As can be understood from eq. (11), the design sensitivity coefficient of modal flexibility is influenced by the characteristics at many other natural modes. This fact means that the modal flexibility f_n is determined by the systematic balance over the complete structure. Hence, the modal flexibility needs systematic analyses.
- (3) As can be understood from eq. (14), the design sensitivity coefficient of the damping ratio at a natural mode does not include the influence of characteristics at the other natural modes. In an approximate sense, the damping ratio at a natural

mode can be changed by adjusting only the characteristics at the natural mode.

(4) As can be understood from eq. (9), the design sensitivity coefficient of natural frequency ω_n does not include the influence of characteristics at the other natural modes.

Higher priority of evaluation must be given to the evaluative parameters which need systematic analyses. If evaluative parameters which can be determined by the local effect are fixed before the systematic evaluation, a great improvement of the product performance cannot be expected. From the above consideration, priority for evaluation of the frequency response should be given in the order of (1) f_s , (2) f_n , and (3) ξ_n and ω_n .

Features of other information for design improvement such as energy distributions, static deformation distributions, and internal vibratory forces are as follows:

(a) In design changes based on energy distributions, it is not necessary to define a specific design variables. Parts of the structure which need increased rigidity or decreased weight can be macroscopically grasped. In usual design practice, first of all, it is required to know where the weak points (regions) in the structure are. In this case, evaluations based on energy distributions (refs. 1 and 2) are effective.

(b) The static displacement distribution can be used as the information for adding elastic structural members.

(c) The magnitude of the internal vibratory force at a natural mode indicates the degree of influence of the structural member or the joint on the vibrational characteristics. That can be used as a sort of sensitivity information.

3. STRATEGIES FOR GREATER IMPROVEMENT OF STRUCTURAL DYNAMICS

In usual design problems, many characteristic and evaluative factors often interact mutually. The relationships between design variables and evaluative factors are very complicated. When the optimum design is required for such design problems, many local optimum solutions often exist in the feasible design space. Therefore, it is very difficult to obtain a design solution which brings about great improvement of the product performance. Table 1 shows the procedures which have been developed for solving those problems. Based on the clarification of competitive and cooperative relationships between characteristics, the procedures are divided into three phases as shown in Table 1 (ref. 5).

In the following, some technical strategies for greater improvement of structural dynamics will be described. Addition of elastic members in Section 3. 1 can be used in the procedures of phases 1 and 2 in Table 1; addition of mass elements in Section 3. 2 can be used in the procedures of phase 2 in Table 1; and substantial changes of joint design variables in Section 3. 3 can be used in the procedures of phase 3 in Table 1.

The improvement or modification of receptance values is most difficult in structural dynamics. Hence, characteristics related with the receptance frequency response will be mainly discussed.

3. 1 Addition of Elastic Structural Members

In the procedures shown in Table 1, first of all, the static compliance is minimized. When sufficient reduction of the static compliance cannot be attained by changes of design variables (such as cross-sectional dimensions of the structural members), addition of new structural members are useful only if change in the framework is possible.

The procedures for decreasing the static compliance $f_{s(C, C)}$ by addition of an elastic structural member are as follows:

Step 1. Detect points P_1 and P_2 having a negative value of the right side part of eq. (24) of which the absolute value is maximum in the feasible region of the machine structural model.

Step 2. Define a thin member region between points P_1 and P_2 , and equalize the Young modulus of the member element with that of the other structural members.

Step 3. Repeat the search for optimum cross-sectional design variables until the objective function converges. At each iteration of the search, the locations of points P_1 and P_2 are slightly moved so that the right side part of eq. (24) has the greatest negative value.

When the objective is to minimize the direct modal flexibility $f_{n(C, C)}$ at the n th natural mode at point C, eq. (13) can be used as the design sensitivity coefficient with respect to the spring stiffness k_p in the axial direction of the hypothetical member between points P_1 and P_2 . The forementioned procedures for the static compliance can also be applied for minimizing the modal flexibility by transforming eq. (24) into eq. (13).

3. 2 Addition of Mass Elements

The design sensitivity coefficient of the modal flexibility $f_{n(C, C)}$ at the n th natural mode at point C of a machine structural system with respect to the small hypothetical mass M_I at point I (such as shown in Fig. 2) is given in eq. (15).

The procedures for reducing the modal flexibility $f_{n(C, C)}$ by means of the addition of a mass element are as follows:

Step 1. In order to detect a point where a mass element should be added, search for a point I having a negative value on the right side part of eq. (15) of which the absolute value is maximum in the feasible region of the machine structural system, and add a small mass element at point I.

Step 2. If the modal flexibility $f_{n(C, C)}$ is sufficiently small or has reached the convergence point, the added mass element is adopted for the final design. Otherwise, go to Step 3.

Step 3. Modify the point I so that the right side part of eq. (15) has a negative maximum absolute value, and increase the magnitude of the mass at point I and return to Step 2.

3.3 Substantial Changes of Joint Design Variables

In a usual searching process for an optimum design solution, initial design variables are slightly changed so that the objective function is most effectively minimized (or maximized). Hence, if an initial design variable has a low sensitivity for changing the objective function and is widely different from the optimum solution, it takes a very long time to reach the optimum solution, and the design variable often converges into some local optimum point without reaching the optimum solution.

From the standpoint of static rigidity (that is, reciprocal of the static compliance), the rigidity of a joint is required to be as great as possible. However, from the standpoint of dynamic characteristics, the rigidity of a point is required to have a specific value or a value within a specific region in the following cases:

- (i) when a change in the ratio f_n/f_s of the modal flexibility f_n to the static compliance f_s is required,
- (ii) when an increase of the damping ratio at the natural mode is required.

When the spring stiffness of a joint in the initial design of a structural model has the value at point H as shown in Fig. 3, the design sensitivity coefficient at the point is very small, and potential energy is scarcely stored at the spring. Hence, the spring stiffness may not be changed largely to the region S, and a sufficient change of the vibrational characteristics cannot be generated. In order to attain objective (i) or (ii), the spring stiffness at the joint should be reduced to the region S. If the internal vibratory force at the spring element is large at point H, there is a high possibility to realize objective (i) or (ii) effectively with this spring element.

The procedures for realizing objective (i) or (ii) are as follows:

Step 1. Detect a spring element having the great internal vibratory force but a small potential energy distribution rate among spring elements of all the joints (the spring stiffness k_j at the spring element has a value within the region T as shown in Fig. 3).

Step 2. Decrease the spring stiffness k_j to a value within the region S as shown in Fig. 3.

Step 3. Start the search for the optimum value after having reduced the spring stiffness k_j to get a new initial value.

4. NUMERICAL EXAMPLE

The procedures described in Section 3 are demonstrated on the machine structural model shown in Fig. 4. Fig. 5 shows the simulation model for structural analysis. At the initial design shown in Fig. 6(a), the spring stiffness values at joints J_1 , J_2 , J_3 and J_4 (see Fig. 5) were large enough for avoiding degradation of the static rigidity. The relative receptance frequency response between points A and B in Y-direction for this initial model is shown in Fig. 7(a). The receptance value at the 1st natural mode is very large, and the ratio f_1/f_s of the modal flexibility f_1 at the 1st natural mode to the static compliance f_s is 0.96. The three kinds of procedures proposed in Section 3 were successively added on the same structural model.

4.1 Addition of an Elastic Member

The objective in this step is to decrease the static compliance f_s by adding a circular tube within the shaded region in Fig. 5. Fig. 6(b) shows the final design obtained according to the procedures described in Section 3.1. The receptance frequency response for the design is shown in Fig. 7(b). The static compliance f_s decreases from 2.36×10^{-6} m/N at the initial design to 1.33×10^{-6} m/N. The incremental percentage of the total weight of the structural model by addition of the elastic member is only 0.0134%.

4.2 Addition of a Mass Element

The objective in this step is to decrease the maximum modal flexibility value at the 1st natural mode. A mass element was added at point I of the model as shown in Fig. 6(c) according to the procedures described in Section 3.2. Fig. 7(c) shows the receptance frequency response after the design change. The maximum modal flexibility value decreased by 6%.

4.3 Substantial Changes of Joint Design Variables

The objective in this step is to minimize the maximum receptance value over the whole frequency range. The modal internal force coefficient h_{EJ1} of the 1st natural mode was large at the spring element in Y-direction of joint J_4 . The spring stiffness k_J of the spring element was 1.0×10^8 N/m. Since the potential energy distribution rate at the spring element was very small (that means the design sensitivity coefficient is also very small), the spring stiffness k_J was greatly reduced to the value of 2.0×10^5 N/m. After this spring stiffness value was set as an initial design variable of k_J , the spring stiffness k_J and the damping coefficients of all joints (J_1 through J_4) were determined so that the maximum receptance value was minimized. Fig. 7(d) shows the receptance frequency response after the proposed procedures. By these procedures, two requirements (i) great reduction of the ratio f_n/f_s of the modal flexibility f_n at the natural mode having the greatest receptance value to the static compliance f_s and (ii) great increase of the damping ratio at the natural mode (described at Section 3.3) were simultaneously accomplished.

It can be understood from comparison of the receptance frequency response in Fig. 7(d) with that in Fig. 7(a) that the proposed procedures are effective for greater improvement of the vibrational characteristics (the maximum receptance value).

5. CONCLUDING REMARKS

Methodologies for greatly improving machine structural dynamics by using design sensitivity analyses and evaluative parameters were proposed. The features are as follows:

- (1) Addition of elastic members and mass elements is carried out using information of displacement distributions and design sensitivity analyses for altering the initial framework of a structural model.
- (2) Substantial changes of joint design variables are conducted using information of internal vibratory forces and potential energy distributions for the improvement of the poor initial design variables.

REFERENCES

1. Yoshimura, M.: Analysis and Optimization of Structural Dynamics of Machine Tools by a Synthesis of Dynamic Rigidity Program System, Proc. 16th International Machine Tool Design and Research Conference, Sept. 1976, pp. 209–215.
2. Yoshimura, M.: Computer-Aided Design Improvement of Machine Tool Structure Incorporating Joint Dynamics Data, Annals of the CIRP, Vol. 28, No. 1, 1979, pp. 241–246.
3. Yoshimura, M.: Design Sensitivity Analysis of Frequency Response in Machine Structures, ASME Journal of Mechanisms, Transmissions, and Automation in Design, Vol. 106, No. 1, 1984, pp. 119–125.
4. Yoshimura, M.: Optimum Design of Machine Structures with Respect to an Arbitrary Degree of Natural Frequency and a Frequency Interval between Adjacent Natural Frequencies, Bulletin of Japan Society of Precision Engineering, Vol. 14, No. 4, 1980, pp. 236–242.
5. Yoshimura, M.: Design Optimization of Machine-Tool Dynamics Based on Clarification of Competitive-Cooperative Relationships Between Characteristics, ASME Paper No. 86-DET-24, 1986.

Table 1. Procedures for the design optimization method based on clarification of competitive-cooperative relationships between characteristics (ref. 5)

	Design variables	Range of modeling, type of modeling and analytical method
Phase 1	<ul style="list-style-type: none"> ○ Design variables of structural members and elements having an influence on the static rigidity 	<ul style="list-style-type: none"> ○ Modeling for a structure on the static force loop ○ Static rigidity analysis
Phase 2	<ul style="list-style-type: none"> ○ Design variables of structural members and elements and joint stiffnesses having no influence on the static rigidity 	<ul style="list-style-type: none"> ○ Modeling for a complete structure ○ Vibrational analysis for an undamped vibrational system
Phase 3	<ul style="list-style-type: none"> ○ Damping coefficients of all joints 	<ul style="list-style-type: none"> ○ Modeling for a complete structure ○ Vibrational analysis for a non-proportionally damped vibrational system

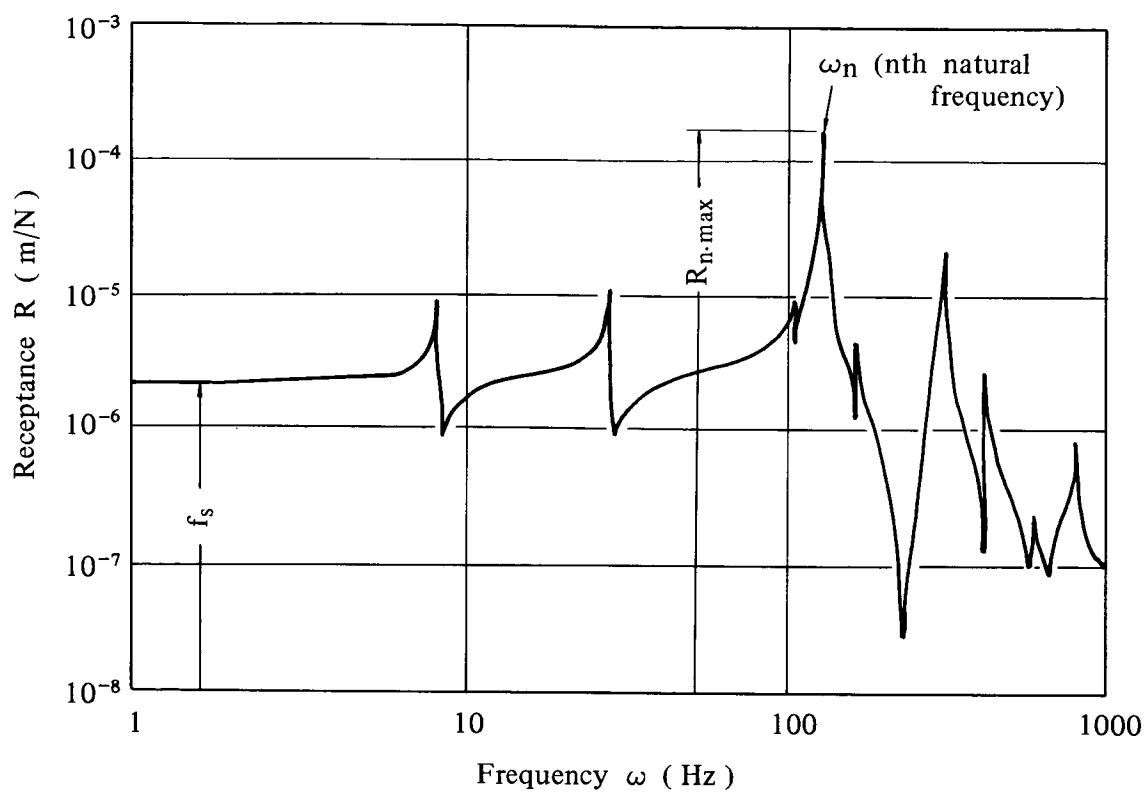


Fig. 1 An example of receptance frequency response

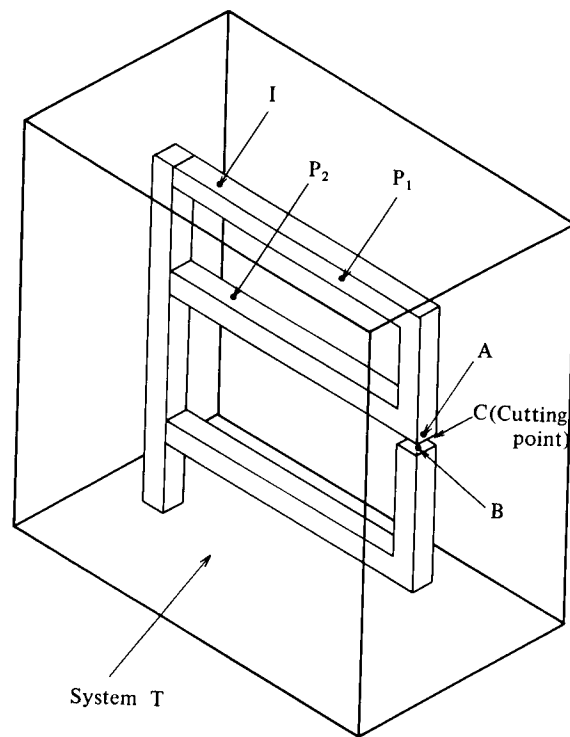


Fig. 2 A structural model in a hypothetical system T

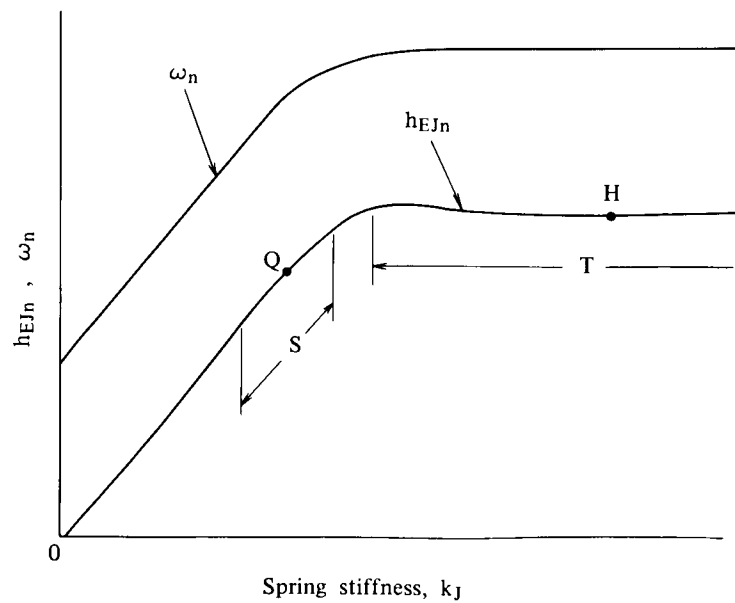


Fig. 3 Relation between the spring stiffness k_J at a joint, and the modal internal force coefficient h_{EJn} and the natural frequency ω_n at the n th natural mode

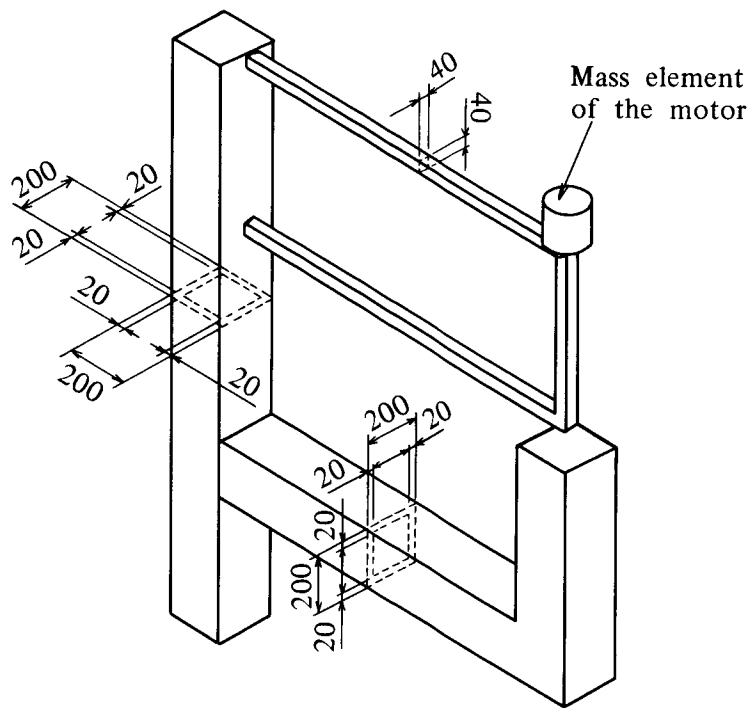


Fig. 4 Structural model of a machine tool
(unit: mm)

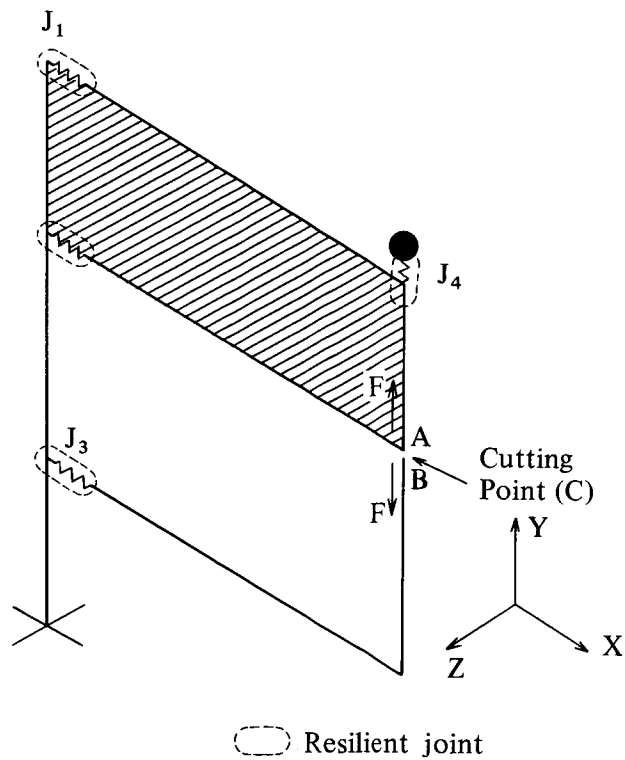


Fig. 5 Simulation model for structural analysis

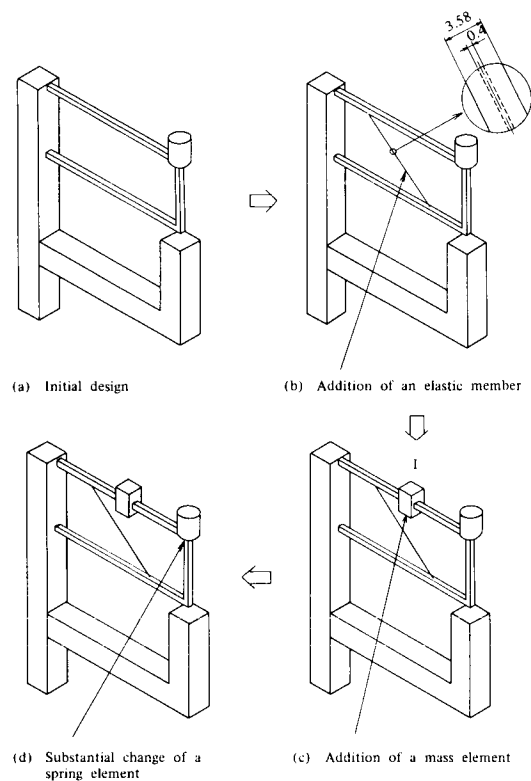


Fig. 6 Alteration of structural configuration by a series of design changes
(unit: mm)

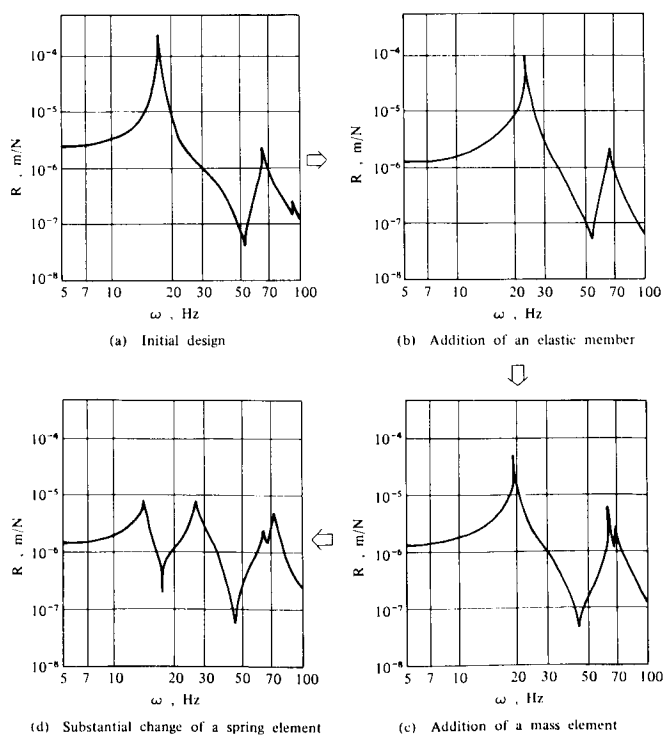


Fig. 7 Relative receptance frequency response R between points A and B corresponding to the design changes shown in Fig. 6

DESIGN SENSITIVITY ANALYSIS OF ROTORCRAFT AIRFRAME STRUCTURES
FOR VIBRATION REDUCTION

T. Sreekanta Murthy
PRC Kentron, Inc.
Hampton, VA

ABSTRACT

As a part of an ongoing NASA/industry rotorcraft structural dynamics program, a study was recently initiated at Langley on optimization of rotorcraft structures for vibration reduction. The objective of this study is to develop practical computational procedures for structural optimization of airframes subject to steady-state vibration response constraints. One of the key elements of any such computational procedure is design sensitivity analysis. A method for design sensitivity analysis of airframes under vibration response constraints is presented. The mathematical formulation of the method and its implementation as a new solution sequence in MSC/NASTRAN are described. The results of the application of the method to a simple finite element 'stick' model of the AH-1G helicopter airframe are presented and discussed. Selection of design variables that are most likely to bring about changes in the response at specified locations in the airframe is based on consideration of forced response strain energy. Sensitivity coefficients are determined for the selected design variable set. Constraints on the natural frequencies are also included in addition to the constraints on the steady-state response. Sensitivity coefficients for these constraints are determined. Results of the analysis and insights gained in applying the method to the airframe model are discussed. The general nature of future work to be conducted is described.

INTRODUCTION

Excessive vibrations have a detrimental influence on the performance, operation and maintenance of helicopters. The primary source of vibration in the airframe arises from the vibratory airloads acting on the main rotor which are transmitted to the airframe at known discrete frequencies. Vibration continues to be a problem in helicopters despite considerable efforts to reduce it. The problem has been attacked by the use of active and passive vibration control devices, by changes to main rotor system and by airframe design. Use of vibration control devices involves weight penalties. Alterations to the rotor by modifying blade stiffness and mass distribution are being studied. Airframes are designed to satisfy strength, vibration and performance requirements. Design for vibrations is based primarily on previous experience. Selection of the best airframe that meets all the requirements, in particular the vibration requirements, is a difficult task. It would appear that structural optimization tools, properly brought to bear by the design engineer, would go a long way toward achieving the goal of an analysis capability for designing a low vibration helicopter.

The use of structural optimization in helicopter airframe design for vibration reduction is a relatively new research topic and has only recently been addressed. Work related to "optimization" of helicopter airframe structures is contained primarily in references 1-6. However, only references 5 and 6 use a nonlinear programming approach. Sciarra (1) used a strain energy approach to guide modification of a structure; Done (2) and Sobey (3) used the Vincent Circle approach; Hanson (4) did a comparative study of the above two approaches; Done and Rangacharyulu (5) and Miura and Chargin (6) used a formal optimization approach for airframe design.

As a part of an ongoing NASA/industry rotorcraft structural dynamics program, a study was recently initiated at Langley on optimization of rotorcraft structures for vibration reduction. The objective of this study is to develop practical computational procedures for optimization of rotorcraft structures subject to steady-state vibratory loads. One of the key elements in the development of a computational procedure for airframe optimization is design sensitivity analysis. A method for design sensitivity analysis of airframes under steady-state response due to rotor-induced dynamic loads is presented. Constraints on airframe dynamic response displacements and natural frequencies are considered. The mathematical formulation of the method and its implementation as a new solution sequence in MSC/NASTRAN are described. The results of the application of the method to a simple finite element 'stick' model of the AH-1G helicopter airframe are discussed. The paper concludes with a short discussion of the direction future in-house work in this area is to take.

DEFINITION OF OPTIMIZATION PROBLEM

The airframe structure of a helicopter is subjected to steady-state rotor-induced harmonic loads acting at the top of the rotor mast. The loads, in general, have six components and occur at frequencies which are integer multiples of the product of the number of blades and the rotor rotational speed. It is assumed that both the magnitude and frequency of the rotor loads acting on the airframe are known and that they are constant during design modifications.

The airframe structure is assumed to have nonuniform stiffness and mass distributions which are functions of the geometry of the structural members. The design variables are taken to be the dimensions which characterize the cross-sectional geometry of a member. In particular, for a beam member having a solid rectangular cross-section the design variable would be the depth and height. Selection of design variables in a large airframe structure containing thousands of members is a difficult task. An experienced airframe designer can suggest candidate members that can be permitted to undergo design modification and the extent to which they can be modified. Studies by Sciarra (Ref.1) and Hanson (Ref.4) have provided some guidelines in the selection of design variables. In particular it has been shown that the design variables that are most likely to bring about changes in the response at specified locations in the airframe are the ones having maximum forced response strain energy. Using this criterion an initial selection of design variables of an airframe can be made. In general, any design change will introduce changes in dynamic response, natural frequencies, mode shapes, static strength, weight, and center of gravity location of an airframe and they in turn indirectly change the performance characteristics of a helicopter as a whole. Therefore, constraints have to be imposed on the allowable response characteristics to restrict design changes within certain bounds. For the work reported in the paper, only constraints on steady-state dynamic response displacements and natural frequencies are considered.

To complete the definition of the optimization problem, an objective function must be defined. This is not an easy task. Should the airframe weight be the objective function or the dynamic response displacement? If the former is selected as the objective function, can the reduced dynamic response be achieved without increasing the stiffness and hence the mass of an airframe? If the latter is the objective function an optimizer may try to drive the response at a point to zero which may not result in reduction of vibration at other points on an airframe. Because this paper is limited to a study of design sensitivity analysis, these additional considerations are not addressed here.

DESIGN SENSITIVITY ANALYSIS OF AIRFRAME

In this section formulation of design sensitivity analysis of an airframe with constraints on steady-state dynamic response displacements is presented and equations for determining the sensitivity coefficients are given. Also, pertinent equations used in the study, such as equations for airframe response analysis and expressions for strain energy, are presented.

The equation of motion (state equation) for determining the steady-state dynamic response is given in the Figure (1). The equation is written in matrix form in terms of the coefficient matrices K (stiffness), M (mass), C (damping), and F (force). The magnitude and frequency of the force F are assumed to be known. Steady-state response X occurs at the same frequency as the forcing frequency. The unknown response vector X is obtained by solving a set of simultaneous linear algebraic equations. The equation of motion for the undamped natural frequencies of an airframe is given. Expressions for modal element strain energy and undamped forced response strain energy are also given in the figure.

To determine the sensitivity coefficients for constraints on the steady-state response X , the design variable b is changed by a small amount db . The structural members associated with the design variables will have new cross-sectional properties and new stiffness, mass and damping matrices for the changed design. Thus, for a small change in a design variable b , new K , M , and C are computed and a new response is generated. The response x for the new design must satisfy the equilibrium requirement $h(b,x)=0$. A linearized version of this requirement is used to derive an expression for the sensitivity coefficients $\partial x/\partial b$ as outlined in Figure (2). The matrices on the left-hand side (LHS) of the equation for the sensitivity coefficients are already known from the finite element analysis for a particular design. In the right-hand side (RHS) the change in force due to a change in design is assumed to be zero. Only the changes in the stiffness, mass and damping matrices due to an increment in design have to be computed. The matrices thus formed are assembled and solved as a set of simultaneous linear algebraic equation for the unknowns $\partial x/\partial b$. An incremental form of the equations for sensitivity coefficients is also given in the figure. The size of the matrix on the RHS is dependent on the number of design variables and number of forcing frequencies used in the analysis. The sensitivity coefficients $\partial x/\partial b$ are obtained in a matrix form with rows corresponding to the number of airframe degrees of freedom and columns corresponding to the number of airframe design variables. The number of matrices of $\partial x/\partial b$ depends on the number of load cases considered.

IMPLEMENTATION OF SENSITIVITY ANALYSIS IN MSC/NASTRAN

NASTRAN is used in the helicopter industry for finite element analysis applications, and therefore it was judged appropriate to implement the sensitivity analysis in that program. A new solution sequence to compute the sensitivity coefficients using NASTRAN Direct Matrix Abstraction Program (DMAP) modules was developed. The incremental form of the equation for the sensitivity coefficients for constraints on steady-state dynamic response displacements was implemented using the DMAP modules and incorporated into MSC/NASTRAN. The solution for the sensitivity coefficients is obtained in the sequence shown in Figure (3). The corresponding DMAP modules are also shown there. The DMAP program uses the data about design variables and constraints specified on NASTRAN bulk data cards (DVAR, DVSET, and DSCONS). The data for the stiffness and mass matrices of the airframe generated in a previous finite element analysis are retrieved from the data base using module DBFETCH. Damping was not considered in the current implementation. The program generates new cross-sectional properties of structural members for an increment in design and rearranges the intermediate data using module DSTA. Using modules EMG and DSVG1, ΔK and ΔM are computed. The RHS of the equations for sensitivity coefficients is assembled using module ADD. The equations are then solved using the FRRD1 module to obtain the sensitivity coefficients for the dynamic response constraints. Several other DMAP modules, such as SSG2, MODACC, SDR1, SDR2, DSMA, DBSTORE and LMATPRT, are used for pre-and post-processing of data used in the solution sequence and also for organizing the stiffness, mass and sensitivity coefficient matrices in a partitioned form.

Numerical results for sensitivity coefficients for constraints on steady-state dynamic response are obtained as follows. First, the airframe dynamic response is obtained from Rigid Format 68. Then, the solution sequence described above is executed.

APPLICATION TO AH-1G HELICOPTER AIRFRAME

Description of the AH-1G Airframe:

The airframe structure of the AH-1G helicopter described in references 4 and 7 was used for the sensitivity analysis application. The airframe structure with its skin panels removed is shown in Figure (4). The fuselage portion of the airframe is built around two main beams which provide the primary vertical bending stiffness in the fuselage structure. The main beams are tied together by the lower horizontal floors, the forward fuel cell cover, and the engine deck to give the fuselage lateral stiffness. The main rotor pylon provides the structural connection between the main rotor and the fuselage. It is attached to the fuselage through five elastomeric mounts and a lift link. The lift link is the primary vertical load path and is pinned to the center wing carry-through beam. The engine, gun turret and the landing gear are attached to the fuselage. The wings (not shown) are designed mainly for carrying external loads and are attached to the fuselage on either side. The tailboom is bolted to the fuselage with four attachment fittings. The tailboom is of semimonocoque construction having aluminium skins, stringers and longerons. The vertical fin is connected to the tailboom through the tail rotor mast.

Elastic Line Model of the AH-1G Airframe:

A built-up finite element model of the AH-1G airframe structure is available (Ref. 7). However, for the initial studies on sensitivity analysis which are the subject of this paper, an elastic line or 'stick' model of the AH-1G airframe (Ref. 4) was used. The model is shown in Figure (5). The dynamic characteristics of this elastic line model are similar to those of the built-up model of the airframe. The fuselage, tailboom, wings and rotor mast structure of the airframe were modelled with beam elements. Scalar spring elements were used in the pylon support structure. The engine and the gun turret mounts were modelled as rigid bar elements. The NASTRAN finite element model of this airframe consists of 42 beam elements, 13 scalar spring elements and 12 rigid elements. There are 56 grid points in the model for a total of 336 degrees of freedom. After applying multi-point and single-point constraints and omitting massless degrees of freedom, the model reduces to one having 130 dynamic degrees of freedom. The airframe mass, both concentrated and distributed, is lumped at the grid points selected as the dynamic degrees of freedom. Structural damping of the airframe was not considered.

The primary vertical vibratory force coming from the rotor acts at grid point 55. The force has a magnitude of 1000 lb and a frequency of 10.8 Hz ('2/rev').

NUMERICAL RESULTS AND DISCUSSIONS

Numerical results from the application of sensitivity analysis to a stick finite element model of the AH-1G helicopter airframe are presented and discussed here.

Finite Element Analysis Results:

A finite element analysis of the elastic line model was made using MSC/NASTRAN. The first few lowest natural frequencies obtained for the model are - 3.02 Hz (pylon pitch), 4.22 Hz (pylon roll), 6.80 Hz (1st airframe lateral bending), 7.85 Hz (1st airframe vertical bending), 16.70 Hz (2nd airframe lateral bending) and 17.10 Hz (2nd airframe vertical bending). The mode shapes corresponding to the vertical bending modes are shown in Figures (6 and 7). The first mode (frequency 7.85 Hz) has two nodes (zero displacement) on the airframe - one near the pilot seat and another near the middle of the tailboom. The second vertical bending mode (frequency 17.1 Hz) has three nodes - near grid points 6, 14, and 28.

The steady-state response of the airframe due to vertical excitation at a frequency of 10.8 Hz is shown in Figure (8). The response shape has two nodes (points of zero displacement) - one near grid point 2 and another near grid point 22. All other points on the airframe vibrate at various levels of acceleration depending on the amount of displacement of the airframe from the undeformed position.

The element strain energies associated with the forced response were also calculated. The distribution of strain energy in the fuselage and tailboom elements is shown in Figures (9-10) and discussed in a later section.

Sensitivity Analysis Results:

Using the strain energy criterion, the structural members which are most likely to influence the natural frequencies and the response were identified. Elements in the rear part of the fuselage and most of the elements in the tailboom were identified as likely candidates. The cross-sectional properties of the elements identified were related to design variables. In particular, design variable 'b' of the beam element was related to the area and moment of inertia of the cross-section (which are linear and cubic functions of b). A small increment was given to b to compute a new value of the design variable.

Constraints on the steady-state dynamic response displacements were imposed at the gun turret and pilot seat grid point locations (4 and 8, respectively). Because only vertical responses were of interest, only the vertical displacements were constrained. Although constraints on lateral and torsional displacements would ultimately also be required in a realistic design analysis, they were not considered in this study. However, they can be easily included.

The sensitivity coefficients for the selected constraints were obtained from the MSC/NASTRAN DMAP program which was discussed earlier. The sensitivity coefficients are plotted in a bar chart format in Figures (11-14). The numerical value of a coefficient indicates the amount of change in constraint value due to a small (positive) change in the design variable (identified by the element number, which also denotes the design variable number). A positive/negative value of a sensitivity coefficient means that an increase in the design variable results in an increase/decrease in the constraint value. To physically interpret the results it is useful to refer to the sensitivity of displacements ($\partial x/\partial b$) rather than the sensitivity of constraints ($\partial h/\partial b$). These sensitivities differ only by a constant.

The results shown in Figures 11-12 indicate that the sensitivity coefficients related to the tailboom elements have magnitudes which are large compared to the fuselage elements. Consider the sign of these coefficients. In the tailboom region the coefficients are negative, whereas they are positive in the fuselage region. This means that an increment in a design variable associated with the members in the tailboom decreases the displacement at the pilot seat (and vice-versa) whereas an increment in a design variable in a fuselage member increases the displacement at the pilot seat (and vice-versa). This shows that the tailboom must be stiffened and/or the fuselage must be softened to reduce the dynamic response displacement at the pilot seat. The sensitivity coefficients obtained for constraints at the gun turret location are shown in Figures 13 and 14. The tailboom elements have coefficients which are an order of magnitude higher than those for the fuselage elements. This indicates that the tailboom elements should be significantly stiffened. The coefficients are negative for the fuselage and all elements in the tailboom (except for element number 1213 which has a positive coefficient). This suggests that the elements of the tailboom and the fuselage (except 1213) require stiffening to reduce the dynamic response at the gun turret location. However, element 1213 requires a reduction in stiffness. Hence, to satisfy the vibration constraint at the gun turret location a stiffening of the airframe structure is required, with an element with reduced stiffness at the junction of the fuselage and the rotor mast (grid 12) of the airframe. In summary, the tailboom requires a significant increase in stiffness to reduce the dynamic response at both the pilot seat and gun turret locations. Thus, rather straightforward considerations have provided the information about the portion of the airframe to be modified, order of magnitude of modification required, and the direction in which the modification (stiffen or soften) is required.

As the forced response of the airframe is a function of the natural frequencies and mode shapes of the structure as well as the excitation forces, any modification to the design variables to control the response will also bring about changes in the natural frequencies. also required. Constraints on the two lowest vertical bending modes (natural frequencies 7.85 and 17.1 Hz) of the airframe were considered here. Upper and lower limits on the first mode were specified at 7.0 and 8.5 Hz, respectively, and at 12.0 and 18.0 Hz, respectively, for the second mode. MSC/NASTRAN Rigid Formats 63 and 53 were used to obtain the sensitivity coefficients for the natural frequency constraints. The results are discussed in the following paragraph.

The sensitivity coefficients for the constraints imposed on the natural frequencies are plotted in Figures 15 and 16. The coefficients obtained all have positive values. The figures indicate that the coefficients related to the tailboom elements are large compared to the coefficients for most of the fuselage elements in the case of the first vertical bending mode. This shows that tailboom design strongly influences the natural frequency of the first vertical bending mode. In the case of the second vertical bending mode, some (aft) fuselage elements and (rear) tailboom elements have sensitivity coefficients larger than other elements of the airframe, and therefore they have a strong influence on the frequency of that mode. In both cases the coefficients are positive indicating that stiffening the elements increases the natural frequency, as might be expected.

Interpretation of Results:

The calculation of sensitivity coefficients for a set of constraints often constitutes a major computational effort in an optimization study. The sensitivity analysis results together with the dynamic characteristics of the airframe must be interpreted carefully to guide iterations to a low vibration design. Proper interpretation of the results will provide insight into the nature of the modifications required for the airframe and the feasibility of such modifications. The results presented above are interpreted and discussed below.

The steady-state response of the airframe is mainly due to excitation of the two lowest vertical bending modes (7.850 and 17.1 Hz) by the vertical force (10.8 Hz). The response shape resembles the first vertical bending mode, with the tailboom responding significantly more than the fuselage. The large motion of the tailboom may be attributed to the fact the tailboom is relatively soft compared to the fuselage. Therefore, to shift the natural frequencies and thereby change the response, the stiffness of the tailboom should be suitably changed. The sensitivity results also suggest that changes should be made to the tailboom design, that is, to increase the tailboom stiffness. Thus, the results on dynamic characteristics and sensitivity analysis are complementary.

Consideration of strain energy results together with sensitivity results can also be meaningful. In particular, compare the distribution of element strain energy densities in the forced response mode shape with the distribution of sensitivity coefficients in the airframe. The element strain energy densities in the tailboom are higher than those in the fuselage elements. This comparison indicates that elements with higher strain energies have higher magnitudes of sensitivity coefficients. Therefore, it would be beneficial to use both strain energy information and sensitivity results in the optimization procedure. There could be two possibilities here - one is to use the strain energy results to select design variables; another is to use the strain energy result to modify the design instead of using a more costly design sensitivity analysis. The later possibility is yet to be investigated. In this regard an explicit relation between the strain energy of elements and sensitivity coefficients would be useful.

The overall dynamics of the airframe has some bearing on the optimization of an airframe for vibration reduction. In a conservative dynamic system, the work done by external forces on a flexible structure is transformed into strain energy and kinetic energy. In a nonuniform structure, the distribution of these energies depends on the stiffness and mass distributions. Often a portion of a structure (for example, the tailboom of the AH-1G helicopter) may vibrate significantly more than other portions. In a sense the portion of the structure which vibrates most acts like a vibration absorber. Therefore, if one tries to reduce vibration in a certain portion of the airframe, some other portion of the airframe will vibrate excessively.

From the above discussion, the following possibilities offer themselves for reducing vibrations in the fuselage:

1. Soften the tailboom so that it acts like a vibration absorber.
2. Stiffen the tailboom and soften the fuselage to reduce vibration at the pilot seat.
3. Stiffen the tailboom and the fuselage and provide a soft spring-like interface structure between them to reduce vibration at the gun turret.

Clearly, these possibilities are not realistic in practice. However, they do suggest the types of modifications required for the airframe to satisfy the design constraints. The magnitudes of the modifications required can be obtained by interfacing the sensitivity analysis program with an optimizer. Careful selection of limits on design variables and constraints is needed, otherwise an optimizer may drive the design to an unrealistic configuration. Also, other types of constraints that must be imposed in a realistic airframe design should be included in the study. Therefore, the airframe optimization problem must be viewed in a broader perspective by considering the total helicopter system and not just a part of it.

CONCLUSIONS

An initial study on design sensitivity analysis of rotorcraft airframe structures for vibration reduction has been made. A mathematical formulation for sensitivity analysis for constraints on steady-state forced response displacements was presented. The equations for the sensitivity coefficients were implemented as a new solution sequence in MSC/NASTRAN. Calculation of sensitivity coefficients was made using an elastic line model of the AH-1G helicopter airframe. The results of this preliminary study indicated the following:

1. Sensitivity coefficient results indicate that tailboom elements significantly influence the vibration response at the pilot seat and gun turret locations.
2. Sensitive elements of the airframe have higher element strain energies.
3. The first two vertical bending modes of the AH-1G airframe have a significant influence on the vertical response of the airframe under '2/rev' vertical rotor excitation loads.
4. Interpretation of the airframe dynamic characteristics together with the sensitivity analysis results has brought out the essential nature of modifications required in the AH-1G airframe to reduce vibration.

DIRECTIONS FOR FUTURE WORK

The initial study on airframe sensitivity analysis indicates that there are several important aspects that must be considered. Based on the study, the following areas are identified for further investigation:

1. Consider constraints on static strength, forced response and natural frequencies simultaneously.
2. Interface an optimizer with the design sensitivity analysis
3. Study built-up finite element models.
4. Include airframe structural damping.
5. Include the effect of change of excitation force due to change in airframe flexibility.
6. Address problem of disjoint design space in forced response constraint formulation.
7. Consider a broader range of constraints (center-of-gravity movement of airframe, crash-loads, etc.,) for more effective use of optimization in actual helicopter design.

REFERENCES

1. Sciarra, J.J., "Use of the Finite Element Damped Forced Response Strain Energy Distribution for Vibration Reduction" Boeing-Vertol Company, Report D210-10819-1, U.S. Army Research Office - Durham, Durham, N.C., July 1974.
2. Done, G.T.S. and Hughes, A.D., "Reducing Vibrations by Structural Modification", Vertica, 1976, Vol. 1, pp 31-38
3. Sobey, A.J., "Improved Helicopter Airframe Response through Structural Change", Ninth European Rotorcraft Forum, Paper No. 59, Sept. 13-15, 1983, Stresa, Italy.
4. Hanson, H.W., "Investigation of Vibration Reduction Through Structural Optimization", Bell Helicopter Textron Report No. USAAVRADCOR - TR-80-D-13, July, 1980.
5. Done, G.T.S., and Rangacharyulu, M.A.V., "Use of Optimization in Helicopter Vibration Control by Structural Modification", Journal of Sound and Vibration, 1981, 74(4), pp, 507-518.
6. Miura, H. and Chargin, M., "Automated Tuning of Airframe Vibration by Structural Optimization", American Helicopter Society, 42nd Annual Forum, Washington D.C., 1986.
7. Cronkhite, J.D., Berry, V.L., and Brunken, J.E., "A NASTRAN Vibration Model of the AH-1G Helicopter Airframe", Volume I and II, Bell Helicopter Report No. 209-099-432, Fort Worth, Texas, June 1974.

PERTINENT EQUATIONS

EQUATIONS FOR STEADY-STATE RESPONSE

$$M\ddot{X} + C\dot{X} + KX = F e^{i\omega t}$$

Where $F = f e^{i\omega t}$ $X = x e^{i\omega t}$

EQUATIONS FOR NATURAL MODES

$$M\ddot{X} + KX = 0$$

Where $X = x e^{i\omega t}$

UNDAMPED FORCED RESPONSE ELEMENT STRAIN ENERGY

$$U = \frac{1}{2} x^T k_e x$$

MODAL ELEMENT STRAIN ENERGY

$$U = \frac{1}{2} x^T k_e x$$

Figure 1.

EQUATIONS FOR SENSITIVITY COEFFICIENTS

CONSTRAINTS ϕ ON STEADY-STATE DYNAMIC DISPLACEMENTS:

$$\phi \equiv \frac{|x|}{|x_a|} - 1 \leq 0$$

STATE EQUATION FOR DYNAMIC DISPLACEMENTS:

$$h(b,x) = (-\omega^2 M + i\omega C + K) x - f = 0$$

Linear approximation to change in h due to change in b:

$$\delta h = \frac{\partial h}{\partial b} \delta b + \frac{\partial h}{\partial x} \delta x \quad \text{ALSO,} \quad \delta x = \frac{\partial x}{\partial b} \delta b$$

EQUATIONS FOR SENSITIVITY COEFFICIENTS:

$$(-\omega^2 M + i\omega C + K) \frac{\partial x}{\partial b} = - \left(-\omega^2 \frac{\partial M}{\partial b} + i\omega \frac{\partial C}{\partial b} + \frac{\partial K}{\partial b} \right) x$$

$$(-\omega^2 M + i\omega C + K) x = \Delta f - (-\omega^2 \Delta M + i\omega \Delta C + \Delta K) x^0$$

Figure 2.

SENSITIVITY ANALYSIS FOR DYNAMIC RESPONSE USING MSC/NASTRAN DMAP SOLUTION SEQUENCE

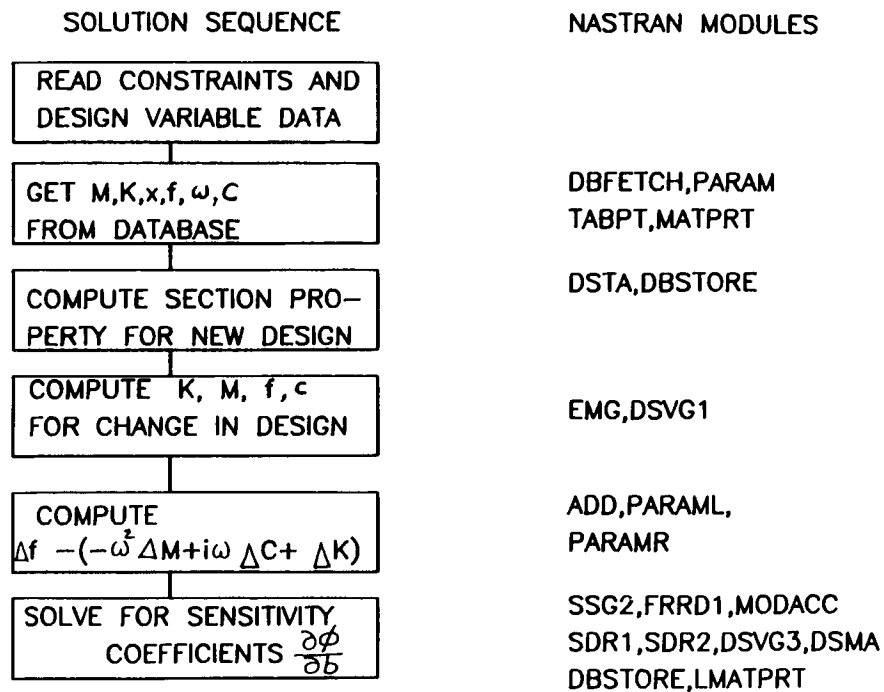


Figure 3.

AIRFRAME STRUCTURE OF THE AH-1G HELICOPTER

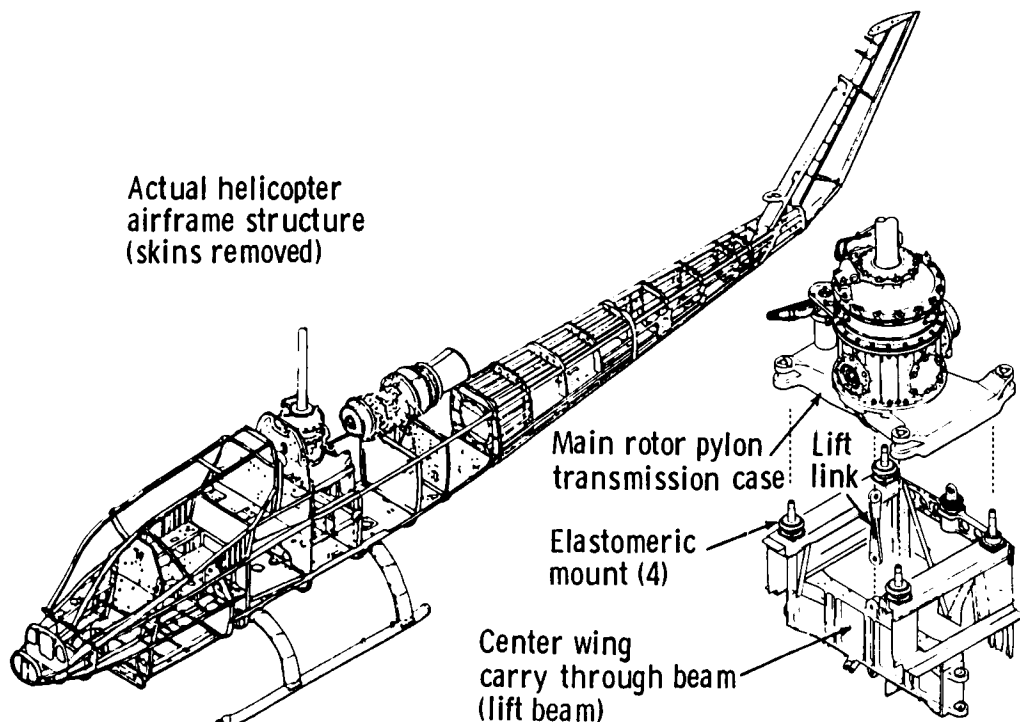


Figure 4.

ELASTIC LINE (STICK) MODEL OF THE AH-1G AIRFRAME

56 grid points
55 structural elements
70 analysis degrees of freedom

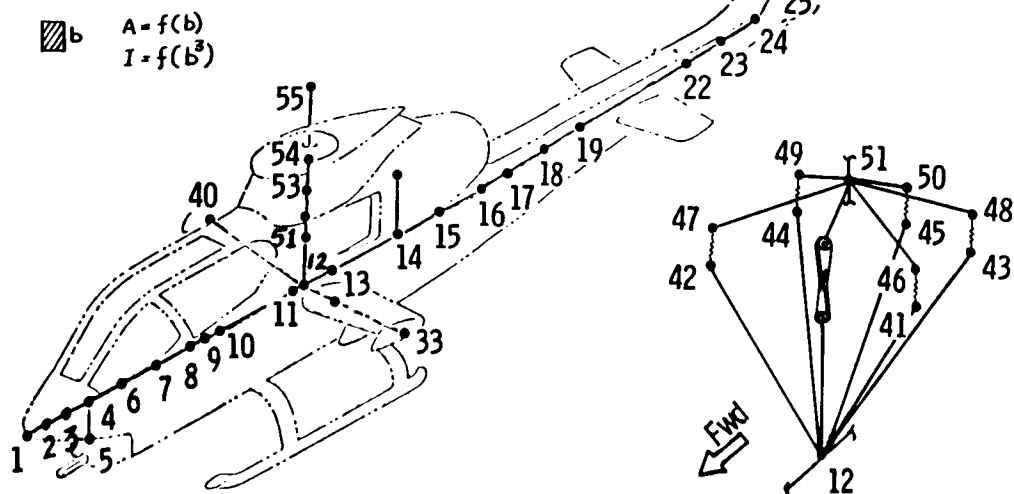


Figure 5.

FIRST VERTICAL BENDING MODE OF AIRFRAME (FREQ.=7.86 HZ)

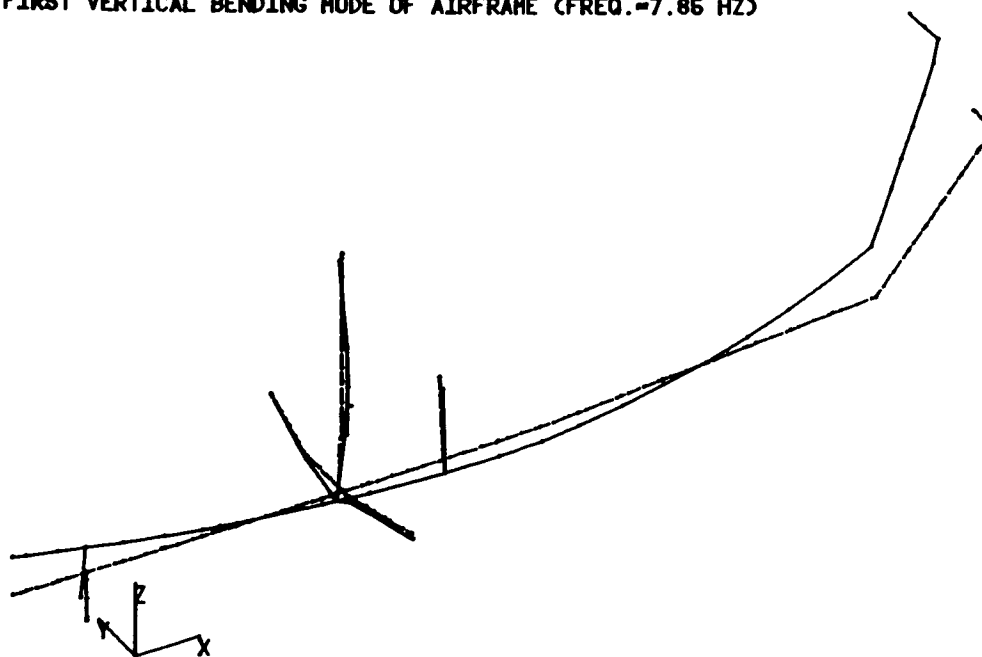


Figure 6.

SECOND VERTICAL BENDING MODE OF AIRFRAME (FREQ.=17.1 HZ)

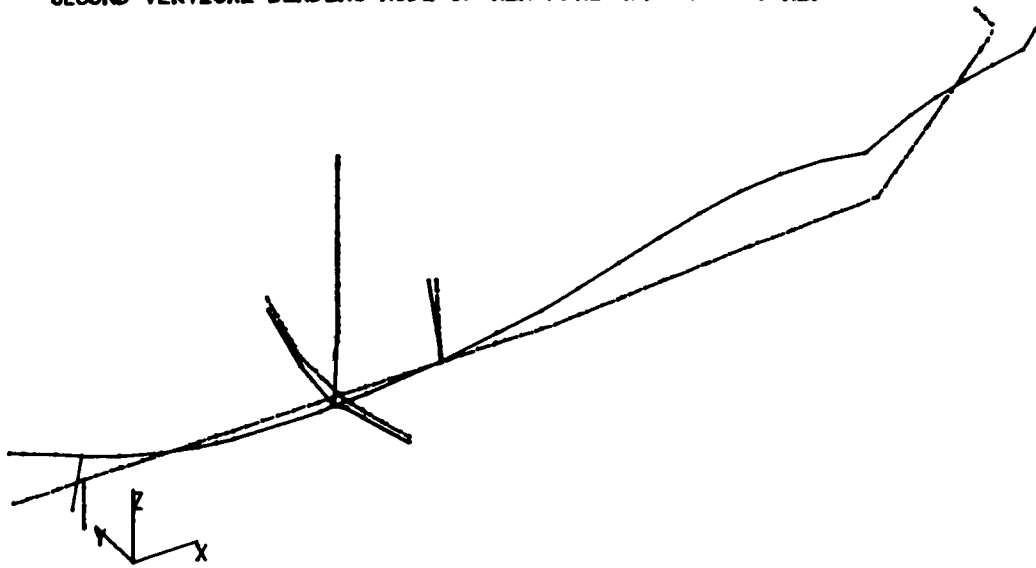


Figure 7.

FORCED RESPONSE MODE OF AIRFRAME
EXCITATION - 1000LB FREQ. 10.8HZ

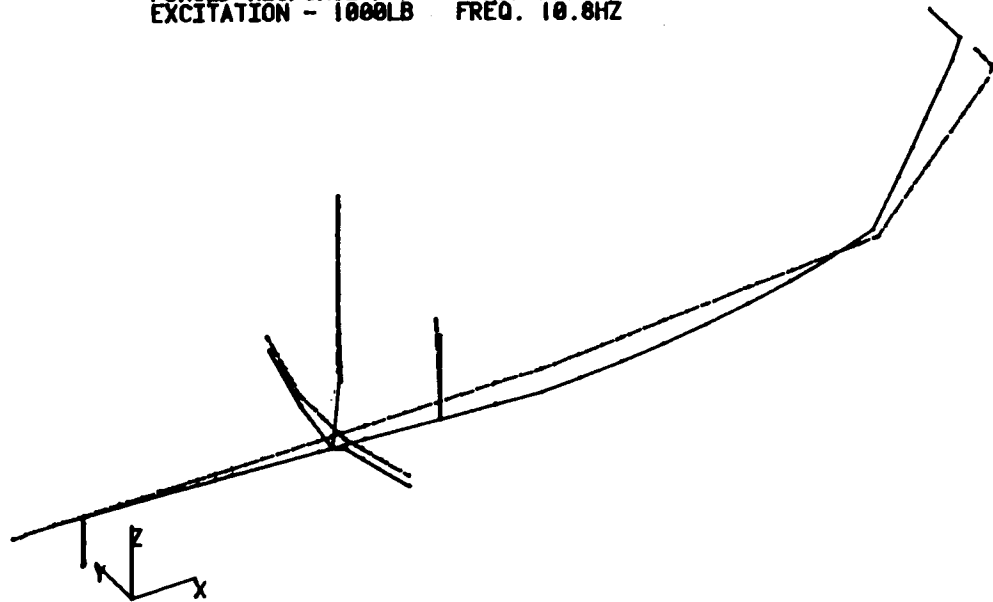


Figure 8.

ELEMENT STRAIN ENERGY DENSITIES
IN FUSELAGE FOR FORCED RESPONSE

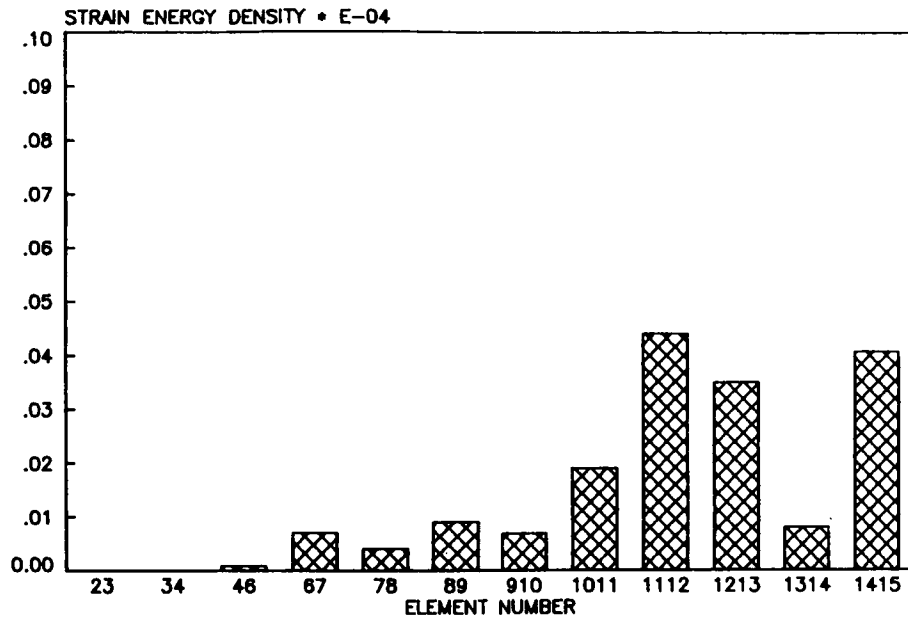


Figure 9.

ELEMENT STRAIN ENERGY DENSITIES
IN TAILBOOM FOR FORCED RESPONSE

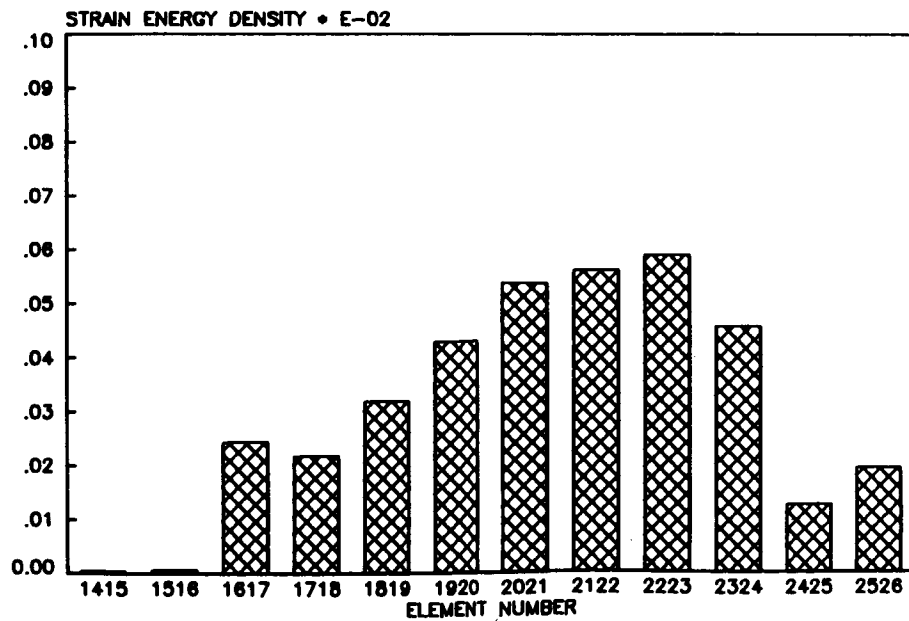


Figure 10.

SENSITIVITY OF DYNAMIC DISPLACEMENT FOR PILOT SEAT LOC. W.R.T. FUSELAGE ELEMENTS

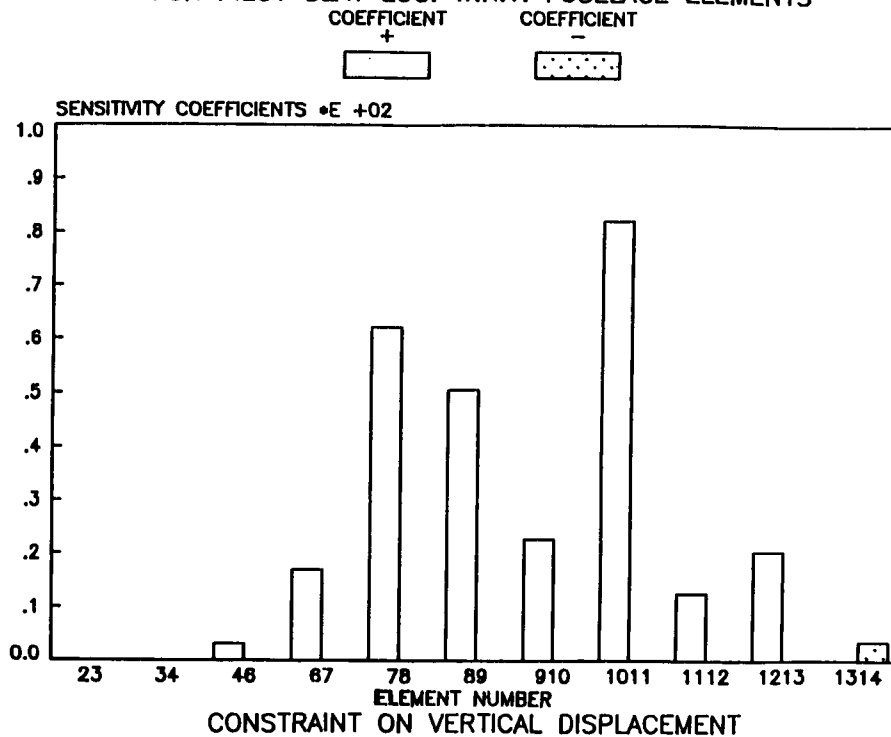


Figure 11.

SENSITIVITY OF DYNAMIC DISPLACEMENT FOR PILOT SEAT LOC. W.R.T. TAILBOOM ELEMENTS

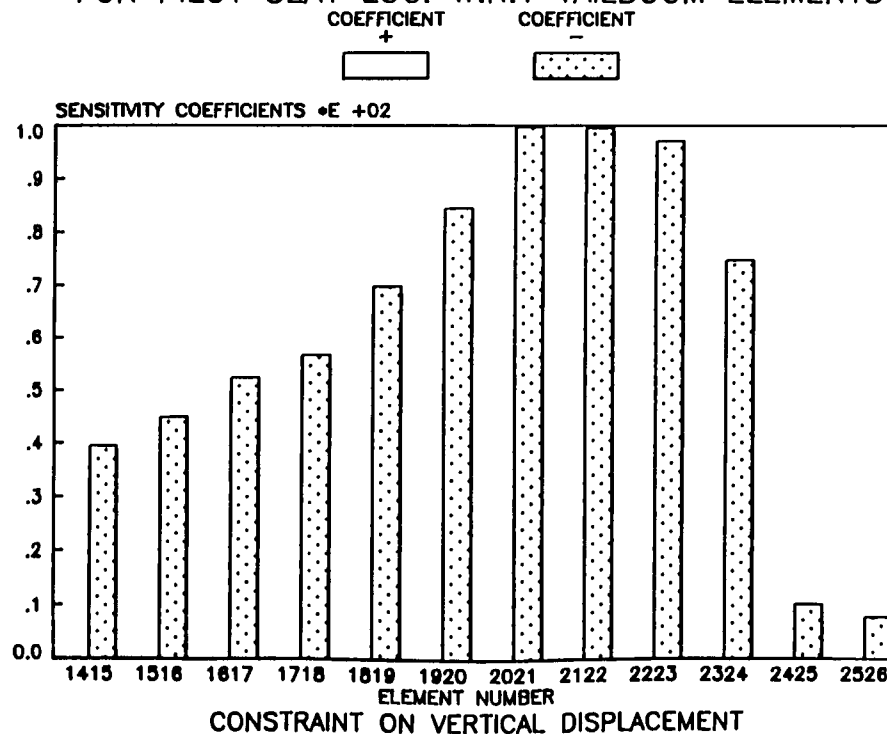


Figure 12.

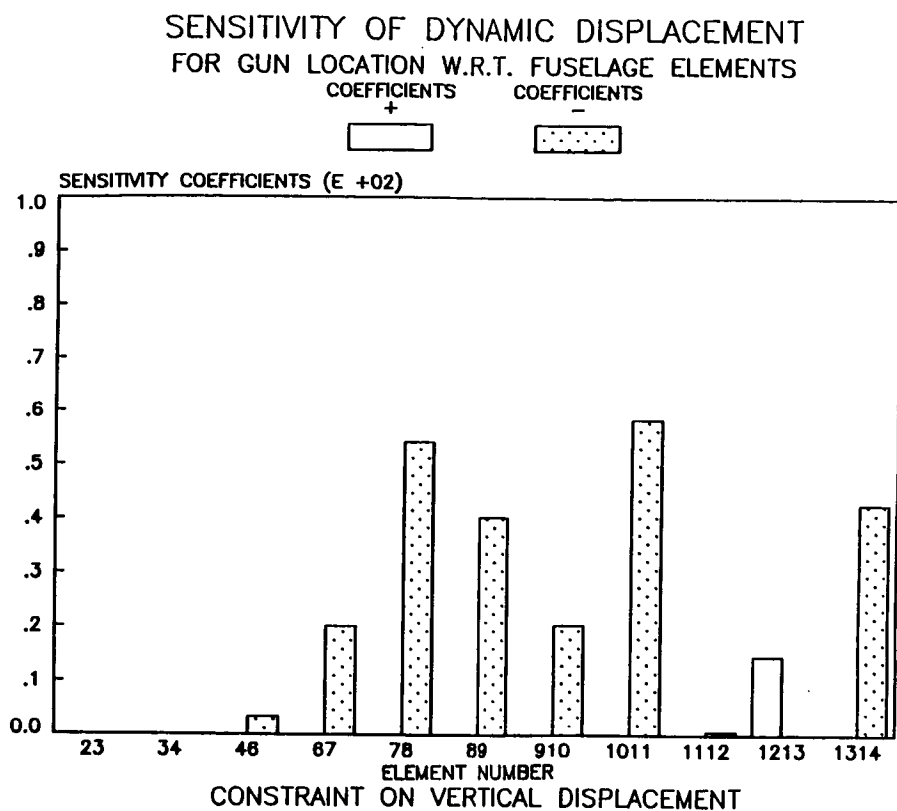


Figure 13.

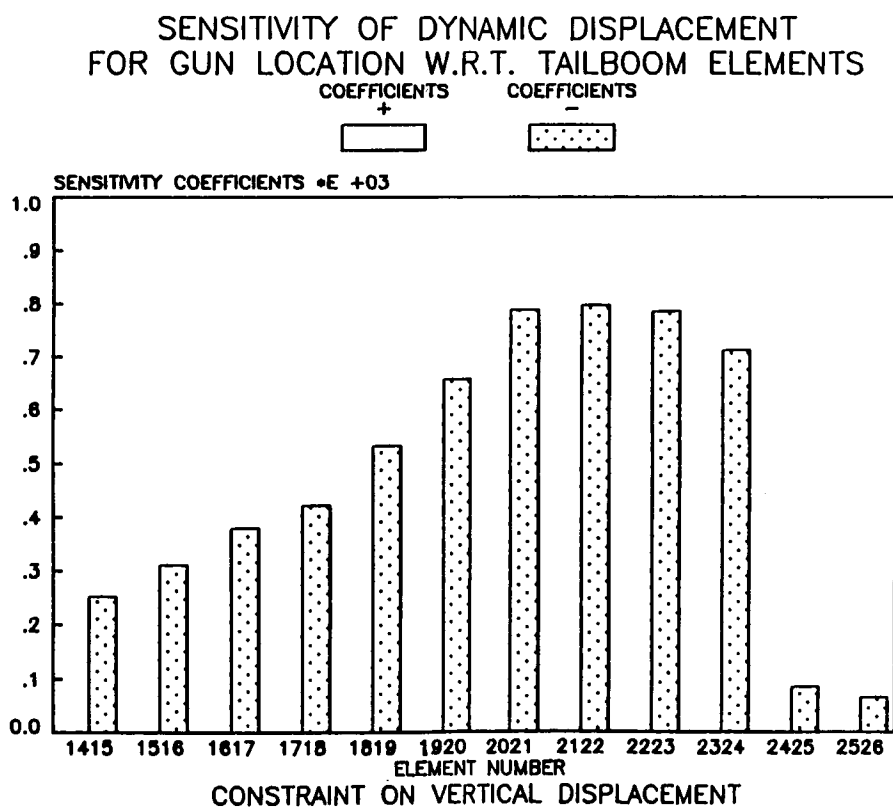


Figure 14.

SENSITIVITY OF FREQUENCIES IN FIRST AND SECOND VERTICAL BENDING MODES

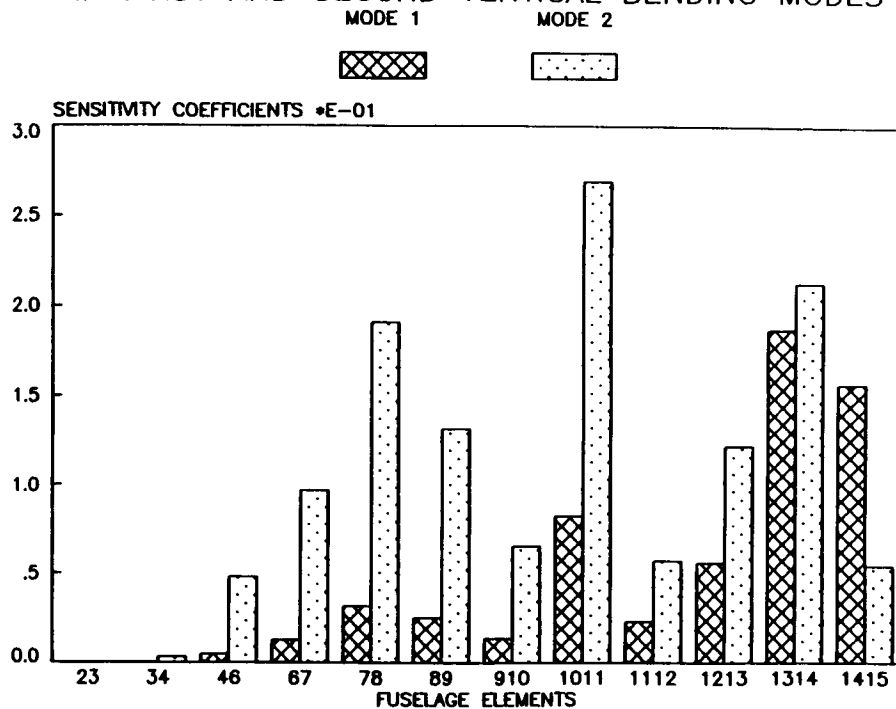


Figure 15.

SENSITIVITY OF FREQUENCIES IN FIRST AND SECOND VERTICAL BENDING MODES

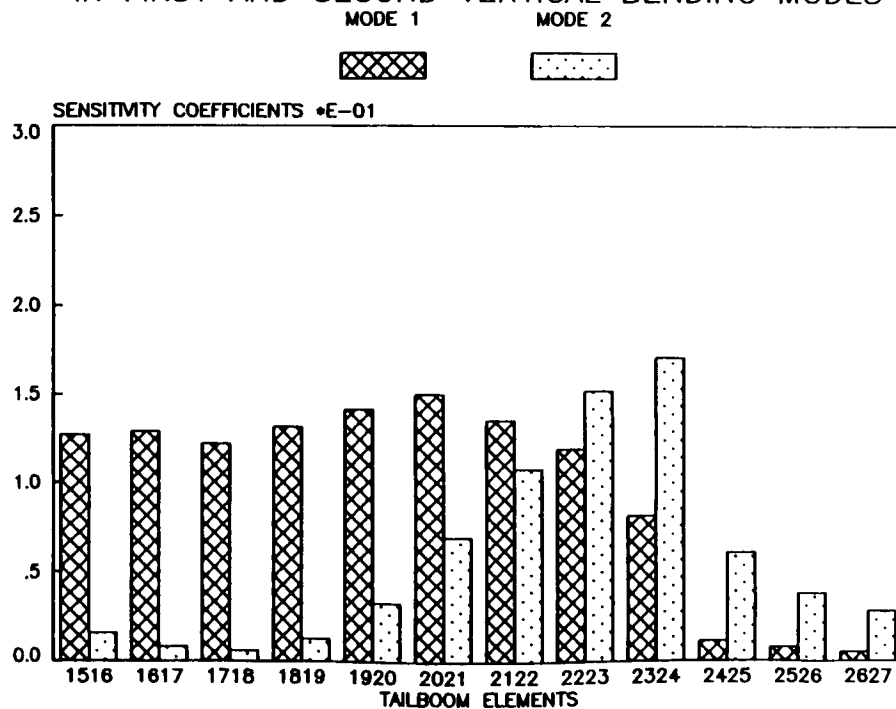


Figure 16.

ON SINGULAR CASES IN THE DESIGN DERIVATIVE
OF GREEN'S FUNCTIONAL*

Robert Reiss
Howard University
Washington, D.C.

SUMMARY

This paper extends the author's prior development of a general abstract representation for the design sensitivities of Green's functional for linear structural systems to the case where the structural stiffness vanishes at an internal location. This situation often occurs in the optimal design of structures. Most optimality criteria require that optimally designed beams be statically determinate. For clamped-pinned beams, for example, this is possible only if the flexural stiffness vanishes at some intermediate location. The Green's function for such structures depends upon the stiffness and the location where it vanishes. A precise representation for Green's function's sensitivity to the location of vanishing stiffness is presented for beams and axisymmetric plates.

INTRODUCTION

This paper is concerned exclusively with the linear self-adjoint differential equation, represented in abstract form by

$$Lu = T^* E T u = f \quad \text{in } \Omega \quad (1a)$$

Here T and T^* are operators which are $L_2(\Omega)$ adjoints of each other, E is a stiffness operator which is symmetric with respect to the $L_2(\Omega)$ inner product, u is the response function and f is a specified disturbance. The open region $\Omega \in \mathbb{R}^n$ is bounded by $\partial\Omega$.

Appropriate mixed inhomogeneous boundary conditions are appended to equation (1a). These are

$$\begin{aligned} B Y u &= g \quad \text{on } \partial\Omega_1 \\ B^* Y^* E T u &= h \quad \text{on } \partial\Omega_2 \end{aligned} \quad (1b)$$

where $\partial\Omega_1 \cup \partial\Omega_2 = \partial\Omega$ and $\partial\Omega_1 \cap \partial\Omega_2 = \emptyset$. The operators Y and Y^* map functions in the domain of L into functions defined on $\partial\Omega_1$ and $\partial\Omega_2$, respectively. And the operators B and B^* map functions defined on $\partial\Omega_1$ and $\partial\Omega_2$, respectively, into functions defined on $\partial\Omega_1$ and $\partial\Omega_2$. Examples of the operators appearing in equations (1a) and (1b) can be found in reference 1 for a number of specific applications.

*This research was supported by the Howard University Large Space Structure Institute through Grant No. NAC-383 from the NASA Langley Research Center.

The stiffness operator E frequently depends upon one or more design parameters, which are collectively denoted by S . The operators T and T^* are generally differential operators which are independent of the design. The boundary operators may or may not be design dependent. There are two important classes of problems for which the boundary operators depend upon S . One class of such problems is usually referred to as shape optimization problems. Here, the boundary is the design variable, and consequently the boundary operators are necessarily design dependent. The other class of such problems occurs in structural optimization theory whenever optimality requires that the stiffness vanish somewhere in the interior of Ω . In this case, equation (1b) must also include an internal boundary where certain jump and/or continuity conditions are specified. This latter class of problems is the primary concern of this paper.

GREEN'S FUNCTION AND FUNCTIONAL

Oden and Reddy (ref. 2) have shown the operator P , which consists of the spatial operator of equation (1a) and the boundary operators of equation (1b), will be self-adjoint if the following integration by parts formula is satisfied

$$(Tu, ETv)_{\Omega} - (u, T^*ETv)_{\Omega} = (\gamma u, B^*\gamma^*ETv)_{\partial\Omega_2} - (B\gamma u, \gamma^*ETv)_{\partial\Omega_1} \quad (2)$$

for every u and v in the domain of P . In equation (2), (\cdot, \cdot) denotes the usual L_2 inner product and the appended subscript the domain of integration. Thus, for example, $(\cdot, \cdot)_{\partial\Omega}$ denotes the $L_2(\partial\Omega)$ inner product. In the remainder of this paper, it will be assumed that the operators specified in equations (1a) and (1b) do indeed satisfy equation (2).

The solution to equations (1a) and (1b) can now be obtained in terms of Green's function G , corresponding to the operator P , i.e.

$$u = (f, G)_{\Omega} + (g, \gamma^*ETG)_{\partial\Omega_1} + (h, \gamma G)_{\partial\Omega_2} \quad (3)$$

Equation (3) may be routinely derived by noting that $G(x, y)$ satisfies

$$T^*ETG(\cdot, y) = \delta_y \quad \text{in } \Omega \quad (4a)$$

and boundary conditions

$$\begin{aligned} B\gamma G(\cdot, y) &= 0 \quad \text{on } \partial\Omega_1 \\ B^*\gamma^*ETG(\cdot, y) &= 0 \quad \text{on } \partial\Omega_2 \end{aligned} \quad (4b)$$

where δ_y represents the Dirac distribution with a singularity at the location y . Upon taking the $L_2(\Omega)$ inner product of both sides of equation (4a) with u and integrating the result twice by parts according to equation (2), equation (3) immediately follows. Several illustrations of equation (3) have been derived by Roach (ref. 3) for specific operator equations.

Green's function $G(x, y)$ is defined on the Cartesian product space $\Omega \times \Omega$ and is generally singular when $x=y$. If any of the operators appearing in equation (4) depend upon the design variable(s) S , then G is a functional of the design S . Reiss (ref. 4) recently presented a compact formula for the

design derivative of G when E is the only operator appearing in equations (1a) and (1b) that depends upon the design S . For, in this case, let S and $S + \Delta S$ denote two designs and define ΔG by

$$\Delta G(x, y; S, \Delta S) = G(x, y; S + \Delta S) - G(x, y, S) \quad (5)$$

It immediately follows from equations (4a), (4b) and (5) that

$$\begin{aligned} T^* \Delta E \Delta G &= F & \text{in } \Omega \\ BY \Delta G &= 0 & \text{on } \partial \Omega_1 \\ B^* \gamma^* \Delta E \Delta G &= H & \text{on } \partial \Omega_2 \end{aligned} \quad (6)$$

where

$$\begin{aligned} F &= - T^* \Delta E T (G + \Delta G) \\ H &= - B^* \gamma^* \Delta E T (G + \Delta G) \end{aligned} \quad (7)$$

A cursory comparison of equation (6) with equation (1) shows that the solution for ΔG is immediately specified by equations (3) and (7); thus

$$\begin{aligned} \Delta G &= - (T^* \Delta E T (G + \Delta G), G)_{\Omega} \\ &\quad - (B^* \gamma^* \Delta E T (G + \Delta G), \gamma G)_{\partial \Omega_2} \end{aligned} \quad (8)$$

After applying the integration by parts formula (2), the variation ΔG simplifies to

$$\Delta G = - (T G, \Delta E T (G + \Delta G))_{\Omega} \quad (9)$$

Equation (9) is an integral equation for ΔG . Considerable simplification results if E is Gateaux differentiable with respect to the design. In this case, by restricting the design variation ΔS to be infinitesimal, ΔE is also infinitesimal and equation (9) may be linearized, i.e.,

$$\delta G = - (T G, \delta E T G)_{\Omega} \quad (10)$$

In equation (10), the symbol Δ has been replaced by δ in order to signify linearization. Equation (10) represents the design sensitivity of Green's functional.

SINGULAR DESIGNS

Beams

As stated at the outset, the primary focus of this paper is on designs whose stiffness vanishes somewhere in the interior of Ω . For beams whose boundary conditions are specified by (1b), the stiffness vanishes, at most, at two internal locations. Let x_0 denote the typical location for which $S(x_0) = 0$.

In terms of conventional notation for beams, the internal boundary condition at x_0 is the prescription of zero moment, while the matching condition is zero jump in both the shear force and the response. Thus

$$S(x) G_{xx}(x, y; x_0) \big|_{x=x_0} = 0 \quad (11a)$$

$$[[S(x)G_{xx}(x, y; x_0)]_x]_{x=x_0} = 0 \quad (11b)$$

$$[[G(x, y; x_0)]]_{x=x_0} = 0 \quad (11c)$$

where the subscripts denote partial differentiation with respect to the indicated arguments, and $[[\cdot]]$ denotes the jump in the quantity within the double brackets. In addition, at the extremities of the beam, G must meet the static and kinematic boundary conditions specified by equation (4b).

If the neighboring design $S + \delta S$ also vanishes at x_0 , then δS is specified by equation (10). If, however, $S + \delta S$ vanishes at $x_0 + \delta x_0$, then δG depends explicitly upon δx_0 as well as δS . Since the sensitivity of G with respect to δS is determined by equation (10), it remains to investigate the sensitivity of G to variations in x_0 .

With x_0 treated as the design variable, the counterpart to equation (5) becomes

$$\Delta G(x, y; x_0, \Delta x_0) \equiv G(x, y, x_0 + \Delta x_0) - G(x, y; x_0)$$

which, upon linearization, simplifies to

$$\delta G = G_{x_0}(x, y; x_0) \delta x_0 \quad (12)$$

It is important to note that G will generally have a slope discontinuity at x_0 , but $G + \delta G$ will have a slope discontinuity at $x_0 + \delta x_0$. It follows from equation (6) that δG satisfies

$$(S\delta G_{xx})_{xx} = 0 \quad 0 < x < x_0, \quad x_0 < x < L \quad (13)$$

plus appropriate homogeneous boundary conditions at $x=0$ and L . Due to the shift in the internal boundary x_0 , care must be taken in determining the internal matching conditions for δG . While G satisfies equations (11a), (11b) and (11c), $G + \delta G$ must satisfy

$$S(G + \delta G)_{xx} \big|_{x=x_0 + \delta x_0} = 0 \quad (14a)$$

$$[[S(G + \delta G)_{xx}]_x]_{x=x_0 + \delta x_0} = 0 \quad (14b)$$

$$[[G + \delta G]]_{x=x_0 + \delta x_0} = 0 \quad (14c)$$

Next, SG_{xx} is expanded in a Taylor series about x_0 to get

$$SG_{xx} \big|_{x_0 + \delta x_0} = SG_{xx} \big|_{x=x_0} + (SG_{xx})_x \big|_{x_0} \delta x_0$$

which, by virtue of equations (11a) and (14a), becomes

$$-S\delta G_{xx} \big|_{x=x_0} = (SG_{xx})_x \big|_{x=x_0} \delta x_0 \quad (15a)$$

Similarly, by expanding $(SG_{xx})_x$ and G about $x = x_0$, and making use of equations (11b), (11c), (13), (14b) and (14c), the following jump conditions are obtained:

$$[[S\delta G_{xx}]_x]_{x=x_0} = 0 \quad (15b)$$

$$[[\delta G]]_{x=x_0} = - [[G_x]]_{x=x_0} \delta x_0 \quad (15c)$$

The sensitivity δG is completely specified by equations (13), (15a), (15b), (15c) and the boundary conditions at $x=0$ and $x=L$. After multiplying both sides of equation (13) by G and integrating the result over the domains $0 < x < x_0$ and $x_0 < x < L$, it is found that

$$\begin{aligned} \delta G(z, y) = & [[G(x, z)(S(x)\delta G_{xx}(x, y))_x]]_{x=x_0} \\ & - [[G_x(x, z)S(x)\delta G_{xx}(x, y)]]_{x=x_0} \\ & + [[S(x)G_{xx}(x, z)\delta G_x(x, y)]]_{x=x_0} \\ & - [[(S(x)G_{xx}(x, z))_x\delta G(x, y)]]_{x=x_0} \end{aligned} \quad (16)$$

Equation (16) can be considerably simplified by making use of the jump conditions (11a,b,c) and (15a,b,c). The first term on the right hand side of equation (16) vanishes by virtue of equations (11c) and (15b); the third term also vanishes as a consequence of equation (11a). Now, substitution of equation (15a) into the second term, and equations (11b) and (15c) into the fourth term yield

$$\begin{aligned} \delta G(y, z) = & - \{ [[G_x(x, z)]]_{x=x_0} \bar{Q}(x_0, y) \\ & + [[G_x(x, y)]]_{x=x_0} \bar{Q}(x_0, z) \} \delta x_0 \end{aligned} \quad (17)$$

where $\bar{Q}(x_0, y)$ is the shear force at x_0 due to a unit load at y . Thus

$$\bar{Q}(x_0, y) = - (S(x) G_{xx}(x, y))_x|_{x=x_0} \quad (18)$$

The design derivative of Green's function, obtained from equations (12) and (18), becomes

$$\begin{aligned} \partial G(x, y; x_0) / \partial x_0 = & - [[G_x(x, z)]]_{x=x_0} \bar{Q}(x_0, y) \\ & - [[G_x(x, y)]]_{x=x_0} \bar{Q}(x_0, z) \end{aligned} \quad (19)$$

Axisymmetric Circular Plates

Thin isotropic elastic plates, like the elastic beams considered above, obey the fundamental equations (4a) and (4b). Consequently, the sensitivity of Green's function with respect to changes in the plate stiffness (thickness) must satisfy equation (10). For simplicity, only circular plates subject to axisymmetric loads and boundary conditions are considered. The plates may be full or annular, and the inner and outer boundaries of the plate will be denoted by a and b , respectively. For full plates, $a=0$. If the stiffness of the plate vanishes over a circle of radius r_0 and this radius is also a design parameter, then the sensitivity of G with respect to r_0 also must be determined.

At a circle of vanishing stiffness, the radial bending moment vanishes, and both the shear force and the response are continuous. Thus the counterparts to equations (11a), (11b) and (11c) are, respectively,

$$\begin{aligned} S(r)\{rG_{rr}(r,\zeta;r_0) + vG_r(r,\zeta;r_0)\}|_{r=r_0} &= 0 \\ [[r(S(r)(rG_{rr}(r,\zeta;r_0) + vG_r(r,\zeta;r_0)))_r \\ - S(r)(G_r(r,\zeta;r_0) + v r G_{rr}(r,\zeta;r_0))]]_{r=r_0} &= 0 \\ [[G(r,\zeta;r_0)]]_{r=r_0} &= 0 \end{aligned} \quad (20)$$

where v is Poisson's ratio. And, of course, Green's function must still satisfy the mixed boundary conditions (4b).

Since r_0 is now the design variable, equation (12) is replaced by

$$\delta G = G_{r_0}(r,\zeta;r_0)\delta r_0 \quad (21)$$

where δr_0 denotes the infinitesimal shift in the location of vanishing stiffness.

It is desired to obtain an explicit representation for δG , analogous to equation (17). Toward this end, it is noted that δG satisfies $L\delta G=0$ and therefore

$$(S(r\delta G_{rr} + v\delta G_r))_{rr} - (S(r^{-1}\delta G_r + v\delta G_{rr}))_r = 0 \quad (22)$$

for $a < r < r_0$ and $r_0 < r < b$. Also δG satisfies the same boundary conditions at a and b as does G .

Before considering the jump conditions for δG at $r=r_0$, some notational simplification can be obtained by noting that $G(r,\zeta;r_0)$ represents the response at the circle of radius r due to a unit load distributed along the circle of radius ζ . Accordingly, let $\bar{M}(r,\zeta;r_0)$ and $\bar{Q}(r,\zeta;r_0)$ denote, respectively, the radial bending moment and shear force per unit length along the radius r due to the same unit load acting along the radius ζ . Thus equations (20) simplify to

$$r\bar{M}(r,\zeta;r_0)|_{r=r_0} = 0 \quad (23a)$$

$$[[\bar{Q}(r,\zeta;r_0)]]_{r=r_0} = 0 \quad (23b)$$

$$[[G(r,\zeta;r_0)]]_{r=r_0} = 0 \quad (23c)$$

For the sake of completeness, it is noted that \bar{M} and \bar{Q} are related to G through

$$\begin{aligned} r\bar{M} &= -S(rG_{rr} + vG_r) \\ r\bar{Q} &= -r(S(rG_{rr} + vG_r)) \\ &\quad + S(G_r + v r G_{rr}) \end{aligned} \quad (24)$$

For the varied design whose stiffness vanishes at $r_0 + \delta r_0$, the jump conditions analogous to (23a), (23b) and (23c) are, respectively,

$$r\bar{M}(r, \zeta; r_0) + r\delta\bar{M}(r, \zeta; r_0)|_{r=r_0+\delta r_0} = 0 \quad (25a)$$

$$[[r\bar{Q}(r, \zeta; r_0) + r\delta\bar{Q}(r, \zeta; r_0)]]_{r=r_0+\delta r_0} = 0 \quad (25b)$$

$$[[G(r, \zeta; r_0) + \delta G(r, \zeta; r_0)]]_{r=r_0+\delta r_0} = 0 \quad (25c)$$

By expanding $r\bar{M}|_{r=r_0+\delta r_0}$, $r\bar{Q}|_{r=r_0+\delta r_0}$ and $G|_{r=r_0+\delta r_0}$ in Taylor series about $r=r_0$, and simplifying the result using equations (25a), (25b) and (25c), the jump conditions

$$r\delta\bar{M}|_{r=r_0} = - (r\bar{M})_r|_{r=r_0} \delta r_0 \quad (26a)$$

$$[[r\delta\bar{Q}]]_{r=r_0+\delta r_0} = 0 \quad (26b)$$

$$[[\delta G]]_{r=r_0} = - [[G_r]]_{r=r_0} \delta r_0 \quad (26c)$$

are readily obtained. The quantities $\delta\bar{M}$ and $\delta\bar{Q}$ are implicitly defined through equations (24). Thus

$$\begin{aligned} r\delta\bar{M} &= - S(r\delta G_{rr} + v\delta G_r) \\ r\delta\bar{Q} &= - r(S(r\delta G_{rr} + v\delta G_r))_r \\ &\quad + S(\delta G_r + vr\delta G_{rr}) \end{aligned} \quad (27)$$

The sensitivity δG may now be determined explicitly by multiplying both sides of equation (22) by G and integrating the result from $r=a$ to $r=b$. Thus

$$\begin{aligned} \delta G(\zeta, \xi) &= + [[r\bar{Q}(r, \zeta)\delta G(r, \xi)]]_{r=r_0} \\ &\quad - [[r\bar{M}(r, \zeta)\delta G_r(r, \xi)]]_{r=r_0} \\ &\quad + [[G_r(r, \zeta) r\delta\bar{M}(r, \xi)]]_{r=r_0} \\ &\quad - [[G(r, \zeta)r\delta\bar{Q}(r, \xi)]]_{r=r_0} \end{aligned} \quad (28)$$

The second and fourth terms on the right hand-side of equation (28) vanish by virtue of equation (23a) and equations (23c) and (26b), respectively. Moreover, equations (26c) and (26b) transform the first term into

$$- r\bar{Q}(r, \zeta)|_{r=r_0} [[G_r(r, \xi)]]_{r=r_0} \delta r_0$$

while the third term, obtained from equation (26a) and the equilibrium equation, becomes

$$- r\bar{Q}(r, \xi)|_{r=r_0} [[G_r(r, \zeta)]]_{r=r_0} \delta r_0$$

Therefore, the design derivative $\partial G/\partial r_0$ is given by

$$\begin{aligned} \partial G(\zeta, \xi; r_0)/\partial r_0 &= - \{ r_0\bar{Q}(r_0, \zeta)[[G_r(r, \xi)]]_{r=r_0} \\ &\quad + r_0\bar{Q}(r_0, \xi)[[G_r(r, \zeta)]]_{r=r_0} \} \end{aligned} \quad (29)$$

The usual method of obtaining structural optimality criteria associated with specific cost functionals relies on developing an appropriate variational formulation of the field equations (1a) and (1b). Moreover, each cost functional requires a different variational formulation. In contrast to the historical approaches, the design derivatives specified by equations (10) and (17) or (29) can be used directly to determine the optimality criteria associated with any cost functional without the need of a variational formulation. In order to illustrate the foregoing claim, structural optimality criteria will be derived for two different cost functionals: minimum response and minimum compliance.

The optimality criteria associated with the design of a fixed-weight structure for minimum response at a specified location is considered first. Boundary conditions and loads are assumed known. It is desired to obtain a complete description of the design variable S including its singular points (locations of vanishing stiffness). Shield and Prager (ref. 5) obtained the optimality condition for this problem only after discovering the principle of stationary mutual potential energy. They did not address the question of locating the singular points. However, at least one author (ref. 6) incorrectly assumed that such points can be obtained by requiring the response to be continuously differentiable everywhere.

Attention is now directed toward equation (1a) and (1b) with $g = h = 0$. According to equation (3), the solution for the response is

$$u = (f, G)_{\Omega}$$

Let the location y be specified and $u(y)$ be a minimum. Thus

$$u(y) = (f(\cdot), G(\cdot, y))_{\Omega} \quad (30)$$

whence

$$\delta u(y) = (f(\cdot), \delta G(\cdot, y))_{\Omega} \quad (31)$$

For the moment, it will be assumed that S is not singular anywhere. After substituting equation (10) into equation (31) and changing the order of the resulting double integration, equation (31) becomes

$$\delta u(y) = - (Tu, \frac{\partial E}{\partial S} \delta STG(\cdot, y))_{\partial \Omega} \quad (32)$$

The volume constraint may be easily handled through a Lagrange multiplier. Let $v(S)$ denote the specific volume and λ a Lagrange multiplier. Then the condition $\delta u(y) = 0$ for all designs consistent with the constant volume constraint requires that the augmented functional

$$- (Tu, \frac{\partial E}{\partial S} \delta STG(\cdot, y))_{\partial \Omega} + \lambda (1, \frac{\partial v}{\partial S} \delta S)_{\Omega} = 0$$

for all variations δS . Thus the optimality condition

$$Tu \cdot \frac{\partial E}{\partial S} \cdot TG(\cdot, y) = \lambda \frac{\partial v}{\partial S} \quad (33)$$

follows immediately. For beams, the equivalent to equation (33) was obtained in reference 5. The constant λ appearing in equation (33) can be determined from the fixed-volume constraint.

It was stated earlier that, in many applications, there can be no solution to the optimality and field equations unless a singular point occurs within the structure. In this case it is not possible to determine the location of the singularity from the optimality condition and field equations. This location must be considered an additional design variable, and consequently its location will be determined from an additional optimality condition.

For simplicity, it will be assumed that the structure is a beam. In this case, equation (17) is substituted into equation (31), and the resulting double integrals are evaluated by reversing the order of the integrations. Thus

$$\begin{aligned} \delta u(y) = & - Q(x_0)[[G_z(z,y)]]_{z=x_0} \delta x_0 \\ & - \bar{Q}(x_0,y)[[u_z(z)]]_{z=x_0} \delta x_0 \end{aligned} \quad (34)$$

Since the specific volume v is independent of x_0 , the optimality condition to determine x_0 is obtained directly from equation (34). Thus

$$\begin{aligned} Q(x_0)[[G_z(z,y)]]_{x=x_0} \\ + \bar{Q}(x_0,y)[[u_z(z)]]_{x=x_0} = 0 \end{aligned} \quad (35)$$

Next, consider the problem of minimizing the compliance of a structure. The compliance C is defined to be the work done by the external loads. Thus

$$C = (u, f)_{\Omega}$$

whence

$$\delta C = (\delta u, f)_{\Omega} \quad (36)$$

Substitution of equation (32) into equation (36) yields

$$\delta C = - (Tu, \frac{\partial E}{\partial S} \delta S Tu)_{\Omega}$$

Consequently, the optimality condition for prescribed volume becomes

$$Tu \cdot \frac{\partial E}{\partial S} \cdot Tu = \lambda \frac{\partial v}{\partial S} \quad (37)$$

Equation (37), in its various specific forms, has been derived by many authors for specific structures. In virtually all instances, the principle of minimum potential energy has been an ingredient necessary to the derivation.

The location of any singular points may be determined in the same way that it was done for the minimum response design. In this case, equation (34) is substituted into equation (36) to yield

$$\delta C = - 2Q(x_0)[[u_z(z)]]_{z=x_0} \delta x_0$$

The optimality condition to determine x_0 , therefore, is

$$[[u_z(z)]]_{z=x_0} = 0 \quad (38)$$

As a final remark, it is pointed out, without elaboration, that the approach taken in this paper is easily generalized to transient structures.

REFERENCES

1. Reiss, R.; and Haug, E.J.: Extremum Principles for Linear Initial-Value Problems of Mathematical Physics. Int. J. Engrg. Sci., vol. 16, 1978, pp. 231-251.
2. Oden, J.T.; and Reddy, J.N.: Variational Methods in Theoretical Mechanics. Springer-Verlag, Berlin, 1976.
3. Roach, G.F.: Green's Functions: Introductory Theory with Applications. Van-Nostrand Reinhold, London, 1970.
4. Reiss, R.: On the Design Derivative of Green's Functional. Eighteenth Mid-western Mechanics Conference, Iowa City, May 1983.
5. Shield, R.T.; and Prager, W.: Optimal Structural Design for Given Deflection J. App. Math. Phys. (ZAMP), vol. 21, 1970, pp. 513-523.
6. Huang, N.C.; and Tang, H.T.: Minimum-Weight Design of Elastic Sandwich Beams with Deflection Constraints, vol. 4, 1969, pp. 277-298.

3-D MODELING AND AUTOMATIC REGRIDDING
IN SHAPE DESIGN SENSITIVITY ANALYSIS*

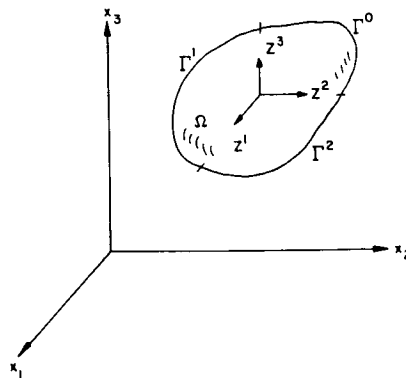
Kyung K. Choi and Tse-Min Yao
The University of Iowa
Iowa City, Iowa

The material derivative idea of continuum mechanics (Ref. 1) and the adjoint variable method of design sensitivity analysis are used to obtain a computable expression for the effect of shape variations on measures of structural performance of three-dimensional elastic solids (Ref. 2).

Consider the three-dimensional elastic solid shown in Figure 1, with the shape of the domain Ω as a design variable. In Figure 1, $z = [z^1, z^2, z^3]^T$ is the displacement field and Γ^0 , Γ^1 , and Γ^2 are clamped, traction free, and loaded boundaries, respectively.

Using the principle of virtual work, the variational equilibrium equation for the elastic solid can be obtained (Ref. 3), where $\sigma^{ij}(z)$ and $\epsilon^{ij}(\bar{z})$ are the stress tensor due to a displacement z and the strain tensor due to a kinematically admissible virtual displacement \bar{z} , respectively, $f = [f^1, f^2, f^3]^T$ is the body force, $T = [T^1, T^2, T^3]^T$ is the traction force, and Z is the space of kinematically admissible virtual displacement. When the Galerkin method is applied to the variational equilibrium equation for approximate solution, an approximate finite-element equation is obtained.

THREE DIMENSIONAL ELASTIC SOLID



- Principle of Virtual Work:

$$\begin{aligned} a_{\Omega}(z, \bar{z}) &= \iiint_{\Omega} \left[\sum_{i,j=1}^3 \sigma^{ij}(z) \epsilon^{ij}(\bar{z}) \right] d\Omega \\ &= \iiint_{\Omega} \left[\sum_{i=1}^3 f^i \bar{z}^i \right] d\Omega + \iint_{\Gamma^2} \left[\sum_{i=1}^3 T^i \bar{z}^i \right] d\Gamma = l_{\Omega}(\bar{z}), \end{aligned}$$

for all $\bar{z} \in Z$

- FEM Equation is an approximate equation of the variational equation.

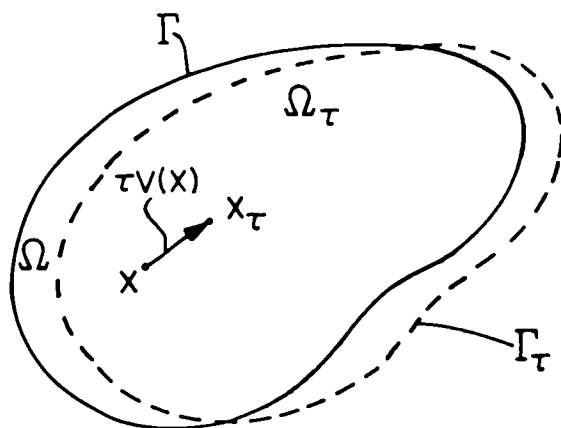
Figure 1

*Research supported by NASA Langley Grant NAG-1-215

Since the shape of domain Ω of the elastic solid is treated as the design variable, it is convenient to think of Ω as a continuous medium and utilize the material derivative idea of continuum mechanics. The process of deforming Ω to Ω_τ by mapping $\Omega_\tau = T(\Omega, \tau)$ may be viewed as a dynamic process of deforming a continuum, with τ playing the role of time. A design velocity field can be considered as a perturbation of design variable (Refs. 2 and 4).

Suppose $z_\tau(x_\tau)$ is a solution of the variational equilibrium equation on the deformed domain Ω_τ . Then the mapping $z_\tau(x_\tau) \equiv z_\tau(x + \tau v(x))$ is defined on Ω and $z_\tau(x_\tau)$ depends on τ in two ways. First, it is the solution of the boundary-value problem on Ω_τ . Second, it is evaluated at a point x_τ that moves with τ . Existence of the pointwise material derivative \dot{z} is shown in Ref. 2. If z_τ has a regular extension to a neighborhood U_τ of the closure $\bar{\Omega}_\tau$ of Ω_τ , then the partial derivative z' exists. One attractive feature of the partial derivative is that, with smoothness assumptions, it commutes with the derivative with respect to x_i (Ref. 2). (Fig. 2.)

VARIATION OF DOMAIN



$$x_\tau = T(x, \tau) = x + \tau V(x)$$

$$\Omega_\tau = T(\Omega, \tau)$$

$$V(x_\tau) \equiv \frac{dx_\tau}{d\tau} = \frac{\partial T(x, \tau)}{\partial \tau}$$

$$\begin{aligned} \dot{z} &= \frac{d}{d\tau} z_\tau(x + \tau V(x)) \Big|_{\tau=0} = \lim_{\tau \rightarrow 0} \frac{z_\tau(x + \tau V(x)) - z(x)}{\tau} \\ &= z'(x) + \nabla z^T V(x) \end{aligned}$$

$$\left(\frac{\partial z}{\partial x_i} \right)' = \frac{\partial}{\partial x_i} (z'), \quad i = 1, 2, 3$$

Figure 2

A common form of structural performance measure involves stress in an elastic solid. Consider a locally averaged stress functional ψ_p over a small subdomain $\Omega_p \subset \Omega$ of the elastic solid, as shown in Figure 3, where $g(\sigma)$ is a stress measure such as von Mises stress or principal stress and m_p is a characteristic function that has a constant value on Ω_p and its integral is 1. The averaged stress measure depends on shape of the domain in two ways; first directly on the domain over which the integral is carried out and second on the stress σ that, in turn, depends on the displacement field z .

Taking the first variation of ψ_p , using material derivative formulas of Refs. 2 and 5, ψ'_p is obtained. To obtain an explicit expression for ψ'_p in terms of the velocity field V , a variational adjoint equation is introduced by replacing $z \in Z$ by a virtual displacement $\bar{\lambda} \in Z$ and equating terms involving $\bar{\lambda}$ to the energy bilinear form $a_\Omega(\lambda, \bar{\lambda})$, yielding the variational adjoint equation for the adjoint variable λ .

STRESS SHAPE SENSITIVITY

$$\begin{aligned}\psi_p &= \iiint_{\Omega_p} g(\sigma(z)) m_p d\Omega = \frac{\iiint_{\Omega_p} g(\sigma(z)) d\Omega}{\iiint_{\Omega_p} d\Omega} \\ \psi'_p &= \iiint_{\Omega_p} \left[\sum_{i,j=1}^3 g_{\sigma^{ij}}(z) \sigma^{ij}(\dot{z}) \right] m_p d\Omega \\ &\quad - \iiint_{\Omega_p} \left[\sum_{i,j=1}^3 \left[\sum_{k,\ell=1}^3 g_{\sigma^{ij}}(z) c^{ijkl} (\nabla z^k \nabla_\ell z) \right] \right] m_p d\Omega \\ &\quad + \iiint_{\Omega_p} g \operatorname{div} V m_p d\Omega - \iiint_{\Omega_p} g m_p d\Omega \iiint_{\Omega_p} m_p \operatorname{div} V d\Omega \\ a_\Omega(\lambda, \bar{\lambda}) &= \iiint_{\Omega} \left[\sum_{i,j=1}^3 g_{\sigma^{ij}}(z) \sigma^{ij}(\bar{\lambda}) \right] m_p d\Omega, \quad \text{for all } \bar{\lambda} \in Z\end{aligned}$$

Figure 3

Using the adjoint variable method of design sensitivity analysis (Refs. 2 and 4) and the domain method of Ref. 5, an explicit and computable expression for ψ'_p in terms of the velocity field V is obtained. Evaluation of the design sensitivity ψ'_p requires the solution z of the original variational equation and the adjoint variable λ of the variational adjoint equation. This is an efficient calculation, using finite-element analysis, if the original variational equation for z has already been solved, requiring only evaluation of the solution of the same set of finite-element equations with a different right side, called an adjoint load.

For problems with smooth data in which stress is continuous, design sensitivity analysis results can be used for a pointwise stress functional. To obtain the formula, shrink the subdomain Ω_p to a point \hat{x} , where $\hat{x} \in \Omega$. In this case, the characteristic function becomes the Dirac delta measure.^p

Even though sensitivity analysis results for only a stress functional are presented here, the method is also applicable for displacement at a specified point \hat{x} and eigenvalue design sensitivity analysis, as shown in Refs. 2 and 5. (Fig. 4.)

$$\begin{aligned}\psi'_p &= \ell'_V(\lambda) - a'_V(z, \lambda) \\ &= \iiint_{\Omega} \sum_{i,j=1}^3 \left[\sum_{k,l=1}^3 g_{\sigma^{ij}}(z) C^{ijkl} (\nabla z^k \nabla^T v_l) \right] m_p d\Omega \\ &\quad + \iiint_{\Omega} g \operatorname{div} v_m d\Omega - \iiint_{\Omega} g m_p d\Omega \iiint_{\Omega} m_p \operatorname{div} v d\Omega \\ a'_V(z, \lambda) &= - \iiint_{\Omega} \sum_{i,j=1}^3 [\sigma^{ij}(z) (\nabla \lambda^i \nabla^T v_j) + \sigma^{ij}(\lambda) (\nabla z^i \nabla^T v_j)] d\Omega \\ &\quad + \iiint_{\Omega} \left[\sum_{i,j=1}^3 \sigma^{ij}(z) \epsilon^{ij}(\lambda) \right] \operatorname{div} v d\Omega \\ \ell'_V(\lambda) &= \iiint_{\Omega} \sum_{i=1}^3 \lambda^i (\nabla f^i \nabla^T v) d\Omega + \iiint_{\Omega} \left[\sum_{i=1}^3 f^i \lambda^i \right] \operatorname{div} v d\Omega \\ &\quad + \iint_{\Gamma^2} \left\{ - \sum_{i=1}^3 T^i (\nabla \lambda^i \nabla^T v) + \left(\nabla \left[\sum_{i=1}^3 T^i \lambda^i \right] \cdot n + H \left[\sum_{i=1}^3 T^i \lambda^i \right] \right) (\nabla^T n) \right\} d\Gamma\end{aligned}$$

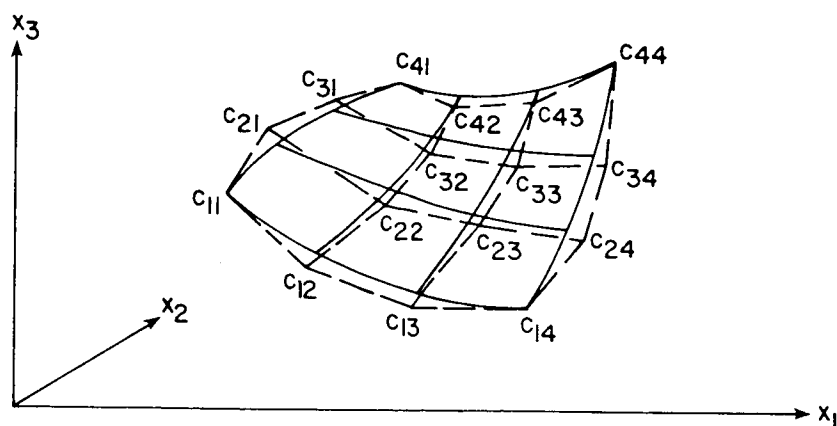
- Pointwise stress functional can be treated for problems with smooth data.

Figure 4

For numerical implementation of shape design sensitivity analysis, the boundary Γ of the domain Ω must be parameterized. There are several methods to parameterize the boundary Γ (Ref. 6). Since the result of shape optimization depends on the parameterization method used, it must be general and flexible enough to represent a large class of structural shapes. It is desirable that the parameterization method has the following properties: smoothness, fairness, required order of continuity, controllability in global and local senses, and a variation diminishing property. Among several parameterization methods, Bezier and B-spline surfaces are commonly used (Ref. 6). Both Bezier and B-spline surfaces use a set of blending functions and are defined in terms of characteristic polyhedra.

Points $p_{x_i}(v,w)$, $i = 1,2,3$, on a Bezier surface are constructed by taking linear combinations of a set of blending functions $B_{m,M}(v)$ and $D_{n,N}(w)$ and x_i coordinates c_{mnx_i} of control points (vertices of the characteristic polyhedron). A Bezier surface represented by a 4×4 array of points is shown in Figure 5. If a Bezier surface is used, positions c_{mnx_i} of the control points are shape design parameters.

MODELING FOR SHAPE (BEZIER SURFACE)



$$p_{x_i}(v,w) = \sum_{m=0}^M \sum_{n=0}^N c_{mnx_i} B_{m,M}(v) D_{n,N}(w), \quad i = 1,2,3$$

- Positions c_{mnx_i} of the control points are shape design parameters.

Figure 5

The next step is to develop a general method of defining and computing a velocity field in the domain, in terms of the perturbations of the positions of control points. It is shown in Ref. 7 that regularity of the velocity field must be at least at the level of regularity of the displacement field of the structure. This suggests use of displacement shape functions to systematically define the velocity field in the domain. Moreover, a velocity field that obeys the governing (elliptic) equation of the structure can be selected. That is, a perturbation of the boundary can be considered as a displacement at the boundary. With no additional external forces and a given displacement at the boundary, the finite-element equation can be used to find the displacement (domain velocity) field, where $\{V_b\}$ is the given perturbation of nodes on the boundary, $\{V_d\}$ is the node velocity vector in the interior of the domain, and $\{f_b\}$ is the fictitious boundary force acting on the varying boundary.

To use ψ' in Figure 4 for sensitivity computation, first perturb design parameter b_i (positions of control points), $i=1, 2, \dots, k$, a unit magnitude to obtain a boundary perturbation $\{V_b\}$. Then domain velocity $\{V_d\}$ is obtained. Using $\{V_d\}$ and displacement shape functions, ψ' in Figure 4 can be evaluated, which gives $\partial\psi/\partial b_i$. This method requires k solutions of the velocity equation. However, much as in adjoint analysis, this is an efficient calculation, requiring only evaluation of the solution of the same set of finite-element equations with a different right side for each unit perturbation of b_i , $i=1, 2, \dots, k$. (Fig. 6.)

AUTOMATIC REGRIDDING FOR SHAPE DESIGN

- Regularity of the velocity field must be the same as that of the displacement field
- Use of displacement shape functions to define velocity field
- Velocity field gives transformation mapping $T(x, \tau)$

$$\begin{bmatrix} K_{bb} & K_{bd}^T \\ K_{bd} & K_{dd} \end{bmatrix} \begin{Bmatrix} V_b \\ V_d \end{Bmatrix} = \begin{Bmatrix} f_b \\ 0 \end{Bmatrix}$$

$$[K_{dd}] \{V_d\} = - [K_{bd}] \{V_b\}$$

- Solve above equation k -times
- Excellent for boundary layer and/or substructuring technique

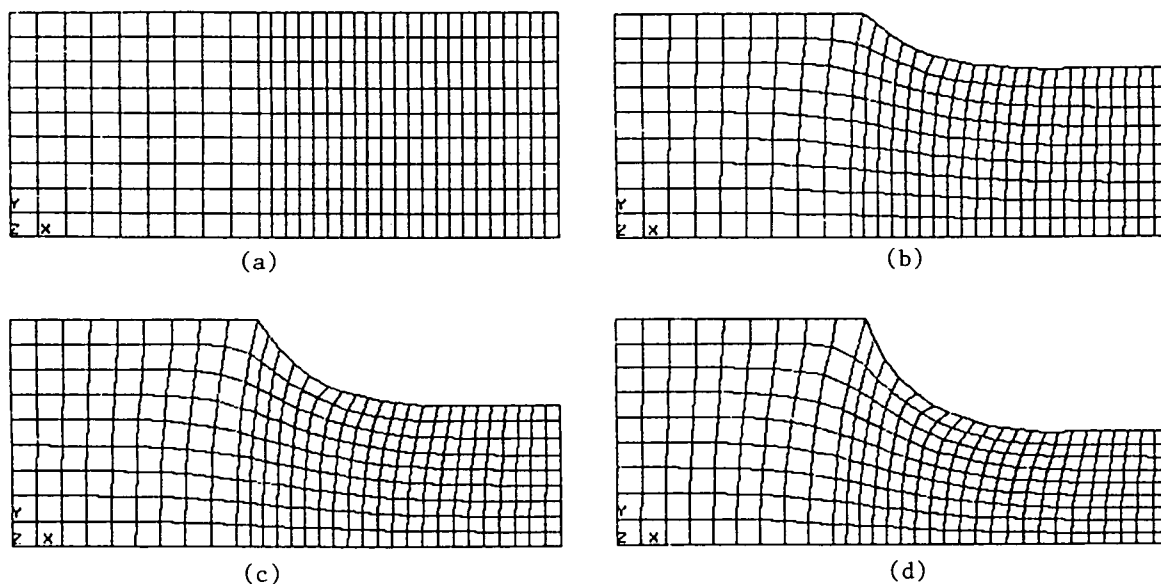
Figure 6

The automatic regridding method presented in Figure 6 can be used with the boundary-layer approach (Ref. 8) and/or substructuring techniques very effectively. That is, if a large portion of the structure is fixed, except for the boundary layer (or substructure), then the part of $\{V_d\}$ that corresponds to the fixed portion can be set equal to zero, thus reducing the dimension of $[K_{dd}]$.

Once a design change has been determined using an iterative design process, regridding of interior grid points can be carried out using $\{V_d\}$. If the initial grid is optimized using an adaptive method (Ref. 9), the regridding method presented will tend to avoid distortion of the finite elements.

To illustrate use of the automatic regridding method, a fillet problem (Figure 7) is used. In Figure 7, regridding is performed at three stages. It is interesting to observe that the method has a tendency to maintain orthogonality of the elements. That is, if the initial grid is regular, then the deformed grid tends to be regular. Also, the method presented can be utilized as mesh generator. That is, starting from a regular shape with a regularly patterned mesh (Figure 7(a)), the present method can be used to generate a mesh (Figure 7(d)) directly (Ref. 10).

AUTOMATIC REGRIDDING FOR FILLET PROBLEM



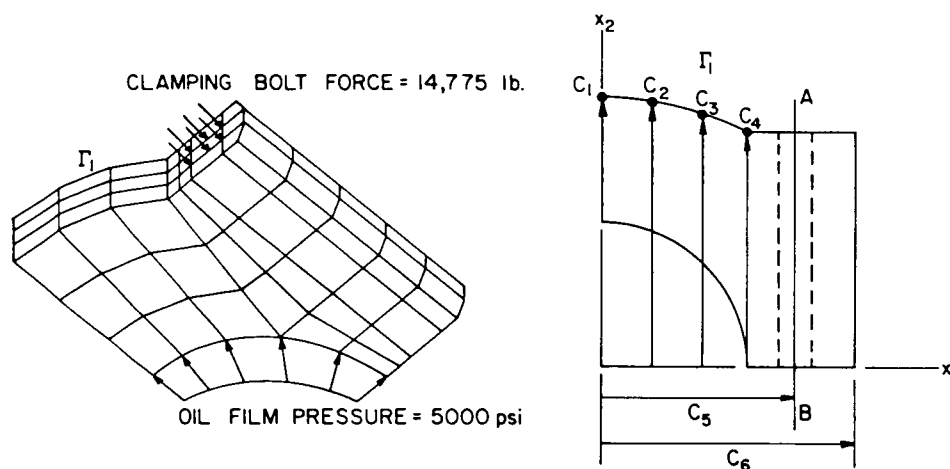
- The method can also be used as a mesh generator.

Figure 7

To demonstrate use of the automatic regriding method for shape design, an engine bearing cap (Ref. 11), subject to oil film pressure and a bolt load, is treated (Figure 8). Oil film pressure is a radial pressure loading, assumed to be uniform. The engine bearing cap is modeled as a three dimensional elastic solid. Due to symmetry, only the right half of the cap is analyzed. The finite-element configuration and loading conditions are shown in Figure 8. The material used is steel, with Young's modulus and Poisson's ratio of $E = 1.0 \times 10^7$ psi and $\nu = 0.3$, respectively. The finite-element model shown in Figure 8 contains 82 elements, 768 nodal points, and 2111 active degrees of freedom. For analysis and design velocity fields, the ANSYS finite-element STIF 95 (Ref. 12), which is a 20-node isoparametric element, is used. As in Ref. 13, implementation of design sensitivity analysis is performed outside the ANSYS finite element code.

The shape design variables for this problem are: The shape of the varying surface Γ_1 , distance c_5 of clamping bolt center line AB, and distance c_6 of edge from the cap centerline. For surface Γ_1 , a Bezier surface with a 4×4 array of points is used. For simplicity, only x_2 -coordinates of four control points c_1 through c_4 are allowed to vary. That is, surface Γ_1 has curvature in the x_1 -direction only.

ENGINE BEARING CAP



- ANSYS STIF95 (20-Node Isoparametric element)
- 82 elements, 768 nodes, and 2111 active DOF

Figure 8

The expression for design sensitivity ψ'_p of averaged von Mises stress over individual finite elements is given in Figure 4, where $g(\sigma)$ is von Mises stress. Define ψ_p^1 and ψ_p^2 as the functional values for the initial design b and modified design $b + \delta b$, respectively. Let $\Delta\psi_p = \psi_p^2 - \psi_p^1$ and let ψ'_p be the predicted difference from sensitivity analysis. The ratio $\psi'_p/\Delta\psi_p$ times 100 is used as a measure of accuracy; i.e., 100% means that the predicted change is exactly the same as the actual change. Notice this accuracy measure will not give meaningful information when $\Delta\psi_p$ is very small compared to ψ_p^1 , because the difference $\Delta\psi_p$ may lose precision due to the subtraction $\psi_p^2 - \psi_p^1$.

Numerical result with a 1% uniform design change; i.e., $\delta b = 0.01 b$, are shown in Figure 9 for randomly selected finite elements. Results given in Figure 9 show excellent agreement between predictions ψ'_p and actual changes $\Delta\psi_p$, except in elements 5 and 57. However, the magnitudes of actual change $\Delta\psi_p$ are small for those elements.

**SHAPE DESIGN SENSITIVITY FOR ENGINE BEARING CAP, $\delta b = 0.01b$
(AVERAGED VON MISES STRESS OVER FINITE ELEMENTS)**

El. No.	ψ_p^1	ψ_p^2	$\Delta\psi_p$	ψ'_p	$(\psi'_p/\Delta\psi_p \times 100)\%$
1	9829.4564	9727.3229	- 102.1335	- 109.7298	107.4
5	11444.4800	11448.0190	3.5390	0.4482	12.7
10	17933.5910	17964.5170	30.9260	29.8750	96.6
14	34270.5140	34294.7650	24.2510	23.7614	98.0
20	12670.2480	12634.3500	- 35.8980	- 38.4216	107.0
26	7311.4083	6999.4094	- 311.9989	- 321.7022	103.1
30	7234.2502	7081.2085	- 153.0417	- 159.7947	104.4
35	13328.4650	13264.9790	- 63.4860	- 59.4243	93.6
39	44231.0680	42109.0220	-2122.0460	-2222.5504	104.7
44	5998.6512	5844.9335	- 153.7177	- 165.1199	107.4
48	6822.9614	6736.9477	- 86.0137	- 90.5011	105.2
53	13634.1000	12964.2560	- 669.8440	- 701.6882	104.8
57	6121.4120	6114.6667	- 6.7453	- 8.1242	120.4
62	7041.7283	6971.4204	- 70.3079	- 79.6051	113.2
66	4787.5653	4761.5085	- 26.0568	- 27.6278	106.0
71	6541.8233	6585.9308	44.1075	45.1422	102.4
75	3820.6962	3843.9362	23.2400	22.5210	96.9
80	6240.3854	6285.3485	44.9631	46.3209	103.0

Unit: psi

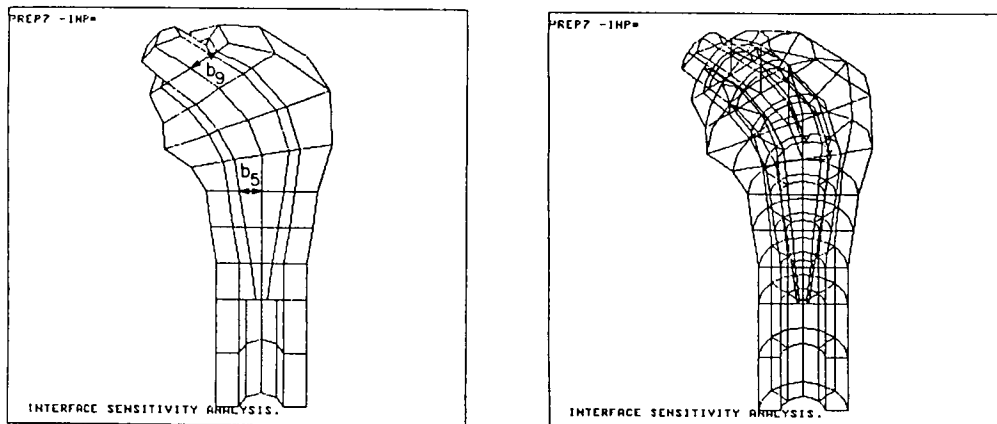
Figure 9

A total hip reconstruction consists of a three-dimensional elastic solid composed of cement, a metal stem, and cortical and trabecular bone (Figure 10). For simplicity, cortical and trabecular bone are modeled with the same material properties. Young's moduli and Poisson's ratios for metal stem, cement, and bone are: $E^1 = 207 \text{ GPa}$, $\nu^1 = 0.3$, $E^2 = 2.07 \text{ GPa}$, $\nu^2 = 0.23$, and $E^3 = 14.0 \text{ GPa}$, $\nu^3 = 0.3$, respectively.

The femur model shown in Figure 10 is obtained by approximating the real cadaver femur model of Ref. 14 with piecewise linear conical solids. For simplicity, structural and loading symmetries are assumed. Therefore, only half of the model is analyzed. A vertical load of 4000 N is applied at the tip of the metal stem.

The finite-element model consists of 16 elements for the metal stem, 28 elements for the cement, and 36 elements for the bone. ANSYS element STIF 95 is used for all finite elements. The model has 525 nodes and 1335 active degrees of freedom. The model is assumed to be fixed at the distal end of the bone.

TOTAL HIP RECONSTRUCTION (IMPLANT DESIGN)



- Pointwise stress and strain energy density at interface.
- 16 elements for stem, 28 elements for cement, and 36 elements for bone (all ANSYS STIF95).
- 525 nodes and 1335 active DOF.

Figure 10

There are 16 shape design parameters: b_1 through b_8 are the radius of the metal stem and b_9 through b_{16} are the radius of the outer surface of the cement, at different locations along the center line. Thus, $b_{i+8} - b_i$, $i=1,2,\dots,8$ is the thickness of the cement at those locations. The shape of the outer surface of the bone does not change.

The principal stress is used as a design failure criteria for the metal stem and bone, whereas strain energy density is considered as the design failure criteria for cement.

Shape design sensitivity results for pointwise principal stress in the stem at the stem-cement interface are given in Figure 11, for a 5% design change in design parameter b_5 . The pointwise stress is measured at a Gauss point (out of 9 Gauss points) on stem-cement interface of each stem finite element.

Results presented in Figure 11 show excellent agreement between predictions ψ'_p and actual changes $\Delta\psi_p$, except in element 6. However, the magnitude of actual change $\Delta\psi_p$ is small compared to the magnitude of ψ_p^1 for this element, so accuracy of the difference is questionable.

SHAPE DESIGN SENSITIVITY FOR IMPLANT DESIGN, $\delta b_5 = 0.05b_5$
(POINTWISE PRINCIPAL STRESS IN THE STEM AT THE STEM-CEMENT INTERFACE)

El. No.	ψ_p^1	ψ_p^2	$\Delta\psi_p$	ψ'_p	$(\psi'_p/\Delta\psi_p \times 100)\%$
1	65.75792800	65.74896400	-0.00896400	-0.00875783	97.70
2	77.13410600	77.24745600	0.11335000	0.11608011	102.41
3	58.03037400	58.53323000	0.50285600	0.52206340	103.82
4	77.00421000	79.96762700	2.96341700	3.01203420	101.64
5	151.71708000	146.27679000	-5.44029000	-5.35753070	98.48
6	234.54156000	234.78980000	0.24824000	0.68237420	274.88
7	288.65995000	291.58509000	2.92514000	3.00576120	102.76
8	149.94087000	149.70614000	-0.23473000	-0.25492036	108.60
9	20.76092900	20.75818400	-0.00274500	-0.00277719	101.17
10	6.23888850	6.22105300	-0.01783550	-0.01811896	101.59
11	3.99426970	3.91787910	-0.07639060	-0.07985700	104.54
12	6.25765390	6.73601410	0.47836020	0.48739250	101.89
13	15.90449700	15.06538300	-0.83911400	-0.91444092	108.98
14	23.77727200	23.71259200	-0.06468000	-0.06987854	108.04

Unit: MPa

Figure 11

Shape design sensitivity results for pointwise strain energy density of cement on the bone-cement interface are given in Figure 12, for a 5% design change in design parameter b_9 . The pointwise strain energy density is measured at one of the Gauss points at the bone-cement interface of each cement finite element.

Results presented in Figure 12 show excellent agreement between predictions ψ'_p and actual changes $\Delta\psi_p$, except in element 41. However, the magnitude of $\Delta\psi_p$ for this element is small compared to others.

Even though results of sensitivity analysis of a pointwise principal stress in the stem and pointwise strain energy density in the cement are given, for variations of one design parameter for each, variations of all other design parameters yield similar results. Shape design sensitivity results for pointwise principal stress in the bone at the bone-cement interface and for pointwise strain energy density in the cement at the stem-cement interface are found to be excellent.

SHAPE DESIGN SENSITIVITY FOR IMPLANT DESIGN, $\delta b_9 = 0.05b_9$
(POINTWISE STRAIN ENERGY DENSITY IN THE CEMENT AT THE BONE-CEMENT INTERFACE)

El. No.	ψ_p^1	ψ_p^2	$\Delta\psi_p$	ψ'_p	$(\psi'_p/\Delta\psi_p \times 100)\%$
17	2.693386	2.864695	0.171309	0.185526	108.30
18	1.324330	1.346854	0.022525	0.025306	112.35
19	1.358676	1.373181	0.014505	0.016123	111.15
20	2.968939	2.965287	-0.003652	-0.003972	108.76
21	6.532172	6.527846	-0.004325	-0.004688	108.39
22	6.197117	6.196119	-0.000998	-0.001068	107.01
23	12.301795	12.302323	0.000528	0.000569	107.74
38	5.474089	5.847445	0.373356	0.398447	106.72
39	2.187812	2.236401	0.048590	0.053682	110.48
40	2.045186	2.077065	0.031879	0.034058	106.83
41	3.616023	3.616629	0.000606	0.000478	78.88
42	10.974028	10.976652	0.002624	0.002725	103.84
43	16.638003	16.640659	0.002656	0.002837	106.81
44	22.454411	22.455967	0.001556	0.001666	107.05

Unit: kJ/m^3

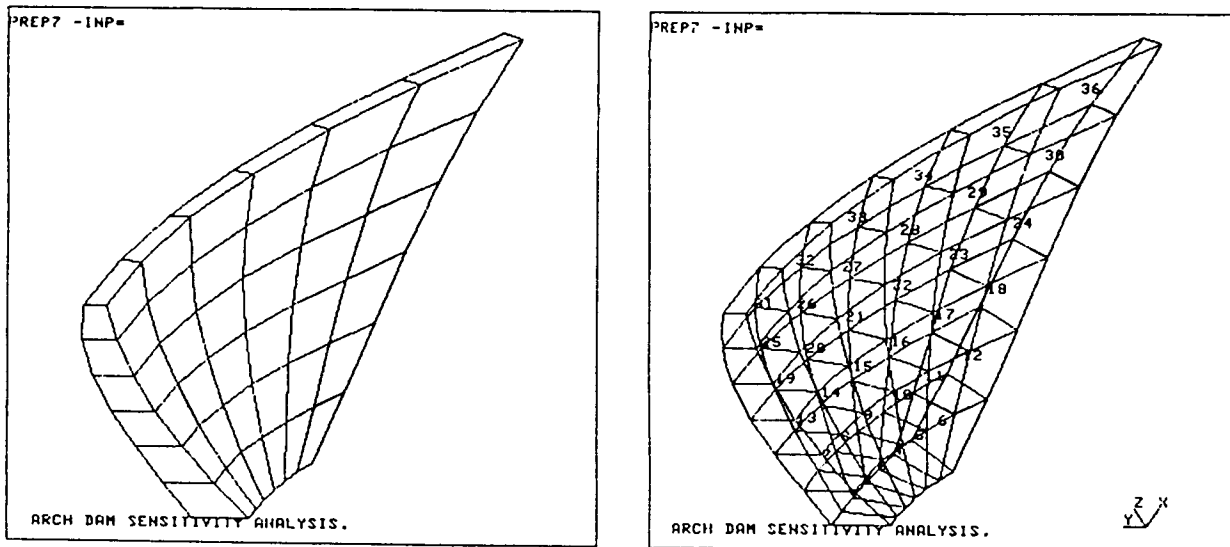
Figure 12

A doubly curved arch dam (Figure 13) that is similar to one treated by Wassermann (Ref. 15) is optimized using higher order finite-element approximation and the continuum shape design sensitivity analysis method presented here.

The dam structure and loading conditions are assumed to be symmetric with respect to the crown cross section. Thus, only half of the dam is analyzed. Also, it is assumed that the dam foundation is rigid, and the gravel concrete is homogeneous and behaves elastically. Concrete's elasticity modulus and Poisson's ratio are $E = 21.0 \text{ GPa}$ and $\nu = 0.2$, respectively. Water and concrete weight densities are 10.0 kN/m^3 and 24.0 kN/m^3 , respectively.

To parameterize two surfaces (water and free sides), Bezier surface parameterization is used with a 4×4 array of points. For a shape design parameter, the x_2 -coordinates of 32 control points are selected. The dam finite-element model contains 36 ANSYS STIF 95 elements, 315 nodal points, and 726 active degrees of freedom.

DOUBLY CURVATURED ARCH DAM



- 36 elements (ANSYS STIF95), 315 nodes, and 726 active DOF.

Figure 13

The principal stress is used as a design failure criteria. Principal stresses are measured at Gauss points on the surface of the dam (8 Gauss points for each finite element). Design sensitivity analysis results are tested for pointwise principal stresses. Excellent agreement between predictions and actual changes is obtained.

The optimal design problem for the doubly curved arch dam is to minimize the volume of the dam, subject to constraints on pointwise principal stress on the surface of dam and thickness at the top of the dam. For iterative optimization, Pshenichny's linearization method (Ref. 16) is used. History of cost function and maximum constraint violation is shown in Figure 14. After 17 design iterations, cost is reduced from an initial value of 253,566 m³ to 182,583 m³ and the maximum tensile stress is reduced from an initial value of 3.084 MPa to 1.981 MPa.

OPTIMIZATION OF DOUBLY CURVATURED ARCH DAM

- Minimize volume subject to:
Principal stress; $-10 \text{ MPa} < \psi_i < 2 \text{ MPa}$, $i = 1, 288$
Dam thickness; $6\text{m} < t_j$, $j = 1, 4$

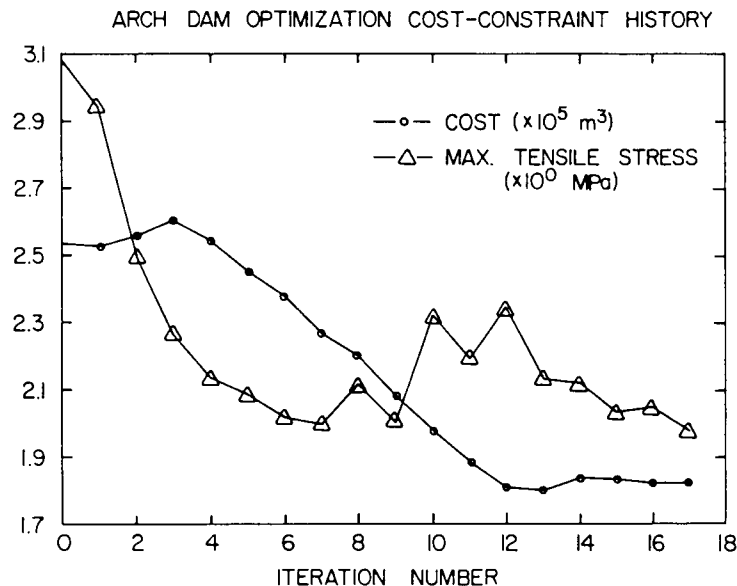


Figure 14

A profile of the final design is shown in Figure 15. The final design shown in Figure 15 is rather different from Wasserman's design (Ref. 15), mainly in the bottom portion of the dam. The final design obtained here had developed a fillet in the bottom corner, which is not observed in Wasserman's design.

In the crown cross section shown in the Figure 15, the middle portion is thinner than the top portion. From stress distribution in the final design, it is observed that the maximum tensile stress in this middle portion is well below the critical value of 2 MPa. Another interesting observation is that the compressive stress limit of -10 MPa has never been violated. In fact, at the final design, the maximum compressive stress is -5.202 MPa.

A PROFILE OF THE FINAL DESIGN

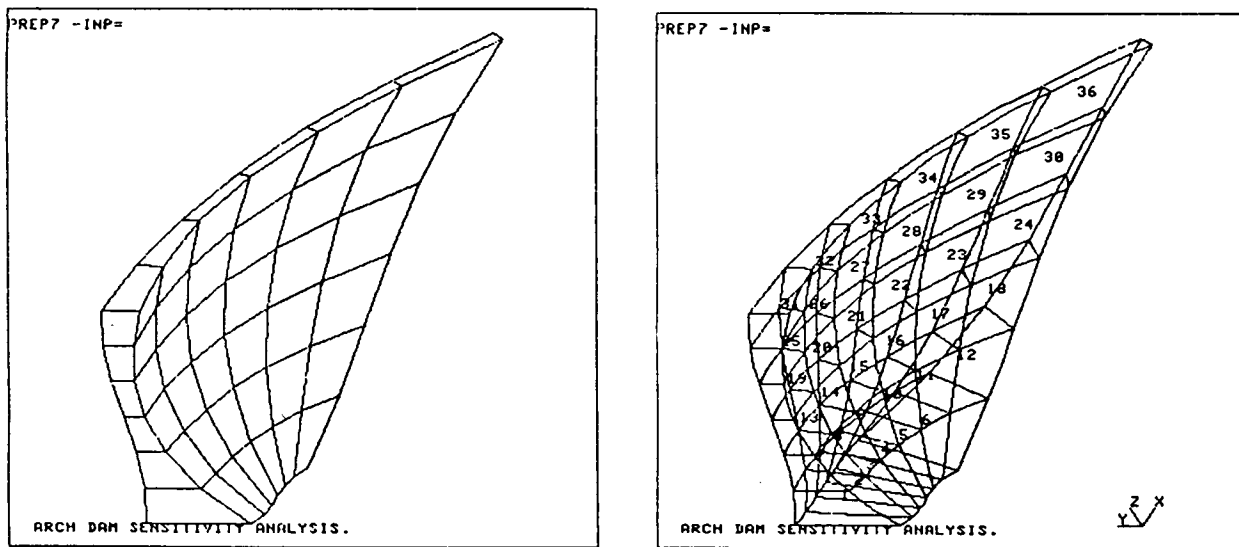


Figure 15

REFERENCES

1. Zolesio, J.P., "The Material Derivative (or Speed) Method for Shape Optimization," Optimization of Distributed Parameter Structures, (Eds., E.J. Haug and J. Cea), Sijthoff and Noordhoff, Alphen ann den Rijn, The Netherlands, 1981, pp. 1089-1151.
2. Haug, E.J., Choi, K.K., and Komkov, V., Design Sensitivity Analysis of Structural Systems, Academic Press, New York, N.Y., 1986.
3. Fung, Y.C., Foundations of Solid Mechanics, Prentice-Hall, Inc., Englewood Cliffs, N.J., 1965.
4. Choi, K.K. and Haug, E.J., "Shape Design Sensitivity Analysis of Elastic Structures," Journal of Structural Mechanics, 11(2), 1983, pp. 231-269.
5. Choi, K.K. and Seong, H.G., "A Domain Method for Shape Design Sensitivity Analysis of Built-Up Structures," Computer Methods in Applied Mechanics and Engineering, 56, 1986.
6. Mortenson, M.E., Geometric Modeling, John Wiley and Sons, New York, N.Y. 1985.
7. Choi, K.K. and Seong, H.G., "A Numerical Method for Shape Design Sensitivity Analysis and Optimization of Built-Up Structures," The Optimum Shape: Automated Structural Design, (Eds. J.A. Bennett and M.E. Botkin), Plenum Press, New York, 1986.
8. Seong, H.G. and Choi, K.K., "Boundary Layer Approach to Shape Design Sensitivity Analysis,": J. of Struct. Mech., 1987.
9. Kikuchi, N., "Adaptive Grid-Design Methods for Finite Element Analysis," Comp. Meth. in Appl. Mech. and Eng., 55, 1986, pp. 129-160.
10. Thompson, J.F., Warsi, Z.U.A., and Mastin, C.W., "Boundary-Fitted Coordinate Systems for Numerical Solution of Partial Differential Equations - A Review," Journal of Computational Physics, 47, 1982, pp. 1-108.
11. Imam, M.H., Three-Dimensional Shape Optimization, General Motors Research Laboratories, Research Publications, GMR3675, 1981.
12. DeSalvo, G.J. and Swanson, J.A., ANSYS Engineering Analysis Systems, Users Manual, Swanson Analysis System, Inc., P.O. Box 65, Houston, PA, Vols. I and II, 1985.
13. Choi, K.K., Santos, J.L.T., and Frederick, M.C., "Implementation of Design Sensitivity Analysis with Existing Finite Element Codes," ASME Journal of Mechanisms, Transmissions, and Automation in Design, 85-DET-77.

14. Crowningshield, R.D. and Wilson, M.A., A Design Analysis of Bone Cements Used in Total Hip Reconstruction, A Report to Howmedica Inc., Biomechanics Laboratory, The University of Iowa, Iowa City, November, 1982.
15. Wassermann, K., "Three Dimensional Shape Optimization of Arch Dams With Prescribed Shape Functions," J. of Struct. Mech., 11(4), 1983, pp. 465-489.
16. Choi, K.K., Haug, E.J., Hou, J.W., and Sohoni, V.N., "Pshenichny's Linearization Method for Mechanical System Optimization," ASME Journal of Mechanisms, Transmissions, and Automation in Design, 106(3), 1984, pp. 415-419.

Accuracy of the Domain Method for the Material Derivative

Approach to Shape Design Sensitivities

R. J. Yang and M. E. Botkin
General Motors Research Laboratories
Warren, Michigan

Abstract

Numerical accuracy for the boundary and domain methods of the material derivative approach to shape design sensitivities is investigated through the use of mesh refinement. The results show that the domain method is generally more accurate than the boundary method, using the finite element technique. It is also shown that the domain method is equivalent, under certain assumptions, to the implicit differentiation approach not only theoretically but also numerically.

Introduction

Haug and Choi et al. ¹⁻⁴ developed a unified theory of structural design sensitivity analysis for linear elastic structures, using a variational formulation of the structural state equations. This theory allows one to take the total derivative, or material derivative, of the variational state equation and to use an adjoint variable technique for design sensitivity analysis. The main attraction of this approach is that it allows one to compute the derivatives of structural performances analytically. No discretization approximations are involved during the derivation, and a step size need not be specified in the calculation. However, the formulation requires evaluating accurate stress quantities on the boundaries which are often difficult to obtain.

Accuracy of the shape design sensitivity theory was studied in Ref. 5 through the equilibrium condition for different types of finite elements. However, a systematic study through the refinement of the finite element mesh was still not found in the literature.

To improve the accuracy of shape design sensitivities, Choi et al. ⁶ proposed a new domain method which transforms the boundary integrals into domain integrals and therefore is less influenced by the the inaccurate boundary stress evaluation. This method takes advantage of the averaging nature of the finite element method, and is found to be more accurate than the boundary approach which evaluates the derivatives using boundary information only ¹⁻³. However, a velocity field for the physical domain needs to be defined. The necessity of defining the domain velocity may indicate that this method is closely related to the implicit differentiation approach which also requires knowledge about the domain change for differentiation of the elemental stiffness matrix ⁷.

In this paper, the accuracy of the design sensitivity is studied through finite element mesh refinement for a cantilever thin plate. Results of the domain and boundary methods for the material derivative approach and the implicit differentiation approach are shown and compared.

In a previous paper ⁸, the boundary integral formulation was shown to be equivalent to the implicit differentiation approach, theoretically. In this report, the domain method is shown to be equivalent to the implicit differentiation method, both in theoretical and numerical aspects.

Shape Design Sensitivity Analysis

Two approaches for shape design sensitivity analysis are found in the literature. One is the well known implicit differentiation approach and the other is the variational or material

derivative approach. Detailed information for these two approaches is available in Refs. 4, 7, and 8. Only a brief background is provided in the following.

For the implicit differentiation approach, the displacement sensitivity is obtained by differentiating the discretized structural system of equations

$$Kz = F \quad (1)$$

By assuming that the force vector F is independent of design, this leads to

$$\frac{\partial z}{\partial b_i} = -K^{-1} \frac{\partial K}{\partial b_i} z \quad (2)$$

where K is the global stiffness matrix, z is the displacement vector, and b_i is the design variable.

The variational design sensitivity theory uses the material derivative concept of continuum mechanics and an adjoint variable method to obtain computable expressions for the effect of shape variation on the functionals arising in the shape design problem. The variation of the displacement functional ψ with respect to shape change is derived by differentiating the variational equilibrium equation and employing the adjoint variable method, to obtain¹⁻⁴

$$\delta\psi = \int_{\Gamma} \sigma^{ij}(z) \epsilon^{ij}(\lambda) V_k n_k d\Gamma \quad (3)$$

where ψ is defined by

$$\psi = \int_{\Omega} z \delta(x - \bar{x}) d\Omega \quad (4)$$

in which \bar{x} is the point of interest, δ the Dirac-measure at zero, Ω the physical domain, σ^{ij} and ϵ^{ij} the stress and strain tensors, respectively, V the design perturbation and can be thought of as velocity, and n_k the unit normal vector of moving boundary Γ . The vectors z and λ are the displacement vectors for state and adjoint equations, respectively, which can be expressed as follows:

$$\int_{\Omega} \sigma^{ij}(z) \epsilon^{ij}(\bar{z}) d\Omega = \int_{\Gamma^2} T_i \bar{z}_i d\Gamma \quad (5)$$

$$\int_{\Omega} \sigma^{ij}(\lambda) \epsilon^{ij}(\bar{\lambda}) d\Omega = \int_{\Omega} \delta(x - \bar{x}) \bar{\lambda} d\Omega \quad (6)$$

where T_i is a traction vector, Γ^2 a loaded boundary, and $-$ indicates the virtual displacements that satisfy the kinematically admissible displacement field. The Einstein summation convention for a repeated index is used throughout this paper.

To obtain Eq. 3, the traction vector T_i , the kinematically constrained boundary, and the loaded boundary are assumed to be fixed during the design process, i.e., they are independent of design. Note that the variation of the displacement functional of Eq. 3 is only affected by the normal movement of the boundary of the physical domain.

Physically, the adjoint equation of Eq. 6 is interpreted by applying a unit load at the point \bar{x} , where the displacement sensitivity is of interest. In Eq. 3, one sees that only the boundary stress information is needed for evaluating the variation of the displacement functional. Unfortunately, finite element analysis usually does not provide high quality stress results, especially on the boundary. It has been shown that better finite element results give better design sensitivity estimates, by examining the equilibrium equations for different finite elements⁵.

Domain Method

The basic idea for the domain integral method is to take advantage of the averaging nature of the finite element method, instead of evaluating the less accurate stresses on the boundary. Since the finite element method is well known to provide better solutions inside the finite element, the domain method has the advantage of predicting better sensitivities.

Applying the same procedure as in obtaining Eq. 3 with the domain method, the first variation of the displacement constraint functional of Eq. 4, is obtained as ^{4,6}

$$\delta\psi = \int_{\Omega} [\sigma^{ij}(\lambda) z_{i,k} V_{k,j} + \sigma^{ij}(z) \lambda_{i,k} V_{k,j} - \sigma^{ij}(z) \epsilon^{ij}(\lambda) V_{k,k}] d\Omega \quad (7)$$

One should note that Eq. 7 is more general than Eq. 3, since only the loaded boundary is assumed to be fixed, while both loaded and kinematically constrained boundaries are assumed to be unchanged in Eq. 3. The kinematically constrained boundary and interface boundary terms appear when the divergence theorem is used to transform the domain integral to the boundary integral. It was shown in Ref. 6 that for an interface or built-up structure problem this method simplifies the formulation and avoids specifying tedious interface conditions and provides increased accuracy for shape design sensitivities.

To have a better understanding of Eq. 7, each term will be examined individually. First, since the stress tensor σ^{ij} is symmetric, the first term of Eq. 7 is divided into two parts and then integrated by parts to obtain

$$\begin{aligned} \int_{\Omega} \sigma^{ij}(\lambda) z_{i,k} V_{k,j} d\Omega &= \int_{\Omega} \sigma^{ij}(\lambda) \frac{1}{2} [z_{i,k} V_{k,j} + z_{j,k} V_{k,i}] d\Omega \\ &= \int_{\Gamma} \sigma^{ij}(\lambda) \frac{1}{2} [z_{i,k} V_{k,j} n_j + z_{j,k} V_{k,i} n_i] d\Gamma \\ &\quad - \int_{\Omega} \sigma^{ij}(\lambda) \frac{1}{2} [z_{i,kj} + z_{j,ki}] V_k d\Omega \end{aligned} \quad (8)$$

By assuming that only the free boundary is varied, the first term of Eq. 8 disappears, since the traction vector is zero, i.e., $\sigma^{ij}(\lambda) n_j = \sigma^{ij}(\lambda) n_i = 0$. The second term of Eq. 8 then can be further modified to

$$\begin{aligned} \int_{\Omega} \sigma^{ij}(\lambda) \frac{1}{2} [z_{i,kj} + z_{j,ki}] V_k d\Omega &= \int_{\Omega} \sigma^{ij}(\lambda) \frac{1}{2} [z_{i,jk} + z_{j,ik}] V_k d\Omega \\ &= \int_{\Omega} \sigma^{ij}(\lambda) \epsilon^{ij}_{,k}(z) V_k d\Omega \end{aligned} \quad (9)$$

where the velocity V_k can be parametrized as $(\partial x_k / \partial b_i) \delta b_i$, in which x_k is the position vector and b_i is the design variable. Since all the integrals are linear in design, one can eliminate δb_i or choose the value as a unit number. By interpreting the adjoint variable λ as the inverse of the reduced stiffness matrix K if all the displacement sensitivities are desired, Eq. 9 is discretized, using the finite element formulation, as⁸

$$\begin{aligned} \int_{\Omega} \sigma^{ij}(\lambda) \epsilon^{ij}_{,k}(z) V_k d\Omega &= K^{-1} \sum_1^{N_e} \int_{\Omega_e} B^T D B_{,k} \frac{\partial x_k}{\partial b_i} z d\Omega \\ &= K^{-1} \sum_1^{N_e} \int_{\Omega_e} B^T D B'_i z d\Omega \end{aligned} \quad (10)$$

where the subscript i with a prime superscript indicates the derivative with respect to the i^{th} design variable. K , D , and B represent the stiffness, elasticity, and strain recovery matrices, respectively. The stress-displacement and strain-displacement relationships are employed in obtaining Eq. 10, which are defined in the following

$$\begin{aligned}\sigma^{ij}(\lambda) &= DB\lambda \\ \epsilon^{ij}(z) &= Bz\end{aligned}\quad (11)$$

Finally, the first term of Eq. 7 is written as

$$\int_{\Omega} [\sigma^{ij}(\lambda) z_{i,k} V_{k,j}] d\Omega = -K^{-1} \sum_1^{N_e} \int_{\Omega_e} B^T DB'_i z d\Omega \quad (12)$$

The second term of Eq. 7 can also be derived in the same way to obtain a similar expression as in Eq. 12 as

$$\int_{\Omega} [\sigma^{ij}(z) \lambda_{i,k} V_{k,j}] d\Omega = -K^{-1} \sum_1^{N_e} \int_{\Omega_e} B_i^{T'} DB z d\Omega \quad (13)$$

Substituting Eqs. 12 and 13 into Eq. 7, the following expressions are obtained

$$\begin{aligned}\delta\psi &= \frac{\partial z}{\partial b_i} \\ &= \int_{\Omega} [\sigma^{ij}(\lambda) z_{i,k} V_{k,j} + \sigma^{ij}(z) \lambda_{i,k} V_{k,j} - \sigma^{ij}(z) \epsilon^{ij}(\lambda) V_{k,k}] d\Omega \\ &= -K^{-1} \sum_1^{N_e} \int_{\Omega_e} B^T DB'_i z + B_i^{T'} DB z + B^T DB z V_{k,k} d\Omega \\ &= -K^{-1} \sum_1^{N_e} \left(\int_{\Omega_e} B^T DB'_i + B_i^{T'} DB + B^T DB V_{k,k} d\Omega \right) z \\ &= -K^{-1} \left(\sum_1^{N_e} \int_{-1}^{+1} \int_{-1}^{+1} \int_{-1}^{+1} [B^T DB'_i + B_i^{T'} DB + B^T DB V_{k,k}] |J| d\xi d\eta d\zeta \right) z\end{aligned}\quad (14)$$

where $|J|$ is the determinant of the Jacobian matrix J which transforms the undeformed configuration into the natural coordinate system. The constraint functional change $\delta\psi$ is equal to $\partial z / \partial b_i$, since all displacement sensitivities are calculated and the design change δb_i is chosen as a unit number.

For the implicit differentiation approach of Eq. 2, the derivative of the global stiffness matrix can be evaluated at the elemental level, i.e.,

$$\begin{aligned}\frac{\partial z}{\partial b_i} &= -K^{-1} \frac{\partial K}{\partial b_i} z \\ &= -K^{-1} \left(\sum_1^{N_e} K_i^{e'} \right) z\end{aligned}\quad (15)$$

where $K_i^{e'}$ is calculated numerically in natural coordinates as ⁷

$$K_i^{e'} = \int_{-1}^{+1} \int_{-1}^{+1} \int_{-1}^{+1} \left[B_i^{T'} DB | J | + B_i^T DB' | J | + B^T DB | J |'_i \right] d\xi d\eta d\zeta \quad (16)$$

Comparing Eqs. 14 and 15, one sees that both are equivalent if the following expression is valid.

$$| J |'_i = | J | V_{k,k} \quad (17)$$

To prove Eq. 17 is true, one should notice that the determinant of the Jacobian can be separated into two parts. The first contribution is from the deformed to undeformed configuration, denoted by $| J |_d$, which depends on design. The other is the contribution of transformation from the undeformed global to local or natural configurations, denoted by $| J |$, which is independent of design. The relationship is expressed in the following form

$$| J |_\tau = | J |_d | J | \quad (18)$$

where τ denotes the deformed configuration. Differentiating Eq. 18 with respect to design, one obtains

$$| J |'_\tau = | J |'_d | J | \quad (19)$$

It was shown in Ref. 4 that $| J |'_d = V_{k,k}$ at $\tau = 0$, if the design change is assumed to be equal to a unit vector. Thus, Eq. 19 is identical to the form of Eq. 17, and the equivalence of Eqs. 14 and 15 is proved.

Another way to prove the validity of Eq. 17 is to carry out the differentiation directly by the definition of the Jacobian. Consider a two-dimensional case as an example, the right side of Eq. 17 is obtained as

$$\begin{aligned} | J | V_{k,k} &= \left(\frac{\partial x}{\partial \xi} \frac{\partial y}{\partial \eta} - \frac{\partial x}{\partial \eta} \frac{\partial y}{\partial \xi} \right) \left(\frac{\partial V_x}{\partial x} + \frac{\partial V_y}{\partial y} \right) \\ &= \frac{\partial y}{\partial \eta} \frac{\partial V_x}{\partial \xi} + \frac{\partial x}{\partial \xi} \frac{\partial V_y}{\partial \eta} - \frac{\partial y}{\partial \xi} \frac{\partial V_x}{\partial \eta} - \frac{\partial x}{\partial \eta} \frac{\partial V_y}{\partial \xi} \end{aligned} \quad (20)$$

where the velocity V_x and V_y are defined as

$$\begin{aligned} V_x &= \frac{\partial x}{\partial b_i} \\ V_y &= \frac{\partial y}{\partial b_i} \end{aligned} \quad (21)$$

Substituting Eq. 21 into Eq. 20, the following expression is obtained

$$\begin{aligned} | J | V_{k,k} &= \frac{\partial}{\partial b_i} \left(\frac{\partial x}{\partial \xi} \frac{\partial y}{\partial \eta} - \frac{\partial y}{\partial \xi} \frac{\partial x}{\partial \eta} \right) \\ &= | J |'_i \end{aligned} \quad (22)$$

This simple calculation also verifies that the relationship of Eq. 17 is valid. Note that the design change δb_i is assumed to be unity in Eq. 17.

Numerical Verification and Comparison

In this section, the equivalence of the domain method and the implicit differentiation is verified through a simple example. The accuracy of design sensitivities will be examined and compared through the refinement of the finite element mesh.

A simple two-dimensional thin plate is considered as an example. The finite element configuration, dimensions, material properties, loading condition, and design variable are shown in Fig. 1. Design variable b is chosen to move the upper traction free boundary. The load of 100 lb is applied parabolically at the right of the plate.

An 8-noded two-dimensional plane stress isoparametric element is employed for analysis. The boundary stresses and strains that appear in Eq. 3 are computed by extrapolating linearly from the stresses at Gauss points, where the optimal or the best approximate stresses are located. Numerical results for design sensitivity of point A in the Y-direction for 1x1, 2x2, 3x3, 4x4, 5x5 and 6x6 meshes are shown in Table 1.

In Table 1, column 1 represents different finite element meshes and column 2 the displacement of point A in the Y-direction for the initial design, b . Columns 3 and 4 represent the displacement sensitivities at point A of Fig. 1, using the boundary method (BM) of Eq. 3 and the domain integral (DM) of Eq. 7, respectively, for different meshes. Column 5 has the results using the implicit differentiation approach (IDA) of Eq. 2. The derivative of the global stiffness matrix is carried out by differentiating the element stiffness matrix, analytically.

Fig. 2 shows the same results as in Table 1. From Fig. 2 and Table 1, one observes that the displacements and the sensitivities for the implicit approach (IDA) do not change much after 3x3 finite element mesh. However, the design sensitivity for the boundary method of the variational approach (BM) is still increasing at the limit of mesh refinement. This implies that the boundary method (BM) is more sensitive to the finite element results, although it provides the analytical formulation for sensitivities. And one concludes that the boundary method of the variational approach tends to yield better gradient estimates, once a more accurate analysis is used and better boundary stresses are obtained. The same conclusion is also found in Refs. 5 and 8.

Comparing column 4 with 5, one sees that the domain method results (DM) are very close to those obtained from the analytical implicit differentiation approach (IDA). Clearer interpretation can be observed from Fig. 2, which plots the displacement and displacement sensitivity versus finite element mesh size. This numerical agreement verifies the equivalence of the two approaches.

In Ref. 8, the boundary **the method was shown to be theoretically equivalent to the implicit approach**, however, they yield slightly different results numerically as also shown in Table 1 and Fig. 2. The difference results from different numerical schemes for these two approaches, i.e., one uses the boundary, and the other the domain information. If consistent numerical schemes are used **for the domain method and the implicit approach as in this report**, they are shown to be equivalent, not only theoretically but also numerically.

The disadvantage of the domain method is in computational aspects. Numerical evaluation of Eq. 7 is more complicated than evaluation of Eq. 3, because Eq. 7 requires integration over the entire domain, whereas Eq. 3 requires integration only over the variable boundary. In addition, a velocity field which satisfies regularity properties must be defined in the domain. The choice of velocity for the physical domain is more difficult than that for the variable boundary. Although, a boundary layer scheme⁹ and a displacement-like velocity field¹⁰ were proposed to alleviate these problems, the domain method still requires more analyst and computational efforts.

Summary

It is shown that accurate finite element analysis results in accurate design sensitivities. For the boundary method of the material derivative approach to shape design sensitivities, the accuracy of the finite element is more crucial, since the finite element method usually does not give accurate stresses on the boundary.

The domain method is generally more accurate than the boundary method in the material derivative approach for evaluating the design sensitivities; however, a velocity field for the physical domain needs to be defined. The necessity of defining a domain velocity field and integrating the domain integral instead of the boundary integral, as in boundary method, requires both more analyst time and computational time.

It is also shown that the domain method is equivalent, under certain assumptions, to the implicit differentiation approach not only theoretically but also numerically. The numerical equivalence is valid only if the numerical methods used for both approaches are consistent.

References

1. Haug, E. J., Choi, K. K., Hou, J. W., and Yoo, Y. M., "A Variational Method for Shape Optimal Design of Elastic Structures," *New Directions in Optimum Structural Design*, Ed. E. Atrek et al., Wiley, New York, 1984.
2. Choi, K. K. and Haug, E. J., "Shape Design Sensitivity Analysis of Elastic Structures," *Journal of Structural Mechanics*, 11(2), pp. 231-269, 1983.
3. Choi, K. K., "Shape Design Sensitivity Analysis of Displacement and Stress Constraints," *Journal of Structural Mechanics*, 13(1), pp. 27-41, 1985.
4. Haug, E. J., Choi, K. K., and Komkov, V., *Design Sensitivity Analysis of Structural Systems*, Academic Press, 1986.
5. Yang, R. J. and Choi, K. K., "Accuracy of Finite Element Based Shape Design Sensitivity Analysis," *Journal of Structural Mechanics*, 13(2), pp. 223-239, 1985.
6. Choi, K. K. and Seong, H. G., "A Domain Method for Shape Design Sensitivity Analysis of Built-up Structures," *Computer Methods in Applied Mechanics and Engineering*, Vol. 57, No. 1, pp. 1-16, 1986.
7. Ramakrishnan, C. V. and Francavilla, A., "Structural Shape Optimization Using Penalty Functions," *Journal of Structural Mechanics*, 3(4), pp. 403-422, 1974-1975.
8. Yang, R. J. and Botkin, M. E., "Comparison between the Variational and Implicit Differentiation Approaches to Shape Design Sensitivities," *AIAA*, Vol. 24, No. 6, pp. 1027-1032, 1986.
9. Haug, E. J. and Choi, K. K., "Material Derivative Methods for Shape Design Sensitivity Analysis," *The Optimum Shape: Automated Structural Design*, Ed. J. A. Bennett and M. E. Botkin, 1986.
10. Choi, K. K. and Seong, H. G., "A Numerical Method for Shape Design Sensitivity Analysis and Optimization of Built-up Structures," *The Optimum Shape: Automated Structural Design*, Ed. J. A. Bennett and M. E. Botkin, 1986.

Table 1. Comparison of Design Sensitivity Accuracy

mesh	displacement	BM	DM	IDA
		dv/db	dv/db	dv/db
1x1	2.495E-5	-4.196E-6	-4.843E-6	-5.248E-6
2x2	2.760E-5	-4.518E-6	-5.167E-6	-5.235E-6
3x3	2.841E-5	-4.856E-6	-5.369E-6	-5.375E-6
4x4	2.845E-5	-4.995E-6	-5.391E-6	-5.394E-6
5x5	2.854E-5	-5.093E-6	-5.412E-6	-5.413E-6
6x6	2.856E-5	-5.158E-6	-5.425E-6	-5.426E-6

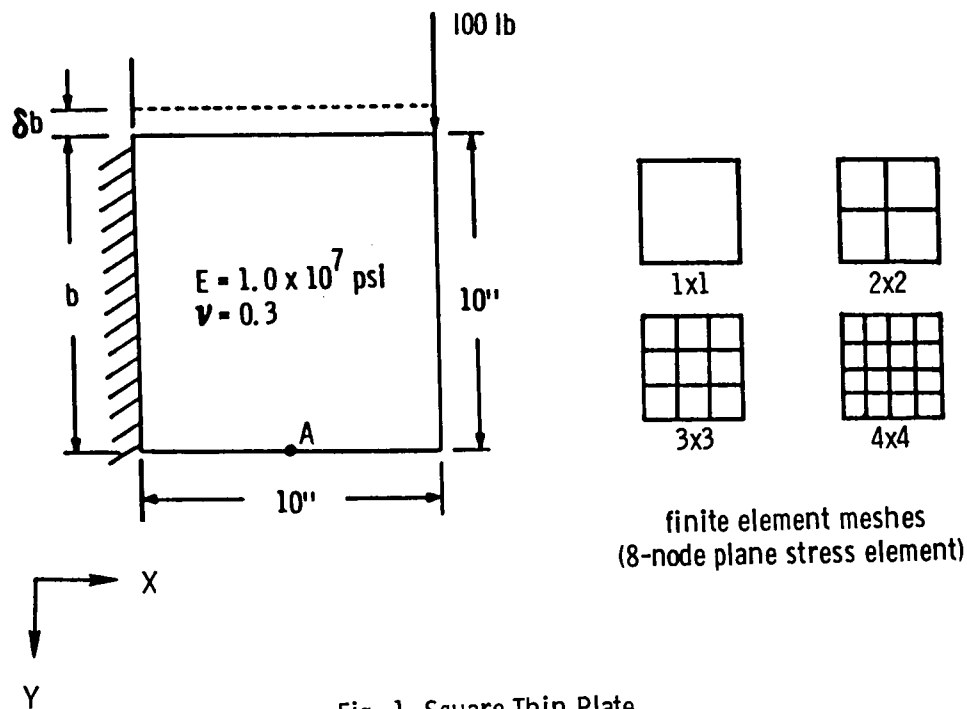


Fig. 1 Square Thin Plate

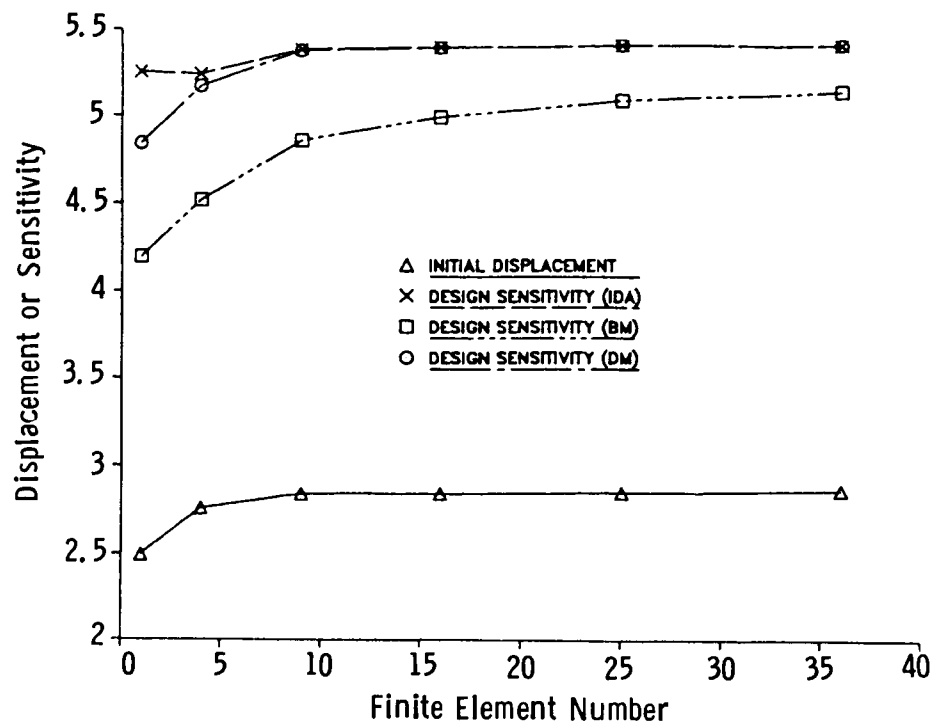


Fig. 2 Accuracy of Design Sensitivity

SENSITIVITY ANALYSIS FOR LARGE-SCALE PROBLEMS

Ahmed K. Noor and Sandra L. Whitworth
George Washington University Center
NASA Langley Research Center
Hampton, Virginia

INTRODUCTION

Due to the wide variety of uses of sensitivity derivatives, the development of efficient computational procedures for the calculation of these derivatives has attracted considerable attention in recent years. The calculation of sensitivity derivatives forms the backbone of many optimization procedures and is the major contributor to the cost and time of optimization of large systems. In addition, sensitivity derivatives have several other applications in structural mechanics including approximate analysis (and reanalysis) techniques, analytical model improvement, and assessment of design trends. A review of the state of the art in sensitivity calculations is contained in a survey paper (Ref. 1), a monograph (Ref. 2), as well as in some papers in these proceedings. Despite all the recent advances made, the calculation of sensitivity derivatives for large structural systems (with large number of degrees of freedom and design variables), is quite expensive even on present-day large computers.

The present study focuses on the development of efficient techniques for calculating sensitivity derivatives. Specifically, the objective and scope of the present paper are listed in Fig. 1. The objective is to present a computational procedure for calculating sensitivity derivatives as part of performing structural reanalysis for large-scale problems. The scope of the paper is limited to framed type structures. Both linear static analysis and free-vibration eigenvalue problems are considered.

Objective

- To present a computational procedure for calculating sensitivity derivatives as part of performing structural reanalysis for large-scale problems

Scope

- Frame-type structures
- Linear static analysis
- Eigenvalue problems

Figure 1

BASIC IDEA AND KEY ELEMENTS OF THE PROPOSED PROCEDURE

The basic idea and the three key elements of the proposed procedure are listed in Fig. 2. The basic idea is to generate the solution of the modified structure using large perturbations from that of the original structure. The three key elements are: a) lumping of the large number of design variables into one (or a small number of) tracing parameters; b) application of operator splitting/reduction technique; and c) for very large problems, use of single-level or multilevel substructuring. Only the first two key elements are discussed in this paper. The application of operator splitting/reduction technique proved to be effective in reducing the computational effort in a number of structural mechanics problems (see, for example, Refs. 3 to 6).

Basic idea

- Solution for modified structure is obtained using large perturbations from that of original structure

Key elements

- Lumping of design variables into tracing parameter(s)
- Application of operator splitting/reduction technique
- Use of multilevel substructuring (for very large problems)

Figure 2

APPLICATION TO LINEAR STATIC ANALYSIS

In Fig. 3 the application of the proposed procedure to linear static analysis is outlined. The governing finite element equations of the original and modified structures are shown. The global stiffness matrices, load vectors, and responses of the original and modified structures are designated by $[K]_0$, $[K]$; $\{P\}_0$, $\{P\}$; and $\{X\}_0$, $\{X\}$, respectively. The original and modified structure characteristics correspond to the values of d_i^0 and d_i^* of the design variables, respectively.

The operator splitting technique is now applied, and the equations of the modified structure are expressed in terms of the original structure equations plus correction terms. A tracing parameter λ is introduced and is attached to the correction terms. The tracing parameter is dimensionless and identifies *all* the design modifications. The original structure equations correspond to $\lambda=0$, and the modified structure equations correspond to $\lambda=1$.

Operator splitting

Original structure

$$[K]_0 \{X\}_0 = \{P\}_0 ; [K]_0 = [K(d_i^0)]_0$$

Modified structure

$$[K] \{X\} = \{P\} ; [K] = [K(d_i^*)]$$

$$\text{or } \left[[K]_0 + \lambda ([K] - [K]_0) \right] \{X\} = \{P\}_0 + \lambda (\{P\} - \{P\}_0)$$

$$\lambda = 0 \rightarrow \text{Original structure}$$

$$\lambda = 1 \rightarrow \text{Modified structure}$$

Figure 3

The response of the modified structure, $\{X\}$, is now expressed as a linear combination of a few preselected global approximation vectors (or modes). This is expressed by the transformation shown in Fig. 4. The columns of the matrix $[\Gamma]$ are the global approximation vectors, and the elements of the vector $\{\psi\}$ are the amplitudes of the approximation vectors which are, as yet, unknowns. Note that the number of global approximation vectors, r , is considerably smaller than the total number of degrees of freedom, n .

A Rayleigh-Ritz technique is now used to approximate the governing equations of the modified structure by a much smaller system of equations in the unknowns $\{\psi\}$.

Basis reduction

$$\{X\}_{n,1} = [\Gamma]_{n,r} \{\psi\}_{r,1} \quad ; \quad r \ll n$$

where $\{\psi\}$ = amplitudes of global approximation vectors

Reduced system of equations

Rayleigh -Ritz technique used to approximate the equations of the modified structure

$$\left[[\tilde{K}]_0 + \lambda \left([\tilde{K}] - [\tilde{K}]_0 \right) \right] \{\psi\} = \{\tilde{P}\}_0 - \lambda \left(\{\tilde{P}\} - \{\tilde{P}\}_0 \right)$$

$$\text{where } [\tilde{K}]_0 = [\Gamma]^t [K]_0 [\Gamma]$$

$$[\tilde{K}] = [\Gamma]^t [K] [\Gamma]$$

$$\{\tilde{P}\}_0 = [\Gamma]^t \{P\}_0$$

$$\{\tilde{P}\} = [\Gamma]^t \{P\}$$

Figure 4

SELECTION AND EVALUATION OF THE GLOBAL APPROXIMATION

The effectiveness of the proposed procedure depends, to a great extent, on the proper choice of the global approximation vectors. In the present study the global approximation vectors are selected to be the response of the original structure, $\{X\}_0$, and its various-order derivatives with respect to the parameter λ . The recursion relations for evaluating the approximation vectors are obtained by successive differentiation of the original finite element equations. Note that the matrix on the left hand sides of these equations, $[K]_0$, is the same (see Fig. 5).

$$\{X\} = [\Gamma] \{\psi\}$$

$$\text{where } [\Gamma] = \left[\{X\}_0 \quad \left\{ \frac{\partial X}{\partial \lambda} \right\}_0 \quad \left\{ \frac{\partial^2 X}{\partial \lambda^2} \right\}_0 \dots \right]$$

$$[K]_0 \{X\}_0 = \{P\}_0$$

$$[K]_0 \left\{ \frac{\partial X}{\partial \lambda} \right\}_0 = - \left([K] - [K]_0 \right) \{X\}_0 + \{P\} - \{P\}_0$$

$$[K]_0 \left\{ \frac{\partial^2 X}{\partial \lambda^2} \right\}_0 = -2 \left([K] - [K]_0 \right) \left\{ \frac{\partial X}{\partial \lambda} \right\}_0$$

.

.

.

.

Same left hand side.

Figure 5

COMPUTATIONAL PROCEDURE

The computational procedure for generating the solution of the modified structure and the sensitivity derivatives is outlined in Fig. 6.

The first step is to generate the global approximation vectors at $\lambda=0$ through decomposition of the stiffness matrix of the original structure. The derivatives with respect to λ provide information about the sensitivity of the response to *all* the design modifications. Because λ is dimensionless, the derivatives with respect to λ have the same dimensions as the original response quantities, and consequently an assessment of the effect of design modifications on the response can be easily made.

The second step is to generate the reduced equations and solve them for the amplitudes of the global approximation vectors.

- Evaluate global approximation vectors at $\lambda = 0$
- Derivatives with respect to λ represent sensitivity of the response to design modifications
- Generate reduced equations
- Solve reduced equations and find amplitudes of global approximation vectors

Figure 6

RELATIONSHIP BETWEEN THE PRECONDITIONED CONJUGATE GRADIENT (PCG) TECHNIQUE AND THE PROPOSED COMPUTATIONAL PROCEDURE

If the proposed computational procedure is contrasted with the preconditioned conjugate gradient (PCG) technique in which the preconditioning matrix is selected to be the global stiffness matrix of the original structure, $[K]_0$, the relationships shown in Fig. 7 can be identified. These relations express the preconditioned residuals $\{y\}_0, \{y\}_1, \dots$ of the PCG technique in terms of the global approximation vectors of the foregoing technique, $\{\frac{\partial X}{\partial \lambda}\}_0, \{\frac{\partial^2 X}{\partial \lambda^2}\}_0, \dots$

Equivalence

$$([K]_0 + \lambda([K] - [K]_0))\{X\} = \{P\}_0 + \lambda(\{P\} - \{P\}_0)$$

$$[K]_0 = \text{preconditioning matrix}$$

PCG	Proposed procedure
$\{X\}_0$	$\{X\}_0$
<u>Preconditioned residuals</u>	
$\{y\}_0$	$\{\frac{\partial X}{\partial \lambda}\}_0$
$\{y\}_1$	$(1 - c_0) \{\frac{\partial X}{\partial \lambda}\}_0 + \frac{c_0}{2} \{\frac{\partial^2 X}{\partial \lambda^2}\}_0$
$\{y\}_i$	$\sum_{j=1}^{i+1} c_j \{\frac{\partial^j X}{\partial \lambda^j}\}_0$

Figure 7

IMPLICATIONS OF THE SIMILARITIES BETWEEN THE PROPOSED PROCEDURE AND THE PCG TECHNIQUE

The implications of the similarities between the proposed computational procedure and the PCG technique are listed in Fig. 8.

For the PCG technique, the similarities can be exploited to provide a rational approach for selecting the preconditioning matrix (as the global stiffness matrix of the original structure), and a physical meaning for the preconditioned residual vectors (in terms of sensitivity derivatives).

For the proposed procedure, some of the work done on parallelizing the PCG on multiprocessor computers can be exploited.

PCG

- Rational choice for preconditioning matrix
- Physical meaning for preconditioned residuals
(in terms of sensitivity derivatives)

Proposed procedure

- Exploiting work done on parallelizing PCG on
multiprocessor computers

Figure 8

APPLICATION TO EIGENVALUE PROBLEMS

The application of the proposed computational procedure to free vibration (eigenvalue) problems is outlined in Fig. 9. The governing equations of the original and modified structures are shown. Again, the operator splitting technique is applied, and the stiffness and mass matrices of the modified structure are written as the sum of the corresponding matrices of the original structure plus correction terms. The correction terms are identified by the tracing parameter λ . When $\lambda=0$, the original structure equations are recovered, and when $\lambda=1$ the modified structure equations are obtained.

Operator splitting

Original structure

$$\left[[K]_0 - \Omega [M]_0 \right] \{X\}_0 = 0$$

Modified structure

$$\left[[K] - \Omega [M] \right] \{X\} = 0$$

or,

$$\left[\left([K]_0 - \Omega [M]_0 \right) + \lambda \left([K]_a - \Omega [M]_a \right) \right] \{X\} = 0$$

$$\lambda = 0 \longrightarrow \text{original structure}$$

$$\lambda = 1 \longrightarrow \text{modified structure}$$

where $[K]_a = [K] - [K]_0$

$$[M]_a = [M] - [M]_0$$

Figure 9

The application of the reduction method to the free vibration problem is outlined in Fig. 10. As in the static analysis, the eigenvectors of the modified structure, $\{X\}$, are approximated by a linear combination of a few global approximation vectors. This is accomplished by the transformation shown. An efficient choice of the approximation vectors was found to be a few eigenvectors for the original structure (corresponding to $\lambda=0$) and their derivatives with respect to λ , evaluated at $\lambda=0$.

Then, the Rayleigh-Ritz technique is used to approximate the original large eigenvalue problem by the reduced one shown in Fig. 10. The solution of the reduced eigenvalue problem gives the amplitudes of the global approximation vectors.

Basis reduction

- Eigenvectors of modified structure, $\{X\}$, are approximated by:

$$\{X\}_{n,1} = [\Gamma]_{n,r} \{\psi\}_{r,1} \quad ; \quad r \ll n$$

where

$$[\Gamma] = \left[\begin{array}{cccc} \{X\}_1 & \left\{ \frac{\partial X}{\partial \lambda} \right\}_1 & \left\{ \frac{\partial^2 X}{\partial \lambda^2} \right\}_1 & \cdots \cdots \{X\}_2 & \left\{ \frac{\partial X}{\partial \lambda} \right\}_2 & \left\{ \frac{\partial^2 X}{\partial \lambda^2} \right\}_2 \cdots \end{array} \right]_{\lambda=0}$$

Reduced system of equations

- Rayleigh-Ritz technique is used to approximate the original eigenvalue problem by a reduced one

$$\left[\left([\tilde{K}]_0 - \Omega [\tilde{M}]_0 \right) + \lambda \left([\tilde{K}]_a - \Omega [\tilde{M}]_a \right) \right] \{\psi\} = 0$$

where

$$[\tilde{K}]_0 = [\Gamma]^t [K]_0 [\Gamma]$$

$$[\tilde{K}]_a = [\Gamma]^t [K]_a [\Gamma]$$

$$[\tilde{M}]_0 = [\Gamma]^t [M]_0 [\Gamma]$$

$$[\tilde{M}]_a = [\Gamma]^t [M]_a [\Gamma]$$

Figure 10

EVALUATION OF GLOBAL APPROXIMATION VECTORS

The recursion equations used in generating the eigenvectors at $\lambda=0$ and their first derivatives with respect to λ are shown in Fig. 11. Note that the left hand sides of all these equations are the same. The expression of the first derivatives of the eigenvalues with respect to λ appearing on the right hand sides of the equations are given in Fig. 11.

Since the matrix on the left hand side of the recursion equations used in evaluating these derivatives is singular, the solution of each set of equations can be expressed as the sum of a homogeneous solution (multiple of the eigenvector) and a particular solution, $\{Q\}_1$. The equations used in evaluating the particular solution $\{Q\}_1$ are given in Fig. 11. The details of this procedure are given in Ref. 5.

Recursion formulas

$$\begin{aligned}
 & \left[[K]_0 - \Omega [M]_0 \right] \{X\} = 0 \\
 & \left[[K]_0 - \Omega [M]_0 \right] \left\{ \frac{\partial X}{\partial \lambda} \right\} = \frac{\partial \Omega}{\partial \lambda} \left[[M]_0 + \lambda [M]_a \right] \{X\} - \left[[K]_a - \Omega [M]_a \right] \{X\} \\
 & \quad \vdots \\
 & \quad \vdots \\
 & \frac{\partial \Omega}{\partial \lambda} = \{X\}^t \left[[K]_a - \Omega [M]_a \right] \{X\} / \{X\}^t \left[[M]_0 + \lambda [M]_a \right] \{X\} \\
 & \quad \vdots \\
 & \quad \vdots \\
 & \left\{ \frac{\partial X}{\partial \lambda} \right\} = \{Q\}_1 + C_1 \{X\} \\
 & \quad \vdots \\
 & \quad \vdots
 \end{aligned}$$

Where $\{Q\}_1$ = particular solution.

Figure 11

COMPUTATIONAL PROCEDURE FOR EIGENVALUE PROBLEMS

The procedure for extracting the eigenvectors of the modified structure and for generating the sensitivity of the eigenvectors to design modifications is outlined in Fig. 12.

First: A few eigenvectors of the original structure (corresponding to $\lambda=0$) are generated.

Second: The derivatives of the eigenvectors with respect to λ are generated at $\lambda=0$. In the process, derivatives of the eigenvalues are also computed. These derivatives provide sensitivity information regarding the effect of all the design modifications on the eigenvectors and eigenvalues. The reduced equations are generated.

Third: The reduced eigenvalue problem is solved at $\lambda=1$.

- Generate eigenvectors for original structure ($\lambda = 0$)
- Generate global approximation vectors (derivatives of eigenvectors w.r.t. λ) and reduced equations. In the process, derivatives of Ω w.r.t. λ are computed
- Solve reduced eigenvalue problem at $\lambda = 1$

Figure 12

CANTILEVERED LATTICE TRUSS

To assess the effectiveness of the proposed computational procedure, a number of problems were solved by this procedure. Comparison was made with the direct solution of the structure. Herein a typical problem of a five-bay cantilevered lattice truss is considered (see Fig. 13). In the original structure all the longerons had the same cross section, and all the battens and diagonals had the same cross section. The design variables consisted of the cross sectional areas, moments of inertia and torsional constants. The characteristics of the original and modified structures are given in Fig. 13.

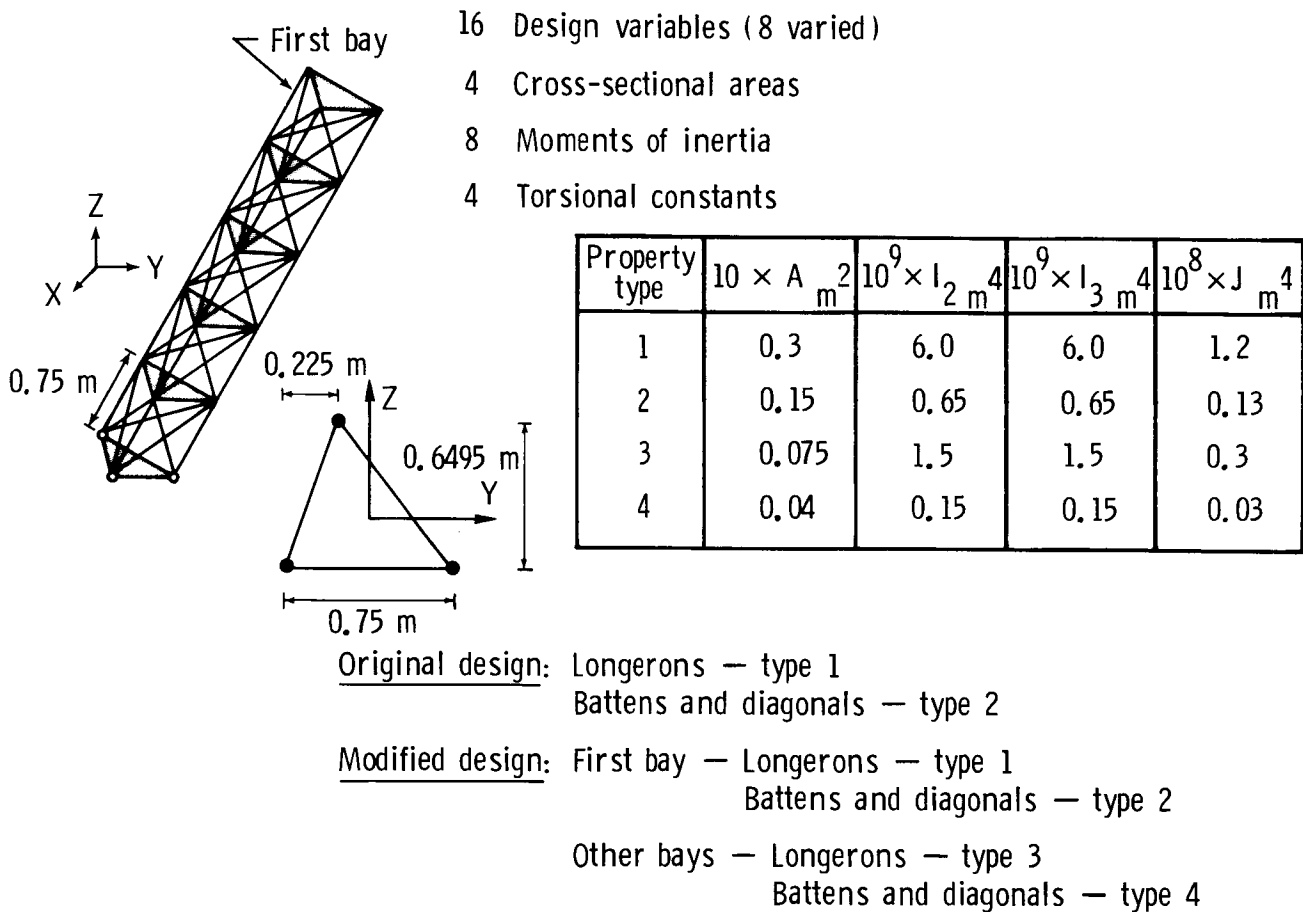


Figure 13

STATIC LOADING

The first problem considered is that of the static response due to a transverse load in the z direction at the free end of the cantilever. Figure 14 shows a summary of the results. The transverse displacement w and rotation at the free end (point a) of the original structure are given. The sensitivity of these quantities to design modifications is provided by $\left\{\frac{\partial X}{\partial \lambda}\right\}_0$ and $\left\{\frac{\partial^2 X}{\partial \lambda^2}\right\}_0$. Also shown in Fig. 14 are the corresponding w and ϕ_2 for the modified structure (which are considerably larger than those for the original structure). The solution obtained using the proposed procedure with four global approximation vectors was identical to the direct solution of the modified structure to at least three significant digits.

Static analysis

			w at a	ϕ_2 at a
Original structure $\lambda = 0$	$\{X\}$		0.102	-0.0397
	$\left\{\frac{\partial X}{\partial \lambda}\right\}_0$		0.0737	-0.0257
	$\left\{\frac{\partial^2 X}{\partial \lambda^2}\right\}_0$		0.110	-0.0388
Modified structure $\lambda = 1$	$\{X\}$	$r = 2$	0.394	-0.142
		$r = 4$	0.394	-0.143
		Full system	0.394	-0.143

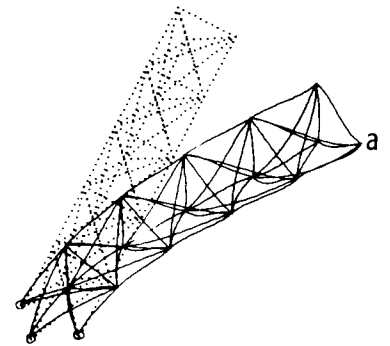


Figure 14

FREE VIBRATIONS

The second problem considered is that of the free vibrations of the same lattice structure. Figure 15 shows a summary of the results. The first three eigenvalues (squares of the vibration frequencies) and their first two derivatives with respect to λ are listed. The corresponding eigenvalues of the modified structure are also listed. The frequencies predicted by the proposed procedure with eight approximation vectors (four eigenvectors and their first derivatives with respect to λ) and twelve approximation vectors (four eigenvectors and their first two derivatives with respect to λ) are listed. The predictions of the eight-vector approximation are accurate for the first two eigenvalues, but not the succeeding ones. On the other hand, the predictions of the twelve-vector approximation are accurate for the first three eigenvalues.

			Mode		
			1	2	3
Original structure $\lambda = 0$	$10^{-5} \times \Omega$		0.324	0.502	1.815
	$10^{-5} \times \frac{\partial \Omega}{\partial \lambda}$		-0.134	-0.207	-0.486
	$10^{-5} \times \frac{\partial^2 \Omega}{\partial \lambda^2}$		-0.0911	-0.141	-0.472
Modified structure $\lambda = 1$	$10^{-5} \times \Omega$	$r = 8$	0.122	0.191	0.583
		$r = 12$	0.122	0.191	0.896
		Full system	0.122	0.191	0.896

Figure 15

MODE SHAPES

The first three mode shapes of the modified structure are shown in Fig. 16. Note that the first two vibration modes are bending modes and the third is a torsional mode.

Free vibrations

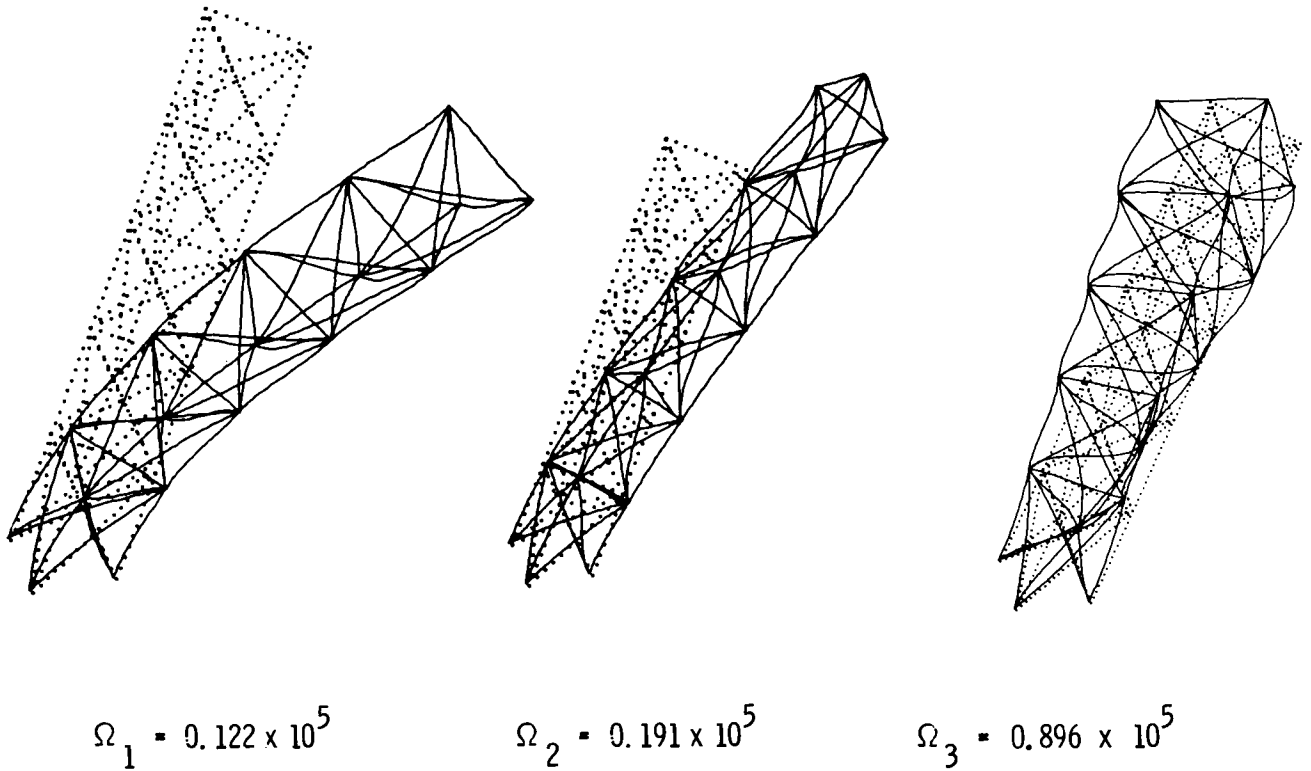


Figure 16

SUMMARY

In summary, a computational procedure has been developed for calculating the sensitivity derivatives of large structural systems as part of structural reanalysis (see Fig. 17). The three key elements of the procedure are:

- a) lumping of the large number of design variables into one (or small number of) tracing parameter(s);
- b) application of operator splitting/reduction technique; and,
- c) for very large problems use of multilevel substructuring technique.

The proposed procedure can be considered as a general computational strategy for generating the response of the modified structure using large perturbations from the response of the original structure.

For static problems the similarities between the proposed procedure and preconditioned conjugate gradient technique are identified and are exploited to provide a rational procedure for selecting the preconditioning matrix and a physical meaning for the preconditioned residual vectors.

Future work includes:

- o extension to more complex structures and to shape design modifications
- o generation of sensitivity information with respect to design variables.

- Computational procedure presented for calculating sensitivity derivatives as part of performing structural reanalysis for large-scale problems
 - Lumping of design variables into tracing parameter(s)
 - Application of operator splitting/reduction technique
 - Use of multilevel substructuring
- Future work includes:
 - Extension to more complex structures and to shape design modifications
 - Generation of sensitivity information w.r.t. design variables

Figure 17

REFERENCES

1. Adelman, H. M. and Haftka, R. T.: Sensitivity Analysis of Discrete Structural Systems. AIAA Journal, vol. 24, no. 5, May 1986, pp. 823-832.
2. Haug, E. J., Choi, K. K., and Komkov, V.: Design Sensitivity Analysis of Structural Systems, Academic Press, New York, 1986.
3. Noor, A. K. and Peters, J. M.: Model Size Reduction Technique for the Analysis of Symmetric Anisotropic Structures. Engineering Computations, vol. 2, no. 4, December 1985, pp. 285-292.
4. Noor, A. K. and Peters, J. M.: Nonlinear Analysis of Anisotropic Panels. AIAA Journal, vol. 24, no. 9, September 1986, pp. 1545-1553.
5. Noor, A. K. and Whitworth, S. L.: Model Size Reduction for the Buckling and Vibration Analyses of Anisotropic Panels. Journal of the Engineering Mechanics Division, ASCE, vol. 113, no. 2, February 1987, pp. 170-185.
6. Noor, A. K. and Whitworth, S. L.: Model Size Reduction for the Analysis of Symmetric Structures with Unsymmetric Boundary Conditions. International Journal for Numerical Methods in Engineering, 1987.

Standard Bibliographic Page

1. Report No. NASA CP-2457		2. Government Accession No.		3. Recipient's Catalog No.	
4. Title and Subtitle Sensitivity Analysis in Engineering				5. Report Date February 1987	
				6. Performing Organization Code 506-43-41-01	
7. Author(s) Howard M. Adelman and Raphael T. Haftka, Compilers				8. Performing Organization Report No. L- 16278	
9. Performing Organization Name and Address NASA Langley Research Center Hampton, VA 23665-5225				10. Work Unit No.	
				11. Contract or Grant No.	
12. Sponsoring Agency Name and Address National Aeronautics and Space Administration Washington, DC 20546-0001				13. Type of Report and Period Covered Conference Publication	
				14. Sponsoring Agency Code	
15. Supplementary Notes Howard M. Adelman: Langley Research Center, Hampton, Virginia. Raphael T. Haftka: Virginia Polytechnic Institute and State University, Blacksburg, Virginia.					
16. Abstract This conference publication contains the proceedings of the NASA/Virginia Polytechnic Institute and State University Symposium on Sensitivity Analysis in Engineering, held at the NASA Langley Research Center, Hampton, VA, September 25-26, 1986. The symposium focused primarily on sensitivity analysis of structural response. However, the first session, entitled "General and Multidisciplinary Sensitivity," focused on areas such as physics, chemistry, controls, and aerodynamics. The other four sessions were concerned with the sensitivity of structural systems modeled by finite elements. Session II dealt with Static Sensitivity Analysis and Applications; Session III with Eigenproblem Sensitivity Methods; Session IV with Transient Sensitivity Analysis; and Session V with Shape Sensitivity Analysis.					
17. Key Words (Suggested by Authors(s)) Sensitivity analysis Optimization Eigenvalue analysis Shape optimization Structural analysis				18. Distribution Statement Unclassified - Unlimited Subject Category 39	
19. Security Classif.(of this report) Unclassified		20. Security Classif.(of this page) Unclassified		21. No. of Pages 379	
				22. Price A17	